



**AUTHOR:**

**TITLE:**

**YEAR:**

**OpenAIR citation:**

This work was submitted to- and approved by Robert Gordon University in partial fulfilment of the following degree:

---

**OpenAIR takedown statement:**

Section 6 of the “Repository policy for OpenAIR @ RGU” (available from <http://www.rgu.ac.uk/staff-and-current-students/library/library-policies/repository-policies>) provides guidance on the criteria under which RGU will consider withdrawing material from OpenAIR. If you believe that this item is subject to any of these criteria, or for any other reason should not be held on OpenAIR, then please contact [openair-help@rgu.ac.uk](mailto:openair-help@rgu.ac.uk) with the details of the item and the nature of your complaint.

This is distributed under a CC \_\_\_\_\_ license.

---



# **Development and application of novel tracers for environmental applications**

**Morgan Adams**

**A thesis submitted in partial fulfilment of the requirement of The Robert Gordon University, Aberdeen for the award of Doctor of Philosophy**

To  
My grandparents

## **Abstract**

Novel glass tracers, organic and inorganic polymers based on narrow band atomic fluorescence, have been developed for deployment as environmental tracers. The use of discrete fluorescent species in an environmentally stable host has been investigated to replace existing toxic, broad band molecular dye tracers. The narrow band emission signals offer the potential for the tracing of a large numbers of signals in the same environment; this has been investigated by examining multiple doped tracers which have the potential for coding to specific effluent sources or particulates.

The concept of using lanthanide doped glasses as environmental tracers has been demonstrated. The spectral characterisation and concentration studies of the lanthanide doped tracer allow the selection of parameters to produce future tracers and detection systems for particular applications. Therefore by altering the chosen lanthanide dopant, number of dopants, dopant concentration and using selective excitation and emission wavelengths there are a huge number of possible unique tracer combinations. The significantly narrower bandwidth emission peaks of the lanthanide based tracers achieve more selective detection of multiple tracers without overlap interference and gives the potential to selectively and simultaneously monitor many different tracers in the same location. The spectral lifetime characteristics of the lanthanide tracers are very different from the lifetime of background fluorescence which is typically molecular in origin. This is an extra discrimination against background interference and is an important additional advantage of using lanthanide based tracers.

Overall this work shows that a very large number of unique environmental tracers can be obtained by varying the concentration, the number of lanthanide ions in a glass and also the possibility of using organic and inorganic lanthanide chelate doped tracers.

**Acknowledgements:**

I would like to thank Professor Pat Pollard and Professor Peter Robertson for their invaluable patience, belief and input over my time at The Robert Gordon University and in undertaking this PhD. Thank you also to the Robert Gordon University for giving me the opportunity with an RDI studentship.

I also wish to thank the School of Engineering and The Center for Research in Energy and Environment for providing a work environment conducive of academic achievement in applied research. I must also thank Dr. Radhakrishna Prabhu, Dr. Cathy McCullagh, Dr. Simon Officer and Dr. Catherine Hunter for their invaluable help.

Special thanks must be given to Dr. Edmund Bellu, Emma Bellu and Rebecca Sadler for their support and encouragement through difficult times.

## Table of Contents

<b>ABSTRACT .....</b>	<b>I</b>
<b>ACKNOWLEDGEMENTS: .....</b>	<b>II</b>
<b>GLOSSARY:.....</b>	<b>XIII</b>
<b>1 INTRODUCTION .....</b>	<b>1</b>
<b>1.1 Tracer Types and Applications .....</b>	<b>1</b>
1.1.1 <i>Fluorescent Dyes</i> .....	4
1.1.2 <i>Fluorescent Particulate Tracers</i> .....	6
1.1.3 <i>Natural Tracers (non injected)</i> .....	7
1.1.4 <i>Lanthanide Tracers</i> .....	7
1.1.5 <i>Isotope Tracers</i> .....	9
<b>1.2 Tracer Matrices.....</b>	<b>10</b>
1.2.1 <i>Glass Matrix</i> .....	10
1.2.2 <i>Borosilicate Glass</i> .....	11
1.2.3 <i>Borosilicate Glass and Sensitisers</i> .....	11
1.2.4 <i>Polymers</i> .....	12
1.2.4.1 <i>Inorganic Polymers - Sol Gel</i> .....	12
1.2.4.2 <i>Organic Polymers</i> .....	12
1.2.5 <i>Chelates</i> .....	13
<b>1.3 Project Aim and Milestones .....</b>	<b>14</b>
1.3.1 <i>Project Aim</i> .....	14
1.3.2 <i>Project Milestones</i> .....	15
<b>1.4 Summary .....</b>	<b>16</b>
<b>2 THEORY .....</b>	<b>19</b>
<b>2.1 Fluorescence .....</b>	<b>19</b>
2.1.1 <i>Molecular Fluorescence</i> .....	19
2.1.2 <i>Concentration and Fluorescence Intensity</i> .....	22
2.1.3 <i>Atomic Fluorescence</i> .....	24
<b>2.2 Lanthanides.....</b>	<b>28</b>
2.2.1 <i>Lanthanide Energy Levels</i> .....	29
2.2.2 <i>Lanthanide Energy Transfer</i> .....	34
<b>2.3 Chelates.....</b>	<b>35</b>
2.3.1 <i>Chelate Energy Transfer</i> .....	35
<b>2.4 Glass Formation.....</b>	<b>36</b>
<b>2.5 Polymerisation.....</b>	<b>39</b>
2.5.1 <i>Inorganic Polymerisation – Silica sol gel</i> .....	39
2.5.2 <i>Doped Sol Gel Sphere Formation</i> .....	40
2.5.3 <i>Organic Polymerisation</i> .....	41

<b>2.6</b>	<b>Particle Size</b> .....	<b>42</b>
<b>2.7</b>	<b>Experimental Design : Chemometrics</b> .....	<b>44</b>
2.7.1	<i>Taguchi Orthogonal Array Fractional Factorial Experimental Design</i> .....	45
<b>3</b>	<b>MATERIALS AND METHODS</b> .....	<b>46</b>
<b>3.1</b>	<b>Glass Tracer Fabrication</b> .....	<b>46</b>
3.1.1	<i>Blank Glass</i> .....	46
3.1.2	<i>Concentration Study Doped Glass Tracer</i> .....	47
<b>3.2</b>	<b>Experimental Design – Chemometrics For Multi-Ion Doping</b> .....	<b>48</b>
3.2.1	<i>Taguchi Orthogonal Array Fractional Factorial</i> .....	48
3.2.2	<i>Design of Experiment to investigate the concentration dependence of the fluorescence lanthanide response and glass host dependence</i> .....	48
3.2.3	<i>Design of Experiment to investigate the effects of fabrication parameters on the glass</i> 50	
<b>3.3</b>	<b>Glass Tracer Fabrication</b> .....	<b>51</b>
3.3.1	<i>Borosilicate Glass 1 Multiple Ion Doped Glass Tracer</i> .....	52
3.3.2	<i>Borosilicate Glass 2 Multiple Ion Doped Glass Tracer</i> .....	53
<b>3.4</b>	<b>Fabrication of Tracer Particles</b> .....	<b>55</b>
3.4.1	<i>Ball Milling</i> .....	56
3.4.2	<i>Size Fractioning</i> .....	56
3.4.2.1	<i>Shaker</i> .....	56
3.4.2.2	<i>Sonic Sifter</i> .....	57
<b>3.5</b>	<b>Particle Size Analysis</b> .....	<b>57</b>
<b>3.6</b>	<b>Inorganic Silica Polymers</b> .....	<b>58</b>
3.6.1	<i>Silica Sol Gel Spheres</i> .....	58
3.6.1.1	<i>Silica Sol Gel Spheres 800 nm</i> .....	58
3.6.1.2	<i>Silica Sol Gel Spheres 200 nm</i> .....	59
3.6.1.3	<i>Doped Sol Gel Spheres</i> .....	59
<b>3.7</b>	<b>Organic Polymers</b> .....	<b>60</b>
3.7.1	<i>Poly-EGDMA-co-MAA</i> .....	60
3.7.2	<i>Poly-EGDMA-co-HEMA</i> .....	60
<b>3.8</b>	<b>Doped Polymer Spheres</b> .....	<b>61</b>
3.8.1	<i>Doped Poly-EGDMA-co-MAA</i> .....	61
<b>3.9</b>	<b>Chelates</b> .....	<b>62</b>
3.9.1	<i>Chelate: 2,6-Pyridinedicarboxylic Acid</i> .....	63
3.9.2	<i>Chelate: Trifluoroacetone</i> .....	63
3.9.3	<i>Chelate: 1,10-Phenanthroline</i> .....	64
3.9.4	<i>Chelate: Thenolytrifluoroacetone</i> .....	64
3.9.5	<i>Chelate: Thenolytrifluoroacetone and 1,10-Phenanthroline</i> .....	64
<b>3.10</b>	<b>Background Study Samples</b> .....	<b>65</b>
3.10.1	<i>Dye Tracers</i> .....	65
3.10.2	<i>Crude Oils</i> .....	65
<b>3.11</b>	<b>Analytical Techniques</b> .....	<b>65</b>
3.11.1	<i>Fluorescence</i> .....	66

3.11.1.1 Perkin Elmer Lambda LS50B .....	66
3.11.1.2 Edinburgh Instruments FLS920P Spectrometer .....	68
<b>3.12 Fluorescent Lifetime Study .....</b>	<b>70</b>
3.12.1 Laser Induced Fluorescence Microscope .....	70
<b>3.13 Scanning Electron Microscopy .....</b>	<b>71</b>
<b>3.14 Detection System Development .....</b>	<b>71</b>
3.14.1 Optical Fibre Heads .....	72
3.14.2 Excitation Sources.....	73
3.14.2.1 Stellarnet Spectrometer .....	74
<b>4 RESULTS AND DISCUSSION .....</b>	<b>75</b>
<b>4.1 Concentration Studies with Spectral Characterisation .....</b>	<b>75</b>
4.1.1 Europium Spectral Characterisation and Single Doped Concentration Study ...	76
4.1.2 Dysprosium Spectral Characterisation and Single Doped Concentration Study	82
4.1.3 Terbium Spectral Characterisation and Single Doped Concentration Study .....	87
<b>4.2 Investigation of the Fabrication Process .....</b>	<b>91</b>
4.2.1 Reproducibility Study .....	91
4.2.2 Investigation of Varying Fabrication Parameters .....	93
4.2.3 Fabrication Process Conclusion .....	97
4.2.3.1 Reproducibility .....	97
4.2.3.2 Parameter Variation .....	97
<b>4.3 Multiple Ion Doped Glass Characterisation and Concentration Study in Borosilicate Glass 1 .....</b>	<b>99</b>
4.3.1 Statistical Analysis of Multi-Ion Doping in Glass 1 .....	101
4.3.2 Trend Analysis of europium, terbium and dysprosium ion interactions in a multi-ion Glass 1 .....	102
4.3.3 Fluorescent Lifetime Study of Multi-Ion Doped Glass 1 .....	107
4.3.4 Glass 1 Characterisation Summary .....	114
<b>4.4 Multiple Ion Doped Glass Characterisation and Concentration Study in Borosilicate Glass 2. ....</b>	<b>115</b>
4.4.1 Statistical Analysis of Multi-Ion Doping in Glass 2 .....	118
4.4.2 Fluorescent Lifetime Study of Multi-Ion Doped Glass 2 .....	123
4.4.3 Investigation into peak wavelength variations with dopant concentrations and glass matrix.....	127
4.4.3.1 Borosilicate glass 1 peak wavelength variations.....	127
4.4.3.2 Borosilicate glass 2 peak wavelength variations.....	129
4.4.4 Conclusions of borosilicate glass 1 and glass 2 .....	131
4.4.4.1 Peak wavelength variations.....	131
4.4.4.2 Spectral Characterisation.....	131
<b>4.5 Lanthanide Glass Tracer Comparison with Existing Molecular Dye Tracers: 132</b>	
4.5.1 Glass Tracer Particles.....	134
<b>4.6 Inorganic Polymers - Sol Gel Spheres.....</b>	<b>135</b>
4.6.1 Undoped Inorganic Polymer Silica Sol Gel Spheres .....	135
4.6.2 Doped Inorganic Polymer Silica Sol Gel Spheres.....	136
4.6.2.1 Spectroscopy Analysis of Eu[ttfa][phen] Beads.....	136
4.6.3 Fluorescent lifetime study of europium chelate in inorganic polymer sol gel ..	140



<b>4.7</b>	<b>Blank Organic Polymer Spheres</b> .....	<b>141</b>
4.7.1	<i>Organic Polymer Poly-EGDMA-co-MAA Spheres</i> .....	141
4.7.2	<i>Organic Polymer Poly-EGDMA-co-HEMA</i> .....	142
4.7.3	<i>Organic Polymer Poly-MMA</i> .....	142
4.7.4	<i>Doped Polymer Spheres</i> .....	143
4.7.4.1	<i>Organic Polymer Poly-EGDMA-co-MAA doped with Eu[ttfa][phen]</i> .....	143
4.7.5	<i>Fluorescent Lifetime Study of Europium Chelate in Polymer</i> .....	146
<b>4.8</b>	<b>Comparison Study</b> .....	<b>148</b>
<b>4.9</b>	<b>Tracer Detection</b> .....	<b>151</b>
4.9.1	<i>Bench Top Detection System – Glass Tracer</i> .....	151
<b>4.10</b>	<b>Background Discrimination</b> .....	<b>152</b>
4.10.1	<i>Fluorescence Lifetime for Background Discrimination</i> .....	152
4.10.2	<i>Background discrimination of the presence of contaminants</i> .....	154
4.10.3	<i>Background Discrimination Conclusion</i> .....	155
<b>4.11</b>	<b>Overall Results and Discussion Summary</b> .....	<b>156</b>
<b>5</b>	<b>CASE STUDY – BOWMORE HARBOUR FEASIBILITY STUDY ...</b>	<b>158</b>
<b>5.1</b>	<b>Introduction: The Proposed Scheme of Work</b> .....	<b>158</b>
<b>5.2</b>	<b>Objectives of the Study</b> .....	<b>160</b>
<b>5.3</b>	<b>Materials and Methods</b> .....	<b>161</b>
5.3.1	<i>Sediment Sampling</i> .....	163
5.3.2	<i>Water Sampling</i> .....	164
5.3.3	<i>Tracer Deployment</i> .....	165
<b>5.4</b>	<b>Case Study Results and Discussion</b> .....	<b>167</b>
5.4.1	<i>Tracer Deployment</i> .....	167
5.4.2	<i>Particle Size</i> .....	170
5.4.3	<i>Weather Influence on Current Direction</i> .....	174
<b>5.5</b>	<b>Conclusions</b> .....	<b>174</b>
<b>6</b>	<b>CONCLUSIONS</b> .....	<b>178</b>
<b>6.1</b>	<b>Overall Conclusion</b> .....	<b>182</b>
<b>7</b>	<b>FUTURE WORK</b> .....	<b>186</b>
<b>7.1</b>	<b>Future Applications</b> .....	<b>186</b>
<b>8</b>	<b>REFERENCES</b> .....	<b>188</b>
	<b>APPENDIX I - PUBLICATIONS</b> .....	<b>196</b>
	<b>Refereed Journals</b> .....	<b>197</b>
	<b>Conferences</b> .....	<b>197</b>

<b>Conference Prizes .....</b>	<b>198</b>
<b>APPENDIX II: SPECTROSCOPIC CHARACTERISATION DATA .....</b>	<b>232</b>
<b>APPENDIX III: LIFETIME DATA .....</b>	<b>233</b>
<b>APPENDIX IV: CASE STUDY GPS DATA .....</b>	<b>234</b>

## **List of Figures**

FIGURE 1 (A) PRODUCED WATER DISCHARGE; (B) TRACER DOPED DISCHARGE.....	2
FIGURE 2 PARTICULATE DYE TRACER DEPLOYMENT IN BOWMORE HARBOUR .....	3
FIGURE 3 ENERGY LEVELS SHOWING RADIATIVE AND NON-RADIATIVE EMISSIONS ...	21
FIGURE 4 ATOMIC FLUORESCENCE PEAKS FROM A GLASS SAMPLE DOPED WITH EUROPIUM, TERBIUM AND DYSPROSIUM .....	24
FIGURE 5 ENERGY LEVELS OF LANTHANIDE 3 <sup>+</sup> IONS EUROPIUM, TERBIUM AND DYSPROSIUM, MODIFIED DIEKE DIAGRAM.....	25
FIGURE 6 EXAMPLES OF GENERAL SET OF <i>f</i> -ORBITALS.....	26
FIGURE 7 EUROPIUM ENERGY LEVELS SHOWING THE TRANSITION OF <sup>5</sup> D <sub>0</sub> TO <sup>7</sup> F <sub>2</sub> WHICH LEADS TO THE EMISSION OF 615 NM.....	29
FIGURE 8 TERBIUM ENERGY LEVELS SHOWING THE TRANSITION OF <sup>5</sup> D <sub>4</sub> TO <sup>7</sup> F <sub>5</sub> WHICH LEADS TO THE EMISSION OF 542 NM.....	30
FIGURE 9 DYSPROSIUM ENERGY LEVELS SHOWING THE TRANSITION OF <sup>4</sup> F <sub>9/2</sub> TO <sup>6</sup> H <sub>13/2</sub> WHICH LEADS TO THE EMISSION OF 575 NM.....	32
FIGURE 10 ENERGY LEVEL DIAGRAM SHOWING THE ENERGY TRANSFER PROCESS FROM DYSPROSIUM TO TERBIUM [59].....	34
FIGURE 11: EXAMPLE OF A BIDENTATE CHELATING AGENTS: 1,10-PHENANTHROLINE AND THENOYLTRIFLUOROACETONE BONDED TO A EU <sup>3+</sup> ION.....	35
FIGURE 12 LUMINESCENCE IN LANTHANIDE CHELATE COMPLEXES .....	36
FIGURE 13 PHASE DIAGRAM FOR AN SiO <sub>2</sub> -B <sub>2</sub> O <sub>3</sub> -Na <sub>2</sub> O SYSTEM [107].....	37
FIGURE 14 SCHEMATIC 2-DIMENSIONAL DRAWING OF THE STRUCTURE OF A SILICON DIOXIDE MATRIX.....	40
FIGURE 15 SCHEMATIC 2-DIMENSIONAL DRAWING OF THE STRUCTURE OF A LANTHANIDE CHELATE DOPED SILICON DIOXIDE MATRIX .....	40
FIGURE 16 CROSS LINKED POLYMER, POLYETHYLENE GLYCOL DIMETHACRYLATE .....	41
FIGURE 17 DOPED CROSS LINKED POLYMER, POLYETHYLENE GLYCOL DIMETHACRYLATE .....	42
FIGURE 18 EXAMPLE OF PARTICLE SIZE ANALYSIS RESULTS. ....	44
FIGURE 19 (I) CONTOUR PLOT (II) EXCITATION (VERTICAL RED LINE) AND (III) EMISSION (HORIZONTAL GREEN LINE) SPECTRA FOR GLASS 1 SAMPLE 7.....	67
FIGURE 20 (A) POWDER SAMPLE CELL IN HOLDER ON MOUNT, (B) GLASS SAMPLE IN HOLDER ON MOUNT .....	68
FIGURE 21 EDINBURGH INSTRUMENTS FLS920P CONFIGURATION INTERFACE .....	69
FIGURE 22 EXAMPLE OF EUROPIUM EMISSION SPECTRA FROM AN EXCITATION OF 393 NM.....	70
FIGURE 23 LASER INDUCED SCANNING FLUORESCENCE MICROSCOPE SETUP FOR FLUORESCENCE LIFETIME STUDY .....	70
FIGURE 24 OPTICAL FIBRE HEAD DESIGN, (I) SHOWING A CUT THROUGH EXAMPLE OF LAYOUT, (II) THE POSITION OF THE OPTICAL FIBRES AND (III) THE COMPLETE HEAD WITH AN EXAMPLE OF LIGHT PATH. ....	72
FIGURE 25 SPECTRAL OUTPUT FROM HARMA 500W UV LAMP.....	74
FIGURE 26 THREE DIMENSIONAL FLUORESCENCE SPECTRUM OF A BLANK SAMPLE OF GLASS 1 .....	75
FIGURE 27 EMISSION AND EXCITATION SPECTRA OF A BLANK SAMPLE OF GLASS 1 ...	75
FIGURE 28 3 DIMENSIONAL FLUORESCENCE SPECTRUM OF A 0.8 MOL % EUROPIUM SAMPLE .....	76
FIGURE 29 EMISSION AND EXCITATION SPECTRA OF A 0.8 MOL % EUROPIUM SAMPLE .....	77
FIGURE 30 EUROPIUM EMISSION INTENSITY AT 612 NM FROM EXCITATION AT 362, 381, 393, 412, 465, 531 AND 579 NM .....	79
FIGURE 31 THICKNESS VARIATION OF EUROPIUM GLASS SAMPLES ACROSS THE CONCENTRATION RANGE.....	80
FIGURE 32 GLASS SAMPLE THICKNESS VARIATION MEASUREMENT PLACEMENT.....	81

FIGURE 33 THREE DIMENSIONAL FLUORESCENCE SPECTRUM OF A 0.6 MOL % DYSPROSIUM SAMPLE .....	82
FIGURE 34 EMISSION AND EXCITATION SPECTRA OF A 0.6 MOL % DYSPROSIUM SAMPLE .....	82
FIGURE 35 DYSPROSIUM EMISSION INTENSITY AT 481 NM FROM EXCITATION AT 324, 352, 354, 391, 426, 452 AND 471 NM .....	84
FIGURE 36 DYSPROSIUM EMISSION INTENSITY AT 575 NM FROM EXCITATION AT 324, 352, 354, 391, 426, 452 AND 471 NM .....	85
FIGURE 37 THICKNESS VARIATION OF DYSPROSIUM GLASS SAMPLES ACROSS THE CONCENTRATION RANGE.....	86
FIGURE 38 THREE DIMENSIONAL FLUORESCENCE SPECTRUM OF A 1.0 MOL % TERBIUM SAMPLE .....	87
FIGURE 39 EMISSION AND EXCITATION SPECTRA OF A 1.0 MOL % TERBIUM SAMPLE	87
FIGURE 40 TERBIUM EMISSION INTENSITY AT 542 NM FROM EXCITATION AT 352, 375 AND 483 NM .....	89
FIGURE 41 THICKNESS VARIATION OF TERBIUM GLASS SAMPLES ACROSS THE CONCENTRATION RANGE.....	90
FIGURE 42 SINGLE LINE EUROPIUM EMISSION SPECTRA FROM 3 MOL % DOPED SAMPLES (EX 465 NM, EM 615 NM).....	92
FIGURE 43 FLUORESCENCE LIFETIME PROFILES OF 3 MOL % EUROPIUM GLASSES .....	93
FIGURE 44 VARIATION OF PEAK EMISSION INTENSITY AT 577 NM FOR 1 MOL % DYSPROSIUM AS THE FABRICATION PROCESSES ARE CHANGED .....	94
FIGURE 45 VARIATION OF THE 577 NM EMISSION PEAK WAVELENGTH FROM 1 MOL % DYSPROSIUM AS THE FABRICATION PROCESSES ARE CHANGED .....	95
FIGURE 46 LIFETIME VARIATION WITH EXPERIMENT OF THE 577 NM DYSPROSIUM EMISSION PEAK AS THE FABRICATION PROCESSES ARE CHANGED .....	96
FIGURE 47 VARIATION OF THE 452 NM EXCITATION WAVELENGTH FROM 1 MOL % DYSPROSIUM AS THE FABRICATION PROCESSES ARE CHANGED .....	96
FIGURE 48 EUROPIUM, TERBIUM AND DYSPROSIUM TRIPLE DOPED TRACER.....	99
FIGURE 49 EMISSION AND EXCITATION SPECTRA OF A EUROPIUM, TERBIUM AND DYSPROSIUM TRIPLE DOPED TRACER.....	99
FIGURE 50 EUROPIUM MEAN INTENSITY TRENDS WITH VARIATIONS IN DOPANT CONCENTRATIONS FOR GLASS 1 SAMPLES .....	102
FIGURE 51 TERBIUM MEAN INTENSITY TRENDS WITH VARIATIONS IN DOPANT CONCENTRATIONS FOR GLASS 1 SAMPLES .....	103
FIGURE 52 DYSPROSIUM MEAN INTENSITY TRENDS WITH VARIATIONS IN DOPANT CONCENTRATIONS FOR GLASS 1 SAMPLES .....	104
FIGURE 53 ENERGY TRANSFER FROM TERBIUM 485 NM EXCITATION TO EUROPIUM 615 NM EMISSION, MEAN INTENSITY AS DOPANT CONCENTRATIONS INCREASED.....	105
FIGURE 54 ENERGY TRANSFER FROM DYSPROSIUM 452 NM EXCITATION TO TERBIUM 545 NM EMISSION, MEAN INTENSITY AS DOPANT CONCENTRATIONS INCREASED .....	106
FIGURE 55 FLUORESCENT LIFETIME PROFILE OF EUROPIUM IONS DOPED IN GLASS 1 SAMPLE 1 .....	108
FIGURE 56 FLUORESCENT LIFETIME PROFILE OF TERBIUM IONS IN GLASS 1 SAMPLE 1 .....	109
FIGURE 57 FLUORESCENT LIFETIME PROFILE OF DYSPROSIUM IONS IN GLASS 1 SAMPLE 1.....	110
FIGURE 58 FLUORESCENT LIFETIME TRENDS OF EUROPIUM IN GLASS 1 GLASS SAMPLES WITH VARYING EUROPIUM, TERBIUM AND DYSPROSIUM CONCENTRATIONS FOR EXCITATION AT 464 NM AND EMISSION AT 615 NM.....	111
FIGURE 59 FLUORESCENT LIFETIME TRENDS IN TERBIUM IN GLASS 1 GLASS SAMPLES WITH VARYING EUROPIUM, TERBIUM AND DYSPROSIUM CONCENTRATIONS FOR EXCITATION AT 483 NM AND EMISSION AT 546 NM.....	112
FIGURE 60 FLUORESCENT LIFETIME TRENDS OF DYSPROSIUM IN GLASS 1 GLASS SAMPLES WITH VARYING EUROPIUM, TERBIUM AND DYSPROSIUM CONCENTRATIONS FOR EXCITATION AT 451 NM AND EMISSION AT 577 NM. ....	113

FIGURE 61 FLUORESCENCE SPECTRUM OF A BLANK SAMPLE OF GLASS 2 .....	115
FIGURE 62 EMISSION AND EXCITATION SPECTRA OF A BLANK SAMPLE OF GLASS 2 ..	115
FIGURE 63 FLUORESCENCE SPECTRUM OF GLASS 2 SAMPLE 13 (1 MOL % EUROPIUM, 1 MOL % TERBIUM, 2 MOL % DYSPROSIUM) .....	116
FIGURE 64 EXCITATION AND EMISSION SPECTRUM OF GLASS 2 SAMPLE 13 (1 MOL % EUROPIUM, 1 MOL % TERBIUM, 2 MOL % DYSPROSIUM).....	116
FIGURE 65 EUROPIUM MEAN INTENSITY TRENDS WITH VARIATIONS IN DOPANT CONCENTRATIONS FOR GLASS 2 SAMPLES .....	118
FIGURE 66 TERBIUM MEAN INTENSITY TRENDS WITH VARIATIONS IN DOPANT CONCENTRATIONS FOR GLASS 2 SAMPLES .....	119
FIGURE 67 DYSPROSIUM MEAN INTENSITY TRENDS WITH VARIATIONS IN DOPANT CONCENTRATIONS FOR GLASS 2 SAMPLES .....	120
FIGURE 68 ENERGY TRANSFER FROM TERBIUM 485 NM EXCITATION TO EUROPIUM 615 NM EMISSION, MEAN INTENSITY AS DOPANT CONCENTRATIONS INCREASED.....	121
FIGURE 69 ENERGY TRANSFER FROM DYSPROSIUM 450 NM EXCITATION TO TERBIUM 545 NM EMISSION, MEAN INTENSITY AS DOPANT CONCENTRATIONS INCREASED .....	122
FIGURE 70 FLUORESCENT LIFETIME TRENDS OF EUROPIUM IN GLASS 2 WITH VARYING CONCENTRATIONS OF EUROPIUM, TERBIUM & DYSPROSIUM FOR EXCITATION AT 464 NM AND EMISSION AT 615 NM.....	123
FIGURE 71 FLUORESCENT LIFETIME TRENDS OF TERBIUM IN GLASS 2 WITH VARYING CONCENTRATIONS OF EUROPIUM, TERBIUM AND DYSPROSIUM FOR EXCITATION AT 483 NM AND EMISSION AT 546 NM.....	124
FIGURE 72 FLUORESCENT LIFETIME TRENDS OF DYSPROSIUM IN GLASS 2 FOR VARYING CONCENTRATIONS OF EUROPIUM, TERBIUM & DYSPROSIUM FOR EXCITATION AT 451 NM AND EMISSION AT 577NM.....	125
FIGURE 73 INVESTIGATION INTO CHANGES IN THE PEAK EXCITATION AND EMISSION WAVELENGTHS FOR EUROPIUM IN GLASS 1 SAMPLES.....	127
FIGURE 74 INVESTIGATION INTO CHANGES IN THE PEAK EXCITATION AND EMISSION WAVELENGTHS FOR TERBIUM IN GLASS 1 SAMPLES .....	128
FIGURE 75 INVESTIGATION INTO CHANGES IN THE PEAK EXCITATION AND EMISSION WAVELENGTHS FOR DYSPROSIUM IN GLASS 1 SAMPLES.....	128
FIGURE 76 INVESTIGATION INTO CHANGES IN THE PEAK EXCITATION AND EMISSION WAVELENGTHS FOR EUROPIUM IN GLASS 2 SAMPLES.....	129
FIGURE 77 INVESTIGATION INTO CHANGES IN THE PEAK EXCITATION AND EMISSION WAVELENGTHS FOR TERBIUM IN GLASS 2 SAMPLES .....	130
FIGURE 78 INVESTIGATION INTO CHANGES IN THE PEAK EXCITATION AND EMISSION WAVELENGTHS FOR DYSPROSIUM IN GLASS 2 SAMPLES.....	130
FIGURE 79 FLUORESCENT EMISSION FROM EUROPIUM DOPED BULK GLASS FROM A 465 NM EXCITATION .....	132
FIGURE 80 FLUORESCENT EMISSION FROM A FLUORESCHEIN DYE TRACER FROM A 475 NM EXCITATION .....	133
FIGURE 81 FLUORESCENT EMISSION FROM RHODAMINE DYE TRACER FROM A 475 NM EXCITATION.....	134
FIGURE 82 COMPARISON OF EMISSIONS FROM 3 MOL % EUROPIUM DOPED GLASS 1 MATRIX, BULK SAMPLE, <5 $\mu$ M, 5-10 $\mu$ M, 10-20 $\mu$ M AND 45-75 $\mu$ M POWDER FROM A 393 NM EXCITATION. ....	135
FIGURE 83 UNDOPED SILICA SOL GEL SPHERES .....	136
FIGURE 84: DOPED SILICA SOL GEL SPHERES .....	137
FIGURE 85 EMISSION SPECTRA FROM EU[TTFA][PHEN] DOPED SILICA SOL GEL 200 NM SPHERE FROM 355 NM EXCITATION.....	137
FIGURE 86 EMISSION SPECTRA FROM EU[TTFA][PHEN] DOPED SILICA SOL GEL 200 NM SPHERES FROM 345, 350, 355, 360, 365 AND 370 NM EXCITATIONS.....	138
FIGURE 87 PEAK INTENSITY VARIATIONS AT 612 NM EMISSION FROM 345, 350, 355, 365 AND 370 EXCITATIONS FROM EU[TTFA][PHEN] SILICA SOL GEL SPHERES. ..	139
FIGURE 88 FLUORESCENCE LIFETIME PROFILES OF 1 WT % EU[TTFA][PHEN] IN INORGANIC POLYMER.....	140

FIGURE 89 BLANK POLY-EGDMA-CO-MAA .....	141
FIGURE 90 BLANK POLY-EGDMA-CO-HEMA SPHERES .....	142
FIGURE 91 BLANK POLY-METHACRYLIC ACID SPHERES .....	143
FIGURE 92 SEM IMAGE OF EU[TTFA][PHEN] POLY-EGDMA-CO-MAA SPHERES .....	144
FIGURE 93 EMISSION SPECTRA OF EU[TTFA][PHEN] DOPED EGDMA-CO-MAA POLYMER SPHERES FROM A 355 NM EXCITATION. ....	144
FIGURE 94 EMISSION SPECTRA OF EU[TTFA][PHEN] DOPED EGDMA-CO-MAA POLYMER SPHERES FROM 345, 350, 355, 360, 365 AND 370 NM EXCITATIONS.....	145
FIGURE 95 PEAK INTENSITY VARIATIONS AT 611 NM EMISSION FROM 345, 350, 355, 365 AND 370 EXCITATIONS FROM EU[TTFA][PHEN] POLYMER SPHERES.....	146
FIGURE 96 FLUORESCENT LIFETIME PROFILE OF EUROPIUM CHELATED IONS IN POLY-EGDMA-CO-MAA .....	147
FIGURE 97 COMPARISON OF EU[TTFA][PHEN] DOPED SILICA SOL GEL AND POLY-EGDMA-CO-MAA AT 355 NM EXCITATION WITH BULK 3 MOL % EUROPIUM DOPED BOROSILICATE GLASS AT 393 NM EXCITATION.....	148
FIGURE 98 COMPARISON OF 612 NM FLUORESCENCE EMISSION FROM EUROPIUM DOPED BULK GLASS, GLASS POWDER, DOPED CHELATE, DOPED POLYMER AND DOPED SOL GEL. ....	149
FIGURE 99 SCHEMATIC OF TRACER DETECTION SYSTEM TRIAL .....	151
FIGURE 100 SURFACE PROJECTION FLUORESCENCE MAP OF EUROPIUM GLASS TRACER ON A COARSE SEDIMENT BED .....	152
FIGURE 101 FLUORESCENT LIFETIME PROFILE OF EUROPIUM IONS IN BOROSILICATE GLASS.....	153
FIGURE 102 FLUORESCENCE EMISSION FROM GULLFAKS CRUDE OIL FROM A 490 NM EXCITATION.....	154
FIGURE 103 FLUORESCENCE EMISSION FROM BRENT CRUDE OIL FROM A 470 NM EXCITATION.....	155
FIGURE 104 BOWMORE HARBOUR SHOWING SILTING .....	158
FIGURE 105 IMAGES OF BOWMORE HARBOUR AT LOW TIDE, PRIOR TO THE 2000 CLEARING.....	159
FIGURE 106 RESEARCH VESSEL JEANIE ANNE .....	161
FIGURE 107 GPS TRACK PLOT OF LOCHINDAAL CRUISE FROM MAPSOURCE VERSION 6.11.6 GARMIN LTD. ....	162
FIGURE 108 DEPLOYMENT OF THE VAN VEEN GRAB SAMPLER.....	164
FIGURE 109 AQUATIC RESEARCH WATER SAMPLER .....	164
FIGURE 110 DEPLOYMENT OF TRACER OFF PIER POINT, TRACER MOVEMENT IN WESTERLY DIRECTION AWAY FROM HARBOUR. ....	166
FIGURE 111 DIAGRAM OF BOWMORE HARBOUR WITH THE 4 TRACER DEPLOYMENT SITES AND THE NOTED DIRECTION OF TRACER MOVEMENT IN RELATION TO TIDE AND WIND DIRECTION. THURSDAY 30-10-08.....	167
FIGURE 112 DEPLOYMENT OF TRACER FROM PIER STEPS, 4 M INSIDE THE HARBOUR MOUTH. TRACER MOVED OUT OF HARBOUR AND AROUND THE PIER END TOWARDS THE WEST. ....	168
FIGURE 113 DIAGRAM OF BOWMORE HARBOUR, SECOND DAY OF TRACER DEPLOYMENT, WITH THE 5 TRACER DEPLOYMENT SITES AND THE NOTED DIRECTION OF TRACER MOVEMENT IN RELATION TO TIDE AND WIND DIRECTION. FRIDAY 31-10-08. ...	169
FIGURE 114 DEPLOYMENT OF TRACER OFF DOG LEG OF BREAK WATER, TRACER MOVEMENT ACROSS HARBOUR MOUTH IN WESTERLY DIRECTION .....	170
FIGURE 115 PARTICLE SIZE DISTRIBUTION PLOT FOR WATER SAMPLE NUMBER 6 .....	171
FIGURE 116 PARTICLE SIZE DATA OBTAINED FROM WATER SAMPLE NUMBER 6 .....	171
FIGURE 117 BOWMORE HARBOUR SAND BAR .....	175
FIGURE 118 SHOWS THE HOLES IN THE BREAK WATER TOWARDS THE NORTH EAST CORNER (INDICATED BY * AND **). THE HOLE AT THE CORNER BEING DOWN TO THE BEACH LEVEL AND THE SECOND BEING SLIGHTLY SHALLOWER.....	176
FIGURE 119 VIEW IN LINE WITH BREAK WATER DOG LEG.....	177
FIGURE 120 VIEW OF BREAK WATER AT HIGH TIDE. ....	177

## **List of Tables**

TABLE 1 ISOTOPES AND THEIR TRACING APPLICATIONS.....	9
TABLE 2 ENERGY TRANSITIONS AND EMISSION WAVELENGTHS FOR EUROPIUM .....	30
TABLE 3 ENERGY TRANSITIONS AND EMISSION WAVELENGTHS FOR TERBIUM.....	31
TABLE 4 ENERGY TRANSITIONS AND EMISSION WAVELENGTHS FOR DYSPROSIUM.....	33
TABLE 5 COMPONENT MATERIALS OF THE BOROSILICATE GLASS MATRIX .....	46
TABLE 6 CONCENTRATION STUDY DOPING CONCENTRATIONS .....	47
TABLE 7 TAGUCHI ORTHOGONAL ARRAY FRACTIONAL FACTORIAL DESIGN OF EXPERIMENT FOR GLASS1 AND GLASS 2 .....	49
TABLE 8 TAGUCHI ORTHOGONAL ARRAY FRACTIONAL FACTORIAL DESIGN OF EXPERIMENT FOR FABRICATION PARAMETER VARIATION .....	50
TABLE 9 EXPERIMENTAL CONDITIONS REQUIRED FOR TAGUCHI ORTHOGONAL ARRAY FRACTIONAL FACTORIAL ANALYSIS .....	51
TABLE 10 CONCENTRATION (MOL %) COMBINATIONS FOR MULTIPLE ION DOPED BOROSILICATE GLASS 1 SAMPLES .....	52
TABLE 11 CONCENTRATION COMBINATIONS FOR MULTIPLE ION DOPED BOROSILICATE GLASS 1 SAMPLES .....	53
TABLE 12 CONCENTRATION (MOL %) COMBINATIONS FOR MULTIPLE ION DOPED BOROSILICATE GLASS 2 SAMPLES .....	54
TABLE 13 CONCENTRATION COMBINATIONS FOR MULTIPLE ION DOPED BOROSILICATE GLASS 2 SAMPLES .....	55
TABLE 14 CHELATE COMPOUNDS INVESTIGATED .....	62
TABLE 15 INSTRUMENT SETTINGS FOR PERKIN ELMER LS50B .....	66
TABLE 16 TECHNICAL SPECIFICATION OF TWIN CORE POLYMER FIBRES.....	73
TABLE 17 EXCITATION AND EMISSION WAVELENGTHS FOUND IN EUROPIUM DOPED GLASS.....	78
TABLE 18 EXCITATION AND EMISSION WAVELENGTHS OF DYSPROSIUM DOPED GLASS .....	83
TABLE 19 EXCITATION AND EMISSION WAVELENGTHS OF TERBIUM DOPED GLASS ....	88
TABLE 20 EXPERIMENTAL PARAMETER CHANGES IN FURNACE TEMPERATURE AND TIME, AND ANNEALING TEMPERATURE AND TIME .....	94
TABLE 21 SPECTRAL CHARACTERISTICS FOR EXPERIMENTS 1-8 .....	97
TABLE 22 FLUORESCENCE PEAKS FROM A TRIPLE DOPED SAMPLES SHOWN IN FIGURE 48. YELLOW DYSPROSIUM, ORANGE TERBIUM AND RED EUROPIUM.....	100
TABLE 23 WAVELENGTHS SELECTED FOR TREND ANALYSIS .....	101
TABLE 24 TABLE OF PEAK WAVELENGTHS FOR FLUORESCENCE EXCITATION, EMISSION AND FILTER .....	107
TABLE 25 TABLE OF FLUORESCENCE PEAKS, THEIR INTENSITY AND PEAK WIDTH FOR GLASS 2 SAMPLE 13.....	117
TABLE 26 FLUORESCENCE EMISSION INTENSITIES FOR 612 NM .....	150
TABLE 27 SEDIMENT AND WATER SAMPLE GPS POSITIONS.....	163
TABLE 28 SEDIMENT SAMPLE PARTICLE SIZE RESULTS.....	172
TABLE 29 WATER SAMPLE PARTICLE SIZE RESULTS OF SUSPENDED SOLIDS (INCLUDING FLOCCULATED MATERIAL) .....	173

**Glossary:**

g	- Gram
km	- kilometer
LASER	- Light Amplified Stimulated Emission of Radiation
mol %	- Mole percent
ms	- Millisecond
Nd:YAG	- Neodymium Yttrium Aluminium Garnet
OPO	- Optical Parametric Oscillator
nm	- Nanometer
PED	- Polymer encapsulated dye
PHEN	- 1,10-phenanthroline
TEOS	- Tetraethyl Orthosilicate
TTFA	Thenoyltrifluoroacetone
TOAFFED	- Taguchi Orthogonal Array Fractional Factorial Experimental Design
μs	- Microsecond
UV	- Ultra-violet



## **1 INTRODUCTION**

The use of compounds or materials in the environment, whether naturally occurring or a by-product of human activity, as “environmental tracers” is well documented with some having been used successfully for more than half a century [1-4]. These include the tracing or tracking of chemicals using compounds indicative of spillage or discharge. Tracing sediments using fluorescent or radioactive particles, tracing soils where the transport of agricultural compounds is monitored and water flow where the application of a fluorescent dye allows visual observation of movement. The type of materials used for these range from naturally occurring isotopes [5-7], fluorescent dyes [8], fluorescent particles [9], chemical indicators and geochemical indicators [10].

This research project aims to develop novel narrow band fluorescent glass, silica sol gel and polymer tracers in the application of multiple source environmental monitoring of environmental parameters/pollutants. The application examples and tracer types found in the literature will be examined more closely to determine the potential applications for novel narrow band fluorescent glass tracers.

### **1.1 Tracer Types and Applications**

Environmental tracing is a vital scientific field in studying the fate of substances in aqueous or soil/sediment environments. This can range from monitoring the fate of industrial and domestic effluents [11] in ecological systems by adding a dye tracer to outflow sources and studying the dispersion, dilution and travel of discharge [10] to monitoring the waste suspension from fish farming and its effect on the local environment [12]. Currently typical fluorescent dye tracers rely on molecular fluorescence for detection which may produce an intense signal but is very broad, typically 80-120nm bandwidth [13-15]. This has several major disadvantages as only a small number of target species can be monitored simultaneously because there is spectral overlap of the broad tracer bandwidths, secondly as these fluorescent molecular dyes have been used as tracers for many years the background levels of these dye tracers in many areas are

elevated, making it very difficult to use then to carry out further tracer studies in areas of need, e.g. contaminant and sediment tracer studies in harbours where temporal studies are needed sometimes requiring comparative tracer studies over 10 or 20 years [16].



**Figure 1 (a) Produced water discharge; (b) Tracer doped discharge**

One of the largest problems associated with fluorescent dye tracers is their ecotoxicological effects within the environment and their effect on human health. Commonly used tracers such as Fluorescein, Lissamine Flavine FF, Rhodamine WT, Rhodamine B, Sulpho Rhodamine G, Sulpho Rhodamine B, eosin, among others, have all been studied for the toxicological effects [5][17]. Many of these may have breakdown products and synergistic effects with compounds within aqueous systems that could produce increased dangers to human health and the environment. Therefore the need for a new type of tracer which can provide environmental stability and minimal toxicological effects is great. Also the application of such tracers in sediment transport monitoring in the North Sea environment where there already exist a large number of possible background contaminant sources such as hydrocarbons [18, 19], which exhibit broad band emission spectra, make monitoring molecular fluorescent tracers challenging. Figure 1 (a) shows an example of produced water discharge from an off shore oil platform and (b) show the use of a molecular fluorescent tracer in produced water.

In an environment where there is the possibility of multiple sources of contamination, e.g. many platforms and cuttings piles [20, 21], the use of

multiple tracers exhibiting discrete fluorescent atomic emissions with wavelength and lifetime discrimination would be a distinct advantage allowing the monitoring of the origin of contaminants from more than one source. Not only allowing real time fluorescence measurements to be made with reduced background interference, but also many studies can be carried out in the same area.

Sediment transport occurs through natural processes such as currents, tides and waves, and through anthropogenic activities such as dredging, dam building and sub sea constructions. These can be studied by placing tracers into the sediment layer to monitor movement and travel [22-24]. With the present public focus on energy conservation and sustainability, governments all over the world are funding projects for wind, tidal and wave energy devices. The trend of placing turbines in coastal waters is causing increasing concern with the general public, not only for aesthetic properties but for their impact upon the local marine environment. The localised effect of sub sea manmade structures on the sea bed can be studied by the monitoring of sediment distribution and movement around the structure [25]. The interrupted movement of sediment on the sea bed can directly impact upon fish [26], crustaceans and other bottom dwelling creatures.



**Figure 2 Particulate dye tracer deployment in Bowmore Harbour**

In the case of dredging, companies undertaking such activity aim to minimise the amount of disturbed sediment entering the water column and its impact upon the local environment [27]. Figure 2 shows the deployment of a particulate dye

tracer for sediment tracing. Tracing allows the close study of where this disturbed sediment may be carried by ambient water currents and where it settles particularly in sensitive areas such as shell fish beds or areas of biodiversity.

This of course needs to be a comparable tracer in terms of size to the particles in the target sediment. The development of the novel tracers allows control of physical properties such as size and density. This can be engineered to mimic the naturally occurring sediment particles and therefore provide a far closer replication of particle behavior [28]. Glass provides an ideal material for use as an environmental tracer where the tracer may be exposed to varying degrees of chemical and biological attack as it protects the lanthanide tracer from water quenching external influences and degradation.

### ***1.1.1 Fluorescent Dyes***

The most common environmental tracers currently used are molecular dye based tracers, normally applied in simulated release studies. For example, applications of dye tracers can be found in the study of groundwater in the Missouri Ozarks where there is reliance upon an abundant supply of potable water found in fractured bedrock [29]. Petroleum products which are stored in underground storage tanks pose a threat to this potable water if a release occurs with contaminated ground water commonly found more than 2000 metres from the source. In this study four of the most commonly used fluorescent tracers, Fluorescein, Rhodamine-WT, Tinopal CBS-X and Pyranine were deployed either singly or used in combinations of two. The samples were analysed by spectrofluorimetry, but it was determined that the background fluorescence from hydrocarbons was too great. Finger printing of the hydrocarbons was utilised instead, this shows the limitation of a molecular broad band tracer.

Rhodamine WT has also been used in the study [9] of residence time of water and suspended particles at Fort Point Channel, a region of Boston Harbour, which contains a combined sewer outflow with highly contaminated sediments. The study involved measured disappearance of fluorescent tracers from the water

column by fluorescence spectroscopy of water samples collected over 7 days. Rhodamine was also used to create fluorescent pigment particles which were used to mimic the sewage particles of interest.

The fluorescent dye Tinopal CBS-X has been used to develop a method for the determination of pesticide residue on soils. It has been estimated that up to one-third of the total amount sprayed onto a crop can be lost to the soil at the time of application, the volume of which is dependant on soil and crop type. A major limitation for use of such fluorescent compounds was found when solutions of Tinopal CBS-X degraded in sunlight by 9.4% in 100 min, making it unreliable for field testing [30].

Onsite sewage and disposal systems are the most common means of wastewater treatment in many countries and are also the source of groundwater contamination. In the American state of Florida an estimated 450 million gallons of wastewater is discharged daily. As part of a study [31] to examine the flow of onsite sewage effluent from a mounded drainfield to a discharge point, several different tracers were employed. Two fluorescent tracers (Fluorescein and Rhodamine WT), an inert gas (sulphur hexafluoride) and a viral tracer (bacteriophage PRD-1) were used in the study.

Sediment transport studies [22] have been undertaken using dyed sediment particles to study the sediment transport pathways at the Ancão Inlet (southern Portugal). An orange fluorescent ink, Glycero Orange Fluo, was used to dye sediment collected from the study area. Determination of tracer presence in the study area was determined by ultra-violet light. For analysis the grain-size was examined to compare the natural sand and the tracer from the study area by computer program. For certain sample areas the fluorescent tracer was manually counted under ultra-violet excitation and for others an automatic system was used. This allowed generation of tracer distribution maps.

Although many users of tracer dyes such as Rhodamine WT and Fluorescein claim them to be safe and non-toxic, with little or no effect on marine life, there has been some research into their potential ecotoxicity effects [32]. 10 other dyes have also been examined for their eco-toxicity; Lissamine Flavine FF, Rhodamine B, Sulpho Rhodamine G, Sulpho Rhodamine B, Eosin, Pyranine,

Phorwite BBH Pure, Tinopal 5BM GX, Tinopal CBS-X, and Diphenyl Brilliant Flavine 7GFF - and a dye-intermediate, Amino G Acid. Based on set criteria for human health and acute ecotoxicity, the study indicated that these tracers have low to moderate levels of concern. This is an interesting observation as the Rhodamine family of dyes and in particular Rhodamine 6G is well documented as a highly toxic compound which has been used for surface water tracing studies.

### ***1.1.2 Fluorescent Particulate Tracers***

Fluorescent particle tracers can be created by dyeing [5] a naturally occurring material such as pebbles, sands and sediments. The application of such fluorescent particles can range from sediment mass transport monitoring [2, 9, 22] to the investigation of sub sea manmade structures [25] on the sea bed, but in general particle tracing is usually sediment based monitoring of some form.

For example over the past few decades, damage to reefs from pollution has accelerated alarmingly, it has been suggested that the reefs of Eilat on the Red Sea have been undergoing deterioration due to pollution. Pollution sources in that region are located 5-8 Km from the coral reefs and it is theorised that current derived mass transport may be responsible for bringing the pollutants in to contact with the coral [33]. To determine the possible occurrence of pollutant pathways and modes of transport fluorescently labelled tracers have been deployed. These were developed to examine mass transport in coastal marine environments. The particle sizes examined ranged from fine sediment particles of 5–10  $\mu\text{m}$  to coarse particles of 100–200  $\mu\text{m}$ .

Fluorescent particle tracing is the main environmental tracing application to which novel fluorescent glass tracers could be easily applied. This is due to the ease at which particle size ranging from 5  $\mu\text{m}$  – 10 mm can be produced and also the potential for tracing large numbers of signals to be monitored in the same environment. The narrow band emission signals will give increased data accuracy allowing for multiple source environmental monitoring which will give a significant competitive advantage over existing dye based particle tracers.

### **1.1.3 Natural Tracers (non injected)**

As previously mentioned naturally occurring tracers are materials or compounds which are already present in the environment. Lanthanides are already utilised as environmental tracers in groundwater flow and soil erosion studies [34-38].

### **1.1.4 Lanthanide Tracers**

Soil erosion is a global problem which sees in the region of 2 – 6.8 billion tonnes of soil lost every year in the US alone. Erosion can be a very visible effect on a localised environment, yet extremely difficult to measure. A monitoring technique investigated has been that of using lanthanides as tracers. The rare earth elements trivalent state and ionic radii allow them to be easily adsorbed onto clays. They are found in many soils in concentrations of up to tens of parts per million with organic soils usually richer in lanthanides than mineral soils. Lanthanide compounds show low toxicity ratings and often are accumulated by plants through roots, although the uptake is too low to cause considerable change in concentration of lanthanide elements in soil. The solubility of these elements tends to increase with decreasing pH, which is a key factor in their mobility in soil [34].

Another use of lanthanides as tracers has been in the investigation of groundwater flow. The study of water mixing from various sources has been undertaken by examining the “shale-normalised” lanthanide patterns. The calculated lanthanide concentrations were subsequently used to determine mixing ratios, the results of which coincided with the initial calculations as well as the previous studies. The results of this study suggest that solution complexation of the lanthanide is sufficient to overcome, to a certain degree, the affinity of the lanthanides to be adsorbed onto surface sites in the aquifers such that distinctive lanthanide signatures develop and persist in solution in ground waters from different aquifers [35].

Another example of lanthanide oxides being used as tracers is in the investigation of their suitability to be used as a sediment tracer for coarse textured soils. This study showed that lanthanides could be successfully used to study soil loss from erosion, but also showed a limitation of using a rare earth

oxide as a tracer. Their ability to bind and form complexes has been shown to be extremely high. This therefore limits the accuracy of such tracing techniques when a percentage of the applied tracer may be lost to non-genuine soil loss, but to complexation with components in the soil [36]

Lanthanide elements have also been used in the study of the distribution of fine sedimentary deposits. A study along the coast of the Bay of Biscay, and was undertaken by studying the deposit sources of the Loire, Gironde and Adour rivers [37]. An estimated 2.4 million tonnes of fine sediments are carried to the Atlantic from these rivers with 80% of this total coming from the Gironde. Analysis of lanthanides by ICP-MS allowed effective characterisation of continental sources of sediments deposited.

Monitoring of a flow system to investigate the behaviour of lanthanides at different stages in fractured basalt and sedimentary aquifers was examined [38]. It was shown that the lanthanide patterns reflect the different types and rates of reactions taking place to those controlling major ion chemistry. In areas where recharge is through sediments, lanthanide concentrations are high and localised processes control lanthanide patterns and concentrations. The observed increase of lanthanide concentrations in ground waters was found to be the result of early stage mobilisation of the lanthanides in the flow system. Lower lanthanide concentrations in the groundwater may be due to progressive lanthanide sorption.

These examples above show how lanthanides are currently employed in tracing applications. They are all very different from the way lanthanides are to be used in this proposed research project. However, interestingly they do demonstrate the low toxicity of rare earths making them suitable for environmental monitoring purposes.



### 1.1.5 Isotope Tracers

Naturally occurring isotopes are used for different environmental studies; Table 1 shows an example for 5 different isotopes.

<b>Isotope</b>	<b>Application</b>
<b><math>^{11}\text{B}</math></b>	Natural sodium borate minerals are used for world production of sodium perborate, an industrially manufactured bleaching agent added to a variety of detergent formulations and cleaning products. During end use, water-soluble boron compounds are discharged with domestic aqueous effluents into sewage treatment plants, where little or no boron is removed and, hence, the anthropogenic boron load is almost entirely released into the aquatic environment. [39]
<b><math>^{15}\text{N}</math></b>	Increased aquaculture production along the eastern Adriatic coast has created some environmental problems by releasing large amounts of effluents into the coastal environment. The negative environmental impacts related to fish farming are due to the increased amounts of dissolved and particulate nutrient loads, especially of organic phosphorus (P) and nitrogen (N) in the form of ammonia that might easily induce eutrophication. [40]
<b><math>^{129}\text{I}</math></b>	The natural radioisotope $^{129}\text{I}$ covers an important age range for applications in geological systems, particularly for fluids derived from or associated with organic material. Crucial for the application of this isotopic system is the initial ratio used for the calculation of ages, the marine input ratio of $^{129}\text{I}/\text{I}$ . Determinations of this ratio, $R$ , in recent marine sediments led to a value $R_i = (1500 \pm 150) \times 10^{-15}$ [41]
<b><math>^{230}\text{Th}</math> and <math>^{238}\text{U}</math></b>	Rates of transport and interaction processes in the ocean can be evaluated with the radioactive decay of the natural Uranium–Thorium radioactive decay series (U–Th). Isotopes of soluble U decay to isotopes of highly particle-reactive Th. In seawater, $^{234}\text{Th}$ and $^{230}\text{Th}$ are removed from the water column by adsorption onto settling particles (scavenging). The resulting U/Th disequilibria can be used to constrain the transport rates of particles and reaction processes between the solution and particulate phases. [42]

**Table 1 Isotopes and their tracing applications**

## **1.2 Tracer Matrices**

The development of novel fluorescent environmental tracers will examine borosilicate glass, silica sol gel hydrolysis and polymer formation as potential carriers for fluorescent species.

### **1.2.1 Glass Matrix**

The most ideal glass host matrix for use as an environmental tracer would be pure silica, because of its low thermal expansion, high thermal stability and high UV transmission. Pure silica however, requires a high temperature furnace of more than 2000 °C because the Si-O bonds are so strong their melting temperature is 1750 °C, this renders silica unworkable for an environmental tracer host due to the dangerous working temperatures and cost.

Based on previous work carried out within the Centre for Research in Energy and the Environment (CREE) at The Robert Gordon University funded by NCR Ltd, a borosilicate glass matrix was found to be a suitable host material for lanthanide based security taggants [43]. The adaptation of these security taggants for applicability as an environmental tracer will be investigated in this proposed research project. However, it is also known that altering the host matrix can alter the spectral response of the rare earth ions [44, 45]. This is due to the change in the surrounding environment of the rare earth ions and the amount of splitting of their energy levels. Changes in this environment can therefore be used to alter the fluorescence peak intensity, fluorescence lifetime and fluorescence peak width of the rare earth ions, such as praseodymium [46], europium [47], holmium [48] and samarium [49]. This could potentially produce new fluorescent emissions using the same concentration of the rare earth ions. The narrow band emission signals offer the potential for tracing of an even larger numbers of signals in the same environment. This will give significant competitive advantage and increased data accuracy and also allow multiple source environmental monitoring of environmental parameters.

### **1.2.2 Borosilicate Glass**

The current glass matrix which was developed for security applications is a borosilicate glass matrix. It provides an environmentally stable host into which the lanthanide ions can be placed. The use of borosilicate as a glass host for lanthanide doping has been studied with eight rare earths which exhibit a visible fluorescent emission e.g. europium, terbium, dysprosium, cerium, samarium, praseodymium, erbium and thulium [50]. A typical borosilicate glass consists of silicon dioxide, boric oxide, sodium oxide and alumina [51] the ratio of these components can affect the glass network formed and therefore the emission wavelengths from dopant ions. When compared with phosphate or fluoride based glasses [52] borosilicate is far more stable in the presence of water. It has been seen though that the use of a phosphate or fluoride composition will yield stronger fluorescence emissions.

### **1.2.3 Borosilicate Glass and Sensitisers**

In order to enhance the spectral response of the rare earth ions the addition of suitable sensitizers can be examined. The addition of sensitizers would involve the excitation of the donor ion which then transfers its energy to the acceptor ion which then undergoes its emission at the desired wavelength. This energy transfer or fluorescence enhancement is not only observed within glass matrices containing rare earth ions [45], but also within polymer matrices [53]. This can increase the emission intensity of the acceptor ion without increasing its concentration whilst simultaneously decreasing the emission intensity of the donor ion [54]. This effect has been observed with dysprosium enhancing terbium [55, 56] and terbium enhancing europium [57]. Energy transfers can produce higher fluorescent emissions from multi-ion doped glasses from lower doping concentrations. The energy transfer effect can also a stimulation of additional emissions, further enhancing the potential coding aspect of lanthanide ion doped tracers. This effect shall be studied in more detail by undertaking multiple ion doping experiments to examine the energy transfer in multiple doped tracers between europium, terbium and dysprosium. Other energy transfers have been seen with terbium enhancing holmium [58] and samarium enhancing europium [59, 60].

#### **1.2.4 Polymers**

##### **1.2.4.1 Inorganic Polymers - Sol Gel**

Conventional glass fabrication requires the melting of component materials, mixed into a homogeneous powder, at high temperatures with rapid cooling. This process restricts the choice of substances which can be incorporated into the glass matrix. Only some inorganic salts and metal oxides can survive the melting process for borosilicate glass, which has a maximum pouring temperature of 1250 °C. This makes the substitution of the lanthanide salt e.g.  $\text{EuCl}_3 \cdot 6\text{H}_2\text{O}$ , with an organic chelated lanthanide [61, 62] complex impossible as the organic complex cannot resist the high temperature and will be destroyed.

An alternative approach to the glass melt fabrication method is the generation of colloidal suspensions (sol) which are converted to gels and then solid or spherical materials [63, 64]. The sol-gel method is based on the hydrolysis of liquid precursors and the formation of colloidal solids. Stöber [65] showed in 1968 the process of producing silica spheres in the region of 800 nm from an organosilicate precursor (tetraethyl orthosilicate, TEOS) with a base catalyst. Sol gel methods have been documented which show the incorporation of traditional dyes such as Rhodamine 6G and B [66, 67], into TEOS based acid hydrolysis thin films.

The choice of a sol-gel method for the fabrication of doped spheres is important due to the size control possible allowing finer sediment to be easily replicated. A limitation of glass particle size production is sub 5 -10  $\mu\text{m}$ , the effort required to produce smaller particles becomes incredibly labour intensive. With the sol-gel process it is possible to produce pure silica spheres in the 50 nm region [68].

##### **1.2.4.2 Organic Polymers**

Reviewing polymer literature for spherical polymerisation preparations has provided several different starting formulations for the production of polymer spheres. These have ranged from polymer sphere production for biomedical applications such as drug carriers [69, 70] and immunoassays [71-74] to polymer optical fibers which are doped [74-76] with lanthanides for

telecommunication developments. The existing use of lanthanide chelates doped into polymer matrices shows the feasibility of the method, although not in combination with sphere formulations.

The majority of polymerisation reactions to produce spheres are monodisperse [77-79] or emulsion reactions [75], which will generally produce spheres in the range of 100 nm – 10 µm. It is possible to have a core and shell [76] formation for a polymer sphere whereby a core could contain the fluorescent species and the shell could provide protection from aggressive attack.

Some polymer particles exist which have been produced containing Rhodamine 6G [77] (already known as a tracer and also as a toxic species) for flow tracing, electronic inks, cell labeling and diagnostic reagents. Another method by which polymer spheres can be produced is by aerosol [78] where instead of a typical monodisperse or emulsion reaction, a vibrating-orifice generator is used which can produce spheres in the region of 5 – 50 µm. It is also possible to produce magnetic micron sized polymer sphere through the encapsulation of iron (Fe) particles [79]. This has wide application in the development of new materials for pollutant removal, water treatment, cell labeling, drug targeting and immunoassaying.

An advantage of using a polymer based carrier for a fluorescent tracer is its ability to be easily modified allowing for surface group alterations [80] which could be used for alternative tracing applications.

### **1.2.5 Chelates**

Chelating agents are organic compounds capable of forming coordinate bonds with metals through two or more atoms from within the organic compound. The complex formed with the binding of chelating agent and metal is called a chelate. Chelating agents such as 1,10-phenanthroline [81] and thenoyltrifluoroacetone [62, 82] are bidentate chelating agents [83, 84] as they have two coordination atoms. The development of spherical polymer and sol gel formulations as potential environmental tracers requires the investigation of lanthanide chelate complex formation. The use of a chelating compound with a lanthanide will produce an organic molecule which can be utilised in polymerisation of organic and inorganic sphere formation. A chelate will absorb energy in the ultra violet

region of the electromagnetic spectrum and transfer the energy to the lanthanide ion [81, 85-87]. By doing this a far higher fluorescence signal can be generated from a much lower concentration of lanthanide ions than would be found in a doped glass sample using only lanthanide chloride. Although the stability and resistance to environmental parameters are undefined for these chelated compounds and therefore may not prove suitable for application as environmental tracing materials.

The synthesis of lanthanide chelated compounds is well documented [61, 73, 74, 81, 86, 88-90] and has been investigated for many years. An initial review of existing literature regarding the use of chelated lanthanides has shown that it is possible for these compounds to be used in combination with both polymer [91, 92] and sol gel (sphere and thin film) [61, 88] matrices.

### **1.3 Project Aim and Milestones**

#### ***1.3.1 Project Aim***

The overall aim of this project is the development of novel tracers, based on narrow band atomic fluorescence which will be examined for deployment as environmental tracers. The use of discrete fluorescent species in an environmentally stable host will be investigated to replace existing mildly toxic, broad band fluorescent, molecular dye tracers. The narrow band emission signals emitted from lanthanide doped glass offer the potential for the tracing of a large numbers of signals in the same environment. This in turn should give significant competitive advantage and increased data accuracy and also allow multiple source environmental monitoring of environmental parameters. An initial sediment study will be undertaken to provide particle size information from a real field site.

### **1.3.2 Project Milestones**

Milestone 1: *Literature review of current environmental tracing techniques and tracers, glass and polymer fabrication and their potential for application in environmental tracing.*

Milestone 2: *Development of current security glass matrix for use as an environmental tracer.*

Milestone 3: *Concentration study of lanthanide doping in to current borosilicate glass matrix Glass 1.*

Milestone 4: *Investigation of new glass matrix Glass 2.*

Milestone 5: *Investigation of chelates for the formation of organic lanthanide complexes for use with polymer and silica sol gel spheres.*

Milestone 6: *Investigation of polymer sphere formation.*

Milestone 7: *Investigation of silica sol gel sphere formation.*

Milestone 8: *Investigation of polymer spheres doped with organic lanthanide complexes.*

Milestone 9: *Investigation of silica sol gel spheres doped with organic lanthanide complexes.*

Milestone 10: *Measurement of novel tracers using a proposed trial detection system.*

Milestone 11: *Determination of sediment particle size from a potential field site.*

## 1.4 Summary

The use of compounds or materials in the environment, whether naturally occurring or a by-product of human activity, as "environmental tracers" is well documented with some having been used successfully for more than half a century. The type of materials used for environmental tracing range from naturally occurring isotopes, fluorescent dyes, fluorescent particles, chemical indicators and geochemical indicators.

Environmental tracing is a vital scientific field in studying the fate of substances in aqueous or soil/sediment environments. Currently typical fluorescent dye tracers rely on molecular fluorescence for detection which may produce an intense signal but is very broad, typically 80-120nm bandwidth. This has several major disadvantages as only a small number of target species can be monitored simultaneously because there is spectral overlap of the broad tracer bandwidths.

One of the largest problems associated with fluorescent dye tracers are their eco-toxicological effects within the environment and their effect on human health. Many of these may have breakdown products and synergistic effects with compounds within aqueous systems that could produce increased dangers to human health and the environment. So the need for a new type of tracer which can provide environmental stability and minimal toxicological effects is great.

In an environment where there is the possibility of multiple sources of contamination the use of multiple tracers exhibiting discrete fluorescent atomic emissions with wavelength and lifetime discrimination would be a distinct advantage allowing the monitoring of the origin of contaminants from more than one source. Not only allowing real time fluorescence measurements to be made with reduced background interference, but also many studies can be carried out in the same area.

Glass provides an ideal material for use as an environmental tracer where the tracer may be exposed to varying degrees of chemical and biological attack as it



protects the lanthanide tracer from water quenching external influences and degradation.

Based on previous work carried out within CREE at The Robert Gordon University funded by NCR Ltd, a borosilicate glass matrix was found to be a suitable host material for rare earth based security taggants. The adaptation of these security taggants for applicability as an environmental tracer will be investigated in this proposed research project. However, it is also known that altering the host matrix can alter the spectral response of the rare earth ions. This is due to the change in the surrounding environment of the rare earth ions and the amount of splitting of their energy levels. Changes in this environment can therefore be used to alter the peak intensity, fluorescence lifetime and peak width of the rare earth ions. Therefore, this potentially could produce new fluorescent emissions using the same concentration of the rare earth ions.

Conventional glass fabrication though requires the melting of component materials, mixed into a homogeneous powder, at high temperatures with rapid cooling. This makes the substitution of the lanthanide salt e.g.  $\text{EuCl}_3 \cdot 6\text{H}_2\text{O}$ , with an organic chelated lanthanide complex impossible as the organic complex cannot resist the high temperature and will be destroyed.

An alternative approach to the glass melt fabrication method is the generation of colloidal suspensions (sol) which are converted to gels and then solid or spherical materials. The Sol-gel method is based on the hydrolysis of liquid precursors and the formation of colloidal solids. Sol gel methods have been documented which show the incorporation of traditional dyes.

The choice of a sol-gel method for the fabrication of doped spheres is important due to the size control possible allowing finer sediment to be easily replicated. A limitation of glass particle size production is sub 5 -10  $\mu\text{m}$ , beyond which becomes incredibly labour intensive. The existing use of lanthanide chelates doped in to polymer matrices show the feasibility has already been carried out, although not in combination with sphere formulations. An advantage of using a polymer based carrier for a fluorescent tracer is its ability to be easily modified allowing for surface group alterations which could be used for alternative tracing applications.

The use of a chelating compound with a lanthanide will produce an organic molecule which can be utilised in polymerisation of organic and inorganic sphere formation. A chelate will absorb energy in the ultra violet region of the electromagnetic spectrum and transfer the energy to the lanthanide ion. By doing this a far higher fluorescence signal should be generated from a much lower concentration of lanthanide, than would be found in a doped glass sample. The stability and resistance to environmental parameters are undefined for these chelated compounds and therefore may not prove suitable for application as environmental tracing materials.

## **2 THEORY**

### **2.1 Fluorescence**

Fluorescence is a phenomenon where the absorption of light of a given wavelength by an atom or molecule is followed by the emission of light at longer wavelengths [93]; high energy photons in with lower energy photons out. The absorption of electromagnetic radiation causes the promotion of an electron from its energy level to a higher energy level. If it loses some of its energy by non radiative decay before returning back down to its ground state it is said to fluoresce. The photon emitted is a lower energy than absorbed. Fluorescence is a highly sensitive technique allowing very low concentrations to be measured, in comparison to measuring the difference between two large signals ( $I$  and  $I_0$ ) in absorption spectrometry. Also, the fluorescence intensity can be increased by increasing the incident radiation  $I_0$  which therefore increases sensitivity, increasing the incident radiation has no effect on absorption as  $I$  is simultaneously increased proportionally therefore no increase in sensitivity. Even with the increased sensitivity of fluorescence methods, they are much less widely applicable than absorption because of the relatively limited number of chemicals that show appreciable fluorescence. More traditional methods of analysing chemical samples such as Gas Chromatography-Mass Spectroscopy (GC-MS), Fourier Transform Infra Red Spectroscopy (FT-IR), Nuclear Magnetic Resonance Spectroscopy (NMR) and Flame Atomic Absorption Spectroscopy (FAAS) are suitable for laboratory situations, but for field analysis where real time data acquisition is required fluorescence spectroscopy is ideal.

#### **2.1.1 Molecular Fluorescence**

When a molecule absorbs radiation (excitation energy) to create an excited state, not only electronic transitions occur, but also energy changes in the vibrational and rotational energy levels. This excited state is the first excited singlet state. A molecule in a high vibrational level of the excited state will quickly fall to the lowest vibrational level of this state by losing energy to other

molecules through collisions and the molecule will also dissipate the excess energy to other modes of vibration and rotation non radiative loss of energy.

Fluorescence occurs when the molecule returns to the electronic ground state, from the excited singlet state, with the emission of a photon [94] which is a lower energy and consequently a longer wavelength, Figure 3. Fluorescence is measured at right angles to the excitation source to avoid swamping the fluorescent signal with incident radiation.

Once a molecule has been excited to a higher energy level, there are several processes which can occur that causes the molecule to lose the excess energy. The most important of these mechanisms are non-radiative relaxation and fluorescence emission. The non-radiative relaxation methods are: vibrational relaxation which occurs during collisions between excited molecules and molecules of the solvent or lattice and internal conversion which is the process of non-radiative relaxation between the lower vibrational levels of an excited electronic state and the higher vibrational levels of another electronic state.

Most fluorescence transitions occur from the lowest excited electronic state to the ground state. Fluorescence only usually occurs between the lowest vibrational level of  $E_1$  to various vibrational levels of  $E_0$  because internal conversion and vibrational relaxation processes are very rapid in comparison to fluorescence. Therefore a fluorescence spectrum usually consists of only one band with many closely spaced lines representing transitions from the lowest vibrational level of the excited state to the many different vibrational levels of the ground state.

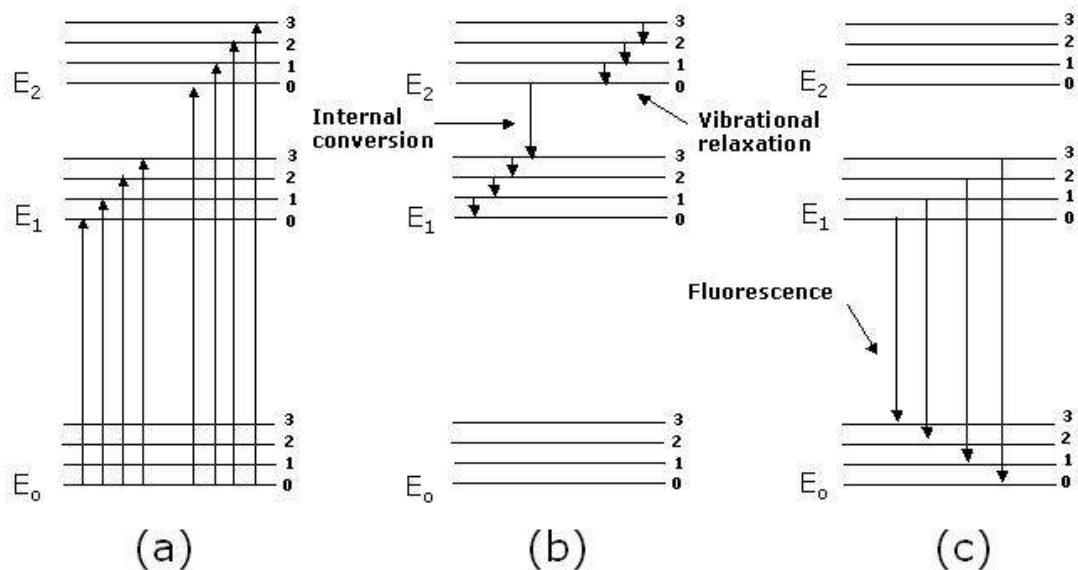


**Figure 3 Energy levels showing radiative and non-radiative emissions**

Figure 3 shows the process of fluorescence, showing internal conversion and vibrational relaxation. Figure 3 (a) shows the excitation of electrons from the ground state ( $E_0$ ) to various vibrational energy levels of  $E_1$  and  $E_2$ . Figure 3 (b) shows the mechanism of non-radiative processes including vibrational relaxation and internal conversion. Figure 3 (c) shows fluorescence from the higher energy levels back down to the ground state.

The energy from the absorbed radiation promotes an electron from the outer shell of the atom to a higher energy level. Equation 1 states that the energy of a photon is proportional to its frequency and to Planck's constant.

**Equation 1:** 
$$E = h\nu = \frac{hc}{\lambda}$$

Where:

E = energy of a photon

h = Planck's constant  $6.63 \times 10^{-34}$  Js

$\nu$  = frequency / Hz

c = velocity of light  $2.998 \times 10^8$  ms<sup>-1</sup>

$\lambda$  = wavelength / nm

### **2.1.2 Concentration and Fluorescence Intensity**

Radiant power of fluorescence (F), Equation 2, is proportional to the radiant power of the excitation beam absorbed ( $I_0 - I$ ) and the fluorescence efficiency ( $\phi$ ) of the fluorescent species (quantum yield):

**Equation 2:** 
$$F = \phi(I_0 - I)$$

Where:

$I_0$  = radiant power of beam incident on the sample

I = power after it traverses a path length l of the medium

$\phi$  = fluorescence quantum efficiency = ratio of number of photons fluorescing to the number absorbed

To relate the fluorescence intensity to the concentration requires Beer's law, Equation 3:

**Equation 3:** 
$$\text{Log}(I_0 / I) = \epsilon lc$$

Where:

$\epsilon$  = molar absorptivity of the fluorescence species / m<sup>2</sup> mol

$\epsilon lc$  = absorbance

By multiplying both sides of  $\text{Log}(I_0/I) = \epsilon lc$  by -1 and taking the antilog, this can be written as:

$$I/I_0 = 10^{-\epsilon lc}$$

$$1 - (I/I_0) = 1 - 10^{-\epsilon lc}$$

$$(I_0/I_0) - (I/I_0) = 1 - 10^{-\epsilon lc}$$

$$I_0 - I = I_0 (1 - 10^{-\epsilon lc})$$

Substituting this into  $F = \phi(I_0 - I)$ :

**Equation 4:** 
$$F = \phi I_0 (1 - 10^{-\epsilon lc})$$

### 2.1.3 Atomic Fluorescence

The fluorescence studied in this work is atomic since the lanthanide ions doped in to the borosilicate glass, silica sol gel and polymers are  $\text{Eu}^{3+}$ ,  $\text{Tb}^{3+}$  and  $\text{Dy}^{3+}$  with the observed emissions being that of lanthanide energy transitions. Unlike molecular fluorescence which has a broad band excitation and emission due to the large number of vibrational and rotational states, atomic fluorescence produces narrow band fluorescence, Figure 4.

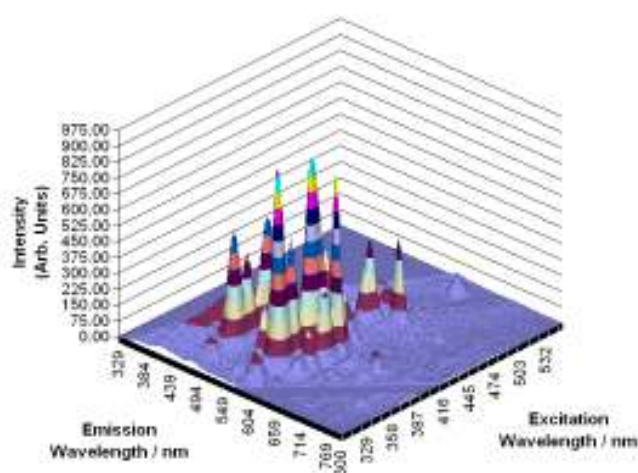


**Figure 4 Atomic fluorescence peaks from a glass sample doped with europium, terbium and dysprosium**

This is because the fluorescence is caused only by the electronic transitions of the outmost electrons. Figure 5 show an example of the energy levels of the lanthanide ions europium, terbium and dysprosium [95]. The closeness of the 4f-4f energy levels strongly influence the sharp nature of the emissions. Only Lanthanides and Actinides exhibit these narrow atomic fluorescence emissions because of closeness of the band levels in their 4f-4f and 5f-5f energy levels respectively. However Actinides are radioactive and thus were not investigated as this research is aimed at the development of more environmentally friendly tracers.



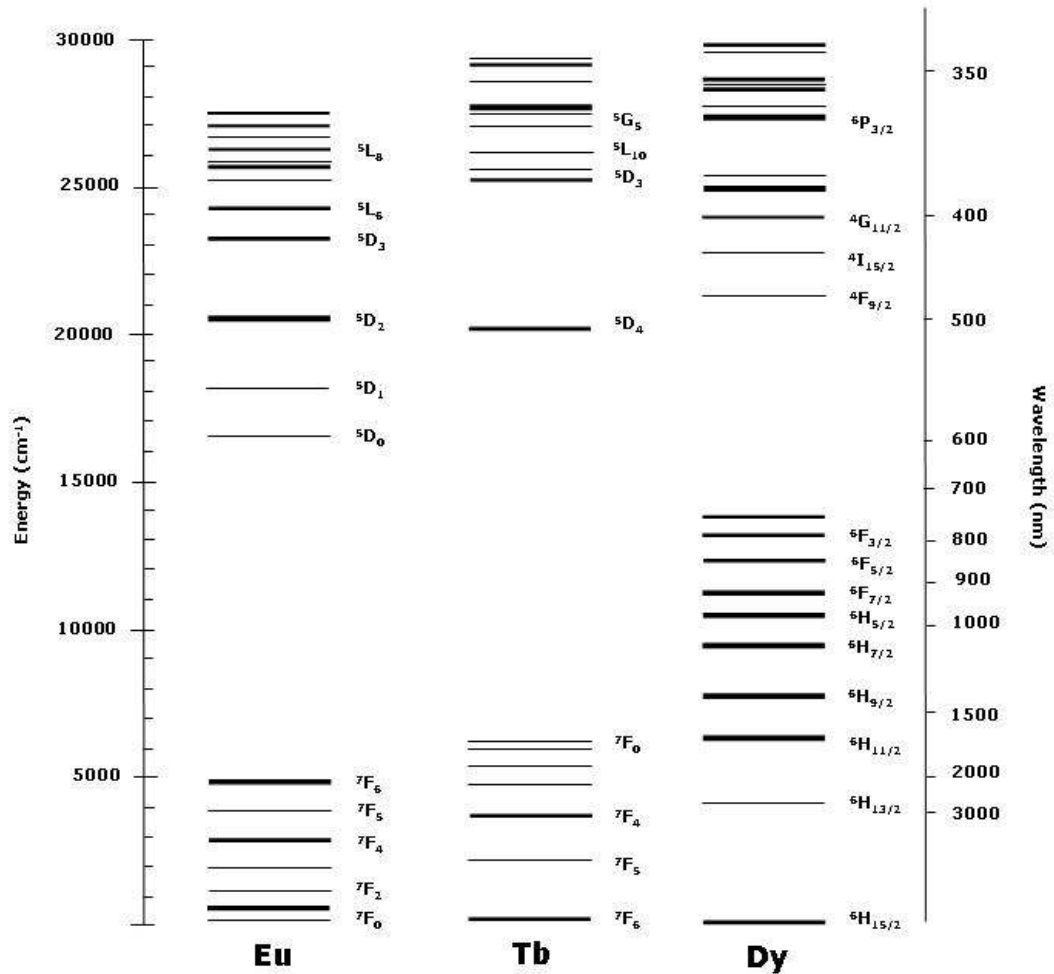


**Figure 5 Energy Levels of Lanthanide 3<sup>+</sup> Ions europium, terbium and dysprosium, modified Dieke diagram**

The lanthanides discrete fluorescence process occurs because of electronic transitions from their 4*f* electrons. For any electronic transition to occur, there are certain selection rules that need to be obeyed [96]:

**Spin electron rule:**  $\Delta S=0$  (changes in multiplicity are forbidden)

**Laporte selection rule (transition rule):** there must be a change in parity

- Allowed transitions:  $g \leftrightarrow u$  ( $g$ =even and  $u$ =odd)
- Forbidden transitions:  $g \leftrightarrow g$   $u \leftrightarrow u$

**This leads to the selection rule:**  $\Delta l = \pm 1$  (where  $l$  is the orbital quantum number and determines the shape of the atomic orbital)

- Allowed transitions are:  $s \rightarrow p$ ,  $p \rightarrow d$ ,  $d \rightarrow f$
- Forbidden transitions are:  $s \rightarrow s$ ,  $p \rightarrow p$ ,  $d \rightarrow d$ ,  $f \rightarrow f$ ,  $s \rightarrow d$ ,  $p \rightarrow f$ , etc

Figure 6 shows an example of the general set of  $4f$  -orbitals.

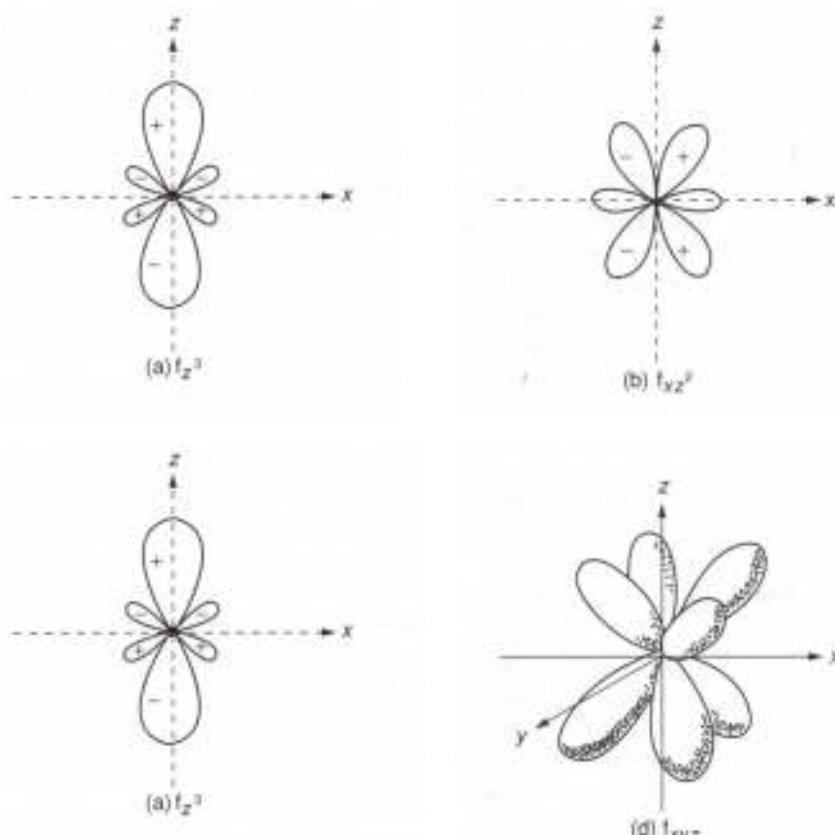


**Figure 6 Examples of general set of  $f$ -orbitals**

The  $f$ - $f$  transitions occur due to spin-orbit coupling [97], which is more significant than crystal-field splitting [98]. Crystal-field splitting is due to the arrangement and type of ligands surrounding the ion which have differing strengths of effect on the different atomic orbitals of the ion. If the effect was spherical, then all the energies of the electrons would be affected by the same amount and raised uniformly, although this is not generally the case [99]. If the effect was

octahedral, then this causes the energy of electrons in the 4f level that point directly at the ligand to be raised whilst lowering those electrons that point between the ligands with respect to the spherical field [100]. Spin orbit coupling (also called LS coupling) involves the interaction, when several electrons are present in a subshell, between the total orbital angular quantum number  $L$  and the spin quantum number  $S$ .  $L$  due to the overall effect of individual orbital angular momentum,  $l$  and  $S$ , due to the overall effect of individual spins,  $m_s$ .

This effect splits the terms into a number of levels ( $J$ ) with  $J=L+S, L+S-1, \dots [L-S]$  [101]. The spin multiplicity is equal to  $2S+1$  and follows the rules:

- For less than half-filled shells, smallest  $J$  lies lowest
- For more than half-filled shells, largest  $J$  lies lowest

Therefore the full level term symbol is written as  $^{2S+1}L_J$ .

As the f orbital of the lanthanides are well shielded by the surrounding 5s and 5p electrons, the various states from the  $f^n$  configurations are only split by approximately  $100 \text{ cm}^{-1}$  by external fields (caused by ligand vibrations). Therefore, the  $f \rightarrow f$  electronic transitions from one  $J$  state to another  $J$  state of the same configuration results in very sharp absorption bands similar to the free atom and have weak intensities due to the low probability of the  $f \rightarrow f$  transitions.

As  $l=3$  for an f electron,  $m_l$  can be 3, 2, 1, 0, -1, -2 or -3 and can give rise to high values of  $L$  for certain lanthanide ions. For example, praseodymium ( $\text{Pr}^{3+}$ ) has two f electrons and the highest values for  $M_L$  of 6, 5, 4, 3, 2, 1 and 0. For two electrons the highest  $S$  value is +1 (as each electron can be +1/2 or -1/2) making  $2S+1=3$ , and the highest  $L$  value with  $S=1$  would be 5. According to Hund's rule, where the term with the highest  $S$  value lies lowest in energy and if there are several terms with the same  $S$ , the one with the highest  $L$  lies lowest, the ground state of  $\text{Pr}^{3+}$  is  $^3H_4$ . Furthermore, the terms S, P, D, F, G and I are also possible (relating to  $M_L$  values of 0, 1, 2, 3, 4 and 6 respectively) and each having many different values of  $J$ . Even taking into account the selection rules mentioned above, the number of possible transitions is large, and therefore, the number of lanthanide absorptions can be large. Furthermore, some lanthanide

$M^{3+}$  ions with greater or equal to three f electrons have one or more transitions that show an increase in intensity when  $H_2O$  is replaced by other ligands. This is because hydroxyl groups have a strong absorption band, which when nearby the lanthanide ion, allows a non-radiative decay mechanism that causes fluorescence quenching.

Although there are a large number of energy transitions possible from lanthanide ions, the number that will produce fluorescent emissions are influenced by the matrix into which the particular ion is doped and also the conjugated chelate molecule.

## **2.2 Lanthanides**

The first discovery of the rare earth element yttria by Johann Gadolin in 1794 and later ceria by M.H. Klaproth, J.J. Berzelius and W. Hisinger heralded the beginning of lanthanide chemistry. These two, yttria and ceria were later separated into the rare earth elements erbium, terbium, ytterbium, cerium and lanthanum [102].

The lanthanides are f block elements and are in the periodic table from 57 – 71, lanthanum, cerium, praseodymium, neodymium, promethium, samarium, europium, gadolinium, terbium, dysprosium, holmium, erbium, thulium, ytterbium and lutetium. Of these, 10 have potentially useful visible fluorescent emissions, with the remainder being unusable due to their emissions being in the infrared, their radioactive nature or toxicity.

The ions of most lanthanide elements absorb in the ultraviolet and visible region of the electromagnetic spectrum. Compared to the spectroscopic behaviour of most inorganic and organic absorbers, their spectra consist of narrow, very well defined absorption peaks. These characteristics are highly stable under varying conditions, glass matrix, chelate matrix etc. This makes them ideal for use as a dopant in varying carrier compositions as their spectral outputs are relatively unaffected by host.

### 2.2.1 Lanthanide Energy Levels

Europium exhibits several energy transitions which result in a visible fluorescent signal. The strongest of these energy transitions for europium is the  $^5D_0$  to  $^7F_2$  which leads to the emission at 615 nm, Figure 7.

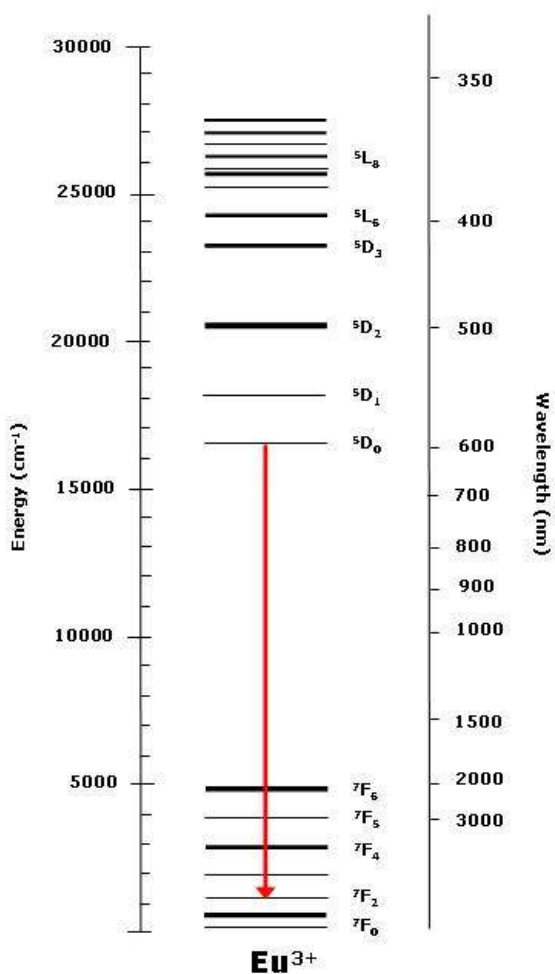


**Figure 7 Europium energy levels showing the transition of  $^5D_0$  to  $^7F_2$  which leads to the emission of 615 nm**

Europium also exhibits visible fluorescence from four other transitions, Table 2. All of these emissions can be clearly seen as discrete fluorescent peaks.

Europium Energy Transition	Emission Wavelength / nm
$^5D_1$ to $^7F_1$	535
$^5D_0$ to $^7F_2$	615
$^5D_0$ to $^7F_3$	635
$^5D_0$ to $^7F_1$	592
$^5D_0$ to $^7F_4$	702

**Table 2 Energy transitions and emission wavelengths for europium**

Terbium, like europium, also exhibits several energy transitions which result in a visible fluorescent signal. The strongest energy transition for terbium is the  $^5D_4$  to  $^7F_5$  which leads to the emission at 542 nm is shown in Figure 8.

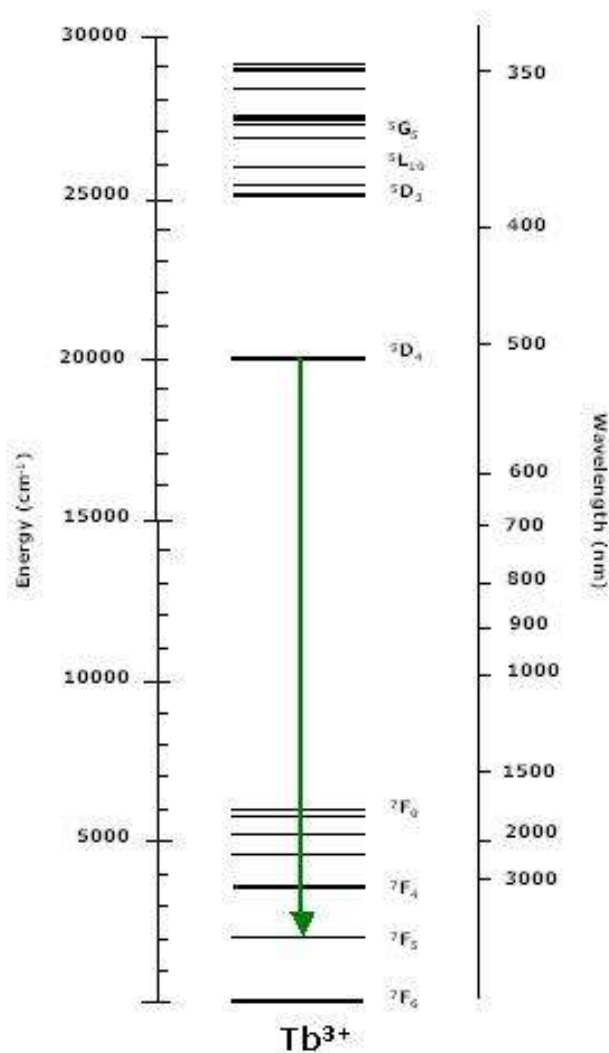


**Figure 8 Terbium energy levels showing the transition of  $^5D_4$  to  $^7F_5$  which leads to the emission of 542 nm**

Terbium also exhibits visible fluorescence from four other energy transitions, Table 3. These can be clearly observed as visible emissions.

<b>Terbium Energy Transition</b>	<b>Emission Wavelength / nm</b>
$^5D_4$ to $^7F_6$	385
$^5D_4$ to $^7F_5$	542
$^5D_4$ to $^7F_3$	546
$^5D_4$ to $^7F_4$	588
$^5D_3$ to $^7F_3$	622

**Table 3 Energy transitions and emission wavelengths for terbium**

Dysprosium also exhibits several energy transitions which result in a visible fluorescent signal. Dysprosium energy levels showing the transition of  ${}^4F_{9/2}$  to  ${}^6H_{13/2}$  which leads to the emission at 575 nm is shown in Figure 9 .

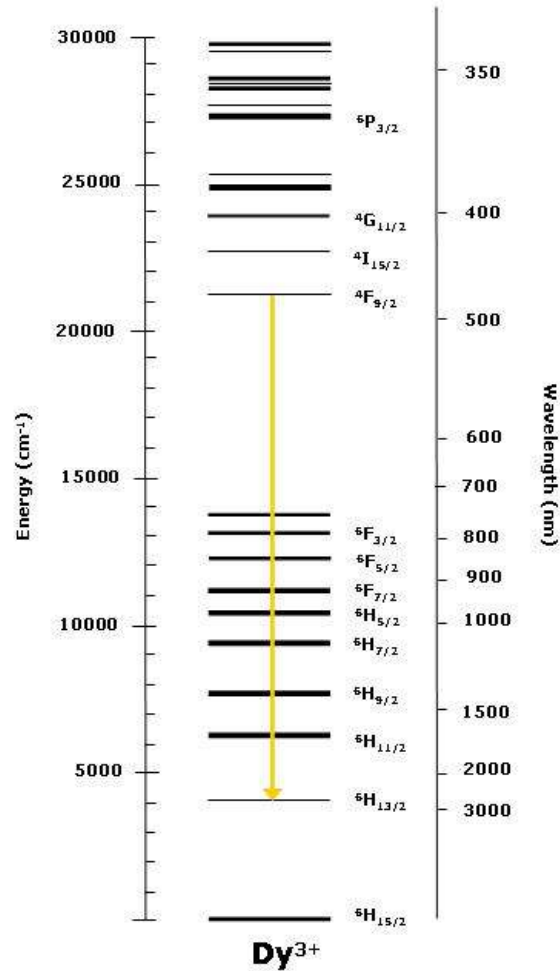


**Figure 9 Dysprosium energy levels showing the transition of  ${}^4F_{9/2}$  to  ${}^6H_{13/2}$  which leads to the emission of 575 nm**



Dysprosium also exhibits visible fluorescence from three other energy transitions, Table 4. These can be clearly observed as visible emissions.

<b>Terbium Energy Transition</b>	<b>Emission Wavelength / nm</b>
${}^4F_{9/2}$ to ${}^6H_{15/2}$	483
${}^4F_{9/2}$ to ${}^6H_{13/2}$	575
${}^4F_{9/2}$ to ${}^6H_{11/2}$	662
${}^4F_{9/2}$ to ${}^6H_{9/2}$	756

**Table 4 Energy transitions and emission wavelengths for dysprosium**

### 2.2.2 Lanthanide Energy Transfer

It is possible for lanthanide ions within the same host matrix to transfer energy from one ion to that of another. For example an energy transfer from terbium to europium will occur from a 485 nm excitation resulting in a 615 nm emission ( $^5D_4 - ^5D_0$ ), and also an energy transfer from dysprosium to terbium where a 452 nm excitation will result in a 545 nm emission ( $^5D_4 - ^4F_{9/2}$ ), Figure 10.

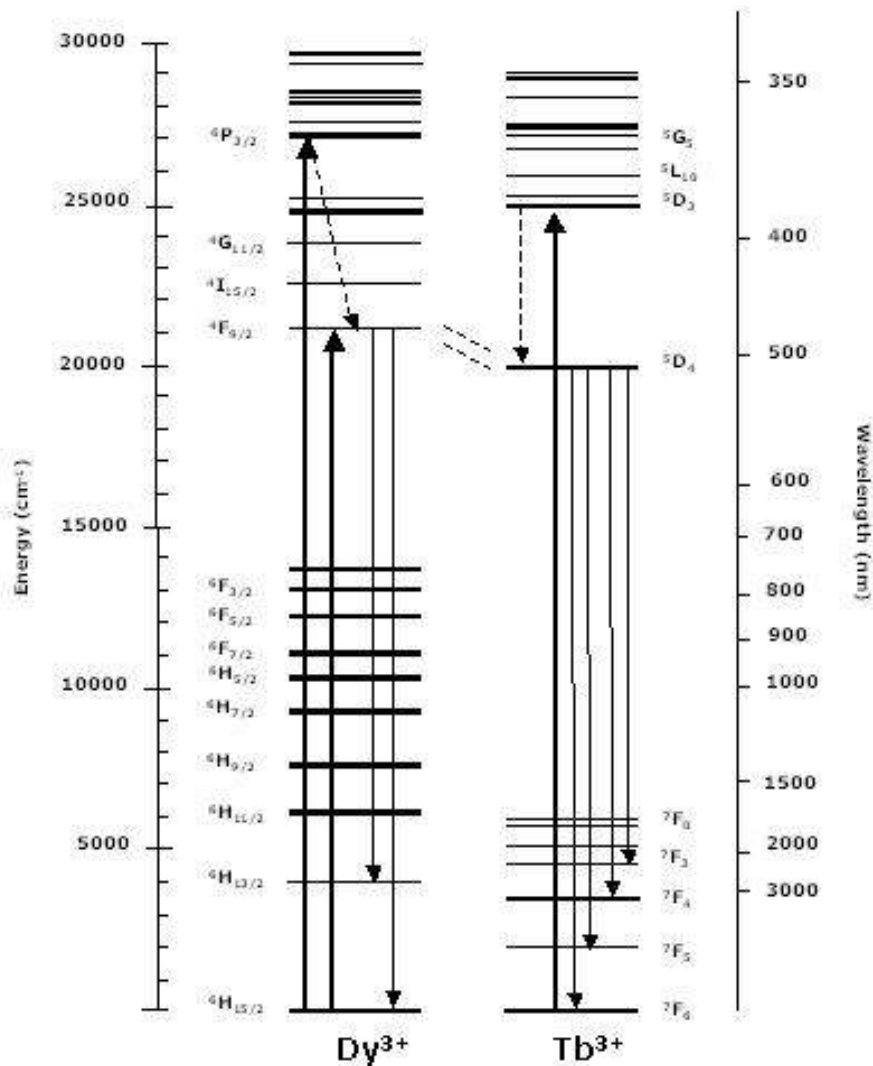


**Figure 10 Energy level diagram showing the energy transfer process from dysprosium to terbium [59]**

These energy transfer effects will be investigated in triple doped glass samples containing europium, dysprosium and terbium.

### 2.3 Chelates

Chelating agents are organic compounds capable of forming coordinate bonds with metals through two or more atoms from within the organic compound. The complex formed with the binding of chelating agent and metal is called a chelate. Chelating agents such as 1,10-phenanthroline and thenoyltrifluoroacetone are bidentate chelating agents as they have two coordination atoms. Figure 11 shows an example of what this structure coordination looks like.

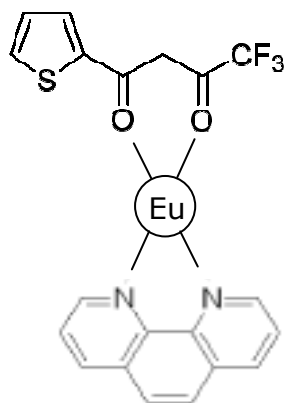


**Figure 11: Example of a bidentate chelating agents: 1,10-phenanthroline and thenoyltrifluoroacetone bonded to a Eu<sup>3+</sup> ion.**

#### 2.3.1 Chelate Energy Transfer

The fluorescent emission observed from lanthanide ions although intense, can be further enhanced with the addition of an organic chelate. The mechanism of luminescence of a lanthanide chelate is shown in Figure 12 [102]. This shows an electron promoted to an excited singlet state in the chelate upon absorption of energy, in this case ultraviolet light. This photon drops back to the lowest state of the excited singlet, from where it can return to the ground state directly

(chelate fluorescence) or follow a non-radiative path to a triplet state of the chelate. From the triplet state it may either return to the ground state by phosphorescence or alternatively undergo non-radiative intersystem crossing, this time to a nearby excited state of a lanthanide ion, where it can return to the ground state either by non-radiative emission or by metal ion fluorescence.

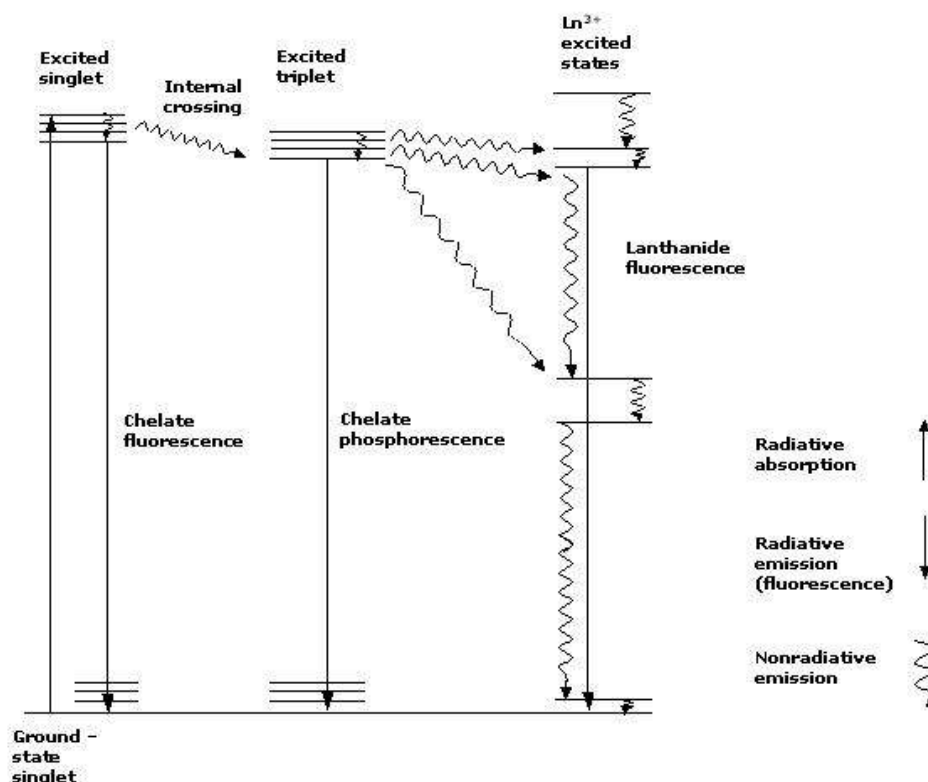


**Figure 12 Luminescence in lanthanide chelate complexes**

## 2.4 Glass Formation

Glass is defined as an amorphous solid which does not exhibit an exacting symmetrical structure. Typically a glass is a sum of its constituent parts, mainly oxides, which play different roles in the glass formation. The borosilicate glass used in this work consists of SiO<sub>2</sub>, Na<sub>2</sub>O, CaO, Al<sub>2</sub>O<sub>3</sub>, MgO, FeO, Fe<sub>2</sub>O<sub>3</sub>, K<sub>2</sub>O and B<sub>2</sub>O<sub>3</sub>. These compounds fall into three categories for glass

formation; network (glass) formers, conditional glass formers and network (glass) modifiers [103].

E.g.

**Network formers** -  $\text{SiO}_2$  and  $\text{B}_2\text{O}_3$

**Condition glass formers** -  $\text{Al}_2\text{O}_3$

**Network modifiers** -  $\text{Na}_2\text{O}$ ,  $\text{CaO}$ ,  $\text{MgO}$ ,  $\text{FeO}$ ,  $\text{Fe}_2\text{O}_3$  and  $\text{K}_2\text{O}$

The network formers can form glasses on their own,  $\text{B}_2\text{O}_3$  for example; will form a pure borate glass. While the conditional glass formers will not form glasses in their own right, they can form glasses when combined with network modifiers. Network modifiers cannot alone form glasses, but in combination with network formers or conditional formers will affect the structure and glass melt properties [104]. These affects include lowering the glass melt temperature [105, 106], for example in the case of pure silica which has a glass melt temperature of  $1715^\circ\text{C}$ , the addition of network modifiers can lower this temperature to below  $1000^\circ\text{C}$  [103]. A tertiary phase diagram for the  $\text{SiO}_2$ - $\text{B}_2\text{O}_3$ - $\text{Na}_2\text{O}$  system, borosilicate glass can be seen in Figure 13. This shows the comparison of  $\text{Na}_2\text{O}$ ,  $\text{K}_2\text{O}$  and  $\text{Li}_2\text{O}$  within a borosilicate system and their effect on melting temperature each component has.

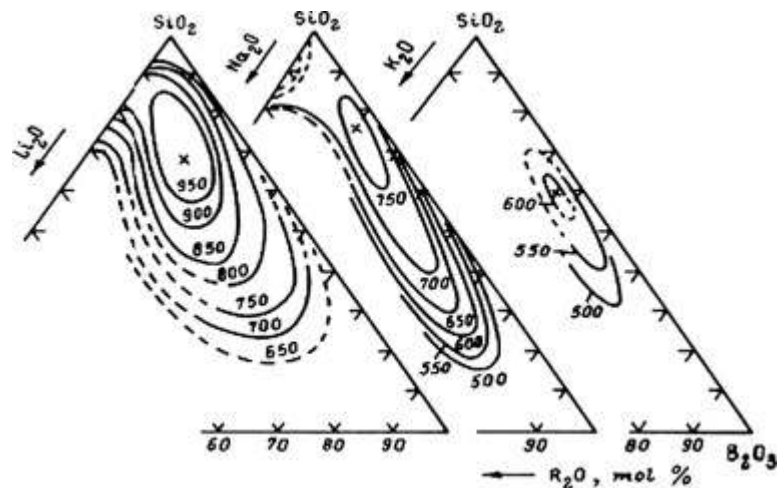


**Figure 13 Phase diagram for an  $\text{SiO}_2$ - $\text{B}_2\text{O}_3$ - $\text{Na}_2\text{O}$  system [107]**

In addition to the affect of network modifiers adding  $\text{B}_2\text{O}_3$  to a silica based glass will allow the glass structure to become more open, forming triangular units

compared to the tetrahedral units of silicates. This will therefore aid the likelihood of producing a glass matrix which could accept a high level of lanthanide doping. The use of  $B_2O_3$  further lowers the silica melting point to below  $800^\circ C$ . The use of alkali metals (network modifiers) further reduces the glass melting temperature and introduces non-bridging oxygens [108]. The available oxygens aid in providing bonding sites for the lanthanide, and can also directly affect the characteristics of the glass e.g tendency to become hydrophilic.

The strongest influence on the ability of lanthanide ions within a glass matrix to emit fluorescence is the phonon energy of the glass [109-111]. A phonon is a vibrational motion in which a structure, in this case glass, uniformly oscillates at the same frequency [112]. Thus a low phonon energy glass will be directly linked to the strength of the structure and conversely high phonon energy will be linked to a more rigid structure. The lowest phonon energy glasses are fluoride and phosphate glasses, soft structure, but these are not environmentally stable. Both fluoride and phosphate have a tendency to absorb water, becoming opaque as the glass absorbs more water, but also potentially allowing doped materials to leach out. Low phonon energy allows more energy transitions to take place within the lanthanide ion, which in turn allows more emissions to occur.

High phonon energy glasses such as silicates or borates have a more rigid structure which provides an extremely robust host for environmental stability and immense physical strength, e.g. Pyrex is a borosilicate glass. This high phonon energy comes at a price for lanthanide doping; the higher energy compromises the number of possible transitions which can occur. This limits the potential number of fluorescent emissions which could be used for tracing studies.

The glass formulation is critical in tailoring the phonon energy, for example Schott 8830 borosilicate glass contains a high percentage of  $SiO_2$  (80.6%) which would create a high phonon energy glass. The glass formulation used in this work contains 51.8 % of  $SiO_2$  which reduces the phonon energy of the glass structure and still produces a glass which exhibits environmental stability.

## 2.5 Polymerisation

Polymerisation can be divided into organic and inorganic polymer formation. Polyethylene glycol dimethacrylate (p-EGDMA) forms an organic polymer [113, 114], tetraethyl orthosilicate (TEOS), silica sol gel precursor, forms an inorganic polymer [115]. The use of monodisperse organic and inorganic polymerisation methods allows the synthesis of size controlled spheres.

### 2.5.1 Inorganic Polymerisation – Silica sol gel

The sol gel method is a colloidal precipitation technique that has its origins in the development of low temperature fabrication methods for glass and ceramics. The use of TEOS provides inorganic silica which produces particles of pure silicon dioxide, highly stable and environmentally robust, an ideal host for a lanthanide doping.

A sol is a dispersion of colloidal particles suspended within a fluid where the particles range between 1 nm and 1000 nm. The formation of particles is influenced by the gravitational and frictional forces upon them and this can be calculated by examining the sedimentation rate and assuming the particles to be spherical [116].

#### Equation 5: Sedimentation rate

$$\begin{aligned} dx / dt &= \left[ \left( \frac{4\pi r^3}{3} \right) (\rho' - \rho) g \right] / 6\pi r \eta \\ &= \left[ 2r^2 (\rho' - \rho) g \right] / 9\eta \end{aligned}$$

Where  $\eta$  = viscosity of surrounding medium /  $\text{Nm}^{-2}\text{s}$

$\rho$  = density of surrounding medium /  $\text{kg m}^3$

$\rho'$  = density of colloid particle material /  $\text{kg m}^3$

$r$  = radius of colloid particle / nm

$g$  = gravity  $9.81 \text{ m/s}^2$

The structure of the sol gel prepared silica sphere will take that of a typical amorphous  $\text{SiO}_2$  matrix, Figure 14 shows a 2 dimensional schematic of this formation.

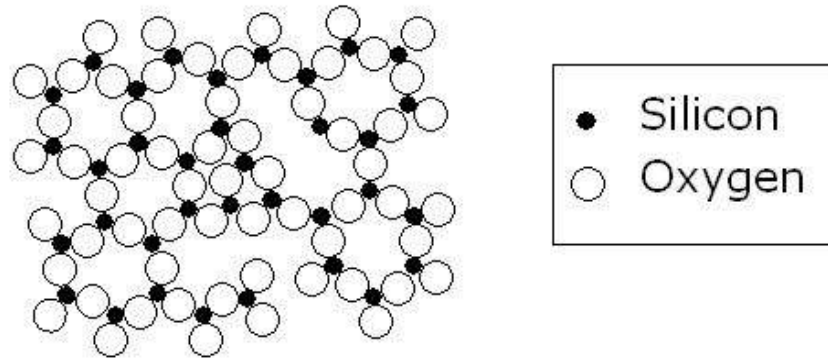


**Figure 14 Schematic 2-dimensional drawing of the structure of a silicon dioxide matrix**

### 2.5.2 Doped Sol Gel Sphere Formation

Following the same principles of the pure silicon dioxide sphere formation, the doped spheres are predicted to follow the Zachariasen random network theory [103] of structure formation.

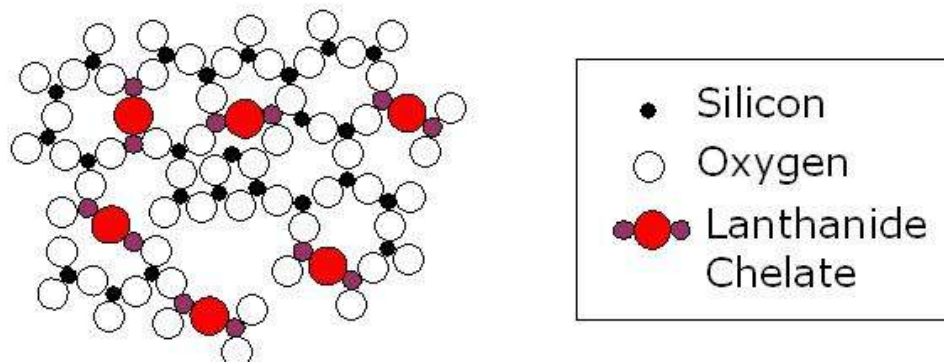


**Figure 15 Schematic 2-dimensional drawing of the structure of a lanthanide chelate doped silicon dioxide matrix**



As a sphere forms the oxygen will bond with the chelate molecule, acting almost as a network modifier within the silica network. The rules of phonon energy apply to silica sol gel particles as it would to silica glasses, resulting in a silica particle having high phonon energy.

As a result experimentally it was found that terbium did not exhibit the  $^5D_4$  to  $^7F_5$  transition which in the borosilicate glass matrix results in a 543 nm (green) emission.

### 2.5.3 Organic Polymerisation

Polymerisation is the process of reacting monomer molecules together to form either long chains or networks. This follows two forms of polymerisation, addition polymerisation and condensation polymerisation. Addition polymerisation is where single monomer molecules are bonded together to form long chain molecules without the loss of any atoms, such as ethylene which forms polyethylene. Condensation polymerisation is where multiple monomers form structures with molecules like polyethylene glycol dimethacrylate and methacrylic acid (a cross linking monomer) form polyethylene glycol dimethacrylate-co-methacrylic acid, Figure 16.

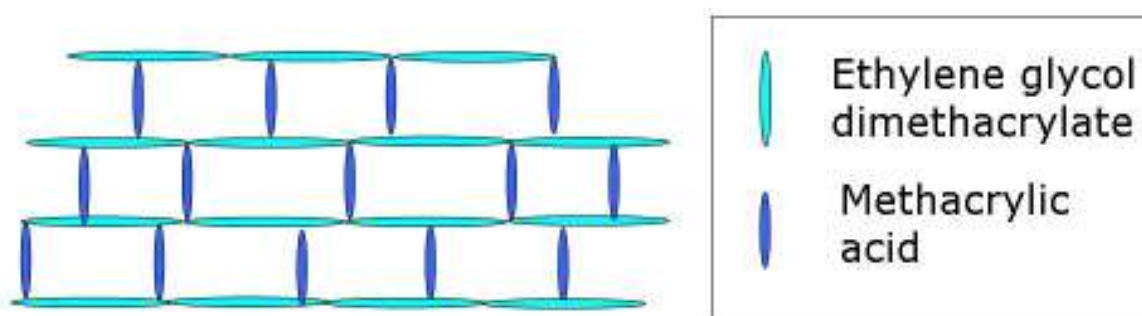


**Figure 16 Cross linked polymer, polyethylene glycol dimethacrylate**

The actual formation of a cross linked polymer is not as structural as indicated by the figure, condensation cross linked polymers take on a randomised "spaghetti

like" form. The use of a cross linking condensation polymerisation reaction allows a great possibility for doping in to the polymer network. The chelated lanthanide molecule will replace the cross linker in the formation of the polymer network.

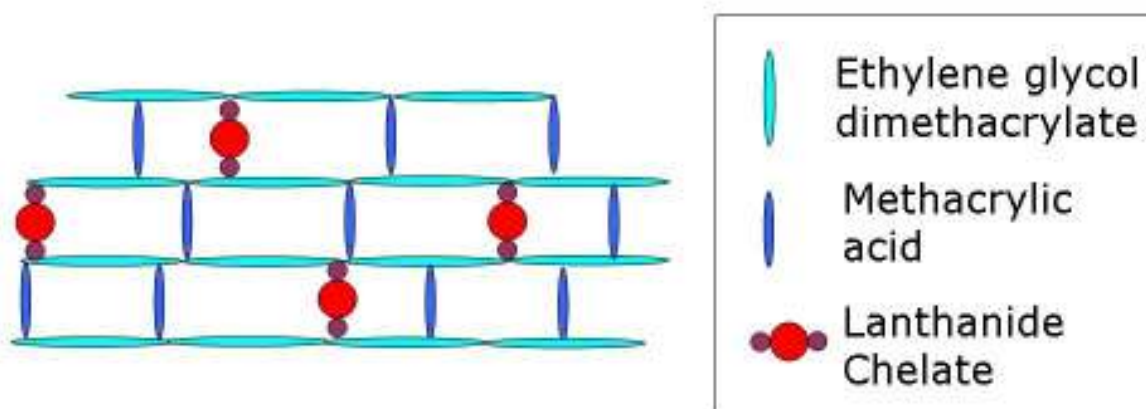


**Figure 17 Doped cross linked polymer, polyethylene glycol dimethacrylate**

A basic structure layout is shown in Figure 17, this indicates the hypothesised location of the lanthanide chelate within the polymer structure.

## 2.6 Particle Size

Particle size determination for sediment samples was determined using a Malvern Mastersizer E. The instrument utilises laser ensemble light scatter as a means of particle size distribution determination. This is based upon two theories of light scattering behaviour, the Fraunhofer Model and the Mie Theory [117]. The Fraunhofer theory can predict the scattering pattern that is created when a solid, opaque disc, of a known size passes through a laser beam. The Mie theory was developed to predict the way light is scattered by spherical particles and deals with the way light passes through, or is adsorbed by, the particle.

A Helium Neon laser (632 nm) is fired through a beam expander to collimate the beam to 18 mm. This collimated laser beam will pass through the sample cell where any particles present in suspension will scatter the laser light. The scattered laser pass through the receiver lens which operates as a fourier transform lens, forming the far field diffraction pattern of the scattered light at its focal plane. The detector used is a series of 31 concentric annular sections

and gathers the scattered light over a range of solid angles of scatter. The unscattered light is focused on the detector and passed through a small aperture in the detector and passes out of the optical system. This process is monitored to allow the determination of the sample volume concentration. Due to the range lens configuration it keeps the diffraction pattern stationary and centered on its optical axis wherever the particle is in the analyser beam. This means it does not matter if the particle is moving through the analyser beam, such as it would in an aqueous suspension. During an analysis many particles are simultaneously present in the beam path and the scattered light measured, equals the sum of all the individual patterns overlaid on the central axis. Typically the number of particles needed in the beam simultaneously to obtain an adequate measurement of the scattering would be 100-10,000 dependent on their size. Therefore measurements are not done by one instantaneous measurement but are averaged over time as the material is continuously passed through the beam, e.g. 2000 in 1 ms.

When the particles scatter the light, they produce unique light intensity characteristics with an angle of observation. The resulting measured peak energy intensity on the detector results in a specific scattering angle related to its diameter. Large particles have peak energies in small angles of scatter while small particles have peak energies in high angles of scatter.

The terms of interest,  $D [v,0.5]$ ,  $D [4,3]$ ,  $D [v,0.1]$  and  $D [v,0.9]$  can be defined as:

- $D [v,0.5]$  – Volume median diameter. This figure has 50 % of the distribution above and 50 % below this value. It divides the distribution exactly in half.
- $D [4,3]$  – Volume mean diameter. This is the diameter of the sphere that has the same volume as an ideal sphere.  $D[4,3] = \frac{\sum d^4}{\sum d^3}$
- $D [v,0.1]$  and  $D [v,0.9]$  – These are 90 % and 10 % cut-offs respectively for the distribution. Where  $D [v,0.9]$  has 90 % of the distribution below this value and  $D [v,0.1]$  has 10 % of the distribution below this value.

A typical particle size distribution plot for a sediment sample from the Case Study of Bowmore Harbour can be seen in Figure 18.

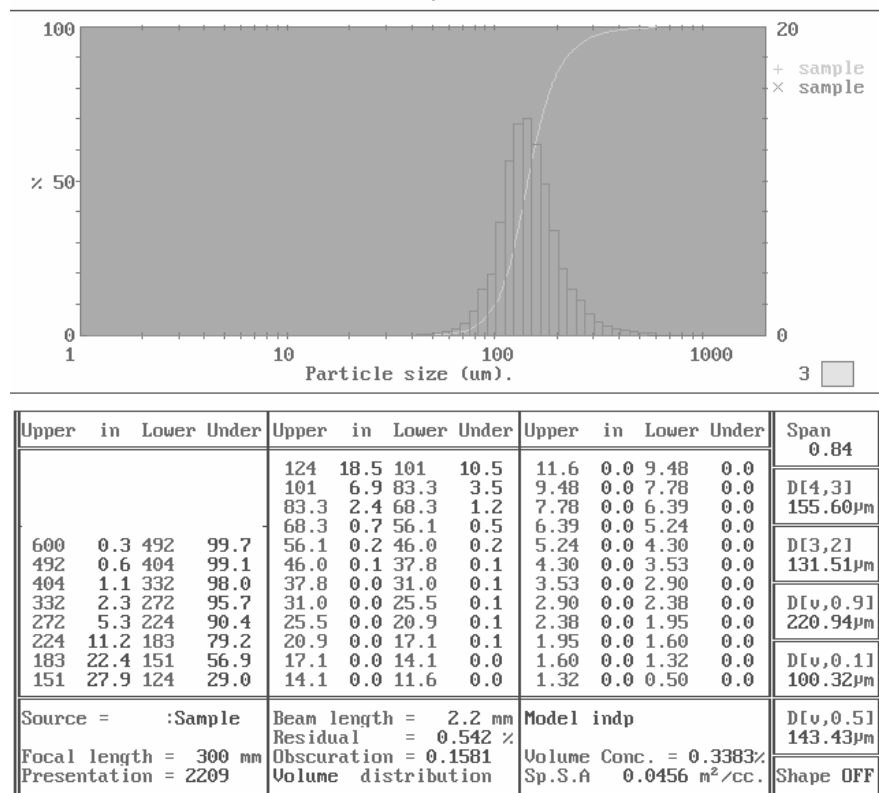


Figure 18 Example of particle size analysis results.

## 2.7 Experimental Design : Chemometrics

Statistical designs of experiment (DOE) are used to optimise the number of experiments that need to be carried out to successfully investigate a given problem. The principle application is to use a statistical planned approach to investigate the influences of variables (called factors in experimental design) on the measurement response, rather than a trial and error approach, which can often lead to a waste of time and can lead to experiments where inadvertently more than one parameter has changed thus making it impossible to assign a cause for any change in response observed [118-121].

### **2.7.1 Taguchi Orthogonal Array Fractional Factorial Experimental Design**

In experimental design a factor is defined as any experimental variable that can affect the result of the 'experiment'. The result or value obtained from an 'experiment' is called a response. The response in this work is complicated in that it includes wavelength, peak intensity and lifetime. The factors known from previous experience are; furnace time, furnace temperature, annealing time and annealing temperature. The different values of a factor are referred to as different levels, so for example in the investigation of the influence of lanthanide concentration (a factor) on the tracer response, some concentration levels will need to be chosen to input into the experimental design. These concentrations were chosen from previous experience with a small input from general trends observed in literature [122-124].

There are a variety of designs; one suitable design uses a complete systematic experimentation, i.e. The Full Design of Experiment, where an experiment is carried out for every combination of factor and level. For example if experiments were carried out to investigate the influence of 5 factors at 3 levels this would require  $3^5$  experiments (243) excluding replicates to comprehensively quantify the dependence, however this is far too many experiments. Statistics can be used further to modify the design to optimise the number of experiments actually required. This full factorial DOE utilises all the main effects and interactions up to order 5 however statistically it is the main to second order effects which are important, this is what is used in the Half Fractional Factorial DOE.

In a Fractional Factorial design, the lower order and higher order effects are paired, and are said to be aliases of each other because they are indistinguishable or confounded. Probability plots are carried out by the DOE software and an array of the statistically significant experiments that have to be carried out to provide a statistically meaningful prediction of the effect being studied is produced.

### 3 MATERIALS AND METHODS

#### 3.1 Glass Tracer Fabrication

##### 3.1.1 Blank Glass

For the production of blank standard borosilicate glass a standard composition was used [104, 125]. Crushed soda lime silica glass (Sigmund Lindner, S-Type Thermal Rounded Soda Lime Glass Beads) and boric acid (Aldrich, 99.99%, 339067-500G) were processed in an Agate ball mill for a total of 8 minutes to produce a homogeneous mixture, which was then transferred to a platinum crucible to produce a 7 g batch.

The composition of the 7 g batch being thus:

*5 g Soda lime silica glass*

*2 g Boric Acid*

*X g Lanthanide*

The breakdown of component materials of the silica glass with boric acid and their percentage weight can be seen in Table 5 below:

<b>Borosilicate Component</b>	<b>Weight / %</b>
SiO <sub>2</sub>	51.8
Na <sub>2</sub> O	9.8
CaO	7
Al <sub>2</sub> O <sub>3</sub>	0.3
MgO, FeO, Fe <sub>2</sub> O <sub>3</sub> and K <sub>2</sub> O	2.5
B <sub>2</sub> O <sub>3</sub>	28.6

**Table 5 Component materials of the borosilicate glass matrix**

The platinum crucible was then placed in to a high temperature muffle furnace where the sample was heated to 550 °C for 30 minutes to allow the boric acid to melt without expansion brought on by rapid heating. The temperature was then raised to 900 °C, 1000 °C and 1100 °C, holding for 1 hour at each point before being raised to pour temperature at 1250 °C. The sample was then poured in to

a brass mould which has been pre-heated on a hot plate to reduce possibility of thermal shock and therefore cracking.

### **3.1.2 Concentration Study Doped Glass Tracer**

For the production of the environmental glass tracer used in the concentration study the appropriate mol % of lanthanide salt (All Aldrich  $\text{EuCl}_3 \cdot 6\text{H}_2\text{O}$ , 99.9%, 212881-25G,  $\text{TbCl}_3 \cdot 6\text{H}_2\text{O}$ , 99.9%, 212903-25G,  $\text{DyCl}_3 \cdot 6\text{H}_2\text{O}$ , 99.9%, 289272-25G), Table 6, was added to the soda lime silica glass and boric acid to produce a 7 g batch as described in 3.1.1.

Mol % of Dopant	Weight of $\text{EuCl}_3 \cdot 6\text{H}_2\text{O}$ / g	Weight of $\text{TbCl}_3 \cdot 6\text{H}_2\text{O}$ / g	Weight of $\text{DyCl}_3 \cdot 6\text{H}_2\text{O}$ / g
2.0	0.8324	0.8484	0.8565
1.8	0.7492	0.7636	0.7709
1.6	0.6659	0.6787	0.6852
1.4	0.5827	0.5939	0.5996
1.2	0.4994	0.5090	0.5139
1.0	0.4162	0.4242	0.4283
0.8	0.3330	0.3393	0.3426
0.6	0.2497	0.2545	0.2570
0.4	0.1665	0.1697	0.1730
0.2	0.0832	0.0848	0.0857

**Table 6 Concentration study doping concentrations**

Taking the weight of component raw materials (weighed by difference) which were placed in the ball mill and what was then transferred to the crucible, after the ball milling process, it was possible to calculate the fabrication loss error which came from the production of the glass. An average of 20 samples showed a loss of 0.47 % or an average of 40 mg. This shows that direct comparison of samples is possible as the error from manufacture is extremely small.

## **3.2 Experimental Design – Chemometrics For Multi-Ion Doping**

### **3.2.1 Taguchi Orthogonal Array Fractional Factorial**

The Fraction Factorial Design of Experiment was chosen to optimise the number of experiments in this work because it confounds the interactions and allows a fraction of the experiments to be carried out and still give a statistically meaningful prediction of response. Using MATLAB 14 a Taguchi Orthogonal Array Fractional Factorial Experimental Design (TOAFFED) was used and produced the DOE arrays shown in Table 7, that optimise the number of experiments required to gain detailed spectral and time resolved fluorescence characterisation of single and multiple lanthanide doped host matrices. The response factors previously identified namely; wavelength, lifetime and intensity, will be measured for the following experiments.

### **3.2.2 Design of Experiment to investigate the concentration dependence of the fluorescence lanthanide response and glass host dependence**

To find the concentration dependence of the fluorescence lanthanide response (peak wavelength, intensity and lifetime) tracers of the same glass host under the current fabrication method and parameters would have to be made containing different concentration levels of multiple lanthanides and the samples would have to be characterised. The chosen 3 lanthanides used as dopants (or sensitiser) are factors in an experimental design and the 5 concentration levels in the Fractional Factorial Design of Experiment. A half fractional design requires  $5^{3-1}$  experiments (25) which are achievable and still utilised second order effects, i.e. it is still using the statistically significant effects. The chosen TOAFFED in Table 7 shows the significant experiments that have to be carried out to provide a statistically meaningful prediction of the effect being studied which in this case is the concentration dependence of the fluorescence lanthanide response and by repeating the array of experiments with a second host it will also show the effect on the response factors of the different glass hosts.



<b>Experiment</b>	<b>A</b>	<b>B</b>	<b>C</b>
<b>1</b>	1	1	1
<b>2</b>	1	2	2
<b>3</b>	1	3	3
<b>4</b>	1	4	4
<b>5</b>	1	5	5
<b>6</b>	2	1	2
<b>7</b>	2	2	3
<b>8</b>	2	3	4
<b>9</b>	2	4	5
<b>10</b>	2	5	1
<b>11</b>	3	1	3
<b>12</b>	3	2	4
<b>13</b>	3	3	5
<b>14</b>	3	4	1
<b>15</b>	3	5	2
<b>16</b>	4	1	4
<b>17</b>	4	2	5
<b>18</b>	4	3	1
<b>19</b>	4	4	2
<b>20</b>	4	5	3
<b>21</b>	5	1	5
<b>22</b>	5	2	1
<b>23</b>	5	3	2
<b>24</b>	5	4	3
<b>25</b>	5	5	4

**Where:**

<b>A</b>	Europium
<b>B</b>	Terbium
<b>C</b>	Dysprosium

	<b>Glass 1</b>	<b>Glass 2</b>
<b>1</b>	0.5 mol%	0 mol%
<b>2</b>	1.0 mol%	0.5 mol%
<b>3</b>	1.5 mol%	1.0 mol%
<b>4</b>	2.0 mol%	1.5 mol%
<b>5</b>	2.5 mol%	2.0 mol%

**Table 7 Taguchi Orthogonal Array Fractional Factorial Design of Experiment for Glass1 and Glass 2**

**3.2.3 Design of Experiment to investigate the effects of fabrication parameters on the glass**

The chosen experimental design, TOAFFED was applied to optimise the experiments required to investigate the effects of factors associated with the fabrication of the glass. Using existing knowledge of glass fabrication 4 factors were identified, furnace temperature, furnace time, annealing temperature and annealing time with the effects of these factors on the spectral emissions will be examined at 2 levels. The experiments required are shown in Table 8.

For these experiments each fabrication factor, A, B, C and D will be altered, e.g. increase time or temperature, Table 9.

<b>Experiment</b>	<b>A</b>	<b>B</b>	<b>C</b>	<b>D</b>
1	1	-1	1	-1
2	1	1	1	1
3	-1	1	-1	1
4	-1	-1	1	1
5	-1	1	1	-1
6	1	-1	-1	1
7	1	1	-1	-1
8	-1	-1	-1	-1

**Where:**

<b>Experiment</b>	<b>Parameter</b>	<b>Setting</b>
<b>A</b>	1	1300 °C
	-1	1200 °C
<b>B</b>	1	60 min
	-1	15 min
<b>C</b>	1	450 °C
	-1	350 °C
<b>D</b>	1	60 min
	-1	30 min

**Table 8 Taguchi orthogonal Array Fractional Factorial Design of Experiment for fabrication parameter variation**

<b>Experiment</b>	<b>A / °C</b>	<b>B / min</b>	<b>C / °C</b>	<b>D / min</b>
<b>1</b>	1300	15	450	30
<b>2</b>	1300	60	450	60
<b>3</b>	1200	60	350	60
<b>4</b>	1200	15	450	60
<b>5</b>	1200	60	450	30
<b>6</b>	1300	15	350	30
<b>7</b>	1300	60	350	30
<b>8</b>	1200	15	350	30

**Table 9 Experimental Conditions required for Taguchi Orthogonal Array Fractional Factorial Analysis**

The fluorescence properties were studied using single scans since this glass contained only dysprosium which had been previously fully characterised in the concentration study, also the dysprosium concentration remained constant. The wavelength used for excitation was 452 nm and the emission peak of interest was at 575 nm.

### **3.3 Glass Tracer Fabrication**

The use of constituent component compounds ball milled together with a lanthanide dopant to produce a homogenous glass matrix is described here. This mixture, when heated to 1250 °C, produces a borosilicate glass melt which is then moulded using the cast and quench method to create reproducible glass samples which can be easily analysed using spectroscopic techniques.

### 3.3.1 Borosilicate Glass 1 Multiple Ion Doped Glass Tracer

To examine the effect of multi-ion doping in the glass tracer the appropriate mol % of lanthanide salt was added to the soda lime silica glass and boric acid to produce a 7 g batch as described in 3.1.1. Using experimental design, the following concentration combinations were used to produce a range of samples, Table 10.

Glass 1 Sample	mol % of Eu	mol % of Tb	mol % of Dy
G1-1	0.5	0.5	0.5
G1-2	0.5	1.0	1.0
G1-3	0.5	1.5	1.5
G1-4	0.5	2.0	2.0
G1-5	0.5	2.5	2.5
G1-6	1.0	0.5	1.0
G1-7	1.0	1.0	1.5
G1-8	1.0	1.5	2.0
G1-9	1.0	2.0	2.5
G1-10	1.0	2.5	0.5
G1-11	1.5	0.5	1.5
G1-12	1.5	1.0	2.0
G1-13	1.5	1.5	2.5
G1-14	1.5	2.0	0.5
G1-15	1.5	2.5	1.0
G1-16	2.0	0.5	2.0
G1-17	2.0	1.0	2.5
G1-18	2.0	1.5	0.5
G1-19	2.0	2.0	1.0
G1-20	2.0	2.5	1.5
G1-21	2.5	0.5	2.5
G1-22	2.5	1.0	0.5
G1-23	2.5	1.5	1.0
G1-24	2.5	2.0	2.0
G1-25	2.5	2.5	1.5

**Table 10 Concentration (mol %) combinations for multiple ion doped borosilicate glass 1 samples**

The masses of europium, terbium and dysprosium used for the multiple ion doped glass 1 experiments can be seen in Table 11.

Glass 1 Sample	Mass of $\text{EuCl}_3 \cdot 6\text{H}_2\text{O}$ / g	Mass of $\text{TbCl}_3 \cdot 6\text{H}_2\text{O}$ / g	Mass of $\text{DyCl}_3 \cdot 6\text{H}_2\text{O}$ / g
G1-1	0.2081	0.2121	0.2141
G1-2	0.2081	0.4242	0.4282
G1-3	0.2081	0.6363	0.6423
G1-4	0.2081	0.8484	0.8564
G1-5	0.2081	1.0605	1.0705
G1-6	0.4162	0.2121	0.4382
G1-7	0.4162	0.4242	0.6423
G1-8	0.4162	0.6363	0.8564
G1-9	0.4162	0.8484	1.0705
G1-10	0.4162	1.0605	0.2141
G1-11	0.6243	0.2121	0.6423
G1-12	0.6243	0.4242	0.8564
G1-13	0.6243	0.6363	1.0705
G1-14	0.6243	0.8484	0.2141
G1-15	0.6243	1.0605	0.4282
G1-16	0.8324	0.2121	0.8564
G1-17	0.8324	0.4242	1.0705
G1-18	0.8324	0.6363	0.2141
G1-19	0.8342	0.8484	0.4282
G1-20	0.8324	1.0605	0.6423
G1-21	1.0405	0.2121	1.0705
G1-22	1.0405	0.4242	0.2141
G1-23	1.0405	0.6363	0.4242
G1-24	1.0405	0.8484	0.6423
G1-25	1.2081	0.4242	0.4282

**Table 11 Concentration combinations for multiple ion doped borosilicate glass 1 samples**

### 3.3.2 Borosilicate Glass 2 Multiple Ion Doped Glass Tracer

It has been seen [126] that the incorporation of the fluoride ion in to a glass matrix is said to increase the maximum concentration of dopant in the glass in comparison to other glass matrices containing other halide elements. This could also lead to increased fluorescence emission from lower concentrations of dopants. This was done by adding 5 mol % (0.2385 g) of sodium fluoride (NaF, Adrich, 99.99%, 450022-25G) to the existing borosilicate glass matrix. As this new

glass composition has not been analysed before, the same Taguchi factorial design of experiment as used for Glass 1 was employed here, except this time sample 1 equalled 0 mol %, see Table 12. This enabled double lanthanide doped samples to be produced without increasing the number of samples, thereby allowing the investigation of any differences in peak wavelengths with the change in host matrix.

Glass 2 Sample	mol % of Eu	mol % of Tb	mol % of Dy
G2-1	0.0	0.0	0.0
G2-2	0.0	0.5	0.5
G2-3	0.0	1.0	1.0
G2-4	0.0	1.5	1.5
G2-5	0.0	2.0	2.0
G2-6	0.5	0.0	0.5
G2-7	0.5	0.5	1.0
G2-8	0.5	1.0	1.5
G2-9	0.5	1.5	2.0
G2-10	0.5	2.0	0.0
G2-11	1.0	0.0	1.0
G2-12	1.0	0.5	1.5
G2-13	1.0	1.0	2.0
G2-14	1.0	1.5	0.0
G2-15	1.0	2.0	0.5
G2-16	1.5	0.0	1.5
G2-17	1.5	0.5	2.0
G2-18	1.5	1.0	0.0
G2-19	1.5	1.5	0.5
G2-20	1.5	2.0	1.0
G2-21	2.0	0.0	2.0
G2-22	2.0	0.5	0.0
G2-23	2.0	1.0	0.5
G2-24	2.0	1.5	1.5
G2-25	2.0	2.0	1.0

**Table 12 Concentration (mol %) combinations for multiple ion doped borosilicate glass 2 samples**

The Glass 2 samples were analysed using the same measurement parameters as used for glass 1. The mass of europium, terbium and dysprosium used for the multiple ion doped glass 2 experiments can be seen in Table 13.

Glass 2 Sample	Mass of $\text{EuCl}_3 \cdot 6\text{H}_2\text{O}$ / g	Mass of $\text{TbCl}_3 \cdot 6\text{H}_2\text{O}$ / g	Mass of $\text{DyCl}_3 \cdot 6\text{H}_2\text{O}$ / g
G2-1	0	0	0
G2-2	0	0.8484	0.8564
G2-3	0	0.4242	0.4282
G2-4	0	0.6363	0.6423
G2-5	0	0.8484	0.8564
G2-6	0.2081	0	0.2141
G2-7	0.2081	0.2121	0.4282
G2-8	0.2081	0.4242	0.6423
G2-9	0.2081	0.6363	0.8564
G2-10	0.2081	0.8484	0
G2-11	0.4162	0	0.4282
G2-12	0.4162	0.2121	0.6423
G2-13	0.4162	0.4242	0.8564
G2-14	0.4162	0.6363	0
G2-15	0.4162	0.8484	0.2141
G2-16	0.6243	0	0.6423
G2-17	0.6243	0.2121	0.8564
G2-18	0.6243	0.4242	0
G2-19	0.6243	0.6363	0.2141
G2-20	0.6243	0.8484	0.4282
G2-21	0.8324	0	0.8564
G2-22	0.8324	0.2121	0
G2-23	0.8324	0.4242	0.2141
G2-24	0.8324	0.6363	0.4282
G2-25	0.8324	0.8484	0.6423

**Table 13 Concentration combinations for multiple ion doped borosilicate glass 2 samples**

### 3.4 Fabrication of Tracer Particles

For a material to be used as a particle tracer it must be of a functional size and fit for purpose, which for a glass based tracer requires the melted glass to be reduced in size through mechanical grinding. This production paradigm, although true for glass based tracers is not the case for all tracer particles, e.g. sol gel or polymer spheres. To turn bulk glass samples of glass into powder they must be ball milled using the same agate ball mill to reduce the possibility of contamination. The pieces of bulk glass are reduced in size using a mechanical fracture method to produce pieces in the region of 2-6 mm in

diameter. These pieces are far easier to ball mill as they will break down in to smaller fragments faster compared to a larger piece of glass which would begin to “round off” much like a pebble on a beach.

### **3.4.1** *Ball Milling*

An agate ball mill was used to grind the glass pieces. The mill comprises two end pieces, two cork o-rings, two agate balls and a central cylinder. One of the end pieces is placed on the bench, the cork o-ring is put in place and the central cylinder is set on top of the cork ring. The glass pieces are added, the second cork o-ring is placed on the central cylinder and the mill is closed by setting the second end piece on top. This is then placed inside Gier Creston ball mill. This device contains an electric motor which drives a belt connected to a steel sample holder. It is this sample holder in to which the agate mill is placed. The ball mill is turned on for 5 minutes and then the agate mill is removed from the holder and emptied.

### **3.4.2** *Size Fractioning*

To separate the glass particles into size fractions which could be used as environmental tracers it is necessary to sieve the glass powder. The first pass of ball milled glass will have a particle distribution of mainly 45  $\mu\text{m}$  and above, this is separated using a Fritsch Analysette shaker. As the particle distribution becomes <20  $\mu\text{m}$  the Endecotts Sonic Sifter is used to separate the particles to <5  $\mu\text{m}$ .

#### **3.4.2.1** Shaker

A Fritsch Analysette 3E used for sifting ball milled glass powders in to different size fractions. Sieves of 75  $\mu\text{m}$ , 45  $\mu\text{m}$ , 32  $\mu\text{m}$  and 20  $\mu\text{m}$  sized mesh were used. These are arranged in a stack with the 75  $\mu\text{m}$  sieve on top and the 20  $\mu\text{m}$  on the bottom, which is placed on to a collection pan. The stack is placed on to the Analysette shaker and held by using a perspex domed top with has



retaining straps. The instrument is adjusted for amplitude by observing the motion of the powder on the top sieve and the time is set for between 5 and 15 minutes. After each period of time it is necessary to examine the fractions in each sieve to ensure the mesh has not become blocked. After 2 or 3 x 15 minute timed shaking the sample which remains in the 75  $\mu\text{m}$  sieve is re-ball milled to reduce the particle size. This is repeated for each of the size fractions.

#### **3.4.2.2 Sonic Sifter**

Once the glass powder has been sifted to a size fraction of less than 20  $\mu\text{m}$  it is necessary to use a different instrument as there is a particle filtration limitation. These samples are placed in an Endecotts Sonic Sifter. The machine uses 10  $\mu\text{m}$  and 5  $\mu\text{m}$  sieves and a collection bag, which as with the shaker, are arranged in a stack. The sieving action of the sonic sifter is controlled by the motion of a vertical column of air which is made to oscillate. The oscillation is variable and can be augmented with mechanical “tapping” on the side of the column to liberate particles which may block the mesh. After 120 minutes 5  $\mu\text{m}$  particles are collected from the bag at the bottom of the stack. This method is slow, laborious and inefficient as the volume of glass powder is very limited.

### **3.5 Particle Size Analysis**

To determine the particle size distribution and average particle size of the ball milled glass, a Malvern Mastersizer/E, Particle Size Analyser was used. The instrument comprises a laser source, focusing optics, sample cell and detector. For the size range 0.5 – 180  $\mu\text{m}$  the focusing lens of 100 mm was used. The sample for analysis is placed in the sample cell which contains a small stirrer to maintain sample suspension. The suspension media is degassed water or degassed water containing a drop of surfactant to maintain an even dispersion of particles. Using the Malvern Particle Size Software the instrument is calibrated on a blank sample of degassed water, using the calibration controls to adjust the “laser intensity” by moving the alignment optics. Once a good signal is obtained powder sample can be added to the sample cell. There is an optimum quantity of sample which should be added and this is found by adding powder a fraction

at a time. Upon the ideal concentration of sample being reached, analysis runs for 15 seconds and is completed with a particle distribution graph and table.

Although the mesh sizes of the sieves which are used for the glass particle sieving, it is important to know the particle distribution within the size fraction.

### **3.6 Inorganic Silica Polymers**

Following a literature review of silica sol gel sphere techniques and methods, the Stöber Method is known [127-133] to be the foundation from which the majority of silica sol gel sphere preparations are based upon. The sol-gel method is based on the hydrolysis of liquid precursors and the formation of colloidal solids.

#### **3.6.1 Silica Sol Gel Spheres**

Stöber showed in 1968 the process of producing 800 nm sized silica spheres from simple reaction of an organosilicate precursor, tetraethyl orthosilicate (TEOS, Aldrich, 99%, 86578-1L) with a base catalyst, ammonium hydroxide (NH<sub>4</sub>OH, Aldrich, 28-30% NH<sub>3</sub>, 320145-1L) 30%, in absolute ethanol (AE, Aldrich, 99.8%, 02875-2.5L). The size of the produced spheres being controlled by the ratio of AE : TEOS : NH<sub>4</sub>OH. This degree of control allows the possible production of spheres down to a minimum size of 50 nm.

##### **3.6.1.1 Silica Sol Gel Spheres 800 nm**

The following combinations of compounds were used to produce 800 nm size range silica sol gel spheres:

*18.7 ml absolute ethanol*

*7.0 ml ammonium hydroxide*

*1.3 ml TEOS in 5 ml absolute ethanol*

The ethanol was added to a small beaker upon a stirring plate where the ammonium hydroxide and TEOS in ethanol was also added. A precipitate begins to form within 15 minutes and reaction reaches completion after 1 hour.

### **3.6.1.2** Silica Sol Gel Spheres 200 nm

To produce smaller spheres the ratio of ammonium hydroxide:TEOS was adjusted to:

*18.7 ml absolute ethanol*  
*2 ml ammonium hydroxide*  
*1.3 ml TEOS in 5 ml absolute ethanol*

From this formulation 200 nm spheres were produced and for all subsequent silica sol gel experiments this ratio was used.

The silica spheres were removed from solution by filtration, 0.2  $\mu\text{m}$  Whatman nylon filter membrane.

### **3.6.1.3** Doped Sol Gel Spheres

To make doped silica spheres using the chelated lanthanides the formulation used was 18.7 ml absolute ethanol into which 0.2 g of  $\text{Eu}[\text{ttfa}][\text{phen}]$  was dissolved:

*18.7 ml absolute ethanol*  
*2 ml ammonium hydroxide*  
*1.3 ml TEOS in 5 ml absolute ethanol*

The doped silica spheres were removed from solution using filtration, 0.2  $\mu\text{m}$  Whatman filter membrane.

### **3.7 Organic Polymers**

#### **3.7.1 Poly-EGDMA-co-MAA**

Following a literature review of monodisperse polymerisation reactions the following preparation was chosen:

*70 ml Distilled acetonitrile*  
*10 ml absolute ethanol*  
*1.2 ml ethylene glycol dimethacrylate (EGDMA)*  
*0.8 ml methacrylic acid (MAA)*  
*0.04 g azobisisobutyronitrile (AIBN)*

A distillation set up was prepared and a 150 ml round bottom flask was used as the reaction vessel. To this the Acetonitrile (Aldrich, 99.8%, 271004-2L) was added, along with the ethanol, EGDMA (Aldrich, 98%, 335681-500ML), MAA (Fisher, 99.5%, 16831-5000) and the AIBN (Aldrich, 98%). The flask was swirled to dissolve the AIBN/initiator and then placed in a heating mantle which was set to a temperature at which distillation of the acetonitrile will begin. The solution will start to turn cloudy when the temperature reaches 80 °C. After 15 – 25 minutes the reaction reached completion.

#### **3.7.2 Poly-EGDMA-co-HEMA**

The polymer spheres produced from this reaction are very similar to that of poly-EGDMA-co-MAA, except they have carboxyl functional groups on the surface.

The following preparation was used:

*70 ml Distilled acetonitrile*  
*10 ml absolute ethanol*  
*1.2 ml EGDMA*  
*0.8 ml hydroxyethyl methacrylate (HEMA)*  
*0.04 g AIBN*

A distillation set up was prepared and a 150 ml round bottom flask was used as the reaction vessel. To this the acetonitrile was added, along with the ethanol, EGDMA, HEMA (Aldrich, 99%, 477028-100ML) and the AIBN. The flask was swirled to dissolve the AIBN/initiator and then placed in a heating mantle which was set to a temperature at which distillation of the acetonitrile will begin. The solution will start to turn cloudy when the temperature reaches 80 °C. After 15 – 25 minutes the reaction reached completion.

### **3.8 Doped Polymer Spheres**

#### **3.8.1 Doped Poly-EGDMA-co-MAA**

Following a literature review of monodisperse polymerisation reactions and the success of experiments examining undoped morphology it was decided to use the following methodology.

*70 ml Distilled acetonitrile*

*10 ml absolute ethanol*

*1.2 ml EGDMA*

*0.8 ml MAA*

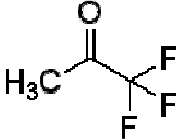
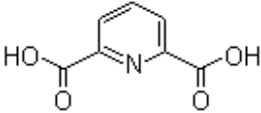
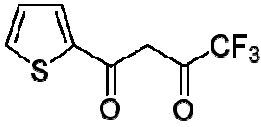

*0.04 g AIBN*

*0.2 g Eu[ttfa][phen]*

A distillation set up was prepared and a 150 ml round bottom flask was used as the reaction vessel. To this, 0.2 g of Eu[ttfa][phen] was dissolved into the 10 ml of absolute ethanol (as Eu[ttfa][phen] is only partially soluble in Acetonitrile). The acetonitrile was the added, along with EGDMA, MAA and the AIBN. The flask was swirled to dissolve the AIBN/initiator and then placed in a heating mantle which was set to a temperature at which distillation of the acetonitrile will begin. The solution will start to turn cloudy when the temperature reaches 80 °C. After 15 – 25 minutes the reaction reached completion.

### 3.9 Chelates

The use of chelates combined with lanthanides to enhance the fluorescent emission has been well documented and the lanthanide complexes have been used in various materials [73, 81, 88, 134]. From literature the following chelate compounds were examined. Europium and terbium were chosen as the test lanthanides as they have typically a strong visible fluorescence emission of red and green which made it easier for quick visual analysis as to whether the experiments were working. The experiments using trifluoroacetone were unsuccessful as they did not yield a precipitate which could be used.

Chelate	Abbreviation	Structure
trifluoroacetone	TFA	
2,6-pyridinedicarboxylic acid	PDA	
thenolytrifluoroacetone	TTFA	
1,10-phenanthroline	PHEN	

**Table 14 Chelate Compounds Investigated**

### **3.9.1** *Chelate: 2,6-Pyridinedicarboxylic Acid*

In to 30ml of distilled water 0.2836 g of  $\text{EuCl}_3 \cdot 6\text{H}_2\text{O}$  was added, dissolved using a sonic bath and then placed on a hot plate. The water was heated to around 50 °C at which point PDA was added in a molar ratio of 3:1. The pH on the solution was raised to 8 from a starting pH of 3 using Sodium Hydroxide solution. At the correct pH the PDA completely dissolved to give a clear solution, at this point the liquid was removed from the hot plate and decanted to a Pyrex petri dish where the water was allowed to evaporate. The removal of water yielded a crystalline solid which under UV excitation produced a bright red glow.

The same process was followed to produce  $\text{Tb}[\text{pda}]_3$ ,  $\text{Sm}[\text{pda}]_3$ ,  $\text{Dy}[\text{pda}]_3$ ,  $\text{Gd}[\text{pda}]_3$ ,  $\text{Ce}[\text{pda}]_3$ ,  $\text{Er}[\text{pda}]_3$  and  $\text{Nd}[\text{pda}]_3$ .

Experiments using 2,6-pyridinedicarboxylic acid produced highly fluorescent precipitates which were crystalline in structure. These had limited application in the formation of doped silica or polymer spheres as they could not be dissolved in the preparation solutions. A variety of solvents were examined e.g. butanol, propanol, ether, chloroform, dichloromethane, but none were suitable. Water was the only solvent in which Lanthanide  $\text{X}[\text{pda}]$  dissolved; future investigation of  $\text{H}_2\text{O}$  based polymerisation reactions may yield a useable method.

### **3.9.2** *Chelate: Trifluoroacetone*

In to 50ml of Absolute Ethanol 0.5672 g of  $\text{EuCl}_3 \cdot 6\text{H}_2\text{O}$  was dissolved, to this solution Trifluoroacetone was added in a 3:1 molar ratio. No precipitate formed. TTA is a highly volatile liquid which made it difficult to work with. This was not carried forward for any further testing.

### **3.9.3** *Chelate: 1,10-Phenanthroline*

In 50 ml absolute ethanol 1.4180 g of  $\text{EuCl}_3 \cdot 6\text{H}_2\text{O}$  was dissolved, to which 1,10-phenanthroline (Aldrich, 99%, 131377-25G) was added in a 2:1 molar ratio. The solution was stirred for 60 minutes, during this time a heavy precipitate formed which was collection via filtration with a Whatman 0.2  $\mu\text{m}$  membrane filter. This was allowed to dry in a desiccator overnight before using to remove all ethanol.

Initial testing of  $\text{Eu}[\text{phen}]_2$  proved to be highly promising until it was discovered that 1,10-phenanthroline was destroyed by water. This would not only cause problems for the main compound, but also for doped spheres as they may come in contact with water and therefore have their fluorescence destroyed.

### **3.9.4** *Chelate: Thenolytrifluoroacetone*

In 50 ml of absolute ethanol 0.4163 g of  $\text{EuCl}_3 \cdot 6\text{H}_2\text{O}$  was dissolved, to which thenoyltrifluoroacetone (Aldrich, 99%, T27006-25G) was added in a 3:1 molar ratio. The solution was stirred for 60 minutes before removing the ethanol with a rotary film evaporator (RFE). This produced a sticky residue in the flask which was collected and placed in a desiccator to dry. The sample of  $\text{Eu}[\text{ttfa}]_3$  was again a promising sample, bright fluorescence but as it would not full dry it was difficult to accurately weigh for comparable doping levels.

### **3.9.5** *Chelate: Thenolytrifluoacetone and 1,10-Phenanthroline*

$\text{Eu}[\text{phen}]_2$  was prepared as the method previously described. To 50 ml of absolute ethanol 0.2 g of  $\text{Eu}[\text{phen}]_2$  was added, to which TTFA was added in a 1:1 molar ratio. The solution was stirred for 60 minutes during which time the initially cloudy  $\text{Eu}[\text{phen}]_2$  solution became clear with the addition of the TTFA. The solution was placed in a RFE where the majority of the ethanol was removed to leave a powder product. This was collected and placed in a desiccator to dry fully. The combination of 1,10-phenanthroline and thenoyltrifluoroacetone



moved the problems of each individually. The lanthanide chelate Eu[ttfa][phen] was a dry powder which was easy to weigh and also resistant to water.

### **3.10 Background Study Samples**

#### **3.10.1**      *Dye Tracers*

Fluorescein (Aldrich, 46955-500G-F) and Rhodamine 6G (Aldrich, R4127-100G) molecular dye samples were prepared with distilled water to produce a stock solution of concentration  $1 \times 10^{-4}$  M (Fluorescein, 0.0332 g in 1L; Rhodamine 6G, 0.0479 g in 1L) from which further dilutions to  $1 \times 10^{-5}$  M were made in 100 ml volumes.

The sample spectroscopic analysis was carried out using an Edinburgh Instruments FLS920P Spectrophotometer.

#### **3.10.2**      *Crude Oils*

Gullfaks and Brent crude oil samples were prepared in dichloromethane (Aldrich, 99.9%, 650463-1L), 0.1ml in 20ml and 5 $\mu$ l in 10ml for the background experiments.

All sample spectroscopic analysis was carried out using an Edinburgh Instruments FLS920P Spectrophotometer for the doped bulk glass samples, molecular dyes and oil samples.

### **3.11 Analytical Techniques**

All spectroscopic analysis was performed using an Edinburgh Instruments FLS920P Spectrometer, powder samples being analysed using the flat quartz cell mount and a Perkin Elmer LS50B Luminescence Spectrometer for analysis of doped bulk glass samples. Scanning Electron Microscopy imagery was carried out using a Leo S430 SEM with samples prepared using a Polaron CC7650 Carbon Coating Unit.

### **3.11.1**      *Fluorescence*

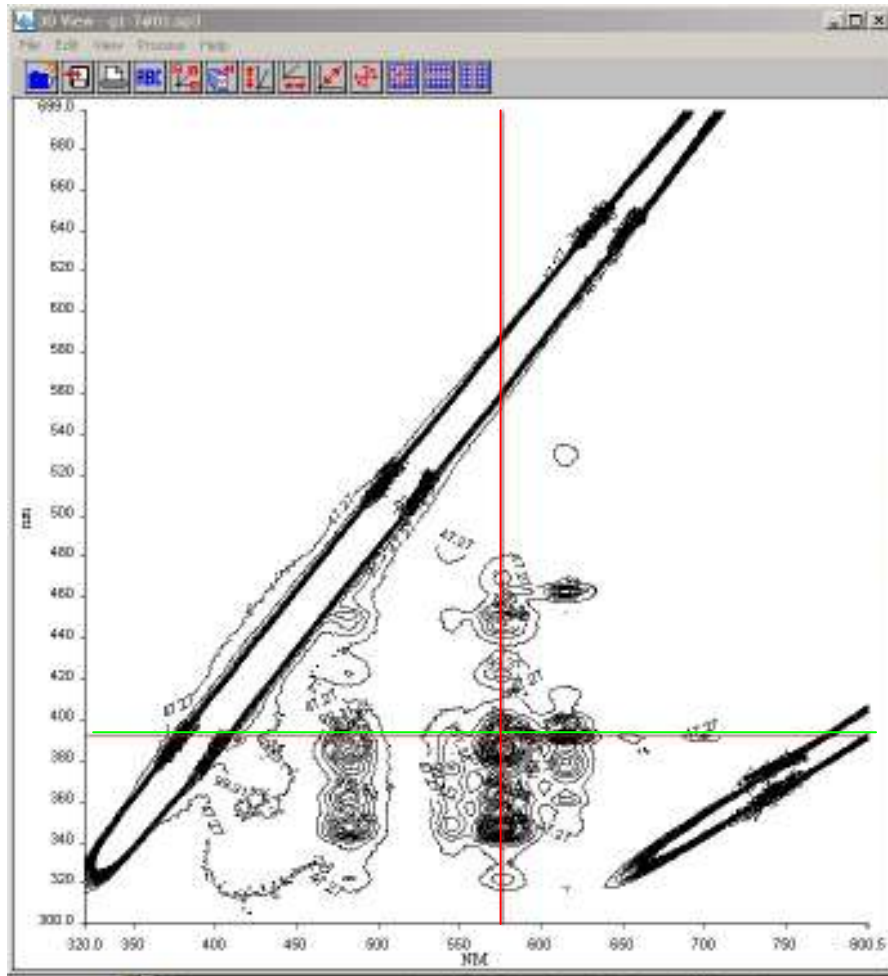
#### **3.11.1.1**    Perkin Elmer Lambda LS50B

All 3 dimensional spectroscopic analysis was performed using the Perkin Elmer LS50B with the FLWinlab software. The LS50B has a wavelength accuracy of +/- 1.0 nm and wavelength reproducibility is +/- 0.5 nm. The instrument settings can be seen in Table 15 and these settings were used to perform all 3D scan analysis of the 50 glass samples. This was done to allow direct comparison of all spectral emissions recorded from each sample, which would not be possible if the instrument settings were altered. Due to maintaining instrument settings there were some slight saturation for some of the Glass 2 samples. A standard 3 mol % europium sample was used as a standard to ensure the spectrometer was performing consistently through the analyses.

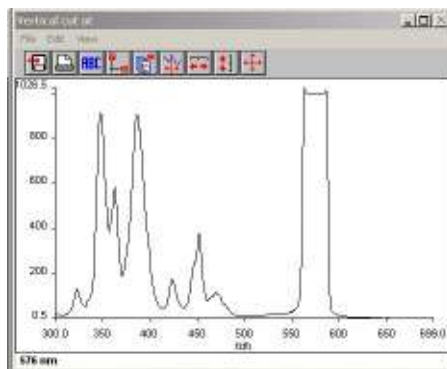
<b>Perkin Elmer LS50B - FLWinlab Settings</b>			
Excitation Setting	300 nm	Scan Speed	1500 nm/min
Wavelength Start	320 nm	Wavelength End	800 nm
Excitation Slit Width	7.5 nm	Emission Slit Width	9 nm
Number of Scans	400	Excitation Increment	1 nm

**Table 15 Instrument Settings for Perkin Elmer LS50B**

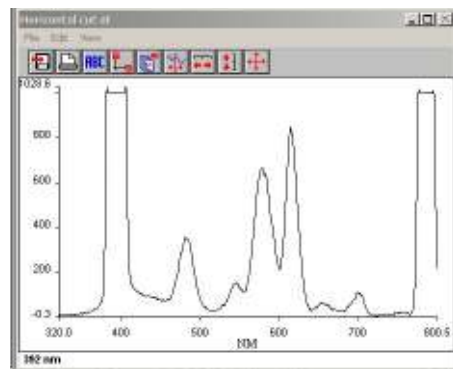
Using the 3D function of the spectrometer it is possible to produce a surface projection of fluorescence, which is an XYZ plot of intensity, emission and excitation. There is a large amount of information contained within this surface projection and the most accurate method of interrogation is to examine the contour plot.



(i)



(ii)



(iii)

**Figure 19 (i) Contour plot (ii) Excitation (vertical red line) and (iii) Emission (horizontal green line) spectra for Glass 1 sample 7**

Figure 19 (i) is an example of a typical contour plot of a doped glass sample, in this case Glass 1 sample 7. The red vertical and green horizontal lines represent the excitation and emission, the information from which can be seen in Figure 19

(ii) and (iii) respectively. Using this method of analysis allows a highly detailed investigation of all the absorption and fluorescence peaks which occur in a lanthanide ion.

The data table produced from the spectroscopic characterisation can be seen in Figure 28 - Figure 86.

### 3.11.1.2 Edinburgh Instruments FLS920P Spectrometer

For the spectroscopic analysis of glass, organic and inorganic polymers, an Edinburgh Instruments FLS920P Spectrometer was used. Initial analysis using the Perkin Elmer LS50B Spectrometer proved futile as the powder samples could only be analysed in a quartz 1 cm path cell. This cell requires a suspension of particles, and due to the scattering nature of particles and the low level of fluorescence from the glass, this proved impossible.

The Edinburgh Instruments FLS920P has 2 main sample cell fittings, one for a 1 cm path standard quartz cell or one for a powder cell, Figure 20. This allows for solid bulk glass sample analysis and powder analysis to be reproducibly undertaken.



**Figure 20 (a) powder sample cell in holder on mount, (b) glass sample in holder on mount**

Using the F900 software the configuration window, Figure 21, allows for the selection of detector and excitation source (Xenon flash lamp or micro second flash lamp) as well as the setting of excitation wavelength, emission wavelength and slit widths for both.

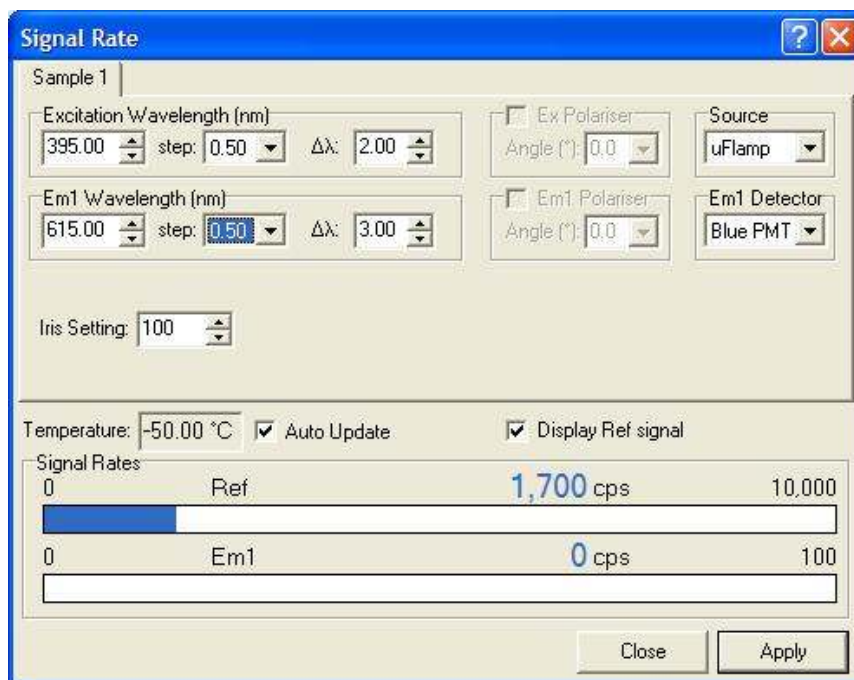


**Figure 21 Edinburgh Instruments FLS920P configuration interface**

The "Ref" counts bar visually displays the intensity of excitation light and the "Em1" counts bar displays the emission fluorescence intensity. After configuration of the Edinburgh Instruments FLS920P a fluorescence emission scan can be obtained, and example of which is shown in Figure 22 which shows the emission spectra for Europium doped glass from an excitation of 393 nm.

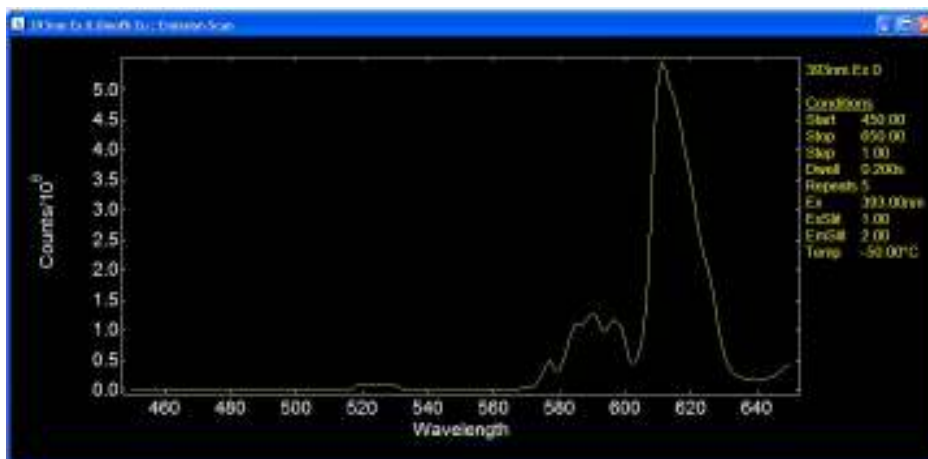


**Figure 22** Example of Europium emission spectra from an excitation of 393 nm

### 3.12 Fluorescent Lifetime Study

#### 3.12.1 Laser Induced Fluorescence Microscope

In order to obtain the fluorescent lifetimes, time resolved fluorescence studies of the lanthanide ions in the borosilicate glass were carried out. A Laser Induced Scanning Fluorescence Microscope (LISFM) was used and the experimental set-up is shown in Figure 23. The lanthanide doped glass samples were placed below a microscope objective.

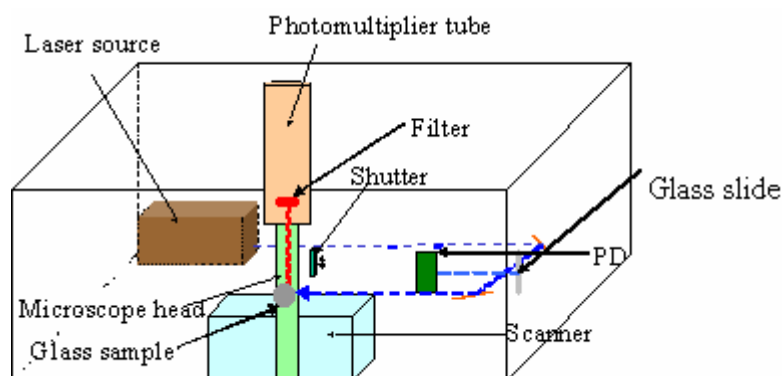


**Figure 23** Laser induced scanning fluorescence microscope setup for fluorescence lifetime study

Short laser pulses ( $\sim 5$  nsec with better than 1 nm wavelength resolution) at the optimum excitation wavelength, generated from an Continuum Nd:YAG OPO (Optical Parametric Oscillator) laser were used to excite the fluorescence from the rare-earth ion doped glass samples. The output wavelength of the laser was tuneable and was selected with the help of a Stellarnet EPP2000 Portable Spectrometer, 3.14.2.1. The temporal fluorescence intensity variations were detected using a high sensitivity photomultiplier tube. The fluorescence wavelength was selected by a set of filters placed in front of the detector. A photodiode in combination with a partially reflecting microscopic glass slide (10% reflectance typically) was used to monitor the laser pulses. A Tektronix TDS 380 400 MHz digital real-time oscilloscope which can sample at 2 gigasamples/s and has a resolution of 1 ns/div was used to view and record the signals from the photomultiplier tube.

### **3.13 Scanning Electron Microscopy**

Scanning electron microscopy was done using a Leo S430 instrument. Samples of powder were prepared by placing a small quantity on a carbon tab on an aluminium stub. The stub was then placed in a Polaron CC7650 carbon coating unit, which by coating the samples in fine graphite make them conductive for SEM analysis.

### **3.14 Detection System Development**

A prototype detection system to test the novel tracers for environmental tracing applications was constructed to be as simple as possible, comprising an excitation source, a delivery system and a detection method. The excitation source for the borosilicate glass tracer was a laser and the excitation source for the polymers was a UV lamp. The delivery system utilised optical fibre heads from a previous project which used the heads to monitor fluorescent dyes such as Rhodamine 6G and Fluorescein as well as particle tracers. The detection method used avalanche photodiode technology which allows greater sensitivity

than traditional photodiodes but without the cost, delicate nature and power limitations of photomultiplier tubes.

### **3.14.1**      *Optical Fibre Heads*

The delivery system optical fibre heads are constructed from high impact plastic. They consist of a two piece body and tail, the body containing two holes drilled at a 20° angle. The tail of the delivery head provides extra protection to the fibres to help prevent them snapping under applied force. Figure 24 shows the set up of the delivery head along with the orientation of the fibres (RS Components Twin Core polymer, 413-374).

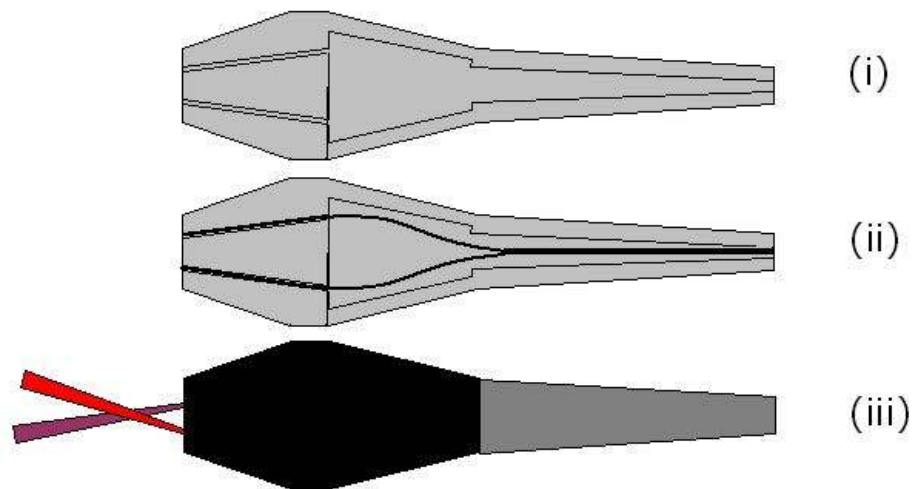


**Figure 24 Optical fibre head design, (i) showing a cut through example of layout, (ii) the position of the optical fibres and (iii) the complete head with an example of light path.**



<b>Fibre material</b>	PMMA (polymethylmethacrylate)
<b>Cladding material</b>	Fluorinated polymer
<b>Sheath</b>	Black PE
<b>Attenuation @ 660nm</b>	200dB/km
<b>Attenuation @ 820nm</b>	1500 dB/km
<b>Numerical aperture (NA)</b>	0.47
<b>Number of fibres</b>	1 or 2
<b>Fibre diameter</b>	1mm
<b>Tensile Strength</b>	5kg
<b>Temperature Range</b>	-30 to +85°C

**Table 16 Technical specification of twin core polymer fibres**

The use of twin core polymer fibre is suited to fluorescence detection work because of its larger diameter, 1mm, compared to more traditional glass optical fibres which generally have  $\mu\text{m}$  range diameters. Table 16 shows the specifications for the fibres used for this work.

### **3.14.2**      *Excitation Sources*

The possibility of using three different lanthanide ion hosts; borosilicate glass, organic and inorganic polymers, presents the need for two different excitation sources. The borosilicate glass based tracer utilises the lanthanide ion discrete narrow band absorption lines, which requires sources such as laser or filtered white light. The organic and inorganic polymers conversely, use the broadband UV absorption of the chelate molecule. This energy is then transferred to the lanthanide ion, which then exhibits stronger fluorescence than the uncomplexed ion.

### 3.14.2.1 Stellarnet Spectrometer

To determine the spectral emission from the Harma 500 W UV light source a Stellarnet Spectrometer was used, Figure 25 shows the spectral characteristics for this excitation source.

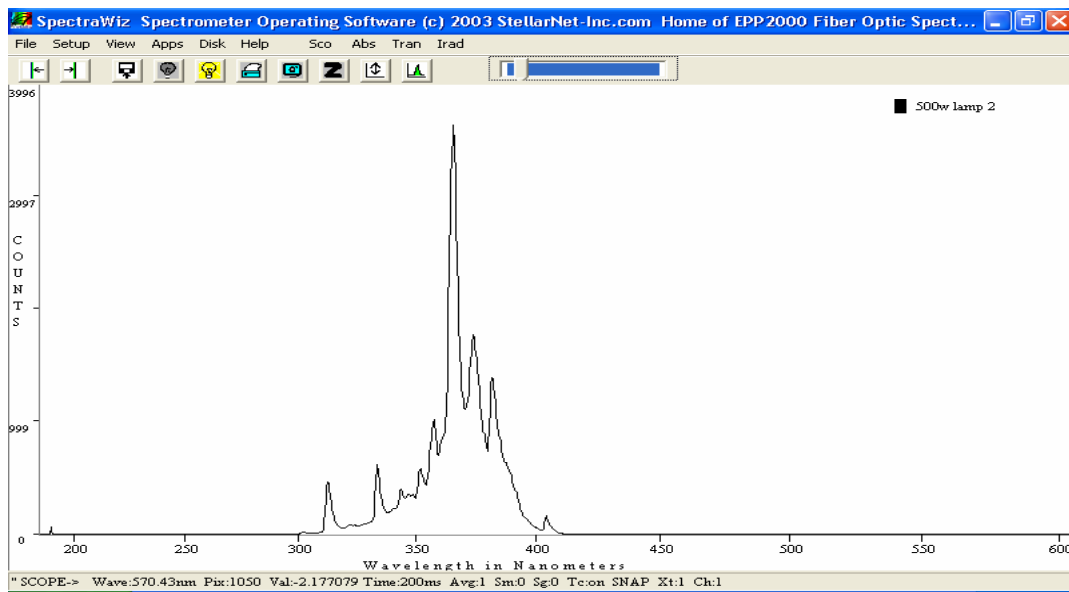


**Figure 25 Spectral output from Harma 500W UV lamp**

The Stellarnet spectrometer has an optical fibre connection which allows the unit to be used as an independent detection source.

## 4 RESULTS AND DISCUSSION

### 4.1 Concentration Studies with Spectral Characterisation

Initially 3 Dimensional spectra of the excitation and emission peaks of a range of single and multiple lanthanide doped glass tracers were recorded to indicate possible useful tracer peaks. Figure 26 shows the fluorescence spectrum of a blank, undoped sample of borosilicate glass which displays no emission or excitation peaks in the visible region, Figure 27.

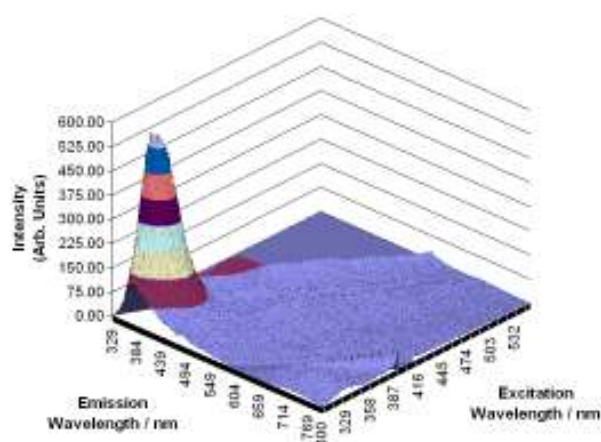


**Figure 26 Three Dimensional Fluorescence spectrum of a blank sample of glass 1**

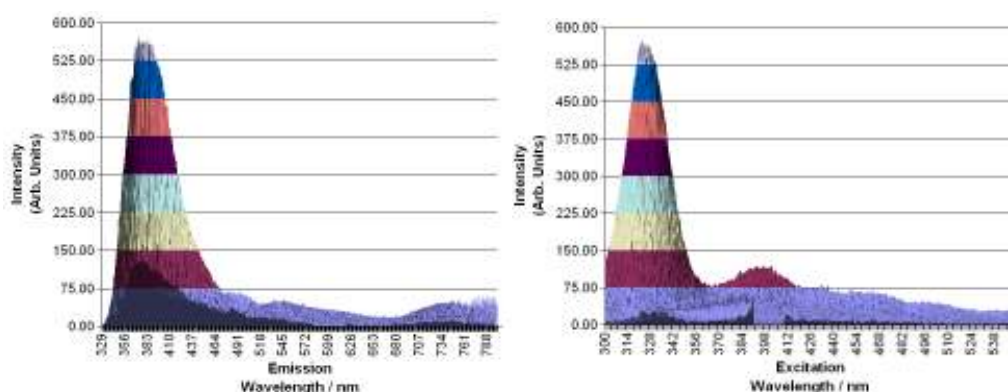


**Figure 27 Emission and Excitation spectra of a blank sample of glass 1**

The blank glass was then doped with a single lanthanide, either Europium, Dysprosium or Terbium ion over a range of concentrations. Tracer dopant studies were then carried out to investigate potential interactions between different concentrations of different dopants affecting the emission characteristics of the tracer and to investigate any quenching effects.

#### **4.1.1 Europium Spectral Characterisation and Single Doped Concentration Study**

Spectral characterisation of a europium doped glass sample can be achieved by detailed examination of the 3D spectra, Figure 28 and Figure 29, which shows all possible excitation (absorbance) and emission (fluorescence) wavelengths from a 0.8 mol% europium glass sample.

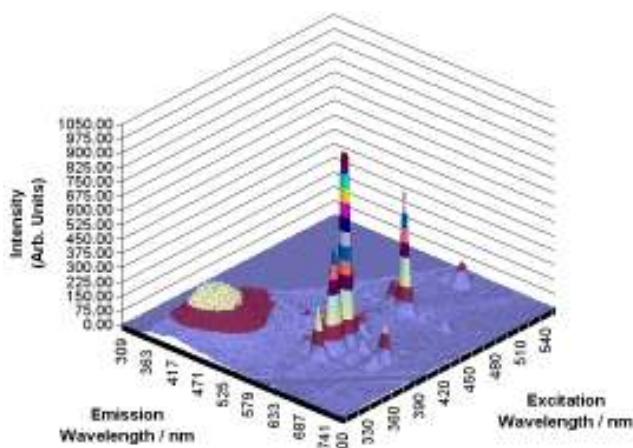


**Figure 28 3 Dimensional Fluorescence Spectrum of a 0.8 mol % europium sample**

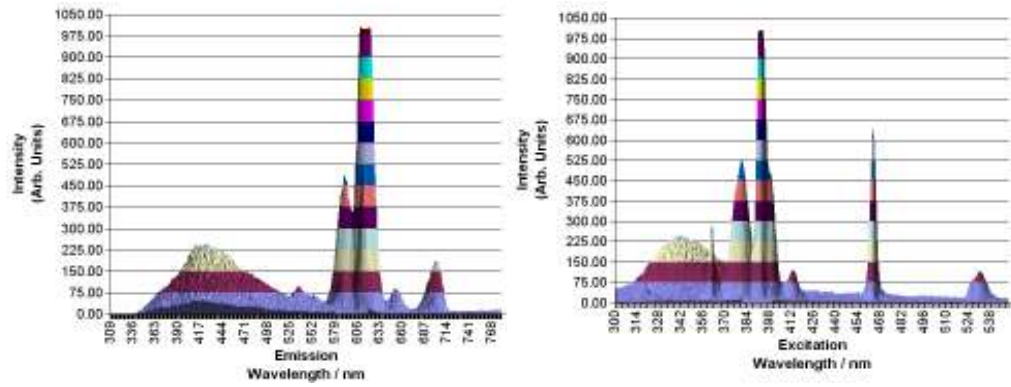


**Figure 29 Emission and Excitation Spectra of a 0.8 mol % europium sample**

From Figure 29 it is possible to determine the precise excitation and emission wavelengths. Table 17 displays the full spectroscopic characterisation for the 0.8 mol % europium doped glass sample, the most intense emission peak being 612 nm. The 7 excitation wavelengths selected for the concentration study are indicated by a (\*).

<b>Excitation Wavelength / nm</b>	<b>Emission Wavelength / nm</b>
362	591
362 *	612
362	654
381	592
381 *	612
381	653
382	702
387	535
393	591
393 *	612
393	702
395	635
412	591
412 *	612
412	635
412	702
444	535
463	592
463	652
463	702
465	535
465 *	612
526	652
531	590
531 *	612
531	702
579 *	616
579	704
580	651

**Table 17 Excitation and Emission wavelengths found in europium doped glass**

During more detailed analysis it was found that higher emission readings were obtained for a 612 nm emission, this was located when a more sensitive fluorescent spectrometer instrument with a high wavelength resolution was purchased.

Figure 30 shows the effect of altering the excitation wavelength on the 612 nm emission line intensity as the europium ion concentration is increased from a dopant level of 0.2 mol % to 2.0 mol %.

The two strongest excitation wavelengths producing a 612 nm emission are 393 nm and 465 nm. In the 0.2, 0.4, 0.6, 0.8, 1.0 and 1.2 mol % samples they all show a higher intensity from the 393 nm excitation compared to 465 nm. This trend changes for 1.4, 1.6, 1.8 and 2.0 mol % with the 465 nm excitation producing a stronger emission. The emission from the 2.0 mol% is 23 % higher with 465 nm than that of 393 nm.

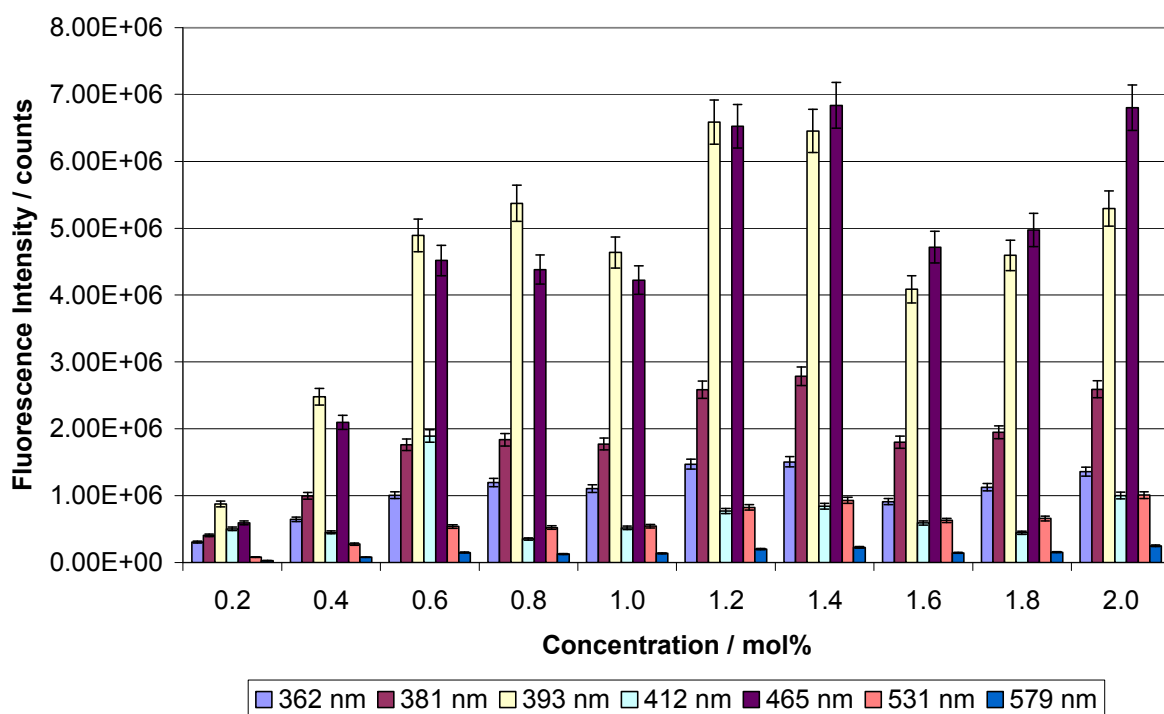


**Figure 30 Europium Emission Intensity at 612 nm from excitation at 362, 381, 393, 412, 465, 531 and 579 nm**

This study to compare one emission wavelength across a range of excitation wavelengths, at each concentration step of doping, found that the resulting emission intensities did not follow the expected trend of a concentration curve. This is possibly due to the density arrangement of the dopant ions within the

glass matrix. As the number of europium ions increase they displace network modifier sodium ions and their increased proximity allows for intra network discrete energy transfer to occur. It could also be due to concentration quenching or more unlikely in-homogeneity of the ions within the glass matrix. Concentration quenching would be unlikely as typically a concentration quench produces a negative effect on the observed fluorescence. An inhomogeneous mixture of the ions within the glass matrix is also unlikely as a separate set of experiments were carried out to determine the reproducibility of glass fabrication methods, taking into account human error and mistakes. These results can be seen in Section 4.2 which clearly shows that there is very little variation over a range of 5 samples producing an experimental error of 6 %.

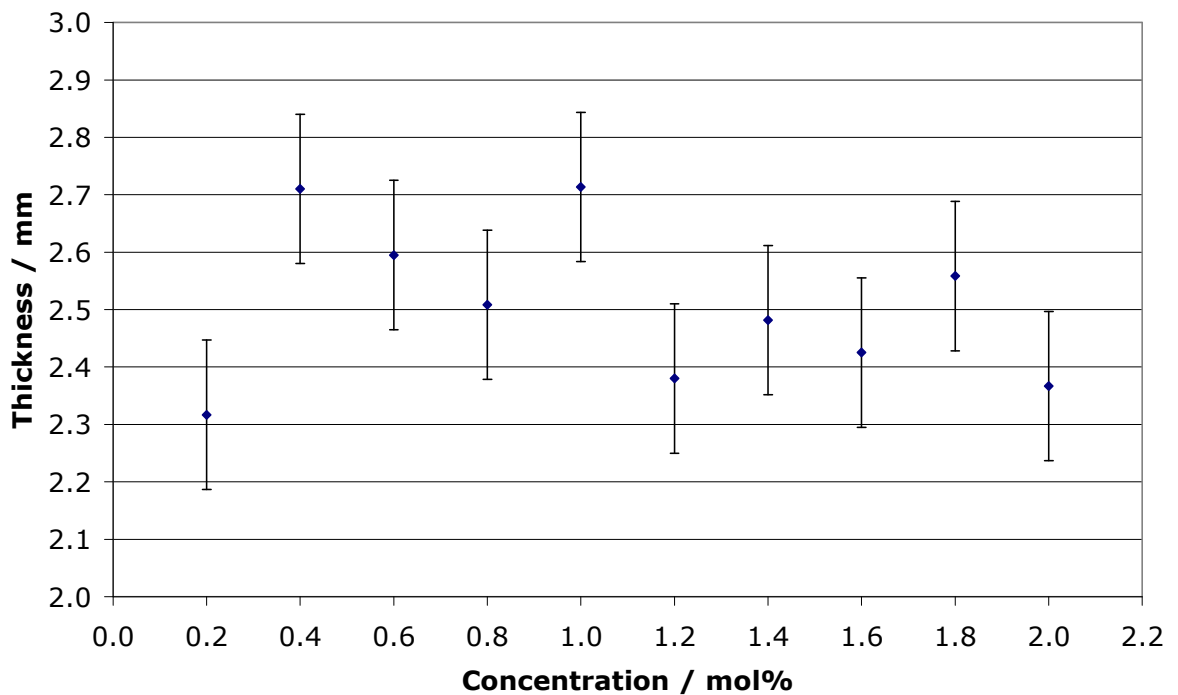


**Figure 31 Thickness variation of Europium glass samples across the concentration range.**

Another possible cause of the concentration trend observed could be due to sample thickness variation during fabrication. As the time between the crucible leaving the furnace, the glass pour and the quench can vary from sample to sample it means the temperature of the glass when it is quenched can also vary.



This variation effects viscosity dramatically with a temperature drop of 200-300 °C, which in turn will influence how easy it is to form each glass sample. To determine the effect of thickness variation on the concentration range, the thickness of each sample was measured in 6 places, Figure 32. The average of this is shown in Figure 31, the trend observed confirms that the variation of thickness has no effect on the fluorescent emission wavelength observed, with a standard deviation of 0.13 mm.



**Figure 32 Glass sample thickness variation measurement placement**

### 4.1.2 Dysprosium Spectral Characterisation and Single Doped Concentration Study

The same investigation has been repeated for dysprosium doped glass samples as shown in Figure 33 and Figure 34.

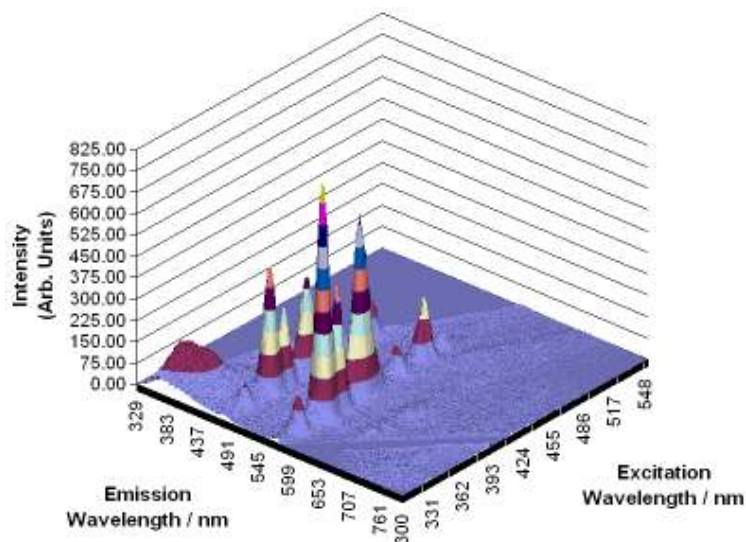


**Figure 33 Three Dimensional Fluorescence Spectrum of a 0.6 mol % dysprosium sample**

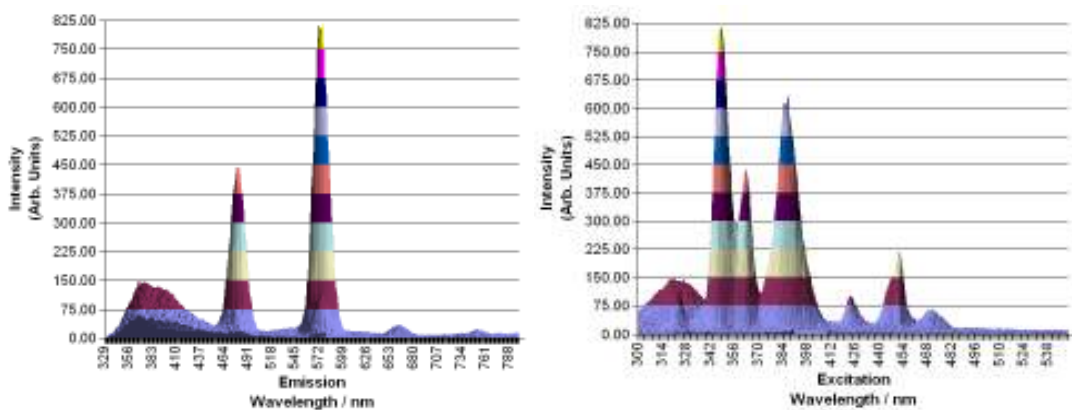


**Figure 34 Emission and Excitation Spectra of a 0.6 mol % dysprosium sample**

As previously discussed it is possible to determine the precise excitation and emission wavelengths from 3D characterisation, Table 18 displays the full spectroscopic characterisation for the 0.6 mol % dysprosium doped glass sample. The excitation wavelengths selected for the concentration study are indicated by a (\*) leading to emission at 481 nm) and (\*\* leading to emission at 575 nm).

<b>Excitation Wavelength / nm</b>	<b>Emission Wavelength / nm</b>
324 **	575
325 *	481
352 *	481
352 **	575
352	662
364 *	481
364 **	575
365	665
391 *	481
391 **	575
391	665
391	752
425	758
426 *	481
426 **	575
426	664
451	758
452 *	481
452 **	575
452	669
470 **	575
471 *	481
471	756

**Table 18 Excitation and Emission wavelengths of dysprosium doped glass**

The spectral excitation and emission detail observed for the lines in dysprosium doped borosilicate glass has shown that the 481 nm and 575 nm emission peaks have the most potential for use as a tracer because of their intensity and separation from the emission lines of europium. The combination of these two factors, allow greater sensitivity and selectivity for potential tracers.

From the spectroscopic analysis of the 0.2 – 2.0 mol% dysprosium doped borosilicate glass Figure 35 displays the emission intensity at 481 nm from each of the following excitation wavelengths 324, 352, 364, 391, 426, 452 and 471 nm. It can be seen that the most intense spectral output was obtained from the 391 nm excitation wavelength with a dysprosium concentration 0.8 mol %. Further analysis of the 0.2 – 2.0 mol% dysprosium doped borosilicate glass was carried out with the other suitable emission peaks at 575 nm.

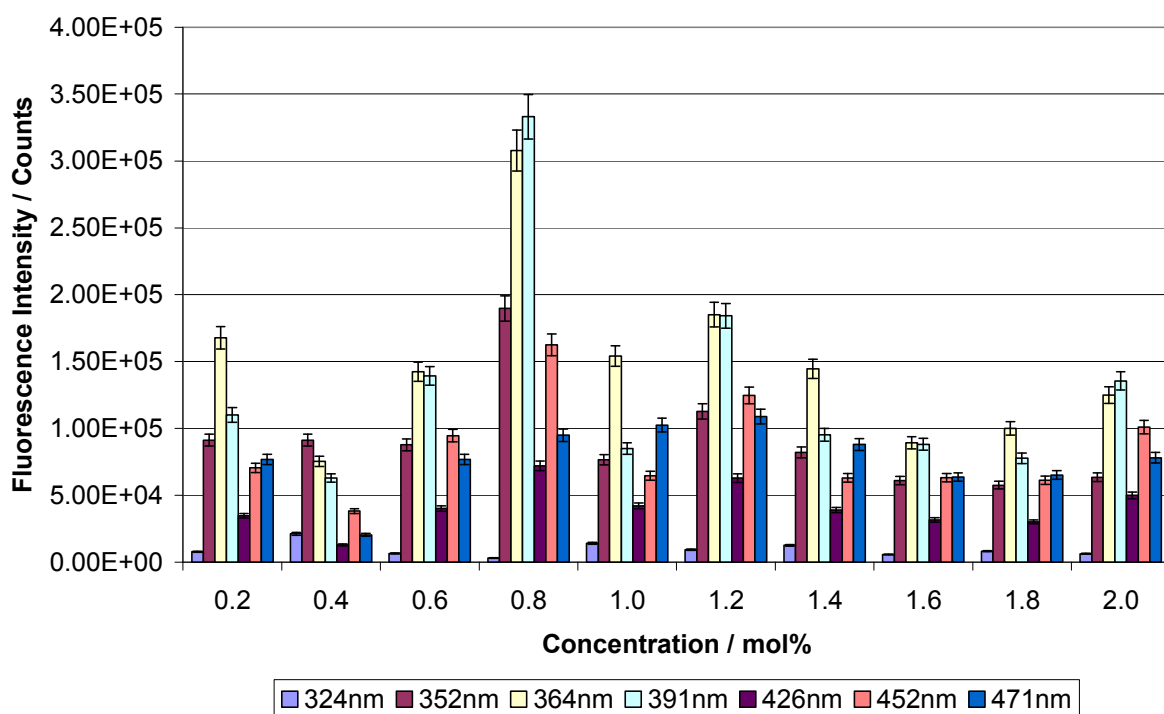


**Figure 35 Dysprosium Emission Intensity at 481 nm from excitation at 324, 352, 354, 391, 426, 452 and 471 nm**

It can be seen in Figure 36 that the most intense spectral emission output was obtained from the 0.8 mol % sample with the 391 nm excitation wavelength. However, comparing Figure 35 and Figure 36 overall the intensity (706,500) of the 575 nm emission peak excited at 391 nm exceeded the best intensity (330,000) of the 481 nm emission peak excited at 391 nm. These experiments have shown that the optimum sensitivity is achieved with an emission of 575 nm

from an excitation of 391 nm. It also shows that the dopant concentration versus emission intensity is different for different excitation wavelengths. Both the 481 nm and 575 nm excitation wavelengths produced a similar trend of fluorescent emission, peaking at 0.8 mol %.

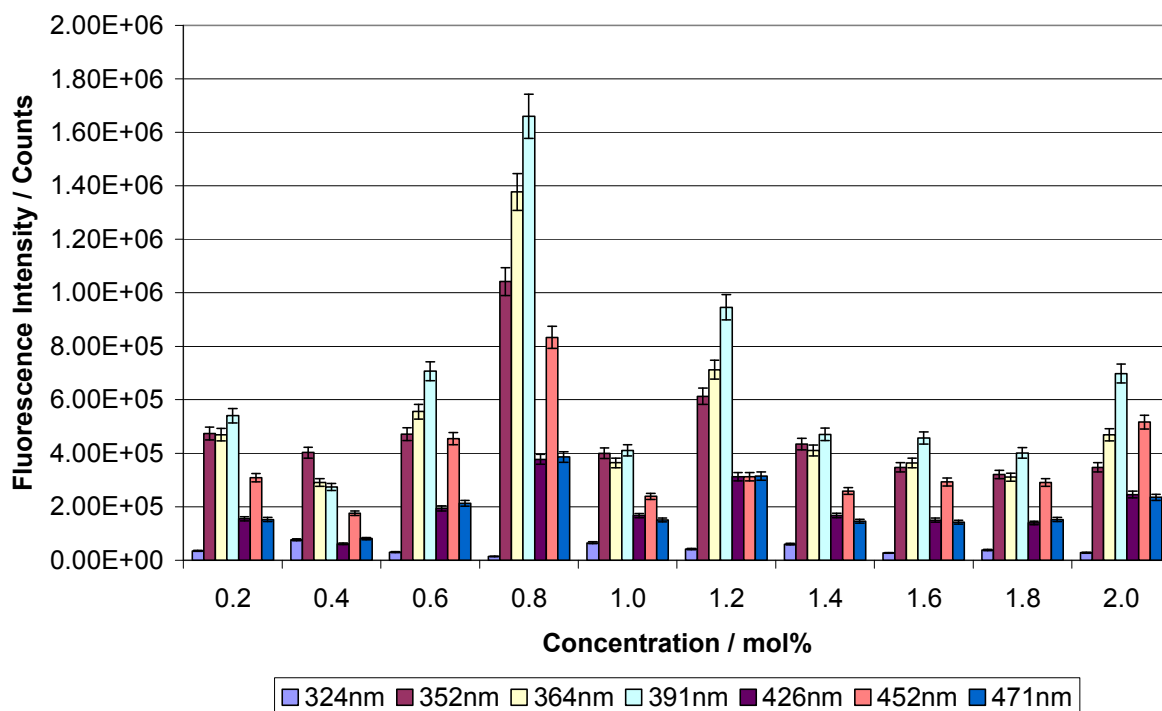


**Figure 36 Dysprosium Emission Intensity at 575 nm from excitation at 324, 352, 354, 391, 426, 452 and 471 nm**

Again from this study the comparison of emission wavelengths across a range of excitation wavelengths shows that the resulting emission intensities did not follow the expected trend of a concentration curve. This is possibly due to the density of the dopant ions within the glass matrix, where as the number of dysprosium ions increase they displace network modifier Sodium ions and their increased proximity allows for intra network discrete energy transfer to occur. As previously shown it is unlikely that the observed variation comes from inhomogeneity in the fabrication process, the reproducibility study shows

conclusively the minimal error, and therefore signal variation, incurred during fabrication.

As with the europium samples another possible cause of the concentration trend observed could be due to sample thickness variation during fabrication. This could have been the case with the 0.8 mol % sample, where the dominant 391 nm excitation creates over twice the intensity of the corresponding wavelength from the 0.6 mol % sample and over 4 times the intensity of the 1.0 mol % sample. To determine the effect of thickness variation on the concentration range, the thickness of each sample was measured 6 times with a standard deviation of 0.13 mm.

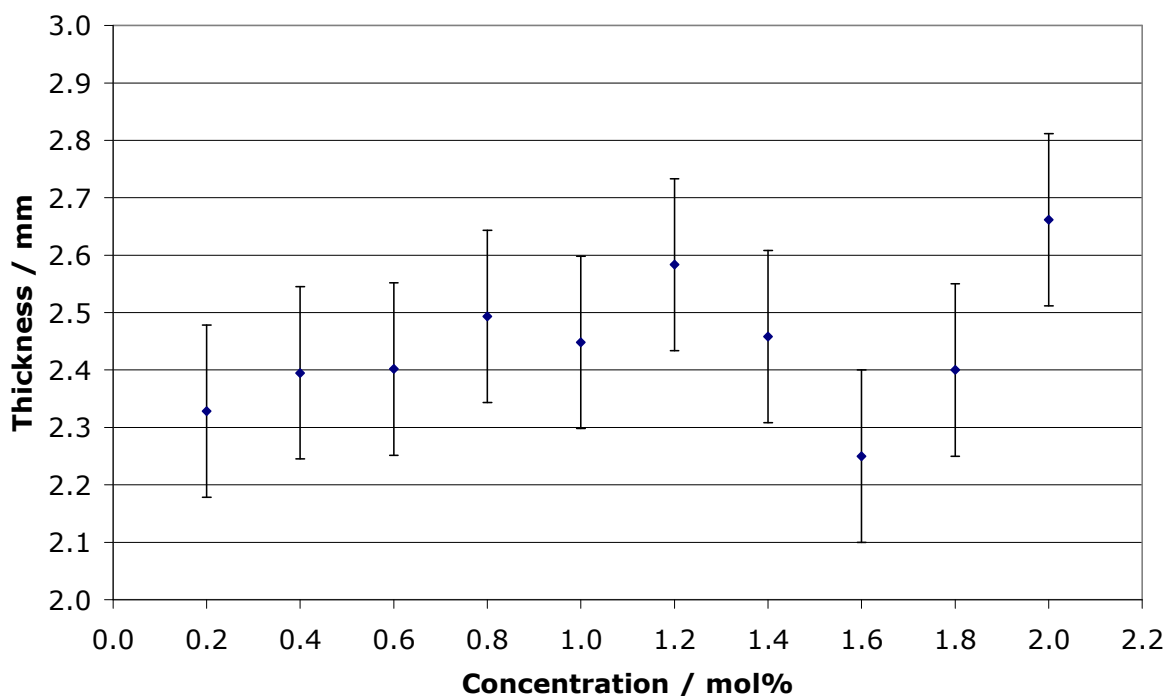


**Figure 37 Thickness variation of dysprosium glass samples across the concentration range.**

The averages of these measurements are shown in Figure 37, the trend observed confirms that the variation of thickness has no effect on the fluorescent emission observed. If it had been, it would be expected that the 0.8 mol % sample was the thickest, this was not the case.

### 4.1.3 Terbium Spectral Characterisation and Single Doped Concentration Study

The same experiment has been repeated for terbium doped glass samples.

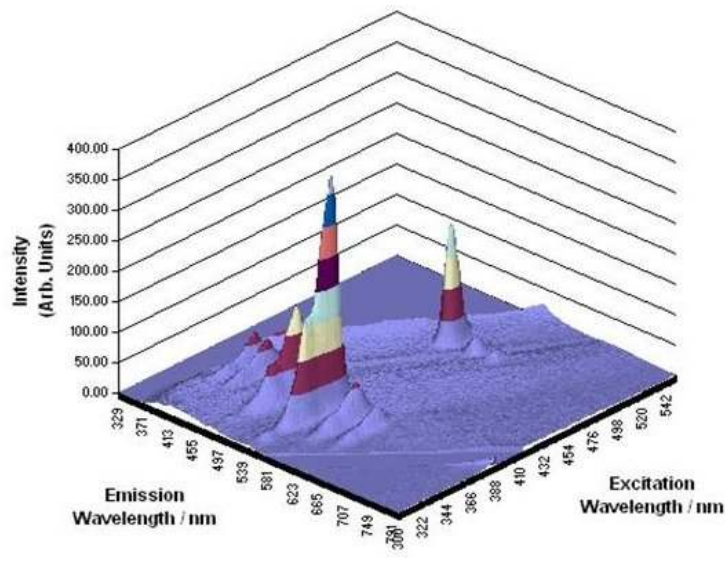


**Figure 38 Three Dimensional Fluorescence Spectrum of a 1.0 mol % terbium sample**

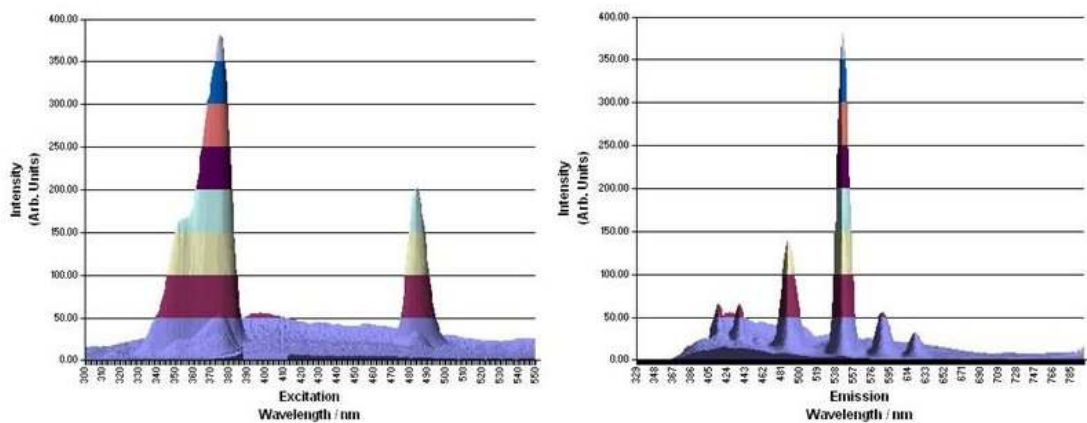


**Figure 39 Emission and Excitation Spectra of a 1.0 mol % terbium sample**

As previously reported the precise excitation and emission wavelengths can be obtained from 3D characterisation, Table 19 displays the full spectroscopic characterisation for the 1.0 mol % terbium doped glass sample which was found from Figure 38 and Figure 39. The excitation wavelengths selected for the

concentration study are indicated by a (\*).

Excitation Wavelength / nm	Emission Wavelength /nm
352	588
352	488
352 *	542
354	622
359	385
375 *	542
375	588
376	415
376	438
376	488
377	622
379	458
483 *	542
483	588
483	622

**Table 19 Excitation and Emission wavelengths of terbium doped glass**

The spectral excitation and emission detail for the most intense excitation and emission lines in terbium doped borosilicate glass have shown that the 542 nm emission line has the most potential for use as a tracer. This is because the 542 nm emission peak is easily resolved in combination with dysprosium and europium in a multi ion tracer. This allows greater sensitivity and selectivity.

From spectroscopic analysis of the 0.2 – 2.0 mol % terbium doped borosilicate glass Figure 40 displays the emission intensities at 542 nm from 352, 375 and 483 nm excitations. It can be seen that the most intense spectral output was obtained from the 1.8 mol % sample with a 375 nm excitation.



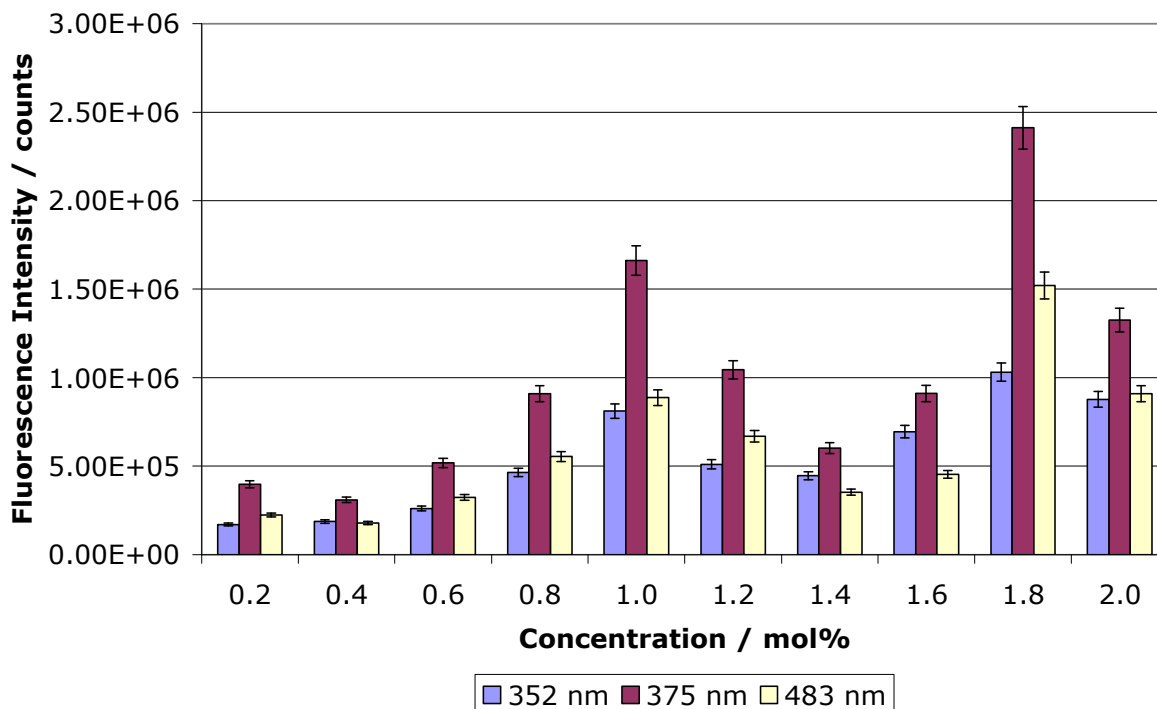


**Figure 40 Terbium Emission Intensity at 542 nm from excitation at 352, 375 and 483 nm**

Again in this study the comparison of emission wavelengths across a range of excitation wavelengths found that the resulting emission intensities did not follow the expected trend of a concentration curve. This is possibly due to the density of the dopant ions within the glass matrix, where as the number of terbium ions increase they displace network modifier sodium ions and their increased proximity allows for intra network discrete energy transfer to occur. As previously shown it is unlikely that the observed variation comes from inhomogeneity in the fabrication process, the reproducibility study shows conclusively the minimal error, and therefore signal variation, incurred during fabrication.

As with the europium and dysprosium samples another possible cause of the concentration trend observed could be due to sample thickness variation during fabrication. This could have been the case with the 1.8 mol % sample, where the dominant 375 nm excitation creates over twice the intensity of the corresponding wavelength from the 1.6 mol % and 2.0 mol % sample. To

determine the effect of thickness variation on the concentration range, the thickness of each sample was measured 6 times with a standard deviation of 0.15 mm.

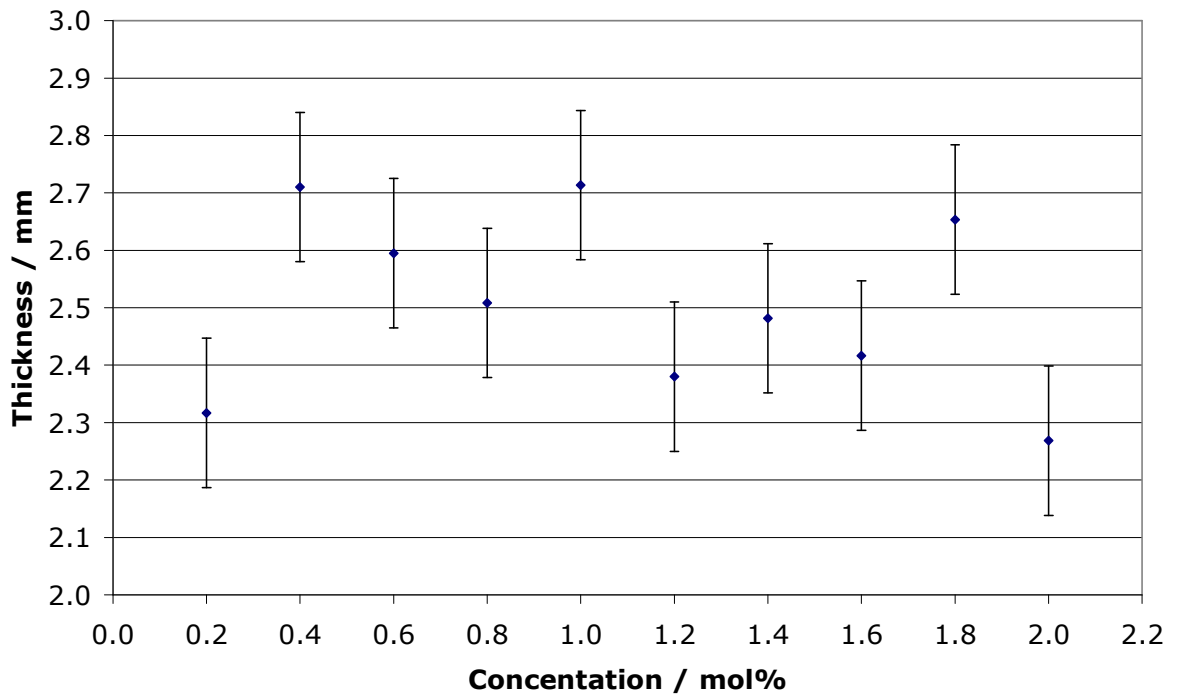


**Figure 41 Thickness variation of terbium glass samples across the concentration range.**

The averages of these measurements are shown in Figure 41, the trend observed confirms that the variation of thickness has no effect on the fluorescent emission observed. If it had been, it would be expected that the 1.8 mol % sample was the thickest, this was not the case.

## **4.2 Investigation of the Fabrication Process**

The glass fabrication process is an area where many errors can be introduced which could strongly influence the spectral characteristics of the doped glasses. It was determined that the most robust way to assess the influence of all the “human error” factors concerning glass fabrication was to undertake a reproducibility study. During this assessment it was proposed to examine the influence of furnace pouring temperature, time held at this temperature, annealing temperature and the annealing time.

### **4.2.1 Reproducibility Study**

To determine the reproducibility of the doped glasses, a study of the fabrication process was undertaken. For this, five Glass 1 samples doped with 3 mol % europium were manufactured using the cast and quench method, then analysed using fluorescence spectroscopy and lifetime analysis.

3D fluorescence analysis was carried out using the same experimental parameters as for the single and multiple doped samples. From the resultant spectral characterisation analysis of the europium doped samples, a strong absorption peak at 465nm with an emission peak at 615nm was observed. Each sample was then analysed with those parameters to produce single line spectra, Figure 42, which illustrates the reproducibility of the spectral fluorescence for the 3 mol % europium doped glass.

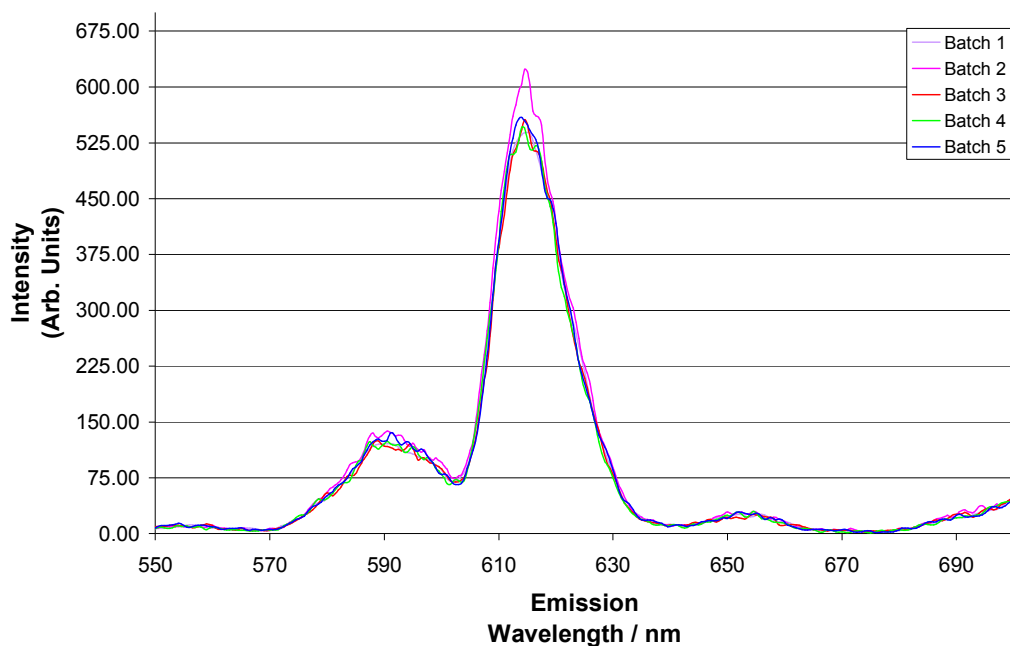


**Figure 42 Single line europium emission spectra from 3 mol % doped samples (Ex 465 nm, Em 615 nm)**

With potential errors coming from the human factor during the weighing, ball milling and dry component powder transfer to the crucible, plus the potential variables from the glass pour with cast and quench, it can be seen that the 5 batches produced exhibited very similar emission spectra. The standard deviation of the intensity of the 615 nm emission wavelength was 6 %, with the peak wavelength position variation of  $\pm 1$  nm.

The fluorescent lifetimes of the 3 mol % europium doped glasses were analysed using a modified LISFM system. Figure 43 shows that for the first three batches, the lifetime reproducibility was 2.15 ms and for batches 4 and 5 the lifetime was 2.2 ms. The average for the five batches was 2.17 ms. The maximum variation from the average was  $\pm 1.3$  %.

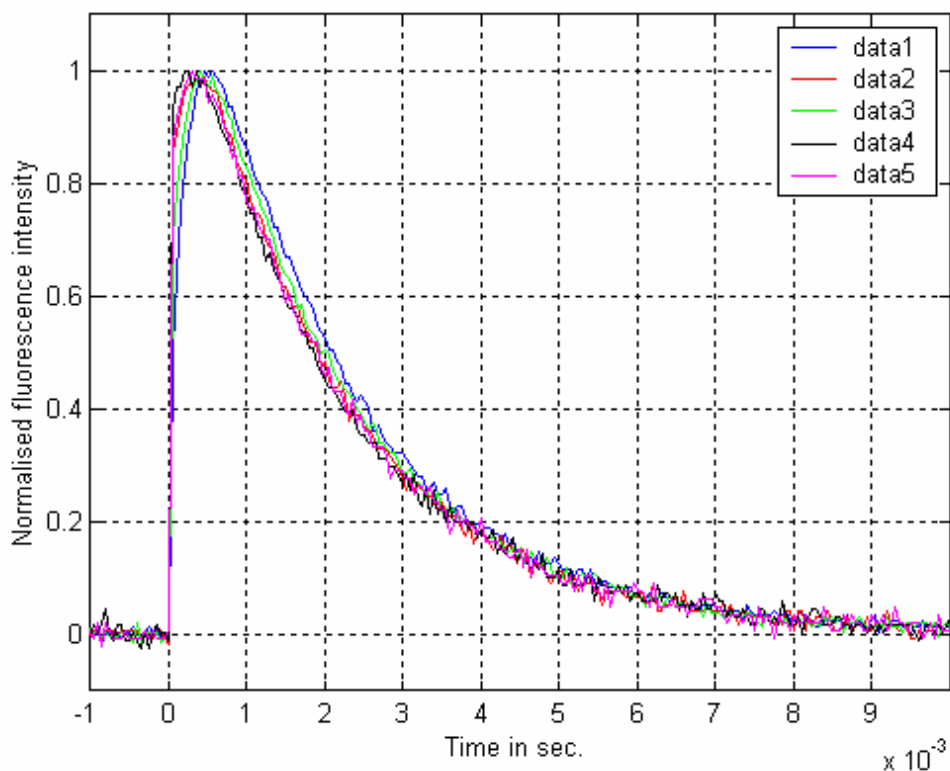


**Figure 43 Fluorescence lifetime profiles of 3 mol % europium glasses**

#### **4.2.2 Investigation of Varying Fabrication Parameters**

Leading on from determining the reproducibility of the fabrication process, it was proposed to investigate the effects of altering the fabrication parameters on the fluorescence emission characteristics and fluorescence lifetime of the glass 1 matrix. Using experimental design a series of experiments were planned with 4 factors (parameters), Table 20 shows the experimental parameters with the variables A – furnace temperature, B –furnace time, C – annealing temperature and D – annealing time. For each of the Experiments 1-8 the excitation wavelength, the emission wavelength, the emission peak intensity and the fluorescent lifetime were measured to allow full characterisation of the effect of the fabrication parameters. For this set of experiments single doped 1 mol % dysprosium samples were prepared, this was purely down to economics as europium is the most expensive of the lanthanide salts.

<b>Experiment</b>	<b>A / °C</b>	<b>B / min</b>	<b>C / °C</b>	<b>D / min</b>
<b>1</b>	1300	15	450	30
<b>2</b>	1300	60	450	60
<b>3</b>	1200	60	350	60
<b>4</b>	1200	15	450	60
<b>5</b>	1200	60	450	30
<b>6</b>	1300	15	350	30
<b>7</b>	1300	60	350	30
<b>8</b>	1200	15	350	30

**Table 20 Experimental parameter changes in furnace temperature and time, and annealing temperature and time**

The plot of 577 nm emission intensity from each dysprosium sample is shown in Figure 44, which clearly indicates that there is no significant change in emission intensity with the alteration of fabrication parameters.

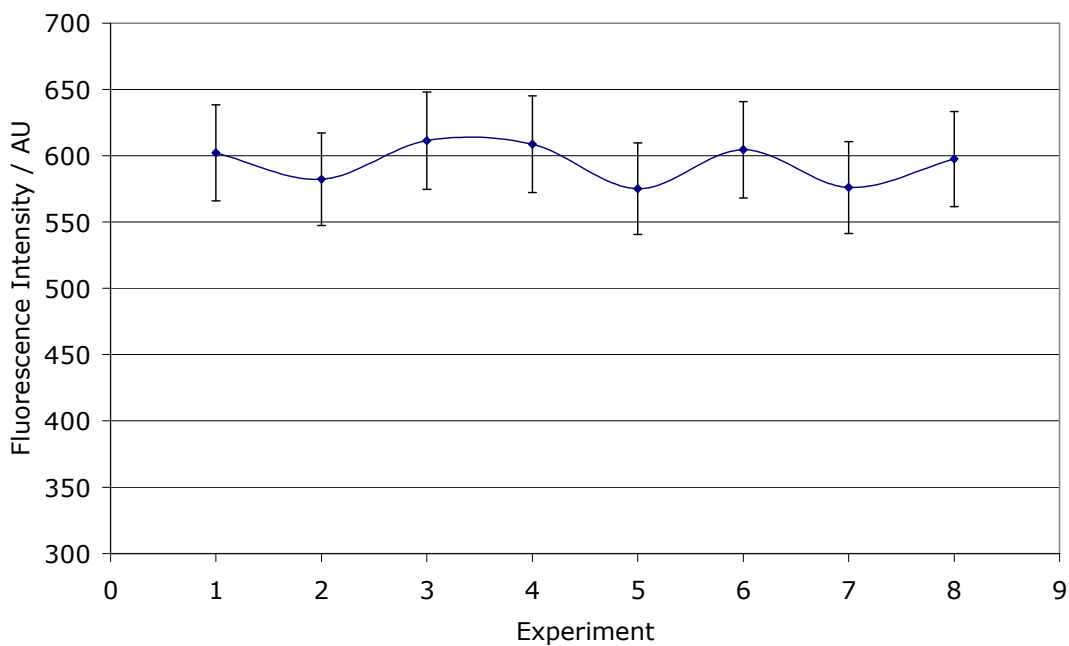


**Figure 44 Variation of peak emission intensity at 577 nm for 1 mol % dysprosium as the fabrication processes are changed**

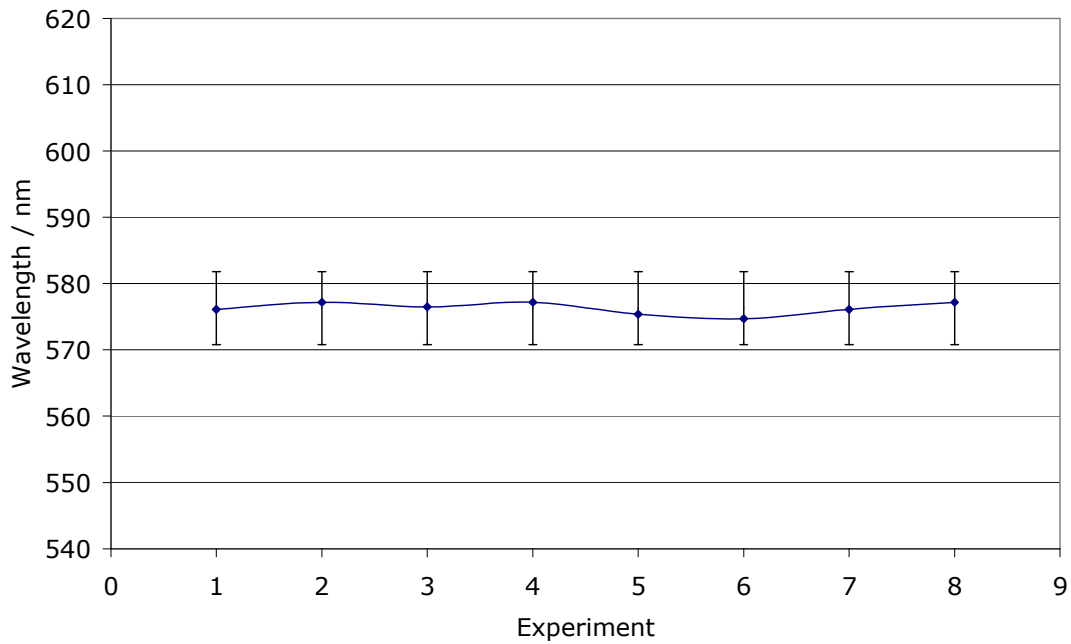


**Figure 45 Variation of the 577 nm emission peak wavelength from 1 mol % dysprosium as the fabrication processes are changed**

A similar plot for the 452 nm excitation wavelength of dysprosium was found, Figure 47, which again shows there is no significant difference caused by varying temperatures and times. The 577 nm emission wavelength and the fluorescent lifetime are shown in Figure 45 and Figure 46 respectively, which further confirms no significant effect from the fabrication parameter variations.

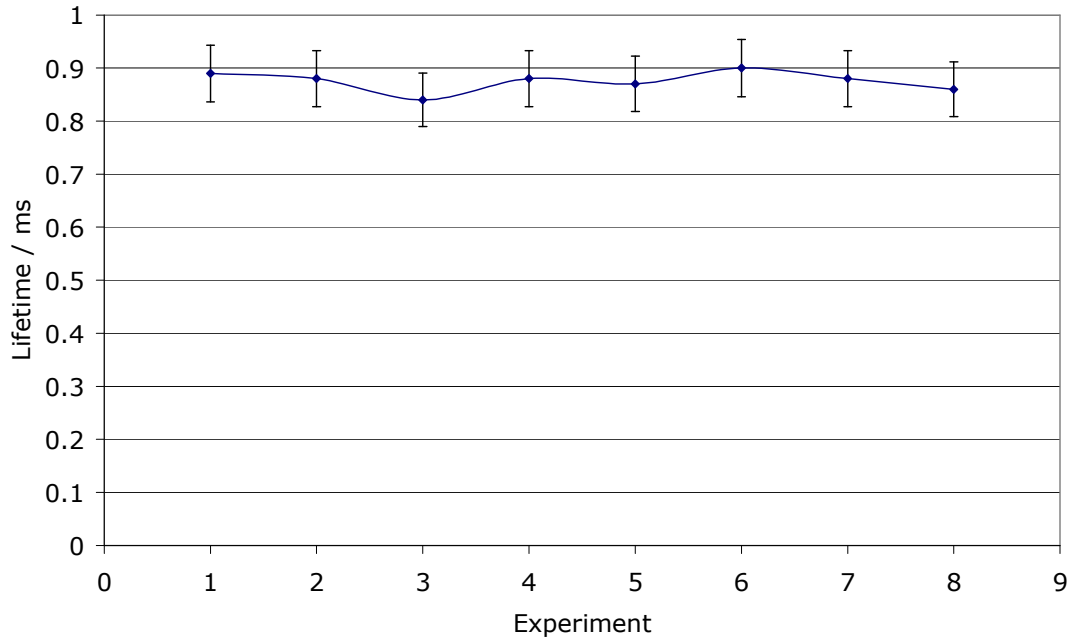


**Figure 46 Lifetime Variation with Experiment of the 577 nm dysprosium emission peak as the fabrication processes are changed**

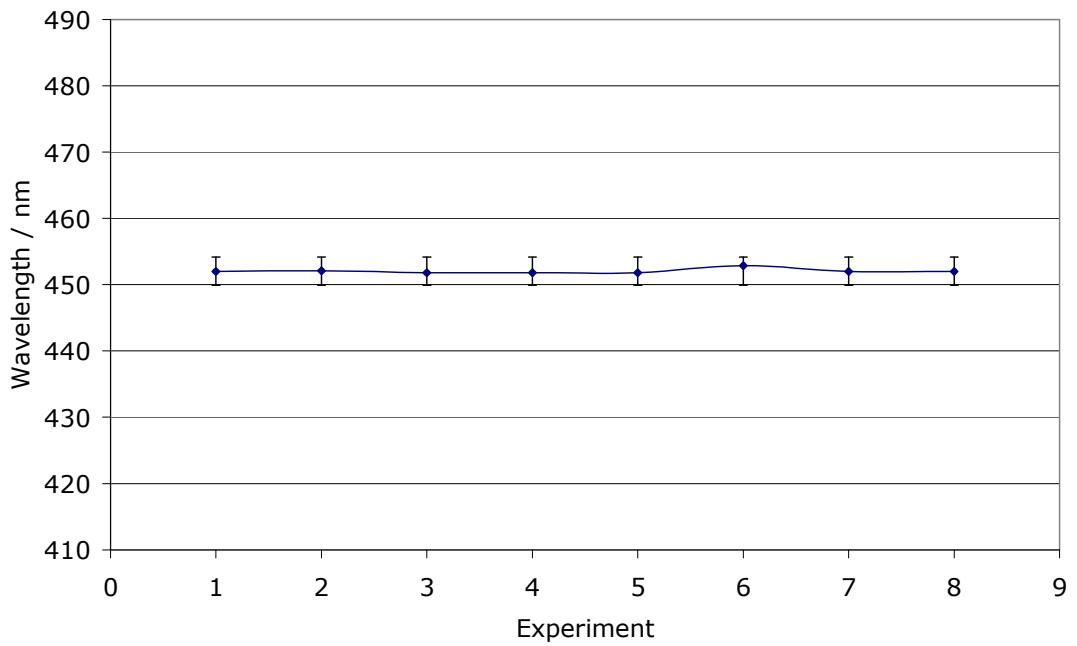


**Figure 47 Variation of the 452 nm excitation wavelength from 1 mol % dysprosium as the fabrication processes are changed**



For all figures, any variation in the values is within the expected experimental error. The results are summarised in Table 21.

<b>Experiment</b>	<b>Excitation /nm</b>	<b>Emission / nm</b>	<b>Normalised Peak Intensity</b>	<b>Lifetime /ms</b>
1	452	576	602	0.8933
2	452	577	582	0.88
3	451	576	611.	0.84
4	451	577	608	0.88
5	451	575	575	0.8733
6	452	574	604	0.9
7	452	576	576	0.88
8	452	577	597	0.86

**Table 21 Spectral Characteristics for Experiments 1-8**

### **4.2.3 Fabrication Process Conclusion**

#### **4.2.3.1 Reproducibility**

The results obtained for the reproducibility study confirmed the incredibly low “human error” losses incurred during the physical preparation of the samples. Given the weighing, balling milling, sample powder transferred to crucible, pouring and quenching all possible points at which to introduce great variation and error, to achieve a sample error of 6 % is very good. This gives great confidence in the results obtained from the glass samples, as the variations in signal observed can be judged as genuine spectral characteristics of the lanthanide ions within the glass.

#### **4.2.3.2 Parameter Variation**

The values for furnace and annealing temperature and also the furnace and annealing time were chosen using phase diagrams, Chapter 2 Section 2.4. The high and low levels were chosen with the expectation that successful glass

samples could still be produced. An entirely different result might have been observed if for example an annealing temperature had been chosen which was greater than the glass transition temperature of borosilicate, 650 °C. The wrong choice of fabrication parameters would probably have resulted in the production of a partially crystalline sample and an entirely different spectral response would have occurred.

The results obtained confirm that within the range of parameters selected, in this work, they can be used as the guide for the manufacturing limits. Within these limits the spectral responses of the glasses are controlled by the concentration of the lanthanide ion and the composition of the host glass matrix and not by changes in the fabrication parameters. It means that variations in manufacture will not influence the monitored fluorescent emissions and lifetimes. This is vital information, however, for the large scale production of glass as an environmental tracer it will probably be necessary to take samples to check the responses to ensure homogeneous results are obtained for the scaled up batches.

### 4.3 Multiple Ion Doped Glass Characterisation and Concentration Study in Borosilicate Glass 1

To investigate the potential effects of multi-ion doping, a range of 25 samples were prepared. The main advantage of using multi-ion doping is the added benefit of an increased number of “coded” tracers, which for example could be “coded” for a specific discharge sources or effluent streams. Figure 48 shows a europium, terbium and dysprosium triple doped tracer with dopant concentrations of 1 mol % europium, 1 mol % terbium and 1.5 mol % dysprosium (sample no.7 from Table 10).

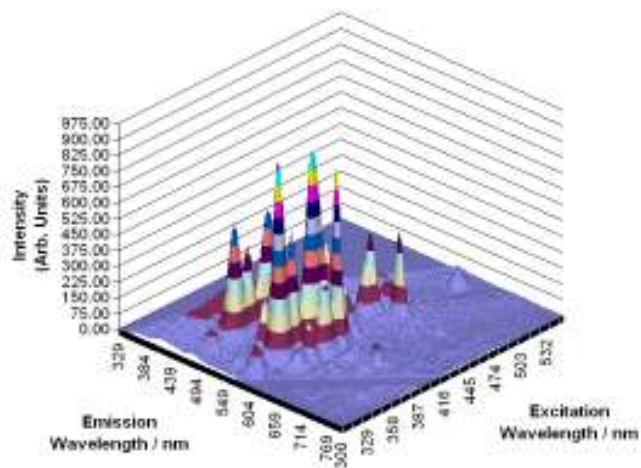


Figure 48 Europium, terbium and dysprosium Triple doped tracer

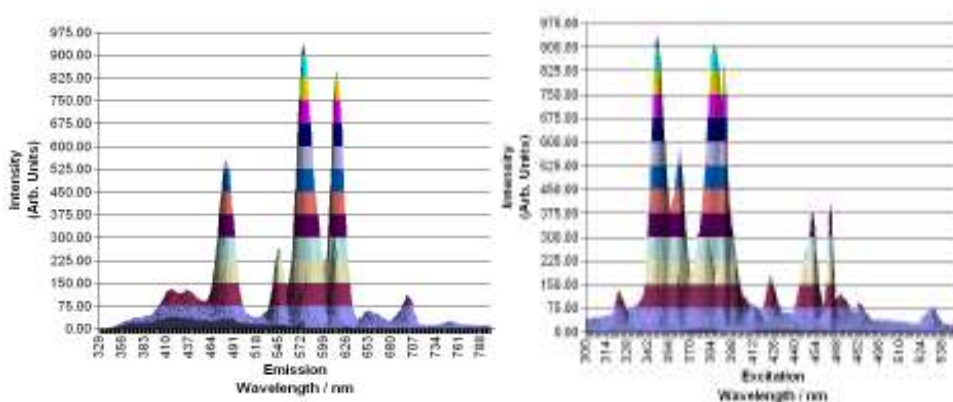


Figure 49 Emission and excitation spectra of a europium, terbium and dysprosium triple doped tracer

Tracer dopant concentration studies were carried out to investigate potential interactions between different dopant ions, which may affect the emission characteristics of the tracer through energy transfer.

Excitation Wavelength / nm	Emission Wavelength / nm	Intensity	Peak width					
			Ex Wavelength			Em Wavelength		
			From	To	PW	From	To	PW
324	482	102.65	313.0	329.0	16.0	461.0	505.0	44.0
348	481.5	559.35	335.0	357.0	22.0	457.5	505.0	47.5
363	483	414.65	357.0	371.0	14.0	459.0	501.0	42.0
387	483	525.60	371.0	409.0	38.0	459.0	505.0	46.0
424	481.5	104.01	416.0	430.0	14.0	461.0	499.0	38.0
452	483.5	239.50	438.0	458.0	20.0	472.5	507.0	34.5
322	545.5	46.83	310.0	330.0	20.0	545.5	554.5	9.0
348	545.5	241.58	332.0	357.0	25.0	531.5	556.5	25.0
365	545	219.26	359.0	370.0	11.0	528.0	558.5	30.5
377	545	268.63	373.0	381.0	8.0	528.0	558.5	30.5
384	545.5	204.00	382.0	390.0	8.0	531.5	554.5	23.0
391	546	166.07	390.0	404.0	14.0	531.5	554.5	23.0
424	548	41.83	417.0	430.0	13.0	531.5	554.5	23.0
452	544.5	76.58	438.0	460.0	22.0	533.5	556.5	23.0
463	544	33.62	461.0	467.0	6.0	528.0	549.0	21.0
472	544	37.17	468.0	475.0	7.0	529.5	554.5	25.0
482	545	90.66	475.0	494.0	19.0	529.5	562.0	32.5
322	576	128.39	313.0	330.0	17.0	558.5	598.5	40.0
348	574.5	937.70	338.0	357.0	19.0	556.5	604.0	47.5
363	576	582.79	357.0	371.0	14.0	558.5	602.0	43.5
386	576	907.61	371.0	408.0	37.0	554.5	602.0	47.5
424	575	178.37	414.0	435.0	21.0	556.5	602.0	45.5
452	575.5	380.59	436.0	460.0	24.0	556.5	602.0	45.5
471	575	119.16	462.0	485.0	23.0	556.5	598.5	42.0
319	617	47.38	311.0	330.0	19.0	602.0	619.0	17.0
349	616	90.01	340.0	355.0	15.0	604.0	638.5	34.5
362	615.5	171.66	355.0	368.0	13.0	602.0	638.5	36.5
379	615.5	323.62	368.0	387.0	19.0	602.0	638.5	36.5
393	614.5	845.71	387.0	406.0	19.0	600.5	640.5	40.0
412	614	82.77	408.0	420.0	12.0	602.0	636.5	34.5
451	614.5	47.17	449.0	455.0	6.0	606.0	632.5	26.5
463	615.5	387.79	455.0	468.0	13.0	600.5	640.5	40.0
482	616	32.08	479.0	496.0	17.0	604.0	631.0	27.0
531	616	76.13	520.0	544.0	24.0	600.5	636.5	36.0
579	615.5	21.02	569.0	582.0	13.0	608.0	634.5	26.5
349	662.5	42.02	340.0	359.0	19.0	638.5	680.5	42.0
362	663	29.97	359.0	370.0	11.0	644.0	680.5	36.5
386	663.5	49.11	371.0	389.0	18.0	644.0	680.5	36.5
392	662	53.32	390.0	402.0	12.0	640.5	671.0	30.5
427	661.5	13.01	416.0	433.0	17.0	657.5	672.5	15.0
452	654	25.17	447.0	455.0	8.0	650.0	682.5	32.5
465	653.5	30.27	458.0	468.0	10.0	644.0	663.0	19.0
362	696	22.14	357.0	368.0	11.0	688.0	707.0	19.0
381	696	36.83	370.0	387.0	17.0	682.5	714.5	32.0
393	698.5	105.98	387.0	405.0	18.0	680.5	718.5	38.0
463	699.5	34.88	457.0	469.0	12.0	682.5	716.5	34.0
533	699.5	13.52	520.0	544.0	24.0	648.0	724.0	76.0

**Table 22 Fluorescence peaks from a triple doped samples shown in Figure 48. Yellow dysprosium, Orange terbium and Red europium**

Unlike the single ion doped glass samples, where a limited number of emission peaks would be expected, a multiple ion doped sample exhibits many more. Table 22 shows a full interrogation of all the peaks present from a europium, dysprosium and terbium ion doped glass sample.

#### **4.3.1 Statistical Analysis of Multi-Ion Doping in Glass 1**

Due to the high number of possible combinations of dopant and dopant concentrations it was necessary to use Chemometrics to optimise the number of experiments to observe the dependence of the response parameters. A fractional experimental design was used to obtain meaningful results with a manageable and cost effective number of experiments. Statistical analysis was carried out on the data to determine the trends and how the concentration of each dopant affected the fluorescence intensity and peak wavelength of the three chosen peak wavelengths, Table 23.

The wavelength selection was made from the single ion doped concentration analysis, the 3D spectral characterisation (Section 4.1), and the observed interactions between the dopants causing energy transfer signals thus enhancing certain emission peaks. It should be noted that the discrepancy between the optimum excitation wavelengths found and the selected excitation wavelength for some of the experiments was due to the limitation presented by the availability of laser excitation sources with a limited budget.

<b>Lanthanide Ion</b>	<b>Optimum Excitation Wavelength / nm</b>	<b>Selected Excitation Wavelength / nm</b>	<b>Emission Wavelength / nm</b>
<b>Europium</b>	393	465	615
<b>Terbium</b>	375	485	545
<b>Dysprosium</b>	453	453	577

**Table 23 Wavelengths selected for trend analysis**

Minitab 14 was used to analyse either the peak wavelenghts or the peak intensity against the Taguchi Orthogonal Array table, Table 10 and Table 12.

This produced charts showing the interaction of each dopant concentration against the mean intensity values, with each statistical plot representing data from 25 samples.

#### 4.3.2 Trend Analysis of europium, terbium and dysprosium ion interactions in a multi-ion Glass 1

The first trend analysis examined the europium intensity as the concentrations of europium, terbium and dysprosium increased. Figure 50 (a) shows as the concentration of europium increased, the europium 615 nm emission intensity increased. Figure 50 (b) shows that increasing the terbium concentration had no significant effect on the europium 615 nm peak intensity but Figure 50 (c) shows that increasing dysprosium concentration did cause a small decrease in 615 nm peak intensity.

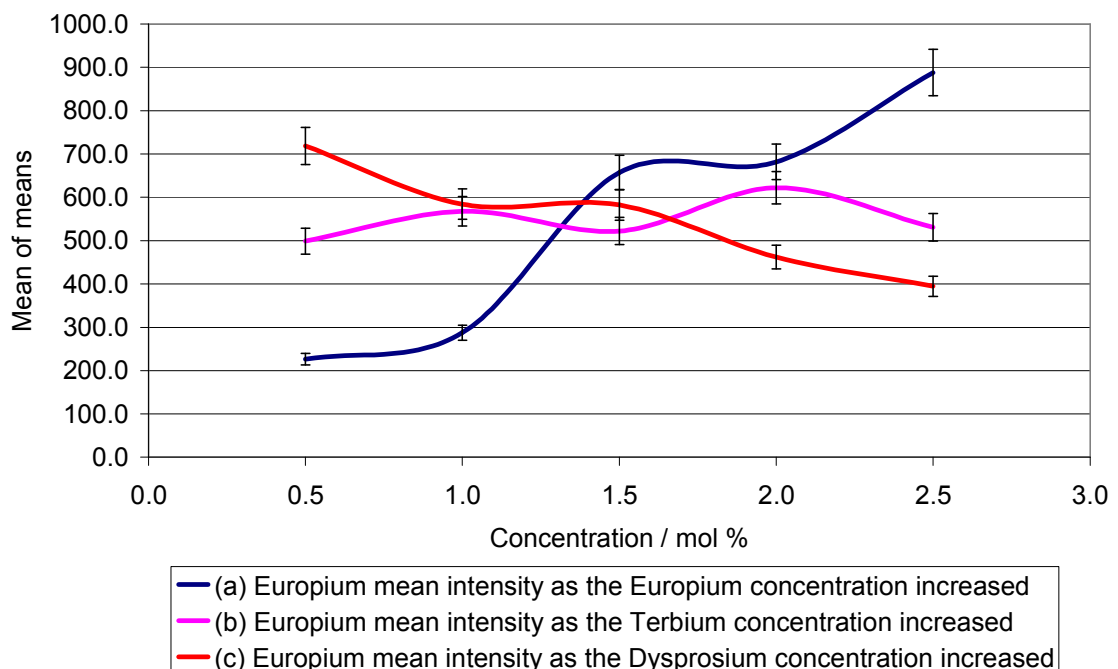


**Figure 50 Europium mean intensity trends with variations in dopant concentrations for Glass 1 samples**

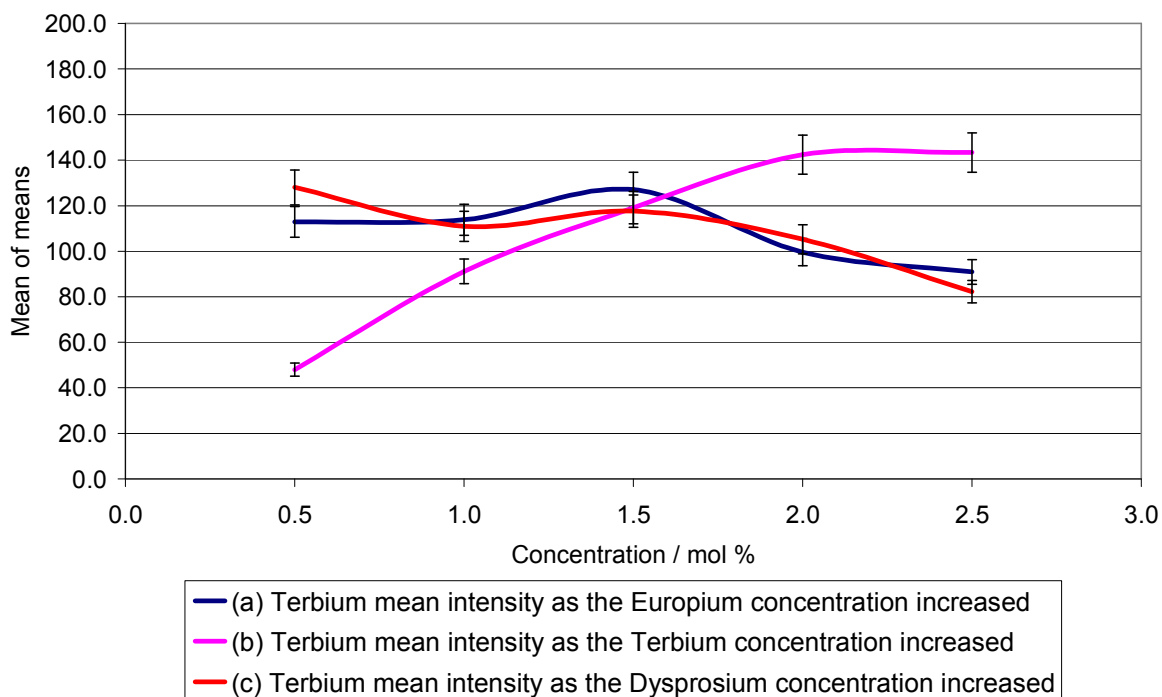


**Figure 51 Terbium mean intensity trends with variations in dopant concentrations for Glass 1 samples**

The next trend analysis examined the terbium fluorescence peak intensity. Figure 51 (a) and (c) show that with increasing europium or dysprosium concentration the 545 nm peak intensity of terbium stayed fairly stable up to 1.5 mol % but at 2.0 mol % the terbium intensity decreased. Increasing the terbium concentration increased the terbium peak intensity linearly up to 2.0 mol %, above this did not appear to effect intensity, Figure 51 (b). This suggests the maximum doping concentrations should be 2.0 mol % of terbium, with no more than 1.5 mol % of europium or dysprosium.

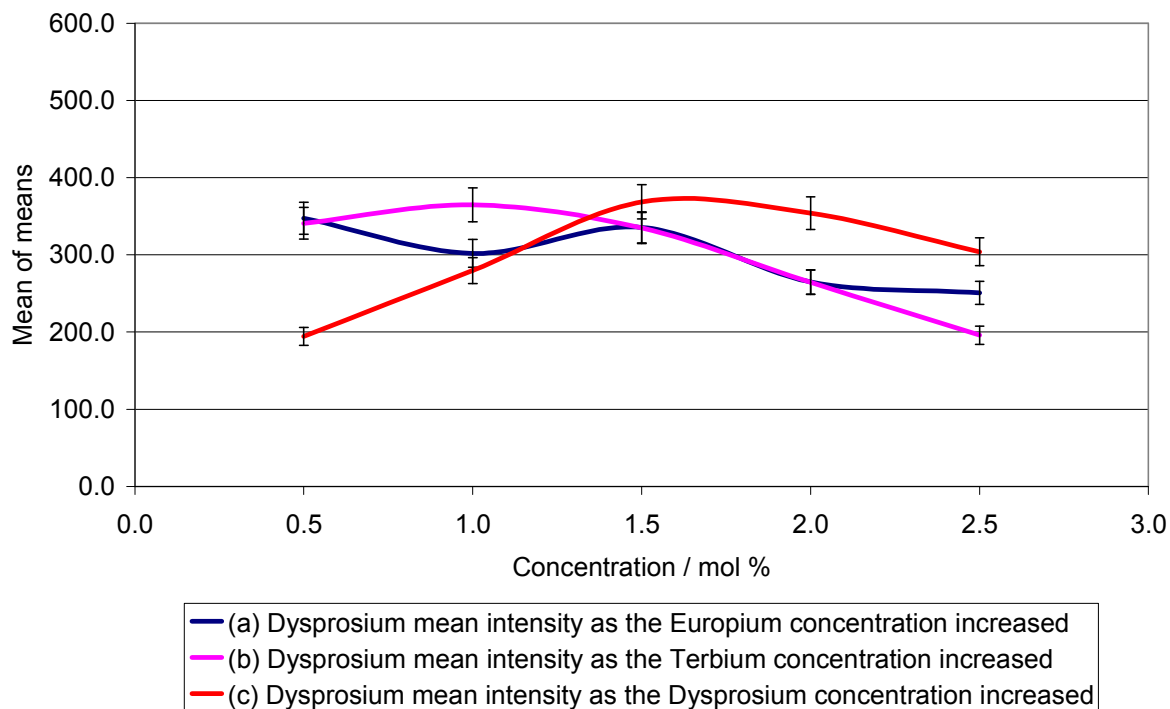


**Figure 52 Dysprosium mean intensity trends with variations in dopant concentrations for glass 1 samples**

The final trend analysis of glass 1 was for dysprosium, the results for which are shown in Figure 52. The dysprosium 577 nm peak intensity decreased with an increase in europium concentration, Figure 52 (a), while increasing terbium concentration peaked at 1.0 mol% before decreasing with higher concentrations, Figure 52 (b). The 577 nm peak intensity of dysprosium increased linearly up to a concentration level of 1.5 mol%, Figure 52 (c) before energy transfer, or possible fluorescence quenching, occurred.

These results indicate that there are interactions between the dopants resulting in the fluorescence signal changing with varying dopant concentrations. From the literature [57], energy transfer peaks were found from a terbium 485 nm excitation wavelength producing a europium 615 nm emission wavelength. Also, a dysprosium 450 nm excitation wavelength was found to induce a terbium 545 nm emission wavelength. These peak enhancements were caused by energy transferring between the lanthanide ions which produce a new unique response



signal for this particular glass and therefore would provide added feature for a tracer. To further investigate this, the intensity of the terbium 485nm enhancing the intensity of the europium 615nm peak was statistically analysed as each dopant concentration was increased as shown in Figure 53.

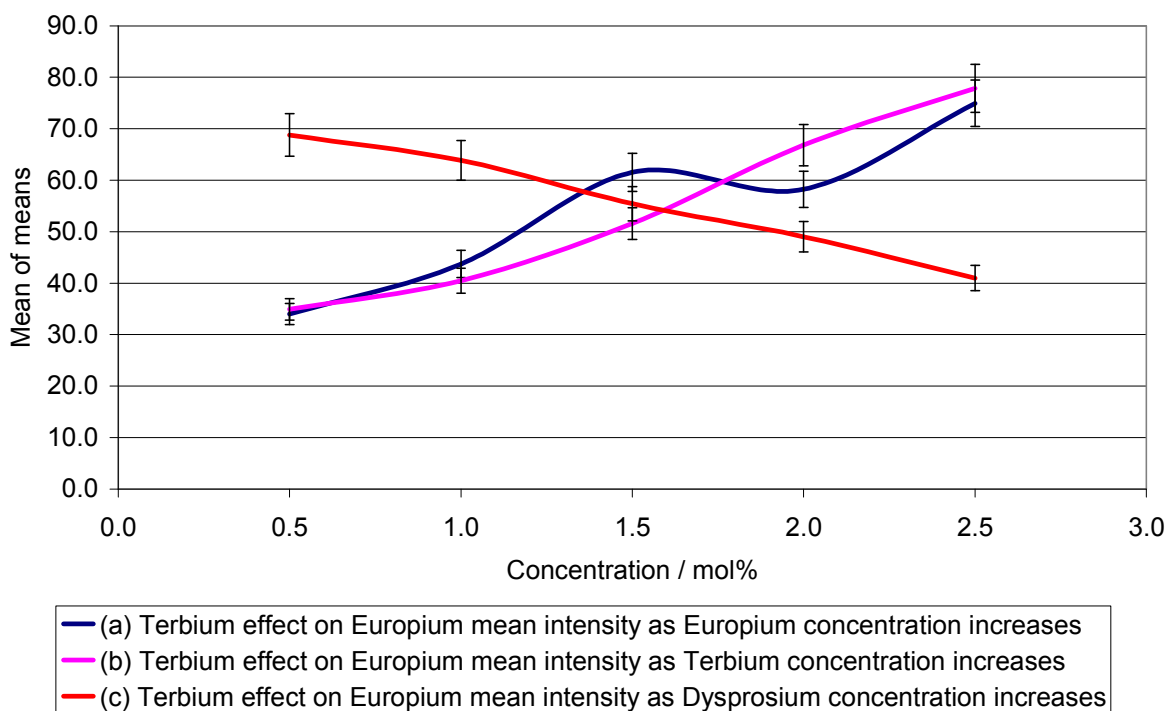


**Figure 53 Energy transfer from terbium 485 nm excitation to europium 615 nm emission, mean intensity as dopant concentrations increased**

These plots show that as the europium or terbium concentration increases, the 615 nm emission peak intensity increases. Whereas increasing the dysprosium concentration caused the 615 nm emission peak intensity to decrease as had been seen in previous studies [43]. The probability of terbium and europium ions coming into close enough proximity within the glass network to undergo energy transfer increases as their concentration increases. This occurs by the dopant ions substituting sodium network modifier ions with the glass network. However, as dysprosium concentrations increase the 615 nm peak intensity decreased, which indicates a further interaction between all three dopants. It is possible that dysprosium ions are entering between terbium and europium ions

reducing the possibility of the energy transfer occurring between terbium and europium.

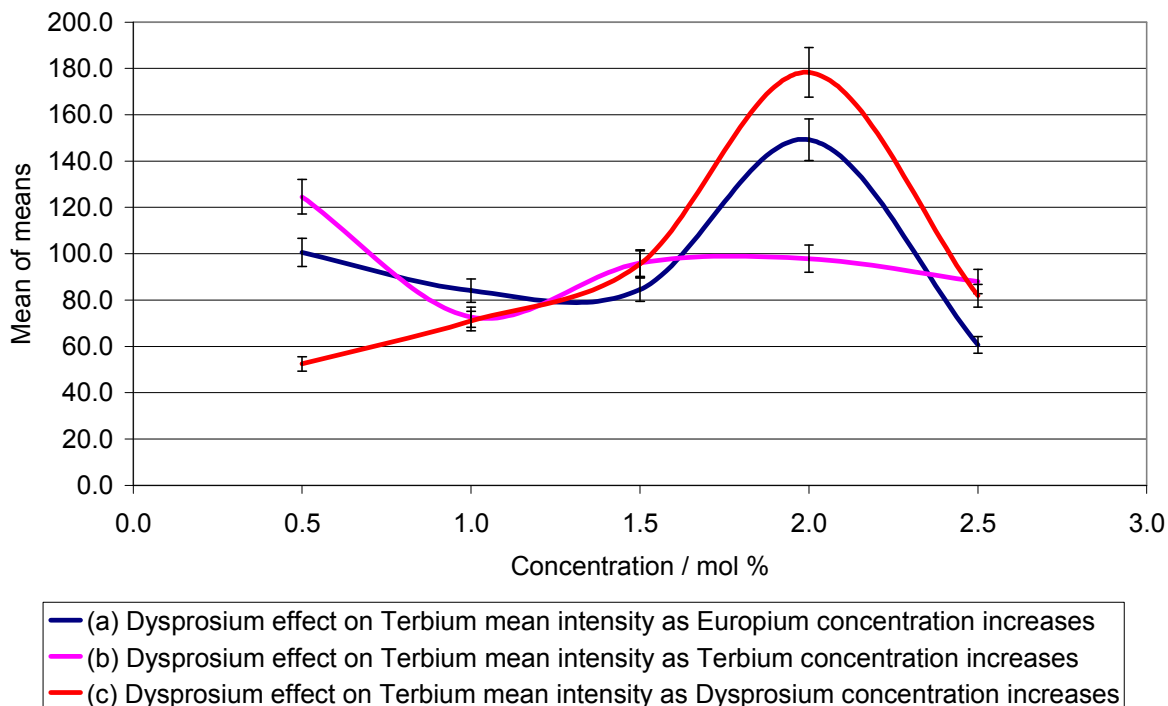


**Figure 54 Energy transfer from dysprosium 452 nm excitation to terbium 545 nm emission, mean intensity as dopant concentrations increased**

The second energy transfer analysed was the emission caused by dysprosium (452 nm excitation) enhancing terbium (545 nm emission) and the results are shown in Figure 54. As the europium concentration was increased the trend appeared to go down, reducing the intensity except at 2 mol %. This point was odd and could be an outlier result. Increasing terbium concentration produced a slightly decreasing trend whilst increasing dysprosium concentration increased the intensity peaking at 2 mol % before decreasing again.

Literature shows the energy transfer from dysprosium to terbium had been reported in phosphate glasses [55] and in boroaluminosilicate glasses [56] with dysprosium reportedly undergoing concentration quenching.

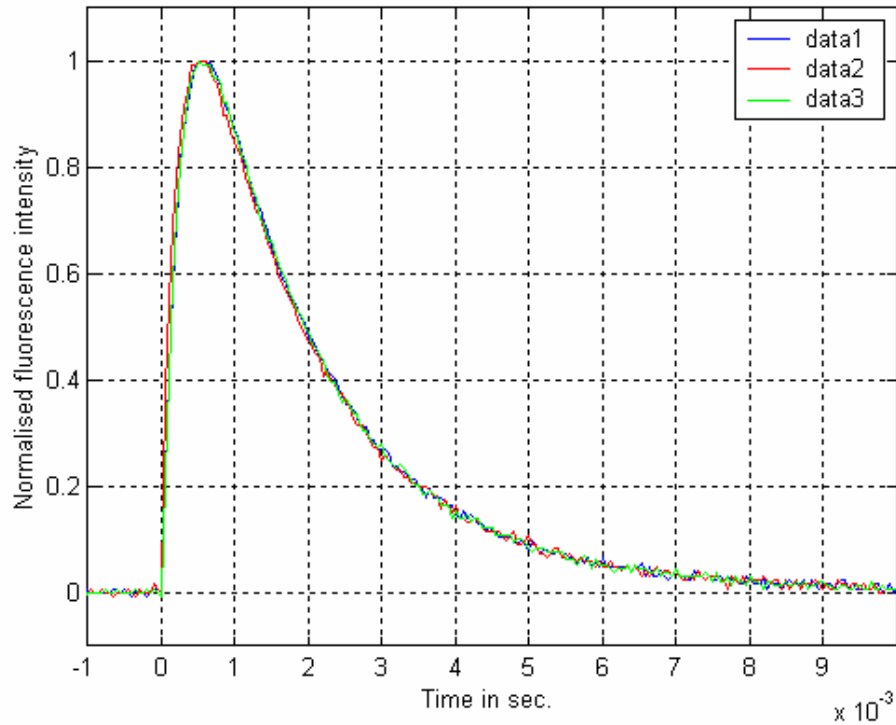
### 4.3.3 Fluorescent Lifetime Study of Multi-Ion Doped Glass 1

An additional feature of using lanthanides as tracers is their unique fluorescent lifetime (long, millisecond range) compared to traditional tracers (short, nanosecond range) and possible pollutants or background molecular fluorescence (short, nanosecond range). A list of selected excitation and fluorescence wavelengths corresponding to each of the doped lanthanides ions, identified from fluorescence spectra, along with the transmission peak of interference filter (10 nm bandwidth), is given in the table below, Table 24.

Lanthanide ions	Excitation laser wavelength/nm	Fluorescence emission peak/nm	Interference filter peak/nm
Europium	464	615	620
Terbium	483	546	546
Dysprosium	451	577	578

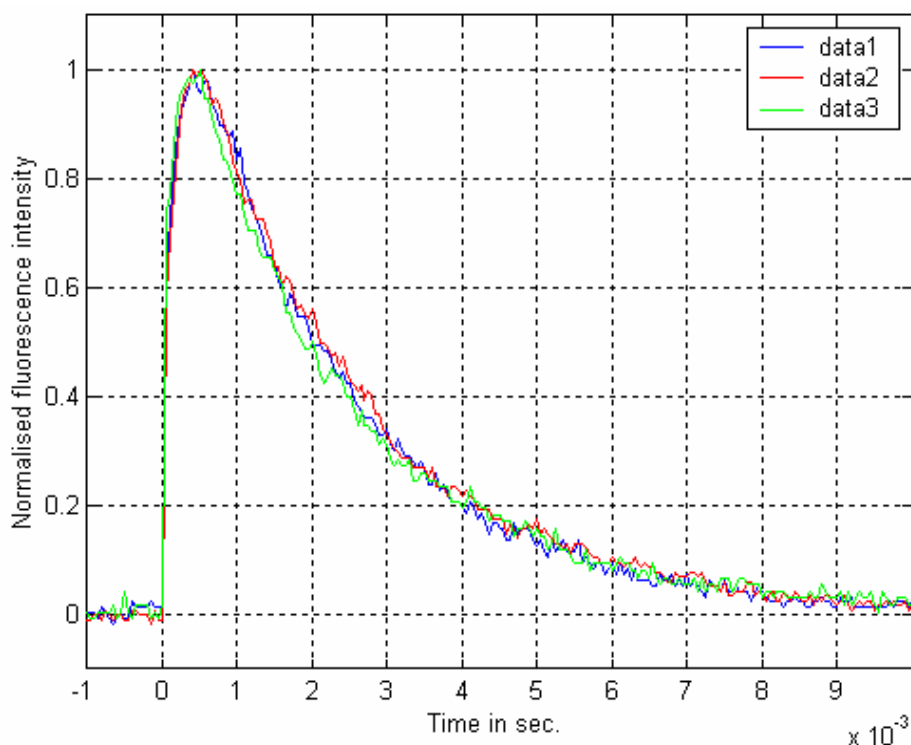
**Table 24 Table of peak wavelengths for fluorescence excitation, emission and filter**

A typical normalised fluorescence pulse from europium in the Glass 1 sample 1, for 464 nm laser excitation and fluorescence emission at 615 nm (filtered through an interference filter with transmission peak at 620 nm and bandwidth of 10 nm) is shown in the Figure 55. It shows a fast rising pulse with a long exponentially decaying tail corresponding to the long fluorescence lifetime of the europium. The lifetime was calculated based on single exponential fluorescence decay and the characteristic lifetime constant of the exponential curve as the fluorescent lifetime of the particular lanthanide ions. From each sample, three data sets were used to calculate an average fluorescent lifetime of europium and this sample shows an average lifetime of  $1.95 \text{ ms} \pm 0.11 \text{ ms}$ .



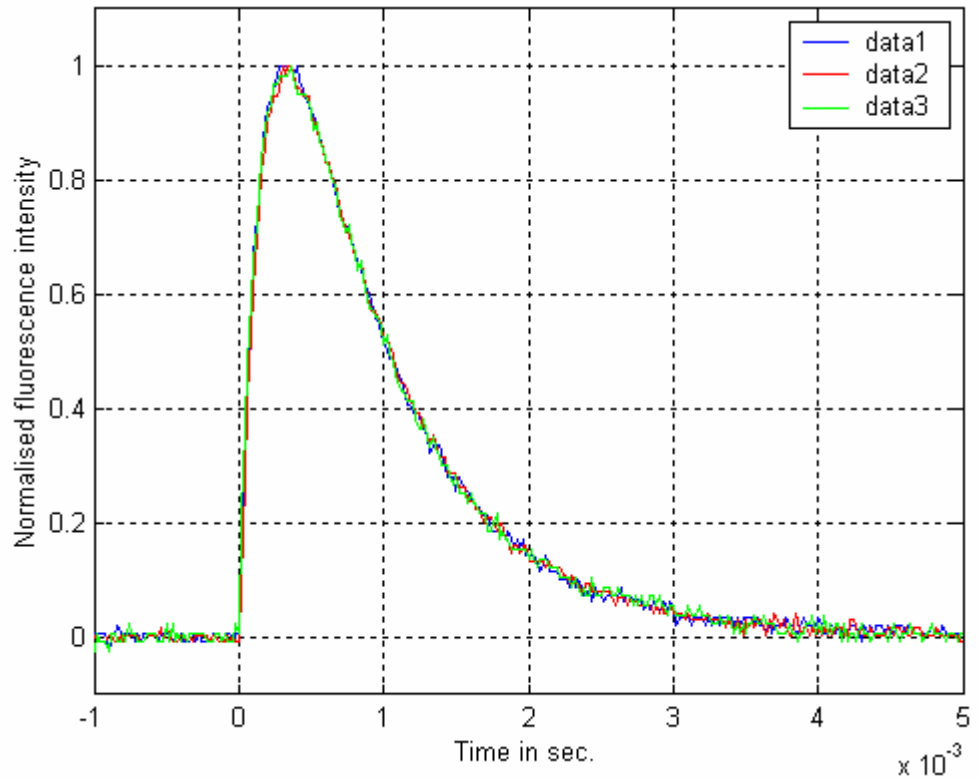
**Figure 55 Fluorescent lifetime profile of europium ions doped in Glass 1 sample 1**

A similar approach was followed on all the glass samples to calculate the lifetime corresponding to terbium and dysprosium. A decay profile of terbium in Glass 1 sample 1 at 546 nm for the 483 nm excitation is shown in Figure 56 and it indicates an average lifetime of  $2.27 \text{ ms} \pm 0.13 \text{ ms}$ .



**Figure 56 Fluorescent lifetime profile of terbium ions in Glass 1 sample 1**

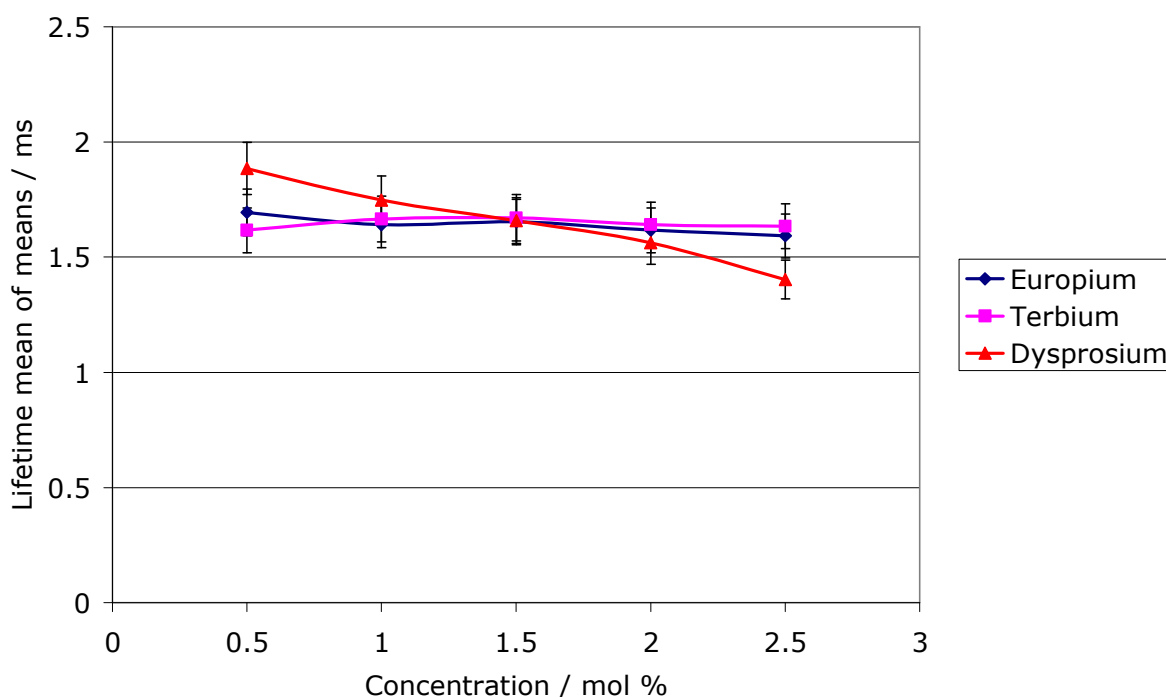
The fluorescent decay profile from dysprosium ions in Glass 1 sample 1 is shown in Figure 57. In this case, laser pulses at 451 nm were used to excite the fluorescence and fluorescence emission at 577 nm was filtered through an interference filter with transmission peak at 578 nm to record the decaying pulse using a photomultiplier tube. It shows an average lifetime of  $0.95 \text{ ms} \pm 0.05 \text{ ms}$ . Following a similar procedure all 25 samples of the Glass 1 matrix were characterised for the fluorescent lifetime of europium, terbium and dysprosium ions.



**Figure 57 Fluorescent lifetime profile of dysprosium ions in Glass 1 sample 1**

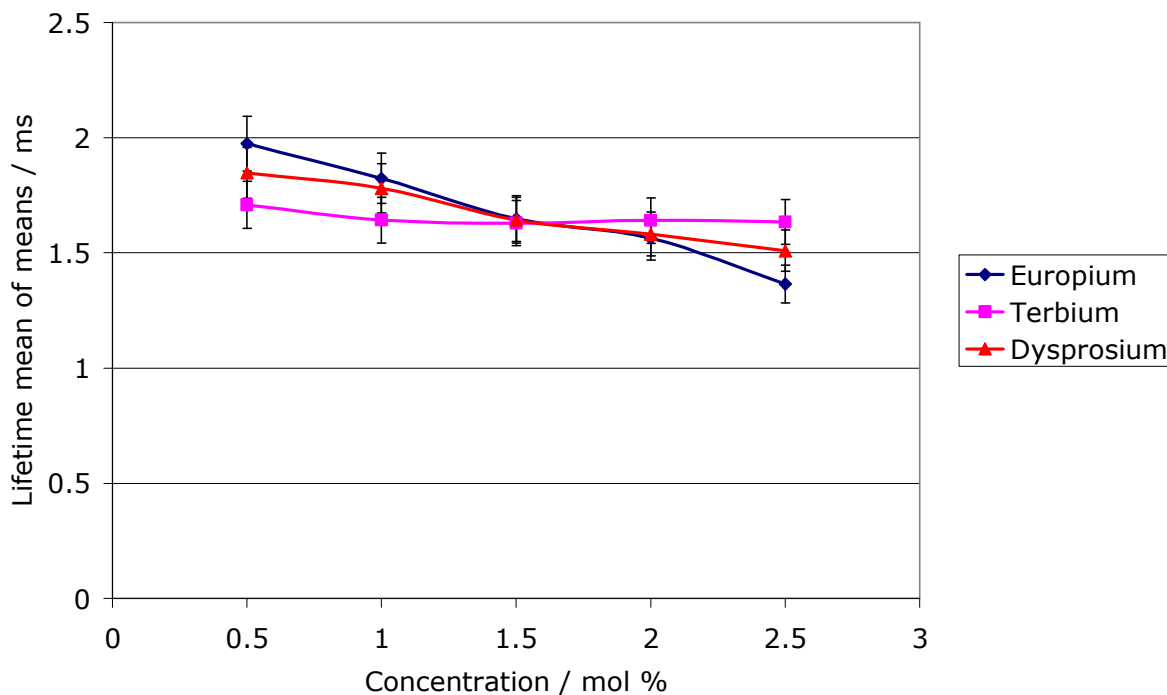
Minitab14, as explained previously in the spectral trend analysis, was used to analyse the tabulated lifetime (in milliseconds) data of europium, terbium and dysprosium the 25 glass 1 glass samples, to study the concentration dependent lifetime variations.

Figure 58 shows the trends for mean lifetimes of the europium in Glass 1 glass for different concentrations of europium, terbium and dysprosium (for excitation at 464 nm and emission at 615 nm). It shows a linearly decreasing trend for fluorescent lifetime of europium with the europium concentration and this may be due to the concentration dependant self quenching of the fluorescence. In addition to this, the effect of terbium and dysprosium, on europium lifetime is also plotted in the figure. The terbium provides a small increase in europium lifetime up to 1 mol % of terbium but as the dysprosium concentration increases indicating a much faster reduction in europium lifetime, over the same range of concentrations.



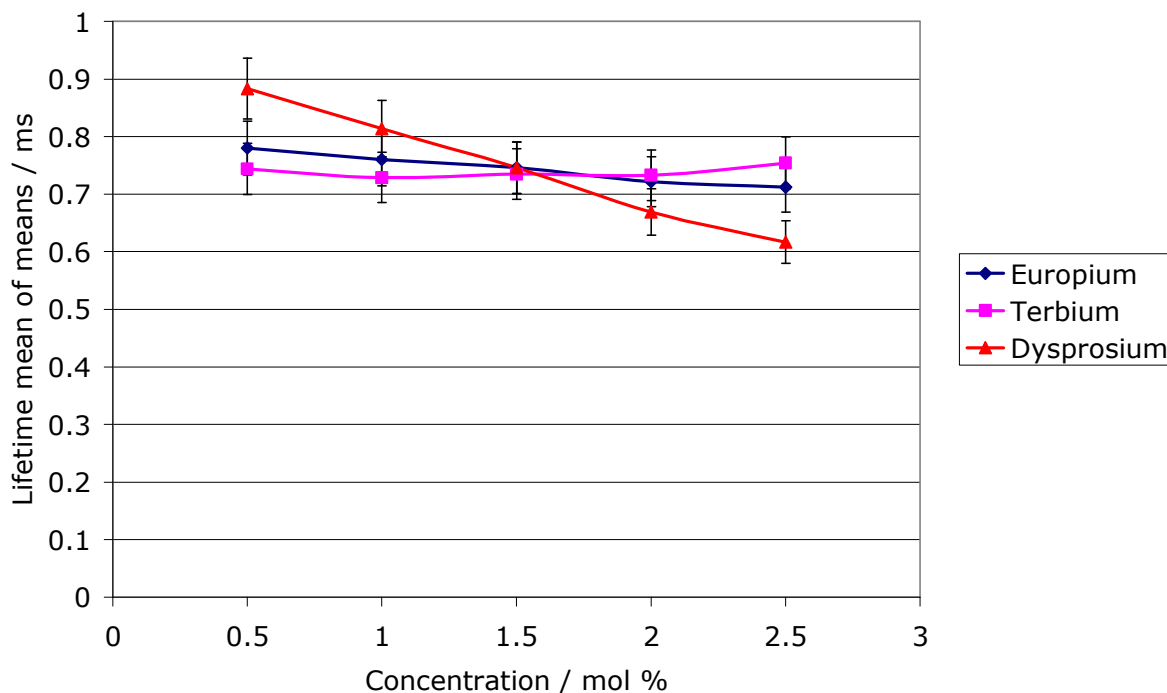
**Figure 58 Fluorescent lifetime trends of europium in glass 1 glass samples with varying europium, terbium and dysprosium concentrations for excitation at 464 nm and emission at 615 nm.**

Figure 59 shows the effect of europium, terbium and dysprosium concentration on terbium lifetime plotted for the excitation at 483 nm and fluorescence emission at 545 nm. It indicates a gradual reduction in terbium lifetime with the increase of all the three lanthanide ion concentrations. A similar trend is also observed in the dysprosium lifetime (for 451 nm excitation and 577 nm emission) and is shown in Figure 60.



**Figure 59 Fluorescent lifetime trends in Terbium in glass 1 glass samples with varying europium, terbium and dysprosium concentrations for excitation at 483 nm and emission at 546 nm.**





**Figure 60 Fluorescent lifetime trends of dysprosium in glass 1 glass samples with varying europium, terbium and dysprosium concentrations for excitation at 451 nm and emission at 577 nm.**

A general conclusion on the individual ion interactions is that all three lanthanide ions have shown a negative trend with the increase in their own ion concentration and this can be attributed to the concentration quenching effect. Regarding the lanthanide interactions, a similar trend is observed from all the three lanthanide ions due to the increase in the other two lanthanide ion concentrations. Comparing the three lanthanide ions in glass 1 borosilicate glass, terbium has shown the longest fluorescent lifetime (nearly 2.0 ms) with dysprosium the least (nearly 0.8 ms). Based on these observations, these long lifetime characteristics can be used as an additional differentiating feature for the environmental tracer application in the glass 1 matrix.

#### **4.3.4** *Glass 1 Characterisation Summary*

A large number of narrow excitation and emission peak wavelengths are available to choose from.

There is a very strong relationship between lanthanide concentrations and emission peak intensities. This means that different environmental tracer combinations can be achieved by altering the concentrations of the lanthanide dopants in the glass matrix. The data indicates the possibility that 0.1 mol% concentration differences could be utilised to produce different emission combinations.

Further unique codes should be achievable as additional excitation/emission peak wavelengths previously forbidden are observed due to energy transfer (sensitisation) of certain combinations of lanthanides.

Long lifetime characteristics can be used as one of the discrimination features for the environmental tracer in the glass matrix. With lanthanides exhibiting lifetimes in the millisecond region compared to that of conventional molecular tracers typically in the nanosecond region.

#### 4.4 Multiple Ion Doped Glass Characterisation and Concentration Study in Borosilicate Glass 2.

To investigate the effect of altering the glass matrix, a range of 25 samples were prepared with the addition of NaF. The addition of NaF is an attempt to alter the position, ratio and fluorescence intensity of emission wavelengths produced. To investigate this effect, 3D spectra of the excitation and emission peaks of a range of multiple lanthanide doped glass tracers were recorded to indicate possible changes in useful tracer peaks. Figure 61 shows the fluorescence spectrum of a blank, undoped sample of borosilicate glass which displays no emission or excitation peaks in the visible region.

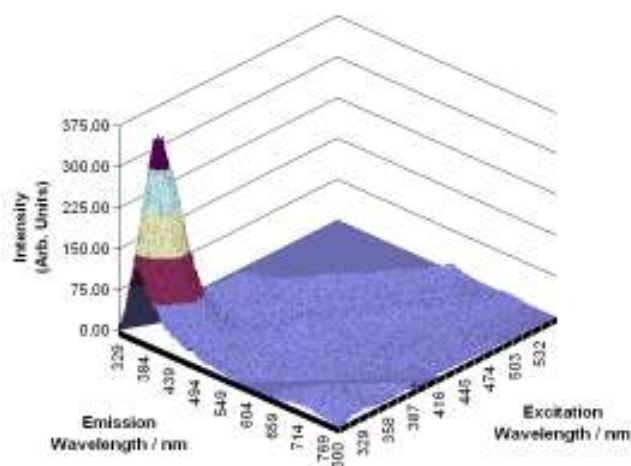


Figure 61 Fluorescence spectrum of a blank sample of glass 2

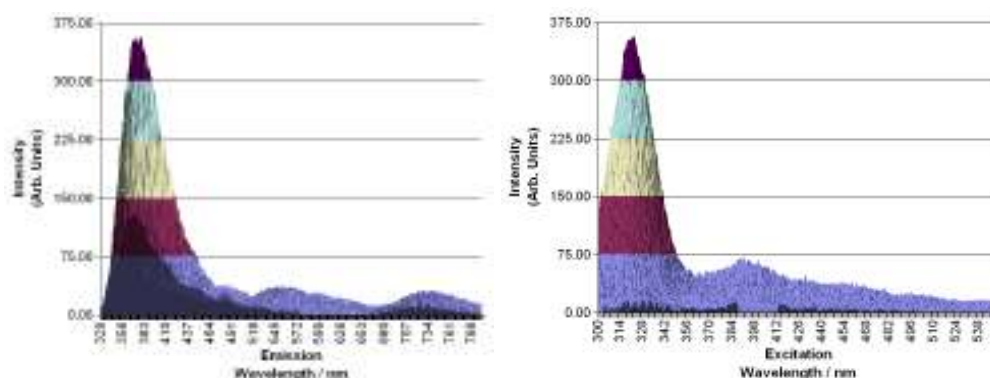
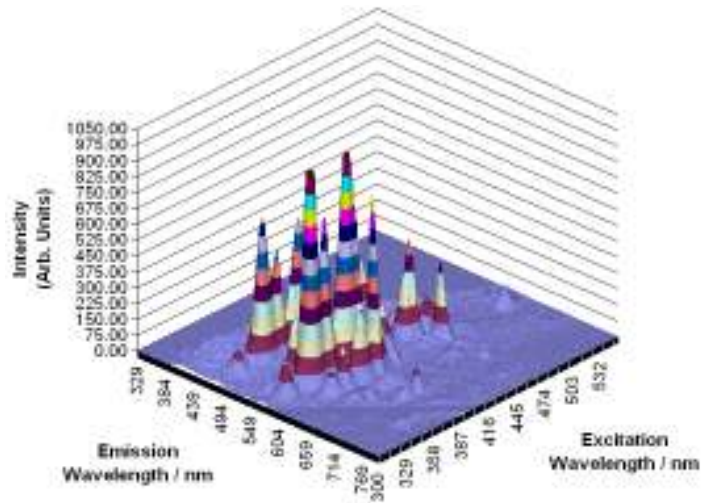
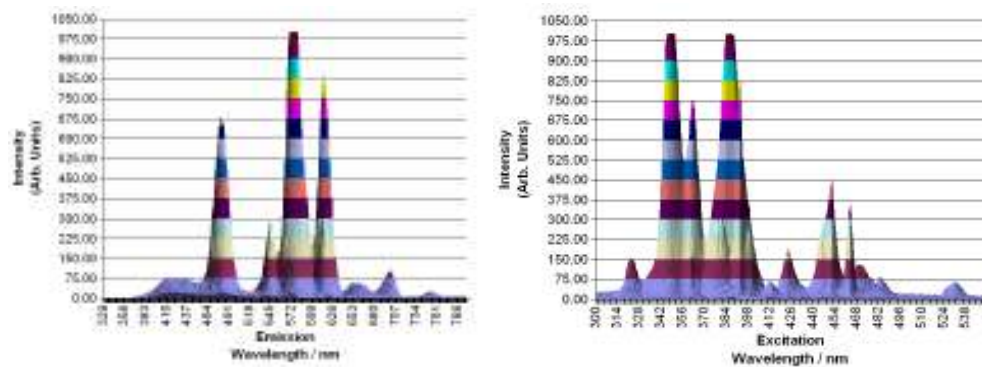


Figure 62 Emission and Excitation spectra of a blank sample of glass 2

As discussed previously the added advantage of using multi-ion doping is the added benefit of an increased number of “coded” tracers, which for example could be “coded” for a specific discharge sources or effluent streams. Figure 63 and Figure 64 show the 3D fluorescence spectra from europium, terbium and dysprosium multi-ion doped tracer with dopant concentrations of 1 mol % europium, 1 mol % terbium and 2 mol % dysprosium.



**Figure 63 Fluorescence Spectrum of Glass 2 sample 13 (1 mol % europium, 1 mol % terbium, 2 mol % dysprosium)**



**Figure 64 Excitation and Emission Spectrum of Glass 2 sample 13 (1 mol % europium, 1 mol % terbium, 2 mol % dysprosium)**

Excitation Wavelength / nm	Emission Wavelength / nm	Intensity	Peak width					
			Ex Wavelength			Em Wavelength		
			From	To	PW	From	To	PW
323	481	116.44	312.0	331.0	19.0	466.5	506.5	40.0
349	481	677.09	331.0	357.0	26.0	459.5	506.5	47.0
363	481	473.49	357.0	371.0	14.0	465.5	506.5	41.0
386	481	581.58	371.0	411.0	40.0	457.5	506.5	49.0
423	481	100.80	416.0	431.0	15.0	459.5	501.5	42.0
452	481	242.19	436.0	460.0	24.0	468.5	501.5	33.0
324	546	43.06	312.0	329.0	17.0	529.0	554.5	25.5
349	546	288.18	332.0	356.0	24.0	527.0	555.5	28.5
364	546	241.89	358.0	370.0	12.0	531.0	555.5	24.5
378	546	257.01	373.0	382.0	9.0	529.0	557.5	28.5
385	546	206.25	382.0	409.0	27.0	529.0	552.5	23.5
424	546	37.81	417.0	434.0	17.0	531.0	554.5	23.5
445	546	51.32	437.0	448.0	11.0	531.0	553.5	22.5
452	546	74.35	448.0	459.0	11.0	530.0	553.5	23.5
485	546	71.52	475.0	495.0	20.0	531.0	558.5	27.5
323	577.5	161.20	311.0	331.0	20.0	559.5	600.5	41.0
349	577.5	999.99	331.0	357.0	26.0	555.5	603.0	47.5
363	577.5	753.64	357.0	371.0	14.0	556.5	603.0	46.5
385	577.5	1002.58	371.0	412.0	41.0	555.5	602.0	46.5
423	577.5	182.23	412.0	436.0	24.0	556.5	603.0	46.5
452	577.5	435.82	436.0	460.0	24.0	555.5	601.5	46.0
471	577.5	127.47	461.0	491.0	30.0	555.5	595.5	40.0
318	615	41.26	312.0	328.0	16.0	603.0	631.5	28.5
351	615	89.54	341.0	355.0	14.0	606.0	635.5	29.5
361	615	186.19	355.0	368.0	13.0	602.0	636.5	34.5
380	615	314.30	368.0	387.0	19.0	602.0	636.5	34.5
393	615	844.77	387.0	406.0	19.0	600.5	640.5	40.0
412	615	65.72	407.0	419.0	12.0	603.0	634.5	31.5
464	615	356.67	457.0	471.0	14.0	600.5	636.5	36.0
532	615	65.51	520.0	545.0	25.0	600.5	635.5	35.0
322	658	5.76	317.0	326.0	9.0	654.0	664.5	10.5
347	658	44.04	332.0	357.0	25.0	637.5	691.0	53.5
362	658	29.61	357.0	369.0	12.0	643.5	683.5	40.0
384	658	51.24	371.0	386.0	15.0	642.5	682.5	40.0
392	658	51.69	389.0	407.0	18.0	638.5	674.0	35.5
425	658	10.13	418.0	429.0	11.0	652.0	687.0	35.0
451	658	21.39	439.0	457.0	18.0	644.0	688.0	44.0
464	658	20.28	460.0	468.0	8.0	646.0	676.5	30.5
485	658	9.65	482.0	487.0	5.0	665.5	682.5	17.0
320	700.5	3.73	311.0	328.0	17.0	685.5	710.5	25.0
352	700.5	9.31	336.0	356.0	20.0	693.0	711.5	18.5
361	700.5	19.40	356.0	368.0	12.0	688.0	712.5	24.5
380	700.5	36.30	368.0	387.0	19.0	683.5	716.5	33.0
392	700.5	100.73	387.0	406.0	19.0	678.5	723.5	45.0
414	700.5	10.38	406.0	420.0	14.0	685.5	714.5	29.0
464	700.5	30.19	458.0	469.0	11.0	677.5	716.5	39.0
530	700.5	8.40	521.0	540.0	19.0	676.5	716.5	40.0
349	754	24.80	338.0	357.0	19.0	731.0	786.0	55.0
363	754	14.26	357.0	367.0	10.0	744.0	781.0	37.0
422	754	8.27	412.0	435.0	23.0	739.0	773.0	34.0
448	754	10.07	440.0	462.0	22.0	728.0	781.0	53.0

**Table 25 Table of fluorescence peaks, their intensity and peak width for Glass 2 sample 13**

Unlike the single ion doped glass samples, where a limited number of emission peaks would be expected, a multiple ion doped sample exhibits many more. Table 25 shows a full interrogation of all the peaks present from a europium, dysprosium and terbium ion doped glass 2 sample 13.

#### 4.4.1 Statistical Analysis of Multi-Ion Doping in Glass 2

Statistical analysis of the response trends for the triple doped glass 2 was achieved using Minitab14 as was carried out for the glass 1 samples. The europium intensity trends of glass 2 based glasses with dopant concentrations are shown in Figure 65. For the triple doped glass increasing the europium concentration, Figure 65(a), showing a clear concentration dependence of the peak intensity. This showed a linearly increasing trend with increasing europium concentration. No significant interaction effect was observed with increasing terbium concentration Figure 65(b) however, increasing the dysprosium decreased the europium intensity Figure 65(c).

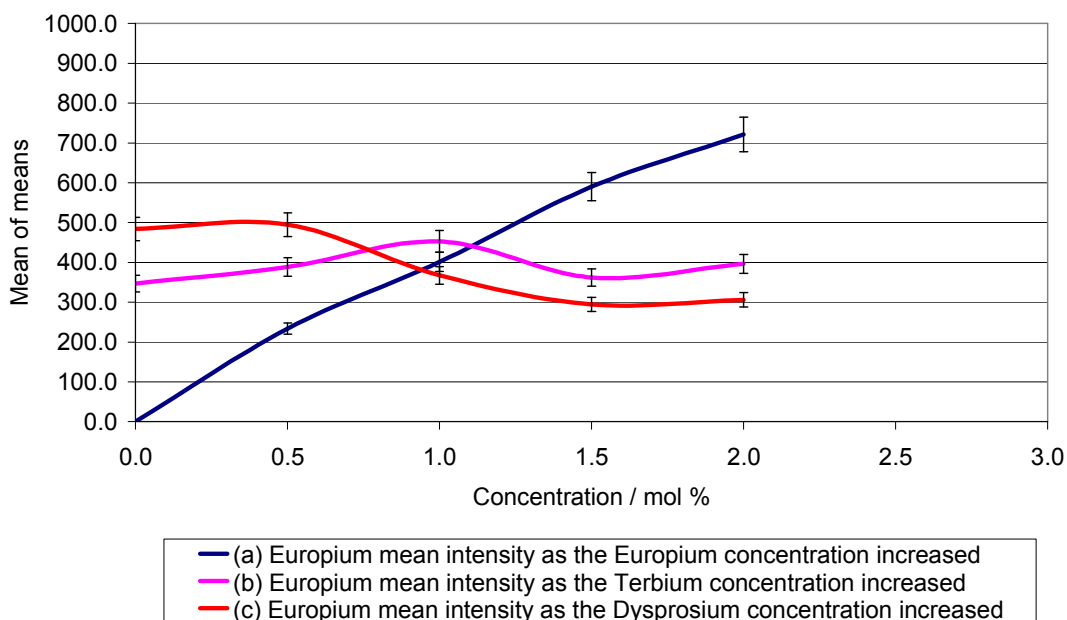


**Figure 65 Europium mean intensity trends with variations in dopant concentrations for glass 2 samples**

The terbium intensity trends are shown in Figure 66 where an increase in europium concentration caused a slight decrease in terbium peak height. The terbium peak intensity increased with concentration, showing a clear concentration dependence of the terbium peak intensity. Increasing dysprosium concentration showed no effect on the terbium intensity.

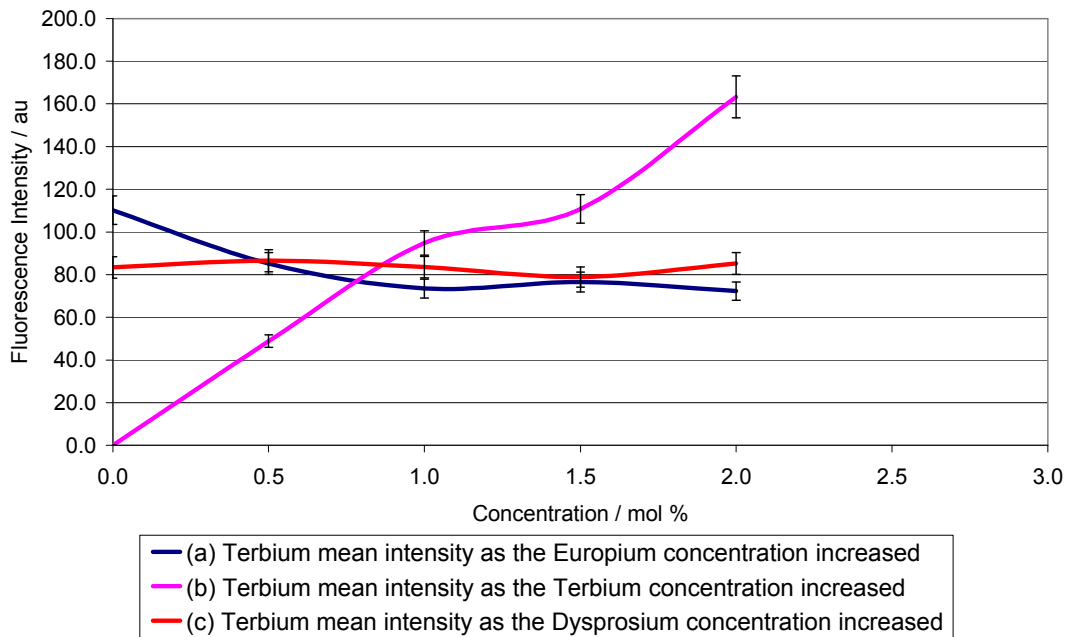


**Figure 66 Terbium mean intensity trends with variations in dopant concentrations for glass 2 samples**

Figure 67(a) and (b) shows the dysprosium trends which indicated a decrease with increasing either europium or terbium concentration. However, an increase was found with increasing dysprosium concentration up to 1 mol % with a plateau from 1 – 2 mol %, Figure 67(c).

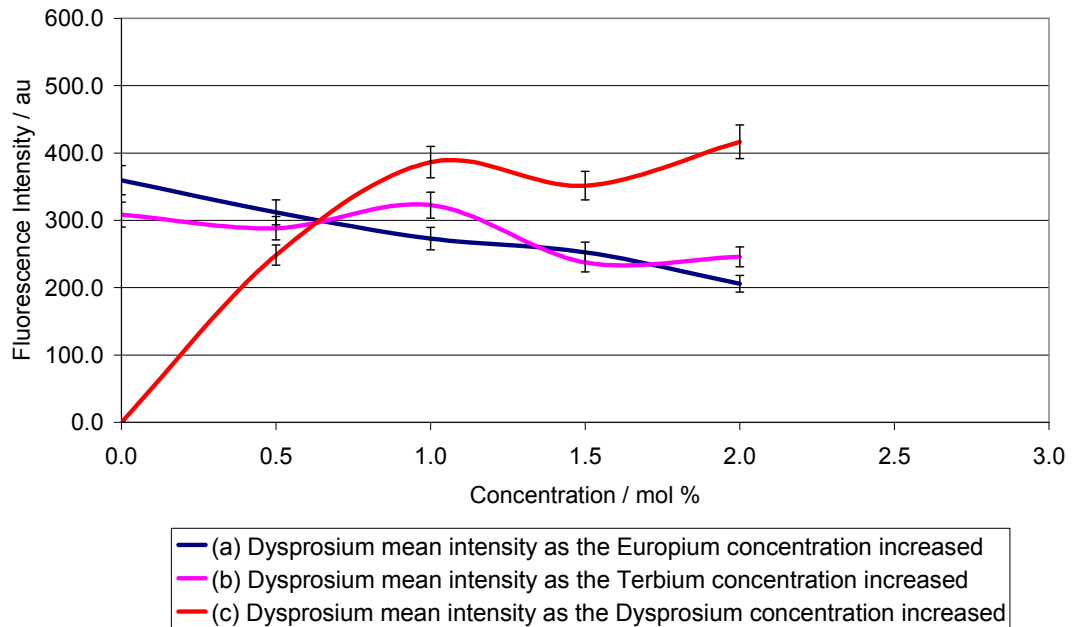


**Figure 67 Dysprosium mean intensity trends with variations in dopant concentrations for glass 2 samples**

As with the analysis of glass 1 significant, energy transfer peaks were observed in the glass 2 samples. Therefore the same analysis was carried out to look at the trends for the terbium energy transfer to europium and dysprosium energy transfer to terbium.



The first analysis shows that as either the europium or dysprosium concentration was increased, the peak intensity increased Figure 68 (a) and (c). However, no peak was found when the terbium concentration was 0 or 0.5 mol % therefore there is insufficient data to obtain the terbium trend, Figure 68 (b). These results did however show a large interaction between the europium and dysprosium concentrations influencing the terbium to europium energy transfer.

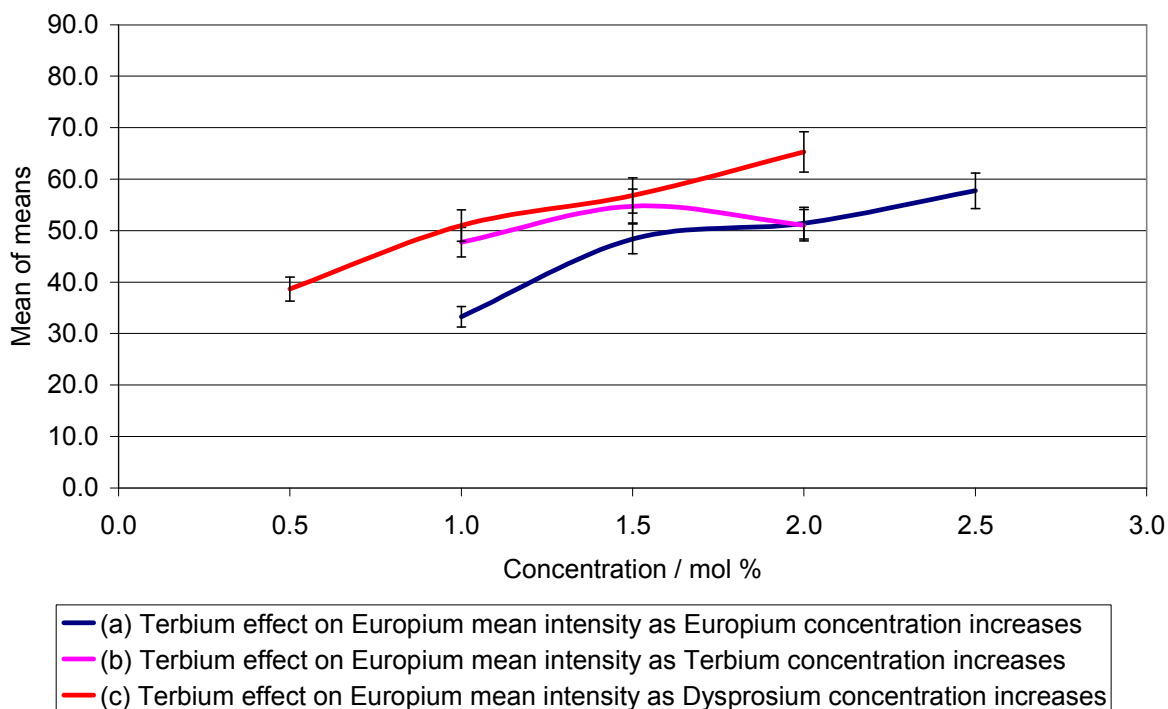


**Figure 68 Energy transfer from terbium 485 nm excitation to europium 615 nm emission, mean intensity as dopant concentrations increased**

The energy transfer results from dysprosium to terbium are shown in Figure 69. With increasing europium concentration a decrease in peak emission intensity (545 nm) was found up until 1 mol %, Figure 69 (a). However, with an increase in either the terbium or dysprosium concentration there was a large increase in 545 nm europium peak intensity, Figure 69 (b) and (c). Therefore the europium has a significant negative effect on the peak intensity as it may enhance the probability of the energy transfer from terbium to europium instead of enhancing terbium due to the three way interaction between dopants.

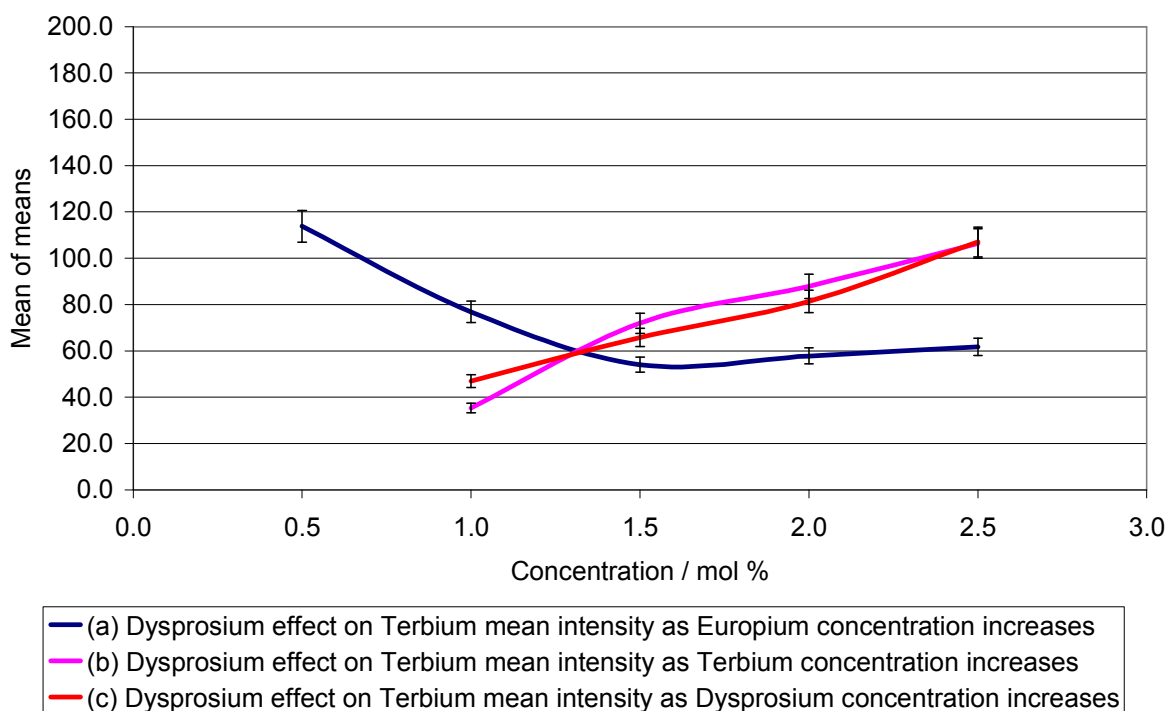


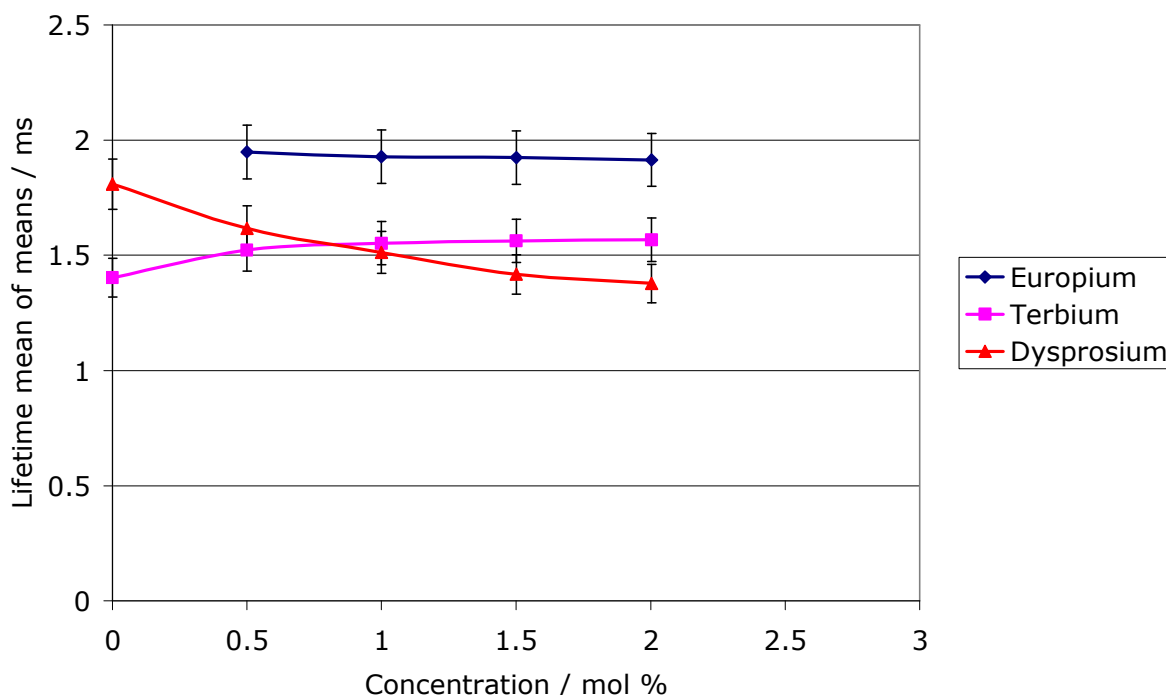
**Figure 69 Energy transfer from dysprosium 450 nm excitation to terbium 545 nm emission, mean intensity as dopant concentrations increased**

Overall the glass 2 data showed that generally the peak intensity was proportional to the concentration of the lanthanide dopant with differences of 0.1 mol % concentration changes generating measurable changes in peak intensity. The data also showed that some significant interactions between the lanthanide dopants occurred with some of the glass samples generating more potential tracer combinations.

#### 4.4.2 Fluorescent Lifetime Study of Multi-Ion Doped Glass 2

As explained in the case of glass 1 lifetime analysis, a similar set of fluorescent lifetime trend analyses was carried out with the glass 2 triple doped glass samples. All the 25 glass 2 triple doped glass samples were tested at the specific wavelengths and tabulated in Table 25 selected using the Minitab14 Taguchi Chemometric statistical model. Since no significant spectral peak shift was observed by changing the host glass matrix, the same excitation and emission wavelengths, as in glass 1, were utilised. The resulting trend plots are presented and discussed in this subsection.

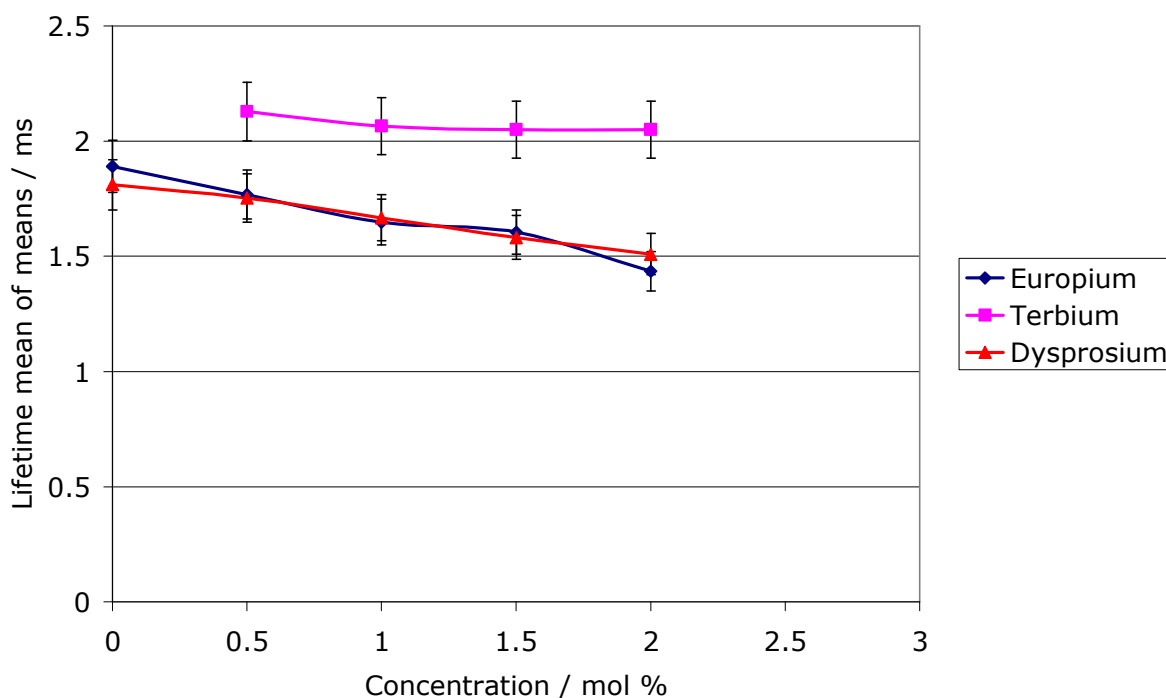
A range of lanthanide concentrations were examined for the lifetime trend analysis in the glass 2 matrix at 0, 0.5, 1.0, 1.5, 2.0 mol %. The lifetime trend for europium ions in the glass 2 composition, for varying concentrations of europium, terbium and dysprosium is shown in Figure 70.



**Figure 70 Fluorescent lifetime trends of europium in Glass 2 with varying concentrations of europium, terbium & dysprosium for excitation at 464 nm and emission at 615 nm.**

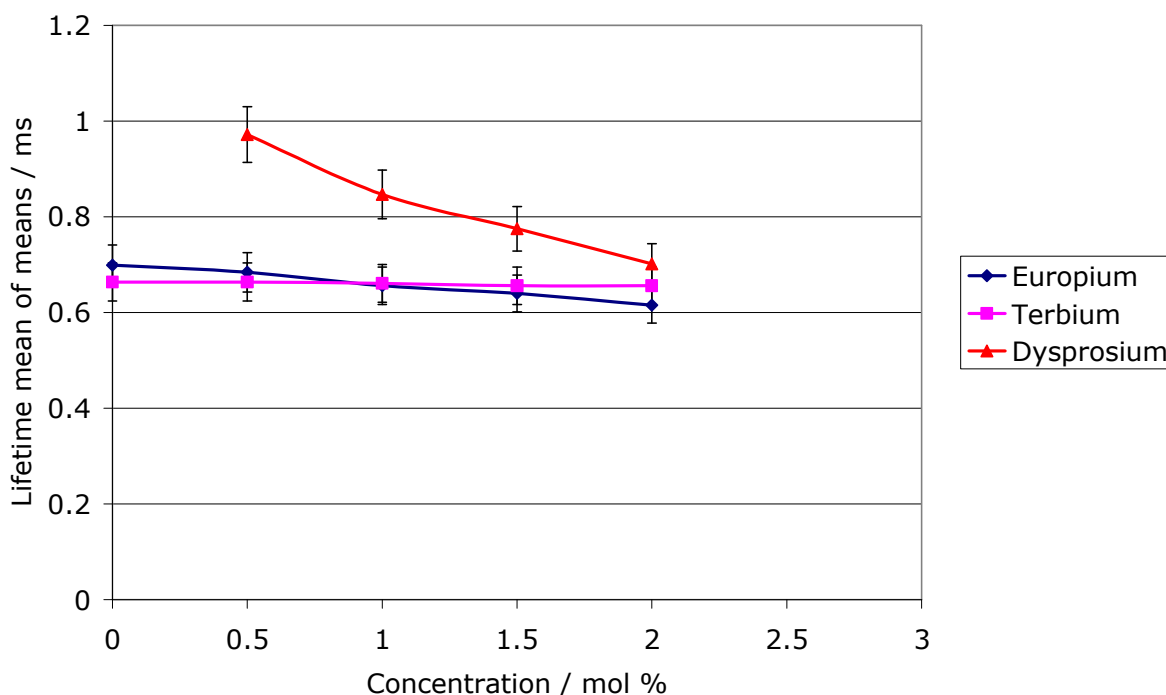
During the lifetime study experiments, short laser pulses at 464 nm were used for fluorescence excitation and emission at 615 nm was detected using a PMT. The optimum excitation wavelengths for europium, terbium and dysprosium and the “best fit” excitation sources available are shown in Table 23 on p101. As there is no 395 nm laser available for use as an excitation source the second strongest excitation wavelength for Europium is 465 nm. As can be observed from the trend plot the europium lifetime decreases as the dysprosium concentration increases. As the terbium and europium concentration increases, the europium lifetime has shown a slight increase followed by saturation, although this is not statistically significant as the error bars show.

Figure 71 shows the lifetime trends for the terbium ions in glass 2 triple doped samples and indicates a gradual reduction in terbium lifetime with any increase in the europium and dysprosium concentration. With terbium itself the trend is very gradual decrease but statistically flat.



**Figure 71 Fluorescent lifetime trends of Terbium in Glass 2 with varying concentrations of europium, terbium and dysprosium for excitation at 483 nm and emission at 546 nm.**

A similar plot for dysprosium is shown in Figure 72. It shows a strong negative dependency of dysprosium lifetime as the dysprosium concentration increases and a level trend as the europium concentration increases. The terbium concentration has shown no significant effect on dysprosium lifetime within the selected concentration limit.



**Figure 72 Fluorescent lifetime trends of dysprosium in glass 2 for varying concentrations of europium, terbium & dysprosium for excitation at 451 nm and emission at 577nm.**

From this analysis, it can be concluded that the lanthanide ion lifetime in glass 2 multi doped glass depends on the lanthanide concentration. All three ions exhibit self quenching to varying degrees, with dysprosium showing a strong negative trend and very little with europium and terbium which statistically level. Generally a negative lifetime trend was observed for the interactions between the lanthanides with the exception of europium lifetime due to terbium concentration. In this case, a very small increase in europium lifetime due to terbium ions was observed. The same trend had been observed in glass 1 glasses. The results demonstrate the long and stable nature of the lifetimes, for this range of lanthanide concentrations, it can be concluded that the fluorescent

lifetime of lanthanide ions could be used as one of the background discrimination features for the lanthanide ion based environmental tracer. The potential to use this lifetime variation as a determination between lanthanide doped glass tracers in a real world application would only be possible if a large variation in lifetime were possible. As the results show here, it would be almost impossible to attempt to differentiate between a 0.5 mol % and 1 mol % europium if using more than one tracer dopant combination. This would suggest that using fluorescent emission and dopant lifetime of the glass tracer could be used as the method of identification in a single tracer study. If more than one tracer combination were to be used then only fluorescent emission could be exploited as a monitoring method, using lifetime as a pure background discriminatory feature.

#### 4.4.3 Investigation into peak wavelength variations with dopant concentrations and glass matrix

To determine whether the peak wavelength changed with changes in dopant concentrations, the mean and standard deviations were calculated for each of the peaks of interest. The influence of the glass matrix is observed by comparison of glass 1 and glass 2 data.

##### 4.4.3.1 Borosilicate glass 1 peak wavelength variations

Using the spectroscopy data from the 25 glass 1 samples, europium had a mean peak excitation at 463.68 nm with a standard deviation of 0.56 nm and mean peak emission at 615.24 nm with a standard deviation of 1.37 nm, Figure 73.

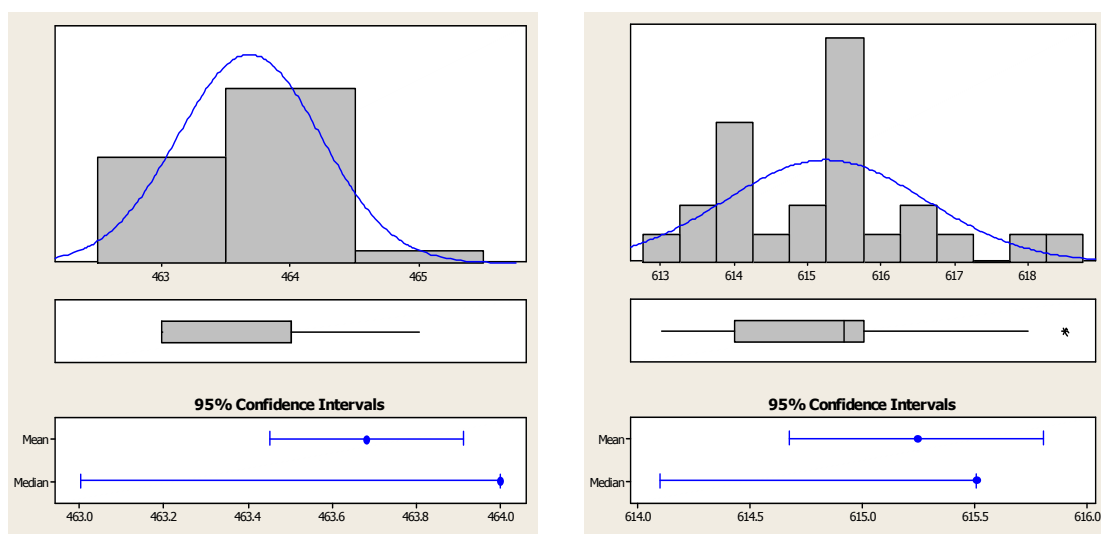


**Figure 73 Investigation into changes in the peak excitation and emission wavelengths for europium in glass 1 samples**

Terbium had a mean peak excitation at 483.32 nm with a standard deviation of 0.75 nm and a mean peak emission at 545.32 nm with a standard deviation of 1.06 nm, Figure 74.

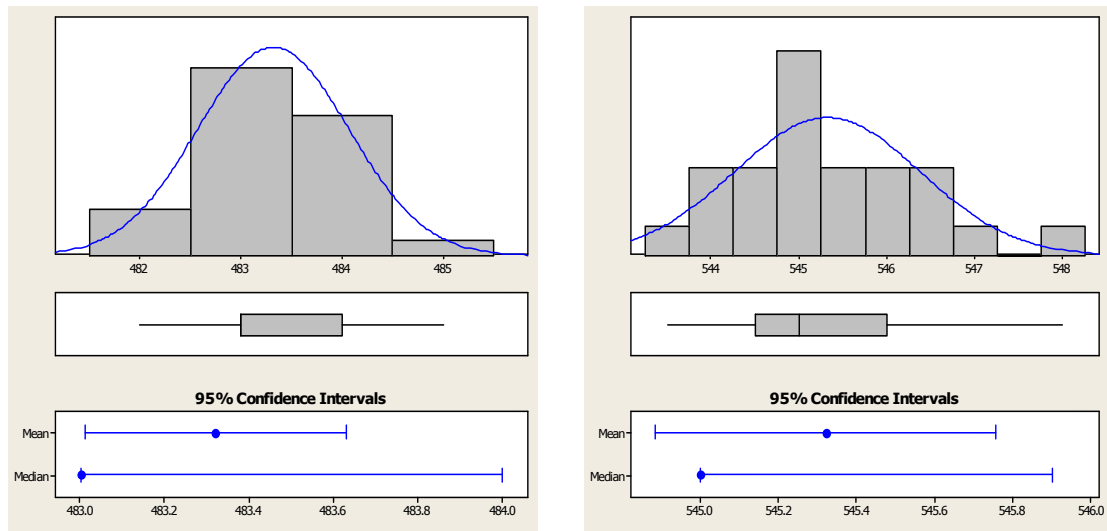


**Figure 74 Investigation into changes in the peak excitation and emission wavelengths for terbium in glass 1 samples**

Dysprosium had a mean peak excitation at 451.96 nm with a standard deviation of 0.20 nm and a mean peak emission at 576.29 nm with a standard deviation of 1.17 nm Figure 75.

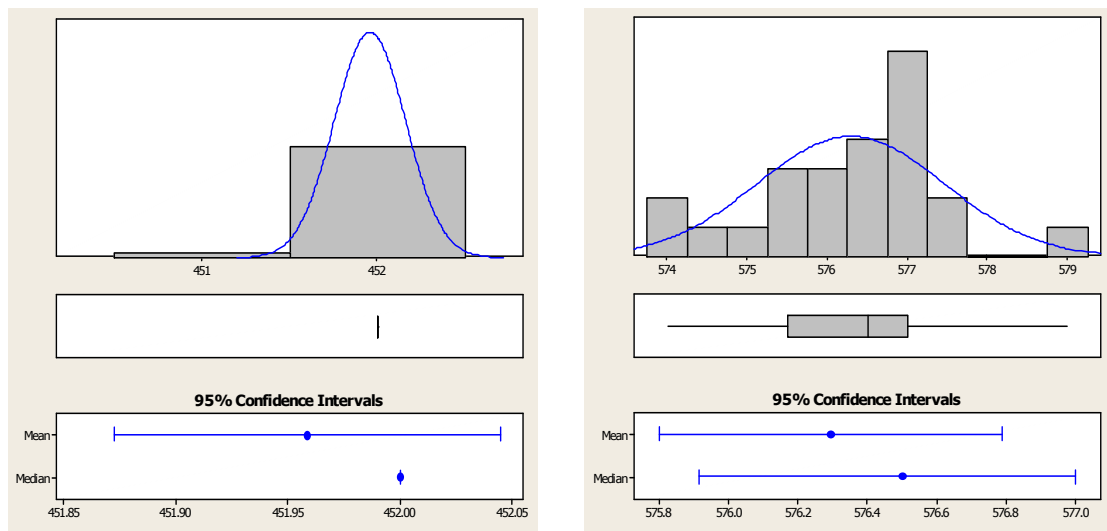


**Figure 75 Investigation into changes in the peak excitation and emission wavelengths for dysprosium in glass 1 samples**



#### 4.4.3.2 Borosilicate glass 2 peak wavelength variations

For the glass 2 samples, europium had a mean peak excitation at 464.05 nm with a standard deviation of 0.39 nm and mean peak emission at 614.70 nm with a standard deviation of 0.73 nm, Figure 76.

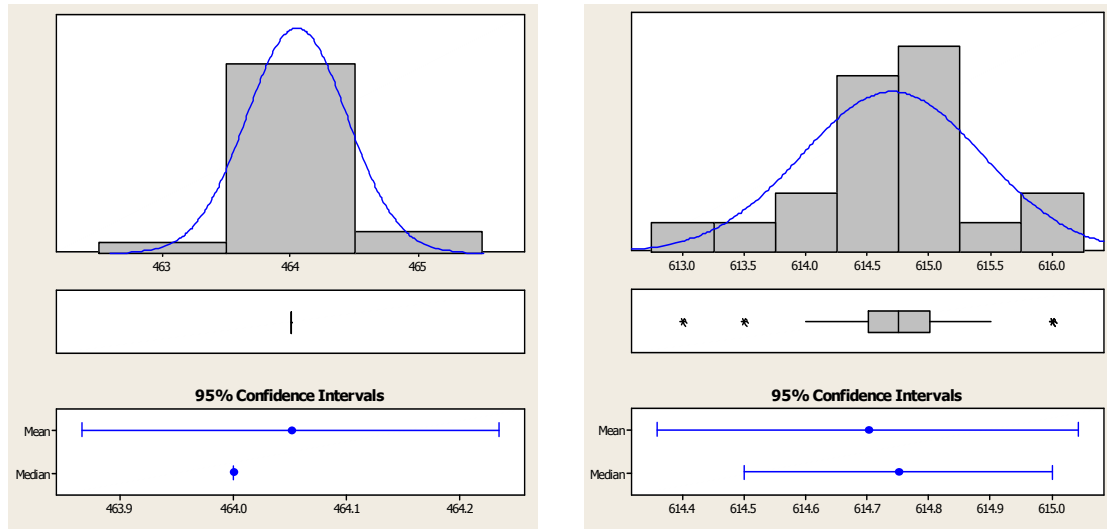


**Figure 76 Investigation into changes in the peak excitation and emission wavelengths for europium in glass 2 samples**

Terbium had a mean peak excitation at 483.30 nm with a standard deviation of 0.73nm and a mean peak emission at 545.08 nm with a standard deviation of 0.85nm, Figure 77.

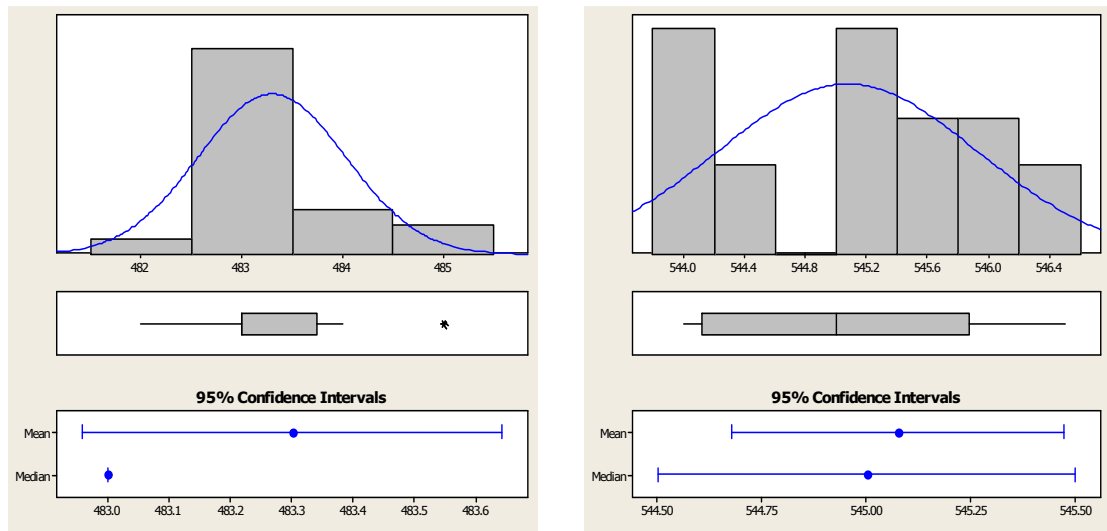


**Figure 77 Investigation into changes in the peak excitation and emission wavelengths for terbium in glass 2 samples**

Dysprosium had a mean peak excitation at 451.95 nm with a standard deviation of 0.39nm and a mean peak emission at 575.83 nm with a standard deviation of 1.23nm, Figure 78.

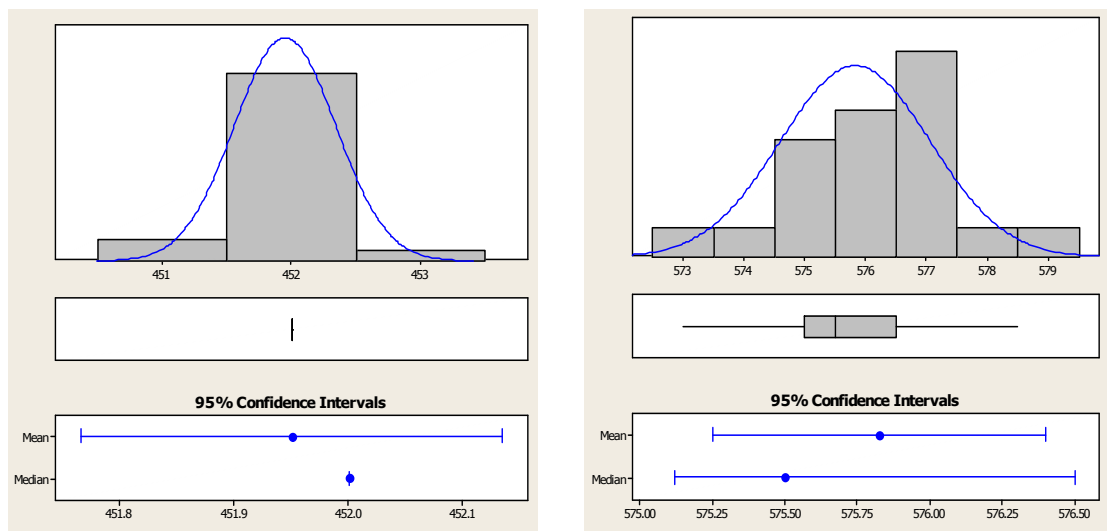


**Figure 78 Investigation into changes in the peak excitation and emission wavelengths for dysprosium in glass 2 samples**

#### **4.4.4** *Conclusions of borosilicate glass 1 and glass 2*

##### **4.4.4.1** Peak wavelength variations

For all of these results in the 25 glass 1 and 25 glass 2 multi doped samples, the peak emission and excitation wavelengths were very consistent with small standard deviations of between 0.2 to 0.75 nm for glass 1 excitation and 0.39 to 0.73 nm for glass 2 excitation; and 1.06 to 1.37 nm for glass 1 emission and 0.73 to 1.23 nm for glass 2 emission. This means that a confident measurement of concentration of the dopants based on their emission peak wavelength should be readily achieved with a suitable detector system. However the addition of NaF to the matrix has not significantly changed the peak wavelengths to distinguish between the two glass matrices by wavelength although NaF should allow higher concentrations of dopants to be added. This means that addition of the small amount of NaF is an insufficient change to create a whole new set of tracers. However the addition of NaF had the effect of reducing the glass melt temperature which resulted in the glass being less viscous and so easier to work with when poured at 1250°C.

##### **4.4.4.2** Spectral Characterisation

Overall the glass 2 data showed that generally the peak intensity was proportional to the concentration of the lanthanide dopant with differences of 0.1 mol% concentration changes generating measurable changes in peak intensity. The data also showed that some significant interactions between the lanthanide dopants occurred just as with the glass 1 samples leading to an even wider range of useful tracer fluorescent peaks. They also showed useful long lifetime characteristics as with the glass 1 samples which can allow discrimination of the glass peaks of interest from background molecular fluorescence interference.

It can be seen that by altering the chosen lanthanide dopant, number of dopants, dopant concentration and using selective excitation and emission wavelengths there are a huge number of possible unique tracer combinations.

#### 4.5 Lanthanide Glass Tracer Comparison with Existing Molecular Dye Tracers:

A single line scan of the discrete fluorescent emission from a Europium glass 1 tracer is shown in Figure 79, and shows a FWHM spectral bandwidth of 12 nm. By comparison, Figure 80 and Figure 81, show the commonly used molecular dyes Fluorescein and Rhodamine displaying broader FWHM spectral bandwidths of approximately 50 nm and 60 nm.

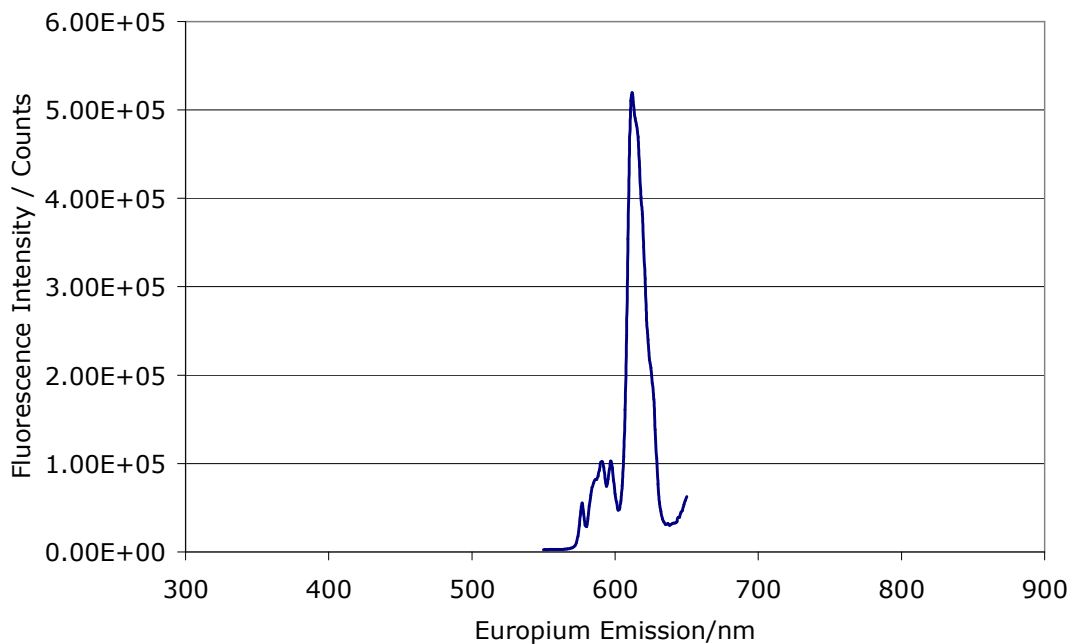


**Figure 79 Fluorescent emission from europium doped bulk glass from a 465 nm excitation**

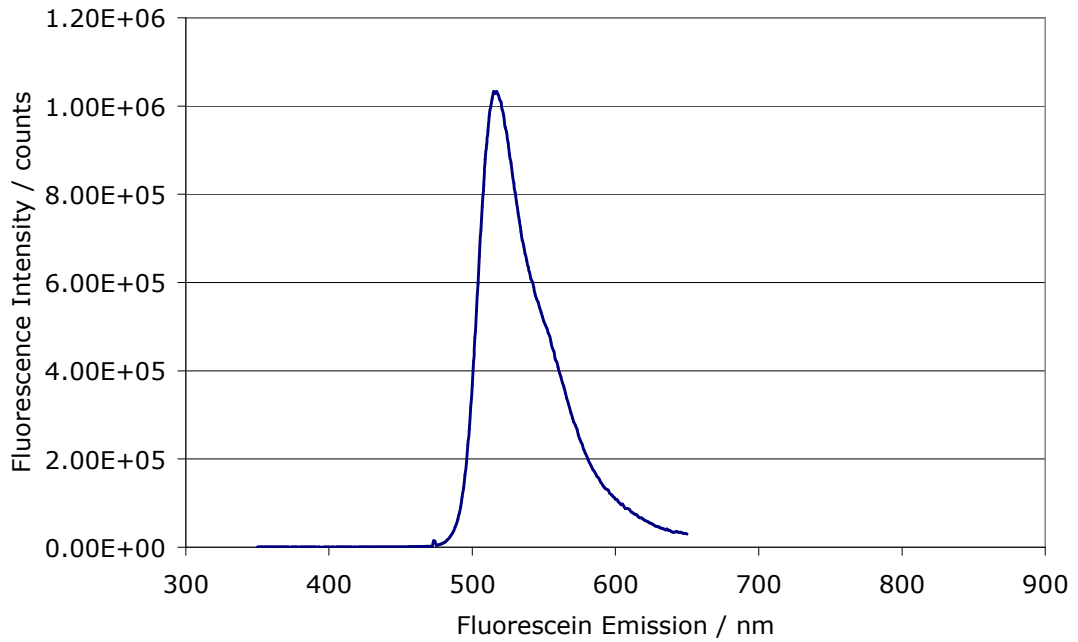


**Figure 80 Fluorescent emission from a Fluorescein dye tracer from a 475 nm excitation**

The significantly narrower bandwidth emission peaks of the lanthanides achieve a more selective detection of multiple tracers without interference from overlapping emissions. Thus giving the potential to selectively simultaneously monitor many different tracer combinations in the same location, this would not be possible using broad bandwidth molecular dye tracers.

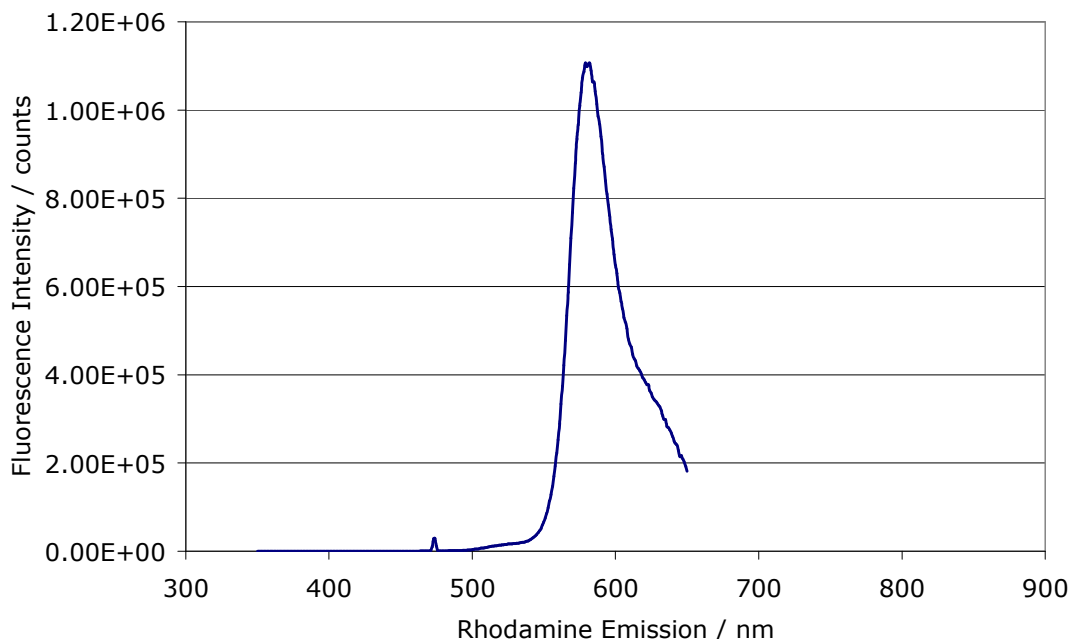


**Figure 81 Fluorescent emission from Rhodamine dye tracer from a 475 nm excitation**

#### **4.5.1 Glass Tracer Particles**

To produce tracer particles from bulk glass, the glass samples were broken into 3-5 mm pieces and repeatedly ball milled and sieved down to <5  $\mu\text{m}$ . The size ranges of <5  $\mu\text{m}$ , 5-10  $\mu\text{m}$ , 10-20  $\mu\text{m}$ , 45-75  $\mu\text{m}$  and a bulk sample were analysed to determine the effect of particle size on the fluorescent emission, shown in Figure 82. The bulk sample (dark blue plot) shows a peak emission of 612 nm, as does the 45-75  $\mu\text{m}$  (pink plot). This peak emission appears to shift toward a maximum of 609 nm and there is also an increasing emission peak of 600 nm. This is most likely due to scattering effects of the glass particles, with the decreasing glass particle size, which also causes an increased background signal. As the glass particles reduce in size the random nature of their shape and surface quality directly effects a reduction in excitation signal and the reduction observed in emission signal.

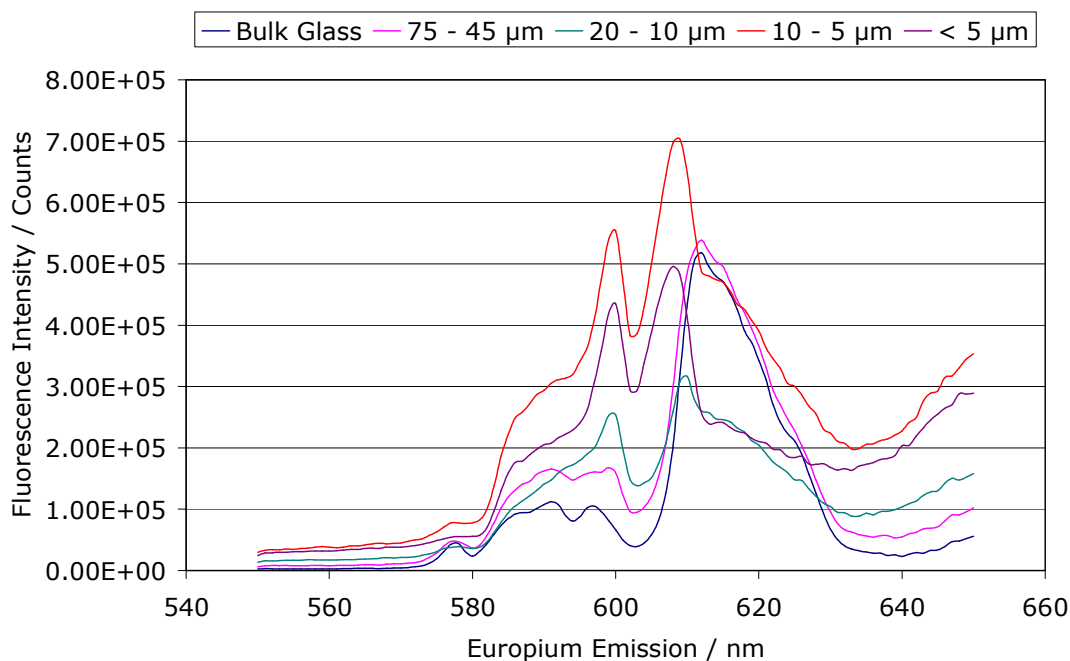


**Figure 82 Comparison of emissions from 3 mol % europium doped glass 1 matrix, bulk sample, <5  $\mu\text{m}$ , 5-10  $\mu\text{m}$ , 10-20  $\mu\text{m}$  and 45-75  $\mu\text{m}$  powder from a 393 nm excitation.**

#### 4.6 Inorganic Polymers - Sol Gel Spheres

To overcome the deterioration in fluorescent emission from the glass tracer particles, and to provide a wider range of environmental tracers, it was proposed to make another range of tracers. The proposal is to use silica sol gel spheres to replace the borosilicate glass as the host matrix of the lanthanide fluorescent species. The use of a methodology which would not only produce <5 $\mu\text{m}$  particles easily, but could be doped with an organic lanthanide species, could produce highly fluorescent particles.

##### 4.6.1 Undoped Inorganic Polymer Silica Sol Gel Spheres

Following the Stöber method for silica sol gel spheres preparation, outlined in Chapter 3, samples of highly spherical particles were produced. Figure 83 shows an SEM image of the spheres produced, where the uniformity of the silica spheres can be seen, with a particle size of 500 nm. By altering the ratio of

base catalyst (ammonium hydroxide), to the organosilicate precursor (TEOS), will vary the size of sphere produced.

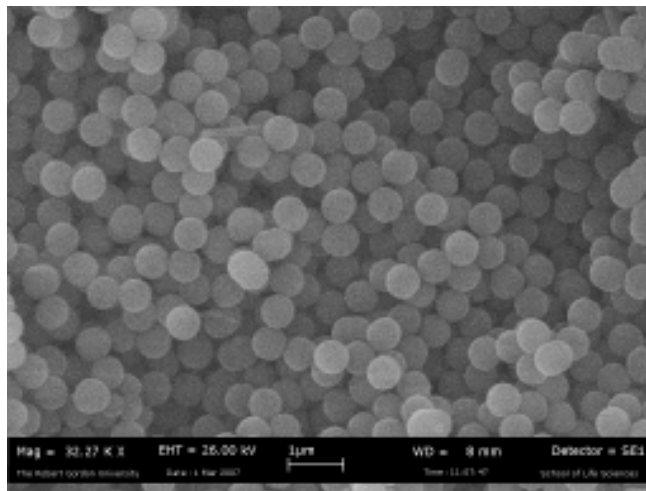


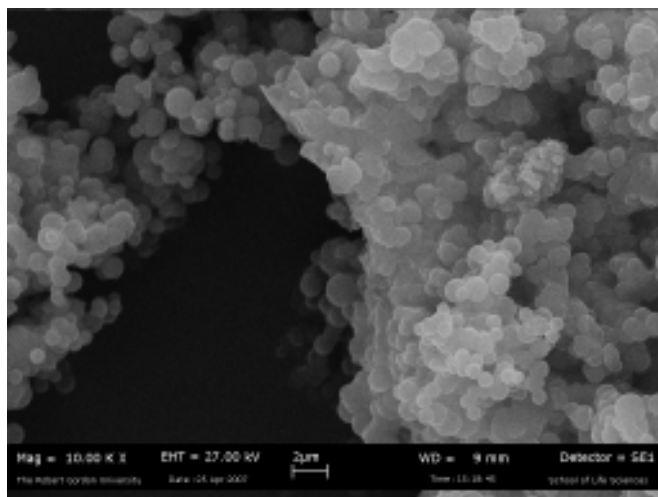
**Figure 83 Undoped silica sol gel spheres**

#### **4.6.2 Doped Inorganic Polymer Silica Sol Gel Spheres**

##### **4.6.2.1 Spectroscopy Analysis of Eu[ttfa][phen] Beads**

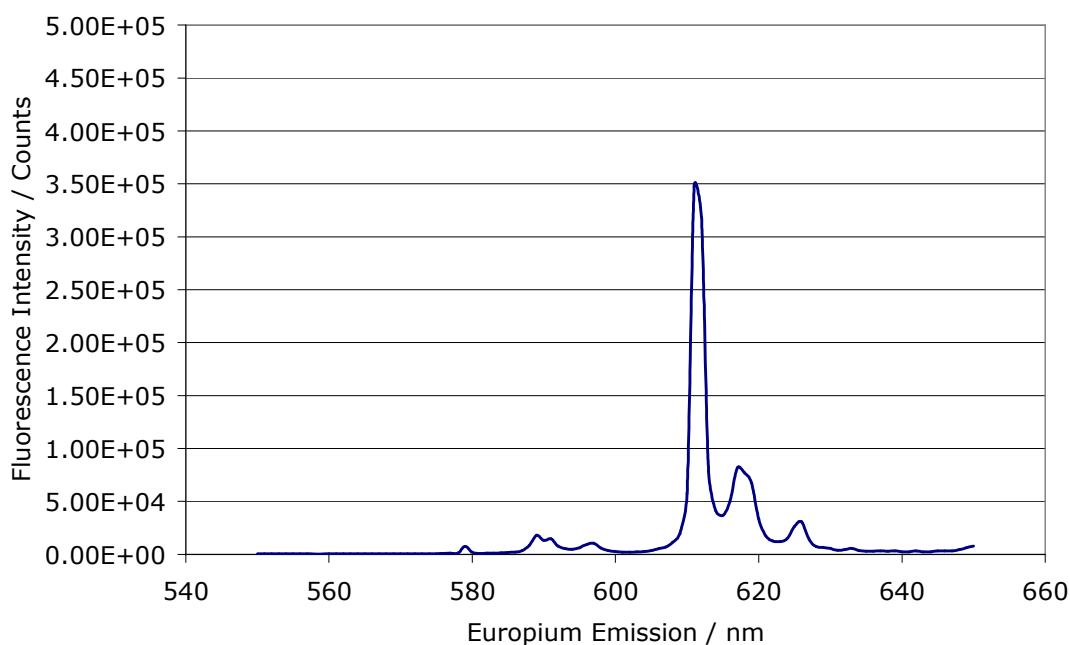
The initial investigation of all the Europium chelate doped sol gel spheres was a visual assessment under UV light. If the sample emitted a bright red/pink glow it was a strong indication the combination of sol gel process and chelate had been successful. The particles produced can be seen in Figure 84 which shows spherical particles and also more amorphous particles.





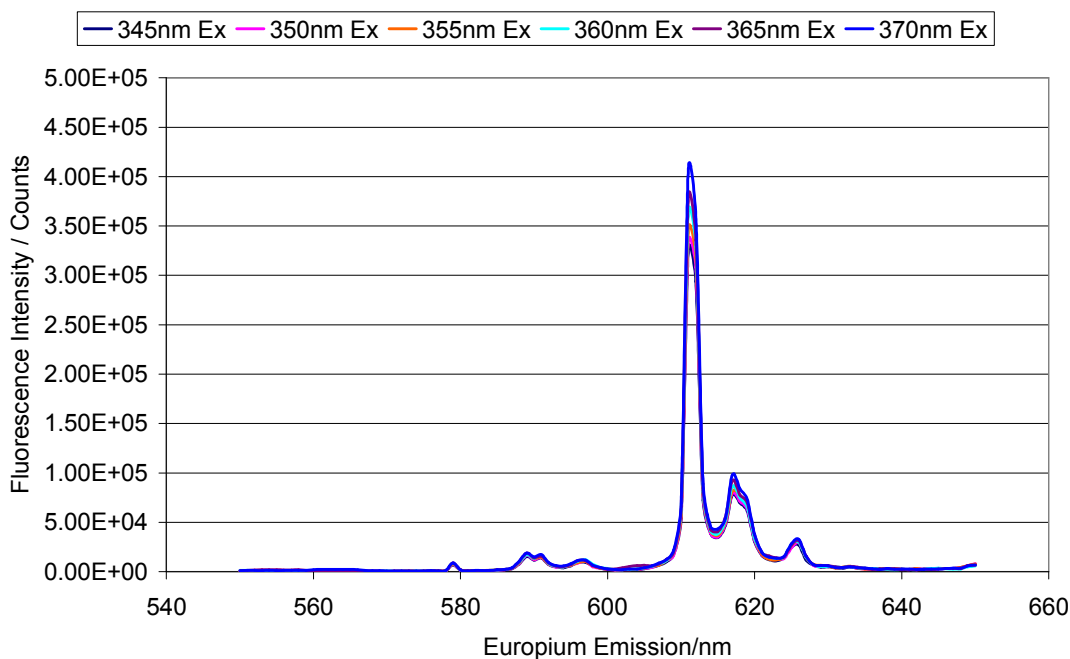
**Figure 84: Doped silica sol gel spheres**

Figure 85 is an example of an emission spectrum obtained from an Eu[ttfa][phen] sol gel sphere sample. The high definition of emission lines at 612 nm, 617 nm and 626 nm is due to the more crystal structure of the lanthanide ion within the chelate/silica matrix.



**Figure 85 Emission Spectra from Eu[ttfa][phen] doped Silica Sol Gel 200 nm sphere from 355 nm excitation.**

A study of a range of excitation wavelengths in the UV region, across the chelate absorption band, was undertaken to establish which gave the most intense emission for the 612 nm line. Figure 86 shows the multiple emission spectra from a range of excitation wavelengths from 345 nm, 350 nm, 355 nm, 360 nm, 365 nm and 370 nm.



**Figure 86 Emission Spectra from Eu[tfa][phen] doped Silica Sol Gel 200 nm Spheres from 345, 350, 355, 360, 365 and 370 nm excitations.**

Figure 87 shows the 612 nm emission intensity increasing through this range; 345 nm to 370 nm. The most intense emission was obtained from a 370 nm excitation, but this may not be a concern if a broader band UV excitation source is utilised.

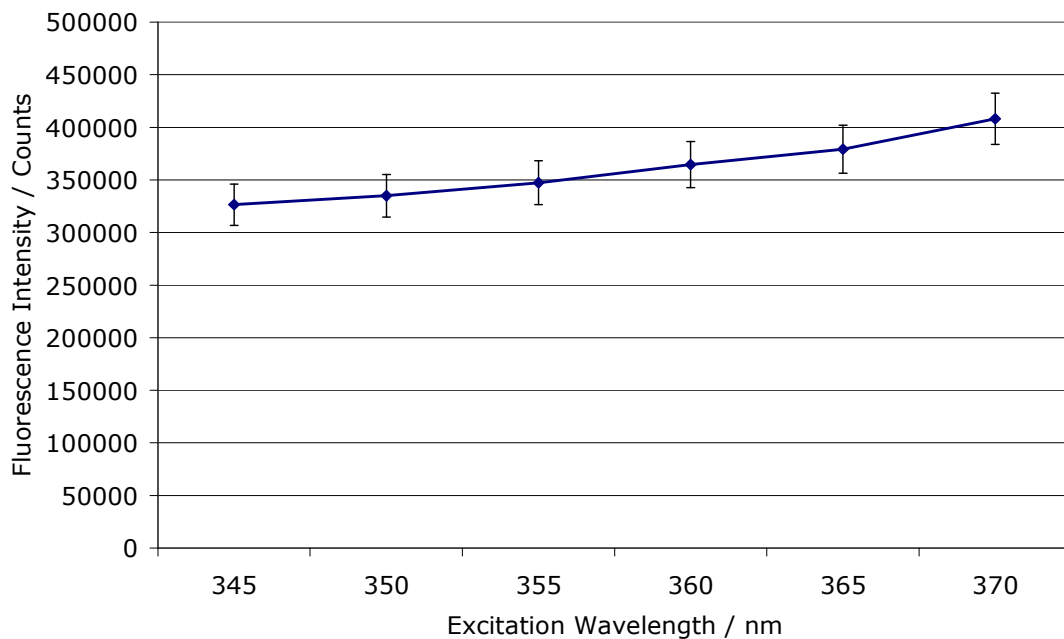


**Figure 87 Peak Intensity variations at 612 nm emission from 345, 350, 355, 365 and 370 excitations from Eu[ttfa][phen] Silica Sol Gel Spheres.**

#### 4.6.3 Fluorescent lifetime study of europium chelate in inorganic polymer sol gel

A typical normalised fluorescence pulse from Eu[ttfa][phen] doped in an inorganic polymer sphere, for 355 nm laser excitation and fluorescence emission at 615 nm (filtered through an interference filter with transmission peak at 620 nm and bandwidth of 10 nm) is shown in the Figure 88. It shows a fast rising pulse with a long exponentially decaying tail corresponding to the long fluorescence lifetime of the europium.

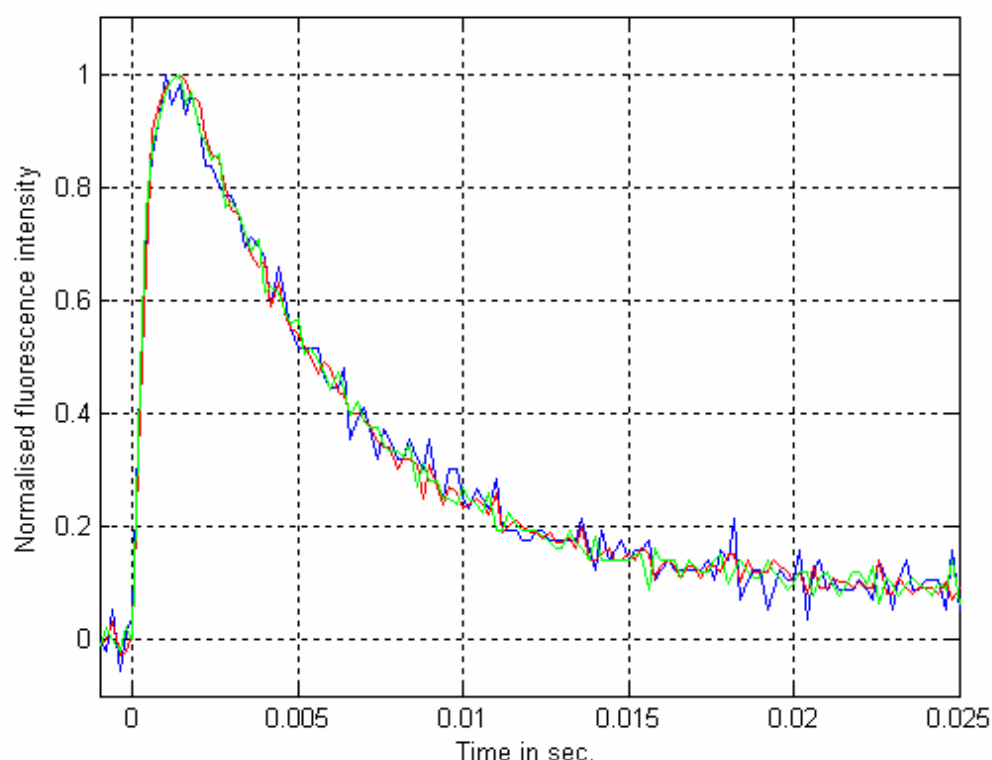


**Figure 88 Fluorescence lifetime profiles of 1 wt % Eu[ttfa][phen] in inorganic polymer**

The lifetime was calculated based on single exponential fluorescence decay and the characteristic lifetime constant of the exponential curve as the fluorescent lifetime of the particular lanthanide ions. From each sample, three data sets were used to calculate an average fluorescent lifetime of Europium and this sample shows an average lifetime of  $1.14 \text{ ms} \pm 0.11 \text{ ms}$ . When this is compared to the 1.95 ms obtained from a europium doped borosilicate glass

sample, the Eu[ttfa][phen] doped inorganic polymer exhibits a lifetime measurably quicker. This lifetime difference could be utilised as a distinguishing feature for tracer applications.

#### **4.7 Blank Organic Polymer Spheres**

To investigate the formation of polymer spheres a series of experiments was carried out to determine the control parameters for the production of 50 – 500 nm diameter spheres. The morphological effect which doping these spheres was unknown, so several different formulations were examined using the following monomers; ethyleneglycol dimethacrylate, methacrylic acid and divinyl benzene.

##### **4.7.1 Organic Polymer Poly-EGDMA-co-MAA Spheres**

Undoped poly-EGDMA-co-MAA spheres were analysed under the SEM and Figure 89 shows an example of the spherical particles produced. The particles are seen to be around 100 nm in diameter which is significantly smaller than the sol gel particles. The particles are also “agglomerated” together which could potentially cause problems when trying to accurately produce a range of tracers with controlled size.

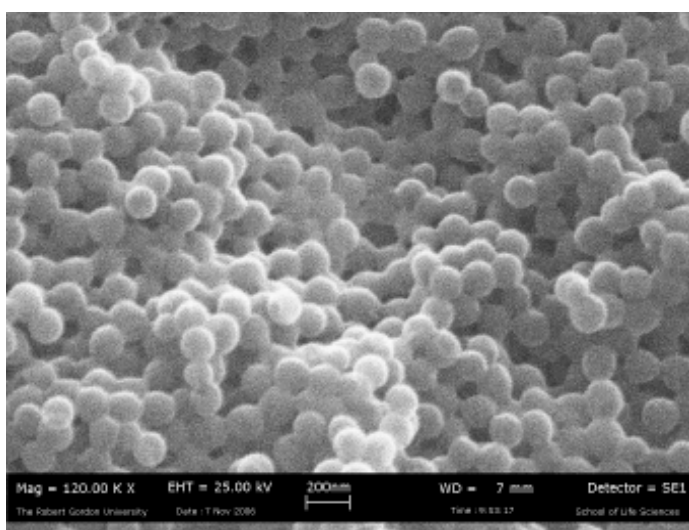


**Figure 89 Blank poly-EGDMA-co-MAA**

#### **4.7.2 Organic Polymer Poly-EGDMA-co-HEMA**

Undoped poly-EGDMA-co-HEMA spheres were analysed under the SEM and Figure 90 shows an example of the agglomerated particles produced. These did not produce particles as easy to define as the poly-EGDMA-co-MAA and also appears to contain a higher portion of excess polymer which is undesirable.

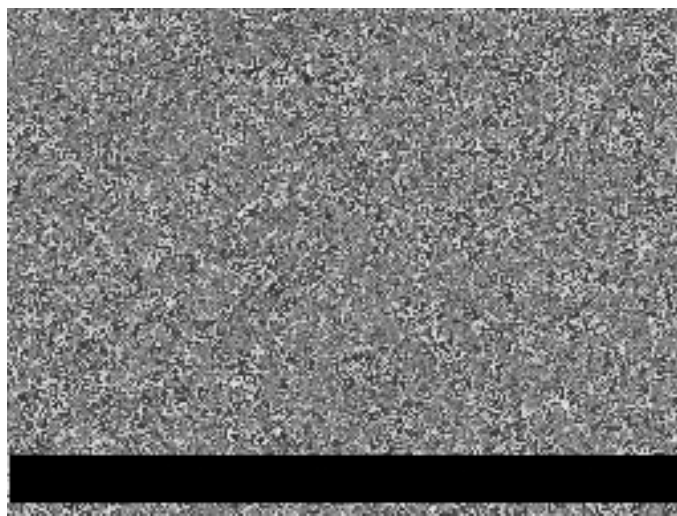


**Figure 90 Blank Poly-EGDMA-co-HEMA spheres**

#### **4.7.3 Organic Polymer Poly-MMA**

The Undoped poly-MMA particles seen in Figure 91 show a far better morphology than previous polymer samples. There is no agglomeration visible and there are clearly defined single particles of polymer. The particles are 400 nm in diameter and there appears to be very little variation of size.

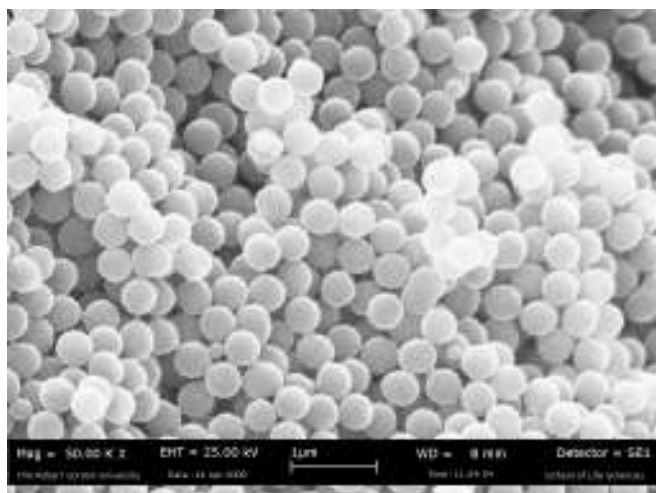


**Figure 91 Blank poly-methacrylic acid spheres**

#### **4.7.4 Doped Polymer Spheres**

After several attempts to produce doped polymers of varying composition it was decided to focus on one formulation. Although poly-MMA has a more reproducible morphology when undoped, the yield is poor compared to that of poly-EGDMA-co-MAA and Poly-EGDMA-co-HEMA. Based on morphology when doped, poly-EGDMA-co-MAA, when compared to other formulations was more productive with good sphere formation. The change in morphology may relate to the manner in which the lanthanide chelate interacts with the polymerisation reaction and influence the spherical formation.

##### **4.7.4.1 Organic Polymer Poly-EGDMA-co-MAA doped with Eu[ttfa][phen]**

The production of doped poly-EGDMA-co-MAA particles with Eu[ttfa][phen] was expected to generate an amorphous mass of spherical particles similar to that seen in the Undoped SEM image. Figure 92 shows the SEM image obtained and the particles found were 200 nm in size and far more individual. The spheres produced are far more regular in appearance than even the undoped spheres. Spectroscopy analysis and characterisation was undertaken to determine

whether the doping process with the incorporation of chelated lanthanide molecules within the polymer matrix had been successful.

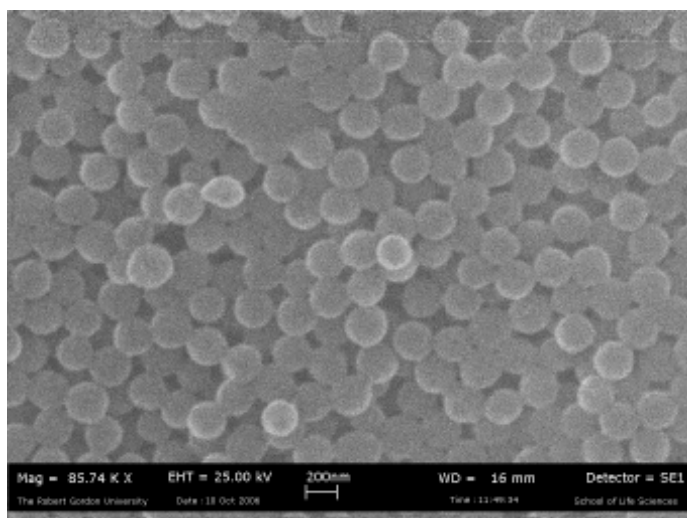


**Figure 92 SEM image of Eu[tffa][phen] poly-EGDMA-co-MAA spheres**

A fluorescence emission plot from a sample of Eu[tffa][phen] is shown in Figure 93, obtained with an excitation of 355 nm.

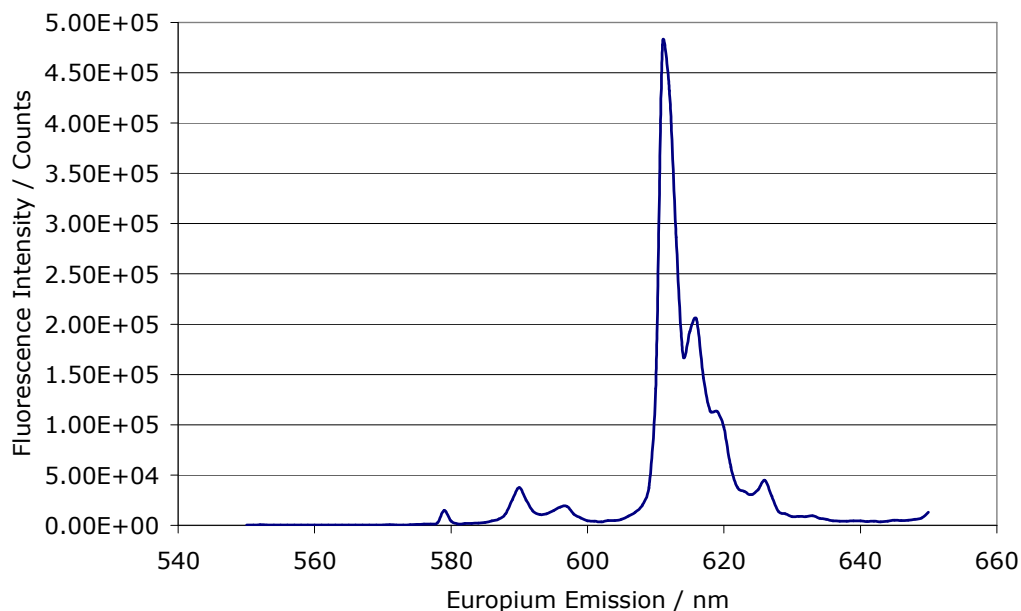


**Figure 93 Emission Spectra of Eu[tffa][phen] doped EGDMA-co-MAA polymer spheres from a 355 nm excitation.**



A study of a range of excitation wavelengths across the chelate absorption band was undertaken to establish the most intense emission for the 611 nm line, the same parameters and settings as for the silica sol gel spheres. Figure 94 shows the multiple emission spectra from 345 nm, 350 nm, 355 nm, 360 nm, 365 nm and 370 nm. The most intense emission was obtained from a 355 nm excitation, which is the UV laser line from the Continuum Nd:YAG OPO Laser. This laser system could potentially be used as an excitation source for the samples as the pulsed laser will allow for low detection limits compared to a steady state UV source such as a Xenon lamp.

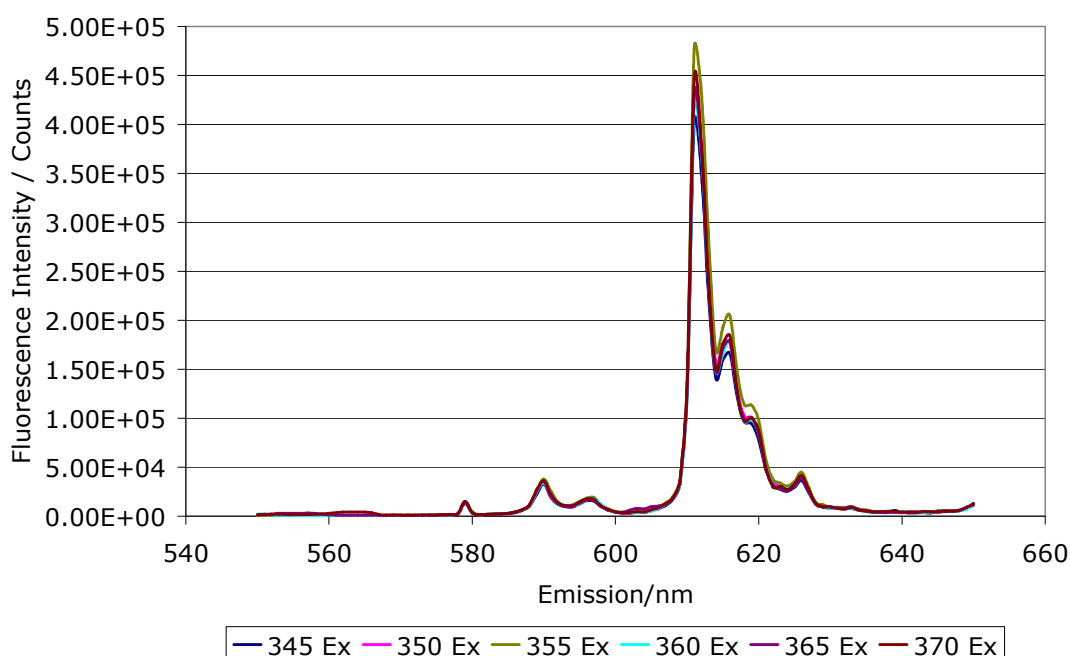


**Figure 94 Emission Spectra of Eu[ttfa][phen] doped EGDMA-co-MAA polymer spheres from 345, 350, 355, 360, 365 and 370 nm excitations.**

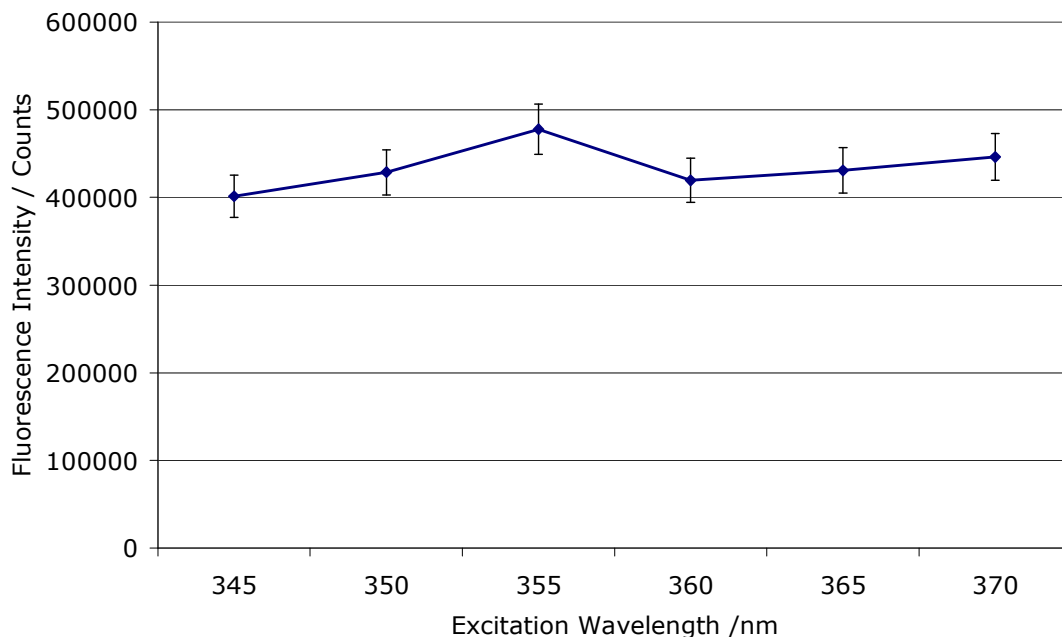


**Figure 95 Peak Intensity variations at 611 nm emission from 345, 350, 355, 365 and 370 excitations from Eu[ttfa][phen] Polymer Spheres.**

The peak emissions from the aforementioned excitation wavelengths can be seen in Figure 95. When compared with the peak intensity graph for the sol gel spheres, Figure 87 it can be seen that the emission across the range of 345 nm – 370 nm is extremely stable. This stability could provide extra excitation energy for heightened sensitivity at lower detection levels.

#### **4.7.5** *Fluorescent Lifetime Study of Europium Chelate in Polymer*

A typical normalised fluorescence pulse from Eu[ttfa][phen] doped in an organic polymer sphere, for 355 nm laser excitation and fluorescence emission at 615 nm (filtered through an interference filter with transmission peak at 620 nm and bandwidth of 10 nm) is shown in Figure 96. It shows a fast rising pulse with a long exponentially decaying tail corresponding to the long fluorescence lifetime of the Europium ion.

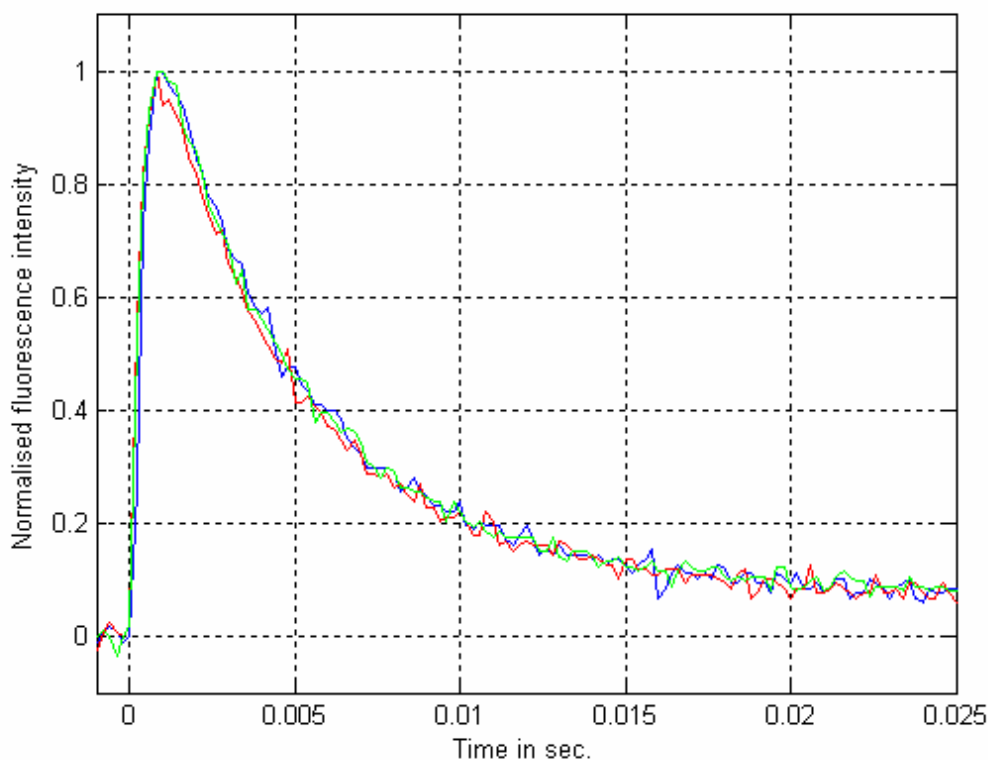


**Figure 96 Fluorescent lifetime profile of europium chelated ions in poly-EGDMA-co-MAA**

The lifetime was calculated based on single exponential fluorescence decay and the characteristic lifetime constant of the exponential curve as the fluorescent lifetime of the particular lanthanide ions. From each sample, three data sets were used to calculate an average fluorescent lifetime of europium and this sample shows an average lifetime of  $0.85 \text{ ms} \pm 0.11 \text{ ms}$ . When this is compared to the  $1.95 \text{ ms}$  obtained from a europium doped borosilicate glass sample, the  $\text{Eu}[\text{ttfa}][\text{phen}]$  doped organic polymer exhibits a lifetime twice as fast.

#### 4.8 Comparison Study

A comparison study was undertaken to examine the fluorescent emission of the europium doped bulk glass, europium doped glass powder, europium chelate doped silica sol gel spheres and europium chelate doped polymer spheres. Figure 97 shows the emission spectra from a 355 nm excitation for the sol gel and polymer and a 393 nm excitation for the glass with the same spectrometer settings. 393 nm was used as europium does not absorb 355 nm and would therefore produce no fluorescent emission at 612 nm.

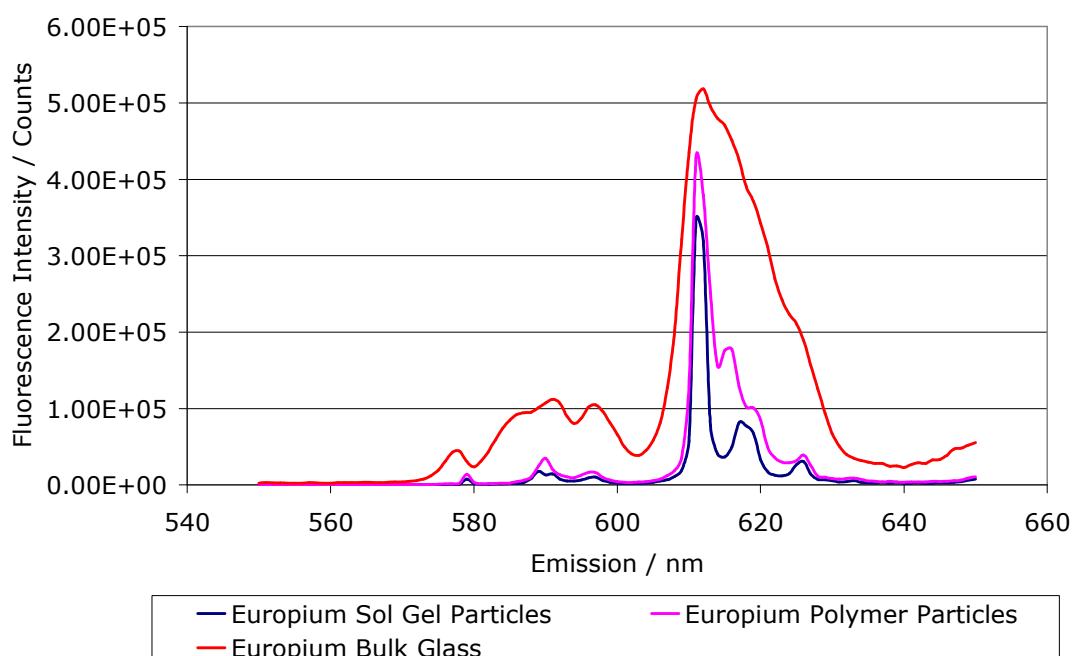


**Figure 97 Comparison of Eu[ttfa][phen] doped silica sol gel and poly-EGDMA-co-MAA at 355 nm excitation with bulk 3 mol % europium doped borosilicate glass at 393 nm excitation**

It can be seen that the sol gel and polymer emissions are narrower and more discrete than that of the doped glass emission spectra. Traditionally lanthanides are known for their discrete fluorescent emissions, and previous experience of lanthanide doped glasses has shown this to be the case. The resolution of 3

distinct emission peaks at 616 nm 619 nm and 626 nm with are normally indefinable in a doped glass emission can be clearly seen. This degree of peak resolution is normally found in crystalline structures containing lanthanide ions [135, 136]. However, the comparison of europium doped bulk glass with the chelate doped sol gel and polymer spheres can't be used for a direct comparison as one sample is solid glass and the others are 500 nanometer sized particles.

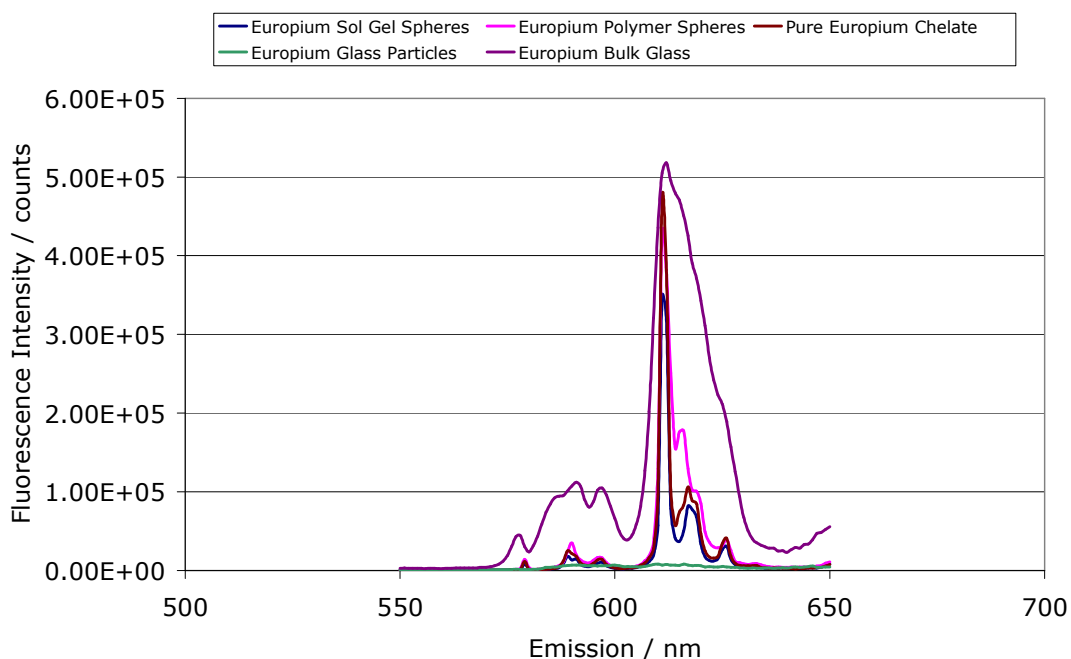


**Figure 98 Comparison of 612 nm fluorescence emission from europium doped bulk glass, glass powder, doped chelate, doped polymer and doped sol gel.**

For a valid comparison it is necessary to examine the smallest fraction of ball milled glass powder, the 5  $\mu\text{m}$ , with the sol gel and polymer powder. Using the same instrument settings samples of pure europium doped chelate, doped sol gel sphere, doped polymer spheres, doped bulk glass and doped ball milled glass are plotted together, Figure 98. From this figure it can be seen that the fluorescent emission from europium doped glass powder is much smaller than that of the parent bulk glass sample.

It can be seen from Table 26 that the 5  $\mu\text{m}$  europium sample has a 98.5 % weaker fluorescent emission than the bulk glass sample.

<b>Europium Sample</b>	<b>Fluorescence Intensity / counts</b>	<b>Percentage Difference to Bulk Glass Emission / %</b>
Bulk Glass	518200	0
5 $\mu\text{m}$ Glass Powder	7618	98.5
Pure Europium Chelate	381900	26.3
Europium Chelate Doped Sol Gel	379500	38.4
Europium Chelate Doped Polymer	318700	26.7

**Table 26 Fluorescence emission intensities for 612 nm**

For use as an environmental tracer, the intensity of the fluorescent signal which was found from the glass powder, would limit its application compared to the doped sol gel and doped polymer spheres.

## 4.9 Tracer Detection

### 4.9.1 Bench Top Detection System – Glass Tracer

The tracer detection system developed for the trial investigation utilised a pulsed 532 nm laser as the excitation source with an optical fibre collector coupled to an avalanche photodiode, fitted with a 10nm band pass filter at 610nm for europium fluorescence as shown in Figure 99. To replicate the process of scanning the sea bed from a moving vessel or a towed sledge, the small tank was placed on an X-Y moving stage the coarse sediment was scanned past the fixed excitation and detection system.

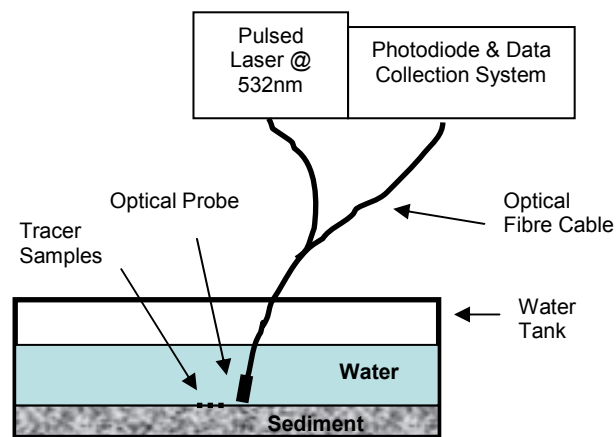


**Figure 99 Schematic of Tracer Detection System Trial**

To demonstrate the potential for using lanthanide doped glass as an environmental tracer a real time detection study was undertaken. The tank contained a North Sea sediment "sea bed" where a europium glass tracer was used. Figure 100 shows a 3D fluorescence map observed for one deployment of tracer, clearly observed in 3 locations in the tank.

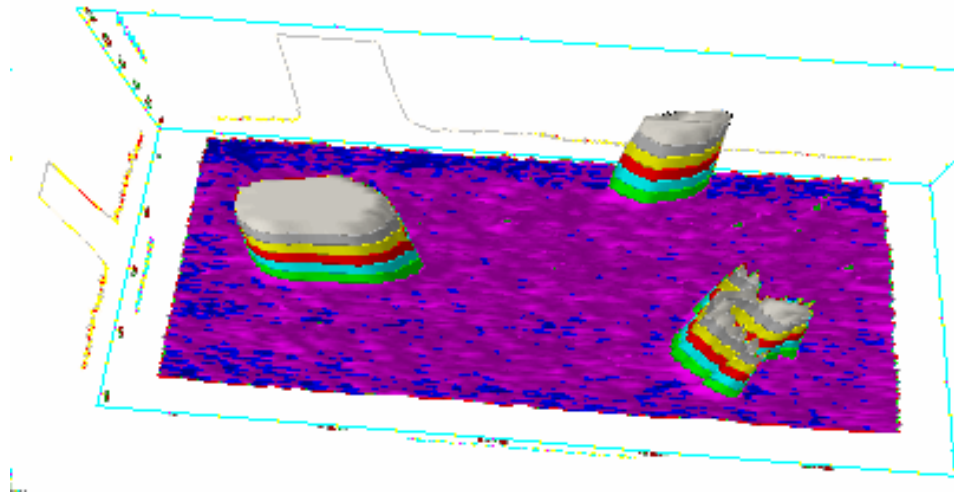


**Figure 100 Surface projection fluorescence map of europium glass tracer on a coarse sediment bed**

Table 17 showed the optimum excitation wavelengths for europium, the excitation used for this experiment was 532 nm which has low quantum efficiency for the europium ion. Even with the lower excitation energy, the detection system shows a slight saturation from one of the doped patches. This preliminary investigation suggests that it should be possible to attain even lower detection limits because there will be an increased quantum efficiency gain when the optimum 465 nm source is used, as opposed to the source that was available for this laboratory trial.

## **4.10 Background Discrimination**

### **4.10.1 Fluorescence Lifetime for Background Discrimination**

A typical normalised fluorescence pulse from europium in the tracer sample, for 465 nm laser excitation and fluorescence emission at 615 nm (filtered through an interference filter with transmission peak at 620 and bandwidth of 10 nm) is shown in Figure 101. It shows a fast rising pulse with a long exponentially decaying tail corresponding to the long fluorescence lifetime of the europium.



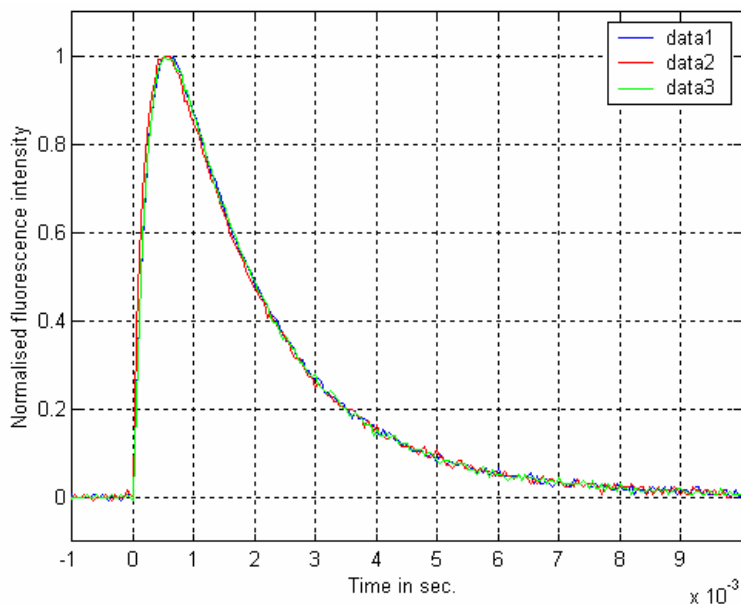


**Figure 101 Fluorescent lifetime profile of europium ions in borosilicate glass**

The lifetime is calculated based on single exponential fluorescence decay and the characteristic lifetime constant of the exponential curve as the fluorescent lifetime of the particular lanthanide ions. Three data sets were used to calculate an average fluorescent lifetime of europium and this sample had an average lifetime of 1.95 ms. The fluorescent lifetime of fluorescein is typically in the region of 4 ns. This is very important because it clearly demonstrates the huge difference in lifetime between an atomic fluorescence peak i.e. Europium and molecular fluorescent lifetimes. Using time gated detection the presence of naturally occurring background fluorescence signals and signals from previously deployed molecular dye tracers can be discriminated against. For example an efficient discrimination against these unwanted signals could be achieved by only measuring the fluorescent signal emitted 1  $\mu$ s after the excitation pulse up to 1 ms. This gives a significant advantage to the use of the lanthanide elements atomic fluorescent tracers in environmental monitoring.

#### **4.10.2**      *Background discrimination of the presence of contaminants*

A great advantage derived from using lanthanide ions for environmental tracing applications (or any tracing application) is the ability to easily discriminate between background signals and tracer signals.

In marine or even river environments it is common to find traces of hydrocarbon contamination from industrial sources. Figure 102 shows the fluorescent emission peak for a sample of Gullfaks crude oil with Figure 103 showing the emission peak for a sample of Brent crude oil.

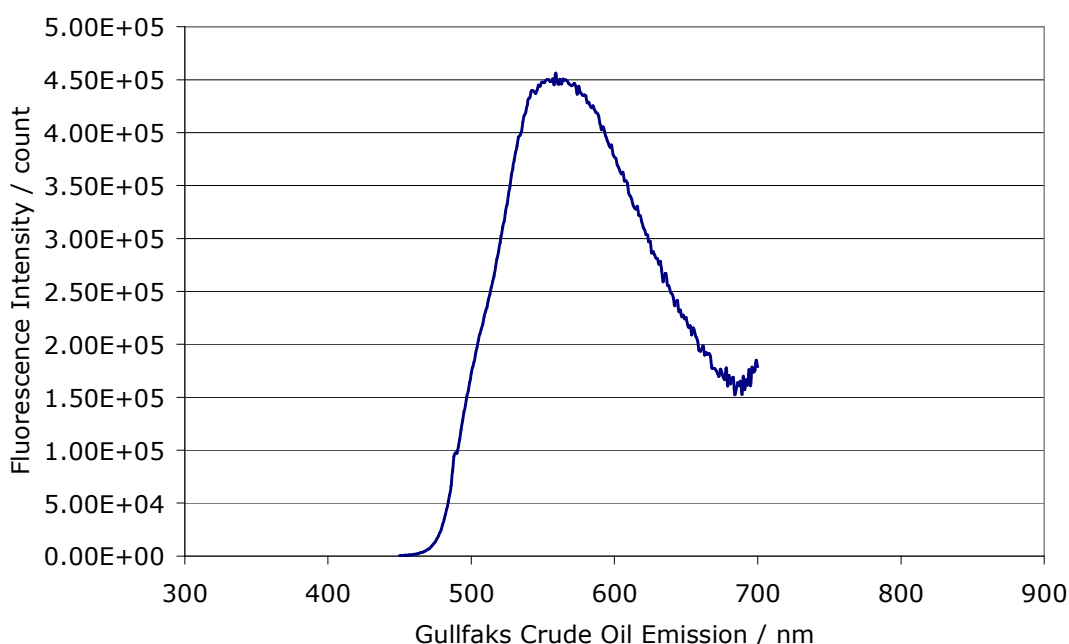


**Figure 102 Fluorescence emission from Gullfaks crude oil from a 490 nm excitation**

Although from off-shore production oil fields; Gullfaks Location: block 34/10 northern North Sea off Norway, Brent Location: block 211/29 between Shetland and Norway, both provide a classic hydrocarbon fluorescence profile.

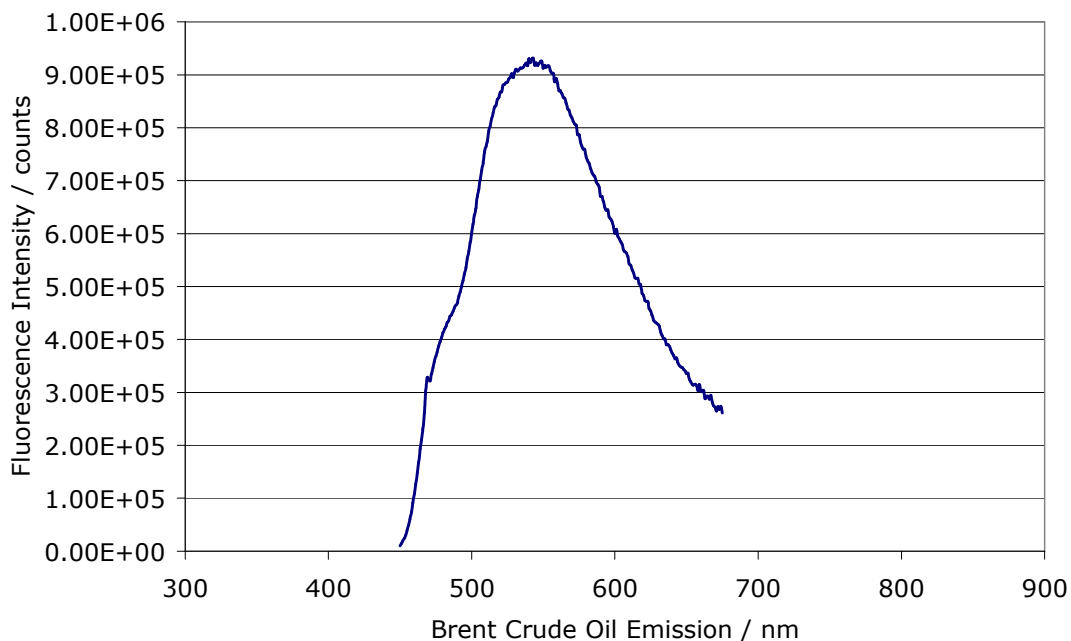


**Figure 103 Fluorescence emission from Brent crude oil from a 470 nm excitation**

#### **4.10.3**      *Background Discrimination Conclusion*

The use of lanthanide doped tracers for environmental applications provides a method for performing tracing studies in areas which contain multiple background fluorescent contaminants. The unique discrete fluorescent signals produced by the lanthanide dopants allow for discrimination between various background sources exhibiting broadband fluorescence, e.g. hydrocarbons. The presence of compounds which may fluoresce are highly likely in waste water streams or marine environments.

An additional feature to using lanthanides in tracing studies is the possibility of using fluorescence lifetime as a discrimination method. The atomic fluorescence lifetimes of lanthanide ions are in the millisecond range, compared to that of molecular fluorescence which is in the range of nanoseconds. Using time gated detection the presence of naturally occurring background fluorescence signals and signals from previously deployed molecular dye tracers can be discriminated against.

#### **4.11 Overall Results and Discussion Summary**

25 samples containing different concentrations of the lanthanides europium, dysprosium and terbium in the glass host matrix glass 1 were successfully made. 25 samples containing different concentrations of the lanthanides europium, dysprosium and terbium in the glass host matrix glass 2 were successfully made.

A large number of narrow lanthanide excitation and emission peak wavelengths are available to choose from as environmental tracer response peaks.

There is a very strong relationship between lanthanide concentrations and emission peak intensities. This means that different environmental tracer combinations can be achieved by altering the concentrations of the lanthanide dopants in the glass matrix. The data indicates the possibility that 0.1 mol % concentration differences could be utilised to produce multiple different tracer combinations.

The addition of NaF to the matrix has not significantly changed the peak wavelengths to distinguish between the two glass matrices by wavelength. This means that addition of the small amount of NaF is an insufficient change to create a whole new set of environmental tracers.

Further unique tracers should be achievable as additional excitation/emission peak wavelengths previously forbidden are observed due to energy transfer (sensitisation) of certain combinations of lanthanides.

Long lifetime characteristics can be used as one of the background discrimination features for the environmental tracer in the glass matrix.

For all of these results in the 25 glass 1 and 25 glass 2 samples, the peak emission and excitation wavelengths were very consistent with small standard deviations of between 0.2 to 0.75 nm for glass 1 excitation and 0.39 to 0.73 nm for glass 2 excitation; and 1.06 to 1.37 nm for glass 1 emission and 0.73 to 1.23 nm for glass 2 emission. This means that a confident measurement of

concentration of the dopants based on their emission peak wavelength should be readily achieved with a suitable detector system.

Overall this work shows that a very large number of unique environmental tracers can be obtained by varying the concentration and number of lanthanide dopants in a glass host.

The production of tracer sized glass particles however from the doped glass showed a decreased in the intensity of the fluorescent signal, 98.5% from a bulk sample to  $<5 \mu\text{m}$  particles. The process of producing glass particles and the randomization of the surfaces created greatly diminished excitation and emission efficiency. This would greatly limit its application as an environmental tracer as the huge reduction in fluorescent emission makes it extremely hard to detect in the field.

The investigation of organic and inorganic polymer lanthanide doped spheres to overcome the fluorescence decrease observed in the production of glass particles produced reproducible particles of a  $<800 \text{ nm}$  size.

The combination of organic chelates with the lanthanide ions created highly fluorescent species, which when doped in to the organic and inorganic spheres, produced particles an order of magnitude more fluorescent.

The use of lanthanide doped tracers for environmental applications provides a method for performing tracing studies in areas which contain multiple background fluorescent contaminants. The unique discrete fluorescent signals produced by the lanthanide dopants allow for discrimination between various background sources exhibiting broadband fluorescence, e.g. hydrocarbons. The atomic fluorescence lifetimes of lanthanide ions which are in the millisecond range, compared to that of molecular fluorescence which is in the range on nanoseconds, further allows discrimination. Using time gated detection the presence of naturally occurring background fluorescence signals and signals from previously deployed molecular dye tracers can be discriminated against.

## 5 CASE STUDY – BOWMORE HARBOUR FEASIBILITY STUDY

### 5.1 Introduction: The Proposed Scheme of Work

The Bowmore Harbour Improvement Association (BHIA) wanted to understand the mechanisms which contributed to the sedimentation, Figure 104, of the harbour. The opportunity to undertake a sediment particle study was important for the development of novel tracers as the work provided real world particle size data, as well as providing an area for future detection system deployment.

It was suggested that the sedimentation problem was largely driven by the strong west-going tides that flow past Lochindaal's entrance to the Irish Sea, colliding with the submerged rocks that make up a continuation of the Rhinns of Islay, and that these flows will induce a clockwise circulation at the head of the loch. This combined with wave and wind action may contribute significantly to the sedimentation process.



**Figure 104 Bowmore Harbour showing silting**

The original harbour was itself modified for military use during the Second World War. The harbour wall was extended to its current stature and the breakwater was added. Early photographs (late 1800's early 1900's) of the harbour show large ships docked which suggests the depth of water to be good.

It has been noted that the head of Lochindaal has indeed been becoming shallower over the years. A depth chart dating from the early 1900's of the area indicates the degree to which sedimentation has occurred, with some points having a 6-8 foot difference. This shows that there has been a natural sedimentation process occurring over the past 100 years, so the sedimentation problems are not limited to just the harbour.

The degree to which the harbour had become silted can be seen in the photographs taken prior to the 2000 clearing, Figure 105, where at low water the entire harbour area is above sea level.



**Figure 105 Images of Bowmore Harbour at low tide, prior to the 2000 clearing**

The proposed study was to sample water and sediment around Lochindaal and Bowmore Harbour. The sediment samples would give an indication of the average particle size in each location with the water samples giving an indication of the suspended material particle size. Although suspended materials can be flocculation particles which would give a larger particle size than the particles which are part of the floc. The particle size distribution data gathered could then be utilised by producing a tailor made glass, sol gel of polymer particle which could be fabricated to accurately mimic the naturally occurring sediments.

The commonly used definitions and sizes of particles found are:

1. Very coarse sand: 2.0 – 1.0 mm (2000 – 1000  $\mu\text{m}$ )
2. Coarse sand: 0.5 – 1.0 mm (500 – 1000  $\mu\text{m}$ )
3. Medium sand: 0.25 – 0.5 mm (250 - 500  $\mu\text{m}$ )
4. Fine sand: 0.1 – 0.25 mm (100 - 250  $\mu\text{m}$ )
5. Very fine sand: 0.05 – 0.1 mm (50 -100  $\mu\text{m}$ )
6. Silt: 0.002 – 0.05 mm (2- 50  $\mu\text{m}$ )
7. Clay: <0.002 mm (< 2  $\mu\text{m}$ )

Typically sedimentation (silting) occurs with particles in the 0.05 – 0.002 mm size range. The glass particles can be manufactured to have a particle size range from 2000  $\mu\text{m}$  - 20  $\mu\text{m}$  (very fine sand) and the sol gel and polymer to have 20  $\mu\text{m}$  – 100 nm.

## **5.2 Objectives of the Study**

1. To determine the tidal patterns in Loch Indaal and around the Bowmore harbour area which affect the movement of silt and sediment.
2. Investigate the practical steps which the Bowmore Harbour Improvement Association (BHIA) can take to keep the harbour as a valuable community asset by preventing silting which will lead to the harbour becoming unusable.
3. Investigate what effect the existing breakwater, and its outer section, has on the silting of the Harbour.
4. Recommend the most cost effective method of removing the existing sand and silt from the Harbour basin and disposing of it.
5. Investigate the most economical method of replacing the existing pontoons and mooring trots which are nearing the end of their useful life.



### 5.3 Materials and Methods

The planned practical work to study the sedimentation processes going on around Bowmore Harbour and Lochindaal was to sample both sediment and water from around the Loch. Michael MacNaughton kindly volunteered not only his time to assist, but also his boat "Jeanie Anne" as the research vessel for this study, Figure 106.



**Figure 106 Research Vessel Jeanie Anne**

The weather conditions on the day were to dictate strongly the distance travelled in the boat and also the amount of sampling done. Fortunately the weather was excellent the conditions were settled.

Plan of work:

- Sample around the circuit of Lochindaal, gathering both water and sediment at each sample site.
- Deploy tracer at points around the harbour entrance on an in coming tide
- Deploy tracer at points around the harbour entrance on an out going tide
- Gather sediment samples after tracer deployment

Figure 107 shows the route navigated during the sediment and water sampling run, the red dots indicate each point where a sample was taken and the smaller black dots indicate where a GPS data point was stored.

Table 27 details the GPS points where each sample was taken during the circuit of Lochindaal.



**Figure 107 GPS track plot of Lochindaal cruise from MapSource Version 6.11.6 Garmin Ltd.**

Unfortunately the Van Veen sampler was lost while gathering samples across the centre of Lochindaal at the end of the first circuit. This meant no further sediment samples could be collected and no sediment samples could be gathered after tracer deployment. Initially this was a cause for concern as the entire tracer deployment study may have had to be called off completely, but fortunately the calm conditions and the highly visible tracer proved useful without the need to sample sediment.

A full track detail of the course travelled during the sampling run can be found on **CD Appendix IV**.

<b>Sample</b>	<b>Date</b>	<b>GPS Position</b>
1	30/10/2008 09:13	N55 45.686 W6 17.489
2	30/10/2008 09:42	N55 44.420 W6 22.273
3	30/10/2008 09:49	N55 45.337 W6 21.802
4	30/10/2008 09:59	N55 45.822 W6 21.353
5	30/10/2008 10:09	N55 46.528 W6 20.797
6	30/10/2008 10:22	N55 46.564 W6 20.400
7	30/10/2008 10:32	N55 46.819 W6 19.092
8	30/10/2008 10:41	N55 46.769 W6 17.994
9	30/10/2008 10:48	N55 46.695 W6 17.182
10	30/10/2008 11:02	N55 46.104 W6 16.647
11	30/10/2008 11:10	N55 45.812 W6 16.742
12	30/10/2008 11:17	N55 45.573 W6 17.261
13	30/10/2008 11:24	N55 45.537 W6 17.389
14	30/10/2008 11:25	N55 45.534 W6 17.376
15	30/10/2008 11:32	N55 45.504 W6 17.521
16	30/10/2008 11:38	N55 45.399 W6 17.968
17	30/10/2008 11:50	N55 45.743 W6 18.487
18	30/10/2008 11:54	N55 45.946 W6 17.639
19	30/10/2008 12:04	N55 45.167 W6 19.099
20	30/10/2008 12:10	N55 44.925 W6 19.887
21	30/10/2008 12:16	N55 44.689 W6 20.317
22	30/10/2008 12:24	N55 44.631 W6 21.098
23	30/10/2008 12:31	N55 44.646 W6 21.098
24	30/10/2008 13:54	N55 46.797 W6 20.108
25	30/10/2008 14:02	N55 46.792 W6 17.980

**Table 27 Sediment and water sample GPS positions.**

### **5.3.1 Sediment Sampling**

The sediment sampling was undertaken using a Van Veen grab sampler which was on loan from SAMS Aberdeen Marine Laboratory. Figure 108 shows the Van Veen grab being deployed from the side of the boat. The sampler uses a simple bucket scoop mechanism which stays open under the weight of the sampler, but closes when it hits the sea floor and closes upon lifting. The Van Veen grab is a simple and effective device for gathering sediment. During the cruise a few sampling points yielded no sediment as the floor of the Loch was quite stony.



**Figure 108 Deployment of the Van Veen grab sampler**

### ***5.3.2 Water Sampling***

The water sampling was undertaken using an Aquatic Research water sampler. The sampler is primed much like a mouse trap, with the two end caps held in an open position on a trigger. This device was attached to a line with a “sender weight” which tripped the closing mechanism trigger when the sampler reached the desired depth of water. Figure 109 shows an example of the sampler used for this study. Each fill of water is 2.2 L, but only 100 ml of water will be required for this study to give an indication of suspended material within the water column.

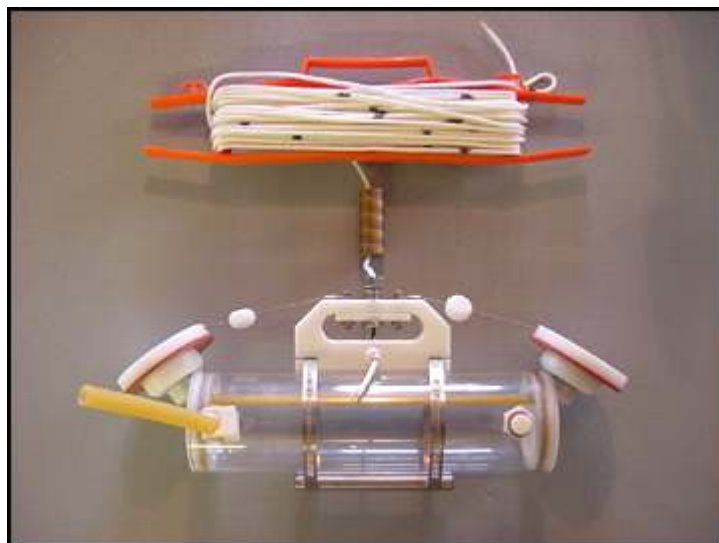


**Figure 109 Aquatic Research water sampler**

### **5.3.3** *Tracer Deployment*

The tracer which was chosen for this study is a PED (polymer encapsulated dye) particle tracer, which is a polymer encapsulated dye. It is typically used as a pigment colour in paint manufacture. The tracer was prepared ahead of time in 500 ml volumes which contained 100 g of tracer in a 1:1 mix with a surfactant (washing up liquid). This made handling easier as the tracer powder is extremely difficult to handle in breezy conditions.

The tracer bottles were mixed with 5L of sea water in a bucket to give a suitable quantity of tracer to give a visible contrast in the Loch. Figure 110 shows the deployment of the orange tracer off the side of the Jeannie Anne, it can be seen how bright the tracer is in the water and how easy it is to track visually through the sequence of photographs.



**Figure 110 Deployment of tracer off pier point, tracer movement in westerly direction away from harbour.**

## 5.4 Case Study Results and Discussion

### 5.4.1 Tracer Deployment

Figure 111 shows the positions of tracer deployments around Bowmore Harbour, the orange circles representing the point of deployment and the orange arrow indicating the direction in which the tracer travelled. The wind direction and tide directions are also indicated.

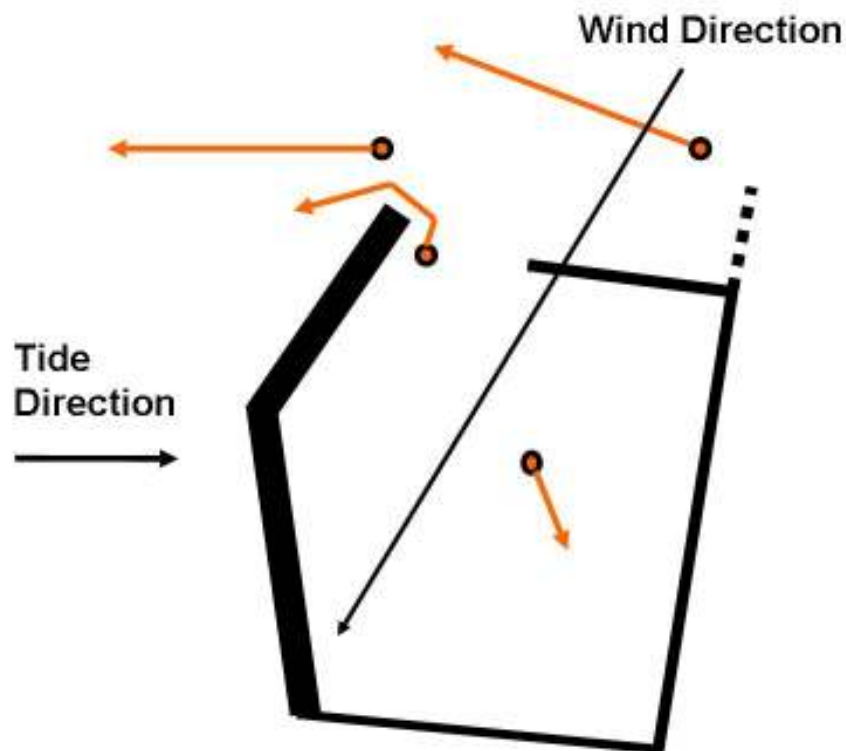


**Figure 111 Diagram of Bowmore Harbour with the 4 tracer deployment sites and the noted direction of tracer movement in relation to tide and wind direction. Thursday 30-10-08.**

It was expected that with an incoming tide the tracer would be carried with the tidal flow and be carried in to the harbour. This was not the case. Each of the 3 deployments outside the harbour entrance moved easterly, against the direction of tidal flow and also perpendicular to the wind (which was blowing in a strong northerly direction). Dismissing the possibility that a surface effect of wind driven movement had caused the direction of the tracer movement observed in Figure 111.



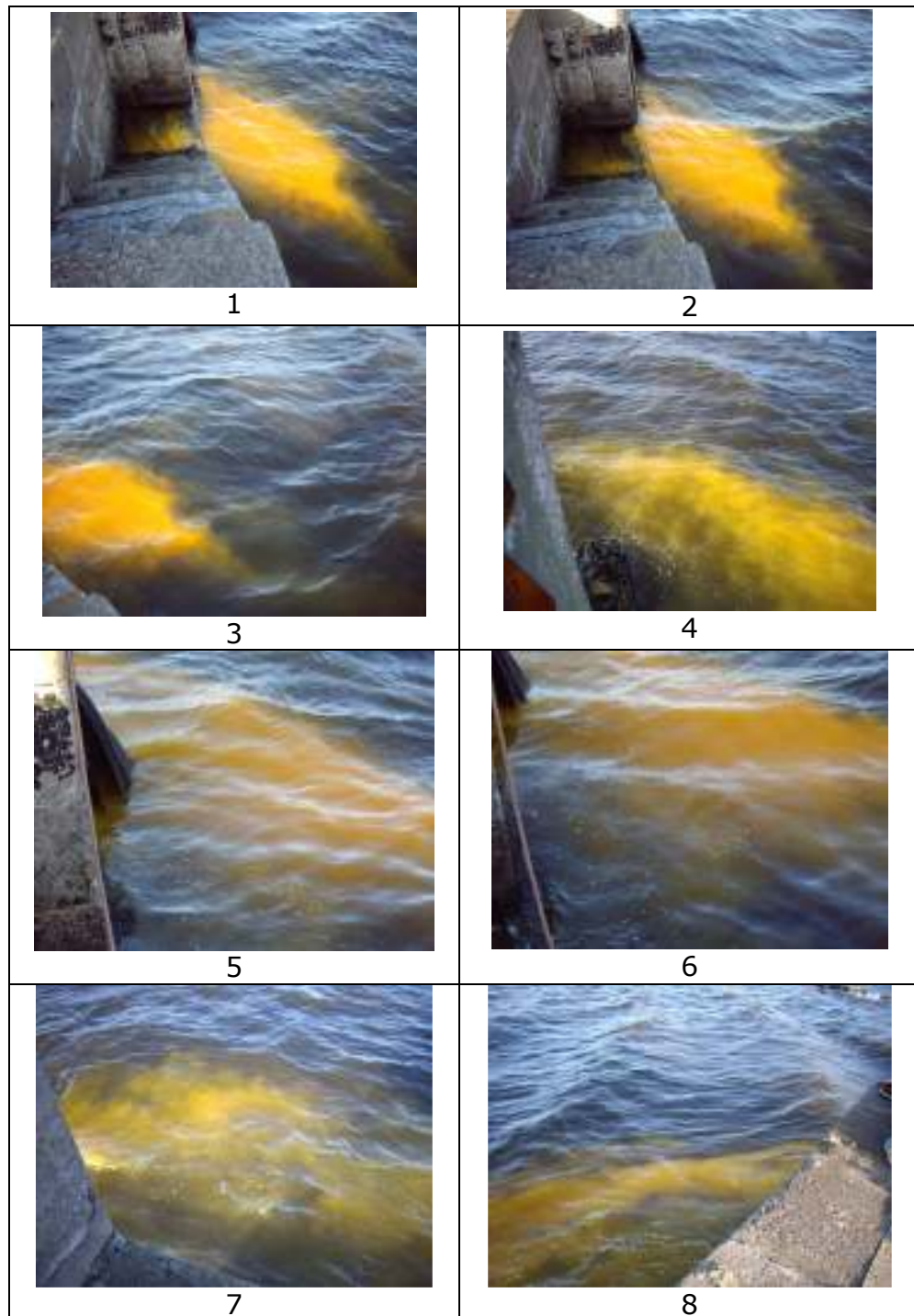


**Figure 112 Deployment of tracer from pier steps, 4 m inside the harbour mouth. Tracer moved out of harbour and around the pier end towards the West.**

A second day of tracer deployment was proposed depending on weather conditions. It was planned to coincide with an outgoing tide to provide



comparative data to the in coming tide, Figure 113. As with the previous deployment, each of the 5 deployments outside the harbour entrance moved easterly, going with the direction of tidal flow and also perpendicular to the wind (which was again blowing in a strong northerly direction). This confirmed what was seen the previous day, that any potential surface effect of wind driven movement was not a concern.

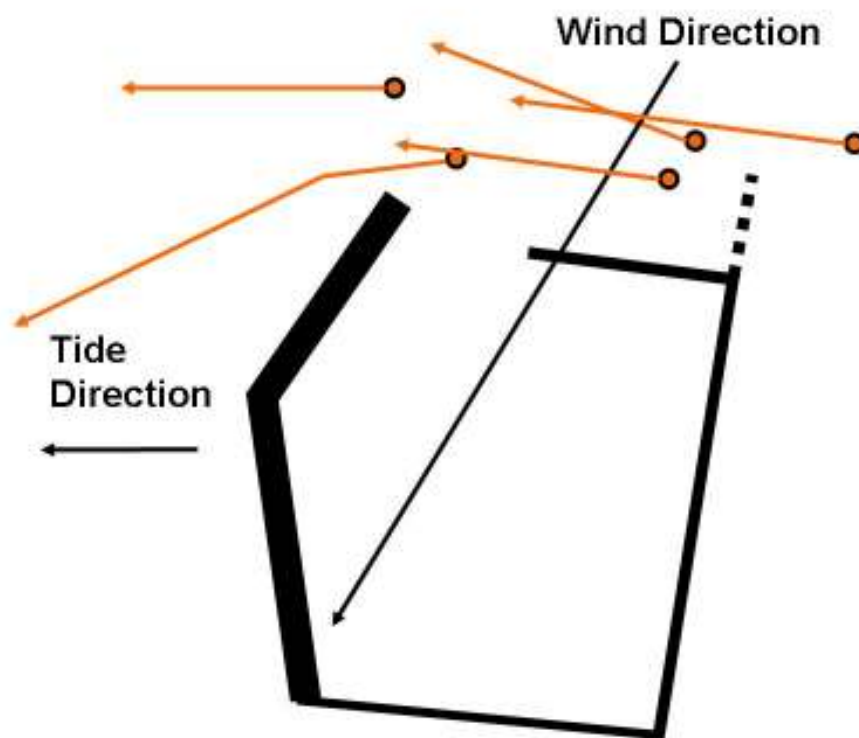


**Figure 113 Diagram of Bowmore Harbour, second day of tracer deployment, with the 5 tracer deployment sites and the noted direction of tracer movement in relation to tide and wind direction. Friday 31-10-08.**

It can be seen in Figure 114 with the orange tracer was unaffected by the prevailing wind and was indeed carried across the mouth of the harbour, going with the currents.



**Figure 114 Deployment of tracer off dog leg of break water, tracer movement across harbour mouth in westerly direction**

#### **5.4.2 Particle Size**

Particle sizing experiments were carried out using a Malvern Particle Size Analyzer. For the sediment samples a small amount was taken and placed in distilled water. This was then added drop wise to the particle size cell until a suitable concentration of particles were detected. The particle size data from the sediment samples collected can be seen in Table 28. Sample 5 and 17 did not yield a sediment sample as the loch floor was stony. Samples 19-25 could not be gathered as this was after the grab sampler was lost. Samples 26 and 27 were gathered on foot at low tide from inside the harbour and outside the breakwater. Sample 27 is possibly a sample of the material which was dredged from the harbour in 2000, but is of a much finer particle distribution compared to the current harbour sediment. Table 29 shows the particle size data for the collected water samples, samples 1 and 20 were extremely clean and did not register particles on the instrument.

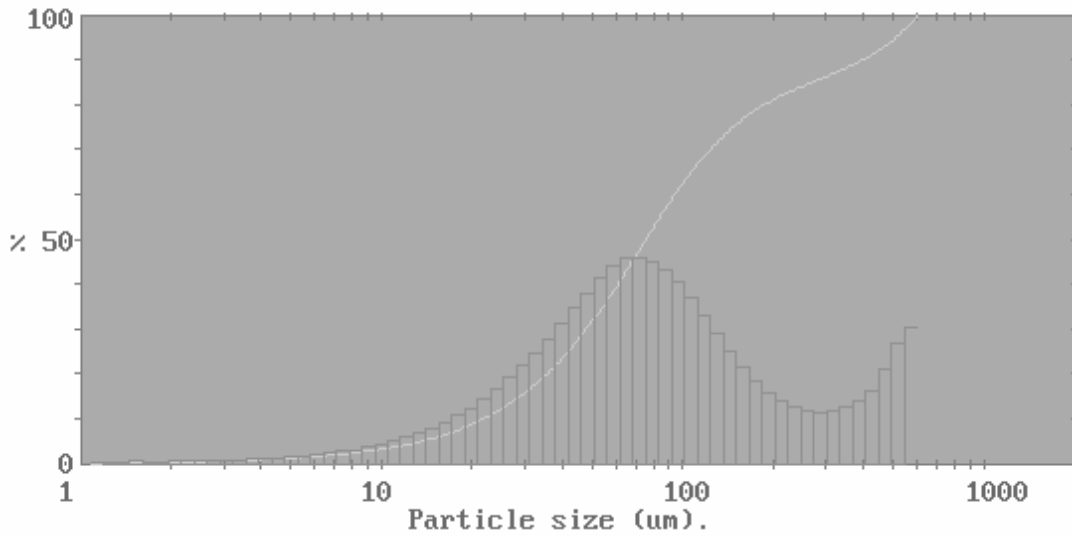


**Figure 115 Particle size distribution plot for water sample number 6**

Upper	in	Lower	Under	Upper	in	Lower	Under	Upper	in	Lower	Under	Span
				124	7.0	101	63.3	11.6	1.0	9.48	3.1	4.94
				101	8.5	83.3	54.8	9.48	0.7	7.78	2.4	D[4,3]
				83.3	9.1	68.3	45.7	7.78	0.5	6.39	1.9	131.58µm
				68.3	9.0	56.1	36.6	6.39	0.4	5.24	1.5	
600	5.8	492	94.2	56.1	8.0	46.0	28.7	5.24	0.3	4.30	1.2	D[3,2]
492	3.8	404	90.5	46.0	6.6	37.8	22.0	4.30	0.2	3.53	1.0	37.67µm
404	2.7	332	87.7	37.8	5.3	31.0	16.7	3.53	0.2	2.90	0.8	
332	2.4	272	85.4	31.0	4.1	25.5	12.6	2.90	0.2	2.38	0.6	D[u,0.9]
272	2.5	224	82.9	25.5	3.1	20.9	9.5	2.38	0.2	1.95	0.4	392.12µm
224	3.0	183	79.9	20.9	2.4	17.1	7.2	1.95	0.1	1.60	0.3	
183	4.1	151	75.8	17.1	1.7	14.1	5.4	1.60	0.1	1.32	0.2	D[u,0.11]
151	5.5	124	70.3	14.1	1.3	11.6	4.1	1.32	0.2	0.50	0.0	21.65µm
Source = :Sample				Beam length = 2.2 mm				Model indep				D[u,0.5]
Focal length = 300 mm				Residual = 0.406 %				Volume Conc. = 0.2031%				74.98µm
Presentation = 2209				Obscuration = 0.3174				Sp.S.A 0.1593 m <sup>2</sup> /cc.				Shape OFF
				Volume distribution								

**Figure 116 Particle size data obtained from water sample number 6**

<b>Sediment Sample</b>	<b>D [v,0.5]</b>	<b>D [4,3]</b>	<b>D [v,0.1]</b>	<b>D [v,0.9]</b>
1	159.19	175.95	104.25	266.90
2	138.54	200.48	20.87	499.23
3	91.91	167.86	15.53	482.26
4	67.53	198.15	12.20	557.44
5	<b>stones</b>	<b>stones</b>	<b>stones</b>	<b>stones</b>
6	55.87	193.40	6.78	537.65
7	48.04	116.81	9.79	461.64
8	143.43	155.60	100.32	220.94
9	150.66	158.49	105.20	217.95
10	134.84	143.76	94.69	197.00
11	126.80	233.04	40.95	566.79
12	140.48	148.90	102.13	203.63
13	152.88	169.02	107.56	247.86
14	153.18	181.66	99.15	302.68
15	204.44	234.13	96.77	430.82
16	151.58	232.68	75.93	538.36
17	<b>stones</b>	<b>stones</b>	<b>stones</b>	<b>stones</b>
18	272.95	328.63	119.88	573.76
19	<b>n/a</b>	<b>n/a</b>	<b>n/a</b>	<b>n/a</b>
20	<b>n/a</b>	<b>n/a</b>	<b>n/a</b>	<b>n/a</b>
21	<b>n/a</b>	<b>n/a</b>	<b>n/a</b>	<b>n/a</b>
22	<b>n/a</b>	<b>n/a</b>	<b>n/a</b>	<b>n/a</b>
23	<b>n/a</b>	<b>n/a</b>	<b>n/a</b>	<b>n/a</b>
24	<b>n/a</b>	<b>n/a</b>	<b>n/a</b>	<b>n/a</b>
25	<b>n/a</b>	<b>n/a</b>	<b>n/a</b>	<b>n/a</b>
26 - Breakwater Sediment (in harbour)	152.50	167.19	98.92	250.53
27 - Breakwater Dredged Sediment (out of harbour)	14.37	24.22	3.49	54.20

**Table 28 Sediment sample particle size results**

<b>Water Sample</b>	<b>D [v,0.5]</b>	<b>D [4,3]</b>	<b>D [v,0.1]</b>	<b>D [v,0.9]</b>
1	n/a	n/a	n/a	n/a
2	450.67	324.71	33.03	576.83
3	491.39	390.63	64.08	579.93
4	480.06	342.77	30.81	579.34
5	548.87	526.78	477.15	589.95
6	74.98	131.58	21.65	392.12
7	113.30	219.85	27.70	554.68
8	142.71	261.87	32.17	567.76
9	500.86	410.45	43.50	581.18
10	503.20	359.50	38.30	582.09
11	487.24	403.85	80.77	579.07
12	384.94	347.71	81.06	566.37
13	188.32	237.48	45.92	513.31
14	458.68	408.57	168.77	574.61
15	486.07	427.49	183.46	578.78
16	489.51	415.33	112.79	579.52
17	307.49	296.46	44.75	565.38
18	486.48	407.80	89.74	579.10
19	90.35	265.83	25.56	572.76
20	n/a	n/a	n/a	n/a
21	84.98	230.31	27.10	566.81
22	122.03	258.16	27.78	567.28
23	532.70	469.08	117.31	586.79
24	212.56	248.59	62.08	502.91
25	461.68	447.32	325.83	536.13

**Table 29 Water sample particle size results of suspended solids (including flocculated material)**

The terms from Table 28 and Table 29, D [v,0.5], D [4,3], D [v.0.1] and D [v,0.9] can be defined as:

- D [v,0.5] – Volume median diameter. This figure has 50 % of the distribution above and 50 % below this value. It divides the distribution exactly in half.
- D [4,3] – Volume mean diameter. This is the diameter of the sphere that has the same volume as an ideal sphere.  $D[4,3] = \frac{\sum d^4}{\sum d^3}$

- D [v,0.1] and D [v,0.9] – These are 90 % and 10 % cut-offs respectively for the distribution. Where D [v,0.9] has 90 % of the distribution below this value and D [v,0.1] has 10 % of the distribution below this value.

The cells in Table 28 and Table 29 which have light grey shading are the particle sizes which fall within the fine particle range responsible for silting.

#### **5.4.3 Weather Influence on Current Direction**

A potentially strong influence on current direction and intensity can be localised weather patterns. Examining weather data from the Gartbreck landfill site showed there was a fairly fast moving low pressure area moving across Lochindaal, up to and during the sample period. It was noted that a southerly wind was blowing around noon on the 29<sup>th</sup> October 2008. However, there is insufficient duration of any one direction to significantly influence the local currents.

### **5.5 Conclusions**

The water samples analysed for particle size show a higher number of samples exhibiting fine “silt” sized particles in the D [v,0.1]; samples 2, 3, 6-10, 13, 17, 19, 21 and 22 all have a range from 21 – 44 µm. The D [v,0.9] fell between 392 – 589 µm with the average particle size ranging from 74 – 548 µm. These large particle sizes may not be due to actual particles, but due to agglomerations or flocculation of particles.

This is confirmed by the particle size results, showing that a small portion of the sediment samples gathered fall within the river “silt” size range of 2 – 50 µm. Only samples 3, 4, 6, 7, 11 and 27 recorded particles within the silt range and that is within the D [v,0.1] which is 10 % of the distribution. The 90 % of the distribution, D [v,0.9], fell between 392 – 589 µm which are classed as medium-coarse sands. As average particle size ranged from 48 – 204 µm, this confirms that the silting problem in the harbour is not due to the river. This investigation shows that it is coarser sand causing the silting problem in the harbour, which

you would only get with high velocity currents, keeping the heavier particles suspended. The high velocity currents within Lochindaal would keep medium coarse sands (particulates) suspended. As there was a relatively low volume (percentage in the samples analysed) of sedimentary particles so, the accumulation of particles in the harbour would be slow.

The tracer deployments on the incoming tide (Figure 111) went directly against the tide and was unaffected by wind direction, this ruled out surface influence for the particle tracer movement. Tracer deployment on an outgoing tide (Figure 112) showed exactly the same behaviour as that of the incoming, with zero wind affect. The tracer study has confirmed the cyclical current pattern within Lochindaal, but only from the point of the area assessed. Further examination of the waters to the South West of Bowmore would pin point the interface between the cyclical currents and the tidal driven currents.

What these results also show is that there is not a high percentage of fine "silt" particles in suspension around Lochindaal. Although this is low, there is still enough suspended material, which with time, will add to silting problem observed in the harbour.

In conclusion it can be said that the circular motion of the currents within Lochindaal overwhelm any effect an incoming or outgoing tide would have upon sediment movement.



**Figure 117 Bowmore Harbour Sand bar**

The current sand bar looks similar to Figure 117, showing that the sand bar is again starting to build up, along with deposits within the harbour boundary from the break water side. There are two major problems with the current break water, firstly there are the two holes which can be seen in Figure 118 indicated by a \* and \*\*, and also in Figure 119. These two holes were created for machinery to access the outer harbour area during the last sediment clearing.



**Figure 118 Shows the holes in the break water towards the North East corner (indicated by \* and \*\*). The hole at the corner being down to the beach level and the second being slightly shallower.**

There is significant build up of sediment/sand in that corner of the harbour purely because of those two holes, as the tide comes in it is possible to see material in the water being carried in to the harbour. Secondly, the height of the break water is far too low to be an effective method of keeping the harbour clear of sedimentary material. Figure 120 shows a view of the break water at almost high tide and the dog leg is barely visible above the surface of the water. This lack of height can be even more of a problem during stormy weather when there is naturally more material carried in the water column from the bottom of the Loch. Therefore the break water would be completely swamped during the season high tides and stormy weather.





**Figure 119 View in line with break water dog leg**



**Figure 120 View of break water at high tide.**

## 6 CONCLUSIONS

The work presented here was achieved by completing the milestones originally defined in the project plan. The development of lanthanide doped borosilicate glass, silica sol gel glass and polymers have all been investigated for their potential application as environmental tracer.

Milestone 1: *Literature review of current environmental tracing techniques and tracers, glass and polymer fabrication and their potential for application in environmental tracing.*

This milestone has been achieved by an extensive search of literature sources to examine historic and current documents. This has provided useful information regarding existing tracers, potential glass matrices for use as environmental tracers which could provide increased fluorescent output and also details on potential polymerisation experiments which can be used as starting points for modification to produce 'fine sediment' mimicking tracers.

Milestone 2: *Development of current security glass matrix for use as an environmental tracer.*

This milestone was achieved by producing 45 $\mu$ m sized particles of doped borosilicate glass and developing a basic laser based detection system. The design of which can be seen in Section 3.3. The initial results have shown that it is possible to use a laser as an excitation source coupled to an optical fiber detection device. The laser used had an output wavelength of 532 nm, which, in terms of Europium absorbance is only the 5<sup>th</sup> strongest wavelength, compared to 393 nm or 465 nm which are far higher. The detection limit possible using these alternative excitation wavelengths is greatly improved.

Milestone 3: Concentration study of lanthanide doping in to current borosilicate glass matrix Glass 1.

This milestone was achieved by producing a range of borosilicate glass samples doped from 0.2 mol% - 2.0 mol% with europium, dysprosium and terbium in 0.2 mol% increments. One sample from each dopant was then analysed by 3D spectral characterisation to find the optimum excitation and emission wavelengths for each lanthanide. This information was used to produce concentration graphs which detail the strongest emission wavelengths for europium, dysprosium and terbium. These were then probed with a range of excitation wavelengths to produce the concentration graphs reported.

Further investigation in to the current glass matrix (Glass 1) was undertaken by carrying out a series of 25 multiple ion doped experiments to investigate the effect of ion sensitisation. This was achieved by preparing multi ion doped samples containing europium, dysprosium and terbium with concentrations of 0.5, 1.0, 1.5, 2.0 and 2.5 mol % in varying combinations thereof. Fractional factorial experimental design was used to select the concentration combinations used.

The results showed that a large number of narrow excitation and emission peak wavelengths are available to choose from, with a very strong relationship between lanthanide concentrations and emission peak intensities. This means that different environmental tracer combinations can be achieved by altering the concentrations of the lanthanide dopants in the glass matrix. The data indicates the possibility that 0.1 mol% concentration differences could be utilised to produce different emission combinations.

Milestone 4: Investigation of new glass matrix Glass 2.

This milestone was achieved by examining the influence of adding sodium fluoride (NaF) to the standard borosilicate glass matrix. It was proposed that the addition of NaF would have the effect of allowing a higher level of rare earth ion doping. This was investigated by producing a range of doped samples using the modified Glass 1 matrix with the addition of 5 mol% NaF. The preparation

of multi ion doped samples (double and triple) containing europium, dysprosium and terbium with concentrations of 0.5, 1.0, 1.5 and 2.0 mol % in varying combinations thereof. Fractional factorial experimental design was again used to select the concentration combinations used.

The results showed that the addition of NaF to the glass matrix did not significantly alter the large number of narrow excitation and emission peak wavelengths which were observed in glass 1. It did however effect the glass melt producing a less viscous sample, this could potentially save time and energy in the production of the tracer by lowering the maximum melt temperature.

Milestone 5: *Investigation of chelates for the formation of organic lanthanide complexes for use with polymer and silica sol gel spheres.*

This milestone was achieved by reviewing existing literature for chelate compounds which were known to work in combination with sol gel or polymer formulations. As the varying stability of chelate compounds can be difficult to utilise if the complex formed dissolves in aqueous solutions or is destroyed in the presence of ammonia. The chelates chosen to investigate produced robust lanthanide complexes which formed sol gel and polymer particles easily. A characteristic of a chelating molecule is that it allows a broad absorption of ultraviolet light. This energy is then transferred to the rare earth and produces a stronger fluorescence. This fluorescence is orders of magnitude greater than the emission seen from a discrete excitation of the ion itself. The most promising chelates were found to be TTFA and PHEN, which in combination with europium produced a highly fluorescent lanthanide complex.

Milestone 6: *Investigation of polymer sphere formation.*

This milestone was achieved by reviewing literature for methods of producing monodisperse polymer particles. SEM analysis showed the spherical formation and uniformity of polymer particles of differing composition, made from the final modified polymers of this research.

Milestone 7: Investigation of silica sol gel sphere formation.

This milestone was achieved by reviewing current literature, where it was found that the most referenced method of silica sol gel sphere formation was the Stöber method or modified Stöber method. This method was found to be extremely reproducible and allowed reasonable yield of beads from each experiment. SEM analysis showed the spherical formation and uniformity of silica particles produced in this research.

Milestone 8: Investigation of polymer spheres doped with organic lanthanide complexes.

This milestone was achieved by incorporating the chelate materials investigated in Milestone 5 in to the polymerisation formulations investigated in Milestone 6. This combination of lanthanide complex and polymer allowed the production of <800 nm sized highly fluorescent particles. SEM analysis showed the amorphous formation and variety of polymer particles produced. Spectroscopic interrogation of the particles found a high fluorescent emission of the lanthanide ion, in the case of this study Europium, due to the energy transfer between the chelate molecule and the rare earth ions within the complex in the polymer matrix the observed fluorescence is much greater than that observed from the glass.

Milestone 9: Investigation of silica sol gel spheres doped with organic lanthanide complexes.

This milestone was achieved by incorporating the chelate materials investigated in Milestone 5 in to the silica sol gel sphere method investigated in Milestone 7. This combination of lanthanide complex and sol gel allowed the production of <400 nm sized highly fluorescent particles. SEM analysis showed the amorphous formation of silica particles produced. Spectroscopic interrogation of the particles found a high fluorescent emission of the lanthanide ion, in the case of this study Europium. Due to the energy transfer between the chelate molecule and the rare earth ions within the complex in the silica sol gel matrix

the observed fluorescence is much greater than that observed from the first glass.

Milestone 10: *Measurement of novel tracers using a proposed trial detection system.*

This milestone was achieved by performing laboratory based tests to simulate tracer deployment in an aqueous environment. The trial detection system used optical fibre delivery for both the laser excitation and fluorescence emission detection. The use of optical fibres would allow for a real time detection system to be developed for deployment in any aqueous environment. Single point and multiple point detection would be possible using the tracers developed in this work.

Milestone 11: *Determination of sediment particle size from a potential field site.*

This milestone was achieved by undertaking a field study of Loch Indaal on the isle of Islay, which formed part of a feasibility study to determine why the Bowmore Harbour continually silted. Water and sediment sampling was taken from around Loch Indaal and from within the confines of the harbour itself. This allowed detailed information to be gathered regarding the particle size distribution within the aquatic system and also what may have been responsible for the silting of the harbour. Also it provided valuable particle size information for future tracer development work, allowing a tracer with specific characteristics to be designed.

## **6.1 Overall Conclusion**

The development of lanthanide doped borosilicate glass, silica sol gel glass and polymers have all been investigated for their potential application as environmental tracers by examining their spectroscopic and lifetime properties.

Naturally occurring and artificially introduced materials within aqueous, geological and industrial environments have been used for many years in the

monitoring of currents, sediments, waste effluent streams, soils and pollutants. The range of existing tracing methods includes fluorescent dyes, fluorescent particles, isotopes, naturally occurring compounds and rare earth tracers. These tracing techniques have their advantages and disadvantages within their specific application range.

The work reported here provides a new tracer for use in environments which would normally be problematic for real time online monitoring. Increased background signal and overlapping broadband fluorescent signals make monitoring a complex, unreliable and expensive process. The development of a new tracer, using borosilicate glass, organic polymer and inorganic polymer methods has been examined. The incorporation of lanthanide ions to a glass host matrix produces an environmentally stable and inert tracer. This allows a tracer which will exhibit highly discrete narrow band atomic fluorescence, which is the key feature of using a lanthanide ion.

Further investigation of the limitations of lanthanide doped glass particles as an environmental tracer showed that with decreasing particle size, the greater the reduction in the effective fluorescent signal became. This is due not to the particle itself but to the scattering of excitation light and emitted fluorescence with the increased surface area. A further limiting issue with lanthanide ions in a crushed glass particle is quenching with water. If the dopant ion is near the surface of the particle and in an aqueous solution the fluorescence will be quenched.

Also the process of producing sub 5  $\mu\text{m}$  particles was time consuming and too labour intensive, producing incredibly small quantity (20 mg) from many hours of grinding and sieving. The loss of fluorescence and loss of resolution of the discrete atomic emission from the rare earth ion showed that glass was not going to be an ideal tracer unless it was possible to increase the signal. The production of tracer sized glass particles of  $<5\mu\text{m}$  from the doped glass showed a decrease in the intensity of the fluorescent signal, 98.5% less intense compared to a bulk sample. This is not an ideal situation for a tracer where distinct fluorescent intensity is vital. This would greatly limit its application as a real

time monitoring environmental tracer as the huge reduction in fluorescent emission would make it extremely hard to detect in the field.

This led to the investigation in to ways in which it would be possible to increase the observed fluorescence from the lanthanide ions. Increasing concentration did not itself yield a large enough variation in bulk glass signal to warrant further experimentation. Multiple ion doping was examined in an attempt to produce "sensitised", ion enhanced fluorescence. This again did not produce orders of magnitude higher fluorescence. Reviewing literature it was noted that producing a complex molecule of a rare earth produced a significant increase in emitted fluorescence from the rare earth ion. This is achieved by the chelating molecule acting as an "antenna" which directly channels the energy it absorbs in to the rare earth energy level. This allows a greatly increased range of energy to be absorbed by an ion which would normally have only a narrow band excitation.

This increase of fluorescence although great, presented a new problem, as an organic complex such as  $\text{Eu}[\text{ttfa}][\text{phen}]$  would not be capable of being incorporated to a standard type inorganic glass matrix. The 1250°C upper limit pouring temperature far outstrips the maximum tolerance level for an organic molecule. This major limitation of inorganic glass initiated the need for an organic host matrix, or an inorganic host with low working temperatures. Reviewing literature produced two extremely promising possibilities for an alternative to a glass host. Two different forms of polymerisation, organic and inorganic were investigated. Both forms were low temperature methods, room temperature and 80 °C. The investigation of these particles found it was far simpler to produce sub 5  $\mu\text{m}$  particles, in a one step process. The ability to produce particles in the 250-500 nm range was highly desirable and impossible with the borosilicate glass.

The concept of using lanthanide doped glasses as environmental tracers has been demonstrated. The spectral characterisation and concentration studies of the lanthanide doped tracer allow the selection of parameters to produce future tracers and detection systems for particular applications. By altering the chosen lanthanide dopant, number of dopants, dopant concentration and using selective excitation and emission wavelengths there are a huge number of possible unique



tracer combinations. The significantly narrower bandwidth emission peaks of the lanthanide based tracers achieve more selective detection of multiple tracers without overlap interfere and gives the potential to selectively simultaneously monitor many different tracers in the same location. The spectral lifetime characteristics of the lanthanide tracers are very different from the lifetime of background fluorescence which is typically molecular in origin. This is an extra discrimination against background interference and is an additional advantage of using lanthanide based tracers.

Through the analysis of 50 triple lanthanide ion doped tracers a large number of narrow lanthanide excitation and emission peak wavelengths are available to choose from as environmental tracer response peaks. This research clearly demonstrated a linear relationship between lanthanide concentrations and emission peak intensities for a variety of peak emission wavelengths. The addition of NaF to the glass matrix did not significantly change the peak wavelengths to distinguish between the two glass matrices by wavelength. Further unique tracers should be achievable as additional excitation/emission peak wavelengths previously forbidden are observed due to energy transfer (sensitisation) of certain combinations of lanthanides.

Overall this work shows that a very large number of unique environmental tracers can be obtained by varying the concentration, the number of lanthanide ions in a glass and also the possibility of using organic and inorganic lanthanide chelate doped tracers.

## **7 FUTURE WORK**

The work presented here clearly demonstrated the immense potential for lanthanide doped materials to be used as environmental tracers. The work though, has reached the stage where the following developments could take it to the next stage.

- Investigation of glass matrices which would allow an increase in signal from the lanthanide ions doped into it
- Development of new chelate molecules to provide more energy efficient transfers to the lanthanide ions, therefore lowering doping levels of ions but increasing signal
- Fabrication of sufficient quantities of tracer to allow field trials
- Further development of specific tracer particle size to match that of sedimentary silts
- Development of a field trial detection system which can incorporate atomic spectral and lifetime differentiation so that a study such as that in Chapter 5 can be carried out using the novel lanthanide chelate silica sol gel tracers developed in this work

### **7.1 Future Applications**

The development of these tracers has focused mainly on environmental applications, such as marine, river, sediments, pollution etc. The nature of glass /silica sol gel and polymer as tracer hosts has wider applications.

Offshore applications could be an area for the use of these tracers to replace radioactive and molecular dye tracers currently applied for downhole testing. Existing flow-through fluorometers are already in use in many places and could be adapted (see above) to monitor the lanthanide doped glasses. Currently

these fluorescent nano-sized particles are being used in the development of bio-assay technology.

The detection system being developed for that application could be adapted for environmental applications.

## 8 REFERENCES

1. Ambulatov, N.A.P., V. V. , *On the influence of luminophoric and agaroid films on the hydrodynamic properties of tracer sand*. . Okeanologia, 1963. **3**: p. 921–924.
2. Crickmore, M.J., *Measurement of sand transport in rivers with special reference to tracer methods.*, in *Sedimentology*. 1967. p. 175-228.
3. Cummins, R.S.a.I., L. F. , *Tracing sediment movement with radioisotopes*. Military Engineering, 1963(55): p. 161-164.
4. Byass, J.B., *Equipment and methods for orchard spray application research III: The measurement of spray deposits on leaves using light from fluorochromes on the surface*. Journal of Agricultural Engineering Research, 1969. **14**(1): p. 78-88.
5. McCulloch, M., et al., *Tracing the source of sediment and phosphorus into the Great Barrier Reef lagoon*. Earth and Planetary Science Letters, 2003. **210**(1-2): p. 249-258.
6. Santos, I.R., et al., *Extended time series measurements of submarine groundwater discharge tracers ( $^{222}\text{Rn}$  and  $\text{CH}_4$ ) at a coastal site in Florida*. Marine Chemistry, 2009. **113**(1-2): p. 137-147.
7. Liu, Y., H. Ren, and B. Wang, *Application Prospect of Environmental Isotopes and Tracing Techniques for Earthquake Prediction*. Earth Science Frontiers, 2009. **16**(2): p. 369-377.
8. Nestmann, E.R., D.J. Kowbel, and J. Ellenton, *Mutagenicity in Salmonella of fluorescent dye tablets used in water tracing*. Water Research, 1980. **14**(7): p. 901-902.
9. Adams, E.E., et al., *Deposition of Contaminated Sediments in Boston Harbor Studied Using Fluorescent Dye and Particle Tracers*. Estuarine, Coastal and Shelf Science, 1998. **46**(3): p. 371-382.
10. Bachtiar, T., J.P. Coakley, and M.J. Risk, *Tracing sewage-contaminated sediments in Hamilton Harbour using selected geochemical indicators*. Science of The Total Environment, 1996. **179**: p. 3-16.
11. Seguel, C.G., et al., *Tracing Sewage in the Marine Environment: altered signatures in Concepción Bay, Chile*. Water Research, 2001. **35**(17): p. 4166-4174.
12. Cromey, C., et al., *Validation of a fish farm waste resuspension model by use of a particulate tracer discharged from a point source in a coastal environment*. Estuaries and Coasts, 2002. **25**(5): p. 916-929.
13. Malley, M.M. and G. Mourou, *The picosecond time-resolved fluorescence spectrum of rhodamine 6G*. Optics Communications, 1974. **10**(4): p. 323-326.
14. Martin, M.M. and L. Lindqvist, *The pH dependence of fluorescein fluorescence*. Journal of Luminescence. **10**(6): p. 381-390.
15. Kasten, F.H. and W.T. Mason, *Introduction to Fluorescent Probes: Properties, History and Applications*, in *Fluorescent and Luminescent Probes for Biological Activity (Second Edition)*. 1999, Academic Press: London. p. 17-39.
16. Thomas, A.J., *Input of artificial radionuclides to the Gulf of Lions and tracing the Rhône influence in marine surface sediments*. Deep Sea Research Part II: Topical Studies in Oceanography, 1997. **44**(3-4): p. 577-595.

17. Behrens, et al., *Toxicological and ecotoxicological assessment of water tracers*. Hydrogeology Journal, 2001. **9**(3): p. 321-325.
18. Ryder, A.G., et al., *Characterization of crude oils using fluorescence lifetime data*. Spectrochimica Acta Part A: Molecular and Biomolecular Spectroscopy, 2002. **58**(5): p. 1025-1037.
19. Russell, M., et al., *The effects of oil exploration and production in the Fladen Ground: Composition and concentration of hydrocarbons in sediment samples collected during 2001 and their comparison with sediment samples collected in 1989*. Marine Pollution Bulletin, 2005. **50**(6): p. 638-651.
20. Ahmed, A., Webster, L., Pollard, P., Davies, I., Russell, M., Walsham, P., Packer, G. and Moffat, C., *The distribution and composition of hydrocarbons in sediments from the Fladen ground, North Sea, an area of oil production*. J. Environ. Monit., 2006. **8**: p. 307 - 316.
21. McStay, D., Robertson, P.K.J., Pollard, P., Edwards, I., Bonsen, E., Al-Obaidi, A. and Tait. D., *A multicability sensor for hydrocarbons, synthetic based fluids and heavy metals: Applications for environmental monitoring during removal of drill cutting piles*. Underwater Technology, 2002. **25**: p. 69-75.
22. Vila-Concejo, A., et al., *Tracer studies on the updrift margin of a complex inlet system*. Marine Geology, 2004. **208**(1): p. 43-72.
23. Anfuso, G., *Sediment-activation depth values for gentle and steep beaches*. Marine Geology, 2005. **220**(1-4): p. 101-112.
24. Silva, A., et al., *Longshore drift estimation using fluorescent tracers: New insights from an experiment at Comporta Beach, Portugal*. Marine Geology, 2007. **240**(1-4): p. 137-150.
25. Tan, S.-K., Yu, G., Lim, S-Y and Ong, M-C. , *Flow Structure and Sediment Motion around Submerged Vanes in Open Channel*. J. Wtrwy., Port, Coast, and Oc. Eng., , 2005. **131**(3).
26. de Groot, S.J., *The impact of laying and maintenance of offshore pipelines on the marine environment and the North Sea fisheries*. Ocean Management, 1982. **8**(1): p. 1-27.
27. Cooper, K., et al., *Recovery of the seabed following marine aggregate dredging on the Hastings Shingle Bank off the southeast coast of England*. Estuarine, Coastal and Shelf Science, 2007. **75**(4): p. 547-558.
28. Kevin S. Black, S.A., Peter Wilson and Darren Evans, *The use of particle tracking in sediment transport studies : a review*. Journal of the Geological Society of London, 2007. **274**: p. 73-91.
29. Fels, J.B., *Source-identification investigations of petroleum contaminated groundwater in the Missouri Ozarks*. Engineering Geology, 1999. **52**(1-2): p. 3-13.
30. Barber, J.A.S. and C.S. Parkin, *Fluorescent tracer technique for measuring the quantity of pesticide deposited to soil following spray applications*. Crop Protection, 2003. **22**(1): p. 15-21.
31. Harden, H.S., et al., *Comparison of sulfur hexafluoride, fluorescein and rhodamine dyes and the bacteriophage PRD-1 in tracing subsurface flow*. Journal of Hydrology, 2003. **277**(1-2): p. 100-115.
32. Field M. S., W.R.G., Quinlan J. F., Aley T. J. , *An assessment of the potential adverse properties of fluorescent tracer dyes used for groundwater tracing*. Environmental Monitoring and Assessment, 1995. **38**: p. 75-96.
33. Abelson, A., et al., *Mass transport from pollution sources to remote coral*

- reefs in Eilat (Gulf of Aqaba, Red Sea). *Marine Pollution Bulletin*, 1999. **38**(1): p. 25-29.
34. Polyakov, V.O. and M.A. Nearing, *Rare earth element oxides for tracing sediment movement*. *CATENA*, 2004. **55**(3): p. 255-276.
  35. Johannesson, K.H., K.J. Stetzenbach, and V.F. Hodge, *Rare earth elements as geochemical tracers of regional groundwater mixing*. *Geochimica et Cosmochimica Acta*, 1997. **61**(17): p. 3605-3618.
  36. Kimoto, A., et al., *Applicability of rare earth element oxides as a sediment tracer for coarse-textured soils*. *CATENA*, 2006. **65**(3): p. 214-221.
  37. Jouanneau, J.-M., et al., *Pb, Zn, Cs, Sc and rare earth elements as tracers of the Loire and Gironde particles on the Biscay shelf (SW France)*. *Oceanologica Acta*, 1998. **21**(2): p. 233-241.
  38. Tweed, S.O., et al., *Behavior of rare earth elements in groundwater during flow and mixing in fractured rock aquifers: An example from the Dandenong Ranges, southeast Australia*. *Chemical Geology*, 2006. **234**(3-4): p. 291-307.
  39. Barth, S., *Application of boron isotopes for tracing sources of anthropogenic contamination in groundwater*. *Water Research*, 1998. **32**(3): p. 685-690.
  40. Dolenc, T., et al., *Nitrogen stable isotope composition as a tracer of fish farming in invertebrates *Aplysina aerophoba*, *Balanus perforatus* and *Anemonia sulcata* in central Adriatic*. *Aquaculture*, 2007. **262**(2-4): p. 237-249.
  41. Fehn, U., et al., *The initial  $^{129}\text{I}/\text{I}$  ratio and the presence of 'old' iodine in continental margins*. *Nuclear Instruments and Methods in Physics Research Section B: Beam Interactions with Materials and Atoms*, 2007. **259**(1): p. 496-502.
  42. Coppola, L., et al., *Thorium isotopes as tracers of particles dynamics and deep water circulation in the Indian sector of the Southern Ocean (ANTARES IV)*. *Marine Chemistry*, 2006. **100**(3-4): p. 299-313.
  43. Ross, G.A., Pollard, P.M., Hunter, C., Officer, S. and Prabhu, G.R., *Optically detectable security feature*. 2006.
  44. Shen, S., et al., *Compositional effects and spectroscopy of rare earths ( $\text{Er}^{3+}$ ,  $\text{Tm}^{3+}$ , and  $\text{Nd}^{3+}$ ) in tellurite glasses*. *Comptes Rendus Chimie*, 2002. **5**(12): p. 921-938.
  45. Rai, V.K., S.B. Rai, and D.K. Rai, *Optical studies of  $\text{Dy}^{3+}$  doped tellurite glass: Observation of yellow-green upconversion*. *Optics Communications*, 2006. **257**(1): p. 112-119.
  46. Rai, V.K., S.B. Rai, and D.K. Rai, *Spectroscopic properties of  $\text{Pr}^{3+}$  doped in tellurite glass*. *Spectrochimica Acta Part A: Molecular and Biomolecular Spectroscopy*, 2005. **62**(1-3): p. 302-306.
  47. Kumar, A., D.K. Rai, and S.B. Rai, *Optical studies of  $\text{Eu}^{3+}$  ions doped in tellurite glass*. *Spectrochimica Acta Part A: Molecular and Biomolecular Spectroscopy*, 2002. **58**(10): p. 2115-2125.
  48. Rai, S.B., A.K. Singh, and S.K. Singh, *Spectroscopic properties of  $\text{Ho}^{3+}$  ions doped in tellurite glass*. *Spectrochimica Acta Part A: Molecular and Biomolecular Spectroscopy*, 2003. **59**(14): p. 3221-3226.
  49. Kumar, A., D.K. Rai, and S.B. Rai, *Optical properties of  $\text{Sm}^{3+}$  ions doped in tellurite glass*. *Spectrochimica Acta Part A: Molecular and Biomolecular Spectroscopy*, 2003. **59**(5): p. 917-925.
  50. Zhoutang Li, P.W., Xueyin Jiang, Zhilin Zhang and Shaodong Xu, *The synthesis of rare earth borosilicate glasses and their luminescence*

- properties*. Journal of Luminescence, 1988. **40&41**: p. 135-136.
51. Zhu, D., et al., *Preparation of fluorescent glasses with variable compositions*. Ceramics International, 2007. **33**(4): p. 563-568.
  52. Noriyuki Wada, K.K., Kazuhiko Ozutsumi, *Glass composition dependence of Eu<sup>3+</sup> polarization in oxide glasses*.
  53. Jiu, H., et al., *Fluorescence enhancement of europium complex co-doped with terbium complex in a poly(methyl methacrylate) matrix*. Journal of Non-Crystalline Solids, 2006. **352**(3): p. 197-202.
  54. Huang, C., et al., *Multiple Energy Transfers in Rare Earth Complex-Doped SiO<sub>2</sub> Spheres*. Journal of Rare Earths, 2006. **24**(2): p. 134-137.
  55. Sobha, K.C. and K.J. Rao, *Luminescence of, and energy transfer between Dy<sup>3+</sup> and Tb<sup>3+</sup> in NASICON-type phosphate glasses*. Journal of Physics and Chemistry of Solids, 1996. **57**(9): p. 1263-1267.
  56. Yan, Z., et al., *Optical Properties of Dy<sup>3+</sup> Doped in Boroaluminasilicate Glass*. Journal of Rare Earths, 2007. **25**(Supplement 1): p. 99-103.
  57. Tanner, P.A., et al., *Non-resonant energy transfer from the 5D<sub>4</sub> level of Tb<sup>3+</sup> to the 5D<sub>0</sub> level of Eu<sup>3+</sup>*. Journal of Alloys and Compounds, 1994. **207-208**: p. 83-86.
  58. Rai, S. and S. Hazarika, *Fluorescence dynamics of Tb<sup>3+</sup> and Tb<sup>3+</sup>/Ho<sup>3+</sup> doped phosphate glasses*. Optical Materials, 2008. **30**(9): p. 1343-1348.
  59. Lin, H., et al., *Intense visible fluorescence and energy transfer in Dy<sup>3+</sup>, Tb<sup>3+</sup>, Sm<sup>3+</sup> and Eu<sup>3+</sup> doped rare-earth borate glasses*. Journal of Alloys and Compounds, 2005. **390**(1-2): p. 197-201.
  60. Reisfeld, R. and L. Boehm, *Energy transfer between samarium and europium in phosphate glasses*. Journal of Solid State Chemistry, 1972. **4**(3): p. 417-424.
  61. Cybinska, J., et al., *The orange emission of single crystals and sol gels based on Sm<sup>3+</sup> chelates*. Journal of Alloys and Compounds, 2008. **451**: p. 94-98.
  62. Qian, G., Z. Yang, and M. Wang, *Time-resolved spectroscopic study of Eu(TTA)<sub>3</sub>(TPPO)<sub>2</sub> chelate in situ synthesized in vinyltriethoxysilane-derived sol-gel-processed glass*. Journal of Luminescence, 2002. **96**(2-4): p. 211-218.
  63. Lee, M.H., F.L. Beyer, and E.M. Furst, *Synthesis of monodisperse fluorescent core-shell silica particles using a modified Stober method for imaging individual particles in dense colloidal suspensions*. Journal of Colloid and Interface Science, 2005. **288**(1): p. 114-123.
  64. Reisfeld, R., et al., *Spectroscopic properties of cerium in glasses and their comparison with crystals*. Spectrochimica Acta Part A: Molecular and Biomolecular Spectroscopy, 1998. **54**(13): p. 2143-2150.
  65. Stober, W., A. Fink, and E. Bohn, *Controlled growth of monodisperse silica spheres in the micron size range*. Journal of Colloid and Interface Science, 1968. **26**(1): p. 62-69.
  66. Avnir, D., D. Levy, and R. Reisfeld, *The nature of the silica cage as reflected by spectral changes and enhanced photostability of trapped Rhodamine 6G*. The Journal of Physical Chemistry, 2002. **88**(24): p. 5956-5959.
  67. da Silva, A.A., J. Flor, and M.R. Davolos, *Rhodamine B-containing silica films from TEOS precursor: Substrate surface effects detected by photoluminescence*. Surface Science, 2007. **601**(4): p. 1118-1122.
  68. Buining, P.A., L.M. Liz-Marzan, and A.P. Philipse, *A Simple Preparation of Small, Smooth Silica Spheres in a Seed Alcosol for Stober Synthesis*.

- Journal of Colloid and Interface Science, 1996. **179**(1): p. 318-321.
69. Avichezer, D., B. Schechter, and R. Arnon, *Functional polymers in drug delivery: carrier-supported CDDP (cis-platin) complexes of polycarboxylates -- effect on human ovarian carcinoma*. *Reactive and Functional Polymers*, 1998. **36**(1): p. 59-69.
  70. Torchilin, V.P. and V.S. Trubetskoy, *Which polymers can make nanoparticulate drug carriers long-circulating?* *Advanced Drug Delivery Reviews*, 1995. **16**(2-3): p. 141-155.
  71. Kawaguchi, H., *Functional polymer microspheres*. *Progress in Polymer Science*, 2000. **25**(8): p. 1171-1210.
  72. Szurdoki, F., K.L. Michael, and D.R. Walt, *A Duplexed Microsphere-Based Fluorescent Immunoassay*. *Analytical Biochemistry*, 2001. **291**(2): p. 219-228.
  73. Härmä, H., et al., *Luminescent energy transfer between cadmium telluride nanoparticle and lanthanide(III) chelate in competitive bioaffinity assays of biotin and estradiol*. *Analytica Chimica Acta*, 2007. **604**(2): p. 177-183.
  74. Hemmila, I., V.-M. Mikkala, and H. Takalo, *Development of luminescent lanthanide chelate labels for diagnostic assays*. *Journal of Alloys and Compounds*, 1997. **249**(1-2): p. 158-162.
  75. Akiva, U. and S. Margel, *Surface-modified hemispherical polystyrene/polybutyl methacrylate composite particles*. *Journal of Colloid and Interface Science*, 2005. **288**(1): p. 61-70.
  76. Qi, D., et al., *Synthesis of core-shell polymer microspheres by two-stage distillation-precipitation polymerization*. *European Polymer Journal*, 2005. **41**(10): p. 2320-2328.
  77. Nagao, D., et al., *Preparation of highly monodisperse poly(methyl methacrylate) particles incorporating fluorescent rhodamine 6G for colloidal crystals*. *Journal of Colloid and Interface Science*, 2006. **298**(1): p. 232-237.
  78. Esen, C., T. Kaiser, and G. Schweiger, *Photopolymerization reactions in aerosols: a simple method to the synthesis of monodisperse microspheres*. *Journal of Aerosol Science*, 1996. **27**(Supplement 1): p. S371-S372.
  79. Santa Maria, L.C., et al., *Preparation and characterization of polymer metal composite microspheres*. *Materials Letters*, 2006. **60**(2): p. 270-273.
  80. Partouche, E., D. Waysbort, and S. Margel, *Surface modification of crosslinked poly(styrene-divinyl benzene) micrometer-sized particles of narrow size distribution by ozonolysis*. *Journal of Colloid and Interface Science*, 2006. **294**(1): p. 69-78.
  81. Reisfeld, R., et al., *Spectroscopic properties and luminescence enhancement of lanthanide mixed complexes Ln[beta]3L in zirconia glasses*. *Optical Materials*, 2004. **26**(2): p. 191-198.
  82. Maind, S.D., et al., *Analysis of Indian blue ballpoint pen inks tagged with rare-earth thenoyltrifluoroacetates by inductively coupled plasma-mass spectrometry and instrumental neutron activation analysis*. *Forensic Science International*, 2006. **159**(1): p. 32-42.
  83. Morizzi, J., M. Hobday, and C. Rix, *Gallium(III) organophosphonate adducts with the bidentate amines 2,2'-bipyridyl and 1,10-phenanthroline*. *Inorganica Chimica Acta*, 2001. **320**(1-2): p. 67-74.
  84. Warrenner, R.N., et al., *Rigid molecular racks featuring the 1,10-phenanthroline ligand especially those co-functionalised with redox-active groups or other bidentate ligands*. *Tetrahedron*, 1997. **53**(11): p. 3991-



- 4012.
85. Marriott, G., et al., *Time-resolved delayed luminescence image microscopy using an europium ion chelate complex*. Biophysical Journal, 1994. **67**(3): p. 957-965.
  86. Georges, J., *Investigation of fluorescence efficiency in the europium-thenoyltrifluoroacetone chelate in aqueous and ethanolic solutions by laser-induced fluorescence and photothermal spectroscopic methods*. Analytica Chimica Acta, 1995. **317**(1-3): p. 343-351.
  87. Kokko, L., et al., *Europium(III) chelate-dyed nanoparticles as donors in a homogeneous proximity-based immunoassay for estradiol*. Analytica Chimica Acta, 2004. **503**(2): p. 155-162.
  88. Streck, W., et al., *Optical properties of Eu(III) chelates trapped in silica gel glasses*. Optical Materials, 1999. **13**(1): p. 41-48.
  89. Arnaud, N. and J. Georges, *Comprehensive study of the luminescent properties and lifetimes of Eu<sup>3+</sup> and Tb<sup>3+</sup> chelated with various ligands in aqueous solutions: influence of the synergic agent, the surfactant and the energy level of the ligand triplet*. Spectrochimica Acta Part A: Molecular and Biomolecular Spectroscopy, 2003. **59**(8): p. 1829-1840.
  90. Hirokawa, T., et al., *Isotachophoretic separation behavior of rare-earth EDTA chelates and analysis of minor rare-earth elements in an iron ore by bidirectional isotachopheresis-particle-induced X-ray emission*. Journal of Chromatography A, 2001. **919**(2): p. 417-426.
  91. Slooff, L.H., et al., *Optical properties of lissamine functionalized Nd<sup>3+</sup> complexes in polymer waveguides and solution*. Optical Materials, 2000. **14**(2): p. 101-107.
  92. Ken Kuriki, T.K., Nana Imai, Toshihiko Tamura, Susumu Nishihara, Akihiro Tagaya, Yasuhiro Koike and Yoshi Okamoto, *Fabrication and Properties of Polymer Optical Fibres Containing Nd-Chelate*. IEEE Photonics Technology Letters, 2000. **12**(8): p. 989-991.
  93. Skoog, D.A., et al., *Principles of Instrumental Analysis*. Thomson Press, 5th Edition, 1997(ISBN: 8131501167).
  94. Atkins, P.W. and J.d. Paula, *Atkins' Physical Chemistry*. Oxford University Press, 7th Edition, 2002(ISBN: 0198792859).
  95. Gerhard H. Dieke and H.H. Crosswhite, *Spectra and Energy Levels of Rare Earth Ions in Crystals*. Wiley-Interscience, New York, 1968.
  96. Harris, D.C. and M.D. Bertolucci, *Symmetry and Spectroscopy: Introduction to Vibrational and Electronic Spectroscopy*. 1980: Oxford University Press.
  97. Griffiths, D.J., *Introduction to Quantum Mechanics*. 2nd ed. 2004: Prentice Hall.
  98. Miessler, G.L. and D.A. Tarr, *Inorganic Chemistry*. 3rd ed. 2003: Pearson Prentice Hall.
  99. Campbell, R.J.K.a.J.A., *Strain modulation of optical f-f transitions of lanthanide ions*. 1980. p. 5341.
  100. Koenig, E. and S. Kremer, *Octahedral d<sub>4</sub>, d<sub>6</sub> ligand field spin-orbit energy level diagrams*. The Journal of Physical Chemistry, 1974. **78**(1): p. 56-59.
  101. Doggett, G. and B. Sutcliffe, *A Modern Approach to L-S Coupling in the Theory of Atomic Spectra*. Journal of Chemical Education, 1998. **75**(1): p. 110.
  102. Cotton, S., *Lanthanide and Actinide Chemistry*. John Wiley & Sons, 2006(ISBN-13: 978-0-470-01005-1).
  103. Shelby, J.E., *Introduction to Glass Science and Technology*. The Royal

- Society of Chemistry, 2005(ISBN: 0-85404-639-9).
104. Manara, D., A. Grandjean, and D.R. Neuville, *Structure of borosilicate glasses and melts: A revision of the Yun, Bray and Dell model*. Journal of Non-Crystalline Solids, 2009. **355**(50-51): p. 2528-2531.
  105. Rao, K.J., S. Kumar, and P. Vinatier, *Can any material form a glass?* Solid State Communications, 2004. **129**(10): p. 631-635.
  106. Song, S., et al., *Influence of dopants on the crystallization of borosilicate glass*. Ceramics International, 2009. **35**(8): p. 3037-3042.
  107. Wang, Z., et al., *Dielectric properties and crystalline characteristics of borosilicate glasses*. Journal of Non-Crystalline Solids, 2008. **354**(12-13): p. 1128-1132.
  108. Chowdari, B.V.R. and Z. Rong, *The role of Bi<sub>2</sub>O<sub>3</sub> as a network modifier and a network former in xBi<sub>2</sub>O<sub>3</sub> · (1 - x)LiBO<sub>2</sub> glass system*. Solid State Ionics, 1996. **90**(1-4): p. 151-160.
  109. Bhutta, T., Chardon, A.M., Shepherd, D.P., Daran, E., Serrano, C. and Munoz-Yague, A. , *Low phonon energy Nd:LaF<sub>3</sub> channel waveguide lasers fabricated by molecular beam epitaxy*. Journal of Quantum Electronics, 2001(37): p. 1469-1477.
  110. Lin, H., et al., *Infrequent blue and green emission transitions from Eu<sup>3+</sup> in heavy metal tellurite glasses with low phonon energy*. Physics Letters A, 2006. **358**(5-6): p. 474-477.
  111. Liao, M., et al., *Relaxation process of the 4I<sub>13/2</sub> level of Er<sup>3+</sup> in a borosilicate glass*. Journal of Non-Crystalline Solids, 2009. **355**(2): p. 96-100.
  112. Rae, A.I.M., *Quantum Mechanics*. Taylor & Francis, 5th Edition, 2007(ISBN: 1584889705).
  113. Bai, F., X. Yang, and W. Huang, *Preparation of narrow or monodisperse poly(ethyleneglycol dimethacrylate) microspheres by distillation-precipitation polymerization*. European Polymer Journal, 2006. **42**(9): p. 2088-2097.
  114. Bai, F., et al., *Monodisperse hydrophilic polymer microspheres having carboxylic acid groups prepared by distillation precipitation polymerization*. Polymer, 2006. **47**(16): p. 5775-5784.
  115. Basudeb Karmakar, Goutam De, and D. Ganguli, *Dense silica microspheres from organic and inorganic acid hydrolysis of TEOS*. Journal of Non-Crystalline Solids, 2000. **272**: p. 119-126.
  116. Wright, J.D. and N.A.J.M. Sommerdijk, *Sol-Gel Materials: Chemistry and Applications* 1st ed. 2000: CRC Press.
  117. Nai-Ning, W., Z. Hong-Jian, and Y. Xian-Huang, *A versatile Fraunhofer diffraction and Mie scattering based laser particle sizer*. Advanced Powder Technology, 1992. **3**(1): p. 7-14.
  118. Venkata Mohan, S., et al., *Bioslurry phase remediation of chlorpyrifos contaminated soil: Process evaluation and optimization by Taguchi design of experimental (DOE) methodology*. Ecotoxicology and Environmental Safety, 2007. **68**(2): p. 252-262.
  119. Maghsoodloo, S., et al., *Strengths and limitations of taguchi's contributions to quality, manufacturing, and process engineering*. Journal of Manufacturing Systems, 2004. **23**(2): p. 73-126.
  120. Taghizadeh, M., et al., *Selective zirconium stripping of a loaded Cyanex 272 using Taguchi orthogonal array design*. Minerals Engineering, 2007. **20**(15): p. 1401-1403.
  121. Azin, M., R. Moravej, and D. Zareh, *Production of xylanase by Trichoderma*

- longibrachiatum on a mixture of wheat bran and wheat straw: Optimization of culture condition by Taguchi method.* Enzyme and Microbial Technology, 2007. **40**(4): p. 801-805.
122. Ebendorff-Heidepriem, H. and D. Ehrhart, *Formation and UV absorption of cerium, europium and terbium ions in different valencies in glasses.* Optical Materials, 2000. **15**(1): p. 7-25.
123. Kucuk, A. and A.G. Clare, *Optical properties of cerium and europium doped fluoroaluminate glasses.* Optical Materials, 1999. **13**(3): p. 279-287.
124. Wada, N. and K. Kojima, *Glass composition dependence of Eu<sup>3+</sup> ion red fluorescence.* Journal of Luminescence, 2007. **126**(1): p. 53-62.
125. Martens, R. and W. Müller-Warmuth, *Structural groups and their mixing in borosilicate glasses of various compositions - an NMR study.* Journal of Non-Crystalline Solids, 2000. **265**(1-2): p. 167-175.
126. Mishra, R.K., et al., *Effect of fluoride ion incorporation on the structural aspects of barium-sodium borosilicate glasses.* Journal of Non-Crystalline Solids, 2009. **355**(7): p. 414-419.
127. Bringley, J.F., et al., *Silica nanoparticles encapsulating near-infrared emissive cyanine dyes.* Journal of Colloid and Interface Science, 2008. **320**(1): p. 132-139.
128. Lu, Z., et al., *Facile synthesis of Fe<sub>3</sub>O<sub>4</sub>/SiO<sub>2</sub> composite nanoparticles from primary silica particles.* Colloids and Surfaces A: Physicochemical and Engineering Aspects, 2008. **317**(1-3): p. 450-456.
129. Chen, H. and J. He, *Rapid evaporation-induced synthesis of monodisperse budded silica spheres.* Journal of Colloid and Interface Science, 2007. **316**(2): p. 211-215.
130. Liu, G., et al., *Facile synthesis of silica/polymer hybrid microspheres and hollow polymer microspheres.* Polymer, 2007. **48**(20): p. 5896-5904.
131. Lu, Z., et al., *Robust fluorescein-doped silica nanoparticles via dense-liquid treatment.* Colloids and Surfaces A: Physicochemical and Engineering Aspects, 2007. **303**(3): p. 207-210.
132. An, Y., et al., *Preparation and self-assembly of carboxylic acid-functionalized silica.* Journal of Colloid and Interface Science, 2007. **311**(2): p. 507-513.
133. Petit, L., et al., *Luminescence properties of Eu<sup>3+</sup> or Dy<sup>3+</sup>/Au co-doped SiO<sub>2</sub> nanoparticles.* Materials Letters, 2007. **61**(14-15): p. 2879-2882.
134. Du, X., et al., *Comparative study on fluorescence enhancement and quenching of europium and terbium chelate anions in cationic micelles.* Spectrochimica Acta Part A: Molecular and Biomolecular Spectroscopy, 2003. **59**(2): p. 271-277.
135. Oczko, G. and P. Starynowicz, *Comparison of optical properties and crystal structures of the praseodymium and europium chloroderivatives of acetates.* Journal of Molecular Structure, 2005. **740**(1-3): p. 237-248.
136. Fedosseev, A.M., et al., *Crystal structure and luminescence properties of europium-doped iodo- and telluromolybdate compounds.* Journal of Luminescence, 2000. **87-89**: p. 1065-1068.

**Appendix I - Publications**

### Refereed Journals

1. Cathy McCullough, Peter K.J. Robertson, **Morgan Adams**, Pat M. Pollard and Abdulrahman Mohammed, "Development of a slurry continuous flow reactor for photocatalytic treatment of industrial waste water", *Journal of Photochemistry and Photobiology A: Chemistry*, Article in press February 2010
2. Pat Pollard, **Morgan Adams**, Peter K.J. Robertson, Konstantinos Christidis, Simon Officer, Gopala R. Prabhu, Kenneth Gow and Andrew R. Morrisson, "Environmental forensic investigations: The potential use of a novel heavy metal sensor and novel taggants", *Criminal and Environmental Soil Forensics*, Springer Netherlands, ISBN 978-1-4020-9203-9, 2009
3. Peter K.J. Robertson, Kenneth D. Black, **Morgan Adams**, Kate Willis, Fraser Buchan, Heather Orr, Linda Lawton, Cathy McCullagh, "A new generation of biocides for control of crustacea in fish farms", *Journal of Photochemistry and Photobiology B: Biology*, Volume 95, Issue 1, 2 April 2009, Pages 58-63
4. **Morgan Adams**, Ian Campbell and Peter K.J. Robertson, "Novel photocatalytic reactor development for removal of hydrocarbons from water", *International Journal of Photoenergy Special Publication*, Volume 2008, Article ID: 674537

### Conferences

1. **Morgan Adams**, Naomi Turner and Pat Pollard, "A study of annulus lubrication for oil well completion using scale model tests", *IEEE/MTS Oceans 08 Quebec City Conference, Oceans, Poles and Climate: Technological Challenges*, 2008
2. **Morgan Adams** and Pat Pollard, "Novel tracers for environmental monitoring", *IEEE Oceans 07 Conference, Marine Challenges: Coastline to Deep Sea*, ISBN: 1-4244-0635-8, 2007
3. Pat Pollard, **Morgan Adams**, Simon Officer, Gopala R. Prabhu and Catherine Hunter, "Sensitive novel fluorescent tracers for environmental monitoring", *IEEE Oceans 07 Conference, Marine Challenges: Coastline to Deep Sea*, ISBN: 1-4244-0635-8, 2007
4. Abdulrahman Mohammed, Cathy McCullough, Patricia Pollard, Peter K.J. Robertson and **Morgan Adams**. "Photocatalytic destruction of a model pollutant in a novel continuous flow photocatalytic reactor" SP-2 The Second International Conference on Semiconductor Photochemistry, 23025 July 2007, The Robert Gordon University, Aberdeen.
5. Morgan Adams, Ian Campbell and Peter K.J. Robertson, "Novel photocatalytic reactor for the removal of hydrocarbons from water"

SP-2 The Second International Conference on Semiconductor Photochemistry, 23-25 July 2007, Poster Competition, The Robert Gordon University, Aberdeen.

### **Conference Prizes**

1. Second Prize of \$200, IEEE/MTS Oceans 08 Quebec City Conference Poster Competition, Oceans Poles and Climate: Technological Challenges, 2008
2. Second Prize of £200, IEEE Oceans 07 Conference Poster Competition, Marine Challenges: Coastlines to Deep Sea, 2007

# Novel Tracers for Environmental Applications

M. Adams and P. Pollard

**Abstract**— Novel glass tracers, based on narrow band atomic fluorescence, have been developed for deployment as environmental tracers. The use of discrete fluorescent species in an environmentally stable host has been developed to replace existing toxic, broad band molecular dye tracers. The narrow band emission signals offer the potential for the tracing of a large numbers of signals in the same environment. This will give significant competitive advantage and increased data accuracy and also allow multiple source environmental monitoring of environmental parameters. The work presented here aims to outline potential parameters for using lanthanide doped borosilicate glass as environmental tracers.

**Index Terms**— environmental, tracer, particle, sediment, fluorescence, lanthanides

## I. INTRODUCTION

Environmental tracing is a vital scientific field in studying the fate of substances in aqueous environments. This can range from monitoring the fate of industrial and domestic effluents in ecological systems by adding a dye tracer to outflow sources and studying the dispersion, dilution and travel of the discharge [1]. At the moment typical fluorescent dye tracers rely on molecular fluorescence for detection. This, which although strong, is very broad with typically 80-120nm bandwidth. This has several major disadvantages firstly as these fluorescent molecular dyes have been used as tracers for many years the background levels in many areas are elevated, making it very difficult to carry out these kind of tracer studies in areas of need, e.g. pollutant and sediment tracer studies in harbours where temporal studies are needed sometimes requiring comparative tracer studies over 10 or 20 years. An example of which is seen in Figure 1.

One of the largest problems associated with fluorescent dye tracers are their eco-toxicological effects within the environment and their effect on human health. Commonly used tracers such as fluorescein, Lissamine Flavine FF, Rhodamine WT, Rhodamine B, Sulpho Rhodamine G, Sulpho

Rhodamine B, eosin, among others, have all been studied for the toxicological effects [2].



Figure 1. Typical dye tracer being deployed

Many of these may have breakdown products and synergistic effects with compounds within aqueous systems that could produce increased dangers to human health and the environment. So the need for a new type of tracer which can provide environmental stability and minimal toxicological effects is great. Also the application of such tracers in sediment transport monitoring in the North Sea environment where there already exist a large number of possible background contaminant sources such as hydrocarbons, which exhibit broad band emission spectra, make monitoring fluorescent tracers challenging. In this environment the use of a tracer exhibiting discrete fluorescent emissions would be a distinct advantage, allowing not only real time fluorescence measurements to be made without background interference but also several studies to be carried out in the same area.

Sediment transport occurs through natural processes such as currents, tides and waves, and through anthropogenic activities such as dredging, dam building and sub sea constructions. These can be studied by placing tracers in to the sediment layer to monitor movement and travel. With the current air of energy conservation and sustainability, governments all over the world are funding projects for wind, tidal and wave energy devices. The trend of placing turbines in coastal waters is causing increasing concern with the general public, not only for aesthetic properties but for their impact upon the local marine environment. The localised effect of sub sea manmade structures on the sea bed can be studied by the monitoring of sediment movement and distribution around the

M. Adams and P. Pollard are in The Centre for Research in Energy and the Environment, The Robert Gordon University, Schoolhill, Aberdeen, AB10 1FR

Contact: M. Adams – Email: [m.adams@rgu.ac.uk](mailto:m.adams@rgu.ac.uk) Tel: (+44) 01224 262840



structure [3]. The interrupted movement of sediment on the sea bed can directly impact upon crustaceans and other bottom dwelling creatures. Another example is the case of dredging, companies undertaking such activity aim to minimise the amount of disturbed sediment entering the water column. Tracing allows the close study of where this disturbed sediment, which may be carried by ambient water currents to sensitive areas such as shell fish beds or areas of biodiversity, settles. Of course this needs to be a comparative tracer in terms of size to the particles in the sediment, if not there is no way of accurately duplicating the movement of the natural particles [4].

## II. MATERIALS AND METHODS

### 2.1 Glass Tracer Production

For the production of the single doped glass tracer a standard borosilicate glass composition was used [5]. To this the appropriate mol % (0.2 – 2.0) of rare earth salt was added to produce a 7 g batch. This volume of sample is processed in an Agate ball mill for a total of 8 minutes to produce a homogeneous mixture, which was then transferred to a platinum crucible.

The platinum crucible was then placed in to a 1500 °C furnace the sample is heated to 550 °C for 30 minutes to allow the boric acid to melt without expansion brought on by rapid heating. The temperature is then raised to 900 °C, 1000 °C and 1100 °C, holding for 1 hour at each point before rising to pour temperature at 1250 °C. The sample is then poured in to a brass mould which has been pre-heated on a hot plate to reduce possibility of thermal shock.

### 2.2 Spectral Characterisation

Spectral characteristics were studied in 10 x 30 mm glass samples using a Perkin Elmer Lambda Spectrophotometer to produce the 3D spectrum which allowed specific selection of excitation and emission wavelengths. An Edinburgh Instruments FLS920P Spectrophotometer was used for the concentration study using the excitation and emission wavelengths obtained.

## III. RESULTS AND DISCUSSION

The spectroscopic analysis of a 0.6 mol% Dysprosium doped borosilicate glass sample generated a 3D fluorescence spectrum, Figures 2 and 3, which can be used to select the most appropriate wavelengths for different environmental applications.

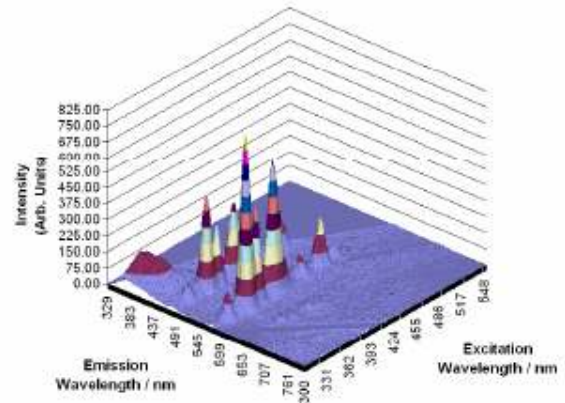


Figure 2. Fluorescence Spectrum of a 0.6 mol% Dysprosium sample

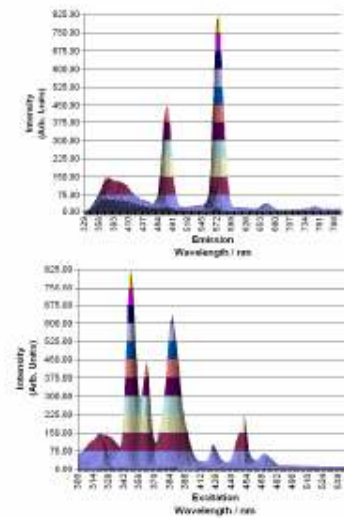


Figure 3. Emission and Excitation Spectra of a 0.6 mol% Dysprosium sample

The spectral excitation and emission detail for the most intense lines in Dysprosium doped borosilicate glass which have been investigated for possible use as a tracer are seen in Table 1.

Rare Earth Ion	Excitation Wavelength / $\lambda$	Emission Wavelength / $\lambda$
Dy	324	481 and 575
Dy	352	481 and 575
Dy	364	481 and 575
Dy	391	481 and 575
Dy	426	481 and 575
Dy	452	481 and 575
Dy	471	481 and 575

Table 1. Excitation and Emission wavelengths for Dysprosium



3.1 Concentration Study of Dysprosium Ions in Borosilicate Glass

From spectroscopic analysis of the 0.2 – 2.0 mol% Dysprosium doped borosilicate glass Figure 4 displays the emission intensities at 481 λ from 324, 352, 364, 391, 426, 452 and 471 λ excitations. It can be seen that the most intense spectral output was obtained from the 0.8 mol% sample with a 391nm excitation.

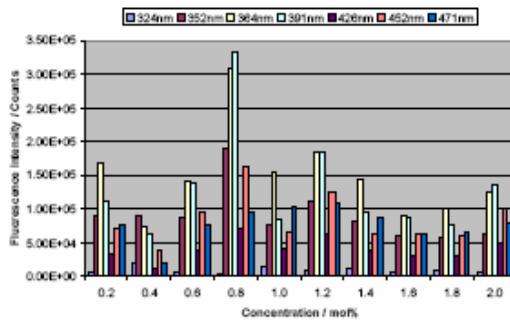


Figure 4. Dysprosium Emissions at 481 λ from 324, 352, 354, 391, 426, 452 and 471 λ Ex

Further analysis of the 0.2 – 2.0 mol% Dysprosium doped borosilicate glass Figure 5 displays the emission intensities at 575 λ from 324, 352, 364, 391, 426, 452 and 471 λ excitations. It can be seen that the most intense spectral output was obtained from the 0.8 mol% sample with a 391 λ excitation.

The emission signal obtained from the 391 λ excitation was far greater at 575 λ (706500) when compared to that of 481 λ (333000).

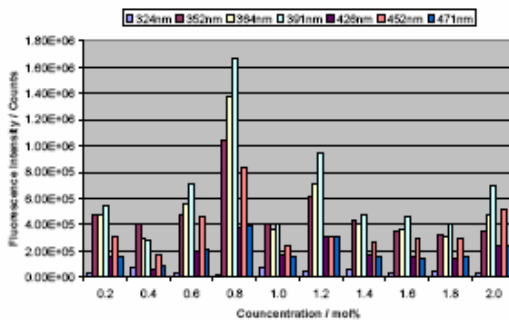


Figure 5. Dysprosium Emissions at 575 λ from 324, 352, 354, 391, 426, 452 and 471 λ Ex

IV. CONCLUSIONS

The use of borosilicate glass doped with lanthanide ions has the potential to produce a novel environmental tracer exhibiting highly discrete fluorescent emissions. The initial concentration study of dysprosium ions in a glass matrix shows the level of useful doping possible within the borosilicate glass matrix, in this case 0.8 mol% with an excitation of 391 λ and emission of 575 λ. Although the potential to use 352, 364, 391 and 452 λ excitations allows the possibility of avoiding excitation wavelengths of other fluorescent species which could generate background signals.

The glass matrix provides an environmentally stable and inert host for use within a variety of aqueous and hostile environments, in an environment where there is the possibility of multiple sources of contamination, e.g. platforms and cuttings piles, the use of multiple tracers exhibiting discrete fluorescent emissions would be a distinct advantage to monitor the origin of a contaminant from more than one source. The incorporation of fluorescent ions within a glass matrix has another major benefit, the glass protect the lanthanide ions from external influences such as water quenching or environmental degradation. This provides an ideal material for use an environmental tracer where the tracer may be exposed to varying degrees of chemical and biological attack. Glass can also be formed in to many shapes and forms to mimic naturally occurring media.

References:

- [1] Bachtar, T., Conkley, J.P., Risk, M.J., 1996. Tracing sewage-contaminated sediments in Hamilton Harbour using selected geochemical indicators. *The Science of the Total Environment*, Volume 179, Pages 3-16.
- [2] Field, M.S., Wilhelm, R.G., Quinlan, J.F., Aley, T.J., 1995. An assessment of the potential adverse properties of fluorescent tracer dyes used for groundwater tracing. *Environmental Monitoring and Assessment*, Volume 38, Pages 75-96.
- [3] Tan, S-K, Yu, G., Lim, S-Y and Ong, M-C. 2005. Flow structure and sediment motion around submerged vanes in open channel. *J. Watrwy., Port, Coast, and Oc. Eng.*, Volume 131, Issue 3, Pages 132-136.
- [4] Black, K.S., Athey, S., Wilson, P., Evans, D. 2006. The use of particle tracking in sediment transport studies: a review. *Journal of the Geological Society (Special Issue) Measuring Sediment Transport on the Continental Shelf. Coastal and Sediment Shelf Transport*, GSL Special Publications, ISBN 978-1-86239-217-5.
- [5] Zhu, D., Zhou, W., Day, D.E., Ray, C.S., 2007. Preparation of fluorescent glasses with variable compositions. *Ceramics International*, Volume 33, Issue 4, Pages 563-568.

# Sensitive Novel Fluorescent Tracers for Environmental Monitoring

P. Pollard, M. Adams, G.R. Prabhu, S. Officer, and C. Hunter

**Abstract**—This paper discusses the development and use of novel glass and polymer tracers, based on narrow band atomic fluorescence, which have been developed for deployment as environmental tracers. The use of discrete fluorescent species in an environmentally stable host has been developed to replace existing toxic, broad band molecular dye tracers. The narrow band emission signals offer the potential for the tracing of a large numbers of signals in the same environment. This will give significant competitive advantage and increased data accuracy and also allow multiple source environmental monitoring of environmental parameters. These novel environmental tracers exhibiting highly discrete fluorescent emissions can also be formed into many shapes, forms and densities to mimic naturally occurring media.

**Index Terms**— environmental, tracer, particle, sediment, fluorescence, lanthanides

## I. INTRODUCTION

Currently typical fluorescent dye tracers rely on molecular fluorescence for detection which may produce an intense signal but is very broad, typically 80-120nm bandwidth. This has several major disadvantages as only a small number of target species can be monitored simultaneously because there is spectral overlap of the broad tracer bandwidths, secondly as these fluorescent molecular dyes have been used as tracers for many years the background levels of these dye tracers in many areas are elevated, making it very difficult to use them to carry out these kind of tracer studies in areas of need, e.g. contaminant and sediment tracer studies in harbours where temporal studies are needed sometimes requiring comparative tracer studies over 10 or 20 years. Also the application of such tracers in sediment transport monitoring in the North Sea environment where there already exist a large number of possible background contaminant sources such as

hydrocarbons, which exhibit broad band emission spectra, make monitoring molecular fluorescent tracers challenging. Figure 1 (a) and (b) show the use of a molecular fluorescent tracer in produced water.

In an environment where there is the possibility of multiple sources of contamination, e.g. many platforms and cuttings piles, the use of multiple tracers exhibiting discrete fluorescent atomic emissions with wavelength and lifetime discrimination would be a distinct advantage allowing the monitoring of the origin of contaminants from more than one source. Not only allowing real time fluorescence measurements to be made with reduced background interference, but also many studies can be carried out in the same area.



(a)



(b)

Figure 1. (a) Produced water discharge, (b) Tracer doped discharge

Sediment transport occurs through natural processes such as

P. Pollard, M. Adams, G. R. Prabhu S. Officer and C. Hunter are in The Centre for Research in Energy and the Environment, The Robert Gordon University, Schoolhill, Aberdeen, AB10 1FR  
Contact: P. Pollard – Email: [p.pollard@rgu.ac.uk](mailto:p.pollard@rgu.ac.uk) Tel: (+44) 01224 262836



currents, tides and waves, and through anthropogenic activities such as dredging, dam building and sub sea constructions. These can be studied by placing tracers in to the sediment layer to monitor movement and travel. With the present public focus on energy conservation and sustainability, governments all over the world are funding projects for wind, tidal and wave energy devices. The trend of placing turbines in coastal waters is causing increasing concern with the general public, not only for aesthetic properties but for their impact upon the local marine environment. The localised effect of sub sea manmade structures on the sea bed can be studied by the monitoring of sediment distribution and movement around the structure. The interrupted movement of sediment on the sea bed can directly impact upon crustaceans and other bottom dwelling creatures.



(a)



(b)

Figure 2. (a) and (b) Dye tracer deployment in a bay

Another example is the case of dredging, companies undertaking such activity aim to minimise the amount of disturbed sediment entering the water column. Figure 2 (a) and (b) show the deployment of a dye tracer for sediment tracing. Tracing allows the close study of where this disturbed sediment may be carried by ambient water currents and where it settles particularly in sensitive areas such as shell fish beds or areas of biodiversity, settles.

Of course this needs to be a comparative tracer in terms of size to the particles in the target sediment. The development of these novel tracers allows control of physical properties such as size and density. This can be engineered to mimic the naturally occurring sediment particles and therefore provide a

far closer replication of particle behaviour. Glass also provides an ideal material for use as an environmental tracer where the tracer may be exposed to varying degrees of chemical and biological attack as it protects the lanthanide tracer from water quenching external influences and degradation.

## II. MATERIALS AND METHODS

For the production of the glass tracer a standard borosilicate glass composition was used [4]. To this the appropriate mol% of rare earth salt was added to produce a 7 g batch. This volume of sample is processed in an Agate ball mill for a total of 8 minutes to produce a homogeneous mixture, which was then transferred to a platinum crucible.

The platinum crucible was then placed in to a 1500 °C furnace the sample is heated to 550 °C for 30 minutes to allow the boric acid to melt without expansion brought on by rapid heating. The temperature is then raised to 900 °C, 1000 °C and 1100 °C, holding for 1 hour at each point before rising to pour temperature at 1250 °C. The sample is then poured in to a brass mould which has been pre-heated on a hot plate to reduce possibility of thermal shock.

The production of doped borosilicate glass particles was achieved by crushing pieces of the doped bulk glass and ball milling them before sieving. The tracers used in the investigation reported in this paper were 75 µm – 500 µm although tracers of larger and much smaller size have been made.

Lanthanide chelate doped polymer spheres [5,6,7,8] were prepared by using a typical procedure for a distillation-precipitation polymerization.

The Rhodamine and Fluorescein molecular dye samples were prepared in a stock solution of distilled water at a concentration of  $1 \times 10^{-5}$  M. The crude oil samples were diluted in dichloromethane, 0.1ml in 20ml and 5µl in 10ml for the background experiments.

All sample spectroscopic analysis was carried out using an Edinburgh Instruments FLS920P Spectrophotometer for the doped bulk glass samples, doped polymer, molecular dyes and oil samples.

In order to test the fluorescent lifetimes, time resolved fluorescence studies of the lanthanide doped tracers were carried out. A Laser Induced Scanning Fluorescence Microscope was used. Short laser pulses (~ 5nsec.) of appropriate wavelength, generated from an OPO laser were used to excite the fluorescence from the rare-earth ion doped samples. The temporal fluorescence intensity variations were detected using a highly sensitive photomultiplier tube. The fluorescence wavelength was selected by a set of filters placed in front of the detector. A photodiode (PD) in combination with a partially reflecting microscopic glass slide was used to

070131-042

3

monitor the laser pulses. A Tektronix TDS 380 digital real-time oscilloscope was used to view and record the signals from the photomultiplier tube.

### III. RESULTS AND DISCUSSION

#### 3.1 Europium Spectral Characterisation and Concentration Studies:

Initially 3D spectra of the excitation and emission peaks of a range of single and multiple lanthanide doped glass tracers were recorded to indicate possible useful tracer peaks. Figure 3 shows a Europium, Terbium and Dysprosium Triple doped tracer. Tracer dopant concentration studies were then carried out to investigate potential interactions between different concentrations of different dopants affecting the emission characteristics of the tracer and to investigate any quenching effects. Figure 4 shows the effect of altering the excitation wavelength on the 612 nm emission line as the Europium ion concentration is increased from a tracer dopant level of 0.2 mol% to 2.0 mol%. From Figures 3 and 4 it can be seen that by altering the chosen lanthanide dopant, number of dopants, dopant concentration and using selective excitation and emission wavelengths there are a huge number of possible unique tracer combinations.

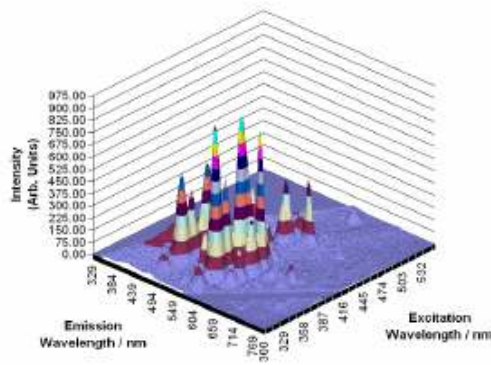


Figure 3. Europium, Terbium and Dysprosium Triple doped tracer

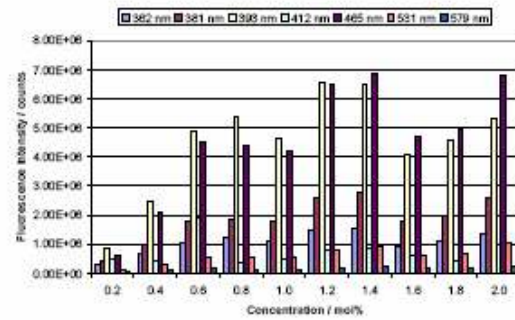


Figure 4. Europium Emissions at 612 nm from 362, 381, 393, 412, 465, 531 and 579 nm ex

#### 3.2 Lanthanide Glass Tracer Comparison with Existing Molecular Dye Tracers:

The discrete fluorescent emission from a Europium glass tracer is shown in Figure 5 and Figure 6 shows the discrete fluorescence emission from a Europium chelate doped polymer. The chelate acts as an energy transfer molecule which absorbs ultra violet light and transfers it to the europium ion. Figures 7 and 8 show the commonly used molecular dyes Fluorescein and Rhodamine with much broader FWHM spectral bandwidths of approximately 50 nm and 60 nm compared to the lanthanide FWHM spectral bandwidths of 12 nm and 8 nm. The significantly narrower bandwidth emission peaks of the lanthanide based tracers achieve more selective detection of multiple tracers without overlap interfere and gives the potential to selectively simultaneously monitor many different tracers in the same location.

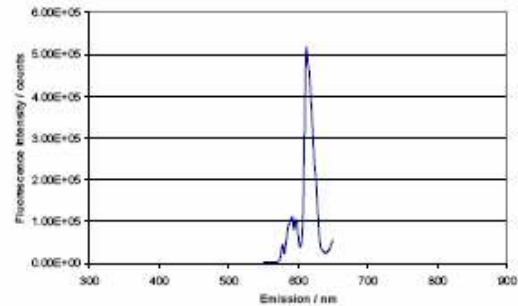


Figure 5. Fluorescent Emission from Europium doped bulk glass @ 465 nm ex

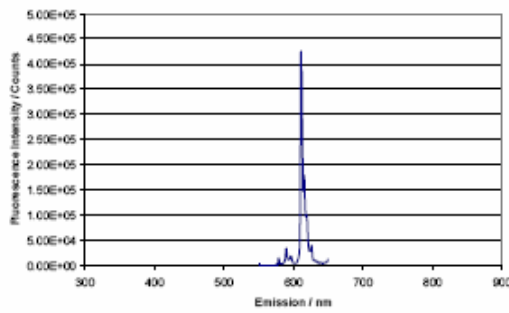


Figure 6. Fluorescent Emission from a Europium Chelate doped polymer @ 355 λ ex

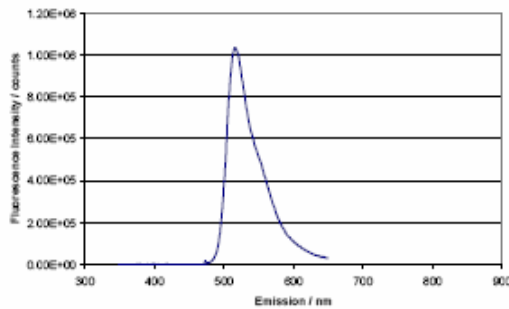


Figure 7. Fluorescent emission from a Fluorescein dye tracer @ 475 λ ex

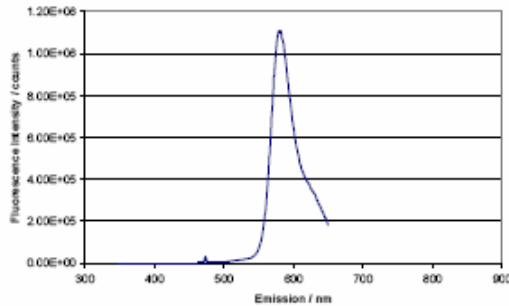


Figure 8. Fluorescent emission from a Rhodamine dye tracer @ 475 λ ex

### 3.3 Background Fluorescence Discrimination:

The use of environmental tracers doped with lanthanide ions have the distinct advantage of their discrete fluorescent emissions which has already been shown in Figures 5 and 6. The extremely broad fluorescence of oil samples can be seen in Figures 9 and 10, this can be highly problematic for dye tracers which emit in the same region. Figure 11 shows a sample of Europium chelate doped polymer spheres in Brent

Crude and it can clearly be seen that the presence of oil posed no background problem. However the spectral lifetime characteristics of the lanthanide tracers are very different from the lifetime of background fluorescence which it typically molecular in origin. This is an extra discrimination against background interference and is an additional advantage of using lanthanide based tracers.

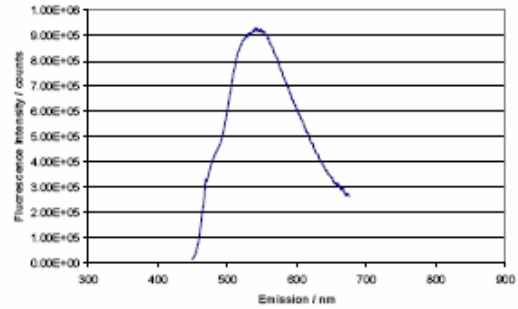


Figure 9. Fluorescent emission from Brent Crude Oil @ 470 λ ex

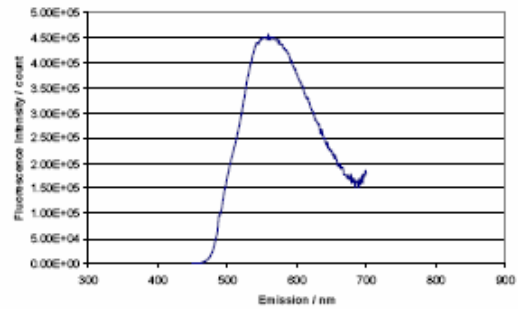


Figure 10. Fluorescent emission from Gullfaks Crude oil @ 490 λ ex

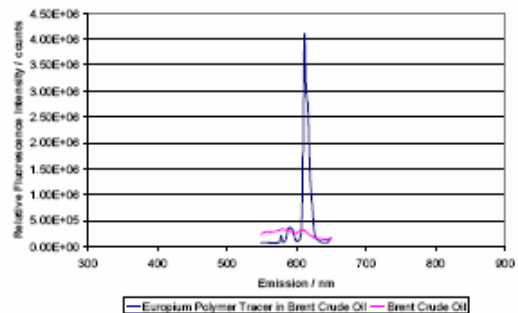


Figure 11. Europium Polymer Tracer analysed in a 5 μl Brent Oil in 10ml DCM @ 355 λ ex

#### 3.3.1 Lifetime Discrimination



A typical normalised fluorescence pulse from Europium in the tracer sample, for 464nm laser excitation and fluorescence emission at 615 nm (filtered through an interference filter with transmission peak at 620 and bandwidth of 10 nm) is shown in Figure 12. It shows a fast rising pulse with a long exponentially decaying tail corresponding to the long fluorescence lifetime of the Europium. The lifetime is calculated based on single exponential fluorescence decay and the characteristic lifetime constant of the exponential curve as the fluorescent lifetime of the particular lanthanide ions. Three data sets were used to calculate an average fluorescent lifetime of Europium and this sample shows an average lifetime of 1.95 ns.

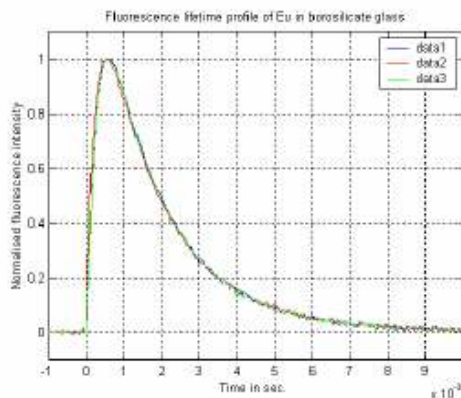


Figure 12. Fluorescent lifetime profile of Europium ions in borosilicate glass

3.4 Tracer Detection:

The tracer detection system developed for the trial investigation utilised a pulsed 532 nm laser as the excitation source with an optical fibre collector coupled to an avalanche photodiode, fitted with a 10nm band pass filter at 610nm for Europium fluorescence. To replicate the process of scanning the sea bed from a moving vessel or a towed sledge, the coarse sediment was scanned past the fixed excitation and detection system. See Figure 13 for schematic.

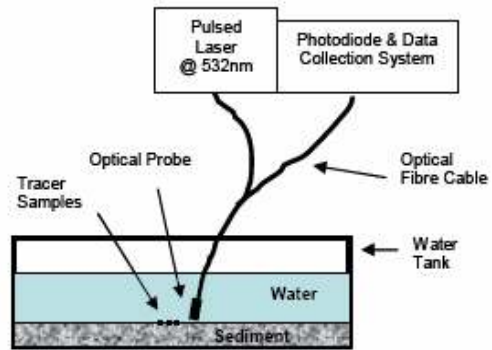


Figure 13. Schematic of Tracer Detection System Trial

To demonstrate the potential for using lanthanide doped glass as an environmental tracer a real time detection study was undertaken. The tank contained a North Sea sediment “sea bed” where a Europium glass tracer was used. Figure 14 shows a 3D fluorescence map observed for one deployment of tracer, clearly observed in 3 locations in the tank.

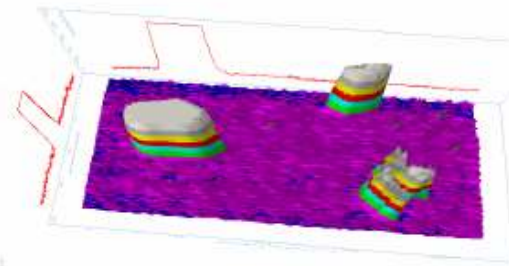


Figure 14. 3D fluorescence map of Europium glass tracer on a coarse sediment bed

Figure 4 showed the optimum excitation wavelengths for Europium, the excitation used for this experiment was 532nm which has low quantum efficiency for the Europium ion. Even with the lower excitation energy, the detection system show slight saturation from one of the doped patches, this shows that with increased quantum efficiency gained from a 465nm source could in theory allow even lower detection limits.

#### IV. CONCLUSION

The concept of using lanthanide doped glasses and polymers environmental tracers has been demonstrated. The spectral characterisation and concentration studies of the lanthanide doped tracer allows the selection of parameter to produce future tracers and detection systems for particular applications. By altering the chosen lanthanide dopant, number of dopants, dopant concentration and using selective excitation and emission wavelengths there are a huge number of possible unique tracer combinations. The significantly narrower bandwidth emission peaks of the lanthanide based tracers achieve more selective detection of multiple tracers without overlap interfere and gives the potential to selectively simultaneously monitor many different tracers in the same location. The spectral lifetime characteristics of the lanthanide tracers are very different from the lifetime of background fluorescence which it typically molecular in origin. This is an extra discrimination against background interference and is an additional advantage of using lanthanide based tracers.

The use of discrete fluorescent species in an environmentally stable host has been developed to replace existing toxic, broad band molecular dye tracers. The narrow band emission signals offer the potential for the tracing of a large numbers of signals in the same environment. This will give significant competitive advantage and increased data accuracy and also allow multiple source environmental monitoring of environmental parameters. These novel environmental tracers exhibiting highly discrete fluorescent emissions can also be formed into many shapes, forms and densities to mimic naturally occurring media.

#### V. REFERENCES

- [1] Cromey, C., Nickell, T., Black, K., Provost, P. and Griffiths, C., "Validation of a fish farm waste resuspension model by use of a particulate tracer discharged from a point source into coastal environment", *Estuaries*, 2002, 25 No 5, 916-929
- [2] Ahmed, Abdulwaheed, Webster, L., Pollard, P., Davies, I., Russell, M., Walsham, P., Packer, G. and Moffat, C., "The distribution and composition of hydrocarbons in sediments from the Fladen ground, North Sea, an area of oil production" *J. Environ. Monit.*, 2006, 8, 307-316.
- [3] D. McStay, P.K.J. Robertson, P. Pollard, I. Edwards, E. Bensen, A. Al-Obaidi, and D. Tait. "A multicapability sensor for hydrocarbons, synthetic based fluids and heavy metals: Applications for environmental monitoring during removal of drill cutting piles", *Underwater Technology*, 2002, 25, 69-75.
- [4] Zhu, D., Zhou, W., Day, D.E., Ray, C.S., 2007. Preparation of fluorescent glasses with variable compositions. *Ceramics International*. Volume 33. Issue 4. Pages 563-568.
- [5] Qi, Donglai, Bai, Feng, Yang, Xinlin, Huang, Wenqiang. 2005. Synthesis of core-shell polymer microspheres by two-stage distillation-precipitation polymerization. *European Polymer Journal*. Volume 41. Issue 10. Pages 2320-2328.
- [6] Ken Kuriki, Takeyuki Kobayashi, Nana Imai, Toshihiko Tamura, Susumu Nishihara, Akihiro Tagaya, Yasuhiro Koike and Yoshi Okamoto. 2000. Fabrication and Properties of Polymer Optical Fibres Containing Nd-Chelate. *IEEE Photonics Technology Letters*. Volume 12. Issue 8. Pages 989-991.
- [7] Arnaud, N., Georges, J., Comprehensive study of the luminescent properties and lifetimes of Eu<sup>3+</sup> and Tb<sup>3+</sup> chelated with various ligands in aqueous solutions: influence of the synergic agent, the surfactant and the energy level of the ligand triplet. 2003. *Spectrochimica Acta Part A: Molecular and Biomolecular Spectroscopy*. Volume 59. Issue 8. Pages 1829-1840.
- [8] Bai, Feng, Yang, Xinlin, Huang, Wenqiang, 2006. Preparation of narrow or monodisperse poly(ethyleneglycol dimethacrylate) microspheres by distillation-precipitation polymerization. *European Polymer Journal*. Volume 42. Issue 9. Pages 2088-2097.

## **Environmental Forensic Investigations: The Potential use of a Novel Heavy Metal Sensor and Novel Taggants**

P. Pollard, M. Adams, P.K.J. Robertson, K. Christidis, S. Officer, G.R. Prabhu, K. Gow and A. Morrisson.

Centre for Research in Energy and Environment, The Robert Gordon University,  
Schoolhill, Aberdeen, AB10 1FR

### **ABSTRACT**

This chapter presents a novel hand-held instrument capable of real-time *in situ* detection and identification of heavy metals, along with the potential use of novel taggants in environmental forensic investigations. The proposed system provides the facilities found in a traditional laboratory-based instrument but in a hand held design, without the need for an associated computer. The electrochemical instrument uses anodic stripping voltammetry, which is a precise and sensitive analytical method with excellent limits of detection. The sensors comprise a small disposable plastic strip of screen-printed electrodes rather than the more common glassy carbon disc and gold electrodes. The system is designed for use by a surveyor on site, allowing them to locate hotspots, thus avoiding the expense and time delay of prior laboratory analysis. This is particularly important in environmental forensic analysis when a site may have been released back to the owner and samples could be compromised on return visits. The system can be used in a variety of situations in environmental assessments, the data acquired from which provides a metals fingerprint suitable for input to a database. The proposed novel taggant tracers, based on narrow band atomic fluorescence, are under development for potential deployment as forensic environmental tracers. The use of discrete fluorescent species in an environmentally stable host has been investigated to replace existing toxic, broad band molecular dye tracers. The narrow band emission signals offer the potential for tracing a large number of signals in the same environment. This will give increased data accuracy and allow multiple source environmental monitoring of environmental parameters.



Keywords: environmental, forensic, heavy metal, sensor, tracer, taggant, fluorescence

## **INTRODUCTION**

### **Heavy metals sensor and contaminated land**

Historical urban and industrial activity such as steel making, coal gas manufacture, mining and ship building, have left a legacy of land and water contamination from highly toxic heavy metals which seriously affect human health and the environment (ICRCL 1987). This represents not only a threat to the environment and risks to users of the land but potentially also significant environmental and financial liabilities. Specifically, apart from the direct effects on biological life and the ecosystem in general, water or land contamination can cause economic and financial damage, namely reduced land values, remediation costs and the potential for litigation costs. The Confederation of British Industry has estimated that over 200,000 hectares of land is contaminated in the UK and remediation of these areas could cost up to £20 billion (Department of Environment 1994). Therefore, the necessity of monitoring pollutant levels at various points in industrial and recycling processes is important, particularly prior to the sale or redevelopment of potentially contaminated sites.

Contamination sources are not solely limited to industrial processes. Activities such as agriculture, waste disposal, deposition from the atmosphere, and common practices such as petrol distribution and dry cleaning all add to pollution in natural water and soils. A recent survey of 200 site investigations showed that over 61% of land assessment involved heavy metals (Systems Insight Ltd. 2004). The characterisation of contaminated land through these surveys could provide inputs to a database for use in forensic investigations. Old industrial sites are often in run-down inner city locations, with derelict buildings, providing locations for illicit activities. The Inter-departmental Committee on the

Redevelopment of Contaminated Land (ICRCL) suite of typical laboratory characterisation/analysis of contaminated land includes a range of heavy metals, anions and organic molecules (Table 1).

<b>Class</b>	<b>Contaminant</b>	<b>Planned Use</b>	<b>Concentration Range mg/Kg (air-dried soil) Threshold</b>
Metals	Cu, Ni, Pb, Cd, Hg, Zn, As	Domestic gardens, allotments, parks and playing fields	40 to 2000
Anions	S, SO <sub>4</sub> <sup>2-</sup> , S <sub>2</sub> <sup>2-</sup> , CN <sup>-</sup> , B	Domestic gardens, any uses where plants grow	3 to 5000
Organics	TEM, TPHs, PAHs, PCBs, BTEX, Phenols, Volatile Organics	Domestic gardens, landscaped areas	5 to 1000
Others	pH, Asbestos	Domestic gardens, landscaped areas, hardcover	<5 pH

Table 1. Excerpt from Inter-departmental Committee on the Redevelopment of Contaminated Land (ICRCL) 59/83 Trigger Concentrations.

These metals are most commonly measured by Inductively Coupled Plasma Atomic Emission Spectroscopy (ICPAES) following microwave digestion, as the detection limits required (Table 1) are not demanding, at 40 to 2000 mg/Kg (air-dried soil), for even domestic use. ICPAES detection limits range from 0.008 mg/L Arsenic to 0.0004 mg/L Nickel in aristar nitric acid digest. Inductively Coupled Plasma Mass Spectroscopy (ICPMS) is also sometimes used, but detection limits in the µg/Kg range are not necessary. Hydride Generation Atomic Absorption Spectroscopy (HGAAS) has been used for the very selective measurement of metals which forms volatile hydrides, and Cold Vapour Atomic Absorption Spectroscopy (CVAAS) can measure Mercury at as low as 5 ng/L. However, all of these methods use laboratory instruments which require highly trained staff and are not suitable for on-site monitoring. Two

methods which could be used for the measurement and analysis of a range of heavy metals, in the field, are Electrochemistry and X-ray fluorescence (XRF).

The use of small, safe, x-ray tubes to replace dangerous radioactive sources has allowed the development of field portable X-ray fluorescence (XRF) systems. When an X-ray passes through a sample, absorption by an inner shell electron of an X-ray quantum produces an excited ion which spontaneously emits a characteristic x-ray fluorescent spectrum. Current field portable XRF systems are capable of monitoring 25 elements simultaneously. Detection limits for a field portable XRF system are typically: 10 to 100 mg/Kg for Cu, Ni, Pb, Cr, Hg, Se, Zn, As and 50 to 150 mg/Kg for Cd (Innovxsys 2007).

All systems have their own advantages and disadvantages. For example, XRF does not have the potential to differentiate between the oxidation states of an element which is a very significant factor in its level of toxicity. Cr(VI) has an oral toxicity of 0.003 mg/Kg/d compared to Cr(III) which has an oral toxicity of 1.5 mg/Kg/d. One of the major problems of quantitative XRF is matrix effects, the extent of which depends on the mass absorption coefficients of all the elements present in the matrix.

<b>Analytical Technique</b>	<b>Sensitivity</b>	<b>Cost</b>	<b>Real Time Detection</b>	<b>Ease of Use</b>	<b>Instrument Size</b>
GFAA	Good	Medium	No	Expert Required	Large, complex laboratory instrument
ICPAES	Good	High	No	Expert Required	Large, complex laboratory instrument
ICPMS	Good	High	No	Expert Required	Large, complex laboratory instrument
LCMS	Good	High	No	Expert Required	Large, complex laboratory instrument
XRF (laboratory instrument)	Good	Medium	No	Expert Required	Large, complex laboratory instrument
XRF (field portable instrument)	Good	High	Yes	Non-expert	Small, simple field portable instrument
Electrochemistry (laboratory instrument)	Good	Medium	No	Expert Required	Large, complex laboratory instrument
Electrochemistry (field portable)	Good	Medium	Yes	Non-expert	Small, simple field portable instrument

**Table 2. Comparison of analytical techniques used for heavy metal detection.**

Stripping analysis is an electroanalytical method which involves a pre-electrolysis step to pre-concentrate a substance onto the surface of an electrode. After the electro-deposition the material is stripped from the electrode, in this case, by differential pulse voltammetry. The potential at which a metal is stripped (oxidised) from the electrode is characteristic of not only the metal but also of its oxidation state. The peak is proportional to the concentration of the metal species and their separation is important for quantification. Research on the detection of heavy metals using electrochemical measurements has focused on computer-based systems (Bersier 1994; Rossmeis 2008). The advantages of these systems can be summarised thus:

- The ability to manage experiments involving sophisticated measurement techniques
- Storage of large amounts of data
- Data can be manipulated in complex ways
- Digital filtering can be performed
- Results can be presented in a convenient format.

Several general purpose electro-analytical instruments based on computer systems are available commercially. However, these instruments, are expensive, complicated to operate and bulky. Some 'portable' instruments are impractical for use in the field, requiring, procedures normally carried out in a laboratory, such as pipetting. It follows that a fast, reliable, relatively inexpensive, portable (hand-held) and independent instrument, capable of the direct monitoring of heavy metal contaminants *in situ* (Christidis 2006 & 2007), without the need for an analytical chemist, is very desirable.

This chapter describes the development of such an electrochemical instrument which is capable of gathering real-time quantitative data on a range of heavy metal contaminants, and recent research on the potential application of novel fluorescent taggant tracers (Pollard 2007) as an additional tool in environmental forensic investigations.

### **Environmental taggants**

One of the largest problems associated with current fluorescent dye tracers is their eco-toxicological effects within the environment and their effect on human health. Commonly used tracers such as Fluorescein, Lissamine Flavine FF, Rhodamine WT, Rhodamine B, Sulpho Rhodamine G, Sulpho Rhodamine B, and eosin, amongst others, have been studied for the toxicological effects (Field 1995). Many of these may have breakdown products and synergistic effects with compounds within soil and aqueous systems which could produce increased dangers to human health and the environment. So, the need for a new type of tracer which can provide environmental stability and minimal toxicological effects is great. The application of such tracers in soil and sediment transport monitoring in industrial environments, where there is already a number of possible background contaminant sources, makes monitoring molecular fluorescent tracers challenging.

In environments where there might be multiple sources of contamination, the use of multiple tracers, exhibiting discrete fluorescent atomic emissions with wavelength and lifetime discrimination, would be a distinct advantage. This would allow the monitoring of the origin of contaminants from more than one source and for real time fluorescence measurements to be made with reduced background interference.

Examples of glass-based environmental taggants already in use are glass microspheres, which have been applied to the identification of the source of explosives. In this, the chemical composition of the glass microsphere allows tracking of the place and date of manufacture of the explosives, allowing quicker analysis of residue.

The current research glass matrix, developed for security applications, is a borosilicate matrix which provides an environmentally stable host into which lanthanide ions can be placed. Borosilicate glass and rare earth ions can resist temperature and pressure variations under which traditional molecular dye tracers would degrade. When compared to

phosphate or fluoride based glasses (Wada 2007) borosilicate is a far more stable host and much less susceptible to water attack. This is important when a taggant is applied in soil forensics, where there may be a range of environmental conditions which may significantly compromise fluorescence from dye tracers.

## **HEAVY METAL SENSOR**

### **Heavy metal solutions and samples**

The heavy metal solutions used in the initial part of the research were prepared from standard 1000 ppm in 1 M aristar nitric acid (HNO<sub>3</sub>) solutions, with the supporting electrolyte of sodium chloride (NaCl), also from a 1.0 M stock solution. Test solutions of lead<sup>II</sup>, cadmium<sup>II</sup>, zinc<sup>II</sup>, nickel<sup>II</sup>, mercury<sup>II</sup> and copper<sup>II</sup> were prepared at different concentration levels in the range of 1 to 50 mg/Kg and used to dope sub-samples of a clean sediment sample. The ions selected for examination were chosen due to their availability, and are all in the ICRCL suite of measurements required for contaminated land. Two modes of operation were used in the initial experiments. Firstly, to maintain controlled conditions, the doped sediment samples were placed in a sample holder with a 0.1 M NaCl supporting electrolyte at a controlled pH prior to measurement. Secondly, when the calibration had been established, containing the data at a wide range of pH values, and the electrode system had been adapted to incorporate a silver/silver chloride (Ag/AgCl) reference electrode, pH was measured. Then, the samples were measured directly.

The heavy metals were measured by pushing the screen printed electrode cartridge directly into the doped sediment sample (or directly in to the soil in the field), without the need for extraction of metals from the soils, as required by conventional laboratory methods such as ICPAE measurements. The pre-concentration (deposition) time was 60 seconds at -1400 mV potential. The scanning voltage range used was from -1400 to +1000 mV, with a step potential of 2 mV, pulse height of 25 mV, a scan rate of 120 ms and pulse duration of 50 ms. Thirty two independent

measurements of the electrical potential and peak amplitude of each of the metals species were recorded. The instrument displays the concentration on the liquid crystal display (LCD) display but the data is stored for download onto a personal computer.

The detection and identification of metals in multi-metal mixtures was also investigated. Further sub -samples of the clean sediment were doped with 5 ppm of each of the four different metal species. 30 mg/Kg doped samples were also made and measure as above.

### **Instrumentation and methods**

The schematic diagram for the electrochemical instrument as developed is shown in Figure 1 (Gow 2008). It consists of five main units: the waveform generator, the potentiostat, the cell (sensor), the data acquisition system (comprising the Programmable Gain Amplifier, ADC and data interfaces) and the microcontroller.

From the different electrochemical techniques suitable for heavy metal detection, differential-pulse anodic stripping voltammetry (DPASV) was chosen in preference over the others. It is a precise analytical method which has been widely used for the trace determinations of several heavy metals (Wang 1985; Bersier 1994) with excellent limits of detection.



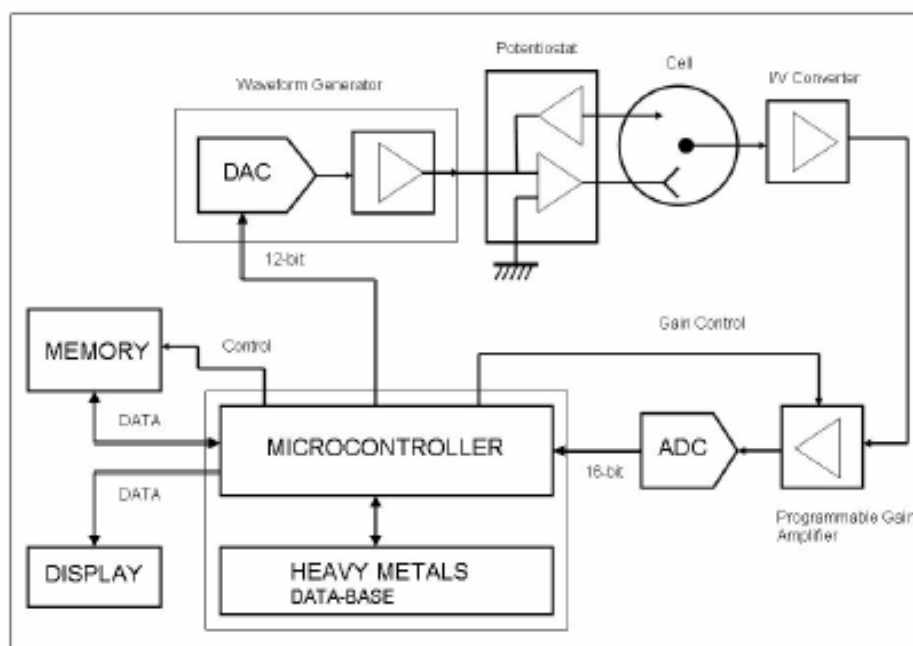


**Figure 1. Block diagram of the electrochemical instrumentation system.**

The excitation signal for DPASV consists of two stages. The first stage is a pre-concentration step of a fixed duration (60 seconds) for the application of a negative potential. For example, -1.4 V causes the deposition stage where the analyte species are reduced and plated onto the working electrode surface. The second analysis stage is where each metal is oxidised back into its original state by means of a time-controlled excitation waveform with the applied potential scanned from the negative starting voltage towards a positive end voltage of +1.0 V. The excitation waveform consists of small pulses (120 ms period and 50 ms duration) of constant amplitude (25 mV) superimposed on a staircase waveform of 2 mV step potential. This waveform is provided by a specially designed waveform generator. The signal generator function is provided by the 16-bit microcontroller which synthesises the excitation signal from its digital data equivalent. The approach allows signal generation to be very flexible, as all of the parameters can be re-programmed and a complex waveform can be generated very easily.

The signal in a digital form undergoes a digital to analogue conversion with a 12-bit resolution. The excitation signal is applied to the sensor via

a potentiostatic circuitry, which controls the voltage potential applied to the cell. It also acquires and amplifies the current flowing through the cell. The current is sampled twice in each pulse period (once before the potential step, and then again just at the end of the pulse). The difference between these two current samples is recorded. This process is repeated for all pulses of the signal.

The sensor (cell) uses solid (screen-printed) working electrodes rather than the more common hanging mercury drop electrode (HMDE) used by most traditional laboratory instruments. Apart from the size and cost difference, an important advantage of solid electrodes is that they do not require the use of mercury which is toxic.

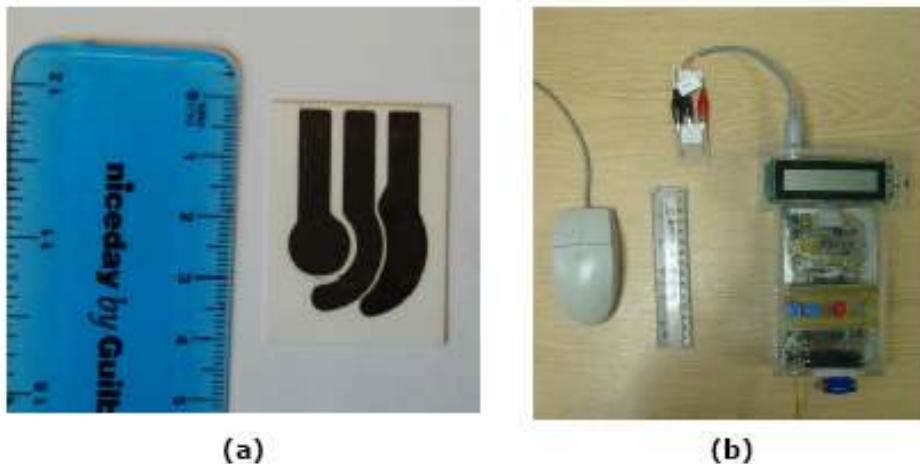


**Figure 2 (a) Screen printed carbon electrode and (b) Electrochemical instrumentation system first prototype**

In the data acquisition process, the electrochemical response current is firstly converted to a voltage, and then amplified before being converted, at fixed time intervals, to digital data using a 16-bit analogue to digital converter. The resultant 16-bit binary words which convey the current information are stored in the microcontroller memory. The full scale range (FSR) and resolution of the data acquisition unit is set by a programmable amplifier under the control of the microcontroller.

For very small signal amplitudes, the system FSR is set to 400  $\mu\text{A}$  corresponding to a 6.1 nA resolution; for higher amplitudes the FSR is set to 30 mA giving a resolution of 458 nA. An important characteristic of the system is its portability, so it is designed for battery operation. DC to DC converters supply internal logic (5 V) and linear ( $\pm 12$  V) supplies from a single battery. The battery capacity of 1.4 Ah delivers approximately eight hours of continuous operation at a power consumption rate of approximately 2 W.

### Detection and identification of heavy metals

An identification technique based on the probability density functions (PDF) of oxidation potential measurements has been developed. PDF curves have been used in the development of decision algorithms for feature selection in various applications (Gunarathne 2002; Bahlman 2006) Data are first arranged into a numerical order from which various statistical features are obtained, such as minimum, maximum, mean, median and standard deviation. These are then used as a basis for classification.

The probability ( $p$ ) for a feature which assumes a value between  $f_1$  and  $f_2$  is given by Stanley 1973:

$$p(f_1 \leq f \leq f_2) = \int_{f_1}^{f_2} p(f) df \quad \text{Equation 1}$$

Where,  $p(f)$  is the probability density function of  $f$ .

In the case of a Gaussian distribution, the probability density function  $p(f)$  is given below:

$$p(f) = \left[ 1 / (\sigma \sqrt{2 \cdot \pi}) \right] \cdot e^{-\frac{(f-\mu)^2}{2\sigma^2}} \quad \text{Equation 2}$$

Where  $\mu$  is the mean value and  $\sigma$  is the standard deviation.

As the potential of the excitation signal approaches the oxidation potential of one of the metals plated onto the electrode surface, it undergoes oxidation, and the current increases rapidly and reaches a maximum value (peak current) when the applied potential approximates to the metal's oxidation potential ( $E_p$ ). When an actual test is carried out, the oxidation potential  $E_p$  is assessed and examined against the PDF to determine the probability of membership of that analyte with all the analytes stored in a database of PDF measurements. The analyte representing the highest probability of likeliness is thus identified. Analytes identified in this way are automatically given a probability of likeliness, indicating the prediction accuracy.

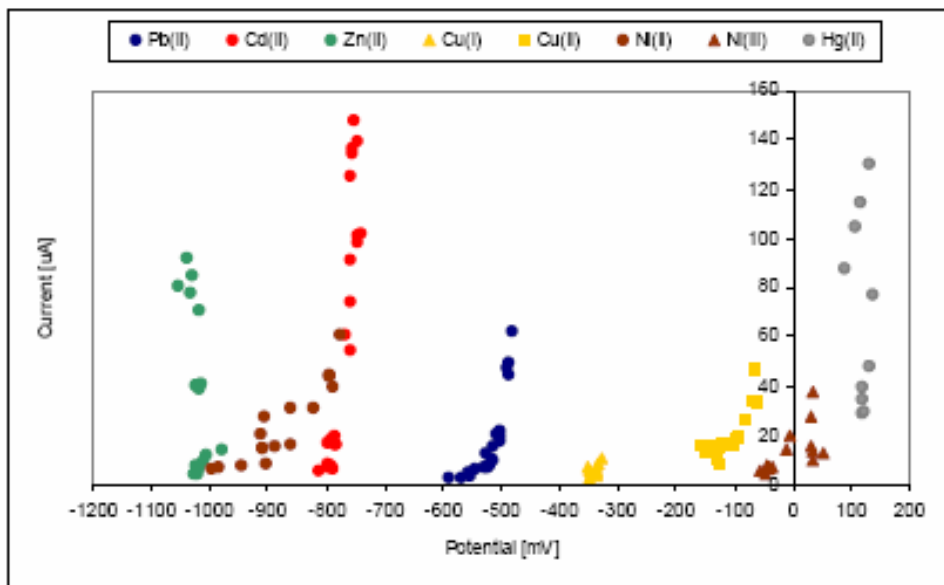


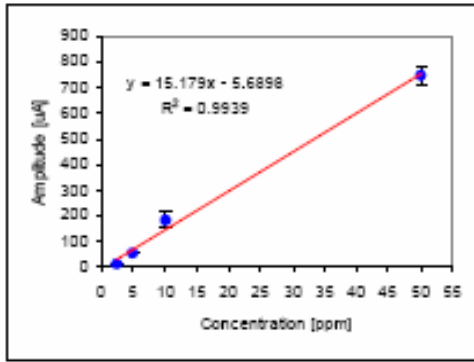
**Figure 3. Amplitude peak versus oxidation potential for all metals including oxidative states for Cu and Ni**

From the dataset obtained from the 32 measurements described above, the points of the peak current amplitude, and associated oxidation potential, can be extracted. The plot shown in Figure 3 is a space scatter diagram, as used in the field of pattern recognition (Prutton 1990),

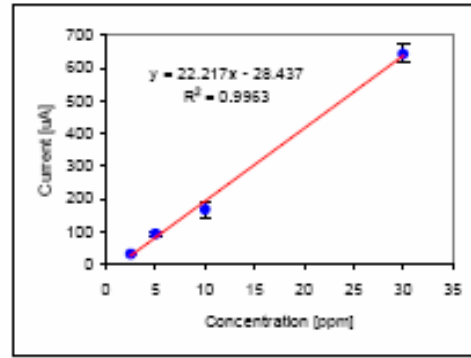
allowing interpretation of any clustering of the data into groups that have strong likeness or similarity. The separation of clusters can then be undertaken using tools such as artificial neural networks (De Carvalho 2000; Cukrowska 2001).

### **Measurements and results**

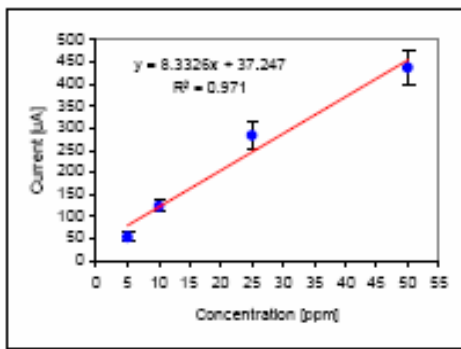
Initial calibration curves were obtained using the single element test solutions, example graphs of which are shown in Figure 4. The coefficients of the first order curve-fitting equations (calibration curves) were stored in system memory and used to obtain the concentration level of the metal, if identified. These equations have been updated as the instrument has been refined and the concentration range extended, down to 250 µg/Kg, and up to 100 mg/Kg.



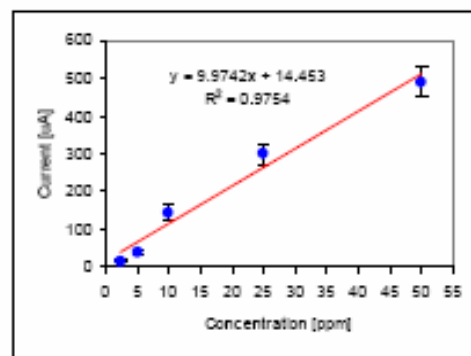
(a) Lead<sup>II</sup>



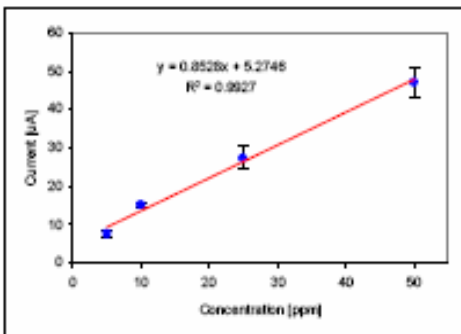
(b) Cadmium<sup>II</sup>



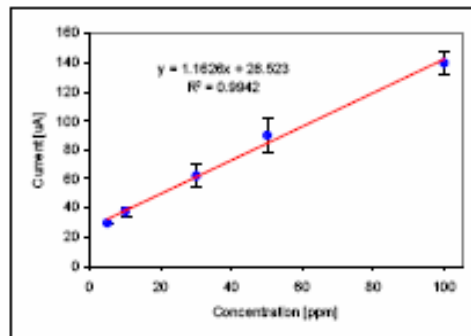
(c) Copper<sup>II</sup>



(d) Zinc<sup>II</sup>



(e) Nickel<sup>II</sup>



(f) Mercury<sup>II</sup>

Figure 4. Examples of calibration curves of six metal species. (a) lead; (b) cadmium; (c) Copper; (d) zinc; (e) nickel; (f) mercury.

Peak position and peak height can vary with pH. Measurements of a 30 mg/Kg lead standard doped clean sediment were carried out for 28 runs on 28 days to check the reproducibility of the peak position and peak height. The peak position was  $-0.564 \pm 0.005$  mV above pH -0.7. More variation was seen with peak height but this was overcome when the electrode system was adapted to incorporate an Ag/AgCl central electrode to replace the central carbon reference electrode. This allowed the pH to be measured prior to the metal analysis cycle. A set of experiments to measure the peak height for each metal as the pH was varied was carried out.

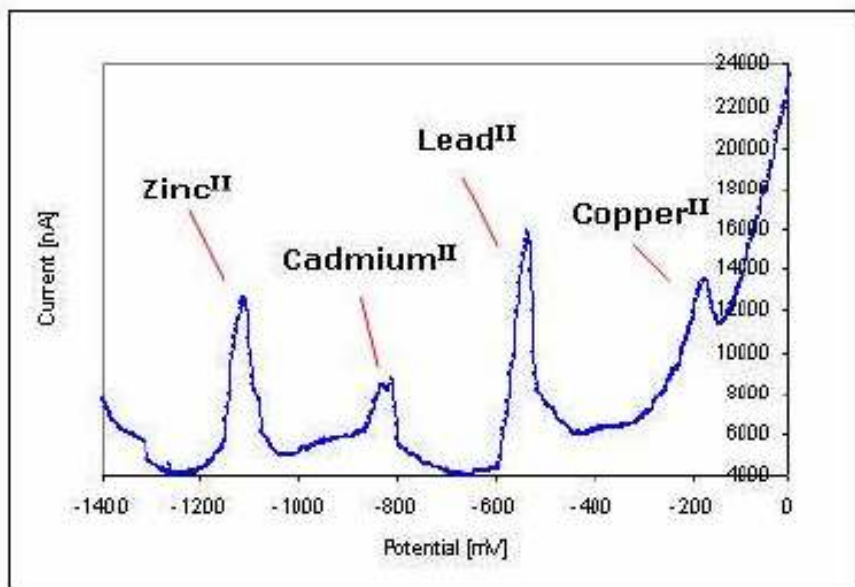


**Figure 5. Differential pulse voltammogram for a solution with a multi-metal mixture containing Cd, Pb, Cu at 5 mg/Kg and Zn at 10 mg/Kg.**

Figure 5 shows the differential pulse voltammogram taken by the instrument. The four peaks representing the oxidation potential of the metals can be interpreted. Using the identification algorithm, the system reported the following results: cadmium<sup>II</sup> at 4 mg/Kg concentration, lead<sup>II</sup> at 7 mg/Kg concentration, copper<sup>II</sup> at 6 mg/Kg concentration and zinc<sup>II</sup> at 8 mg/Kg concentration with a maximum error of 3 mg/Kg. The instrument was also used to examine possible contamination of field



samples. Four contaminated samples (supplied by SureClean Ltd., Aberdeen) were examined for heavy metal contamination as described earlier. The samples were tested using the first prototype instrument, and were analysed using a Perkin Elmer Optima 3300 DV ICPAES which gave the following presented results (Table 3).

<b>Sample No.</b>	<b>Metal Present</b>	<b>Concentration mg/kg Heavy Metal Sensor</b>	<b>Concentration mg/Kg ICPAES</b>
1	zinc II	137	140
2	zinc II	117	119
3	zinc II	98	101
4	zinc II	83	88

**Table 3 Comparison of zinc II contaminated samples using the heavy metal sensor and ICPAES.**

## **NOVEL TAGGANTS**

### **Novel taggants**

A typical borosilicate glass (Zhu 2007) consists of Silicon Dioxide, Boric Oxide, Sodium Oxide and Alumina. The ratio of these components can affect the glass network formed and therefore the emission wavelengths from dopant ions. When compared with phosphate or fluoride, glass using borosilicate as a host matrix is far more stable to water attack. The use of borosilicate formulations as glass hosts for lanthanide doping has been studied with eight rare earths which exhibit a visible fluorescent emission e.g. europium, terbium, dysprosium, cerium, samarium, praseodymium, erbium and thulium (Zhoutang Li 1988).



In light of these above advantages, production of the glass taggants used a borosilicate glass composition doped with rare earth salt, and the samples were produced using the traditional 'melt quench' method (Ramkumar 2008). These samples were then ball milled to produce taggant particles in the region of 5  $\mu\text{m}$  to 75  $\mu\text{m}$ .

### **Novel taggant detection**

The proposed use of novel taggants in environmental forensic investigations is made possible by the discrete, highly intense, fluorescent emissions. These make it possible to differentiate between background molecular fluorescence signals and the target taggant fluorescence. These taggants have the potential to be used to trace the source and/or final destination of contaminants in environmental contamination litigation to 'make the polluter pay'.

### **Taggant detection system**

The taggant detection system, developed for the trial investigation, utilised a pulsed 532 nm laser as the excitation source with an optical fibre collector coupled to an avalanche photodiode, fitted with a 10 nm band pass filter at 610 nm for Europium fluorescence. To replicate the process of scanning across contaminated land, a contaminated soil sample with integrated taggants was scanned past the fixed excitation and detection system.

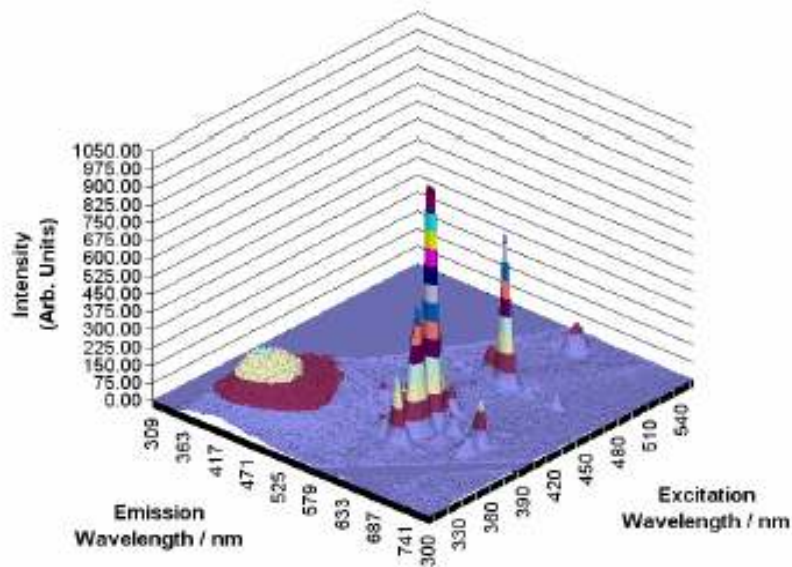


**Figure 6. Europium 615 nm intensity variations with a range of excitations wavelengths.**

It is possible to determine that from a single doped Europium taggant sample there are a large number of potential excitation wavelengths, with several emission wavelengths, which could be monitored to track the movement of contamination (Figure 6). The strongest emission wavelength observed for Europium is 615 nm, a range of excitation wavelengths produce emission; 362, 381, 393, 412, 465, 531 and 579 nm.

The added advantage of using any of the previously mentioned lanthanide series as a doped taggant is the potential to improve the sensitivity of the tracer measurements by using fluorescent lifetime discrimination. In the environment, background fluorescent signals predominately originate from the molecular fluorescence signal of organics. These molecular fluorescent signals are very short lived, in the region of nanoseconds, compared to atomic fluorescence where the lifetime of the signal is in the region of milliseconds. This means that lifetime discrimination in the instrument can effectively remove the background signals improving the

sensitivity of the measurement system. Figure 7 shows an example of a Europium lifetime profile.

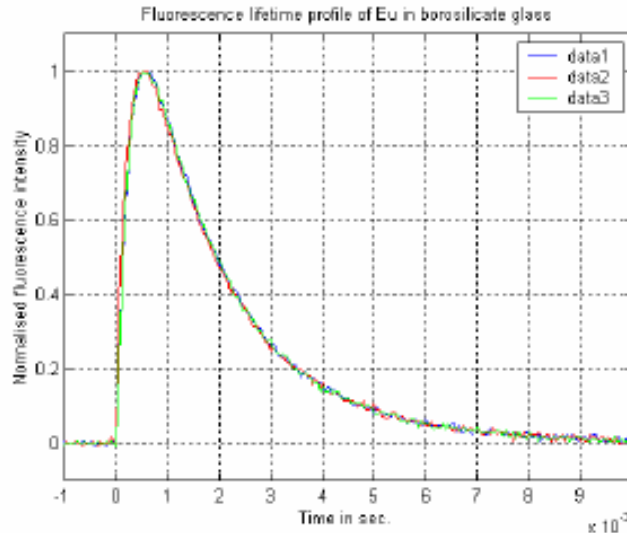


**Figure 7. Fluorescent lifetime profile of Europium ions in borosilicate glass measured in triplicate; data1, data 2 and data 3.**

## CONCLUSIONS

A novel hand-held, easy to use electrochemical instrument capable of real-time *in situ* detection, identification and measurement of concentrations of heavy metals directly in soil samples has been developed. The sensitivity of the system has been assessed and showed that metals can be detected at low concentrations currently down to 1 mg/kg for Pb<sup>II</sup>, Cd<sup>II</sup>, Cu<sup>II</sup> and 3 mg/kg Zn<sup>II</sup>, which fits the ICRC requirements.

The system was field tested, where it was able to assay the contamination of four samples in a fast, easy and accurate procedure, and the results verified by a commercially available laboratory instrument. The surveyor was able to locate hotspots on site, thus avoiding the expense and time delay in having to make a return trip to site after laboratory analysis

highlights hotspots. This is particularly important in environmental forensics when a site may have been released back to the owner and samples on a return visit could be compromised. The system can be used in a variety of situations in environmental assessment and the data acquired provides a metals fingerprint which can be input to databases for subsequent forensic investigations.

The proposed novel taggants, based on narrow band atomic fluorescence, are under development for potential deployment as forensic environmental tracers. The use of discrete fluorescent species in an environmentally stable host has been investigated to replace existing toxic, broad band molecular dye tracers. The narrow band emission signals offer the potential for the tracing of a large numbers of signals in the same environment. This will give increased data accuracy and also allow multiple source environmental monitoring of environmental parameters.

## REFERENCES

Bahlman C (2006). Directional features in online handwriting recognition. *Pattern Recognition* 39: 115-125.

Bersier PM, Howell J and Brunlett C (1994). Tutorial review. Advanced electroanalytical techniques versus atomic absorption spectrometry, inductively coupled plasma atomic emission spectrometry and inductively coupled plasma mass spectrometry in environmental analysis. *Analyst* 119: 219-232.

Christidis K, Pollard P, Gow K and Robertson PKJ (2006). On-site monitoring and cartographical mapping of heavy metals. *Instrumental Science and Technology* 34: 489-499.

Christidis K, Robertson P, Gow K and Pollard P (2007). Voltammetric in situ measurements of heavy metals in soil using a portable electrochemical instrument. *Measurement* 40(9-10): 960-967.

Cukrowska E, Trnková L, Kizek R and Havel J (2001). Use of artificial neural networks for the evaluation of electrochemical signals of adenine and cytosine in mixtures interfered with hydrogen evolution. *Journal of Electroanalytical Chemistry* 503(1-2): 117-124.

De Carvalho RM, Mello C and Kubota LT (2000). Simultaneous determination of phenol isomers in binary mixtures by differential pulse voltammetry using carbon fibre electrode and neural network with pruning as a multivariate calibration tool. *Analytica Chimica Acta* 420(1): 109-121.

Department of Environment (1994). *Paying for our Past. Arrangements for Controlling Contaminated Land and Meeting the Costs of Remedying the Damage to the Environment.* Consultation Paper by Department of the Environment and The Welsh Office, London.

Field MS, Wilhelm RG, Quinlan JF and Aley TJ (1995). An assessment of the potential adverse properties of fluorescent tracer dyes used for groundwater tracing. *Environmental Monitoring and Assessment* 38: 75-96.

Gow K, Robertson PKJ, Pollard P, and Christidis K (2008). Measurement method and apparatus for analysing the metal or metal ion content of a sample. European Patent: EP1904838.

Gunarathne GPP and Christidis K (2002). Material Characterisation in Situ Using Ultrasound Measurements. *IEEE Transactions on Instrumentation and Measurement* 50: 368-373.

ICRCL (1987). Inter-departmental Committee on the Redevelopment of Contaminated Land (ICRCL), 59/83 Guidance on the assessment and redevelopment of contaminated land. 2nd Edition. Available From:

<http://www.ContaminatedLAND.co.uk/std-guid/icrcl-1.htm>. Accessed 27-02-2008.

Innovxsys (2007). Detection Limits for Innov-x Classic Field Portable XRF Instrument in Low Density Soil Types. <http://www.innovxsys.com/products/detect>. Accessed 10-06-08.

Pollard P, Adams M, Prabhu GR, Officer S and Hunter C (2007). Sensitive Novel Fluorescent Tracers for Environmental Monitoring. (Digital Object Identifier 10.1109/OCEANSE.2007.4302448): 1-6.

Prutton M, Gomati MME and Kenny PG (1990). Scatter diagrams and hotelling transforms: application to surface analytical microscopy. *Journal of Electron Spectroscopy and Related Phenomena* 52: 197-219.

Ramkumar J, Sudarsan V, Chandramouleeswaran S, Shrikhande VK, Kothiyal GP, Ravindran PV, Kulshreshtha SK and Mukherjee T (2008). Structural studies on boroaluminosilicate glasses. *Journal of Non-Crystalline Solids* 354(15-16): 1591-1597.

Systems Insight Ltd. (2004). RGU Heavy Metal Detection Technology, Market Research Report, Final Project Report - Volume 2 Appendices A to D, Report Ref: CR RGUC/040615.

Rossmeisl J and Nørskov JK (2008). Electrochemistry on the computer: Understanding how to tailor the metal overlayers for the oxygen reduction reaction. *Surface Science* [doi:10.1016/j.susc.2008.05.015](https://doi.org/10.1016/j.susc.2008.05.015).

Stanley LT (1973). *Practical Statistics for Petroleum Engineers*. The Petroleum Publishing Company USA: 15-20.

Wada N and Kojima K (2007). Glass composition dependence of  $\text{Eu}^{3+}$  polarization in oxide glasses. *Journal of Luminescence* 126(1): 53-62.

Wang J (1985). *Stripping Analysis: Principles, Instrumentation, and Applications*. VCH Publishers Deerfield Beach, FA: pp. 119.

Zhoutang Li PW, Xueyin J, Zhilin Z and Shaodong X (1988). The synthesis of rare earth borosilicate glasses and their luminescence properties. *Journal of Luminescence* 40&41: 135-136.

Zhu D, Zhou W, Day DE and Ray CS (2007). Preparation of fluorescent glasses with variable compositions. *Ceramics International* 33(4): 563-568.

## **Appendix II: Spectroscopic Characterisation Data**



Excitation Wavelength / nm	Emission Wavelength / nm	Intensity	Peak width					
			Ex Wavelength			Em Wavelength		
			From	To	PW	From	To	PW
323	478.5	167.95	318.0	327.0	9.0	467.0	497.5	30.5
452	480.5	228.03	440.0	456.0	16.0	476.5	505.0	28.5
363	482	458.38	357.0	370.0	13.0	461.0	503.0	42.0
423	482	105.68	419.0	433.0	14.0	467.0	499.0	32.0
385	482.5	509.32	373.0	409.0	36.0	461.0	505.0	44.0
347	483	37.71	339.0	357.0	18.0	459.0	507.0	48.0
377	545	208.14	369.0	382.0	13.0	528.0	558.5	30.5
350	545.5	191.16	331.0	357.0	26.0	529.5	556.5	27.0
453	545.5	48.03	440.0	459.0	19.0	535.5	554.5	19.0
484	545.5	70.55	475.0	495.0	20.0	529.5	560.5	31.0
364	546	172.45	360.0	371.0	11.0	531.5	556.5	25.0
348	575.5	950.02	338.0	357.0	19.0	556.5	602.0	45.5
471	576	97.71	466.0	477.0	11.0	554.5	596.5	42.0
452	576.5	286.35	436.0	460.0	24.0	556.5	600.5	44.0
465	576.5	89.12	460.0	466.0	6.0	562.0	598.5	36.5
363	577	552.25	358.0	370.0	12.0	558.5	602.0	43.5
385	577	777.75	371.0	407.0	36.0	554.5	602.0	47.5
323	577.5	136.54	312.0	330.0	18.0	558.5	600.5	42.0
424	578.5	154.98	418.0	430.0	12.0	556.5	596.5	40.0
362	613	136.42	355.0	368.0	13.0	604.0	640.5	36.5
379	614	275.45	367.0	387.0	20.0	602.0	638.5	36.5
395	614	401.50	387.0	406.0	19.0	602.0	636.5	34.5
412	614.5	76.46	406.0	419.0	13.0	604.0	636.5	32.5
463	614.5	287.35	455.0	471.0	16.0	600.5	640.5	40.0
530	615	56.43	520.0	542.0	22.0	600.5	636.5	36.0
308	618.5	25.93	305.0	313.0	8.0	608.0	632.5	24.5
348	618.5	55.47	341.0	354.0	13.0	608.0	636.5	28.5
319	619	39.36	313.0	324.0	11.0	602.0	627.0	25.0
349	655	35.08	341.0	355.0	14.0	646.0	680.5	34.5
465	656	35.21	460.0	468.0	8.0	642.0	663.0	21.0
386	656.5	50.31	371.0	389.0	18.0	644.0	684.0	40.0
392	657	60.78	389.0	409.0	20.0	644.0	676.5	32.5
362	658	33.57	359.0	368.0	9.0	640.5	682.5	42.0
392	700.5	97.69	387.0	403.0	16.0	678.5	724.0	45.5
381	701	38.03	368.0	387.0	19.0	690.0	714.5	24.5
465	701	27.15	457.0	469.0	12.0	688.0	716.5	28.5
533	701	15.49	520.0	538.0	18.0	678.5	716.5	38.0

**Table 1 Multiple ion doped sample Glass1-1 – 0.5 mol % Eu, 0.5 mol % Tb and 0.5 mol % Dy**

Development and Application of Novel Tracers for Environmental Applications  
 Appendix II: Spectroscopic Characterisation Data

Excitation Wavelength / nm	Emission Wavelength / nm	Intensity	Peak width					
			Ex Wavelength			Em Wavelength		
			From	To	PW	From	To	PW
324	483	189.00	308.0	330.0	22.0	467.0	503.0	36.0
348	483	998.92	339.0	357.0	18.0	459.0	509.0	50.0
363	484	684.78	357.0	370.0	13.0	461.0	509.0	48.0
387	484	791.92	371.0	410.0	39.0	457.5	509.0	51.5
424	483	133.65	415.0	435.0	20.0	463.0	507.0	44.0
452	483.5	313.74	438.0	460.0	22.0	470.5	505.0	34.5
323	545.5	74.21	311.0	329.0	18.0	533.5	554.5	21.0
351	545.5	462.93	330.0	357.0	27.0	529.5	558.5	29.0
364	545	411.01	358.0	371.0	13.0	528.0	558.5	30.5
377	545	442.56	371.0	381.0	10.0	531.5	560.5	29.0
384	545.5	319.24	382.0	405.0	23.0	529.5	556.5	27.0
414	545.5	34.70	412.0	417.0	5.0	541.0	554.5	13.5
423	544.5	50.82	417.0	433.0	16.0	529.5	554.5	25.0
452	544.5	102.21	438.0	460.0	22.0	528.0	554.5	26.5
484	545.5	137.14	474.0	494.0	20.0	528.0	564.0	36.0
323	577	204.40	316.0	330.0	14.0	560.5	600.5	40.0
350**	576.5	1000.00	339.0	358.0	19.0	558.5	604.0	45.5
363	576.5	920.48	358.0	371.0	13.0	558.5	602.0	43.5
386**	576.5	1000.00	371.0	409.0	38.0	556.5	604.0	47.5
423	576	232.29	416.0	432.0	16.0	554.5	606.0	51.5
452	576	506.93	437.0	460.0	23.0	556.5	606.0	49.5
470	576.5	153.37	461.0	490.0	29.0	556.5	602.0	45.5
349	616	104.20	339.0	356.0	17.0	606.0	636.5	30.5
361	616	183.48	357.0	368.0	11.0	604.0	634.5	30.5
379	616	297.10	368.0	387.0	19.0	604.0	638.5	34.5
393	616	837.21	387.0	407.0	20.0	602.0	638.5	36.5
413	615	68.59	407.0	420.0	13.0	602.0	638.5	36.5
464	616.5	338.07	458.0	470.0	12.0	600.5	638.5	38.0
451	616.5	44.04	442.0	456.0	14.0	610.0	642.0	32.0
484	616.5	29.35	479.0	497.0	18.0	606.0	638.5	32.5
532	615.5	62.10	519.0	545.0	26.0	600.5	640.5	40.0
579	618	15.10	571.0	582.0	11.0	611.5	627.0	15.5
348	664	70.69	340.0	355.0	15.0	648.0	680.5	32.5
363	663.5	47.56	358.0	367.0	9.0	642.0	686.0	44.0
388	663	65.55	371.0	405.0	34.0	642.0	690.0	48.0
424	662.5	15.03	417.0	430.0	13.0	648.0	686.0	38.0
450	663	25.07	439.0	457.0	18.0	646.0	692.0	46.0
464	661.5	21.06	460.0	469.0	9.0	648.0	674.5	26.5
361	702.5	26.56	360.0	367.0	7.0	690.0	705.0	15.0
381	701.5	39.49	369.0	386.0	17.0	693.5	718.5	25.0
393	701.5	105.28	388.0	405.0	17.0	680.5	720.5	40.0
464	699	28.40	457.0	469.0	12.0	686.0	716.5	30.5
530	700	11.39	523.0	539.0	16.0	674.5	724.0	49.5

**Table 2 Multiple ion doped sample Glass1-2 – 0.5 mol % Eu, 1.0 mol % Tb and 1.0 mol % Dy**

Development and Application of Novel Tracers for Environmental Applications  
 Appendix II: Spectroscopic Characterisation Data

Excitation Wavelength / nm	Emission Wavelength / nm	Intensity	Peak width					
			Ex Wavelength			Em Wavelength		
			From	To	PW	From	To	PW
342	483	114.78	313.0	330.0	17.0	467.0	510.5	43.5
349	484.5	823.07	336.0	357.0	21.0	453.5	510.5	57.0
363	483	628.61	357.0	371.0	14.0	461.0	507.0	46.0
385	483	779.23	371.0	406.0	35.0	461.0	507.0	46.0
423	484.5	135.45	418.0	435.0	17.0	461.0	505.0	44.0
452	484	312.68	438.0	460.0	22.0	470.5	503.0	32.5
325	545.5	62.99	311.0	327.0	16.0	431.5	558.5	127.0
349	546.5	597.01	330.0	357.0	27.0	429.5	558.5	129.0
365	545	526.60	358.0	369.0	11.0	531.5	560.5	29.0
377	546.5	609.21	371.0	381.0	10.0	529.5	560.5	31.0
384	546	435.51	382.0	405.0	23.0	529.5	556.5	27.0
424	545	76.78	418.0	432.0	14.0	529.5	556.5	27.0
452	544.5	161.14	437.0	461.0	24.0	531.5	556.5	25.0
470	545.5	66.13	466.0	475.0	9.0	531.5	558.5	27.0
485	545.5	166.82	475.0	496.0	21.0	529.5	564.0	34.5
322	575	127.47	313.0	330.0	17.0	558.5	604.0	45.5
349**	578	1000.00	338.0	358.0	20.0	558.5	604.0	45.5
363	578	850.96	358.0	370.0	12.0	558.5	602.0	43.5
387**	578	1000.00	371.0	407.0	36.0	556.5	602.0	45.5
424	577	233.94	415.0	431.0	16.0	556.5	604.0	47.5
452	576	536.76	437.0	460.0	23.0	556.5	602.0	45.5
471	575	156.27	462.0	491.0	29.0	556.5	602.0	45.5
320	615	30.00	313.0	331.0	18.0	604.0	632.5	28.5
350	617	113.62	341.0	356.0	15.0	606.0	640.5	34.5
361	615	169.68	357.0	367.0	10.0	606.0	638.5	32.5
380	615	276.25	369.0	387.0	18.0	602.0	640.5	38.5
393	615	679.96	387.0	406.0	19.0	602.0	638.5	36.5
414	615	66.55	407.0	419.0	12.0	602.0	638.5	36.5
424	615	32.93	421.0	430.0	9.0	606.0	632.5	26.5
446	614.5	43.60	442.0	448.0	6.0	608.0	634.5	26.5
452	615	49.34	448.0	456.0	8.0	606.0	631.0	25.0
464	615.5	298.29	457.0	469.0	12.0	600.5	636.5	36.0
484	616	40.00	477.0	496.0	19.0	608.0	634.5	26.5
531	617.5	55.75	520.0	544.0	24.0	598.5	636.5	38.0
348	663.5	59.65	339.0	357.0	18.0	642.0	682.5	40.5
362	664.5	42.56	358.0	370.0	12.0	642.0	682.5	40.5
386	664	63.68	371.0	403.0	32.0	640.5	686.0	45.5
423	664.5	14.98	415.0	433.0	18.0	650.0	684.0	34.0
451	665.5	29.91	440.0	457.0	17.0	644.0	686.0	42.0
362	699	20.36	359.0	364.0	5.0	692.0	709.0	17.0
380	699	32.25	369.0	386.0	17.0	692.0	718.5	26.5
393	701	81.25	387.0	405.0	18.0	680.5	722.5	42.0
464	701	25.59	456.0	470.0	14.0	690.0	718.5	28.5
533	700.5	11.88	522.0	543.0	21.0	688.0	711.0	23.0

**Table 3 Multiple ion doped sample Glass1-3 – 0.5 mol % Eu, 1.5 mol % Tb and 1.5 mol % Dy**

Development and Application of Novel Tracers for Environmental Applications  
 Appendix II: Spectroscopic Characterisation Data

Excitation Wavelength / nm	Emission Wavelength / nm	Intensity	Peak width					
			Ex Wavelength			Em Wavelength		
			From	To	PW	From	To	PW
322	483	85.56	313.0	330.0	17.0	463.0	505.0	42.0
349	483.5	425.82	338.0	357.0	19.0	459.0	507.0	48.0
363	483	333.80	357.0	371.0	14.0	459.0	507.0	48.0
387	482	416.91	371.0	409.0	38.0	457.5	505.0	47.5
424	480.5	81.56	414.0	433.0	19.0	463.0	505.0	42.0
452	483.5	189.96	436.0	458.0	22.0	472.5	503.0	30.5
324	543.5	64.24	310.0	329.0	19.0	529.5	556.5	27.0
349	543	392.09	332.0	357.0	25.0	528.0	558.5	30.5
365	545.5	350.46	357.0	370.0	13.0	529.5	558.5	29.0
377	545	388.32	371.0	381.0	10.0	529.5	560.5	31.0
385	545.5	310.11	382.0	387.0	5.0	528.0	556.5	28.5
389	545.5	286.51	387.0	406.0	19.0	529.5	556.5	27.0
424	543	55.45	417.0	433.0	16.0	531.5	554.5	23.0
452	543	118.28	438.0	460.0	22.0	529.5	556.5	27.0
471	543	52.30	463.0	474.0	11.0	529.5	558.5	29.0
484	544.5	126.10	474.0	496.0	22.0	526.0	562.0	36.0
322	573.5	97.52	316.0	330.0	14.0	558.5	602.0	43.5
348	574	673.92	336.0	357.0	21.0	558.5	602.0	43.5
363	575	421.76	357.0	371.0	14.0	558.5	600.5	42.0
387	575.5	655.40	371.0	409.0	38.0	556.5	602.0	45.5
424	576.5	129.83	416.0	431.0	15.0	554.5	602.0	47.5
452	574	274.46	438.0	460.0	22.0	556.5	604.0	47.5
471	574	88.78	462.0	493.0	31.0	558.5	596.5	38.0
319	615.5	24.85	313.0	331.0	18.0	604.0	629.0	25.0
350	615	72.93	338.0	356.0	18.0	604.0	638.5	34.5
361	614.5	94.88	357.0	368.0	11.0	604.0	638.5	34.5
379	614.5	146.83	369.0	387.0	18.0	602.0	634.5	32.5
393	614.5	359.73	387.0	405.0	18.0	600.5	636.5	36.0
412	614	40.36	408.0	417.0	9.0	602.0	634.5	32.5
452	613.5	39.68	438.0	455.0	17.0	604.0	636.5	32.5
463	614	147.10	458.0	471.0	13.0	598.5	640.5	42.0
482	615.5	32.58	477.0	496.0	19.0	602.0	636.5	34.5
571	615.5	29.15	520.0	542.0	22.0	598.5	632.5	34.0
348	660	31.16	339.0	357.0	18.0	640.5	680.5	40.0
363	659	21.97	357.0	358.0	1.0	642.0	678.5	36.5
389	659	33.56	373.0	405.0	32.0	642.0	680.5	38.5
408	659.5	13.30	405.0	411.0	6.0	655.5	665.0	9.5
424	658	13.73	419.0	427.0	8.0	653.5	665.0	11.5
451	657	18.58	443.0	455.0	12.0	648.0	674.5	26.5
372	700.5	15.47	369.0	374.0	5.0	688.0	711.0	23.0
381	700.5	20.74	374.0	384.0	10.0	692.0	716.5	24.5
393	701.5	45.34	388.0	407.0	19.0	680.5	718.5	38.0
464	702	18.13	455.0	470.0	15.0	688.0	713.0	25.0

**Table 4 Multiple ion doped sample Glass1-4 – 0.5 mol % Eu, 2.0 mol % Tb and 2.0 mol % Dy**

Excitation Wavelength / nm	Emission Wavelength / nm	Intensity	Peak width					
			Ex Wavelength			Em Wavelength		
			From	To	PW	From	To	PW
324	482		313.0	330.0	17.0	465.5	509.5	44.0
349	482		333.0	357.0	24.0	463.5	503.5	40.0
364	483		357.0	371.0	14.0	462.0	507.0	45.0
387	481		374.0	408.0	34.0	462.0	510.0	48.0
425	483		416.0	433.0	17.0	460.0	505.0	45.0
452	483		436.0	456.0	20.0	470.5	509.0	38.5
322	545		310.0	330.0	20.0	531.0	556.5	25.5
350	544		340.0	358.0	18.0	529.0	538.5	9.5
365	544		358.0	369.0	11.0	531.0	559.5	28.5
377	544		372.0	382.0	10.0	532.0	559.5	27.5
387	544		382.0	415.0	33.0	532.0	557.5	25.5
423	544		418.0	436.0	18.0	530.0	557.5	27.5
452	544		439.0	460.0	21.0	529.0	588.5	59.5
483	544		477.0	497.0	20.0	530.0	561.0	31.0
323	573.5		315.0	330.0	15.0	557.5	598.5	41.0
348	576		338.0	357.0	19.0	557.5	602.0	44.5
362	576		357.0	570.0	213.0	559.5	602.0	42.5
386	576		371.0	414.0	43.0	557.5	602.0	44.5
424	576		415.0	437.0	22.0	557.5	635.5	78.0
452	579		439.0	461.0	22.0	557.5	604.0	46.5
469	579		461.0	492.0	31.0	557.5	596.5	39.0
362	618		359.0	365.0	6.0	604.0	635.0	31.0
351	618		332.0	354.0	22.0	608.0	635.0	27.0
380	618		370.0	386.0	16.0	600.0	631.0	31.0
393	618		389.0	405.0	16.0	600.5	635.0	34.5
464	618		459.0	469.0	10.0	599.0	662.0	63.0
531	618		517.0	541.0	24.0	602.0	635.0	33.0
349	664		341.0	354.0	13.0	645.0	676.5	31.5
363	661.5		358.0	371.0	13.0	640.5	677.5	37.0
384	662.5		378.0	414.0	36.0	650.0	664.0	14.0
424	662.5		420.0	427.0	7.0	659.0	666.5	7.5
451	662.5		442.0	457.0	15.0	658.0	684.5	26.5
380	693		369.0	386.0	17.0	687.0	697.0	10.0
393	696.5		389.0	397.0	8.0	682.0	715.0	33.0
463	695.5		458.0	468.0	10.0	679.5	715.5	36.0
533	697.5		530.0	538.0	8.0	678.0	715.0	37.0

**Table 5 Multiple ion doped sample Glass1-5 – 0.5 mol % Eu, 2.5 mol % Tb and 2.5 mol % Dy**

Excitation Wavelength / nm	Emission Wavelength / nm	Intensity	Peak width					
			Ex Wavelength			Em Wavelength		
			From	To	PW	From	To	PW
323	482	79.89	313.0	328.0	15.0	460.0	496.0	36.0
348	482	426.12	334.0	357.0	23.0	456.0	503.5	47.5
363	482	286.38	357.0	371.0	14.0	456.0	506.5	50.5
386	482	353.52	371.0	415.0	44.0	456.0	510.5	54.5
424	481.5	71.83	415.0	435.0	20.0	464.0	498.5	34.5
452	481.5	150.03	439.0	461.0	22.0	471.5	506.5	35.0
350	544.5	99.44	338.0	358.0	20.0	532.0	554.5	22.5
364	544.5	89.47	359.0	368.0	9.0	533.0	554.5	21.5
377	544.5	105.50	370.0	382.0	12.0	531.0	557.5	26.5
452	544.5	25.88	441.0	460.0	19.0	530.0	553.0	23.0
484	544.5	33.06	475.0	494.0	19.0	533.0	557.0	24.0
323	574	85.13	316.0	330.0	14.0	557.0	599.0	42.0
349	574	699.03	335.0	357.0	22.0	553.0	603.0	50.0
362	574	399.38	357.0	371.0	14.0	554.0	601.5	47.5
386	574	607.94	371.0	412.0	41.0	553.0	601.0	48.0
424	574	110.82	413.0	436.0	23.0	554.0	606.0	52.0
452	574	233.45	436.0	460.0	24.0	548.0	601.0	53.0
471	574	72.74	463.0	489.0	26.0	553.0	597.0	44.0
318	613	34.22	311.0	323.0	12.0	603.0	626.0	23.0
349	613	44.21	341.0	356.0	15.0	604.0	637.0	33.0
361	613	134.27	356.0	368.0	12.0	601.0	634.0	33.0
379	613	243.17	368.0	387.0	19.0	601.5	638.0	36.5
393	613	662.69	387.0	408.0	21.0	600.0	641.0	41.0
413	613	58.62	408.0	422.0	14.0	600.0	630.0	30.0
464	613	283.67	455.0	470.0	15.0	600.0	638.0	38.0
533	613	55.23	519.0	549.0	30.0	601.0	635.0	34.0
348	662	30.06	340.0	356.0	16.0	640.0	678.0	38.0
362	662	21.58	356.0	370.0	14.0	644.0	678.0	34.0
385	662.5	32.73	370.0	408.0	38.0	640.0	681.0	41.0
824	665	8.03	418.0	427.0	9.0	660.0	671.0	11.0
450	668	12.94	441.0	459.0	18.0	664.0	671.0	7.0
381	701	33.53	366.0	386.0	20.0	682.0	723.0	41.0
393	701	81.50	388.0	404.0	16.0	674.0	721.0	47.0
415	701	9.71	409.0	420.0	11.0	684.0	714.0	30.0
464	701	25.21	456.0	469.0	13.0	676.0	721.0	45.0
535	701	7.36	522.0	542.0	20.0	678.0	716.0	38.0

**Table 6 Multiple ion doped sample Glass1-6 – 1.0 mol % Eu, 0.5 mol % Tb and 1.0 mol % Dy**

Development and Application of Novel Tracers for Environmental Applications  
 Appendix II: Spectroscopic Characterisation Data

Excitation Wavelength / nm	Emission Wavelength / nm	Intensity	Peak width					
			Ex Wavelength			Em Wavelength		
			From	To	PW	From	To	PW
324	482	102.65	313.0	329.0	16.0	461.0	505.0	44.0
348	481.5	559.35	335.0	357.0	22.0	457.5	505.0	47.5
363	483	414.65	357.0	371.0	14.0	459.0	501.0	42.0
387	483	525.60	371.0	409.0	38.0	459.0	505.0	46.0
424	481.5	104.01	416.0	430.0	14.0	461.0	499.0	38.0
452	483.5	239.50	438.0	458.0	20.0	472.5	507.0	34.5
322	545.5	46.83	310.0	330.0	20.0	545.5	554.5	9.0
348	545.5	241.58	332.0	357.0	25.0	531.5	556.5	25.0
365	545	219.26	359.0	370.0	11.0	528.0	558.5	30.5
377	545	268.63	373.0	381.0	8.0	528.0	558.5	30.5
384	545.5	204.00	382.0	390.0	8.0	531.5	554.5	23.0
391	546	166.07	390.0	404.0	14.0	531.5	554.5	23.0
424	548	41.83	417.0	430.0	13.0	531.5	554.5	23.0
452	544.5	76.58	438.0	460.0	22.0	533.5	556.5	23.0
463	544	33.62	461.0	467.0	6.0	528.0	549.0	21.0
472	544	37.17	468.0	475.0	7.0	529.5	554.5	25.0
482	545	90.66	475.0	494.0	19.0	529.5	562.0	32.5
322	576	128.39	313.0	330.0	17.0	558.5	598.5	40.0
348	574.5	937.70	338.0	357.0	19.0	556.5	604.0	47.5
363	576	582.79	357.0	371.0	14.0	558.5	602.0	43.5
386	576	907.61	371.0	408.0	37.0	554.5	602.0	47.5
424	575	178.37	414.0	435.0	21.0	556.5	602.0	45.5
452	575.5	380.59	436.0	460.0	24.0	556.5	602.0	45.5
471	575	119.16	462.0	485.0	23.0	556.5	598.5	42.0
319	617	47.38	311.0	330.0	19.0	602.0	619.0	17.0
349	616	90.01	340.0	355.0	15.0	604.0	638.5	34.5
362	615.5	171.66	355.0	368.0	13.0	602.0	638.5	36.5
379	615.5	323.62	368.0	387.0	19.0	602.0	638.5	36.5
393	614.5	845.71	387.0	406.0	19.0	600.5	640.5	40.0
412	614	82.77	408.0	420.0	12.0	602.0	636.5	34.5
451	614.5	47.17	449.0	455.0	6.0	606.0	632.5	26.5
463	615.5	387.79	455.0	468.0	13.0	600.5	640.5	40.0
482	616	32.08	479.0	496.0	17.0	604.0	631.0	27.0
531	616	76.13	520.0	544.0	24.0	600.5	636.5	36.0
579	615.5	21.02	569.0	582.0	13.0	608.0	634.5	26.5
349	662.5	42.02	340.0	359.0	19.0	638.5	680.5	42.0
362	663	29.97	359.0	370.0	11.0	644.0	680.5	36.5
386	663.5	49.11	371.0	389.0	18.0	644.0	680.5	36.5
392	662	53.32	390.0	402.0	12.0	640.5	671.0	30.5
427	661.5	13.01	416.0	433.0	17.0	657.5	672.5	15.0
452	654	25.17	447.0	455.0	8.0	650.0	682.5	32.5
465	653.5	30.27	458.0	468.0	10.0	644.0	663.0	19.0
362	696	22.14	357.0	368.0	11.0	688.0	707.0	19.0
381	696	36.83	370.0	387.0	17.0	682.5	714.5	32.0
393	698.5	105.98	387.0	405.0	18.0	680.5	718.5	38.0
463	699.5	34.88	457.0	469.0	12.0	682.5	716.5	34.0
533	699.5	13.52	520.0	544.0	24.0	648.0	724.0	76.0

**Table 7 Multiple ion doped sample Glass1-7 – 1.0 mol % Eu, 1.0 mol % Tb and 1.5 mol % Dy**

Excitation Wavelength / nm	Emission Wavelength / nm	Intensity	Peak width					
			Ex Wavelength			Em Wavelength		
			From	To	PW	From	To	PW
323	482	88.04	314.0	328.0	14.0	465.5	499.5	34.0
348	482	530.25	329.0	357.0	28.0	457.0	518.0	61.0
363	482	416.87	357.0	371.0	14.0	454.0	514.0	60.0
387	482	54.08	371.0	414.0	43.0	450.0	514.0	64.0
424	482	112.75	414.0	433.0	19.0	462.0	503.0	41.0
452	482	260.22	438.0	460.0	22.0	472.0	505.0	33.0
324	546	50.32	311.0	331.0	20.0	530.0	557.0	27.0
349	546	353.61	332.0	358.0	26.0	528.0	557.5	29.5
365	546	332.76	358.0	371.0	13.0	529.0	558.0	29.0
377	546	395.00	373.0	382.0	9.0	529.0	560.5	31.5
386	546	303.44	382.0	417.0	35.0	527.0	556.5	29.5
424	546	59.54	417.0	432.0	15.0	530.0	555.5	25.5
452	546	120.92	438.0	460.0	22.0	530.0	556.5	26.5
484	546	130.20	476.0	492.0	16.0	531.0	563.0	32.0
323	576.5	114.21	308.0	331.0	23.0	563.0	603.0	40.0
349	576.5	883.20	332.0	358.0	26.0	557.5	603.0	45.5
363	576.5	600.67	358.0	371.0	13.0	558.5	602.0	43.5
386	576.5	971.84	371.0	412.0	41.0	556.5	602.0	45.5
424	576.5	202.43	412.0	436.0	24.0	556.5	601.5	45.0
452	576.5	416.12	436.0	460.0	24.0	556.5	604.0	47.5
471	576.5	121.85	465.0	494.0	29.0	556.5	596.5	40.0
319	615	34.49	313.0	330.0	17.0	602.0	626.5	24.5
350	615	112.66	339.0	357.0	18.0	604.0	635.5	31.5
62	615	196.60	357.0	368.0	11.0	601.5	635.5	34.0
380	615	342.66	368.0	388.0	20.0	601.5	635.5	34.0
393	615	890.82	388.0	407.0	19.0	600.5	640.5	40.0
412	615	86.14	407.0	421.0	14.0	601.5	632.5	31.0
464	615	392.93	456.0	476.0	20.0	600.5	640.5	40.0
484	615	42.61	478.0	496.0	18.0	602.0	637.5	35.5
531	615	71.83	519.0	546.0	27.0	600.5	635.5	35.0
348	664.5	45.08	340.0	357.0	17.0	640.5	680.5	40.0
363	664.5	32.07	357.0	371.0	14.0	638.5	676.5	38.0
387	664.5	49.07	371.0	415.0	44.0	643.5	679.5	36.0
423	664.5	13.72	416.0	435.0	19.0	639.5	679.5	40.0
451	664.5	23.29	436.0	459.0	23.0	643.5	687.0	43.5
380	700	38.20	370.0	387.0	17.0	683.5	728.0	44.5
393	700	110.14	387.0	407.0	20.0	677.5	719.5	42.0
413	700	14.70	409.0	417.0	8.0	676.5	718.5	42.0
464	700	38.20	458.0	469.0	11.0	674.5	715.5	41.0
532	700	13.27	521.0	540.0	19.0	681.5	717.5	36.0

**Table 8 Multiple ion doped sample Glass1-8 – 1.0 mol % Eu, 1.5 mol % Tb and 2.0 mol % Dy**



Excitation Wavelength / nm	Emission Wavelength / nm	Intensity	Peak width					
			Ex Wavelength			Em Wavelength		
			From	To	PW	From	To	PW
323	482.5	53.30	311.0	327.0	16.0	458.0	506.5	48.5
348	482.5	377.92	332.0	357.0	25.0	457.0	515.5	58.5
363	482.5	327.02	357.0	371.0	14.0	459.0	510.5	51.5
387	482.5	455.70	371.0	412.0	41.0	458.0	511.0	53.0
423	482.5	88.60	413.0	434.0	21.0	459.5	502.5	43.0
452	482.5	201.55	438.0	461.0	23.0	471.0	507.5	36.5
323	545	34.75	311.0	330.0	19.0	533.0	561.0	28.0
350	545	340.48	331.0	357.0	26.0	527.0	559.5	32.5
364	545	360.77	357.0	371.0	14.0	530.0	559.5	29.5
377	545	420.43	371.0	381.0	10.0	529.0	560.5	31.5
386	545	333.06	381.0	413.0	32.0	529.0	556.5	27.5
424	545	56.38	417.0	433.0	16.0	534.0	556.5	22.5
452	545	131.71	438.0	460.0	22.0	531.0	557.5	26.5
483	545	134.97	476.0	496.0	20.0	532.0	561.0	29.0
323	575.5	57.92	311.0	330.0	19.0	562.0	598.5	36.5
348	575.5	605.66	337.0	357.0	20.0	557.0	602.0	45.0
363	575.5	451.86	357.0	371.0	14.0	558.5	602.0	43.5
387	575.5	777.71	371.0	413.0	42.0	557.5	602.0	44.5
423	575.5	148.26	414.0	436.0	22.0	557.5	605.0	47.5
452	575.5	338.15	436.0	460.0	24.0	558.5	603.0	44.5
471	575.5	100.31	460.0	493.0	33.0	558.5	602.0	43.5
319	618.5	22.99	312.0	328.0	16.0	603.0	630.5	27.5
352	618.5	100.92	340.0	355.0	15.0	603.0	643.5	40.5
362	618.5	163.69	355.0	369.0	14.0	602.0	642.5	40.5
380	618.5	279.64	369.0	387.0	18.0	601.5	640.5	39.0
393	618.5	699.58	387.0	408.0	21.0	601.5	640.5	39.0
413	618.5	53.18	408.0	419.0	11.0	602.0	637.5	35.5
452	618.5	47.55	440.0	457.0	17.0	604.0	639.5	35.5
464	618.5	285.60	457.0	472.0	15.0	598.5	641.5	43.0
483	618.5	39.17	478.0	498.0	20.0	602.0	633.5	31.5
532	618.5	51.97	518.0	545.0	27.0	645.0	678.5	33.5
350	663	29.67	339.0	357.0	18.0	643.5	680.5	37.0
362	663	23.81	358.0	371.0	13.0	641.5	680.5	39.0
387	663	41.23	371.0	414.0	43.0	648.0	686.0	38.0
423	663	9.23	417.0	431.0	14.0	640.5	694.0	53.5
452	663	17.65	437.0	459.0	22.0	643.5	688.0	44.5
381	700.5	38.17	368.0	388.0	20.0	684.5	719.5	35.0
393	700.5	91.10	388.0	406.0	18.0	679.5	719.5	40.0
413	700.5	10.27	407.0	422.0	15.0	674.0	717.5	43.5
464	700.5	25.46	459.0	471.0	12.0	681.5	718.5	37.0
531	700.5	9.26	515.0	547.0	32.0	674.0	731.0	57.0

**Table 9 Multiple ion doped sample Glass1-9 – 1.0 mol % Eu, 2.0 mol % Tb and 2.5 mol % Dy**

Development and Application of Novel Tracers for Environmental Applications  
 Appendix II: Spectroscopic Characterisation Data

Excitation Wavelength / nm	Emission Wavelength / nm	Intensity	Peak width					
			Ex Wavelength			Em Wavelength		
			From	To	PW	From	To	PW
324	483	54.71	311.0	328.0	17.0	472.5	509.0	36.5
349	483.5	302.79	337.0	357.0	20.0	461.0	509.0	48.0
363	485	252.96	357.0	369.0	12.0	463.0	509.0	46.0
378	487	236.11	372.0	380.0	8.0	463.0	512.5	49.5
358	487	195.78	356.0	359.0	3.0	463.0	512.5	49.5
385	484	249.13	381.0	412.0	31.0	459.0	507.0	48.0
423	482.5	53.20	417.0	432.0	15.0	468.5	499.0	30.5
452	482.5	111.27	438.0	456.0	18.0	476.5	507.0	30.5
317	544	45.86	309.0	328.0	19.0	528.0	562.0	34.0
350	545	360.31	330.0	357.0	27.0	528.0	560.5	32.5
365	544.5	374.61	360.0	369.0	9.0	529.5	562.0	32.5
358	544	271.33	357.0	359.0	2.0	528.0	560.5	32.5
376	543.5	479.43	371.0	404.0	33.0	529.5	562.0	32.5
424	543.5	36.00	417.0	430.0	13.0	531.5	556.5	25.0
452	545	65.23	438.0	459.0	21.0	528.0	556.5	28.5
465	544.5	30.93	460.0	468.0	8.0	526.0	549.0	23.0
483	545	180.32	474.0	496.0	22.0	528.0	564.0	36.0
322	578	42.91	311.0	329.0	18.0	560.5	598.5	38.0
348	574	372.42	340.0	357.0	17.0	560.5	604.0	43.5
363	577.5	242.37	358.0	370.0	12.0	560.5	602.0	41.5
385	577	374.41	370.0	405.0	35.0	558.5	602.0	43.5
423	574	81.08	416.0	435.0	19.0	556.5	598.5	42.0
452	575.5	141.03	437.0	459.0	22.0	556.5	600.5	44.0
464	591.5	113.53	458.0	469.0	11.0	564.0	600.5	36.5
470	576.5	47.57	467.0	479.0	12.0	556.5	594.5	38.0
319	615.5	49.32	321.0	328.0	7.0	602.0	627.0	25.0
351	617.5	130.04	341.0	356.0	15.0	602.0	634.5	32.5
361	616	254.92	357.0	365.0	8.0	602.0	640.5	38.5
379	615	423.42	368.0	386.0	18.0	600.5	638.5	38.0
397	616	1002.06	387.0	404.0	17.0	602.0	638.5	36.5
413	613	91.45	407.0	421.0	14.0	602.0	634.5	32.5
453	614	40.82	440.0	454.0	14.0	602.0	636.5	34.5
464	614	438.43	458.0	470.0	12.0	600.5	640.5	40.0
483	615.5	61.06	475.0	500.0	25.0	604.0	638.5	34.5
530	613.5	77.76	516.0	544.0	28.0	600.5	634.5	34.0
576	614	20.65	568.0	579.0	11.0	608.0	631.0	23.0
350	653.5	19.50	338.0	355.0	17.0	642.0	674.5	32.5
363	653	21.89	357.0	386.0	29.0	642.0	674.5	32.5
379	651	36.00	369.0	387.0	18.0	644.0	671.0	27.0
391	649	50.09	387.0	404.0	17.0	642.0	669.0	27.0
464	649	33.40	456.0	469.0	13.0	642.0	661.5	19.5
361	700	34.98	358.0	366.0	8.0	686.0	705.0	19.0
379	701	52.95	369.0	387.0	18.0	676.5	718.5	42.0
393	701.5	140.43	387.0	404.0	17.0	674.5	724.0	49.5
413	701	15.20	407.0	420.0	13.0	688.0	713.0	25.0
464	702	39.75	456.0	470.0	14.0	678.5	718.5	40.0
484	701.5	10.10	476.0	492.0	16.0	693.5	714.5	21.0
532	702	12.71	519.0	536.0	17.0	682.5	716.5	34.0

**Table 10 Multiple ion doped sample Glass1-10 – 1.0 mol % Eu, 2.5 mol % Tb and 0.5 mol % Dy**

Excitation Wavelength / nm	Emission Wavelength / nm	Intensity	Peak width					
			Ex Wavelength			Em Wavelength		
			From	To	PW	From	To	PW
322	485	94.01	316.0	328.0	12.0	463.0	505.0	42.0
349	484.5	552.96	336.0	357.0	21.0	457.5	518.5	61.0
363	482.5	411.66	357.0	471.0	114.0	459.0	516.5	57.5
387	483	543.00	371.0	410.0	39.0	455.5	509.0	53.5
423	484	101.63	415.0	434.0	19.0	461.0	503.0	42.0
451	482.5	227.87	437.0	459.0	22.0	470.5	501.0	30.5
325	547.5	22.29	309.0	327.0	18.0	535.5	552.5	17.0
350	547.5	123.59	332.0	357.0	25.0	529.5	556.5	27.0
364	546.5	117.54	358.0	368.0	10.0	528.0	554.5	26.5
370	546.5	106.23	369.0	372.0	3.0	528.0	556.5	28.5
377	547	142.94	372.0	405.0	33.0	529.5	556.5	27.0
423	547	28.95	420.0	427.0	7.0	533.5	554.5	21.0
452	545.5	47.07	440.0	459.0	19.0	533.5	554.5	21.0
464	544	34.29	460.0	470.0	10.0	524.0	550.5	26.5
483	544	50.95	476.0	494.0	18.0	529.5	560.5	31.0
322	576.5	113.94	315.0	330.0	15.0	558.5	600.5	42.0
349	576	995.58	338.0	358.0	20.0	554.5	606.0	51.5
363	577	623.55	358.0	370.0	12.0	556.5	602.0	45.5
385	576.5	999.72	371.0	407.0	36.0	554.5	602.0	47.5
423	576.5	184.84	415.0	434.0	19.0	554.5	600.5	46.0
452	577.5	414.79	437.0	460.0	23.0	554.5	604.0	49.5
471	573.5	120.39	461.0	491.0	30.0	556.5	598.5	42.0
463	597.5	137.26	458.0	470.0	12.0	564.0	598.5	34.5
530	590.5	33.56	520.0	541.0	21.0	573.5	598.5	25.0
318	615	57.69	312.0	331.0	19.0	602.0	631.0	29.0
349	615.5	91.71	336.0	355.0	19.0	606.0	640.5	34.5
361	615	265.93	356.0	366.0	10.0	602.0	640.5	38.5
380	615.5	485.01	368.0	387.0	19.0	602.0	640.5	38.5
392	615.5	1000.00	387.0	405.0	18.0	600.5	640.5	40.0
414	615.5	112.97	408.0	421.0	13.0	600.5	640.5	40.0
452	615.5	45.58	449.0	455.0	6.0	608.0	638.5	30.5
464	615.5	581.83	457.0	470.0	13.0	600.5	640.5	40.0
483	615.5	31.50	479.0	495.0	16.0	604.0	634.5	30.5
532	615	117.84	518.0	546.0	28.0	600.5	638.5	38.0
577	616	25.62	568.0	583.0	15.0	604.0	632.5	28.5
349	662.5	43.77	340.0	356.0	16.0	642.0	682.5	40.5
363	664.5	31.06	357.0	368.0	11.0	644.0	684.0	40.0
385	661	54.49	371.0	388.0	17.0	642.0	680.5	38.5
393	656.5	75.52	388.0	407.0	19.0	644.0	674.5	30.5
424	656.5	13.33	417.0	429.0	12.0	644.0	674.5	30.5
449	657	20.60	439.0	457.0	18.0	644.0	682.5	38.5
463	654.5	44.12	457.0	471.0	14.0	646.0	671.0	25.0
528	655.5	11.71	524.0	539.0	15.0	642.0	667.0	25.0
361	700.5	30.89	358.0	367.0	9.0	684.0	707.0	23.0
381	700.5	56.91	368.0	388.0	20.0	684.0	720.5	36.5
393	700	156.53	387.0	405.0	18.0	676.5	722.5	46.0
414	700	19.99	408.0	420.0	12.0	690.0	714.5	24.5
463	701.5	47.44	457.0	471.0	14.0	678.5	718.5	40.0
533	701.5	15.56	517.0	547.0	30.0	678.5	716.5	38.0

**Table 11 Multiple ion doped sample Glass1-11 – 1.5 mol % Eu, 0.5 mol % Tb and 1.5 mol % Dy**

Development and Application of Novel Tracers for Environmental Applications  
 Appendix II: Spectroscopic Characterisation Data

Excitation Wavelength / nm	Emission Wavelength / nm	Intensity	Peak width					
			Ex Wavelength			Em Wavelength		
			From	To	PW	From	To	PW
322	480.5	81.36	311.0	329.0	18.0	463.0	507.0	44.0
348	481	530.10	337.0	356.0	19.0	457.5	512.5	55.0
363	483	408.14	358.0	371.0	13.0	459.0	510.5	51.5
387	483.5	559.37	372.0	407.0	35.0	455.5	510.5	55.0
423	483.5	115.13	416.0	432.0	16.0	463.0	503.0	40.0
452	482.5	268.76	436.0	458.0	22.0	472.5	503.0	30.5
322	545.5	31.26	311.0	329.0	18.0	529.5	556.5	27.0
349	546	228.26	332.0	357.0	25.0	529.5	556.5	27.0
366	546	212.29	359.0	370.0	11.0	529.5	558.5	29.0
377	546.5	257.20	371.0	381.0	10.0	529.5	558.5	29.0
384	545.5	215.05	383.0	413.0	30.0	529.5	554.5	25.0
424	547	46.35	419.0	431.0	12.0	529.5	554.5	25.0
452	546.5	86.41	437.0	459.0	22.0	533.5	554.5	21.0
463	546	38.16	460.0	464.0	4.0	522.0	550.5	28.5
483	546.5	91.03	476.0	497.0	21.0	529.5	562.0	32.5
323	576.5	110.45	313.0	328.0	15.0	558.5	600.5	42.0
348	575.5	916.13	336.0	357.0	21.0	556.5	602.0	45.5
362	576	603.88	358.0	370.0	12.0	558.5	600.5	42.0
387	577.5	989.42	371.0	408.0	37.0	556.5	602.0	45.5
423	576	210.27	415.0	435.0	20.0	554.5	600.5	46.0
452	577	433.37	436.0	460.0	24.0	556.5	602.0	45.5
464	583	157.23	460.0	468.0	8.0	560.5	600.5	40.0
470	575.5	129.93	466.0	488.0	22.0	558.5	594.5	36.0
530	576.5	24.23	519.0	539.0	20.0	570.0	589.0	19.0
531	596	35.15	520.0	542.0	22.0	591.0	600.5	9.5
317	616	41.26	313.0	330.0	17.0	602.0	625.0	23.0
351	616	116.46	336.0	354.0	18.0	604.0	636.5	32.5
361	616.5	270.74	356.0	367.0	11.0	602.0	640.5	38.5
380	616	475.23	368.0	387.0	19.0	602.0	638.5	36.5
394	616	1000.28	387.0	405.0	18.0	600.5	640.5	40.0
413	616.5	119.27	408.0	420.0	12.0	600.5	638.5	38.0
423	615.5	38.79	421.0	429.0	8.0	606.0	640.5	34.5
452	617	59.52	447.0	455.0	8.0	608.0	634.5	26.5
464	617	594.24	458.0	470.0	12.0	600.5	640.5	40.0
483	618	47.65	479.0	493.0	14.0	602.0	634.5	32.5
531	616	111.92	518.0	546.0	28.0	600.5	636.5	36.0
552	615.5	10.43	549.0	558.0	9.0	602.0	632.5	30.5
577	613	31.62	569.0	582.0	13.0	608.0	632.5	24.5
350	665.5	42.70	341.0	355.0	14.0	642.0	682.5	40.5
362	666	34.31	358.0	369.0	11.0	644.0	676.5	32.5
387	664.5	51.47	371.0	409.0	38.0	644.0	680.5	36.5
422	663.5	14.76	416.0	430.0	14.0	646.0	674.5	28.5
453	663	25.22	441.0	457.0	16.0	646.0	690.0	44.0
463	660.5	28.35	459.0	469.0	10.0	642.0	669.0	27.0
521	661	15.38	517.0	540.0	23.0	640.5	671.0	30.5
361	697.5	30.17	358.0	366.0	8.0	690.0	705.0	15.0
387	699	55.27	369.0	386.0	17.0	680.5	720.5	40.0
393	700.5	154.94	386.0	405.0	19.0	678.5	720.5	42.0
410	699.5	20.12	407.0	418.0	11.0	690.0	716.5	26.5
426	700	12.28	423.0	430.0	7.0	692.0	711.0	19.0
463	701.5	49.42	456.0	470.0	14.0	678.5	722.5	44.0
532	700.5	17.84	520.0	541.0	21.0	684.5	718.5	34.0

**Table 12 Multiple ion doped sample Glass1-12 – 1.5 mol % Eu, 1.0 mol % Tb and 2.0 mol % Dy**

Development and Application of Novel Tracers for Environmental Applications  
 Appendix II: Spectroscopic Characterisation Data

Excitation Wavelength / nm	Emission Wavelength / nm	Intensity	Peak width					
			Ex Wavelength			Em Wavelength		
			From	To	PW	From	To	PW
322	482.5	58.14	310.0	330.0	20.0	461.0	510.5	49.5
350	482.5	365.17	339.0	357.0	18.0	455.5	512.5	57.0
364	482.5	293.98	357.0	370.0	13.0	459.0	514.5	55.5
386	483.5	441.09	370.0	411.0	41.0	453.5	512.5	59.0
424	483	90.04	416.0	432.0	16.0	463.0	510.5	47.5
452	483	211.74	437.0	460.0	23.0	470.5	507.0	36.5
322	547	29.58	311.0	330.0	19.0	529.5	556.5	27.0
349	546	226.46	332.0	357.0	25.0	529.5	558.5	29.0
364	546	234.98	359.0	370.0	11.0	528.0	558.5	30.5
376	546	264.32	372.0	381.0	9.0	528.0	558.5	30.5
385	545.5	231.02	382.0	408.0	26.0	529.5	556.5	27.0
412	546	32.06	410.0	415.0	5.0	541.0	556.5	15.5
424	545	47.31	417.0	432.0	15.0	529.5	556.5	27.0
452	544.5	103.22	437.0	460.0	23.0	531.5	556.5	25.0
464	544.5	39.81	461.0	467.0	6.0	522.0	554.5	32.5
471	546.5	41.30	468.0	474.0	6.0	529.5	554.5	25.0
483	546.5	98.36	475.0	495.0	20.0	529.5	564.0	34.5
323	576.5	68.49	312.0	329.0	17.0	560.5	600.5	40.0
349	576.5	622.13	338.0	357.0	19.0	558.5	602.0	43.5
363	576	449.64	358.0	370.0	12.0	560.5	600.5	40.0
386	576.5	743.46	371.0	408.0	37.0	556.5	602.0	45.5
424	577	157.31	415.0	433.0	18.0	556.5	604.0	47.5
452	575	349.21	437.0	460.0	23.0	558.5	602.0	43.5
471	575	107.12	461.0	492.0	31.0	560.5	600.5	40.0
529	580	22.88	518.0	538.0	20.0	570.0	591.0	21.0
464	591.5	135.64	459.0	469.0	10.0	562.0	600.5	38.5
532	591.5	27.08	521.0	541.0	20.0	573.5	598.5	25.0
319	616	35.53	312.0	329.0	17.0	602.0	634.5	32.5
351	616.5	101.44	340.0	355.0	15.0	604.0	636.5	32.5
362	616	214.62	357.0	367.0	10.0	602.0	640.5	38.5
381	615	383.47	358.0	386.0	28.0	602.0	640.5	38.5
393	615	942.70	387.0	405.0	18.0	602.0	640.5	38.5
414	614	87.18	407.0	420.0	13.0	602.0	640.5	38.5
425	615	33.93	421.0	430.0	9.0	604.0	636.5	32.5
450	614.5	49.41	440.0	456.0	16.0	606.0	638.5	32.5
464	615	452.09	457.0	471.0	14.0	600.5	640.5	40.0
482	618	41.25	477.0	497.0	20.0	604.0	638.5	34.5
532	614.5	88.88	519.0	544.0	25.0	602.0	636.5	34.5
577	613	23.60	569.0	582.0	13.0	604.0	634.5	30.5
348	655	25.56	338.0	355.0	17.0	648.0	680.5	32.5
363	655	24.79	357.0	370.0	13.0	644.0	680.5	36.5
384	655.5	37.10	370.0	387.0	17.0	644.0	682.5	38.5
392	654	64.07	387.0	405.0	18.0	642.0	674.5	32.5
450	654.5	17.35	438.0	457.0	19.0	648.0	674.5	26.5
463	651	30.69	457.0	469.0	12.0	642.0	671.0	29.0
412	651	12.79	409.0	416.0	7.0	644.0	665.0	21.0
424	650.5	12.01	420.0	427.0	7.0	646.0	657.5	11.5
449	650	14.41	438.0	457.0	19.0	640.5	686.0	45.5
362	703.5	24.46	359.0	362.0	3.0	686.0	709.0	23.0
381	702	45.70	370.0	387.0	17.0	684.0	720.5	36.5
393	700.5	123.96	389.0	406.0	17.0	680.5	718.5	38.0
414	700.5	13.62	408.0	420.0	12.0	682.5	716.5	34.0
425	700.5	7.52	420.0	428.0	8.0	692.0	716.5	24.5
452	701	8.21	447.0	454.0	7.0	692.0	713.0	21.0
463	700	39.09	457.0	469.0	12.0	678.5	722.5	44.0
481	700	7.63	477.0	490.0	13.0	693.5	713.0	19.5
533	700	12.75	519.0	544.0	25.0	680.5	714.5	34.0

**Table 13 Multiple ion doped sample Glass1-13 – 1.5 mol % Eu, 1.5 mol % Tb and 2.5 mol % Dy**

Development and Application of Novel Tracers for Environmental Applications  
 Appendix II: Spectroscopic Characterisation Data

Excitation Wavelength / nm	Emission Wavelength / nm	Intensity	Peak width					
			Ex Wavelength			Em Wavelength		
			From	To	PW	From	To	PW
323	484	82.32	310.0	328.0	18.0	467.0	507.0	40.0
348	485	472.50	338.0	357.0	19.0	459.0	510.5	51.5
363	485.5	346.23	358.0	370.0	12.0	461.0	510.5	49.5
378	486	315.09	372.0	380.0	8.0	463.0	512.5	49.5
385	484	375.80	380.0	408.0	28.0	457.5	512.5	55.0
423	482.5	72.05	416.0	432.0	16.0	463.0	503.0	40.0
452	481.5	164.58	438.0	459.0	21.0	472.5	55.0	417.5
317	545.5	58.29	311.0	328.0	17.0	528.0	562.0	34.0
351	546	455.50	332.0	357.0	25.0	529.5	560.5	31.0
367	546.5	454.21	360.0	370.0	10.0	529.5	562.0	32.5
377	545	591.00	371.0	385.0	14.0	528.0	564.0	36.0
386	546	235.87	385.0	406.0	21.0	529.5	558.5	29.0
424	547	43.92	419.0	429.0	10.0	533.5	556.5	23.0
452	545	80.56	440.0	458.0	18.0	531.5	558.5	27.0
464	545.5	45.55	460.0	468.0	8.0	522.0	558.5	36.5
433	544	22.02	431.0	435.0	4.0	535.5	554.5	19.0
483	546	222.16	475.0	493.0	18.0	528.0	566.0	38.0
323	576	85.46	314.0	329.0	15.0	562.0	602.0	40.0
349	576.5	674.45	338.0	357.0	19.0	560.5	602.0	41.5
362	578.5	403.95	358.0	369.0	11.0	562.0	602.0	40.0
386	577.5	634.78	370.0	368.0	-2.0	558.5	602.0	43.5
393	591.5	868.95	387.0	406.0	19.0	56.5	600.5	544.0
424	577	121.51	417.0	434.0	17.0	558.5	602.0	43.5
452	577	234.78	438.0	459.0	21.0	556.5	604.0	47.5
463	588	250.35	459.0	470.0	11.0	568.0	600.5	32.5
474	579	77.37	470.0	479.0	9.0	562.0	600.5	38.5
483	585.5	62.33	478.0	496.0	18.0	568.0	604.0	36.0
531	594.5	53.80	518.0	544.0	26.0	568.0	600.5	32.5
319	614	124.38	314.0	332.0	18.0	600.5	627.0	26.5
349	617	237.31	341.0	355.0	14.0	604.0	640.5	36.5
362	617	565.65	355.0	367.0	12.0	602.0	638.5	36.5
379	616	1000.45	368.0	387.0	19.0	602.0	640.5	38.5
395	616	1000.00	387.0	406.0	19.0	602.0	640.5	38.5
414	616.5	199.77	408.0	420.0	12.0	602.0	634.5	32.5
424	616	39.49	422.0	429.0	7.0	604.0	634.5	30.5
446	615	51.87	439.0	448.0	9.0	606.0	636.5	30.5
454	615.5	57.87	449.0	456.0	7.0	606.0	642.0	36.0
463	616.5	996.29	455.0	471.0	16.0	600.5	638.5	38.0
484	615	102.26	476.0	498.0	22.0	604.0	636.5	32.5
533	615	202.44	519.0	545.0	26.0	602.0	640.5	38.5
579	613	40.10	571.0	587.0	16.0	606.0	634.5	28.5
346	654.5	29.28	338.0	355.0	17.0	644.0	674.5	30.5
362	656	43.47	357.0	358.0	1.0	642.0	672.5	30.5
379	656.5	63.78	370.0	385.0	15.0	644.0	671.0	27.0
393	655.5	134.69	387.0	406.0	19.0	642.0	669.0	27.0
414	656	17.00	406.0	419.0	13.0	642.0	665.0	23.0
452	654.5	17.92	441.0	455.0	14.0	652.0	674.5	22.5
463	654.5	60.03	457.0	469.0	12.0	642.0	671.0	29.0
485	655	19.13	477.0	493.0	16.0	644.0	667.0	23.0
530	656	15.55	520.0	544.0	24.0	644.0	671.0	27.0
362	701.5	71.77	359.0	365.0	6.0	684.0	709.0	25.0
381	701	125.74	368.0	387.0	19.0	678.5	720.5	42.0
392	702	334.49	387.0	406.0	19.0	674.5	724.0	49.5
412	701.5	27.47	408.0	420.0	12.0	682.5	716.5	34.0
463	701.5	90.77	455.0	471.0	16.0	678.5	720.5	42.0
484	703.5	16.10	477.0	495.0	18.0	682.5	718.5	36.0
531	703	25.79	519.0	547.0	28.0	686.0	722.5	36.5
576	702	7.35	569.0	595.0	26.0	682.5	724.0	41.5

**Table 14 Multiple ion doped sample Glass1-14 – 1.5 mol % Eu, 2.0 mol % Tb and 0.5 mol % Dy**

Development and Application of Novel Tracers for Environmental Applications  
Appendix II: Spectroscopic Characterisation Data

Excitation Wavelength / nm	Emission Wavelength / nm	Intensity	Peak width					
			Ex Wavelength			Em Wavelength		
			From	To	PW	From	To	PW
322	483.5	64.34	313.0	329.0	16.0	470.5	501.0	30.5
349	484.5	398.53	338.0	357.0	19.0	459.0	512.5	53.5
363	484.5	296.67	357.0	370.0	13.0	461.0	512.5	51.5
377	486	252.91	372.0	379.0	7.0	465.0	512.5	47.5
385	483	350.14	379.0	410.0	31.0	455.5	510.5	55.0
424	482.5	75.35	417.0	433.0	16.0	470.5	503.0	32.5
452	482.5	181.95	437.0	457.0	20.0	472.5	509.0	36.5
323	543.5	45.82	311.0	329.0	18.0	529.5	556.5	27.0
349	544.5	401.08	339.0	356.0	17.0	529.5	560.5	31.0
367	546	390.86	358.0	369.0	11.0	529.5	560.5	31.0
377	545.5	480.95	372.0	382.0	10.0	529.5	562.0	32.5
384	545.5	276.99	382.0	401.0	19.0	531.5	558.5	27.0
423	546	51.88	417.0	432.0	15.0	531.5	556.5	25.0
452	545	105.29	438.0	459.0	21.0	529.5	556.5	27.0
464	544	45.12	461.0	466.0	5.0	520.0	560.5	40.5
484	544.5	172.53	474.0	498.0	24.0	529.5	564.0	34.5
322	581.5	68.90	311.0	330.0	19.0	560.5	598.5	38.0
347	576.5	559.90	338.0	356.0	18.0	558.5	600.5	42.0
363	579.5	376.52	357.0	370.0	13.0	560.5	602.0	41.5
386	576.5	590.68	371.0	408.0	37.0	558.5	602.0	43.5
423	576.5	117.52	417.0	432.0	15.0	558.5	598.5	40.0
452	577	245.56	438.0	459.0	21.0	556.5	602.0	45.5
464	589	175.39	458.0	470.0	12.0	566.0	600.5	34.5
484	588.5	53.32	477.0	494.0	17.0	571.5	600.5	29.0
572	588.5	39.32	521.0	540.0	19.0	573.5	598.5	25.0
319	615.5	75.35	311.0	330.0	19.0	600.5	632.5	32.0
350	616.5	208.42	340.0	356.0	16.0	606.0	632.5	26.5
362	616	379.08	356.0	366.0	10.0	602.0	636.5	34.5
378	616	638.48	369.0	387.0	18.0	602.0	638.5	36.5
391	616	1000.46	387.0	406.0	19.0	600.5	638.5	38.0
413	614.5	132.39	408.0	420.0	12.0	602.0	638.5	36.5
425	615.5	92.29	422.0	431.0	9.0	604.0	634.5	30.5
451	615	64.37	438.0	456.0	18.0	604.0	638.5	34.5
464	615.5	662.05	458.0	470.0	12.0	600.5	638.5	38.0
483	616	85.02	476.0	492.0	16.0	604.0	634.5	30.5
531	615.5	132.40	518.0	545.0	27.0	600.5	636.5	36.0
577	615	33.49	566.0	582.0	16.0	604.0	634.5	30.5
350	655	27.97	337.0	356.0	19.0	642.0	680.5	38.5
362	655.5	33.72	357.0	369.0	12.0	642.0	672.5	30.5
382	657	51.28	370.0	387.0	17.0	644.0	671.0	27.0
393	654	95.70	388.0	405.0	17.0	644.0	671.0	27.0
413	654	17.04	408.0	417.0	9.0	648.0	667.0	19.0
452	654.5	20.95	444.0	455.0	11.0	652.0	671.0	19.0
464	655.5	43.99	458.0	469.0	11.0	644.0	672.5	28.5
485	656	22.49	480.0	490.0	10.0	640.5	671.0	30.5
524	656.5	15.10	521.0	537.0	16.0	642.0	667.0	25.0
362	701.5	52.02	360.0	365.0	5.0	678.5	707.0	28.5
380	700.5	84.91	369.0	387.0	18.0	680.5	718.5	38.0
393	701.5	207.57	387.0	405.0	18.0	676.5	722.5	46.0
414	701	20.21	409.0	420.0	11.0	672.5	720.5	48.0
435	701	10.21	431.0	438.0	7.0	686.0	707.0	21.0
452	701.5	10.55	446.0	455.0	9.0	692.0	718.5	26.5
484	701	12.72	476.0	496.0	20.0	680.5	718.5	38.0
530	701	18.97	517.0	547.0	30.0	682.5	726.0	43.5

**Table 15 Multiple ion doped sample Glass1-15 – 1.5 mol % Eu, 2.5 mol % Tb and 1.0 mol % Dy**

Development and Application of Novel Tracers for Environmental Applications  
 Appendix II: Spectroscopic Characterisation Data

Excitation Wavelength / nm	Emission Wavelength / nm	Intensity	Peak width					
			Ex Wavelength			Em Wavelength		
			From	To	PW	From	To	PW
322	482.5	82.12	311.0	330.0	19.0	463.0	507.0	44.0
348	483.5	505.30	339.0	356.0	17.0	459.0	505.0	46.0
363	482.5	376.69	357.0	371.0	14.0	461.0	505.0	44.0
385	481.5	504.37	372.0	409.0	37.0	463.0	505.0	42.0
424	482.5	114.12	417.0	430.0	13.0	452.0	501.0	49.0
452	482.5	261.90	438.0	457.0	19.0	535.5	507.0	-28.5
323	545.5	23.66	311.0	326.0	15.0	529.5	550.5	21.0
350	545.5	118.19	341.0	356.0	15.0	529.5	554.5	25.0
365	545.5	106.54	359.0	370.0	11.0	529.5	556.5	27.0
377	545	129.85	371.0	380.0	9.0	528.0	556.5	28.5
385	545.5	115.45	381.0	386.0	5.0	524.0	550.5	26.5
387	545.5	111.05	386.0	390.0	4.0	518.5	550.5	32.0
393	543	101.23	390.0	398.0	8.0	531.5	550.5	19.0
452	543	470.07	440.0	458.0	18.0	522.0	549.0	27.0
464	542	43.83	459.0	469.0	10.0	531.5	549.0	17.5
427	542	28.38	419.0	433.0	14.0	531.5	547.0	15.5
472	542.5	31.82	469.0	474.0	5.0	531.5	556.5	25.0
482	545	51.36	477.0	493.0	16.0	556.5	560.5	4.0
323	576	107.97	315.0	331.0	16.0	554.5	600.5	46.0
348	577	957.47	338.0	357.0	19.0	556.5	604.0	47.5
362	577.5	610.95	357.0	370.0	13.0	554.5	602.0	47.5
386	577.5	968.90	371.0	408.0	37.0	554.5	602.0	47.5
424	576.5	196.17	416.0	433.0	17.0	554.5	600.5	46.0
452	577	412.84	436.0	460.0	24.0	554.5	602.0	47.5
463	585	196.93	458.0	469.0	11.0	564.0	598.5	34.5
471	576.5	133.37	466.0	490.0	24.0	558.5	596.5	38.0
533	592	44.87	519.0	544.0	25.0	577.5	600.5	23.0
319	615.5	63.41	313.0	330.0	17.0	602.0	629.0	27.0
349	615.5	107.53	340.0	354.0	14.0	606.0	638.5	32.5
362	615	294.04	355.0	368.0	13.0	604.0	640.5	36.5
379	615	559.74	368.0	387.0	19.0	602.0	640.5	38.5
393	615	1000.00	387.0	406.0	19.0	602.0	640.5	38.5
412	616	148.15	408.0	420.0	12.0	600.5	640.5	40.0
454	616	59.94	438.0	455.0	17.0	606.0	638.5	32.5
484	616.5	38.30	479.0	496.0	17.0	602.0	640.5	38.5
577	614.5	38.03	569.0	582.0	13.0	608.0	636.5	28.5
463	614	684.75	457.0	471.0	14.0	600.5	638.5	38.0
530	615	144.06	519.0	544.0	25.0	600.5	640.5	40.0
348	660	40.88	341.0	357.0	16.0	640.5	680.5	40.0
362	661	34.04	357.0	368.0	11.0	642.0	682.5	40.5
382	660	53.45	370.0	387.0	17.0	642.0	672.5	30.5
392	657	86.49	387.0	406.0	19.0	644.0	674.5	30.5
411	656.5	20.11	406.0	416.0	10.0	650.0	663.0	13.0
424	656.5	14.88	419.0	430.0	11.0	657.5	674.5	17.0
452	665	26.65	439.0	457.0	18.0	642.0	684.0	42.0
463	653.5	44.38	457.0	469.0	12.0	642.0	672.5	30.5
362	702.5	35.08	359.0	367.0	8.0	682.5	707.0	24.5
381	702.5	66.46	368.0	387.0	19.0	682.5	722.5	40.0
393	702	180.51	387.0	406.0	19.0	678.5	722.5	44.0
414	702	20.58	408.0	422.0	14.0	684.0	714.5	30.5
463	701.5	58.03	457.0	471.0	14.0	678.5	720.5	42.0
530	701.5	22.41	520.0	539.0	19.0	686.0	716.5	30.5

**Table 16 Multiple ion doped sample Glass1-16 – 2.0 mol % Eu, 0.5 mol % Tb and 2.0 mol % Dy**



Excitation Wavelength / nm	Emission Wavelength / nm	Intensity	Peak width					
			Ex Wavelength			Em Wavelength		
			From	To	PW	From	To	PW
324	484	70.47	313.0	330.0	17.0	465.0	501.0	36.0
349	482.5	398.57	338.0	357.0	19.0	461.0	503.0	42.0
363	482.5	302.00	357.0	371.0	14.0	461.0	501.0	40.0
387	482	410.86	371.0	409.0	38.0	459.0	505.0	46.0
424	482	103.85	417.0	431.0	14.0	467.0	503.0	36.0
452	481.5	229.02	439.0	458.0	19.0	474.5	499.0	24.5
321	543	27.42	311.0	329.0	18.0	531.5	556.5	25.0
425	542	40.01	419.0	431.0	12.0	533.5	549.0	15.5
465	540.5	46.48	458.0	471.0	13.0	529.5	552.5	23.0
452	544.5	69.45	439.0	458.0	19.0	529.5	556.5	27.0
484	544	72.42	476.0	493.0	17.0	531.5	560.5	29.0
351	546	160.60	340.0	357.0	17.0	528.0	556.5	28.5
367	545.5	151.43	357.0	370.0	13.0	529.5	558.5	29.0
378	544.5	187.73	371.0	382.0	11.0	529.5	558.5	29.0
390	544	158.89	384.0	416.0	32.0	518.5	556.5	38.0
324	579	83.40	313.0	330.0	17.0	558.5	600.5	42.0
349	577.5	653.47	336.0	357.0	21.0	556.5	602.0	45.5
363	577	450.21	357.0	371.0	14.0	556.5	600.5	44.0
386	576.5	726.83	373.0	408.0	35.0	556.5	602.0	45.5
424	574.5	174.66	416.0	435.0	19.0	554.5	604.0	49.5
452	577	342.77	438.0	460.0	22.0	556.5	604.0	47.5
463	577	106.71	461.0	467.0	6.0	562.0	600.5	38.5
471	576	108.04	466.0	489.0	23.0	556.5	598.5	42.0
530	576	29.35	520.0	534.0	14.0	570.0	598.5	28.5
463	587	157.07	458.0	468.0	10.0	562.0	600.5	38.5
531	591	39.82	520.0	539.0	19.0	575.5	598.5	23.0
319	614	54.05	311.0	329.0	18.0	604.0	631.0	27.0
349	615.5	109.47	338.0	354.0	16.0	602.0	636.5	34.5
362	615	244.28	355.0	767.0	412.0	602.0	640.5	38.5
381	615.5	435.15	368.0	387.0	19.0	602.0	638.5	36.5
392	615	1002.82	387.0	406.0	19.0	600.5	640.5	40.0
412	615	113.58	408.0	420.0	12.0	600.5	634.5	34.0
424	614	44.64	420.0	431.0	11.0	606.0	638.5	32.5
452	614.5	70.28	438.0	455.0	17.0	604.0	638.5	34.5
463	614	516.29	457.0	471.0	14.0	600.5	642.0	41.5
484	614	42.56	481.0	495.0	14.0	604.0	632.5	28.5
576	615	30.33	569.0	582.0	13.0	608.0	631.0	23.0
531	614.5	111.19	520.0	545.0	25.0	600.5	636.5	36.0
348	659	30.19	340.0	355.0	15.0	644.0	678.5	34.5
360	658.5	29.25	355.0	368.0	13.0	646.0	672.5	26.5
384	658	48.49	368.0	389.0	21.0	642.0	684.0	42.0
392	657	64.25	389.0	406.0	17.0	642.0	672.5	30.5
423	657	16.25	418.0	427.0	9.0	650.0	671.0	21.0
452	656.5	20.74	446.0	456.0	10.0	644.0	686.0	42.0
465	656.5	35.29	458.0	469.0	11.0	644.0	672.5	28.5
360	701.5	33.83	359.0	366.0	7.0	684.0	705.0	21.0
381	702	55.62	370.0	387.0	17.0	682.5	720.5	38.0
393	701.5	140.24	387.0	405.0	18.0	676.5	724.0	47.5
412	703	24.01	409.0	417.0	8.0	686.0	714.5	28.5
462	704.5	34.95	455.0	471.0	16.0	680.5	720.5	40.0
533	702.5	19.17	520.0	544.0	24.0	695.5	718.5	23.0

**Table 17 Multiple ion doped sample Glass1-17 – 2.0 mol % Eu, 1.0 mol % Tb and 2.5 mol % Dy**

Development and Application of Novel Tracers for Environmental Applications  
Appendix II: Spectroscopic Characterisation Data

Excitation Wavelength / nm	Emission Wavelength / nm	Intensity	Peak width					
			Ex Wavelength			Em Wavelength		
			From	To	PW	From	To	PW
323	483.5	45.57	310.0	330.0	20.0	465.0	503.0	38.0
335	483.5	56.52	332.0	337.0	5.0	476.5	503.0	26.5
349	484	254.86	339.0	356.0	17.0	459.0	514.5	55.5
363	484	191.31	357.0	371.0	14.0	461.0	512.5	51.5
378	484.5	164.68	372.0	380.0	8.0	463.0	512.5	49.5
386	484.5	213.48	380.0	395.0	15.0	455.5	509.0	53.5
423	482	56.32	417.0	430.0	13.0	465.0	499.0	34.0
451	481.5	115.84	442.0	457.0	15.0	476.5	507.0	30.5
317	545.5	24.20	311.0	321.0	10.0	529.5	558.5	29.0
323	545.5	24.76	321.0	327.0	6.0	529.5	556.5	27.0
350	545.5	177.96	343.0	355.0	12.0	529.5	558.5	29.0
358	545	134.73	357.0	360.0	3.0	529.5	558.5	29.0
368	545.5	186.06	360.0	370.0	10.0	528.0	562.0	34.0
376	545.5	236.10	372.0	384.0	12.0	528.0	560.5	32.5
387	545.5	106.37	385.0	397.0	12.0	529.5	556.5	27.0
423	546.5	25.62	418.0	430.0	12.0	535.5	554.5	19.0
452	546.5	39.58	439.0	460.0	21.0	529.5	554.5	25.0
464	546.5	27.89	460.0	470.0	10.0	524.0	547.0	23.0
483	545	102.85	474.0	494.0	20.0	528.0	566.0	38.0
323	579	41.62	313.0	330.0	17.0	560.5	598.5	38.0
349	576.5	374.38	339.0	357.0	18.0	558.5	602.0	43.5
362	576	243.77	357.0	370.0	13.0	558.5	600.5	42.0
387	576	383.36	370.0	406.0	36.0	556.5	600.5	44.0
423	575	83.43	415.0	432.0	17.0	556.5	596.5	40.0
452	574.5	149.86	439.0	458.0	19.0	556.5	602.0	45.5
462	589.5	155.12	458.0	470.0	12.0	564.0	600.5	36.5
500	575.5	12.04	495.0	502.0	7.0	571.5	583.0	11.5
533	591.5	49.53	519.0	544.0	25.0	573.5	598.5	25.0
319	615.5	75.87	312.0	330.0	18.0	600.5	632.5	32.0
351	616	126.61	333.0	355.0	22.0	602.0	638.5	36.5
361	615.5	431.71	357.0	367.0	10.0	602.0	640.5	38.5
380	616	755.17	369.0	387.0	18.0	602.0	640.5	38.5
393**	616	1000.00	387.0	405.0	18.0	600.5	640.5	40.0
413	615.5	179.68	408.0	420.0	12.0	602.0	638.5	36.5
426	615	34.55	424.0	430.0	6.0	604.0	636.5	32.5
444	615.5	42.92	437.0	446.0	9.0	606.0	634.5	28.5
452	615.5	48.48	448.0	455.0	7.0	602.0	642.0	40.0
464	613.5	870.03	458.0	469.0	11.0	600.5	638.5	38.0
483	618.5	61.06	477.0	494.0	17.0	602.0	636.5	34.5
533	618.5	148.80	519.0	545.0	26.0	600.5	638.5	38.0
577	617.5	31.38	570.0	582.0	12.0	604.0	636.5	32.5
348	656.5	23.23	339.0	357.0	18.0	646.0	678.5	32.5
362	656.5	26.37	357.0	368.0	11.0	646.0	665.0	19.0
380	656.5	45.24	368.0	386.0	18.0	640.5	669.0	28.5
392	653	106.46	388.0	406.0	18.0	642.0	671.0	29.0
412	652.5	15.83	408.0	417.0	9.0	644.0	663.0	19.0
464	652.5	47.75	457.0	469.0	12.0	642.0	672.5	30.5
451	653.5	17.17	445.0	455.0	10.0	648.0	671.0	23.0
482	653	21.16	481.0	485.0	4.0	642.0	663.0	21.0
532	652.5	12.48	521.0	540.0	19.0	646.0	667.0	21.0
361	701	54.55	360.0	367.0	7.0	680.5	709.0	28.5
379	702.5	92.83	370.0	387.0	17.0	676.5	718.5	42.0
392	702	242.31	387.0	405.0	18.0	674.5	722.5	48.0
413	702	23.31	407.0	419.0	12.0	674.5	720.5	46.0
485	702.5	10.00	477.0	492.0	15.0	692.0	714.5	22.5
463	701	78.21	457.0	470.0	13.0	676.5	720.5	44.0
531	701	22.59	520.0	549.0	29.0	676.5	718.5	42.0

**Table 18 Multiple ion doped sample Glass1-18 – 2.0 mol % Eu, 1.5 mol % Tb and 0.5 mol % Dy**

Development and Application of Novel Tracers for Environmental Applications  
 Appendix II: Spectroscopic Characterisation Data

Excitation Wavelength / nm	Emission Wavelength / nm	Intensity	Peak width					
			Ex Wavelength			Em Wavelength		
			From	To	PW	From	To	PW
325	482	33.41	316.0	329.0	13.0	467.0	497.5	30.5
348	482	275.53	338.0	357.0	19.0	459.0	512.5	53.5
364	482.5	217.55	357.0	371.0	14.0	459.0	512.5	53.5
386	482	283.69	371.0	404.0	33.0	455.5	509.0	53.5
423	479.5	60.30	416.0	430.0	14.0	465.0	501.0	36.0
452	480	142.97	438.0	457.0	19.0	472.5	503.0	30.5
325	546	24.86	311.0	328.0	17.0	533.5	556.5	23.0
349	545.5	224.08	338.0	356.0	18.0	529.5	558.5	29.0
358	545.5	165.05	357.0	359.0	2.0	529.5	558.5	29.0
366	545.5	231.09	359.0	370.0	11.0	529.5	560.5	31.0
377	546.5	288.46	373.0	382.0	9.0	529.5	560.5	31.0
385	546	178.30	382.0	412.0	30.0	531.5	558.5	27.0
422	546.5	34.34	417.0	430.0	13.0	533.5	554.5	21.0
452	545.5	66.37	439.0	459.0	20.0	529.5	556.5	27.0
464	545	30.83	461.0	467.0	6.0	522.0	556.5	34.5
483	543.5	114.14	474.0	497.0	23.0	529.5	564.0	34.5
323	580	36.18	313.0	330.0	17.0	558.5	592.5	34.0
349	579.5	415.50	338.0	357.0	19.0	560.5	62.0	-498.5
363	577.5	299.90	357.0	370.0	13.0	560.5	600.5	40.0
386	576.5	489.85	372.0	407.0	35.0	558.5	600.5	42.0
412	576.5	43.56	410.0	414.0	4.0	570.0	581.0	11.0
423	578	96.34	416.0	431.0	15.0	554.5	602.0	47.5
452	576	190.74	439.0	458.0	19.0	558.5	602.0	43.5
463	579.5	114.17	459.0	469.0	10.0	572.5	581.0	8.5
482	582.5	36.49	480.0	495.0	15.0	565.5	599.0	33.5
531	582.5	33.77	519.0	539.0	20.0	578.5	589.5	11.0
464	593.5	188.14	458.0	470.0	12.0	572.5	599.0	26.5
531	593	39.18	520.0	540.0	20.0	589.5	598.0	8.5
318	615.5	54.71	312.0	330.0	18.0	602.5	629.0	26.5
350	615.5	161.25	342.0	356.0	14.0	602.5	637.0	34.5
362	616	364.97	356.0	367.0	11.0	601.5	633.5	32.0
380	615.5	665.31	369.0	387.0	18.0	601.5	637.0	35.5
393	615.5	1000.00	388.0	405.0	17.0	600.0	637.0	37.0
412	613.5	140.17	408.0	421.0	13.0	600.0	637.0	37.0
424	614.5	39.89	422.0	428.0	6.0	609.5	620.5	11.0
453	614	57.86	447.0	455.0	8.0	601.5	629.0	27.5
463	614.5	688.57	457.0	471.0	14.0	600.0	638.5	38.5
484	616	67.99	477.0	498.0	21.0	602.5	631.0	28.5
531	615.5	138.73	519.0	547.0	28.0	601.5	636.0	34.5
579	616	32.13	569.0	583.0	14.0	612.0	621.5	9.5
348	656.5	24.16	342.0	354.0	12.0	640.5	675.5	35.0
363	656	24.78	358.0	368.0	10.0	640.5	671.5	31.0
379	654.5	45.14	369.0	387.0	18.0	640.5	671.5	31.0
393	655	86.87	387.0	405.0	18.0	642.0	663.5	21.5
415	655	12.79	409.0	418.0	9.0	646.5	662.0	15.5
447	655.5	16.60	439.0	455.0	16.0	650.5	671.5	21.0
464	654	41.61	457.0	469.0	12.0	642.0	662.0	20.0
484	655	18.44	476.0	487.0	11.0	646.5	658.5	12.0
525	653.5	13.30	523.0	537.0	14.0	643.0	658.5	15.5
362	699.5	42.71	358.0	365.0	7.0	688.5	708.5	20.0
381	700	84.68	370.0	387.0	17.0	679.0	718.0	39.0
393	699.5	212.74	387.0	405.0	18.0	676.5	718.0	41.5
413	700.5	23.65	411.0	420.0	9.0	687.0	711.0	24.0
464	701.5	68.46	457.0	471.0	14.0	676.5	717.0	40.5
451	701	9.87	449.0	456.0	7.0	688.5	707.5	19.0
484	699	12.22	476.0	490.0	14.0	691.0	717.0	26.0
531	700	19.62	521.0	543.0	22.0	676.5	719.5	43.0

**Table 19 Multiple ion doped sample Glass1-19 – 2.0 mol % Eu, 2.0 mol % Tb and 1.0 mol % Dy**

Development and Application of Novel Tracers for Environmental Applications  
 Appendix II: Spectroscopic Characterisation Data

Excitation Wavelength / nm	Emission Wavelength / nm	Intensity	Peak width					
			Ex Wavelength			Em Wavelength		
			From	To	PW	From	To	PW
322	484.5	72.60	316.0	327.0	11.0	482.0	501.0	19.0
348	482.5	399.85	341.0	357.0	16.0	461.0	505.0	44.0
363	484	304.24	359.0	370.0	11.0	461.0	509.0	48.0
378	485	249.15	373.0	380.0	7.0	465.0	507.0	42.0
386	484.5	368.79	380.0	397.0	17.0	459.0	507.0	48.0
424	482.5	83.09	419.0	431.0	12.0	470.5	503.0	32.5
452	484	191.74	443.0	458.0	15.0	474.5	501.0	26.5
323	545	47.39	321.0	324.0	3.0	531.5	558.5	27.0
326	543	41.97	325.0	327.0	2.0	533.5	557.5	24.0
350	546.5	376.47	339.0	356.0	17.0	529.5	558.5	29.0
364	545	354.50	362.0	366.0	4.0	531.5	560.5	29.0
361	545.5	92.13	359.0	362.0	3.0	528.0	558.5	30.5
367	545.5	335.77	366.0	369.0	3.0	531.0	560.0	29.0
377	546	432.97	373.0	380.0	7.0	531.0	560.0	29.0
385	545.5	279.50	383.0	386.0	3.0	531.0	556.0	25.0
424	544.5	51.04	420.0	425.0	5.0	538.0	550.0	12.0
448	544.5	82.10	446.0	449.0	3.0	533.0	556.0	23.0
451	545	100.73	449.0	457.0	8.0	533.0	554.0	21.0
465	544	44.83	463.0	467.0	4.0	543.0	546.0	3.0
472	545.5	50.17	470.0	473.0	3.0	540.0	550.0	10.0
483	546.5	160.92	476.0	492.0	16.0	532.0	561.0	29.0
507	546	24.15	503.0	509.0	6.0	543.0	548.0	5.0
323	579	76.34	316.0	330.0	14.0	572.0	582.0	10.0
349	577.5	624.35	338.0	358.0	20.0	562.0	602.0	40.0
362	578.5	394.31	359.0	369.0	10.0	560.0	600.0	40.0
386	577	662.71	370.0	407.0	37.0	558.0	600.0	42.0
424	576.5	135.60	417.0	432.0	15.0	564.0	598.0	34.0
447	577	188.04	440.0	448.0	8.0	560.0	598.0	38.0
452	576.5	272.58	449.0	457.0	8.0	560.0	598.0	38.0
463	585	179.27	459.0	468.0	9.0	583.0	586.0	3.0
470	585.5	69.99	469.0	472.0	3.0	581.0	592.0	11.0
478	575.5	58.59	476.0	479.0	3.0	568.0	583.0	15.0
319	614	84.30	315.0	322.0	7.0	608.0	627.0	19.0
350	616	242.76	343.0	353.0	10.0	604.0	636.0	32.0
361	615	435.67	358.0	367.0	9.0	602.0	634.0	32.0
380	616	760.89	371.0	387.0	16.0	602.0	636.0	34.0
392	616	999.00	388.0	401.0	13.0	602.0	638.0	36.0
413	615.5	160.44	408.0	419.0	11.0	604.0	631.0	27.0
450	614	74.85	448.0	455.0	7.0	608.0	627.0	19.0
463	613.5	730.25	457.0	470.0	13.0	600.0	634.0	34.0
485	614	81.36	480.0	490.0	10.0	606.0	631.0	25.0
532	616	152.36	527.0	538.0	11.0	606.0	632.0	26.0
527	617	108.85	523.0	528.0	5.0	606.0	629.0	23.0
326	656.5	134.88	321.0	335.0	14.0	646.0	671.0	25.0
350	658.5	34.16	344.0	355.0	11.0	652.0	661.5	9.5
361	657.5	32.53	358.0	365.0	7.0	648.0	667.0	19.0
379	656	53.45	374.0	382.0	8.0	642.0	669.0	27.0
392	654	94.01	387.0	404.0	17.0	642.0	665.0	23.0
464	656	41.16	458.0	468.0	10.0	642.0	665.0	23.0
379	701	86.08	373.0	386.0	13.0	686.0	716.5	30.5
392	701.5	227.75	387.0	400.0	13.0	684.0	716.5	32.5
465	701	62.00	460.0	469.0	9.0	692.0	713.0	21.0
362	701.5	53.23	359.0	365.0	6.0	695.0	709.0	14.0
530	700.5	20.18	523.0	539.0	16.0	693.0	713.0	20.0

**Table 20 Multiple ion doped sample Glass1-20 – 2.0 mol % Eu, 2.5 mol % Tb and 1.5 mol % Dy**

Development and Application of Novel Tracers for Environmental Applications  
Appendix II: Spectroscopic Characterisation Data

Excitation Wavelength / nm	Emission Wavelength / nm	Intensity	Peak width					
			Ex Wavelength			Em Wavelength		
			From	To	PW	From	To	PW
348	482.5	334.15	338.0	357.0	19.0	461.0	499.0	38.0
322	482.5	51.15	313.0	330.0	17.0	467.0	505.0	38.0
363	481	266.59	357.0	371.0	14.0	463.0	505.0	42.0
387	480.5	376.14	371.0	409.0	38.0	455.0	507.0	52.0
424	481.5	78.61	416.0	431.0	15.0	467.0	501.0	34.0
450	481	165.37	438.0	460.0	22.0	467.0	503.0	36.0
324	546.5	14.84	311.0	332.0	21.0	533.0	556.0	23.0
349	545	75.24	332.0	355.0	23.0	533.0	556.0	23.0
363	545	70.58	357.0	370.0	13.0	531.0	556.0	25.0
378	545	85.11	371.0	382.0	11.0	529.0	558.0	29.0
387	545	73.83	384.0	390.0	6.0	533.0	554.0	21.0
425	544	21.03	419.0	430.0	11.0	543.0	550.0	7.0
450	544	31.80	438.0	458.0	20.0	533.0	552.0	19.0
465	544.5	30.89	458.0	471.0	13.0	520.0	550.0	30.0
482	547	34.18	476.0	496.0	20.0	535.0	562.0	27.0
322	575.5	67.88	316.0	332.0	16.0	558.0	604.0	46.0
349	575	631.35	335.0	359.0	24.0	556.0	604.0	48.0
363	576.5	458.02	359.0	370.0	11.0	556.0	602.0	46.0
387	576	755.33	371.0	409.0	38.0	556.0	602.0	46.0
424	575.5	158.18	416.0	433.0	17.0	554.5	602.0	47.5
452	577	356.86	436.0	460.0	24.0	556.0	602.0	46.0
463	587.5	181.72	460.0	473.0	13.0	568.0	602.0	34.0
471	577.5	105.50	468.0	499.0	31.0	562.0	600.0	38.0
530	581.5	29.14	522.0	539.0	17.0	570.0	600.0	30.0
321	615	41.03	313.0	327.0	14.0	600.0	636.0	36.0
349	615.5	85.43	341.0	355.0	14.0	606.0	634.0	28.0
363	617	198.02	355.0	370.0	15.0	602.0	640.0	38.0
381	616	525.21	368.0	387.0	19.0	602.0	640.0	38.0
392	615	999.00	387.0	406.0	19.0	602.0	642.0	40.0
412	614	134.26	408.0	420.0	12.0	602.0	636.0	34.0
450	614	48.14	446.0	455.0	9.0	608.0	634.0	26.0
463	615.5	657.01	457.0	476.0	19.0	600.0	642.0	42.0
531	615	150.16	520.0	544.0	24.0	600.0	632.0	32.0
577	615	28.55	572.0	580.0	8.0	602.0	638.5	36.5
348	663.5	29.52	338.0	357.0	19.0	646.0	686.0	40.0
363	662	21.85	355.0	370.0	15.0	644.0	684.0	40.0
382	651	37.30	370.0	387.0	17.0	644.0	678.0	34.0
392	655	76.42	387.0	405.0	18.0	642.0	676.0	34.0
452	656.5	19.51	444.0	458.0	14.0	646.0	684.0	38.0
463	653	41.04	457.0	469.0	12.0	642.0	672.0	30.0
362	700.5	32.08	357.0	365.0	8.0	684.0	716.0	32.0
379	701	61.47	370.0	389.0	19.0	682.0	722.0	40.0
393	699.5	166.42	387.0	405.0	18.0	680.0	720.0	40.0
463	700.5	65.94	457.0	469.0	12.0	676.0	714.0	38.0
531	700.5	17.44	522.0	542.0	20.0	680.0	724.0	44.0

**Table 21 Multiple ion doped sample Glass1-21 – 2.5 mol % Eu, 0.5 mol % Tb and 2.5 mol % Dy**

Development and Application of Novel Tracers for Environmental Applications  
 Appendix II: Spectroscopic Characterisation Data

Excitation Wavelength / nm	Emission Wavelength / nm	Intensity	Peak width					
			Ex Wavelength			Em Wavelength		
			From	To	PW	From	To	PW
323	481.5	42.98	315.0	330.0	15.0	467.5	500.5	33.0
349	481.5	250.67	335.0	357.0	22.0	459.5	506.5	47.0
363	481.5	174.86	357.0	372.0	15.0	460.5	505.0	44.5
387	481.5	206.24	372.0	407.0	35.0	460.5	505.0	44.5
423	481.5	48.68	418.0	435.0	17.0	466.5	498.5	32.0
452	481.5	108.53	439.0	458.0	19.0	474.5	503.5	29.0
317	548	16.34	311.0	323.0	12.0	536.0	558.0	22.0
349	548	117.50	332.0	356.0	24.0	533.0	556.5	23.5
365	548	111.77	356.0	369.0	13.0	556.5	557.5	1.0
377	548	112.38	371.0	384.0	13.0	530.0	559.5	29.5
392	548	69.41	388.0	399.0	11.0	523.0	544.5	21.5
453	548	28.72	444.0	457.0	13.0	536.0	552.5	16.5
464	548	27.83	460.0	469.0	9.0	545.5	555.5	10.0
483	548	63.90	477.0	495.0	18.0	531.0	563.0	32.0
323	574.5	56.25	312.0	329.0	17.0	562.0	599.5	37.5
348	575	434.79	337.0	357.0	20.0	557.5	601.5	44.0
363	576.5	266.56	357.0	371.0	14.0	559.5	601.5	42.0
385	579.5	42.90	370.0	388.0	18.0	529.0	556.5	27.5
393	588.5	758.64	388.0	407.0	19.0	519.0	549.5	30.5
414	588.5	69.36	408.0	418.0	10.0	572.0	600.5	28.5
452	588.5	78.53	438.0	457.0	19.0	555.5	599.5	44.0
464	591	275.56	457.0	475.0	18.0	566.0	600.5	34.5
485	591	25.96	475.0	495.0	20.0	575.0	600.5	25.5
532	591	56.78	520.0	543.0	23.0	572.0	601.5	29.5
319	614	132.14	312.0	332.0	20.0	603.0	635.5	32.5
350	614	127.75	341.0	355.0	14.0	602.0	635.5	33.5
361	614	533.64	355.0	368.0	13.0	600.5	640.5	40.0
380	614	969.94	368.0	388.0	20.0	600.5	640.5	40.0
393	614	999.99	388.0	407.0	19.0	600.5	641.5	41.0
413	614	218.45	407.0	423.0	16.0	600.5	635.5	35.0
464	614	1004.39	455.0	476.0	21.0	600.5	640.5	40.0
484	614	50.69	480.0	494.0	14.0	603.0	634.5	31.5
531	614	221.31	519.0	545.0	26.0	600.5	637.5	37.0
577	614	43.90	572.0	581.0	9.0	604.0	632.5	28.5
350	653	15.45	336.0	356.0	20.0	649.0	656.0	7.0
362	653	34.04	356.0	368.0	12.0	640.5	664.0	23.5
381	653	56.84	369.0	387.0	18.0	641.5	665.5	24.0
393	653	136.93	388.0	404.0	16.0	642.5	672.5	30.0
464	653	59.58	458.0	468.0	10.0	643.5	668.5	25.0
319	700	15.13	313.0	331.0	18.0	679.5	711.5	32.0
349	700	15.58	340.0	357.0	17.0	685.5	714.5	29.0
361	700	63.10	357.0	368.0	11.0	685.5	715.5	30.0
382	700	121.17	368.0	387.0	19.0	679.5	717.5	38.0
393	700	334.54	387.0	407.0	20.0	675.5	719.5	44.0
413	700	29.17	408.0	418.0	10.0	681.5	715.5	34.0
464	700	107.53	457.0	474.0	17.0	674.5	719.5	45.0
531	700	25.50	521.0	546.0	25.0	678.5	716.5	38.0

**Table 22 Multiple ion doped sample Glass1-22 – 2.5 mol % Eu, 1.0 mol % Tb and 0.5 mol % Dy**

Excitation Wavelength / nm	Emission Wavelength / nm	Intensity	Peak width					
			Ex Wavelength			Em Wavelength		
			From	To	PW	From	To	PW
323	482	41.63	314.0	328.0	14.0	463.5	504.5	41.0
349	482	295.16	336.0	357.0	21.0	459.5	511.5	52.0
363	482	221.10	357.0	371.0	14.0	460.5	502.5	42.0
386	482	269.64	371.0	410.0	39.0	458.5	505.5	47.0
424	482	68.35	414.0	430.0	16.0	463.5	499.5	36.0
452	482	157.65	439.0	457.0	18.0	475.5	508.5	33.0
350	545	177.83	335.0	357.0	22.0	529.0	556.5	27.5
365	545	173.37	358.0	371.0	13.0	527.0	558.5	31.5
377	545	211.61	371.0	377.0	6.0	529.0	559.5	30.5
453	545	54.78	440.0	457.0	17.0	534.0	559.5	25.5
484	545	97.65	457.0	496.0	39.0	534.0	560.5	26.5
323	575	45.57	315.0	328.0	13.0	557.5	600.5	43.0
349	575	485.88	338.0	357.0	19.0	559.5	600.5	41.0
363	575	321.85	357.0	371.0	14.0	559.5	600.5	41.0
386	575	538.68	371.0	410.0	39.0	556.5	601.5	45.0
392	589.5	673.70	388.0	407.0	19.0	559.5	599.5	40.0
413	593	66.41	409.0	418.0	9.0	568.0	595.5	27.5
423	577.5	111.36	417.0	434.0	17.0	558.5	601.5	43.0
452	577	221.04	437.0	458.0	21.0	555.5	601.5	46.0
464	590.5	266.98	458.0	470.0	12.0	563.0	600.5	37.5
319	616.5	67.23	311.0	323.0	12.0	601.5	638.5	37.0
349	615.5	162.71	341.0	355.0	14.0	600.5	638.5	38.0
361	615.5	470.68	355.0	367.0	12.0	600.5	639.5	39.0
380	615.5	571.14	367.0	387.0	20.0	601.5	641.5	40.0
393	615.5	999.99	387.0	407.0	20.0	601.5	641.5	40.0
413	615.5	206.82	407.0	422.0	15.0	602.0	636.5	34.5
452	615.5	66.29	440.0	455.0	15.0	603.0	633.5	30.5
464	616	985.65	455.0	477.0	22.0	600.5	639.5	39.0
483	616	72.98	477.0	495.0	18.0	603.0	639.5	36.5
532	616	199.15	520.0	545.0	25.0	601.5	639.5	38.0
578	616	46.22	572.0	582.0	10.0	600.5	639.5	39.0
318	652.5	5.72	313.0	327.0	14.0	644.0	659.0	15.0
350	652.5	20.98	338.0	356.0	18.0	640.5	682.5	42.0
361	652.5	29.98	356.0	370.0	14.0	640.5	675.0	34.5
381	652.5	53.87	370.0	375.0	5.0	641.5	670.5	29.0
393	652.5	108.69	387.0	409.0	22.0	693.5	670.5	-23.0
464	652.5	56.69	457.0	470.0	13.0	641.5	668.5	27.0
530	652.5	14.89	521.0	541.0	20.0	645.0	664.0	19.0
320	700.5	7.60	313.0	332.0	19.0	686.0	709.5	23.5
352	700.5	19.25	340.0	355.0	15.0	682.5	712.5	30.0
362	700.5	50.58	357.0	366.0	9.0	681.5	714.5	33.0
381	700.5	107.46	370.0	387.0	17.0	679.5	717.5	38.0
393	700.5	276.51	387.0	407.0	20.0	675.5	719.5	44.0
412	700.5	22.80	409.0	422.0	13.0	675.5	717.5	42.0
463	700.5	95.59	456.0	470.0	14.0	672.5	725.5	53.0
484	700.5	11.27	478.0	491.0	13.0	687.0	711.5	24.5
532	700.5	24.08	521.0	548.0	27.0	675.5	729.0	53.5

**Table 23 Multiple ion doped sample Glass1-23 – 2.5 mol % Eu, 1.5 mol % Tb and 1.0 mol % Dy**

Development and Application of Novel Tracers for Environmental Applications  
 Appendix II: Spectroscopic Characterisation Data

Excitation Wavelength / nm	Emission Wavelength / nm	Intensity	Peak width					
			Ex Wavelength			Em Wavelength		
			From	To	PW	From	To	PW
322	480.5	50.74	311.0	329.0	18.0	478.0	501.0	23.0
349	482.5	351.18	332.0	357.0	25.0	459.0	510.0	51.0
363	482.5	262.00	359.0	371.0	12.0	461.0	506.0	45.0
386	484.5	344.41	371.0	412.0	41.0	463.0	506.0	43.0
424	486.5	78.90	414.0	435.0	21.0	466.0	506.0	40.0
452	485.5	180.31	436.0	460.0	24.0	472.0	505.0	33.0
322	546	32.65	311.0	330.0	19.0	535.0	560.0	25.0
350	545	258.40	330.0	359.0	29.0	535.0	558.0	23.0
364	545	258.26	359.0	372.0	13.0	535.0	560.0	25.0
376	545.5	302.04	370.0	382.0	12.0	531.0	560.0	29.0
386	545.5	200.24	383.0	390.0	7.0	531.0	558.0	27.0
424	545.5	44.01	418.0	436.0	18.0	535.5	554.5	19.0
452	546	92.34	439.0	460.0	21.0	531.5	556.5	25.0
463	546	43.08	461.0	467.0	6.0	541.0	550.5	9.5
484	545	122.47	473.0	496.0	23.0	531.5	562.0	30.5
323	579	63.49	316.0	329.0	13.0	562.0	600.5	38.5
349	576	591.85	336.0	358.0	22.0	560.0	600.0	40.0
363	578	385.63	358.0	370.0	12.0	562.0	600.0	38.0
385	578.5	653.52	371.0	387.0	16.0	560.0	598.0	38.0
389	579	638.88	387.0	406.0	19.0	560.0	600.0	40.0
424	576.5	138.30	415.0	435.0	20.0	562.0	594.5	32.5
451	576.5	280.48	448.0	459.0	11.0	560.0	600.0	40.0
463	591.5	250.36	458.0	475.0	17.0	571.0	600.0	29.0
484	587.5	51.56	479.0	492.0	13.0	573.0	602.0	29.0
531	588.5	56.88	528.0	539.0	11.0	577.0	598.0	21.0
464	392.5	165.34	458.0	471.0	13.0	575.0	600.0	25.0
319	616.5	91.29	312.0	323.0	11.0	608.0	632.0	24.0
349	617	227.41	339.0	355.0	16.0	606.0	636.0	30.0
362	617	482.64	357.0	368.0	11.0	604.0	634.0	30.0
379	616	397.74	369.0	387.0	18.0	602.0	636.0	34.0
393	615	1000.00	387.0	407.0	20.0	602.0	640.5	38.5
413	615	208.19	408.0	421.0	13.0	606.0	631.0	25.0
452	616	90.97	450.0	455.0	5.0	610.0	625.0	15.0
464	615.5	993.34	457.0	472.0	15.0	602.0	636.0	34.0
484	615.5	92.12	478.0	492.0	14.0	606.0	629.0	23.0
532	614.5	209.62	528.0	546.0	18.0	606.0	629.0	23.0
527	616	160.62	521.0	528.0	7.0	604.0	632.0	28.0
577	613.5	47.08	571.0	582.0	11.0	610.0	621.0	11.0
348	655.5	27.89	343.0	354.0	11.0	646.0	663.0	17.0
362	656.5	32.34	357.0	368.0	11.0	642.0	669.0	27.0
382	656.5	57.66	373.0	387.0	14.0	646.0	669.0	23.0
392	653	119.93	387.0	406.0	19.0	644.0	667.0	23.0
464	652.5	58.81	459.0	468.0	9.0	646.0	657.0	11.0
350	700	25.05	340.0	355.0	15.0	693.0	713.0	20.0
362	700	57.78	357.0	367.0	10.0	686.0	713.0	27.0
379	700	112.42	370.0	387.0	17.0	684.0	716.0	32.0
393	701	277.56	387.0	406.0	19.0	680.0	718.0	38.0
413	699.5	27.09	408.0	420.0	12.0	688.0	713.0	25.0
464	702.5	100.13	458.0	468.0	10.0	684.0	716.5	32.5
531	703.5	24.75	523.0	543.0	20.0	690.0	714.0	24.0

**Table 24 Multiple ion doped sample Glass1-24 – 2.5 mol % Eu, 2.0 mol % Tb and 2.0 mol % Dy**



Excitation Wavelength / nm	Emission Wavelength / nm	Intensity	Peak width					
			Ex Wavelength			Em Wavelength		
			From	To	PW	From	To	PW
322	484	43.33	318.0	327.0	9.0	468.0	497.5	29.5
348	484.5	316.86	334.0	358.0	24.0	461.0	509.0	48.0
363	484	249.26	356.0	371.0	15.0	467.0	505.0	38.0
379	485	212.58	371.0	380.0	9.0	468.5	505.0	36.5
386	486	312.73	381.0	394.0	13.0	463.0	505.0	42.0
423	484.5	69.20	415.0	435.0	20.0	474.5	495.5	21.0
448	484.5	115.57	441.0	449.0	8.0	472.5	501.0	28.5
452	484	170.88	449.0	460.0	11.0	472.5	501.0	28.5
322	548	28.75	312.0	330.0	18.0	539.0	552.0	13.0
350	546	288.67	338.0	358.0	20.0	531.0	560.0	29.0
365	545	287.09	360.0	369.0	9.0	531.0	560.0	29.0
377	546	339.61	371.0	381.0	10.0	531.0	562.0	31.0
385	546	251.81	382.0	405.0	23.0	531.0	558.0	27.0
423	545.5	47.28	417.0	435.0	18.0	539.0	552.0	13.0
451	545	95.65	439.0	461.0	22.0	533.0	556.0	23.0
464	547	41.16	463.0	465.0	2.0	541.0	549.0	8.0
483	546	131.27	475.0	494.0	19.0	535.0	560.0	25.0
324	575.5	51.91	318.0	328.0	10.0	568.0	589.0	21.0
348	576.5	522.45	338.0	357.0	19.0	560.5	598.5	38.0
362	578	365.72	358.0	369.0	11.0	562.0	600.0	38.0
386	577.5	640.96	370.0	408.0	38.0	558.0	602.0	44.0
424	579	123.04	418.0	433.0	15.0	562.0	600.0	38.0
448	579	181.60	439.0	448.0	9.0	560.0	600.0	40.0
452	577.5	273.60	449.0	458.0	9.0	562.0	598.5	36.5
464	593.5	226.30	459.0	469.0	10.0	573.0	600.0	27.0
484	593	43.72	478.0	492.0	14.0	489.0	596.0	107.0
530	593	46.64	527.0	532.0	5.0	591.0	596.0	5.0
320	613	60.83	312.0	320.0	8.0	606.0	627.0	21.0
350	616.5	240.47	342.0	354.0	12.0	606.0	632.0	26.0
362	616.5	439.43	356.0	367.0	11.0	602.0	638.0	36.0
379	616	805.50	367.0	387.0	20.0	602.0	638.0	36.0
391	616	1000.00	387.0	405.0	18.0	602.0	638.0	36.0
413	617	174.19	407.0	417.0	10.0	602.0	634.0	32.0
425	617.5	48.96	419.0	425.0	6.0	608.0	631.0	23.0
451	617	88.26	449.0	457.0	8.0	604.0	634.0	30.0
465	615.5	714.95	457.0	473.0	16.0	600.0	638.0	38.0
485	617	83.94	481.0	490.0	9.0	606.0	634.0	28.0
530	616.5	162.78	522.0	542.0	20.0	602.0	634.0	32.0
578	618.5	33.77	574.0	582.0	8.0	606.0	624.0	18.0
350	658	26.19	342.0	356.0	14.0	646.0	676.0	30.0
363	658.5	27.59	358.0	367.0	9.0	644.0	674.0	30.0
381	657	47.29	375.0	385.0	10.0	644.0	669.0	25.0
393	651.5	97.25	387.0	403.0	16.0	648.0	668.0	20.0
463	653	51.92	459.0	469.0	10.0	644.0	667.0	23.0
526	655	13.76	522.0	532.0	10.0	648.0	665.0	17.0
350	689	12.47	342.0	352.0	10.0	687.0	690.0	3.0
362	700	52.14	356.0	367.0	11.0	695.0	702.0	7.0
379	700	93.95	371.0	387.0	16.0	696.0	701.0	5.0
393	702.5	236.36	387.0	405.0	18.0	682.5	716.5	34.0
413	704	21.30	409.0	411.0	2.0	696.0	702.0	6.0
465	704	68.34	459.0	471.0	12.0	702.0	715.0	13.0
485	702.5	12.42	479.0	487.0	8.0	699.0	704.0	5.0
530	702.5	21.98	524.0	538.0	14.0	695.0	705.0	10.0

**Table 25 Multiple ion doped sample Glass1-25 – 2.5 mol % Eu, 2.5 mol % Tb and 1.5 mol % Dy**

Development and Application of Novel Tracers for Environmental Applications  
 Appendix II: Spectroscopic Characterisation Data

Excitation Wavelength / nm	Emission Wavelength / nm	Intensity	Peak width					
			Ex Wavelength			Em Wavelength		
			From	To	PW	From	To	PW
323	483.5	126.61	309.0	331.0	22.0	466.5	504.5	38.0
348	483.5	710.90	334.0	357.0	23.0	455.0	509.5	54.5
363	483.5	393.47	357.0	371.0	14.0	458.5	505.5	47.0
385	483.5	479.30	371.0	411.0	40.0	457.5	505.5	48.0
424	483.5	78.01	417.0	431.0	14.0	457.5	500.5	43.0
452	483.5	181.90	437.0	459.0	22.0	470.5	504.5	34.0
327	546.5	29.79	312.0	328.0	16.0	538.0	557.5	19.5
349	546.5	175.60	338.0	357.0	19.0	530.0	553.5	23.5
364	546.5	130.35	359.0	371.0	12.0	529.0	556.5	27.5
385	546.5	160.87	371.0	382.0	11.0	531.0	558.5	27.5
452	546.5	32.11	440.0	457.0	17.0	533.0	555.5	22.5
484	546.5	64.02	476.0	495.0	19.0	533.0	561.0	28.0
323	576.5	168.98	313.0	329.0	16.0	557.5	601.5	44.0
348	576.5	999.99	339.0	357.0	18.0	553.5	607.0	53.5
363	576.5	642.78	357.0	371.0	14.0	555.5	604.0	48.5
385	576.5	882.41	371.0	411.0	40.0	555.5	604.0	48.5
424	576.5	137.59	414.0	436.0	22.0	545.5	605.0	59.5
452	576.5	323.64	436.0	461.0	25.0	556.5	605.0	48.5
471	576.5	95.65	461.0	490.0	29.0	556.5	597.5	41.0
322	664.5	7.73	318.0	334.0	16.0	641.5	681.5	40.0
348	664.5	52.37	335.0	358.0	23.0	639.5	704.0	64.5
363	664.5	27.58	358.0	370.0	12.0	637.5	696.0	58.5
388	664.5	38.47	370.0	410.0	40.0	637.5	689.0	51.5
423	664.5	9.61	415.0	431.0	16.0	643.5	685.5	42.0
450	664.5	17.05	440.0	458.0	18.0	640.5	691.0	50.5

**Table 26 Multiple ion doped sample Glass 2-2 – 0.0 mol % Eu, 0.5 mol % Tb and 0.5 mol % Dy**

Development and Application of Novel Tracers for Environmental Applications  
 Appendix II: Spectroscopic Characterisation Data

			Peak width					
Excitation Wavelength / nm	Emission Wavelength / nm	Intensity	Ex Wavelength			Em Wavelength		
			From	To	PW	From	To	PW
324	482	145.81	313.0	330.0	17.0	457.5	509.5	52.0
347	482	950.52	339.0	357.0	18.0	457.5	547.0	89.5
363	482	635.76	357.0	371.0	14.0	457.5	512.5	55.0
386	482	738.95	371.0	411.0	40.0	455.0	506.5	51.5
423	482	115.10	417.0	466.0	49.0	459.5	502.5	43.0
452	482	296.33	439.0	460.0	21.0	468.5	506.5	38.0
323	545	53.87	312.0	328.0	16.0	530.0	558.5	28.5
349	545	437.35	332.0	358.0	26.0	530.0	556.5	26.5
364	545	345.90	358.0	370.0	12.0	528.0	558.5	30.5
377	545	402.92	373.0	382.0	9.0	528.0	555.5	27.5
425	545	35.94	416.0	435.0	19.0	527.0	553.5	26.5
452	545	89.59	439.0	461.0	22.0	531.0	559.5	28.5
483	545	134.25	476.0	496.0	20.0	530.0	599.5	69.5
324	575.5	211.02	310.0	330.0	20.0	555.5	606.0	50.5
347	575.5	999.99	337.0	357.0	20.0	556.5	604.0	47.5
363	575.5	936.56	357.0	371.0	14.0	556.5	605.0	48.5
387	575.5	999.99	371.0	412.0	41.0	554.5	600.5	46.0
423	575.5	212.64	414.0	435.0	21.0	555.5	601.5	46.0
452	575.5	545.95	435.0	461.0	26.0	555.5	599.5	44.0
471	575.5	152.92	461.0	491.0	30.0	557.5	628.5	71.0
323	621.5	6.10	315.0	325.0	10.0	611.0	634.5	23.5
349	621.5	44.87	332.0	357.0	25.0	609.0	641.5	32.5
363	621.5	31.20	357.0	371.0	14.0	608.0	641.5	33.5
377	621.5	32.68	371.0	381.0	10.0	611.0	637.5	26.5
384	621.5	26.18	381.0	407.0	26.0	612.0	629.5	17.5
423	621.5	9.24	417.0	435.0	18.0	614.0	629.5	15.5
452	621.5	17.12	439.0	461.0	22.0	611.0	629.5	18.5
481	621.5	15.36	476.0	498.0	22.0	608.0	634.5	26.5
322	665.5	9.11	317.0	328.0	11.0	648.0	681.5	33.5
349	665.5	71.69	335.0	357.0	22.0	640.5	695.0	54.5
363	665.5	40.13	358.0	371.0	13.0	641.5	692.0	50.5
386	665.5	58.53	371.0	414.0	43.0	640.5	698.0	57.5
423	665.5	10.10	417.0	436.0	19.0	642.5	695.0	52.5
452	665.5	23.73	436.0	458.0	22.0	641.5	691.0	49.5

**Table 27 Multiple ion doped sample Glass 2-3 – 0.0 mol % Eu, 1.0 mol % Tb and 1.0 mol % Dy**

Development and Application of Novel Tracers for Environmental Applications  
 Appendix II: Spectroscopic Characterisation Data

			Peak width					
Excitation Wavelength / nm	Emission Wavelength / nm	Intensity	Ex Wavelength			Em Wavelength		
			From	To	PW	From	To	PW
323	484.5	133.92	311.0	330.0	19.0	463.5	503.5	40.0
349	484.5	790.79	330.0	357.0	27.0	456.5	509.5	53.0
362	484.5	539.15	357.0	371.0	14.0	457.5	506.5	49.0
385	484.5	632.05	371.0	411.0	40.0	435.0	506.5	71.5
424	484.5	107.98	416.0	435.0	19.0	458.5	499.5	41.0
452	484.5	235.38	438.0	458.0	20.0	470.5	505.5	35.0
323	545	82.28	312.0	329.0	17.0	530.0	557.5	27.5
349	545	551.08	331.0	358.0	27.0	529.0	557.5	28.5
364	545	439.11	358.0	371.0	13.0	529.0	558.5	29.5
377	545	504.66	371.0	382.0	11.0	529.0	560.5	31.5
385	545	348.76	382.0	409.0	27.0	529.0	556.5	27.5
424	545	61.60	417.0	431.0	14.0	527.0	554.5	25.5
452	545	129.73	439.0	459.0	20.0	532.0	556.5	29.5
471	545	53.54	463.0	476.0	13.0	528.0	554.5	22.5
483	545	144.67	476.0	495.0	19.0	530.0	560.5	32.5
323	576.5	199.76	313.0	328.0	15.0	558.5	602.0	72.0
349	576.5	999.99	329.0	357.0	28.0	557.5	607.0	48.5
363	576.5	765.60	357.0	371.0	14.0	558.5	604.0	46.5
387	576.5	999.99	371.0	411.0	40.0	556.5	606.0	47.5
423	576.5	186.23	414.0	434.0	20.0	557.5	601.5	45.0
452	576.5	434.47	434.0	461.0	27.0	556.5	601.5	44.0
472	576.5	124.04	461.0	492.0	31.0	557.5	596.5	40.0
323	620.5	7.80	311.0	330.0	19.0	608.0	642.5	85.0
349	620.5	49.10	330.0	355.0	25.0	610.0	642.5	34.5
363	620.5	37.72	357.0	371.0	14.0	607.0	642.5	32.5
377	620.5	45.45	371.0	381.0	10.0	608.0	639.5	32.5
386	620.5	36.04	381.0	405.0	24.0	610.0	636.5	28.5
423	620.5	19.93	414.0	429.0	15.0	610.0	637.5	27.5
451	620.5	26.70	435.0	455.0	20.0	609.0	636.5	26.5
482	620.5	19.84	478.0	500.0	22.0	604.0	635.5	26.5
322	664	7.05	315.0	328.0	13.0	641.5	685.5	81.5
348	664	57.94	338.0	357.0	19.0	639.5	696.0	54.5
362	664	33.91	357.0	370.0	13.0	637.5	694.0	54.5
386	664	52.07	370.0	406.0	36.0	637.5	694.0	56.5
424	664	11.42	417.0	433.0	16.0	653.0	684.5	47.0
451	664	20.08	439.0	459.0	20.0	645.0	690.0	37.0

**Table 28 Multiple ion doped sample Glass 2-4 – 0.0 mol % Eu, 1.5 mol % Tb and 1.5 mol % Dy**

Development and Application of Novel Tracers for Environmental Applications  
 Appendix II: Spectroscopic Characterisation Data

Excitation Wavelength / nm	Emission Wavelength / nm	Intensity	Peak width					
			Ex Wavelength			Em Wavelength		
			From	To	PW	From	To	PW
323	482	128.24	313.0	330.0	17.0	459.4	504.5	45.2
349	482	771.99	330.0	357.0	27.0	453.0	513.5	60.5
363	482	573.65	357.0	371.0	14.0	455.0	510.5	55.5
386	482	718.36	371.0	412.0	41.0	455.0	508.5	53.5
424	482	118.23	412.0	435.0	23.0	459.5	503.5	44.0
452	482	287.60	435.0	460.0	25.0	471.5	507.5	36.0
323	545.5	42.93	310.0	329.0	19.0	530.0	558.5	28.5
349	545.5	730.85	330.0	357.0	27.0	528.0	558.5	30.5
364	545.5	626.11	357.0	370.0	13.0	528.0	559.5	31.5
377	545.5	714.57	371.0	382.0	11.0	526.0	561.0	35.0
384	545.5	545.37	382.0	411.0	29.0	529.0	557.5	28.5
423	545.5	85.65	416.0	433.0	17.0	529.0	555.5	26.5
452	545.5	203.56	438.0	461.0	23.0	528.0	557.5	29.5
472	545.5	78.22	461.0	475.0	14.0	530.0	557.5	27.5
483	545.5	208.09	475.0	499.0	24.0	529.0	562.0	33.0
323	576.5	176.96	312.0	331.0	19.0	558.5	603.0	44.5
349	576.5	999.99	331.0	357.0	26.0	558.5	604.0	45.5
363	576.5	819.65	357.0	371.0	14.0	559.5	606.0	46.5
387	576.5	999.99	371.0	411.0	40.0	557.5	605.0	47.5
424	576.5	210.56	414.0	437.0	23.0	558.5	598.5	40.0
452	576.5	493.91	437.0	462.0	25.0	558.5	607.0	48.5
470	576.5	140.88	462.0	492.0	30.0	559.5	594.5	35.0
323	622.5	7.22	312.0	329.0	45.0	605.0	632.0	27.0
349	622.5	66.45	331.0	357.0	60.0	609.0	639.5	30.5
364	622.5	54.94	357.0	391.0	24.0	607.0	636.5	29.5
377	622.5	59.97	371.0	381.0	42.0	609.0	637.5	28.5
386	622.5	47.93	381.0	413.0	53.0	609.0	637.5	28.5
424	622.5	15.38	413.0	434.0	46.0	609.0	637.5	28.5
452	622.5	29.77	439.0	459.0	32.0	608.0	636.5	28.5
469	622.5	21.39	466.0	471.0	37.0	60.0	648.0	43.0
484	622.5	27.55	475.0	503.0	28.0	605.0	644.0	39.0
324	662	6.47	317.0	330.0	40.0	646.0	676.5	34.0
348	662	58.95	337.0	357.0	34.0	642.5	697.0	54.5
363	662	37.60	357.0	371.0	55.0	642.5	696.0	53.5
387	662	52.38	371.0	412.0	66.0	642.5	687.0	43.5
423	662	11.19	415.0	437.0	44.0	643.5	693.0	50.5
452	662	23.80	438.0	459.0	37.0	642.5	687.0	41.0
470	662	12.56	462.0	475.0	13.0	646.0	691.0	45.0

**Table 29 Multiple ion doped sample Glass 2-5 – 0.0 mol % Eu, 2.0 mol % Tb and 2.0 mol % Dy**

Development and Application of Novel Tracers for Environmental Applications  
 Appendix II: Spectroscopic Characterisation Data

Excitation Wavelength / nm	Emission Wavelength / nm	Intensity	Peak width					
			Ex Wavelength			Em Wavelength		
			From	To	PW	From	To	PW
323	480.5	203.52	310.0	329.0	19.0	463.5	508.5	45.0
348	480.5	834.22	329.0	357.0	28.0	457.5	507.5	50.0
363	480.5	501.67	357.0	371.0	14.0	461.5	504.5	43.0
386	480.5	551.86	371.0	413.0	42.0	458.5	505.5	47.0
423	480.5	81.36	416.0	435.0	19.0	463.5	499.5	36.0
452	480.5	200.31	437.0	460.0	23.0	470.5	500.5	30.0
393	535.5	72.39		405.0	405.0	532.5	537.5	5.0
464	535.5	21.83	460.0	468.0	8.0	528.0	539.5	11.5
323	573	201.02	311.0	330.0	19.0	554.5	600.5	46.0
348	573	999.99	330.0	357.0	27.0	549.5	606.0	56.5
363	573	672.44	357.0	371.0	14.0	552.5	601.5	49.0
386	573	907.96	371.0	413.0	42.0	551.5	602.0	50.5
423	573	142.44	413.0	435.0	22.0	555.5	601.5	46.0
452	573	340.68	437.0	460.0	23.0	552.5	601.5	49.0
470	573	92.38	463.0	491.0	28.0	557.5	595.5	38.0
318	614.5	47.30	312.0	331.0	19.0	603.0	634.5	31.5
348	614.5	34.29	339.0	354.0	15.0	607.0	632.5	25.5
361	614.5	130.03	354.0	368.0	14.0	602.0	635.5	33.5
380	614.5	250.34	368.0	387.0	19.0	601.5	638.5	37.0
393	614.5	711.72	387.0	406.0	19.0	601.5	639.5	38.0
412	614.5	56.35	406.0	419.0	13.0	601.5	639.5	38.0
464	614.5	295.48	457.0	470.0	13.0	599.5	639.5	40.0
532	614.5	51.80	521.0	544.0	23.0	599.5	635.5	36.0
322	658	10.18	313.0	332.0	19.0	647.0	675.5	28.5
348	658	46.17	332.0	355.0	23.0	642.5	694.0	51.5
362	658	28.71	358.0	370.0	12.0	644.0	682.5	38.5
384	658	38.89	370.0	387.0	17.0	641.5	682.5	41.0
393	658	49.98	387.0	406.0	19.0	643.5	676.5	33.0
424	658	8.31	419.0	433.0	14.0	647.0	685.5	38.5
452	658	14.87	437.0	457.0	20.0	640.5	689.0	48.5
464	658	16.06	457.0	474.0	17.0	641.5	677.5	36.0
319	699.5	6.67	315.0	323.0	8.0	695.0	711.5	16.5
349	699.5	4.73	347.0	353.0	6.0	693.0	711.5	18.5
362	699.5	12.91	354.0	367.0	13.0	686.0	712.5	26.5
381	699.5	30.47	367.0	387.0	20.0	683.5	716.5	33.0
393	699.5	86.64	387.0	406.0	19.0	676.5	719.5	43.0
464	699.5	72.96	455.0	471.0	16.0	677.5	719.5	42.0
530	699.5	6.40	521.0	542.0	21.0	681.5	711.5	30.0

**Table 30 Multiple ion doped sample Glass 2-6 – 0.5 mol % Eu, 0.0 mol % Tb and 0.5 mol % Dy**

Development and Application of Novel Tracers for Environmental Applications  
 Appendix II: Spectroscopic Characterisation Data

Excitation Wavelength / nm	Emission Wavelength / nm	Intensity	Peak width					
			Ex Wavelength			Em Wavelength		
			From	To	PW	From	To	PW
323	482.5	149.67	316.0	328.0	12.0	465.0	501.0	36.0
348	482	823.72	338.0	356.0	18.0	455.5	507.0	51.5
362	481	542.77	358.0	370.0	12.0	459.0	507.0	48.0
386	481	637.22	372.0	409.0	37.0	457.5	507.0	49.5
423	481	105.77	417.0	433.0	16.0	461.0	503.0	42.0
452	480	238.30	440.0	457.0	17.0	470.5	507.0	36.5
321	548	30.53	312.0	329.0	17.0	541.0	554.5	13.5
350	545.5	186.12	331.0	357.0	26.0	528.0	554.5	26.5
364	545.5	155.20	358.0	370.0	12.0	531.5	554.5	23.0
377	544.5	167.73	372.0	382.0	10.0	531.5	556.5	25.0
385	545	123.94	383.0	387.0	4.0	529.5	552.5	23.0
358	544.5	120.82	357.0	360.0	3.0	529.5	554.5	25.0
371	545	130.77	370.0	372.0	2.0	531.5	558.5	27.0
388	545	116.19	387.0	390.0	3.0	531.5	552.5	21.0
393	545	98.84	391.0	397.0	6.0	526.0	554.5	28.5
422	546	22.61	418.0	434.0	16.0	531.5	552.5	21.0
446	545.5	31.25	437.0	448.0	11.0	531.5	552.5	21.0
452	545	38.85	448.0	458.0	10.0	531.5	552.5	21.0
464	545.5	21.10	461.0	469.0	8.0	522.0	549.0	27.0
482	546	50.77	474.0	493.0	19.0	529.5	560.5	31.0
470	546.5	20.91	469.0	472.0	3.0	531.5	552.5	21.0
323	576	182.48	314.0	330.0	16.0	556.5	602.0	45.5
349**	576	1000.00	338.0	357.0	19.0	554.5	604.0	49.5
363	576.5	811.91	357.0	371.0	14.0	556.5	602.0	45.5
387**	576	1000.00	371.0	407.0	36.0	552.5	602.0	49.5
424	577	188.39	417.0	432.0	15.0	556.5	602.0	45.5
452	578.5	425.21	437.0	459.0	22.0	554.5	604.0	49.5
471	576.5	123.15	461.0	489.0	28.0	556.5	596.5	40.0
464	587.5	93.27	460.0	468.0	8.0	558.5	598.5	40.0
532	589.5	15.11	519.0	539.0	20.0	570.0	598.5	28.5
318	613.5	28.55	313.0	330.0	17.0	604.0	627.0	23.0
349	613	51.50	339.0	355.0	16.0	608.0	636.5	28.5
361	615.5	121.21	356.0	367.0	11.0	604.0	636.5	32.5
381	614	200.65	368.0	387.0	19.0	604.0	638.5	34.5
393	614	557.11	387.0	405.0	18.0	602.0	638.5	36.5
413	614.5	48.71	407.0	418.0	11.0	602.0	636.5	34.5
444	613.5	21.97	439.0	448.0	9.0	608.0	634.5	26.5
452	614	22.70	448.0	455.0	7.0	606.0	636.5	30.5
464	615	222.99	457.0	470.0	13.0	600.5	640.5	40.0
531	613.5	42.02	517.0	544.0	27.0	600.5	634.5	34.0
577	614	11.42	570.0	581.0	11.0	604.0	634.5	30.5
348	664.5	61.43	339.0	357.0	18.0	644.0	682.5	38.5
362	664	39.63	357.0	370.0	13.0	642.0	684.0	42.0
387	662	53.56	373.0	405.0	32.0	644.0	684.0	40.0
424	660.5	11.06	417.0	430.0	13.0	650.0	686.0	36.0
451	660.5	19.66	437.0	458.0	21.0	646.0	692.0	46.0
462	660.5	12.99	458.0	468.0	10.0	650.0	665.0	15.0
470	659.5	13.06	468.0	477.0	9.0	653.5	672.5	19.0
361	696.5	13.92	357.0	367.0	10.0	690.0	703.5	13.5
377	696.5	21.56	368.0	386.0	18.0	688.0	716.5	28.5
393	698	66.81	388.0	405.0	17.0	682.5	716.5	34.0
414	697	8.66	411.0	417.0	6.0	690.0	711.0	21.0
464	699	18.30	456.0	470.0	14.0	678.5	716.5	38.0
526	699	7.06	519.0	537.0	18.0	688.0	713.0	25.0

**Table 31 Multiple ion doped sample Glass 2-7 – 0.5 mol % Eu, 0.5 mol % Tb and 1.0 mol % Dy**

Development and Application of Novel Tracers for Environmental Applications  
 Appendix II: Spectroscopic Characterisation Data

			Peak width					
Excitation Wavelength / nm	Emission Wavelength / nm	Intensity	Ex Wavelength			Em Wavelength		
			From	To	PW	From	To	PW
323	482	104.08	312.0	329.0	17.0	461.5	503.5	42.0
348	482	678.92	332.0	357.0	25.0	456.0	506.5	50.5
363	482	474.89	357.0	371.0	14.0	456.0	505.5	49.5
386	482	583.50	371.0	412.0	41.0	454.0	505.5	51.5
423	482	105.02	417.0	431.0	14.0	461.5	502.5	41.0
452	482	261.75	436.0	459.0	23.0	470.5	505.5	35.0
323	545.5	36.98	312.0	329.0	17.0	531.0	556.5	25.5
349	545.5	286.01	331.0	358.0	27.0	529.0	556.5	27.5
364	545.5	244.32	358.0	371.0	13.0	529.0	557.5	28.5
377	545.5	285.08	371.0	382.0	11.0	530.0	558.5	28.5
385	545.5	212.03	382.0	407.0	25.0	530.0	554.5	24.5
424	545.5	38.76	418.0	431.0	13.0	532.0	554.5	22.5
452	545.5	82.10	438.0	459.0	21.0	532.0	554.5	22.5
465	545.5	32.60	462.0	467.0	5.0	539.5	549.5	10.0
483	545.5	95.17	476.0	496.0	20.0	530.0	562.0	32.0
323	576.5	132.11	311.0	330.0	19.0	557.5	598.5	41.0
348	576.5	999.99	332.0	357.0	25.0	556.5	602.0	45.5
363	576.5	716.86	357.0	371.0	14.0	556.5	603.0	46.5
386	576.5	1000.50	371.0	410.0	39.0	554.5	603.0	48.5
423	576.5	198.02	414.0	436.0	22.0	556.5	601.5	45.0
452	576.5	431.96	436.0	460.0	24.0	555.5	605.0	49.5
472	576.5	126.10	462.0	490.0	28.0	557.5	597.5	40.0
323	614.5	18.26	314.0	328.0	14.0	601.5	635.5	34.0
350	614.5	56.39	338.0	355.0	17.0	605.0	638.5	33.5
362	614.5	98.69	355.0	367.0	12.0	602.0	639.5	37.5
380	614.5	184.71	367.0	387.0	20.0	601.5	637.5	36.0
393	614.5	487.20	387.0	406.0	19.0	601.5	637.5	36.0
413	614.5	45.79	408.0	421.0	13.0	601.5	632.5	31.0
464	614.5	207.23	456.0	473.0	17.0	601.5	636.5	35.0
533	614.5	37.15	521.0	544.0	23.0	602.0	630.5	28.5
322	662	5.80	321.0	328.0	7.0	653.0	676.5	23.5
347	662	50.93	332.0	357.0	25.0	642.5	688.0	45.5
364	662	30.65	357.0	371.0	14.0	643.5	679.5	36.0
385	662	50.50	371.0	411.0	40.0	643.5	686.0	42.5
424	662	13.43	416.0	430.0	14.0	647.0	659.0	12.0
452	662	22.82	438.0	457.0	19.0	640.5	684.5	44.0
351	700	5.69	342.0	355.0	13.0	697.0	710.5	13.5
362	700	11.24	355.0	367.0	12.0	692.0	710.5	18.5
380	700	21.08	367.0	386.0	19.0	691.0	714.5	23.5
393	700	62.49	388.0	406.0	18.0	682.5	716.5	34.0
464	700	19.82	459.0	472.0	13.0	684.5	713.5	29.0
531	700	10.61	522.0	540.0	18.0	685.5	714.5	29.0
349	753.5	23.32	338.0	357.0	19.0	734.0	779.0	45.0
363	753.5	15.51	357.0	367.0	10.0	745.0	783.0	38.0
422	753.5	7.61	414.0	431.0	17.0	742.0	771.0	29.0
451	753.5	12.74	448.0	458.0	10.0	734.0	772.0	38.0

**Table 32 Multiple ion doped sample Glass 2-8 – 0.5 mol % Eu, 1.0 mol % Tb and 1.5 mol % Dy**



Development and Application of Novel Tracers for Environmental Applications  
 Appendix II: Spectroscopic Characterisation Data

Excitation Wavelength / nm	Emission Wavelength / nm	Intensity	Peak width					
			Ex Wavelength			Em Wavelength		
			From	To	PW	From	To	PW
323	483	134.35	312.0	329.0	17.0	462.5	499.5	37.0
348	483	621.36	330.0	358.0	28.0	456.0	508.5	52.5
363	483	439.09	358.0	371.0	13.0	460.5	508.5	48.0
385	483	537.78	371.0	412.0	41.0	454.0	507.5	53.5
423	483	94.41	415.0	434.0	19.0	463.5	502.5	39.0
452	483	225.20	437.0	459.0	22.0	470.5	503.5	33.0
322	544	72.65	310.0	328.0	18.0	529.0	557.5	28.5
350	544	412.91	340.0	358.0	18.0	526.0	556.5	30.5
364	544	329.73	358.0	371.0	13.0	529.0	558.5	29.5
377	544	353.32	371.0	383.0	12.0	527.0	559.5	32.5
385	544	275.81	383.0	405.0	22.0	529.0	555.5	26.5
423	544	49.81	418.0	433.0	15.0	531.0	555.5	24.5
452	544	109.58	438.0	460.0	22.0	531.0	555.5	24.5
485	544	102.74	474.0	491.0	17.0	530.0	562.0	32.0
322	575	180.81	311.0	330.0	19.0	558.5	600.5	42.0
348	575	1000.97	330.0	357.0	27.0	557.5	605.0	47.5
363	575	612.09	357.0	371.0	14.0	558.5	603.0	44.5
386	575	918.53	371.0	412.0	41.0	557.5	603.0	45.5
423	575	163.85	412.0	434.0	22.0	558.5	603.0	44.5
452	575	362.09	436.0	461.0	25.0	555.5	602.0	46.5
471	575	106.30	461.0	492.0	31.0	560.5	600.5	40.0
317	615	33.33	313.0	330.0	17.0	602.0	634.5	32.5
348	615	70.20	337.0	357.0	20.0	606.0	638.5	32.5
361	615	100.85	357.0	366.0	9.0	604.0	639.5	35.5
381	615	167.40	369.0	387.0	18.0	604.0	639.5	35.5
393	615	380.95	387.0	407.0	20.0	601.5	638.5	37.0
413	615	45.53	409.0	418.0	9.0	601.5	626.5	25.0
464	615	171.12	458.0	469.0	11.0	599.5	639.5	40.0
530	615	28.32	521.0	544.0	23.0	602.0	628.5	26.5
322	663	9.41	316.0	330.0	14.0	652.0	676.5	24.5
348	663	47.82	337.0	357.0	20.0	638.5	687.0	48.5
362	663	28.86	357.0	370.0	13.0	642.5	687.0	44.5
386	663	51.38	372.0	411.0	39.0	639.5	681.5	42.0
423	663	12.44	417.0	431.0	14.0	652.0	670.5	18.5
452	663	22.83	436.0	457.0	21.0	640.5	691.0	50.5
349	700.5	6.36	339.0	356.0	17.0	690.0	710.5	20.5
362	700.5	11.23	356.0	366.0	10.0	687.0	710.5	23.5
381	700.5	19.60	369.0	387.0	18.0	684.5	716.5	32.0
393	700.5	50.96	387.0	405.0	18.0	680.5	717.5	37.0
464	700.5	16.34	457.0	468.0	11.0	680.5	717.5	37.0
529	700.5	9.69	512.0	556.0	44.0	685.5	714.5	29.0
325	753	5.21	315.0	328.0	13.0	748.5	760.5	12.0
347	753	24.63	336.0	357.0	21.0	733.0	777.0	44.0
363	753	13.58	358.0	366.0	8.0	745.0	767.5	22.5
452	753	9.36	437.0	459.0	22.0	735.0	769.0	34.0

**Table 33 Multiple ion doped sample Glass 2-9 – 0.5 mol % Eu, 1.5 mol % Tb and 2. mol % Dy**

Development and Application of Novel Tracers for Environmental Applications  
 Appendix II: Spectroscopic Characterisation Data

			Peak width					
Excitation Wavelength / nm	Emission Wavelength / nm	Intensity	Ex Wavelength			Em Wavelength		
			From	To	PW	From	To	PW
318	489.5	38.13	312.0	320.0	8.0	478.0	503.5	25.5
351	489.5	145.80	342.0	362.0	20.0	472.5	507.5	35.0
369	489.5	152.14	362.0	371.0	9.0	470.5	506.5	36.0
377	489.5	186.50	371.0	390.0	19.0	472.5	510.5	38.0
318	546	44.28	312.0	323.0	11.0	534.0	567.0	33.0
341	546	132.47	331.0	343.0	12.0	531.0	561.0	30.0
351	546	309.04	343.0	360.0	17.0	525.0	564.0	39.0
376	546	476.94	360.0	388.0	28.0	519.0	561.0	42.0
393	546	34.40	388.0	400.0	12.0	521.0	563.0	42.0
483	546	177.50	471.0	497.0	26.0	530.0	561.0	31.0
319	589	18.11	313.0	322.0	9.0	568.0	597.5	29.5
351	589	54.17	343.0	356.0	13.0	570.0	602.0	32.0
362	589	77.64	356.0	364.0	8.0	570.0	601.5	31.5
377	589	133.10	369.0	387.0	18.0	569.0	601.5	32.5
393	589	212.63	387.0	407.0	20.0	569.0	639.5	70.5
413	589	24.64	407.0	419.0	12.0	578.0	597.0	19.0
464	589	63.75	457.0	470.0	13.0	572.0	597.5	25.5
483	589	29.63	474.0	497.0	23.0	572.0	601.5	29.5
530	589	12.64	518.0	545.0	27.0	580.0	598.5	18.5
318	615	35.65	311.0	341.0	30.0	601.5	632.5	31.0
338	615	30.25	335.0	341.0	6.0	600.5	633.5	33.0
350	615	58.66	342.0	356.0	14.0	602.0	636.5	34.5
362	615	148.68	356.0	365.0	9.0	602.0	640.5	38.5
378	615	268.20	368.0	388.0	20.0	601.5	640.5	39.0
393	615	738.13	388.0	407.0	19.0	599.5	639.5	40.0
413	615	55.71	407.0	422.0	15.0	603.0	634.5	31.5
464	615	273.06	454.0	472.0	18.0	600.5	639.5	39.0
483	615	33.26	478.0	495.0	17.0	602.0	641.5	39.5
532	615	51.06	518.0	544.0	26.0	601.5	630.5	29.0
318	653.5	2.06	311.0	322.0	11.0			0.0
351	653.5	7.07	346.0	355.0	9.0	649.0	657.0	8.0
362	653.5	9.93	355.0	366.0	11.0	642.5	672.5	30.0
377	653.5	20.83	370.0	384.0	14.0	644.0	664.5	20.5
393	653.5	39.22	388.0	405.0	17.0	639.5	673.5	34.0
413	653.5	5.76	409.0	421.0	12.0	645.0	664.0	19.0
463	653.5	16.39	458.0	469.0	11.0	641.5	664.0	22.5
472	653.5	8.78	469.0	476.0	7.0	645.0	666.5	21.5
483	653.5	9.71	476.0	487.0	11.0	646.0	659.0	13.0
501	653.5	7.48	497.0	506.0	9.0	647.0	664.5	17.5
510	653.5	6.12	506.0	514.0	8.0	643.5	660.0	16.5
527	653.5	4.71	522.0	538.0	16.0	643.5	669.0	25.5
318	698.5	3.78	314.0	321.0	7.0	690.0	712.5	22.5
351	698.5	6.01	349.0	355.0	6.0	688.0	709.5	21.5
362	698.5	18.81	356.0	366.0	10.0	679.5	712.5	33.0
379	698.5	33.89	370.0	386.0	16.0	675.5	716.5	41.0
393	698.5	89.12	388.0	409.0	21.0	673.5	718.5	45.0
411	698.5	7.45	408.0	414.0	6.0	680.5	710.5	30.0
464	698.5	23.52	455.0	471.0	16.0	674.5	716.5	42.0
484	698.5	5.42	479.0	490.0	11.0	686.0	711.5	25.5
532	698.5	7.33	521.0	539.0	18.0	679.5	717.5	38.0

**Table 34 Multiple ion doped sample Glass 2-10 – 2.0 mol % Eu, 0.0 mol % Tb and 2.0 mol % Dy**

Development and Application of Novel Tracers for Environmental Applications  
 Appendix II: Spectroscopic Characterisation Data

Excitation Wavelength / nm	Emission Wavelength / nm	Intensity	Peak width					
			Ex Wavelength			Em Wavelength		
			From	To	PW	From	To	PW
323	484	226.53	310.0	330.0	20.0	463.5	506.5	43.0
348	484	961.72	330.0	357.0	27.0	455.0	507.5	52.5
363	484	576.31	357.0	371.0	14.0	459.5	506.5	47.0
386	484	690.97	371.0	413.0	42.0	454.0	506.5	52.5
423	484	110.90	413.0	434.0	21.0	462.5	502.5	40.0
452	484	275.56	438.0	461.0	23.0	467.5	503.5	36.0
361	536	41.05	356.0	367.0	11.0	527.0	537.0	10.0
380	536	51.57	368.0	388.0	20.0	524.0	539.5	15.5
393	536	93.13	388.0	407.0	19.0	514.5	547.5	33.0
463	536	38.04	459.0	473.0	14.0	518.5	550.5	32.0
322	576.5	292.98	330.0	357.0	27.0	554.5	598.5	44.0
349	576.5	999.99	357.0	371.0	14.0	549.5	602.0	52.5
363	576.5	925.69	371.0	413.0	42.0	550.5	602.0	51.5
386	576.5	999.99	413.0	436.0	23.0	548.5	602.0	53.5
423	576.5	207.27	436.0	459.0	23.0	551.5	602.0	50.5
452	576.5	478.37	459.0	492.0	33.0	550.5	602.0	51.5
471	576.5	138.79	311.0	331.0	20.0	554.5	597.5	43.0
319	616	89.85	340.0	354.0	14.0	601.5	633.5	32.0
346	616	54.41	354.0	368.0	14.0	604.0	634.5	30.5
362	616	210.94	368.0	387.0	19.0	601.5	638.5	37.0
381	616	416.08	387.0	407.0	20.0	602.0	637.5	35.5
393	616	999.99	407.0	422.0	15.0	601.5	641.5	40.0
413	616	97.85	456.0	474.0	18.0	600.5	639.5	39.0
464	616	473.54	456.0	474.0	18.0	600.5	640.5	40.0
533	616	88.11	520.0	546.0	26.0	601.5	640.5	39.0
322	658	13.56	314.0	330.0	16.0	655.0	661.0	6.0
347	658	58.03	337.0	357.0	20.0	638.0	690.0	52.0
362	658	36.58	357.0	369.0	12.0	638.5	688.0	49.5
385	658	54.53	369.0	387.0	18.0	641.5	686.0	44.5
392	658	75.39	387.0	409.0	22.0	643.5	676.5	33.0
411	658	11.55	409.0	416.0	7.0	646.0	664.5	18.5
423	658	12.64	419.0	429.0	10.0	653.0	683.5	30.5
452	658	22.82	438.0	458.0	20.0	645.0	690.0	45.0
464	658	28.98	458.0	470.0	12.0	642.5	671.5	29.0
320	702	9.98	315.0	325.0	10.0	686.0	711.5	25.5
347	702	7.11	341.0	354.0	13.0	691.0	709.5	18.5
362	702	24.61	354.0	367.0	13.0	688.0	712.5	24.5
381	702	47.74	367.0	387.0	20.0	682.5	717.5	35.0
393	702	139.93	387.0	406.0	19.0	679.5	719.5	40.0
412	702	11.89	409.0	422.0	13.0	694.0	717.5	23.5
464	702	39.25	455.0	473.0	18.0	680.5	719.5	39.0
533	702	13.70	520.0	546.0	26.0	692.0	713.5	21.5
323	754.5	10.22	315.0	330.0	15.0	741.0	771.0	30.0
349	754.5	38.99	338.0	358.0	20.0	728.0	788.0	60.0
362	754.5	18.87	358.0	367.0	9.0	742.0	774.0	32.0
424	754.5	8.79	415.0	433.0	18.0	746.0	774.0	28.0
451	754.5	14.40	434.0	458.0	24.0	727.5	782.0	54.5

**Table 35 Multiple ion doped sample Glass 2-11 – 1.0 mol % Eu, 0.0 mol % Tb and 1.0 mol % Dy**

Development and Application of Novel Tracers for Environmental Applications  
 Appendix II: Spectroscopic Characterisation Data

Excitation Wavelength / nm	Emission Wavelength / nm	Intensity	Peak width					
			Ex Wavelength			Em Wavelength		
			From	To	PW	From	To	PW
323	481.5	82.95	311.0	331.0	20.0	458.5	510.5	52.0
349	481.5	439.21	332.0	358.0	26.0	451.0	510.5	59.5
363	481.5	282.92	358.0	371.0	13.0	458.5	507.5	49.0
386	481.5	385.34	371.0	412.0	41.0	456.0	512.5	56.5
424	481.5	67.62	417.0	432.0	15.0	458.5	503.5	45.0
452	481.5	148.18	439.0	458.0	19.0	471.5	507.5	36.0
323	544	20.59	311.0	329.0	18.0	534.0	550.5	16.5
350	544	85.50	333.0	358.0	25.0	528.0	554.5	26.5
363	544	78.37	358.0	370.0	12.0	532.0	555.5	23.5
377	544	89.30	371.0	381.0	10.0	529.0	556.5	27.5
385	544	69.65	384.0	388.0	4.0	531.0	557.5	26.5
390	544	67.32	388.0	417.0	29.0	535.0	553.5	18.5
423	544	15.22	420.0	432.0	12.0	533.0	550.5	17.5
452	544	28.01	440.0	458.0	18.0	530.0	549.5	19.5
465	544	17.66	462.0	467.0	5.0	524.0	549.5	25.5
483	544	29.96	475.0	491.0	16.0	531.0	561.0	30.0
323	575	115.73	312.0	330.0	18.0	557.5	600.5	43.0
349	575	792.55	330.0	358.0	28.0	552.5	601.5	49.0
363	575	459.93	358.0	371.0	13.0	555.5	601.5	46.0
385	575	686.55	371.0	412.0	41.0	553.5	601.5	48.0
424	575	124.26	414.0	435.0	21.0	554.5	596.5	42.0
452	575	261.98	437.0	461.0	24.0	554.5	601.5	47.0
471	575	79.19	461.0	489.0	28.0	555.5	597.5	42.0
319	614.5	33.87	311.0	330.0	19.0	599.5	631.5	32.0
350	614.5	40.29	339.0	354.0	15.0	605.0	632.5	27.5
362	614.5	105.18	354.0	369.0	15.0	599.5	636.5	37.0
381	614.5	201.61	369.0	388.0	19.0	600.5	638.5	38.0
393	614.5	535.35	388.0	407.0	19.0	601.5	639.5	38.0
414	614.5	47.63	407.0	420.0	13.0	600.5	639.5	39.0
464	614.5	232.68	456.0	471.0	15.0	598.5	636.5	38.0
532	614.5	41.31	521.0	544.0	23.0	601.5	633.5	32.0
323	661	4.27	318.0	328.0	10.0	647.0	669.5	22.5
349	661	33.95	331.0	371.0	40.0	636.5	689.0	52.5
363	663.5	19.31	357.0	371.0	14.0	641.5	682.5	41.0
393	653.5	38.84	387.0	395.0	8.0	642.5	678.5	36.0
423	664	7.96	417.0	431.0	14.0	662.0	681.5	19.5
452	664	15.03	437.0	458.0	21.0	637.5	690.0	52.5
317	700	2.83	314.0	322.0	8.0	697.0	706.0	9.0
347	700	3.93	341.0	353.0	12.0	698.0	706.5	8.5
360	700	9.47	357.0	366.0	9.0	686.0	709.5	23.5
376	700	20.04	369.0	378.0	9.0	687.0	716.5	29.5
381	700	22.39	378.0	386.0	8.0	685.5	716.5	31.0
393	700	65.10	388.0	407.0	19.0	679.5	718.5	39.0
412	700	7.36	407.0	420.0	13.0	680.5	714.5	34.0
463	700	20.38	456.0	471.0	15.0	680.5	716.5	36.0
531	700	7.47	521.0	547.0	26.0	691.0	715.5	24.5
323	755	2.13	318.0	326.0	8.0	753.5	758.5	5.0
345	755	14.46	339.0	356.0	17.0	739.0	779.0	40.0
362	755	10.40	359.0	368.0	9.0	740.0	770.0	30.0
422	755	5.53	416.0	429.0	13.0	743.0	779.0	36.0
452	755	8.01	438.0	458.0	20.0	734.0	781.0	47.0

**Table 36 Multiple ion doped sample Glass 2-12 – 1.0 mol % Eu, 0.5 mol % Tb and 1.5 mol % Dy**

Development and Application of Novel Tracers for Environmental Applications  
 Appendix II: Spectroscopic Characterisation Data

Excitation Wavelength / nm	Emission Wavelength / nm	Intensity	Peak width					
			Ex Wavelength			Em Wavelength		
			From	To	PW	From	To	PW
323	481	116.44	312.0	331.0	19.0	466.5	506.5	40.0
349	481	677.09	331.0	357.0	26.0	459.5	506.5	47.0
363	481	473.49	357.0	371.0	14.0	465.5	506.5	41.0
386	481	581.58	371.0	411.0	40.0	457.5	506.5	49.0
423	481	100.80	416.0	431.0	15.0	459.5	501.5	42.0
452	481	242.19	436.0	460.0	24.0	468.5	501.5	33.0
324	546	43.06	312.0	329.0	17.0	529.0	554.5	25.5
349	546	288.18	332.0	356.0	24.0	527.0	555.5	28.5
364	546	241.89	358.0	370.0	12.0	531.0	555.5	24.5
378	546	257.01	373.0	382.0	9.0	529.0	557.5	28.5
385	546	206.25	382.0	409.0	27.0	529.0	552.5	23.5
424	546	37.81	417.0	434.0	17.0	531.0	554.5	23.5
445	546	51.32	437.0	448.0	11.0	531.0	553.5	22.5
452	546	74.35	448.0	459.0	11.0	530.0	553.5	23.5
485	546	71.52	475.0	495.0	20.0	531.0	558.5	27.5
323	577.5	161.20	311.0	331.0	20.0	559.5	600.5	41.0
349	577.5	999.99	331.0	357.0	26.0	555.5	603.0	47.5
363	577.5	753.64	357.0	371.0	14.0	556.5	603.0	46.5
385	577.5	1002.58	371.0	412.0	41.0	555.5	602.0	46.5
423	577.5	182.23	412.0	436.0	24.0	556.5	603.0	46.5
452	577.5	435.82	436.0	460.0	24.0	555.5	601.5	46.0
471	577.5	127.47	461.0	491.0	30.0	555.5	595.5	40.0
318	615	41.26	312.0	328.0	16.0	603.0	631.5	28.5
351	615	89.54	341.0	355.0	14.0	606.0	635.5	29.5
361	615	186.19	355.0	368.0	13.0	602.0	636.5	34.5
380	615	314.30	368.0	387.0	19.0	602.0	636.5	34.5
393	615	844.77	387.0	406.0	19.0	600.5	640.5	40.0
412	615	65.72	407.0	419.0	12.0	603.0	634.5	31.5
464	615	356.67	457.0	471.0	14.0	600.5	636.5	36.0
532	615	65.51	520.0	545.0	25.0	600.5	635.5	35.0
322	658	5.76	317.0	326.0	9.0	654.0	664.5	10.5
347	658	44.04	332.0	357.0	25.0	637.5	691.0	53.5
362	658	29.61	357.0	369.0	12.0	643.5	683.5	40.0
384	658	51.24	371.0	386.0	15.0	642.5	682.5	40.0
392	658	51.69	389.0	407.0	18.0	638.5	674.0	35.5
425	658	10.13	418.0	429.0	11.0	652.0	687.0	35.0
451	658	21.39	439.0	457.0	18.0	644.0	688.0	44.0
464	658	20.28	460.0	468.0	8.0	646.0	676.5	30.5
485	658	9.65	482.0	487.0	5.0	665.5	682.5	17.0
320	700.5	3.73	311.0	328.0	17.0	685.5	710.5	25.0
352	700.5	9.31	336.0	356.0	20.0	693.0	711.5	18.5
361	700.5	19.40	356.0	368.0	12.0	688.0	712.5	24.5
380	700.5	36.30	368.0	387.0	19.0	683.5	716.5	33.0
392	700.5	100.73	387.0	406.0	19.0	678.5	723.5	45.0
414	700.5	10.38	406.0	420.0	14.0	685.5	714.5	29.0
464	700.5	30.19	458.0	469.0	11.0	677.5	716.5	39.0
530	700.5	8.40	521.0	540.0	19.0	676.5	716.5	40.0
349	754	24.80	338.0	357.0	19.0	731.0	786.0	55.0
363	754	14.26	357.0	367.0	10.0	744.0	781.0	37.0
422	754	8.27	412.0	435.0	23.0	739.0	773.0	34.0
448	754	10.07	440.0	462.0	22.0	728.0	781.0	53.0

**Table 37 Multiple ion doped sample Glass 2-13 – 1.0 mol % Eu, 1.0 mol % Tb and 2.0 mol % Dy**

Excitation Wavelength / nm	Emission Wavelength / nm	Intensity	Peak width					
			Ex Wavelength			Em Wavelength		
			From	To	PW	From	To	PW
351	489.5	80.56	345.0	359.0	14.0	477.0	505.5	28.5
377	489.5	110.99	373.0	387.0	14.0	466.5	508.5	42.0
317	545.5	28.05	311.0	322.0	11.0	526.0	560.5	34.5
351	545.5	159.12	341.0	356.0	15.0	529.0	562.0	33.0
376	545.5	249.68	362.0	386.0	24.0	526.0	566.0	40.0
393	545.5	43.13	389.0	397.0	8.0	516.5	564.0	47.5
462	545.5	18.82	458.0	468.0	10.0	541.5	549.5	8.0
483	545.5	103.36	470.0	497.0	27.0	528.0	566.0	38.0
318	590.5	17.86	311.0	324.0	13.0	579.0	597.5	18.5
351	590.5	36.57	344.0	356.0	12.0	569.0	603.0	34.0
362	590.5	79.97	356.0	364.0	8.0	568.0	599.5	31.5
378	590.5	141.45	367.0	388.0	21.0	568.0	600.5	32.5
393	590.5	350.41	388.0	407.0	19.0	568.0	600.5	32.5
414	590.5	37.95	409.0	420.0	11.0	569.0	599.5	30.5
464	590.5	114.13	456.0	470.0	14.0	568.0	599.5	31.5
483	590.5	25.80	474.0	495.0	21.0	571.0	601.5	30.5
532	590.5	25.65	521.0	542.0	21.0	579.0	598.5	19.5
319	613	51.89	311.0	323.0	12.0	601.5	633.5	32.0
351	613	59.06	345.0	354.0	9.0	605.0	636.5	31.5
361	613	214.29	356.0	366.0	10.0	600.5	637.5	37.0
380	613	411.63	367.0	387.0	20.0	600.5	641.5	41.0
393	613	1001.55	387.0	407.0	20.0	601.5	640.5	39.0
413	613	94.41	407.0	422.0	15.0	599.5	638.5	39.0
464	613	450.63	455.0	470.0	15.0	600.5	641.5	41.0
484	613	34.00	478.0	491.0	13.0	604.0	632.5	28.5
531	613	84.46	519.0	544.0	25.0	600.5	635.5	35.0
318	654	3.50	313.0	321.0	8.0	650.0	658.0	8.0
352	654	6.85	345.0	354.0	9.0	652.0	661.0	9.0
361	654	12.23	354.0	366.0	12.0	646.0	667.5	21.5
380	654	27.56	368.0	387.0	19.0	640.5	673.5	33.0
392	654	59.03	387.0	408.0	21.0	640.5	669.5	29.0
414	654	11.07	411.0	417.0	6.0	647.0	666.5	19.5
464	654	30.35	457.0	469.0	12.0	643.5	674.5	31.0
319	700	5.73	314.0	323.0	9.0	688.0	713.5	25.5
352	700	6.64	349.0	355.0	6.0	688.0	712.5	24.5
361	700	28.86	355.0	368.0	13.0	675.5	712.5	37.0
380	700	51.22	368.0	388.0	20.0	671.5	719.5	48.0
393	700	152.97	388.0	405.0	17.0	672.5	721.5	49.0
464	700	44.94	453.0	469.0	16.0	674.5	725.5	51.0
484	700	6.80	478.0	489.0	11.0	693.0	714.5	21.5
532	700	12.31	521.0	545.0	24.0	676.5	716.5	40.0
378	700	5.44	575.0	581.0	6.0	687.0	706.5	19.5

**Table 38 Multiple ion doped sample Glass 2-14 – 1.0 mol % Eu, 1.5 mol % Tb and 0.0 mol % Dy**

Development and Application of Novel Tracers for Environmental Applications  
 Appendix II: Spectroscopic Characterisation Data

			Peak width					
Excitation Wavelength / nm	Emission Wavelength / nm	Intensity	Ex Wavelength			Em Wavelength		
			From	To	PW	From	To	PW
323	481.5	60.21	312.0	328.0	16.0	465.5	571.5	106.0
348	481.5	390.39	328.0	357.0	29.0	456.5	509.5	53.0
363	481.5	274.36	357.0	371.0	14.0	460.5	509.5	49.0
377	481.5	214.29	371.0	380.0	9.0	464.5	510.5	46.0
385	481.5	294.71	380.0	411.0	31.0	460.5	506.5	46.0
423	481.5	46.49	415.0	433.0	18.0	464.5	504.5	40.0
452	481.5	120.33	438.0	457.0	19.0	472.5	504.5	32.0
318	545	39.78	310.0	321.0	11.0	528.0	562.0	34.0
323	545	36.17	321.0	328.0	7.0	532.0	559.5	27.5
350	545	389.28	329.0	356.0	27.0	528.0	559.5	31.5
364	545	354.05	359.0	369.0	10.0	529.0	560.5	31.5
376	545	467.82	371.0	384.0	13.0	529.0	562.0	33.0
423	545	27.09	416.0	431.0	15.0	533.0	556.5	23.5
452	545	59.67	439.0	458.0	19.0	533.0	557.5	24.5
483	545	162.68	473.0	497.0	24.0	530.0	562.0	32.0
323	575.5	61.39	313.0	330.0	17.0	559.5	599.5	40.0
348	575.5	623.28	330.0	358.0	28.0	558.5	603.0	44.5
363	575.5	350.23	358.0	371.0	13.0	559.5	602.0	42.5
386	575.5	500.74	371.0	409.0	38.0	556.5	602.0	45.5
423	575.5	86.57	416.0	433.0	17.0	556.5	601.5	45.0
452	575.5	189.12	438.0	460.0	22.0	557.5	601.5	44.0
393	585.5	485.52	387.0	406.0	19.0	559.5	599.5	40.0
464	585.5	122.55	458.0	469.0	11.0	565.0	598.5	33.5
533	585.5	22.25	521.0	544.0	23.0	571.0	600.5	29.5
319	615.5	49.58	312.0	330.0	18.0	604.0	633.5	29.5
351	615.5	132.84	341.0	356.0	15.0	603.0	638.5	35.5
362	615.5	273.19	356.0	368.0	12.0	601.5	636.5	35.0
379	615.5	487.37	368.0	387.0	19.0	601.5	639.5	38.0
393	615.5	999.99	387.0	407.0	20.0	600.5	642.5	42.0
413	615.5	92.87	407.0	420.0	13.0	602.0	633.5	31.5
464	615.5	493.75	457.0	469.0	12.0	600.5	639.5	39.0
483	615.5	48.37	477.0	493.0	16.0	602.0	635.5	33.5
532	615.5	92.40	520.0	546.0	26.0	601.5	630.5	29.0
319	653.5	2.89	315.0	326.0	11.0	649.0	662.0	13.0
349	653.5	20.48	332.0	357.0	25.0	640.5	683.5	43.0
361	653.5	21.96	357.0	368.0	11.0	642.5	672.5	30.0
381	653.5	32.34	368.0	387.0	19.0	642.5	673.5	31.0
392	653.5	67.74	387.0	407.0	20.0	640.5	675.5	35.0
413	653.5	8.22	410.0	415.0	5.0	644.0	658.0	14.0
425	653.5	5.80	422.0	429.0	7.0	647.0	656.0	9.0
453	653.5	9.63	443.0	454.0	11.0	639.5	685.5	46.0
464	653.5	26.51	457.0	469.0	12.0	641.5	667.5	26.0
485	653.5	10.47	478.0	488.0	10.0	647.0	664.5	17.5
530	653.5	7.23	521.0	538.0	17.0	648.0	665.5	17.5
318	700.5	5.37	315.0	322.0	7.0	693.0	707.5	14.5
351	700.5	11.04	346.0	356.0	10.0	689.0	706.5	17.5
362	700.5	30.56	357.0	365.0	8.0	682.5	714.5	32.0
381	700.5	59.36	368.0	387.0	19.0	679.5	718.5	39.0
393	700.5	155.72	387.0	407.0	20.0	675.5	720.5	45.0
413	700.5	11.46	409.0	420.0	11.0	679.5	718.5	39.0
464	700.5	46.27	456.0	471.0	15.0	675.5	718.5	43.0
483	700.5	6.84	477.0	493.0	16.0	689.0	710.5	21.5
530	700.5	11.18	521.0	537.0	16.0	678.5	714.5	36.0
349	753	14.83	338.0	357.0	19.0	740.0	773.0	33.0
362	753	9.23	357.0	366.0	9.0	741.0	767.5	26.5
425	753	4.05	417.0	428.0	11.0	746.0	764.5	18.5
452	753	6.21	427.0	457.0	30.0	744.0	768.5	24.5

**Table 39 Multiple ion doped sample Glass 2-15 – 1.0 mol % Eu, 2.0 mol % Tb and 0.5 mol % Dy**

Development and Application of Novel Tracers for Environmental Applications  
 Appendix II: Spectroscopic Characterisation Data

Excitation Wavelength / nm	Emission Wavelength / nm	Intensity	Peak width					
			Ex Wavelength			Em Wavelength		
			From	To	PW	From	To	PW
323	481.5	92.26	315.0	330.0	15.0	466.5	499.5	33.0
349	481.5	588.19	334.0	357.0	23.0	458.5	506.5	48.0
363	481.5	372.23	357.0	371.0	14.0	456.0	503.5	47.5
385	481.5	464.16	371.0	411.0	40.0	456.5	504.5	48.0
423	481.5	76.56	417.0	434.0	17.0	461.5	498.5	37.0
452	481.5	203.87	437.0	458.0	21.0	468.5	502.5	34.0
350	535.5	15.51	346.0	354.0	8.0	524.0	545.5	21.5
361	535.5	20.23	356.0	368.0	12.0	524.0	545.5	21.5
383	535.5	30.80	370.0	385.0	15.0	525.0	546.5	21.5
393	535.5	59.89	388.0	407.0	19.0	515.5	546.5	31.0
409	535.5	18.51	407.0	413.0	6.0	532.0	540.5	8.5
464	535.5	32.57	459.0	469.0	10.0	520.0	544.5	24.5
322	577	137.15	313.0	331.0	18.0	548.5	598.5	50.0
347	577	1003.67	331.0	357.0	26.0	550.5	605.0	54.5
363	577	637.23	357.0	371.0	14.0	550.5	600.5	50.0
386	577	896.54	371.0	413.0	42.0	551.5	602.0	50.5
424	577	156.62	415.0	434.0	19.0	554.5	597.5	43.0
452	577	363.00	437.0	460.0	23.0	553.5	602.0	48.5
319	615	47.18	313.0	330.0	17.0	601.5	631.5	30.0
349	615	49.85	341.0	355.0	14.0	606.0	634.5	28.5
361	615	197.66	355.0	368.0	13.0	602.0	636.5	34.5
380	615	363.86	368.0	387.0	19.0	600.5	637.5	37.0
392	615	1002.28	387.0	407.0	20.0	599.5	629.5	30.0
413	615	89.93	407.0	421.0	14.0	600.5	638.5	38.0
464	615	450.86	456.0	471.0	15.0	599.5	633.5	34.0
531	615	84.70	520.0	544.0	24.0	601.5	635.5	34.0
577	615	18.77	569.0	581.0	12.0	603.0	664.0	61.0
322	660	7.00	319.0	326.0	7.0	658.0	685.5	27.5
349	660	39.38	337.0	356.0	19.0	634.5	683.5	49.0
362	660	26.64	356.0	370.0	14.0	640.5	683.5	43.0
386	660	41.79	370.0	388.0	18.0	640.5	683.5	43.0
392	660	48.24	388.0	405.0	17.0	640.5	673.5	33.0
423	660	7.81	417.0	430.0	13.0	645.0	682.5	37.5
444	660	11.77	437.0	447.0	10.0	644.0	675.5	31.5
452	660	18.47	447.0	458.0	11.0	644.0	689.0	45.0
464	660	18.05	458.0	468.0	10.0	642.0	667.5	25.5
531	660	5.79	521.0	537.0	16.0	647.0	664.0	17.0
319	698	3.06	316.0	323.0	7.0	685.5	713.0	27.5
349	698	4.98	342.0	354.0	12.0	689.0	711.5	22.5
361	698	21.42	356.0	368.0	12.0	680.5	712.5	32.0
380	698	39.18	368.0	387.0	19.0	682.5	713.5	31.0
393	698	121.13	387.0	406.0	19.0	677.5	723.5	46.0
412	698	10.20	409.0	420.0	11.0	676.5	711.5	35.0
464	698	32.46	455.0	470.0	15.0	676.5	716.5	40.0
530	698	9.72	520.0	548.0	28.0	685.5	714.5	29.0
348	753.5	25.00	339.0	355.0	16.0	737.0	777.0	40.0
364	753.5	13.12	361.0	367.0	6.0	747.0	775.0	28.0
424	753.5	5.44	413.0	433.0	20.0	742.0	761.5	19.5
452	753.5	5.95	439.0	457.0	18.0	736.0	766.5	30.5
473	753.5	4.69	467.0	477.0	10.0	748.5	759.5	11.0

**Table 40 Multiple ion doped sample Glass 2-16 – 1.5 mol % Eu, 0.0 mol % Tb and 1.5 mol % Dy**



Development and Application of Novel Tracers for Environmental Applications  
 Appendix II: Spectroscopic Characterisation Data

Excitation Wavelength / nm	Emission Wavelength / nm	Intensity	Peak width					
			Ex Wavelength			Em Wavelength		
			From	To	PW	From	To	PW
323	480.5	106.00	312.0	328.0	16.0	463.5	499.5	36.0
348	480.5	597.70	335.0	357.0	22.0	455.0	504.5	49.5
363	480.5	416.04	357.0	371.0	14.0	457.5	504.5	47.0
386	480.5	521.66	371.0	411.0	40.0	458.5	505.5	47.0
423	480.5	102.02	414.0	433.0	19.0	467.5	498.5	31.0
452	480.5	250.89	439.0	459.0	20.0	471.5	501.5	30.0
322	546.5	27.00	310.0	329.0	19.0	532.0	555.5	23.5
249	546.5	122.88	329.0	356.0	27.0	531.0	552.5	21.5
365	546.5	395.41	356.0	368.0	12.0	527.0	555.5	28.5
377	546.5	115.61	372.0	380.0	8.0	524.0	555.5	31.5
386	546.5	106.13	381.0	408.0	27.0	530.0	552.5	22.5
410	546.5	34.10	408.0	415.0	7.0	542.5	549.5	7.0
424	546.5	25.04	419.0	428.0	9.0	540.5	549.5	9.0
451	546.5	42.41	443.0	460.0	17.0	529.0	549.5	20.5
462	546.5	28.30	460.0	468.0	8.0	541.5	549.5	8.0
484	546.5	44.07	476.0	482.0	6.0	528.0	560.5	32.5
323	575.5	172.16	311.0	330.0	19.0	556.5	601.5	45.0
348	575.5	999.99	332.0	357.0	25.0	552.5	603.0	50.5
363	575.5	683.55	357.0	371.0	14.0	553.5	602.0	48.5
385	575.5	998.57	371.0	412.0	41.0	552.5	602.0	49.5
423	575.5	202.78	414.0	437.0	23.0	552.5	603.0	50.5
451	575.5	431.15	437.0	460.0	23.0	552.5	603.0	50.5
470	575.5	130.03	460.0	491.0	31.0	556.5	598.5	42.0
319	614	96.86	312.0	333.0	21.0	604.0	635.5	31.5
349	614	79.61	337.0	355.0	18.0	601.5	635.5	34.0
362	614	207.19	355.0	368.0	13.0	601.5	635.5	34.0
380	614	407.36	368.0	387.0	19.0	601.5	638.5	37.0
392	614	1001.35	387.0	407.0	20.0	600.5	640.5	40.0
412	614	104.25	407.0	420.0	13.0	601.5	633.5	32.0
463	614	486.27	456.0	474.0	18.0	600.5	639.5	39.0
531	614	99.13	520.0	543.0	23.0	600.5	636.5	36.0
324	661.5	7.51	318.0	328.0	10.0	648.0	678.5	30.5
348	661.5	50.25	338.0	357.0	19.0	641.5	692.0	50.5
363	661.5	27.68	357.0	370.0	13.0	640.5	681.5	41.0
384	661.5	44.45	370.0	388.0	18.0	638.5	680.5	42.0
392	654.5	71.64	387.0	408.0	21.0	641.5	673.5	32.0
463	654	33.34	459.0	471.0	12.0	642.5	672.5	30.0
424	665	12.32	419.0	430.0	11.0	649.0	657.0	8.0
452	665	25.57	436.0	459.0	23.0	654.0	685.5	31.5
322	702	5.81	316.0	324.0	8.0	696.0	712.5	16.5
350	702	9.00	340.0	355.0	15.0	690.0	714.5	24.5
362	702	22.95	355.0	368.0	13.0	686.0	714.5	28.5
380	702	46.48	368.0	386.0	18.0	681.5	718.5	37.0
393	702	122.39	388.0	405.0	17.0	676.5	718.5	42.0
413	702	15.38	409.0	420.0	11.0	681.5	715.5	34.0
464	702	47.20	454.0	469.0	15.0	678.5	715.5	37.0
544	702	13.50	519.0	548.0	29.0	677.5	716.5	39.0
348	702	25.01	336.0	356.0	20.0	729.0	776.0	47.0
363	755	16.42	356.0	367.0	11.0	746.0	775.0	29.0
422	755	8.60	414.0	430.0	16.0	732.0	769.0	37.0
451	755	11.14	425.0	460.0	35.0	739.0	769.0	30.0

**Table 41 Multiple ion doped sample Glass 2-17 – 1.5 mol % Eu, 0.5 mol % Tb and 2.0 mol % Dy**

Development and Application of Novel Tracers for Environmental Applications  
 Appendix II: Spectroscopic Characterisation Data

Excitation Wavelength / nm	Emission Wavelength / nm	Intensity	Peak width					
			Ex Wavelength			Em Wavelength		
			From	To	PW	From	To	PW
350	435.5	129.16	344.0	355.0	11.0	431.0	442.0	11.0
377	435.5	145.69	372.0	383.0	11.0	425.0	449.5	24.5
377	412.5	156.39	362.0	382.0	20.0	403.0	425.5	22.5
353	486	92.76	327.0	361.0	34.0	475.5	501.0	25.5
377	486	94.11	372.0	382.0	10.0	471.5	502.5	31.0
402	486	53.04	393.0	418.0	25.0	479.0	494.0	15.0
416	544.5	24.75	310.0	320.0	10.0	532.0	566.0	34.0
352	544.5	118.90	341.0	357.0	16.0	528.0	563.0	35.0
377	544.5	194.95	360.0	385.0	25.0	519.5	561.5	42.0
392	544.5	96.81	389.0	396.0	7.0	542.0	550.0	8.0
464	544.5	29.80	458.0	468.0	10.0	540.2	552.0	11.8
483	544.5	81.02	475.0	494.0	19.0	529.5	566.0	36.5
319	590	33.19	312.0	332.0	20.0	575.5	601.0	25.5
361	590	112.43	356.0	367.0	11.0	570.0	601.0	31.0
381	590	205.61	367.0	387.0	20.0	571.0	598.0	27.0
393	590	536.73	387.0	407.0	20.0	568.5	599.5	31.0
414	590	71.10	407.0	419.0	12.0	582.0	591.0	9.0
464	590	168.25	459.0	472.0	13.0	570.0	599.5	29.5
483	590	26.29	476.0	491.0	15.0	570.0	601.0	31.0
533	590	43.95	522.0	530.0	8.0	574.5	598.0	23.5
319	614	99.53	314.0	330.0	16.0	601.0	623.5	22.5
361	614	348.58	355.0	367.0	12.0	599.5	637.5	38.0
381	614	629.23	367.0	388.0	21.0	599.5	636.0	36.5
393	614	999.99	388.0	407.0	19.0	599.5	639.0	39.5
413	614	144.30	407.0	419.0	12.0	601.0	636.0	35.0
464	614	695.80	455.0	471.0	16.0	601.0	636.0	35.0
482	614	43.99	477.0	491.0	14.0	602.5	643.0	40.5
532	614	126.19	520.0	544.0	24.0	599.5	637.4	37.9
363	650.5	25.33	356.0	366.0	10.0	644.5	665.5	21.0
378	650.5	46.56	366.0	387.0	21.0	639.0	668.0	29.0
392	650.5	91.71	387.0	406.0	19.0	641.5	667.0	25.5
464	650.5	44.57	455.0	468.0	13.0	643.0	671.0	28.0
319	697	13.10	314.0	323.0	9.0	695.0	703.5	8.5
361	697	53.94	358.0	367.0	9.0	685.5	705.0	19.5
380	697	79.85	367.0	387.0	20.0	675.5	715.0	39.5
393	697	223.25	387.0	408.0	21.0	674.0	722.0	48.0
410	697	20.95	408.0	421.0	13.0	688.0	710.5	22.5
464	697	53.05	458.0	472.0	14.0	679.5	717.5	38.0
532	697	17.55	520.0	537.0	17.0	685.5	716.0	30.5

**Table 42 Multiple ion doped sample Glass 2-18 – 1.5 mol % Eu, 1.0 mol % Tb and 0.5 mol % Dy**

Development and Application of Novel Tracers for Environmental Applications  
 Appendix II: Spectroscopic Characterisation Data

Excitation Wavelength / nm	Emission Wavelength / nm	Intensity	Peak width					
			Ex Wavelength			Em Wavelength		
			From	To	PW	From	To	PW
324	483	84.66	315.0	330.0	15.0	464.5	504.0	39.5
348	483	391.12	339.0	356.0	17.0	457.5	507.0	49.5
363	483	257.02	358.0	368.0	10.0	462.0	507.0	45.0
386	483	280.93	371.0	407.0	36.0	462.0	505.5	43.5
424	483	70.60	417.0	434.0	17.0	466.0	497.0	31.0
452	483	144.59	440.0	458.0	18.0	473.0	501.0	28.0
320	544.5	44.35	310.0	327.0	17.0	533.5	556.0	22.5
350	544.5	281.78	332.0	356.0	24.0	530.5	557.5	27.0
366	544.5	240.82	361.0	371.0	10.0	530.5	557.5	27.0
377	544.5	314.29	371.0	386.0	15.0	528.0	561.5	33.5
451	544.5	54.25	442.0	457.0	15.0	535.0	554.5	19.5
484	544.5	114.09	477.0	493.0	16.0	532.0	560.5	28.5
323	576.5	95.55	313.0	331.0	18.0	559.0	599.5	40.5
348	576.5	629.45	339.0	357.0	18.0	557.5	601.0	43.5
361	576.5	309.32	357.0	371.0	14.0	559.0	601.0	42.0
387	576.5	474.24	371.0	407.0	36.0	554.5	601.0	46.5
424	576.5	106.52	418.0	435.0	17.0	557.5	601.0	43.5
452	576.5	189.03	442.0	460.0	18.0	557.5	604.0	46.5
393	589	582.68	387.0	407.0	20.0	559.0	599.5	40.5
464	589	177.08	458.0	469.0	11.0	573.0	597.0	24.0
319	615	115.70	312.0	329.0	17.0	602.5	626.5	24.0
350	615	141.01	339.0	356.0	17.0	602.5	633.5	31.0
361	615	376.98	356.0	367.0	11.0	601.0	634.5	33.5
379	615	634.80	367.0	387.0	20.0	601.0	637.5	36.5
393	615	999.99	387.0	406.0	19.0	599.5	641.5	42.0
413	615	139.23	406.0	422.0	16.0	604.0	633.5	29.5
464	615	683.17	458.0	471.0	13.0	599.5	639.0	39.5
484	615	53.07	477.0	494.0	17.0	605.0	639.0	34.0
532	615	120.47	520.0	545.0	25.0	601.0	634.5	33.5
349	653.5	30.46	338.0	356.0	18.0	646.0	681.0	35.0
361	653.5	34.47	356.0	366.0	10.0	643.0	671.0	28.0
382	653.5	48.20	370.0	386.0	16.0	643.0	672.5	29.5
393	653.5	96.21	386.0	409.0	23.0	640.5	672.5	32.0
465	653.5	41.66	458.0	468.0	10.0	640.5	672.5	32.0
319	698	16.56	312.0	326.0	14.0	686.5	713.5	27.0
361	698	52.52	358.0	368.0	10.0	679.5	705.0	25.5
382	698	78.19	368.0	388.0	20.0	675.5	715.0	39.5
393	698	217.02	388.0	406.0	18.0	674.0	720.5	46.5
414	698	18.88	409.0	418.0	9.0	681.0	715.0	34.0
464	698	64.47	455.0	471.0	16.0	677.0	719.0	42.0
622	698	19.57	519.0	544.0	25.0	692.5	716.0	23.5
348	756.5	21.45	338.0	358.0	20.0	744.5	775.0	30.5

**Table 43 Multiple ion doped sample Glass 2-19 – 1.5 mol % Eu, 1.5 mol % Tb and 0.5 mol % Dy**

Development and Application of Novel Tracers for Environmental Applications  
 Appendix II: Spectroscopic Characterisation Data

Excitation Wavelength / nm	Emission Wavelength / nm	Intensity	Peak width					
			Ex Wavelength			Em Wavelength		
			From	To	PW	From	To	PW
323	482	122.34	312.0	330.0	18.0	462.0	507.0	45.0
349	482	562.34	337.0	357.0	20.0	457.5	508.5	51.0
363	482	359.37	357.0	371.0	14.0	460.5	511.0	50.5
387	482	403.55	371.0	410.0	39.0	460.5	507.0	46.5
423	482	75.94	419.0	431.0	12.0	463.5	501.0	37.5
452	482	173.10	440.0	458.0	18.0	471.5	508.5	37.0
321	544	65.52	312.0	328.0	16.0	530.5	557.5	27.0
349	544	414.46	332.0	357.0	25.0	530.5	557.5	27.0
365	544	353.85	359.0	370.0	11.0	528.0	559.0	31.0
373	544	438.64	371.0	384.0	13.0	528.0	560.5	32.5
424	544	56.63	418.0	430.0	12.0	533.5	557.5	24.0
452	544	76.83	442.0	458.0	16.0	532.0	556.0	24.0
483	544	143.43	436.0	493.0	57.0	530.5	563.0	32.5
322	575	162.11	314.0	330.0	16.0	559.0	599.5	40.5
348	575	930.46	338.0	358.0	20.0	557.5	604.0	46.5
363	575	491.62	358.0	370.0	12.0	559.0	602.5	43.5
386	575	723.23	372.0	410.0	38.0	557.5	601.0	43.5
423	575	117.85	417.0	433.0	16.0	554.5	602.5	48.0
452	575	280.70	439.0	459.0	20.0	556.0	604.0	48.0
472	575	73.43	467.0	493.0	26.0	560.5	594.0	33.5
464	586.5	164.57	459.0	473.0	14.0	566.0	598.0	32.0
319	614.5	149.90	312.0	329.0	17.0	602.5	633.5	31.0
350	614.5	182.98	335.0	355.0	20.0	604.0	636.0	32.0
361	614.5	387.10	357.0	368.0	11.0	602.5	640.5	38.0
380	614.5	620.74	368.0	388.0	20.0	601.0	639.0	38.0
393	614.5	999.99	388.0	406.0	18.0	601.0	640.5	39.5
413	614.5	125.08	410.0	421.0	11.0	601.0	634.5	33.5
464	614.5	634.47	458.0	474.0	16.0	599.5	640.5	41.0
483	614.5	57.22	477.0	493.0	16.0	605.0	637.5	32.5
531	654	111.97	520.0	545.0	25.0	602.5	636.0	33.5
350	654	32.38	339.0	356.0	17.0	641.5	681.0	39.5
361	654	30.62	356.0	370.0	14.0	640.5	678.5	38.0
381	654	43.99	370.0	388.0	18.0	640.5	674.0	33.5
392	654	94.99	388.0	404.0	16.0	640.5	677.0	36.5
453	654	17.06	444.0	457.0	13.0	639.0	679.5	40.5
464	654	37.22	457.0	469.0	12.0	641.5	670.0	28.5
319	699.5	16.81	312.0	330.0	18.0	682.5	713.5	31.0
361	699.5	44.58	358.0	367.0	9.0	681.0	705.0	24.0
380	699.5	77.43	367.0	387.0	20.0	678.5	720.5	42.0
393	699.5	216.14	387.0	407.0	20.0	674.0	719.0	45.0
413	699.5	16.59	407.0	416.0	9.0	684.5	713.5	29.0
464	699.5	60.20	455.0	469.0	14.0	677.0	717.5	40.5
483	699.5	9.90	481.0	491.0	10.0	689.5	710.5	21.0
532	699.5	14.33	522.0	538.0	16.0	677.0	716.0	39.0
323	753.5	6.73	316.0	327.0	11.0	750.0	762.5	12.5
348	753.5	22.54	341.0	355.0	14.0	740.0	776.5	36.5
424	753.5	6.25	415.0	429.0	14.0	737.5	760.0	22.5
452	753.5	9.04	439.0	457.0	18.0	738.5	774.0	35.5

**Table 44 Multiple ion doped sample Glass 2-20 – 1.5 mol % Eu, 2.0 mol % Tb and 1.0 mol % Dy**

Development and Application of Novel Tracers for Environmental Applications  
 Appendix II: Spectroscopic Characterisation Data

Excitation Wavelength / nm	Emission Wavelength / nm	Intensity	Peak width					
			Ex Wavelength			Em Wavelength		
			From	To	PW	From	To	PW
323	481.5	69.91	314.0	329.0	15.0	460.5	498.5	38.0
348	481.5	483.38	338.0	357.0	19.0	452.0	507.0	55.0
363	481.5	344.08	357.0	371.0	14.0	457.5	507.0	49.5
386	481.5	456.92	372.0	409.0	37.0	455.0	508.5	53.5
423	481.5	83.08	418.0	431.0	13.0	460.5	502.5	42.0
452	481.5	199.06	439.0	459.0	20.0	469.0	507.0	38.0
360	534.5	23.75	357.0	368.0	11.0	528.0	543.5	15.5
380	534.5	35.33	368.0	386.0	18.0	518.0	545.0	27.0
393	534.5	65.68	386.0	413.0	27.0	518.0	545.0	27.0
464	534.5	33.89	459.0	471.0	12.0	522.5	547.5	25.0
323	575.5	109.78	316.0	329.0	13.0	554.5	599.5	45.0
349	575.5	934.26	338.0	357.0	19.0	547.5	602.5	55.0
363	575.5	573.05	357.0	371.0	14.0	553.0	602.5	49.5
386	575.5	880.30	371.0	411.0	40.0	553.0	601.0	48.0
424	575.5	160.71	417.0	436.0	19.0	554.5	597.0	42.5
451	575.5	360.81	438.0	459.0	21.0	554.5	601.0	46.5
471	575.5	105.65	467.0	491.0	24.0	557.5	598.0	40.5
320	616	40.53	312.0	331.0	19.0	602.5	629.0	26.5
348	616	53.73	341.0	355.0	14.0	604.0	633.5	29.5
361	616	213.65	355.0	367.0	12.0	602.5	634.5	32.0
380	616	422.58	367.0	388.0	21.0	599.5	637.5	38.0
392	616	1003.39	388.0	407.0	19.0	599.5	637.5	38.0
413	616	97.74	407.0	419.0	12.0	604.0	636.0	32.0
464	616	515.46	455.0	474.0	19.0	599.5	636.0	36.5
532	616	100.54	520.0	545.0	25.0	601.0	640.5	39.5
348	657.5	35.05	338.0	356.0	18.0	643.0	677.0	34.0
361	657.5	26.72	356.0	371.0	15.0	646.0	685.5	39.5
384	657.5	45.69	371.0	387.0	16.0	641.5	679.5	38.0
382	657.5	63.07	387.0	408.0	21.0	639.0	678.5	39.5
452	657.5	19.47	447.0	458.0	11.0	646.0	681.0	35.0
464	657.5	26.60	458.0	469.0	11.0	643.0	668.5	25.5
530	657.5	7.40	524.0	533.0	9.0	646.0	665.5	19.5
319	701	2.90	315.0	326.0	11.0	699.5	712.0	12.5
380	701	52.68	368.0	388.0	20.0	679.5	717.5	38.0
392	701	127.02	388.0	408.0	20.0	678.5	719.0	40.5
413	701	13.56	408.0	422.0	14.0	679.5	723.0	43.5
464	701	43.94	457.0	473.0	16.0	679.5	719.0	39.5
530	701	12.31	520.0	545.0	25.0	684.0	713.5	29.5
348	759	17.52	337.0	355.0	18.0	733.5	776.5	43.0
422	759	6.81	417.0	428.0	11.0	744.5	772.5	28.0
452	759	9.29	447.0	457.0	10.0	730.5	778.0	47.5

**Table 45 Multiple ion doped sample Glass 2-21 – 2.0 mol % Eu, 0.0 mol % Tb and 2.0 mol % Dy**

Excitation Wavelength / nm	Emission Wavelength / nm	Intensity	Peak width					
			Ex Wavelength			Em Wavelength		
			From	To	PW	From	To	PW
393	535	114.83	387.0	413.0	26.0	519.5	549.0	29.5
464	535	61.63	457.0	469.0	12.0	519.5	549.0	29.5
319	545	18.76	309.0	324.0	15.0	529.5	563.0	33.5
351	545	65.07	346.0	357.0	11.0	528.0	564.5	36.5
378	545	107.79	371.0	385.0	14.0	519.5	564.5	45.0
483	545	55.48	475.0	493.0	18.0	529.5	567.5	38.0
320	590.5	38.37	313.0	327.0	14.0	564.5	599.5	35.0
361	590.5	165.63	356.0	368.0	12.0	567.5	601.0	33.5
380	590.5	324.27	368.0	387.0	19.0	570.0	601.0	31.0
393	590.5	877.87	387.0	406.0	19.0	567.5	599.5	32.0
413	590.5	82.01	410.0	419.0	9.0	574.5	599.5	25.0
464	590.5	309.04	455.0	471.0	16.0	570.0	601.0	31.0
532	590.5	65.37	522.0	541.0	19.0	575.5	601.0	25.5
319	614.5	120.10	312.0	329.0	17.0	602.5	632.0	29.5
361	614.5	558.20	353.0	367.0	14.0	602.5	639.0	36.5
380	614.5	1001.84	367.0	388.0	21.0	599.5	639.0	39.5
393	614.5	999.99	388.0	406.0	18.0	599.5	640.5	41.0
413	614.5	241.12	406.0	422.0	16.0	599.5	633.5	34.0
464	614.5	999.99	453.0	474.0	21.0	599.5	640.5	41.0
532	614.5	248.66	522.0	546.0	24.0	599.5	637.5	38.0
578	614.5	48.58	573.0	582.0	9.0	602.5	633.5	31.0
361	652.5	33.29	355.0	366.0	11.0	643.0	668.5	25.5
381	652.5	57.03	366.0	387.0	21.0	641.5	668.0	26.5
393	652.5	151.17	387.0	406.0	19.0	641.5	671.0	29.5
413	652.5	18.31	407.0	419.0	12.0	641.5	672.5	31.0
464	652.5	66.59	457.0	471.0	14.0	643.0	675.5	32.5
316	701.5	15.86	314.0	327.0	13.0	686.5	713.5	27.0
361	701.5	70.04	358.0	368.0	10.0	677.0	709.0	32.0
381	701.5	128.73	368.0	387.0	19.0	677.0	720.5	43.5
393	701.5	366.39	387.0	408.0	21.0	677.0	720.5	43.5
413	701.5	32.75	408.0	421.0	13.0	682.5	719.0	36.5
464	701.5	115.89	457.0	473.0	16.0	674.0	717.5	43.5
532	701.5	28.40	523.0	541.0	18.0	671.0	717.5	46.5

**Table 46 Multiple ion doped sample Glass 2-22 – 0.0 mol % Eu, 0.5 mol % Tb and 0.0 mol % Dy**

Development and Application of Novel Tracers for Environmental Applications  
 Appendix II: Spectroscopic Characterisation Data

Excitation Wavelength / nm	Emission Wavelength / nm	Intensity	Peak width					
			Ex Wavelength			Em Wavelength		
			From	To	PW	From	To	PW
323	482.5	57.95	314.0	330.0	16.0	464.5	501.0	36.5
348	482.5	433.71	330.0	357.0	27.0	460.5	505.5	45.0
363	482.5	283.45	357.0	371.0	14.0	462.0	505.5	43.5
385	482.5	334.33	371.0	410.0	39.0	462.0	505.5	43.5
424	482.5	63.62	416.0	432.0	16.0	463.5	505.5	42.0
452	482.5	146.70	437.0	458.0	21.0	470.5	501.0	30.5
321	544	26.57	310.0	330.0	20.0	530.5	554.5	24.0
349	544	183.33	332.0	357.0	25.0	528.0	554.5	26.5
367	544	174.11	358.0	372.0	14.0	528.0	559.0	31.0
377	544	227.37	372.0	387.0	15.0	522.5	560.0	37.5
453	544	36.44	438.0	455.0	17.0	533.5	553.0	19.5
454	544	41.72	456.0	469.0	13.0	521.0	546.0	25.0
483	544	92.20	476.0	495.0	19.0	530.5	561.5	31.0
324	575.5	79.34	313.0	330.0	17.0	559.0	601.0	42.0
348	575.5	746.20	337.0	358.0	21.0	557.5	601.0	43.5
363	575.5	417.24	358.0	370.0	12.0	557.5	601.0	43.5
385	575.5	631.04	370.0	409.0	39.0	554.5	601.0	46.5
423	575.5	109.94	418.0	433.0	15.0	554.5	602.5	48.0
453	575.5	200.10	438.0	458.0	20.0	557.5	599.5	42.0
464	575.5	99.31	458.0	468.0	10.0	568.5	599.5	31.0
530	575.5	22.95	520.0	538.0	18.0	568.5	597.0	28.5
319	613.5	115.57	312.0	332.0	20.0	601.0	632.0	31.0
350	613.5	141.88	339.0	355.0	16.0	602.5	637.5	35.0
361	613.5	543.10	355.0	367.0	12.0	601.0	641.5	40.5
381	613.5	943.02	367.0	387.0	20.0	601.0	639.0	38.0
394	613.5	999.99	387.0	407.0	20.0	601.0	639.0	38.0
413	613.5	210.32	407.0	421.0	14.0	602.5	636.0	33.5
464	613.5	1002.95	455.0	475.0	20.0	599.5	640.5	41.0
483	613.5	51.49	475.0	494.0	19.0	604.0	636.0	32.0
532	613.5	192.54	520.0	545.0	25.0	599.5	637.5	38.0
577	613.5	39.46	570.0	581.0	11.0	604.0	637.5	33.5
350	654.5	26.39	337.0	355.0	18.0	643.0	682.5	39.5
361	654.5	34.34	355.0	368.0	13.0	643.0	677.0	34.0
381	654.5	60.05	368.0	387.0	19.0	643.0	668.5	25.5
393	654.5	131.69	387.0	407.0	20.0	641.5	668.5	27.0
452	654.5	16.11	447.0	455.0	8.0	646.0	688.5	42.5
464	654.5	57.13	455.0	472.0	17.0	641.5	670.0	28.5
531	654.5	14.64	520.0	540.0	20.0	641.5	671.0	29.5
317	702	41.48	312.0	329.0	17.0	684.0	713.5	29.5
361	702	60.62	359.0	367.0	8.0	682.5	706.5	24.0
380	702	114.28	367.0	388.0	21.0	679.5	720.5	41.0
393	702	322.29	388.0	407.0	19.0	675.5	720.5	45.0
413	702	25.28	407.0	422.0	15.0	678.5	717.5	39.0
464	702	97.25	455.0	471.0	16.0	674.0	720.5	46.5
532	702	23.91	519.0	540.0	21.0	674.0	720.5	46.5
348	758	17.55	337.0	356.0	19.0	738.5	772.5	34.0
453	758	9.11	446.0	457.0	11.0	731.5	767.0	35.5

**Table 47 Multiple ion doped sample Glass 2-23 – 2.0 mol % Eu, 1.0 mol % Tb and 0.5 mol % Dy**

Development and Application of Novel Tracers for Environmental Applications  
 Appendix II: Spectroscopic Characterisation Data

Excitation Wavelength / nm	Emission Wavelength / nm	Intensity	Peak width					
			Ex Wavelength			Em Wavelength		
			From	To	PW	From	To	PW
323	481.5	67.65	313.0	329.0	16.0	461.5	504.5	43.0
348	481.5	357.31	339.0	356.0	17.0	458.5	504.5	46.0
363	481.5	250.40	360.0	370.0	10.0	460.5	500.5	40.0
388	481.5	290.81	372.0	410.0	38.0	458.5	502.5	44.0
423	481.5	72.44	419.0	432.0	13.0	458.5	499.5	41.0
452	481.5	158.87	439.0	459.0	20.0	471.5	505.5	34.0
318	544	31.36	312.0	320.0	8.0	533.0	552.5	19.5
323	544	34.88	320.0	327.0	7.0	530.0	552.5	22.5
350	544	206.18	332.0	355.0	23.0	529.0	556.5	27.5
356	544	188.99	358.0	365.0	7.0	529.0	558.5	29.5
376	544	229.74	372.0	382.0	10.0	513.5	560.5	47.0
424	544	29.74	419.0	430.0	11.0	532.0	552.5	20.5
452	544	58.00	438.0	460.0	22.0	531.0	554.5	23.5
463	544	33.33	460.0	468.0	8.0	540.5	548.5	8.0
483	544	89.17	474.0	475.0	1.0	540.5	563.0	22.5
323	574	78.65	313.0	329.0	16.0	529.0	601.5	72.5
348	574	542.19	337.0	357.0	20.0	560.5	601.5	41.0
363	574	328.38	357.0	370.0	13.0	555.5	600.5	45.0
386	574	515.34	372.0	410.0	38.0	558.5	600.5	42.0
424	574	125.06	417.0	431.0	14.0	555.5	600.5	45.0
452	574	202.48	439.0	459.0	20.0	553.5	600.5	47.0
463	574	73.23	460.0	467.0	7.0	552.5	599.5	47.0
473	574	65.83	467.0	491.0	24.0	567.0	590.5	23.5
318	615	88.98	313.0	329.0	16.0	558.5	627.5	69.0
348	615	128.15	341.0	356.0	15.0	598.5	636.5	38.0
361	615	317.56	356.0	367.0	11.0	602.0	636.5	34.5
381	615	545.95	369.0	388.0	19.0	599.5	638.5	39.0
393	615	999.99	388.0	407.0	19.0	600.5	640.5	40.0
412	615	126.31	407.0	423.0	16.0	600.5	635.5	35.0
465	615	506.05	456.0	474.0	18.0	600.5	637.5	37.0
484	615	56.41	479.0	495.0	16.0	602.0	631.5	29.5
531	615	25.34	519.0	544.0	25.0	599.5	636.5	37.0
578	615	31.77	573.0	581.0	8.0	603.0	627.5	24.5
349	652.5	23.47	341.0	356.0	15.0	643.5	677.5	34.0
362	652.5	27.43	356.0	369.0	13.0	642.5	673.5	31.0
381	652.5	43.84	371.0	388.0	17.0	640.5	665.5	25.0
392	652.5	93.20	388.0	397.0	9.0	640.5	672.5	32.0
463	652.5	40.13	458.0	468.0	10.0	639.5	672.5	33.0
319	699.5	17.86	314.0	325.0	11.0	698.0	702.0	4.0
361	699.5	45.21	358.0	364.0	6.0	691.0	705.0	14.0
381	699.5	76.07	371.0	388.0	17.0	679.5	715.5	36.0
393	699.5	180.18	388.0	406.0	18.0	673.5	719.5	46.0
414	699.5	19.02	410.0	418.0	8.0	688.0	716.5	28.5
465	699.5	45.27	458.0	469.0	11.0	679.5	712.5	33.0
483	699.5	10.90	479.0	490.0	11.0	696.0	704.0	8.0
533	699.5	18.30	522.0	545.0	23.0	694.0	708.5	14.5
351	750.5	15.10	342.0	355.0	13.0	741.0	761.5	20.5
443	750.5	9.60	440.0	463.0	23.0	748.5	752.5	4.0

**Table 48 Multiple ion doped sample Glass 2-24 – 2.0 mol % Eu, 1.5 mol % Tb and 1.0 mol % Dy**



Development and Application of Novel Tracers for Environmental Applications  
 Appendix II: Spectroscopic Characterisation Data

Excitation Wavelength / nm	Emission Wavelength / nm	Intensity	Peak width					
			Ex Wavelength			Em Wavelength		
			From	To	PW	From	To	PW
323	483.5	63.39	311.0	330.0	19.0	464.5	503.5	39.0
348	483.5	426.05	330.0	357.0	27.0	457.5	506.5	49.0
363	483.5	309.81	357.0	371.0	14.0	460.5	508.5	48.0
386	483.5	384.69	371.0	410.0	39.0	458.5	506.5	48.0
423	483.5	78.51	414.0	435.0	21.0	465.5	501.5	36.0
451	483.5	174.54	435.0	459.0	24.0	473.5	503.5	30.0
322	545	38.80	311.0	329.0	18.0	533.0	557.5	24.5
350	545	329.94	332.0	355.0	23.0	530.0	557.5	27.5
365	545	277.04	358.0	371.0	13.0	528.0	560.5	32.5
377	545	354.87	371.0	381.0	10.0	528.0	560.5	32.5
385	545	221.90	381.0	412.0	31.0	530.0	555.5	25.5
424	545	43.96	417.0	431.0	14.0	530.0	555.5	25.5
452	545	85.54	439.0	459.0	20.0	527.0	555.5	28.5
483	545	125.02	477.0	496.0	19.0	530.0	562.0	32.0
323	575	90.69	314.0	329.0	15.0	560.5	596.5	36.0
349	575	729.89	337.0	357.0	20.0	557.5	601.5	44.0
363	575	445.15	357.0	371.0	14.0	558.5	601.5	43.0
385	575	695.69	371.0	411.0	40.0	555.5	600.5	45.0
423	575	136.11	417.0	434.0	17.0	557.5	600.5	43.0
452	575	266.09	437.0	460.0	23.0	557.5	600.5	43.0
463	575	86.34	460.0	467.0	7.0	564.0	600.5	36.5
470	575	90.29	467.0	481.0	14.0	558.5	599.5	41.0
531	575	18.74	519.0	538.0	19.0	568.0	629.5	61.5
319	614.5	83.89	313.0	332.0	19.0	601.5	637.5	36.0
350	614.5	179.49	337.0	355.0	18.0	601.5	640.5	39.0
362	614.5	380.13	355.0	369.0	14.0	601.5	637.5	36.0
381	614.5	646.25	369.0	388.0	19.0	600.5	640.5	40.0
393	614.5	999.99	388.0	406.0	18.0	600.5	637.5	37.0
414	614.5	140.29	406.0	420.0	14.0	600.5	641.5	41.0
465	614.5	580.96	456.0	474.0	18.0	599.5	638.5	39.0
483	614.5	650.30	474.0	495.0	21.0	601.5	640.5	39.0
532	614.5	132.35	521.0	544.0	23.0	600.5	674.5	74.0
348	649	21.27	339.0	357.0	18.0	643.5	672.5	29.0
361	649	28.71	357.0	369.0	12.0	641.5	672.5	31.0
382	649	42.05	369.0	388.0	19.0	639.5	672.5	33.0
392	649	85.60	388.0	405.0	17.0	642.5	673.5	31.0
463	649	41.37	456.0	470.0	14.0	642.5	707.5	65.0
319	700.5	9.58	315.0	325.0	10.0	690.0	706.0	16.0
361	700.5	45.71	358.0	362.0	4.0	682.5	719.5	37.0
381	700.5	77.88	369.0	388.0	19.0	680.5	723.5	43.0
393	700.5	206.96	388.0	407.0	19.0	677.5	715.5	38.0
414	700.5	18.88	410.0	419.0	9.0	677.5	716.5	39.0
465	700.5	57.42	458.0	470.0	12.0	677.5	767.5	90.0
484	700.5	9.68	476.0	493.0	17.0	654.0	711.5	57.5
532	700.5	17.64	522.0	544.0	22.0	690.0	765.5	75.5
348	754.5	17.16	336.0	355.0	19.0	742.0	765.5	23.5
451	754.5	9.13	439.0	456.0	17.0	744.0	765.5	21.5

**Table 49 Multiple ion doped sample Glass 2-25 – 2.0 mol % Eu, 2.0 mol % Tb and 1.5 mol % Dy**

### **Appendix III: Lifetime Data**

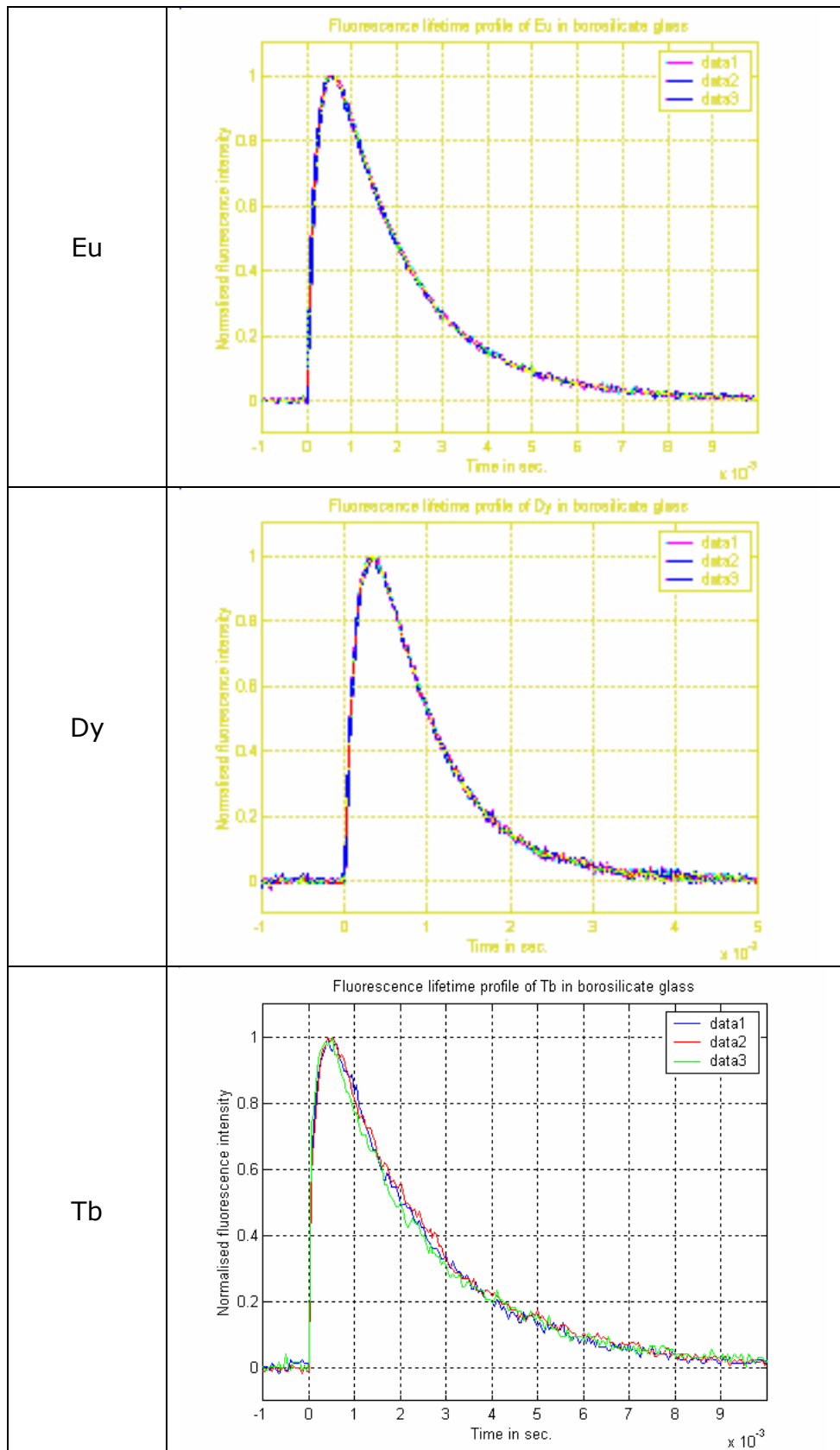


Figure 1 Eu, Dy and Tb fluorescent lifetimes in G1-01

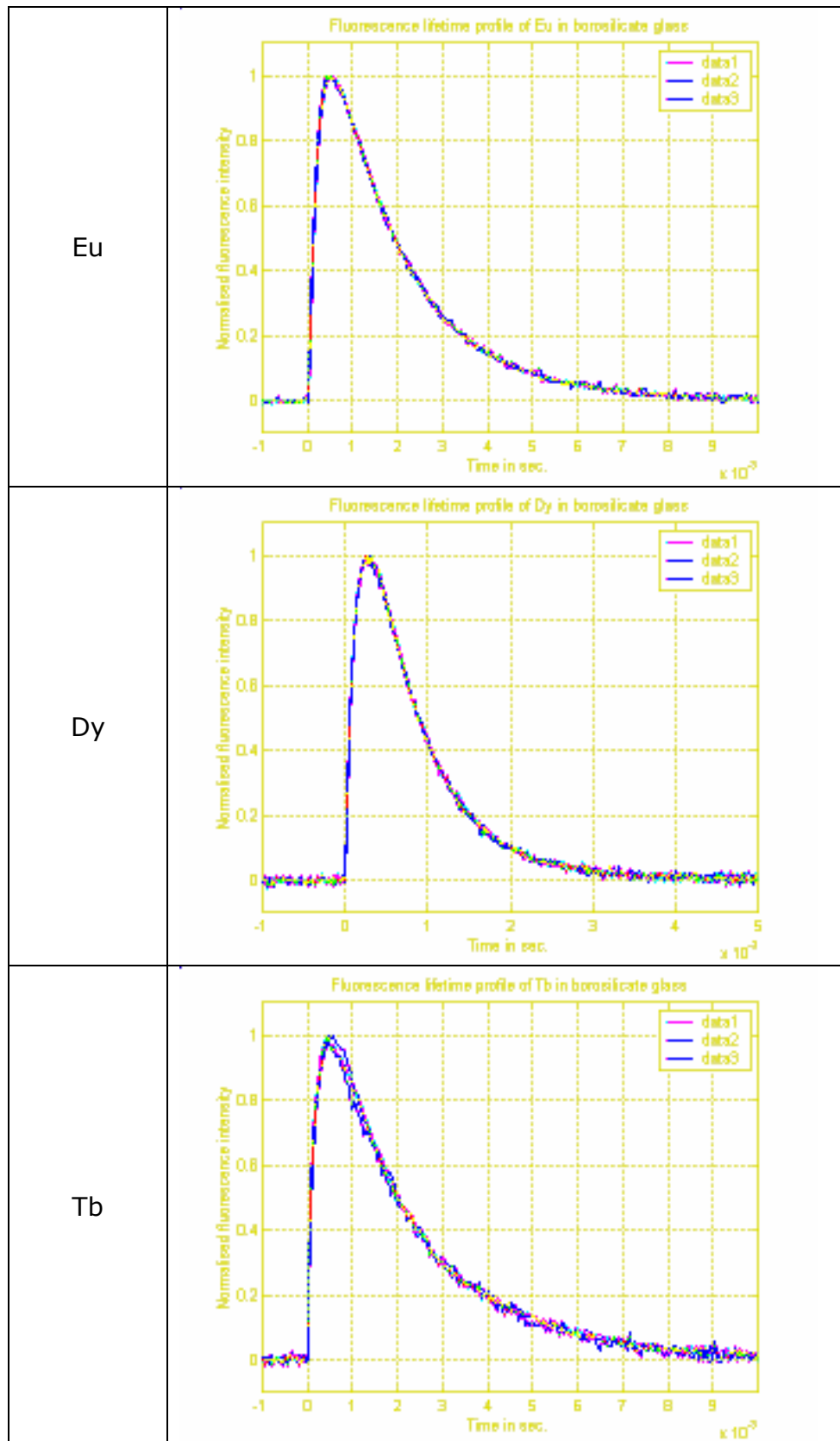


Figure 2 Eu, Dy and Tb fluorescent lifetimes in G1-02

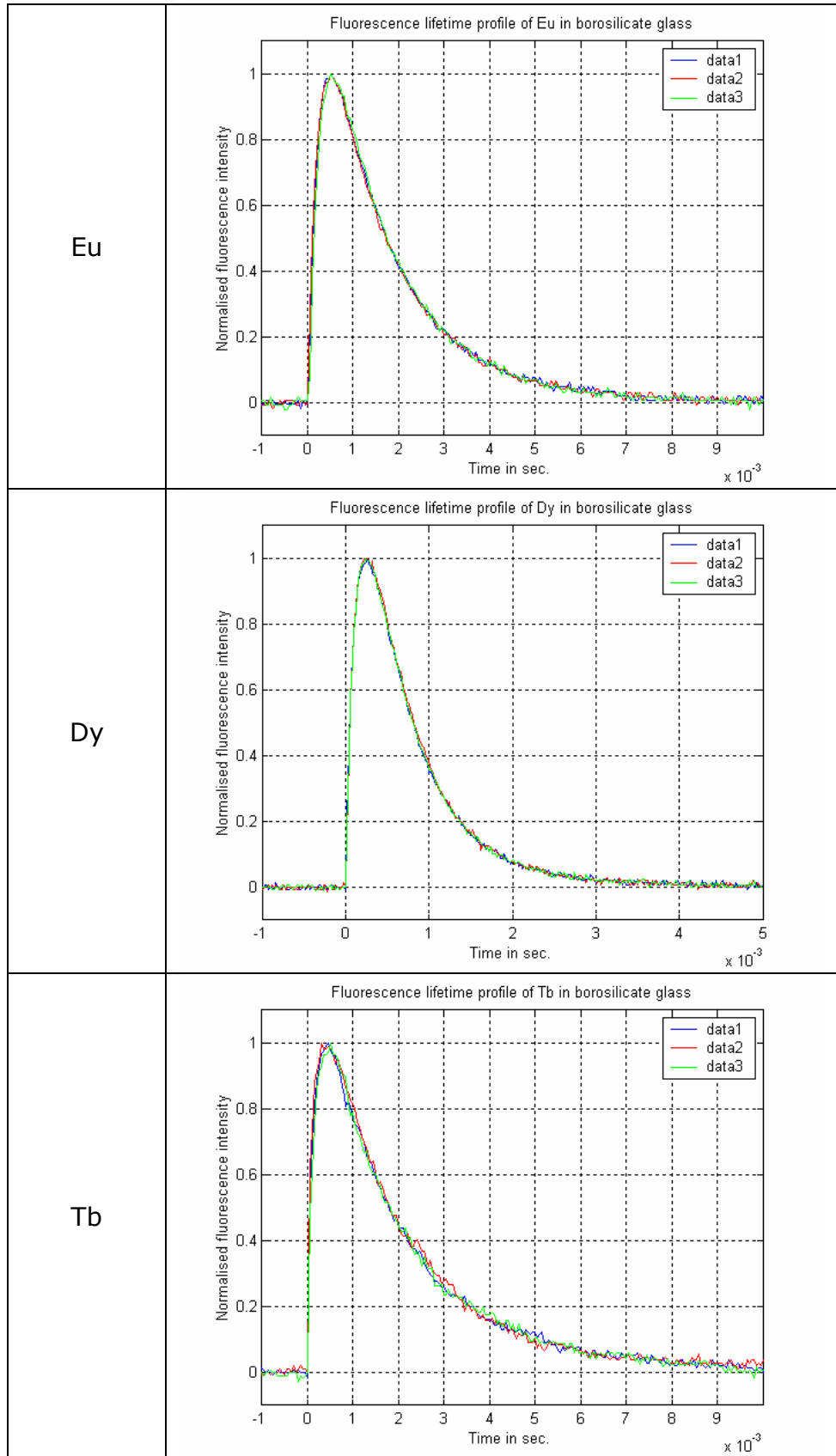


Figure 3 Eu, Dy and Tb fluorescent lifetimes in G1-03

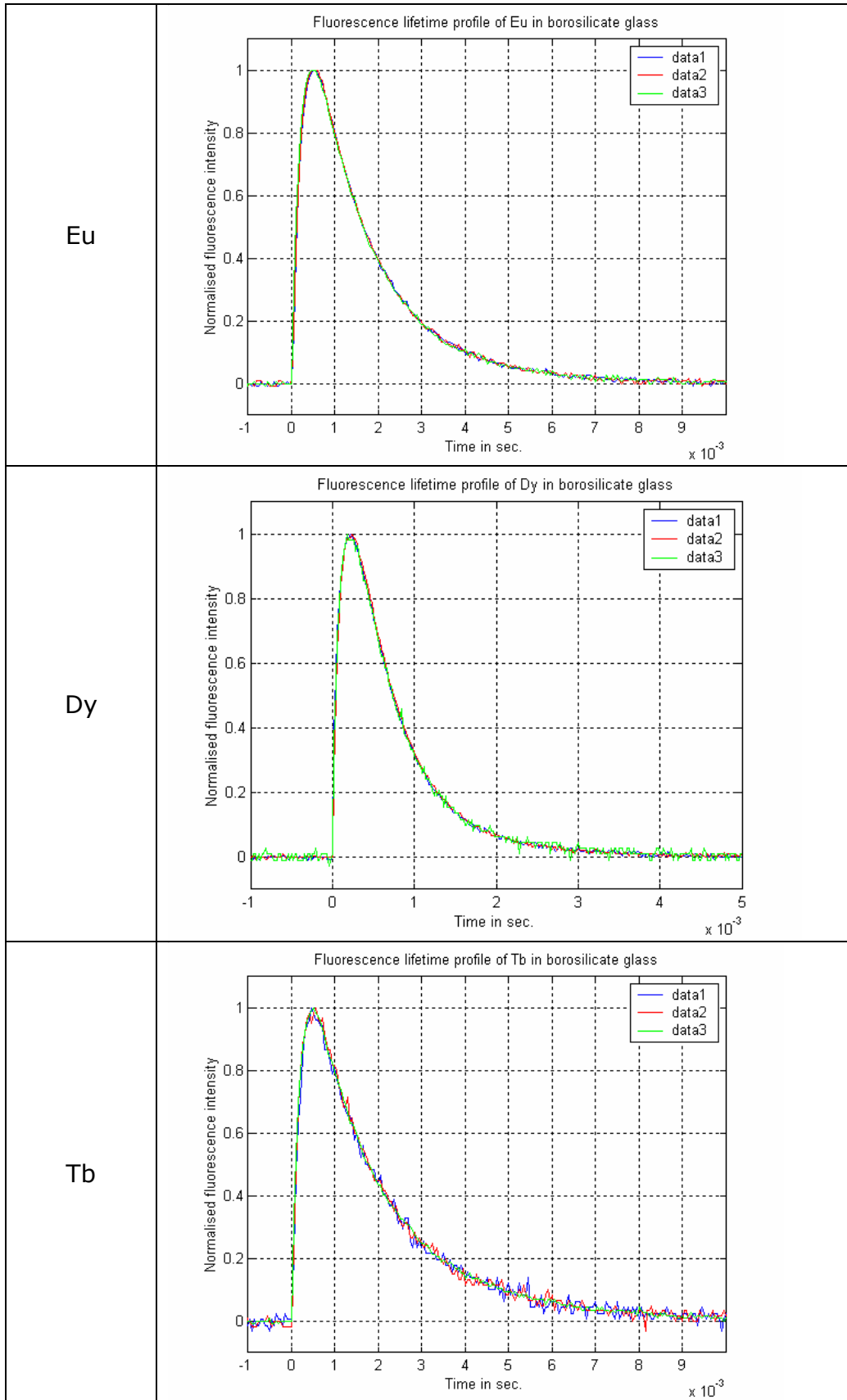


Figure 4 Eu, Dy and Tb fluorescent lifetimes in G1-04

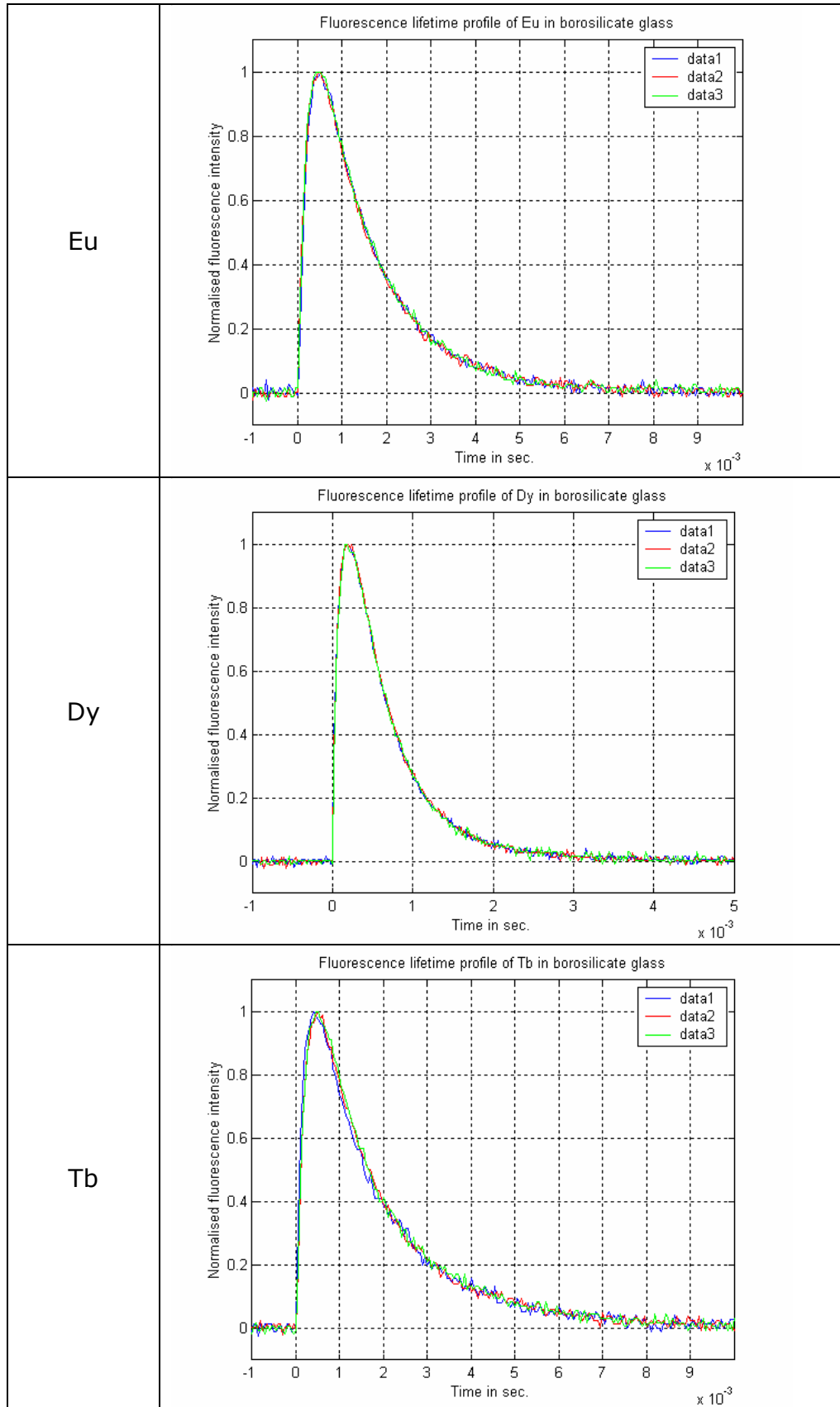


Figure 5 Eu, Dy and Tb fluorescent lifetimes in G1-05

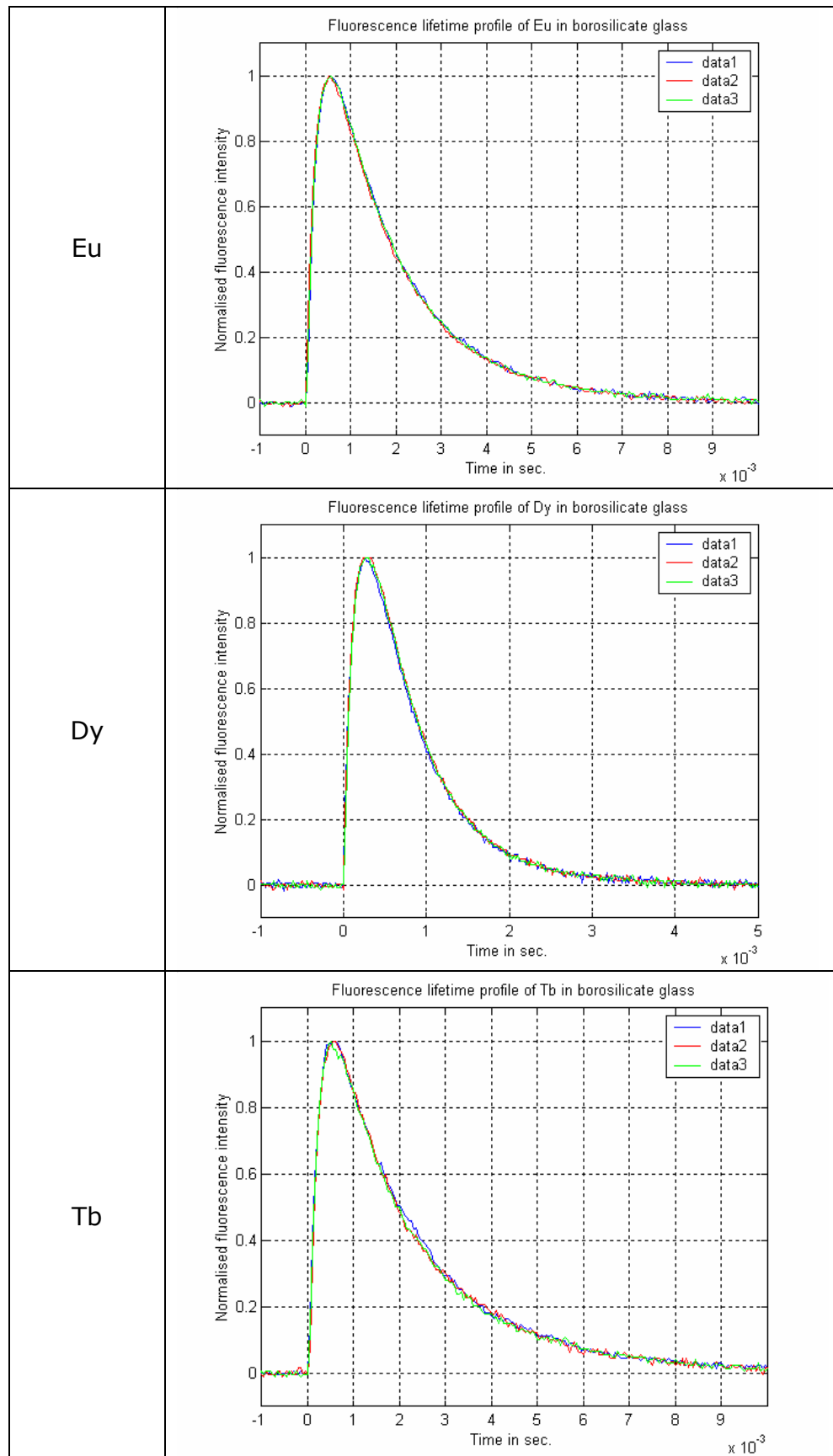


Figure 6 Eu, Dy and Tb fluorescent lifetimes in G1-06



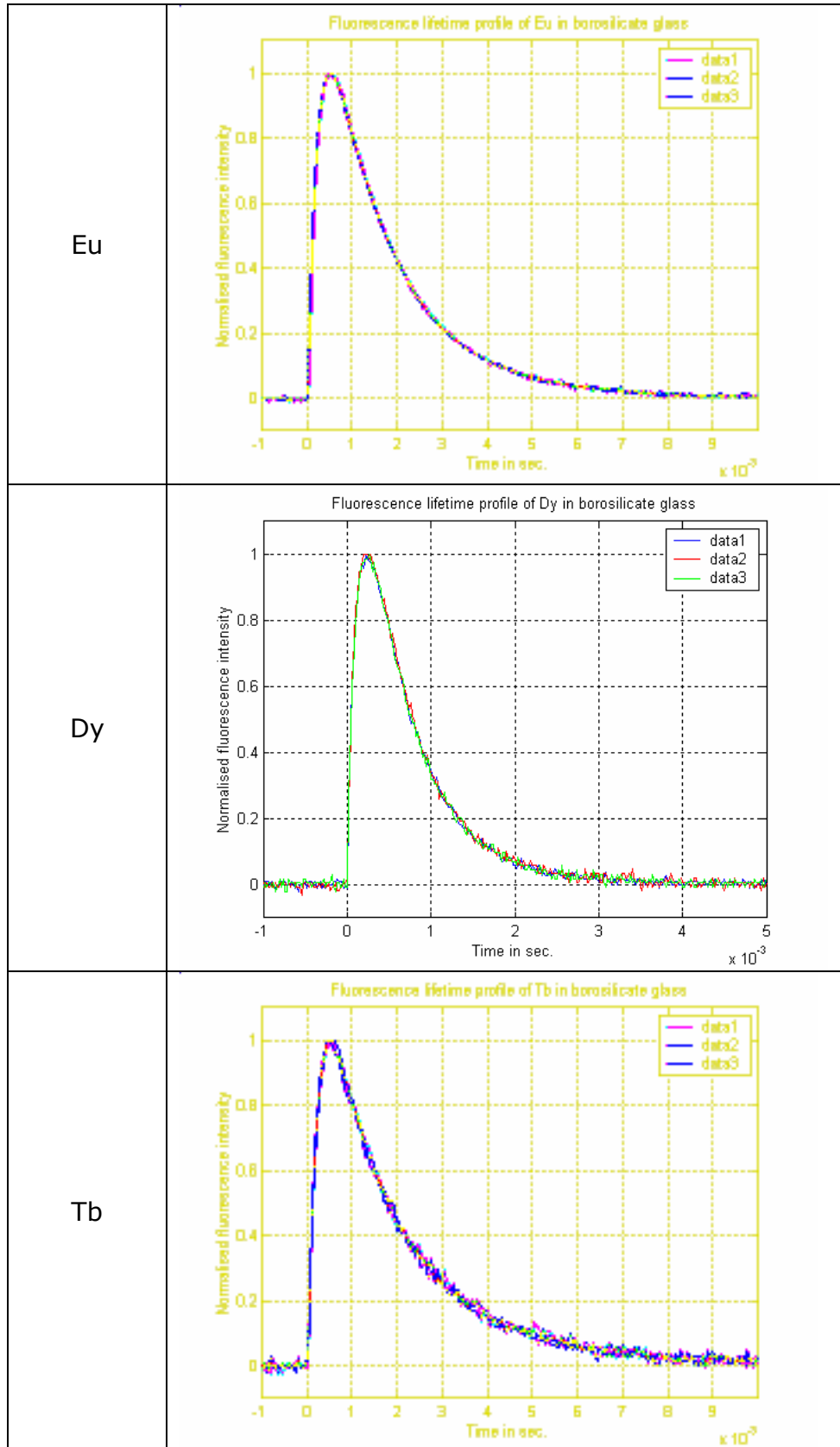


Figure 7 Eu, Dy and Tb fluorescent lifetimes in G1-07

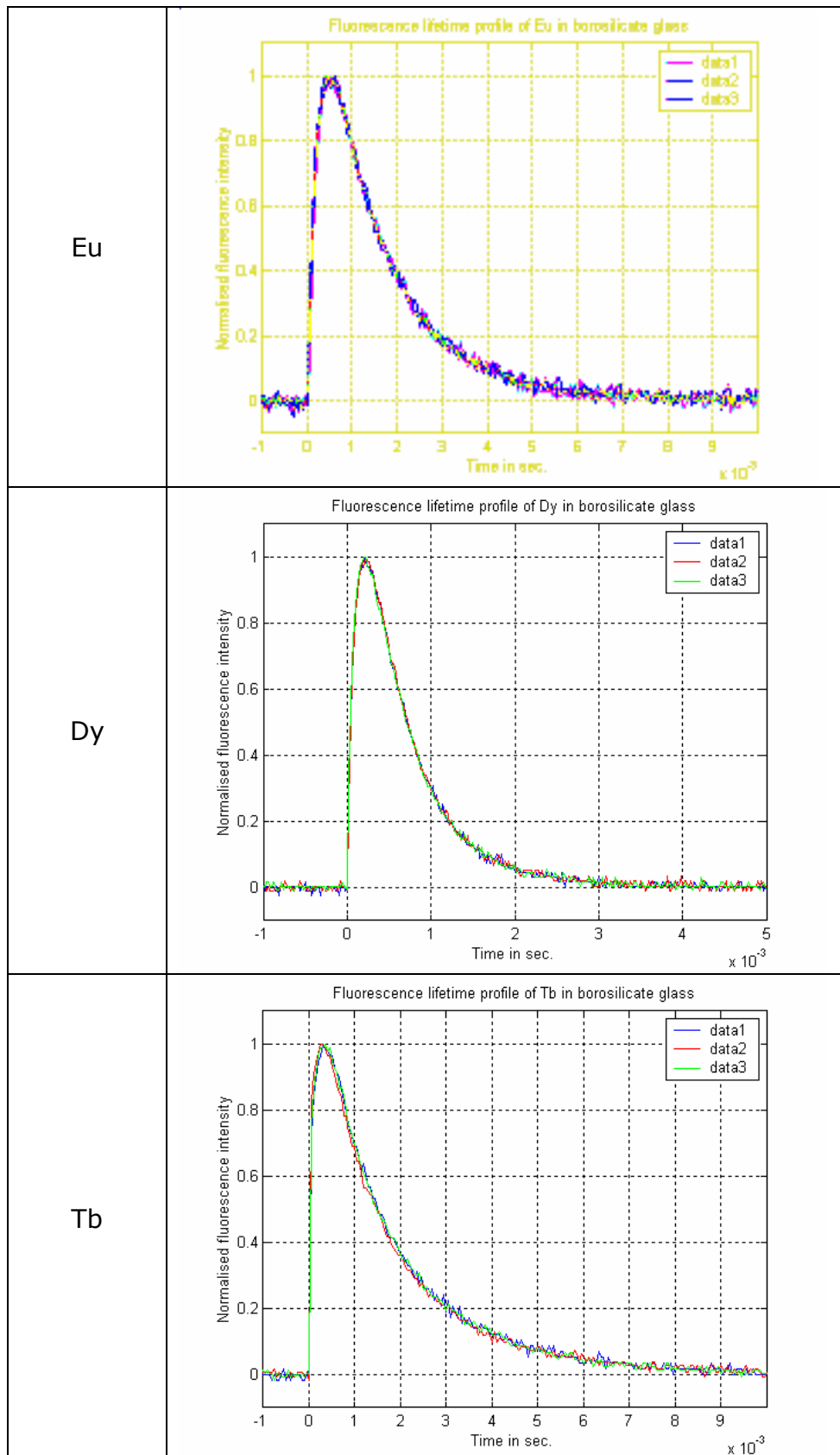


Figure 8 Eu, Dy and Tb fluorescent lifetimes in G1-08

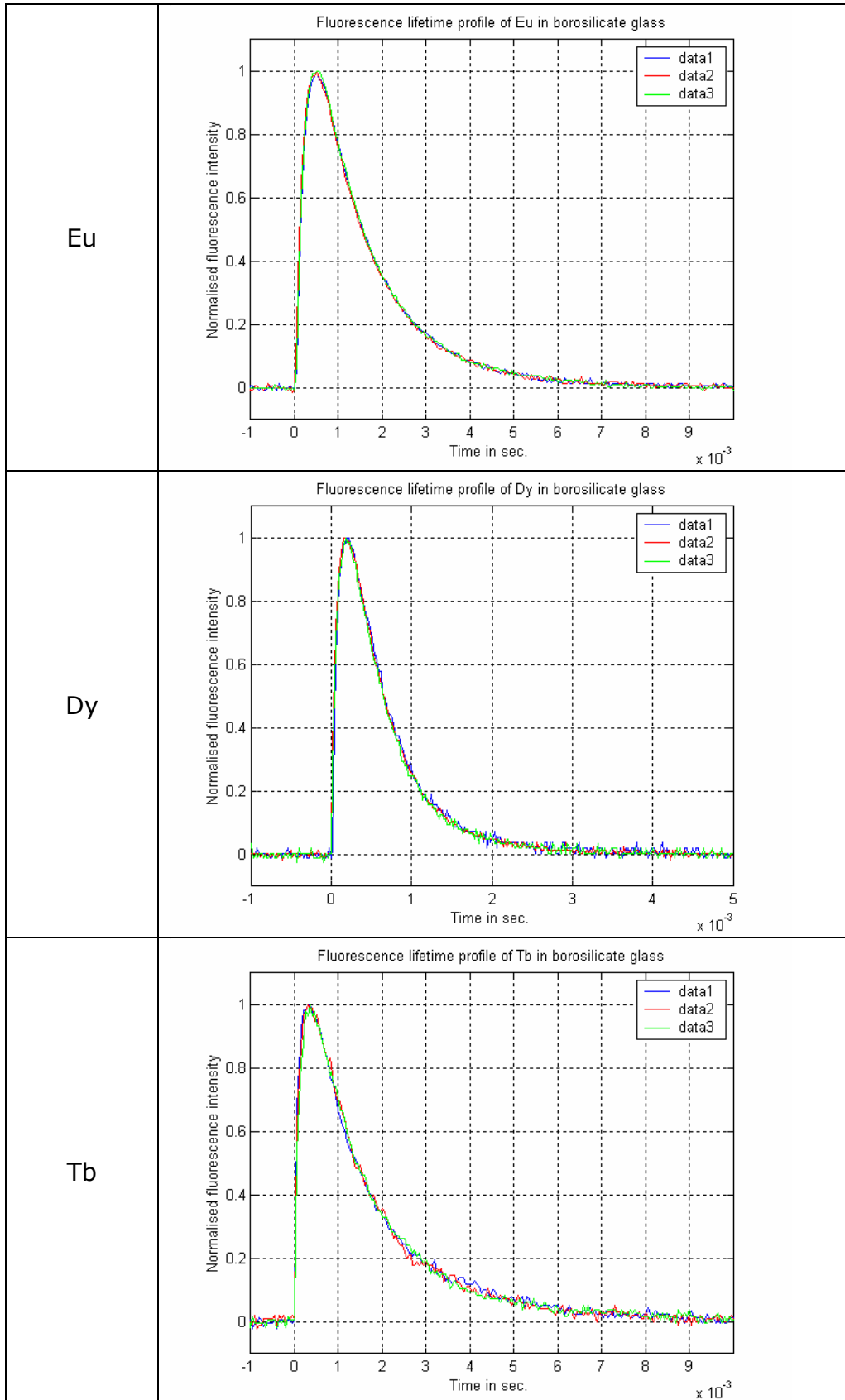


Figure 9 Eu, Dy and Tb fluorescent lifetimes in G1-09

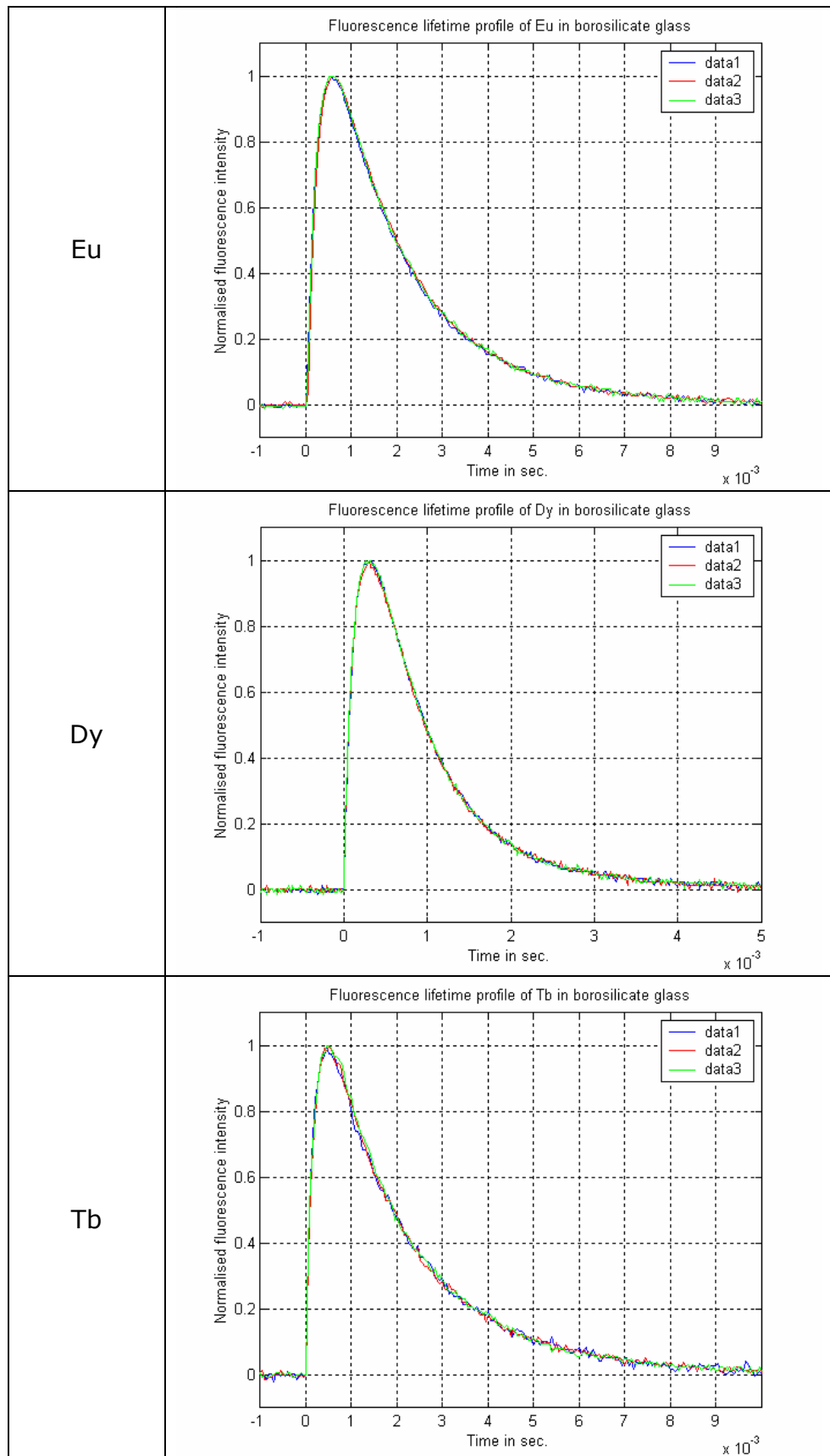


Figure 10 Eu, Dy and Tb fluorescent lifetimes in G1-10

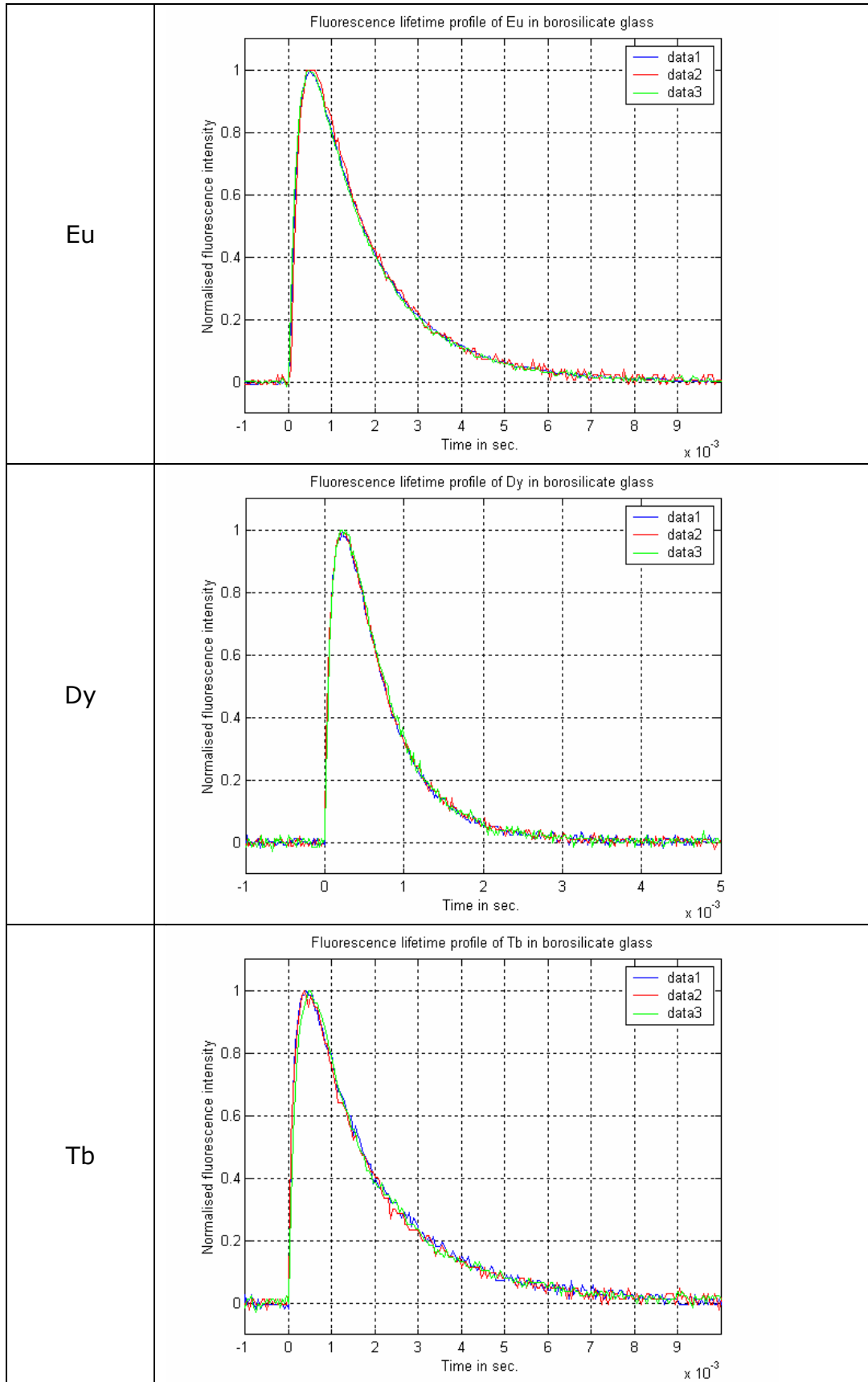


Figure 11 Eu, Dy and Tb fluorescent lifetimes in G1-11

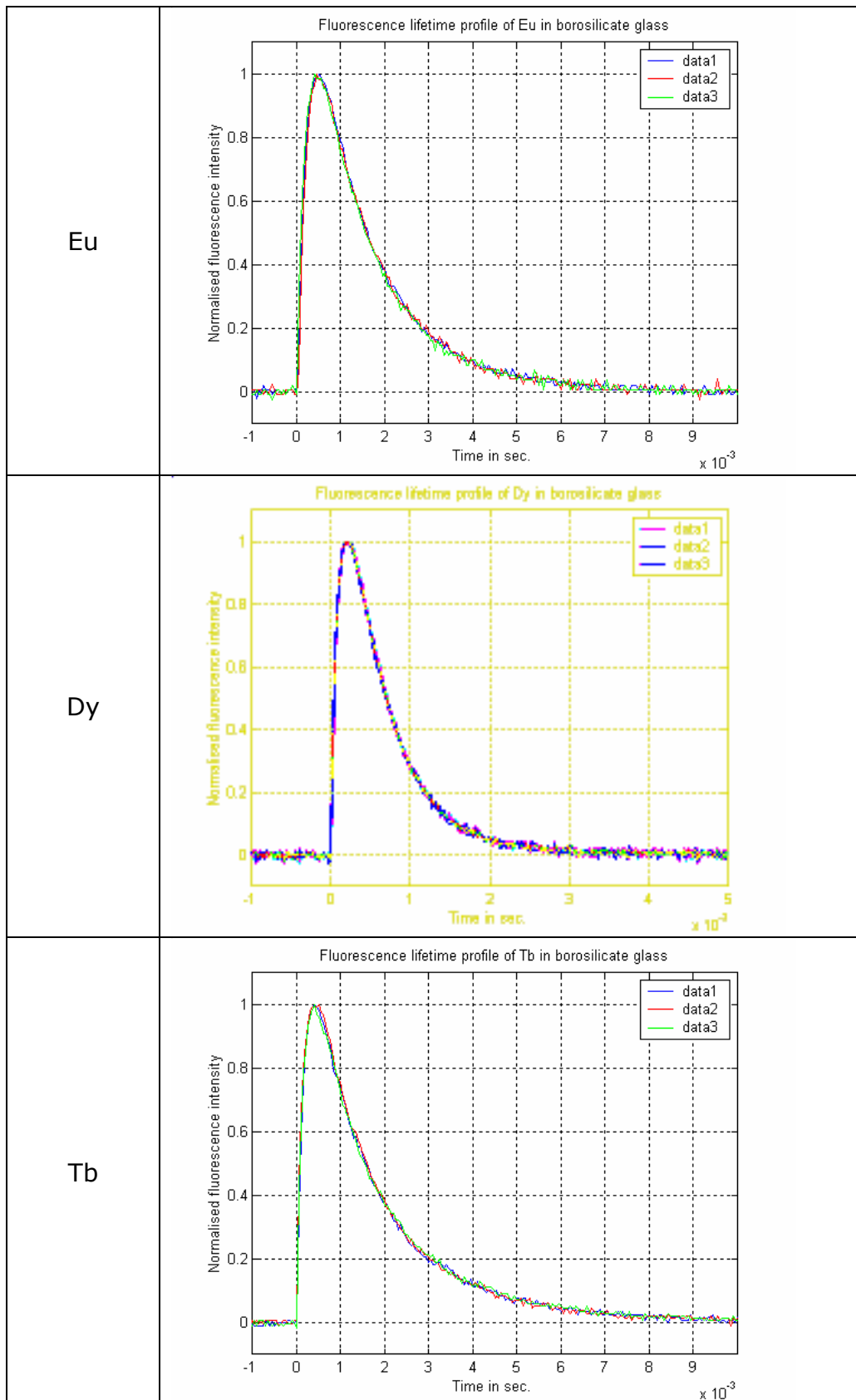


Figure 12 Eu, Dy and Tb fluorescent lifetimes in G1-12

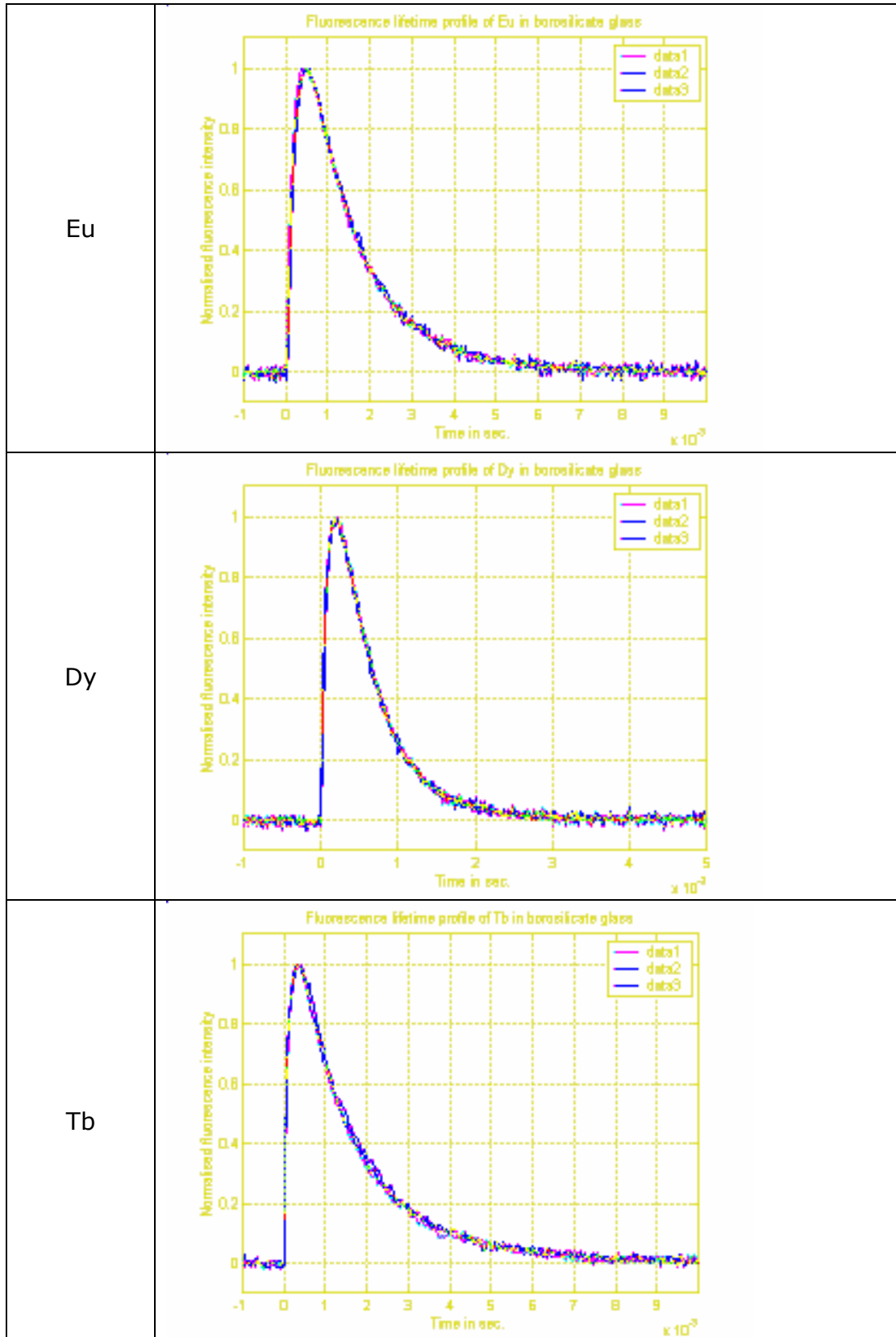


Figure 13 Eu, Dy and Tb fluorescent lifetimes in G1-13

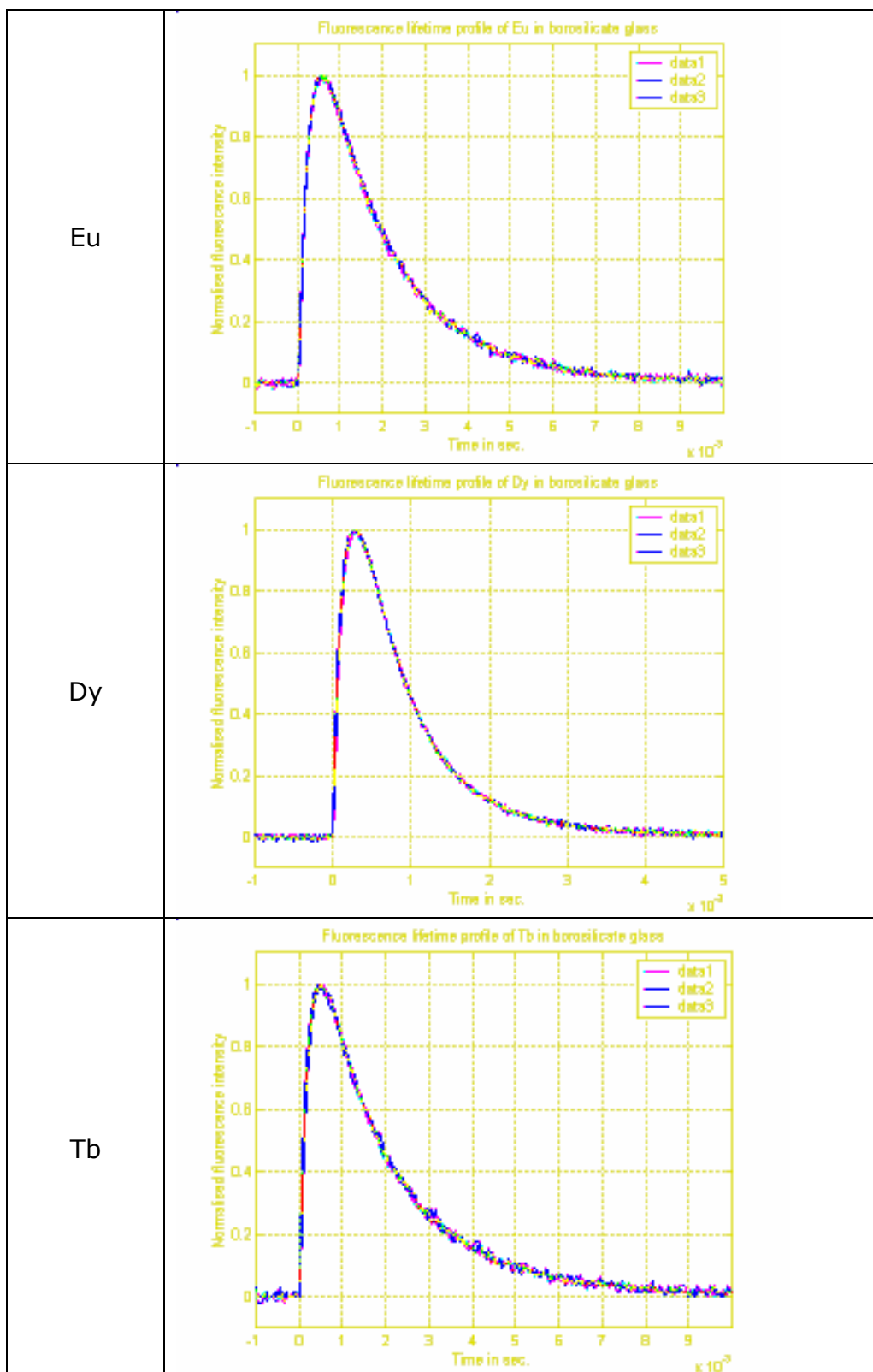


Figure 14 Eu, Dy and Tb fluorescent lifetimes in G1-14



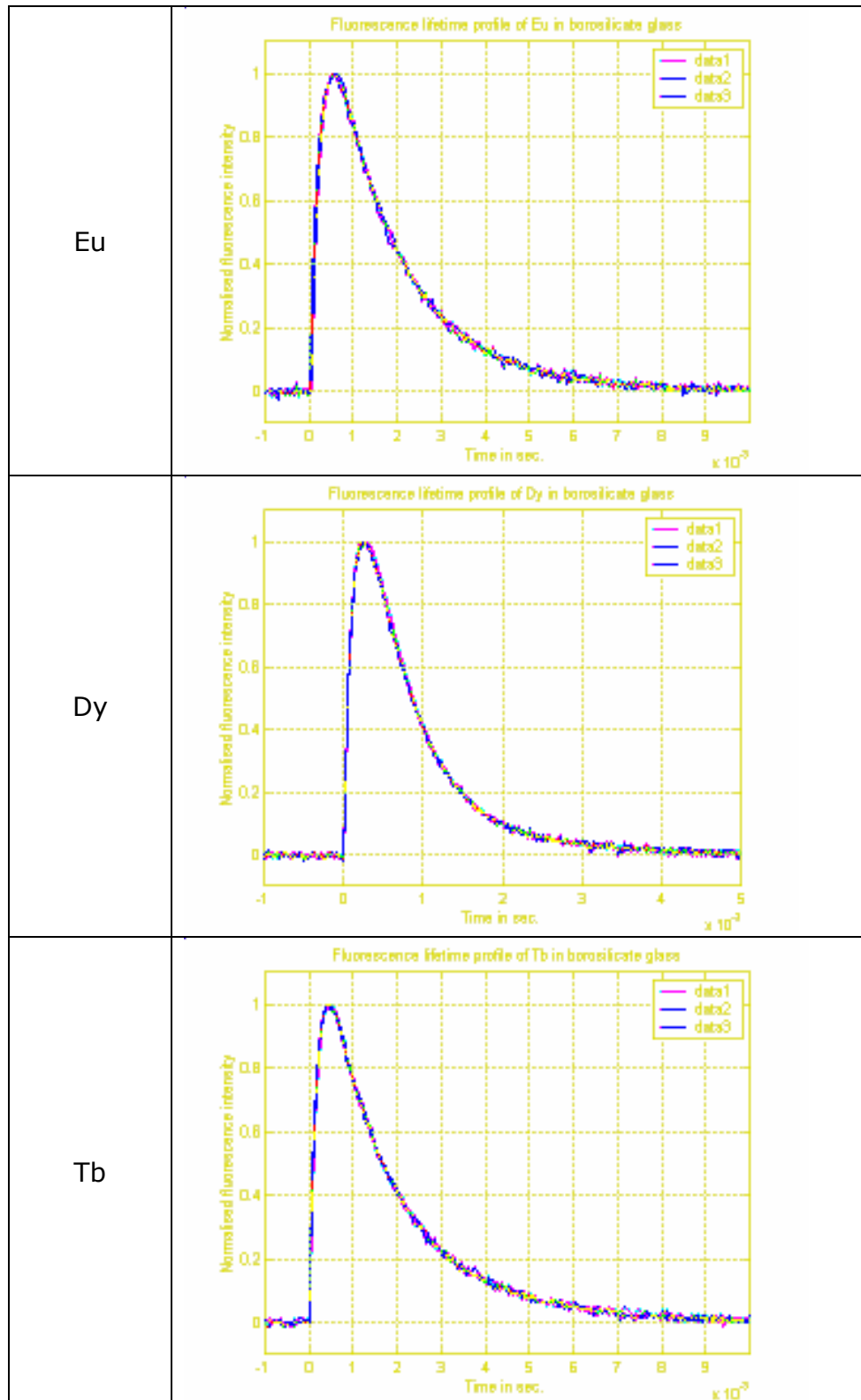


Figure 15 Eu, Dy and Tb fluorescent lifetimes in G1-15

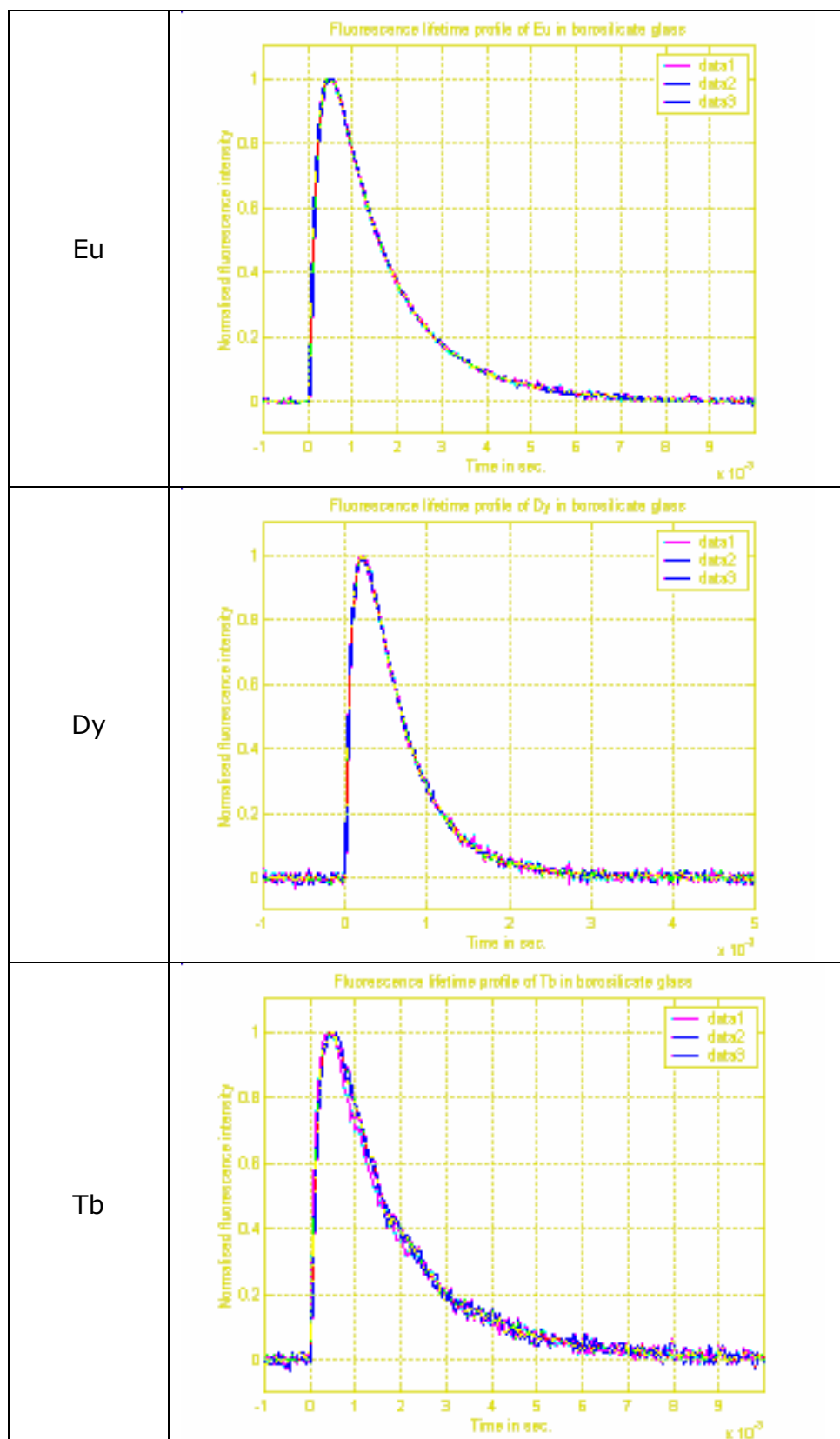


Figure 16 Eu, Dy and Tb fluorescent lifetimes in G1-16

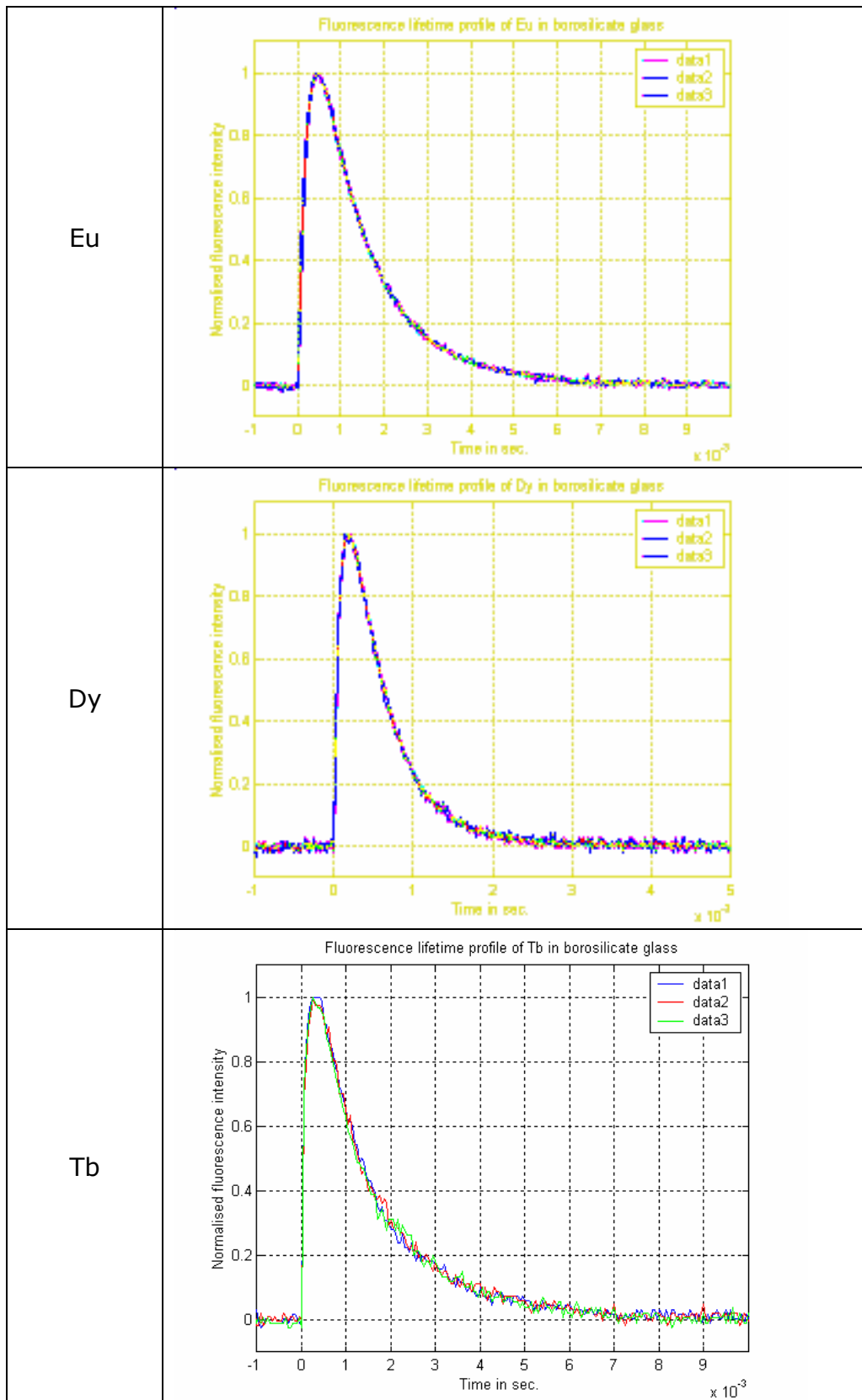


Figure 17 Eu, Dy and Tb fluorescent lifetimes in G1-17

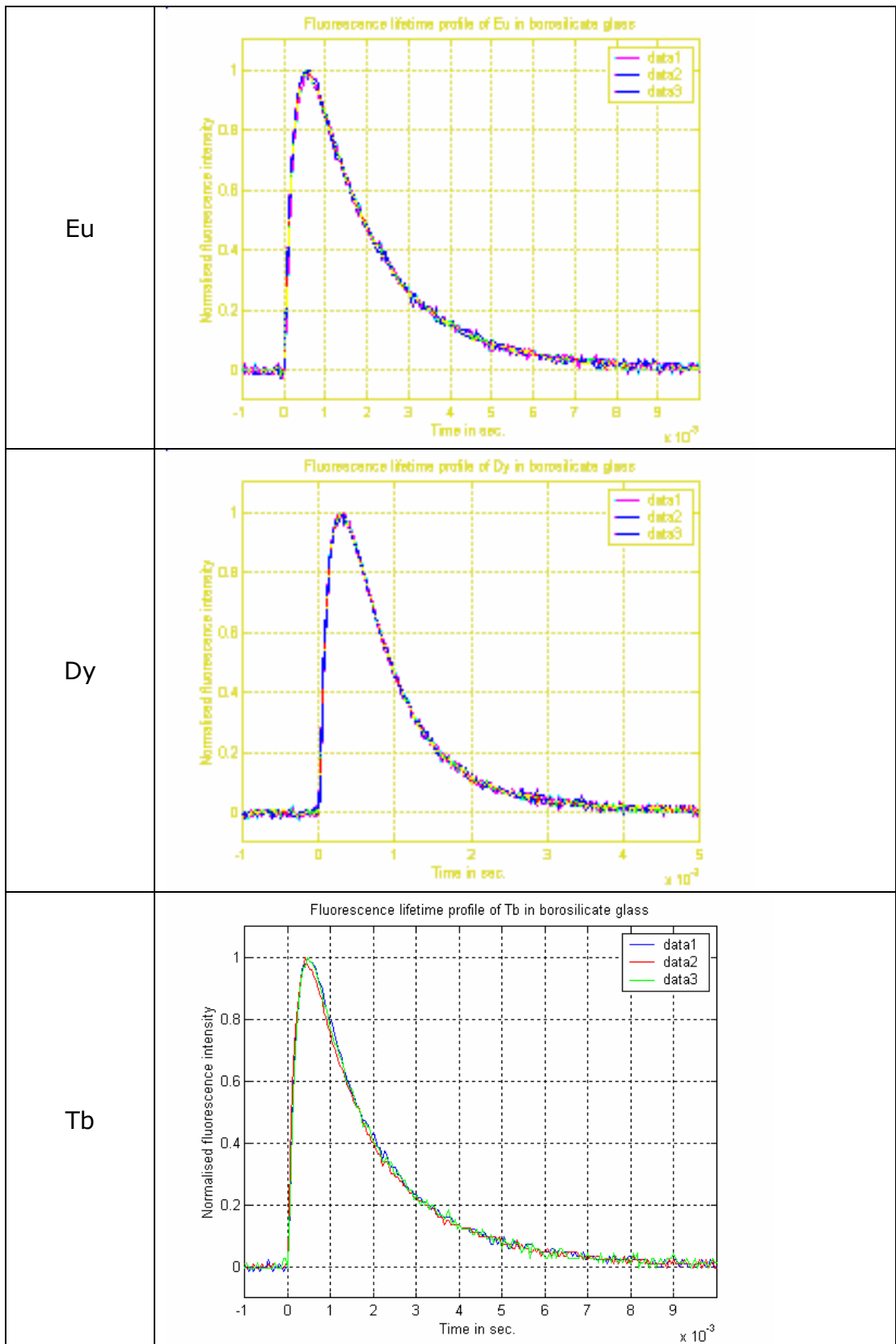


Figure 18 Eu, Dy and Tb fluorescent lifetimes in G1-18

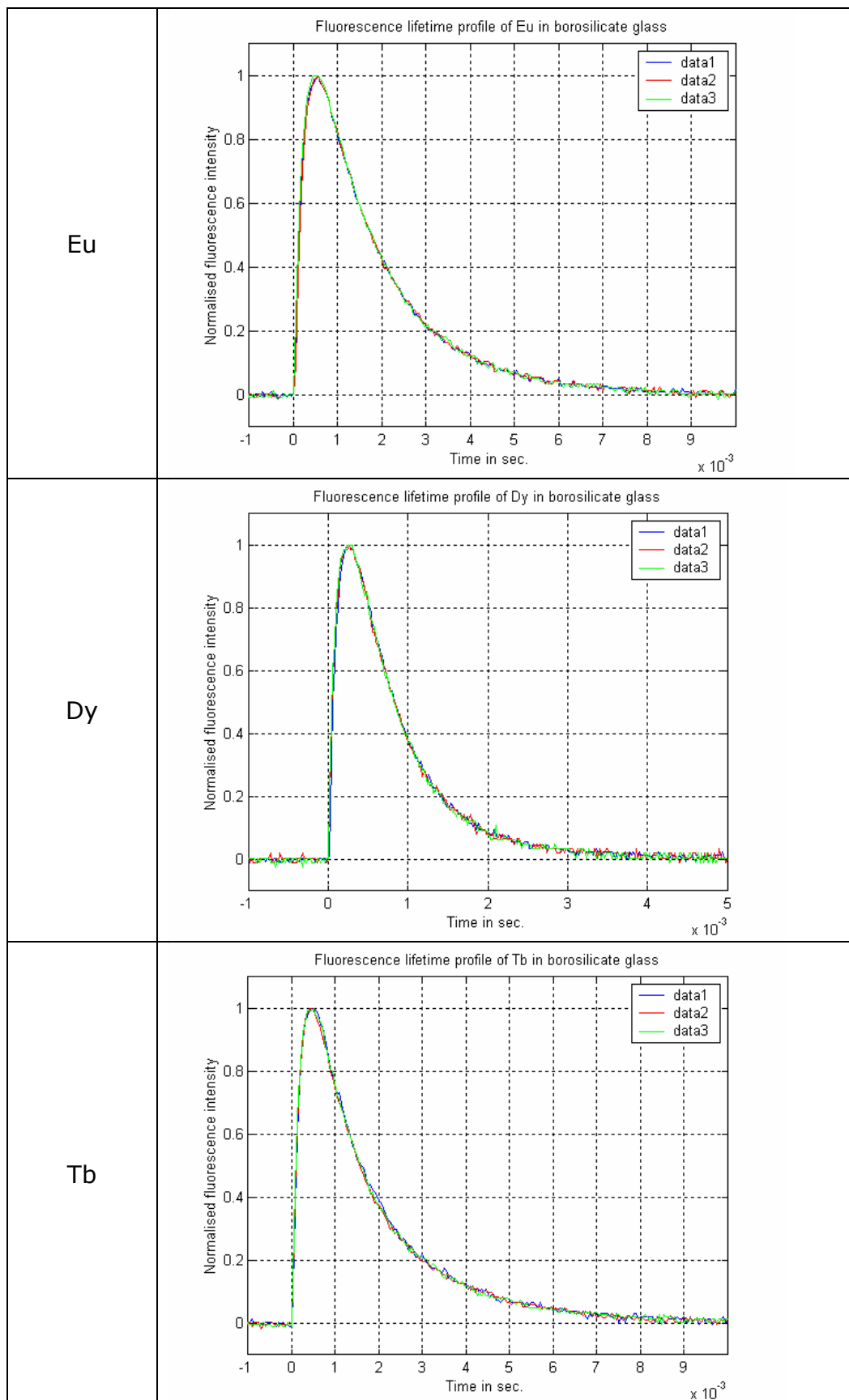


Figure 19 Eu, Dy and Tb fluorescent lifetimes in G1-19

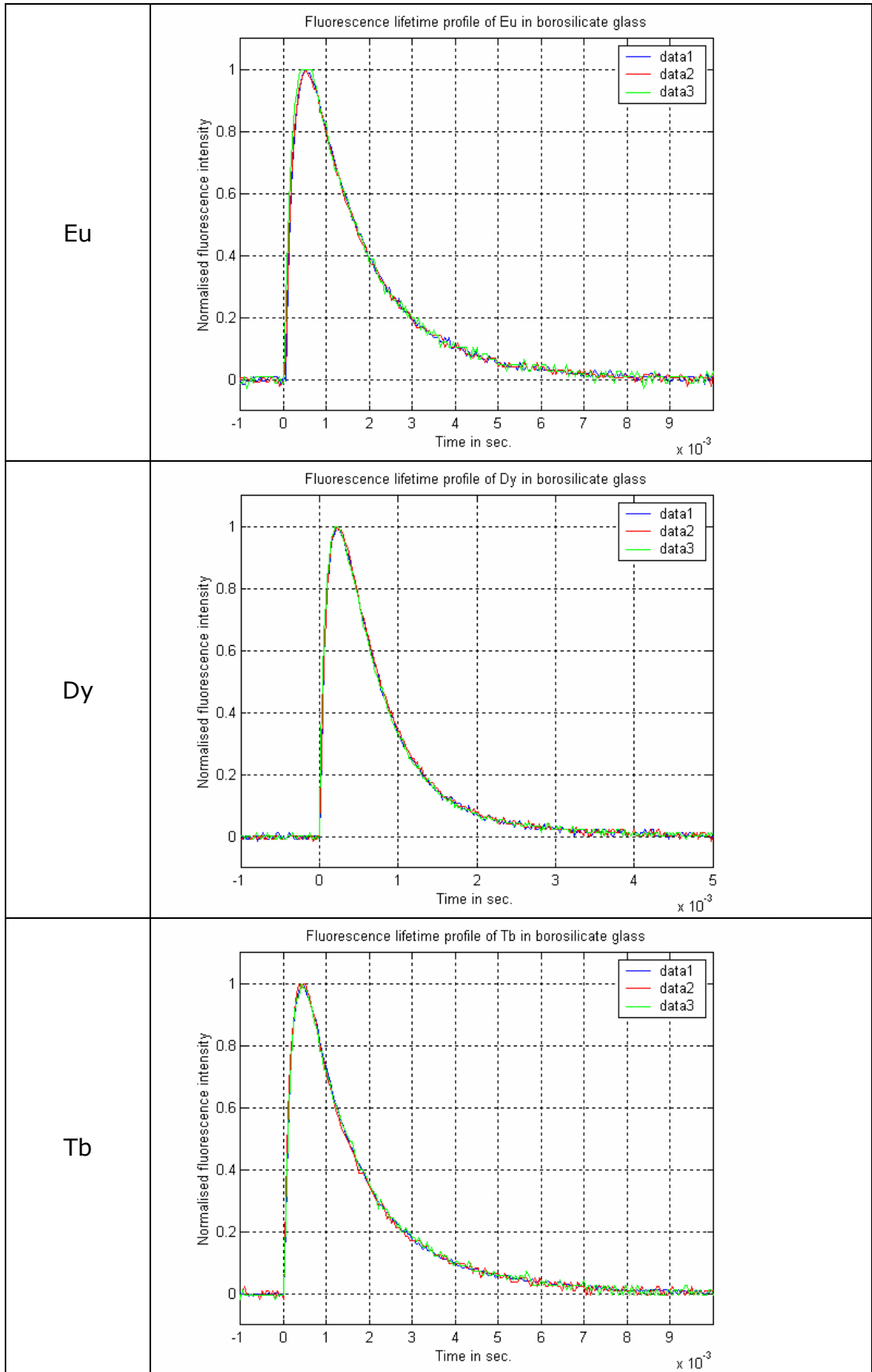


Figure 20 Eu, Dy and Tb fluorescent lifetimes in G1-20

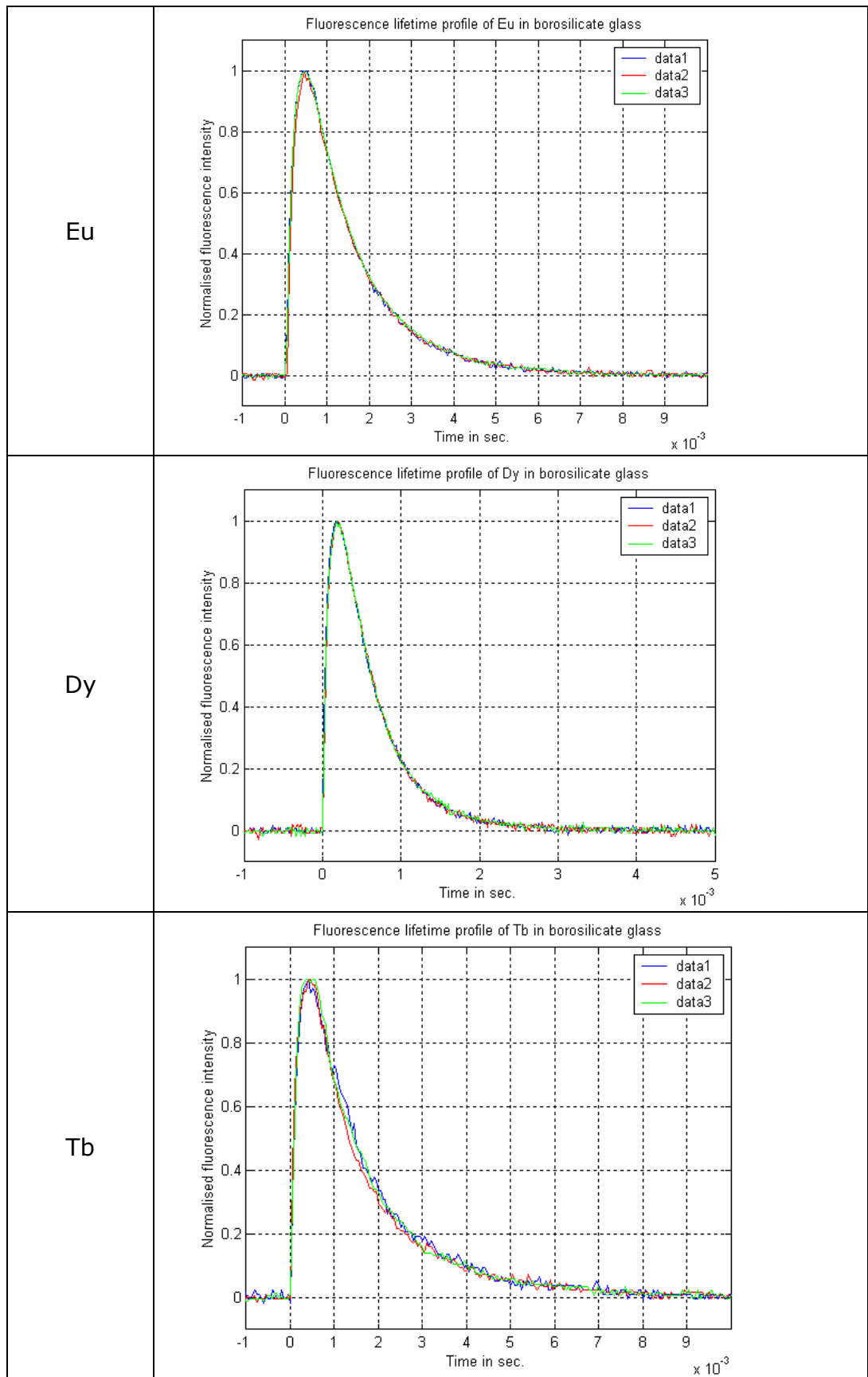


Figure 21 Eu, Dy and Tb fluorescent lifetimes in G1-21

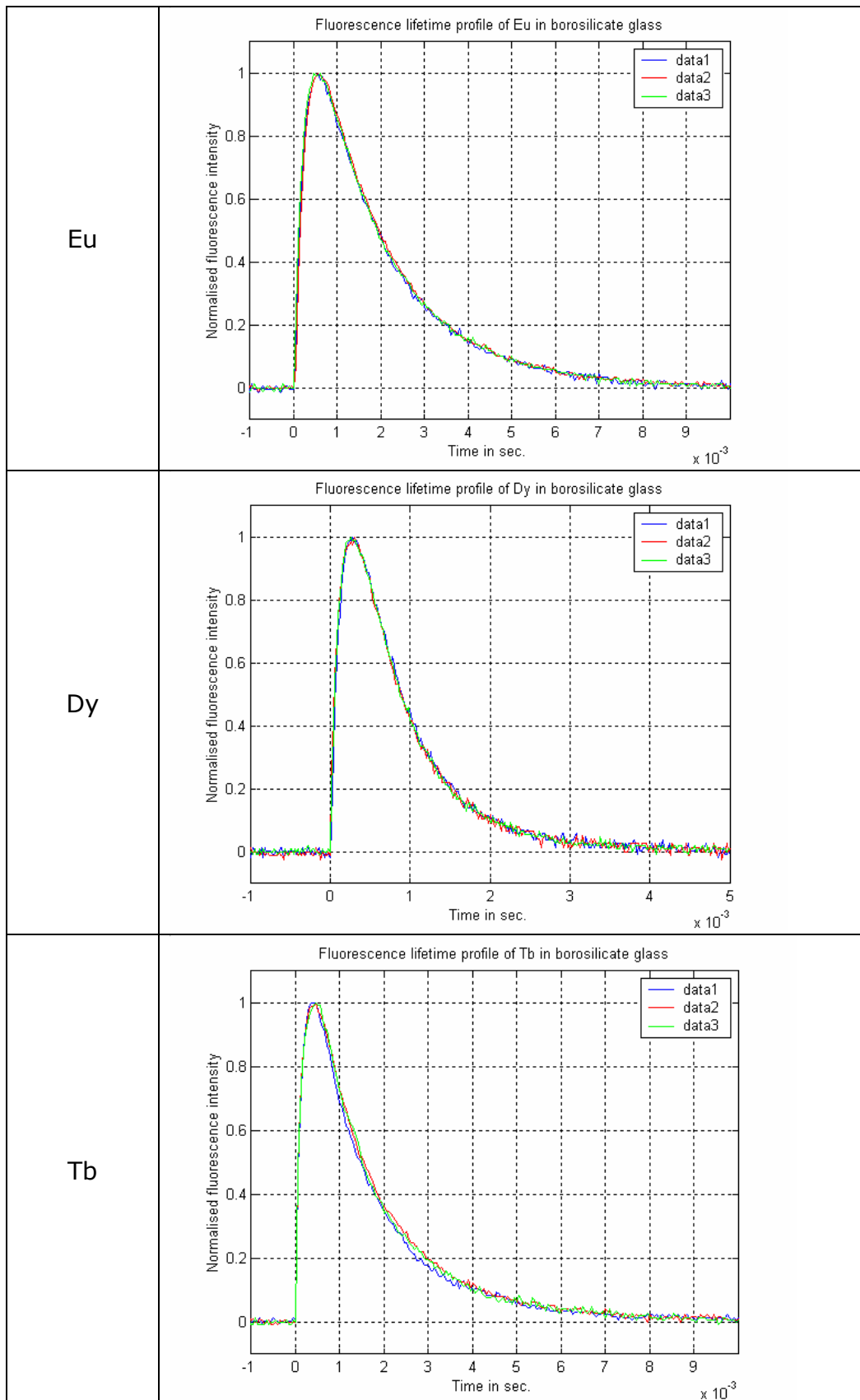


Figure 22 Eu, Dy and Tb fluorescent lifetimes in G1-22



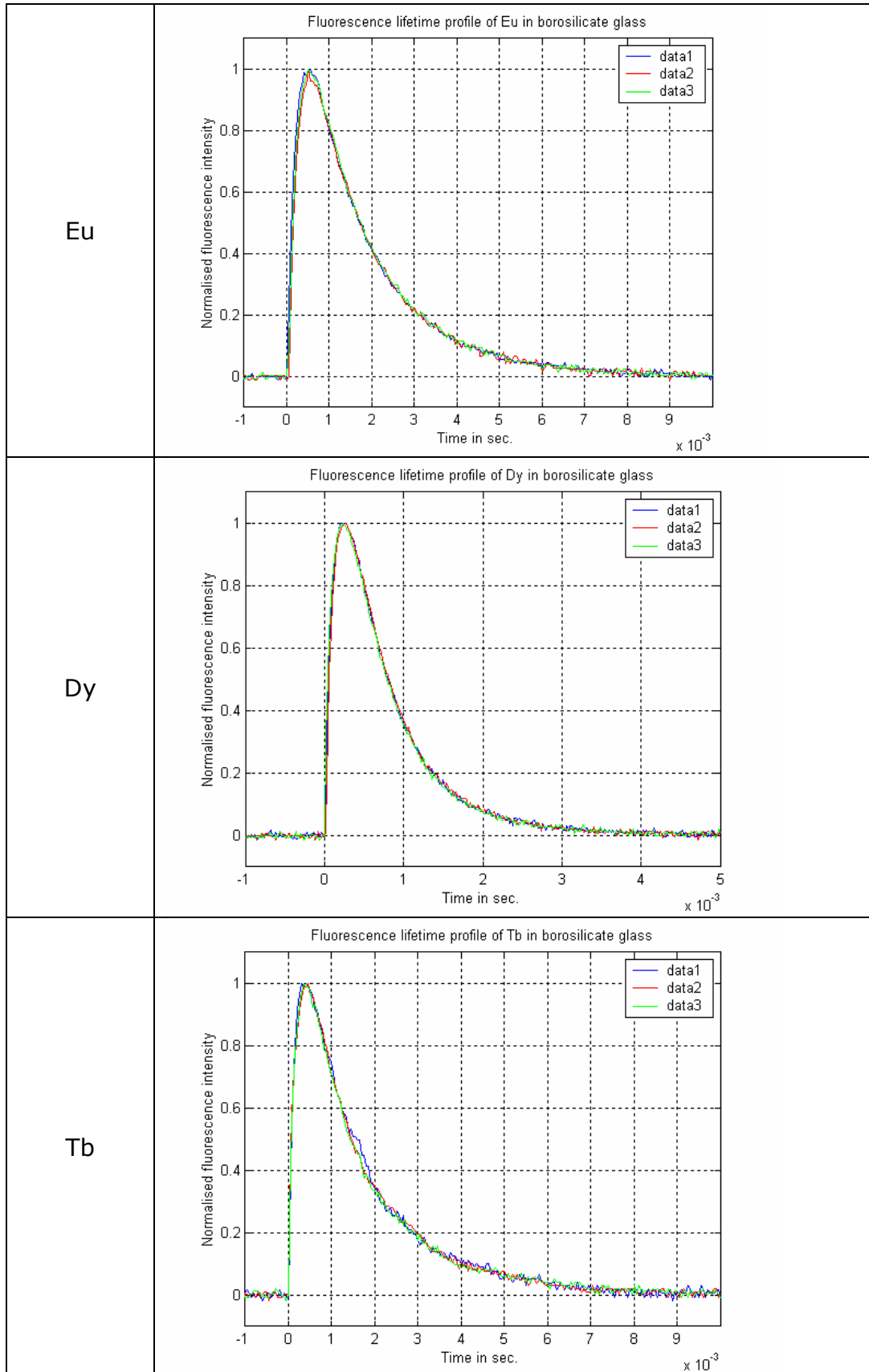


Figure 23 Eu, Dy and Tb fluorescent lifetimes in G1-23

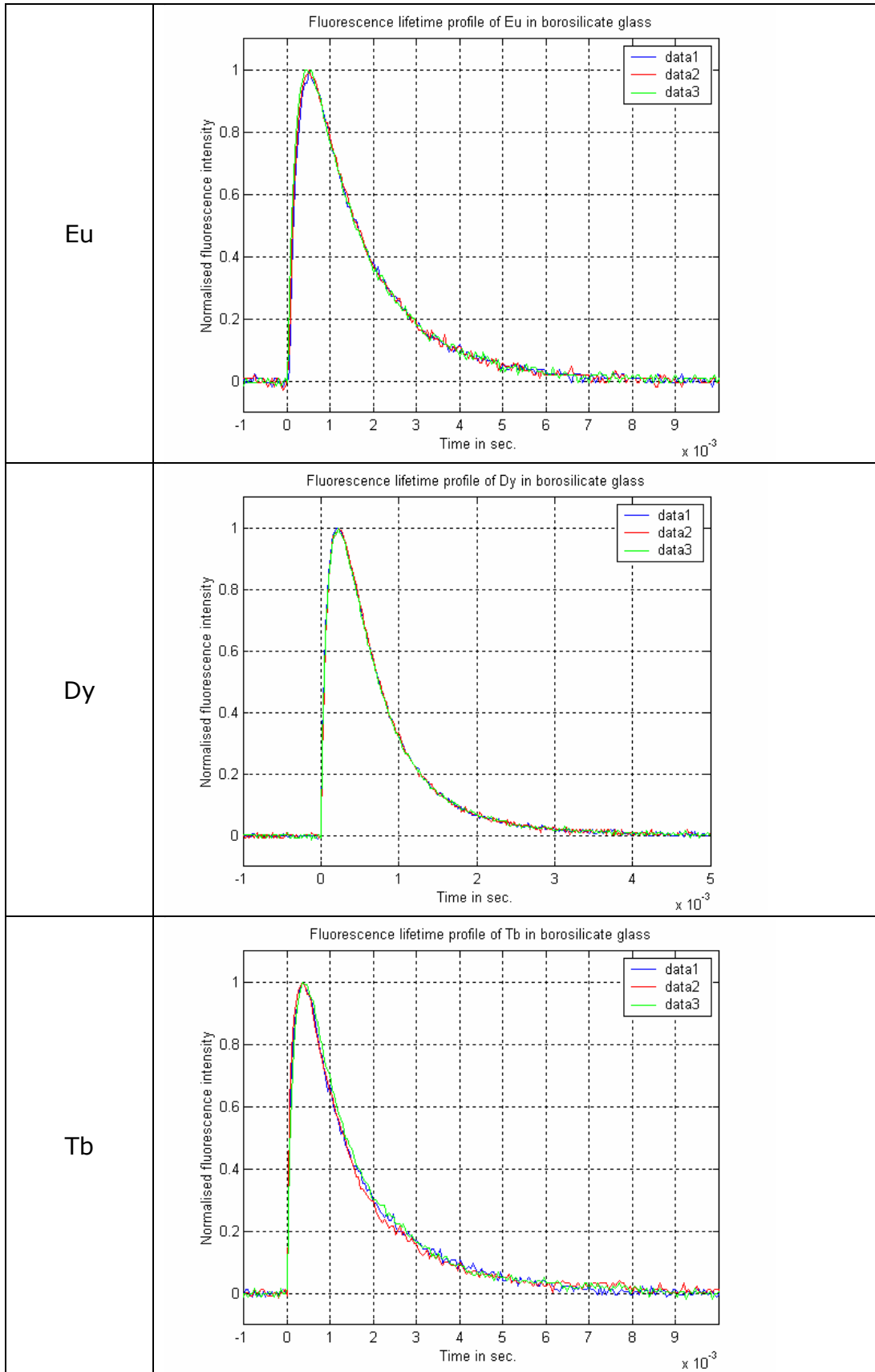


Figure 24 Eu, Dy and Tb fluorescent lifetimes in G1-24

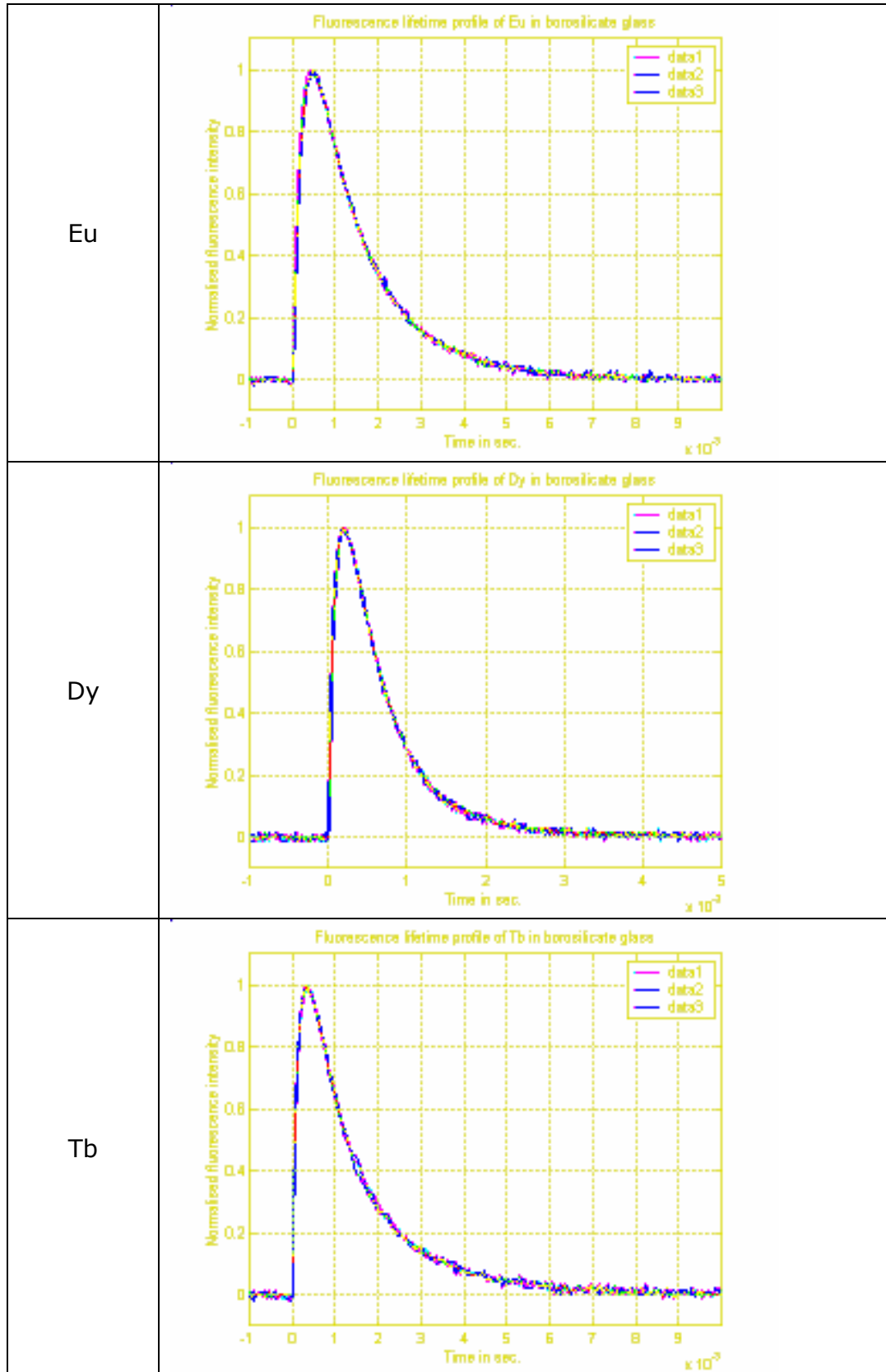


Figure 25 Eu, Dy and Tb fluorescent lifetimes in G1-25

Eu	
Dy	
Tb	

**Figure 26 Eu, Dy and Tb fluorescent lifetimes in G2-01**

Eu	
----	--

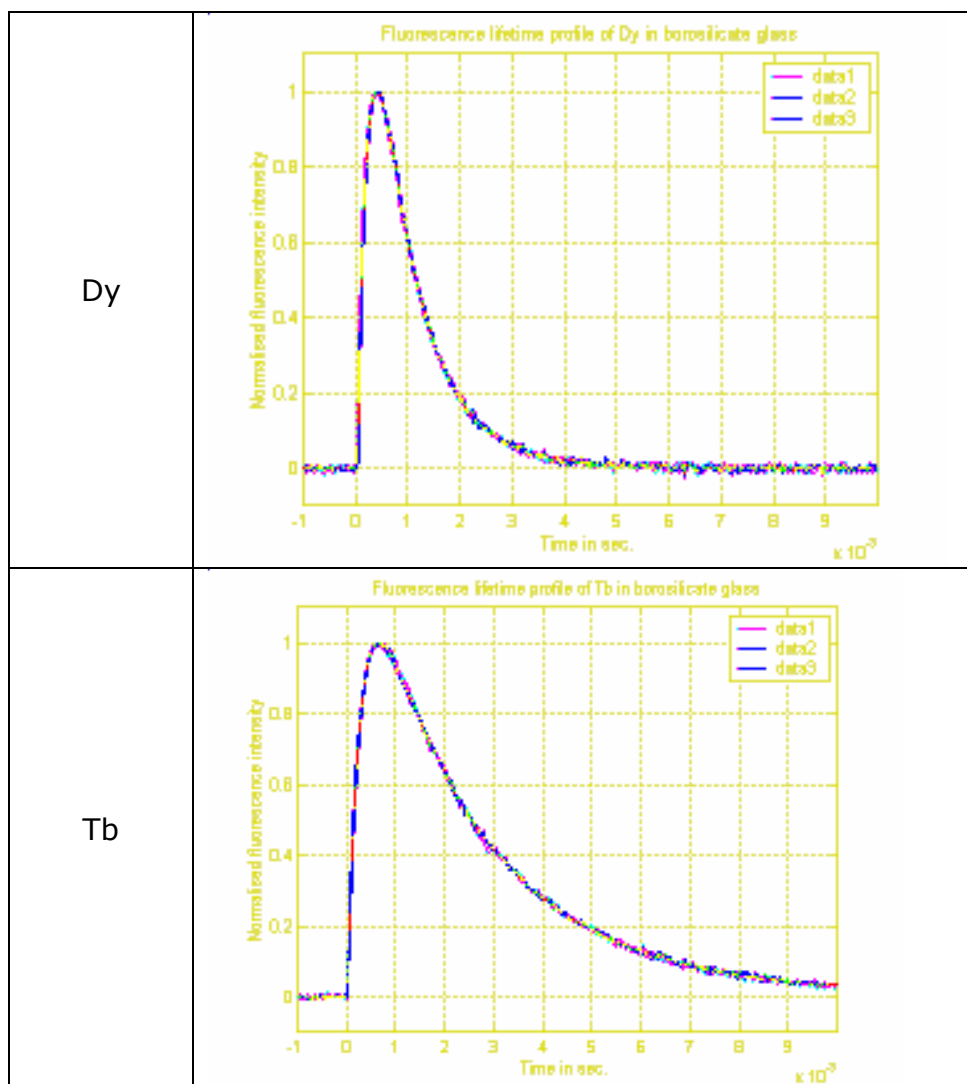


Figure 27 Eu, Dy and Tb fluorescent lifetimes in G2-02

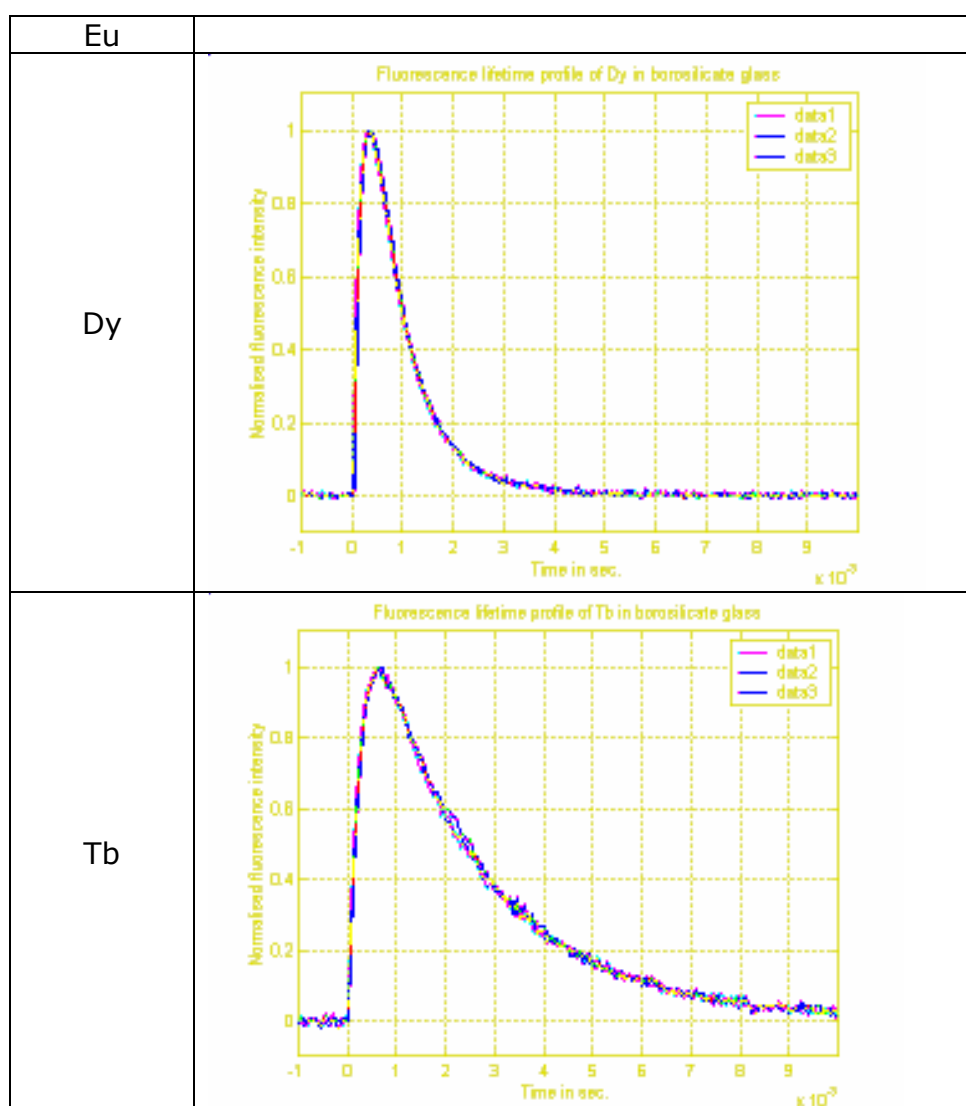
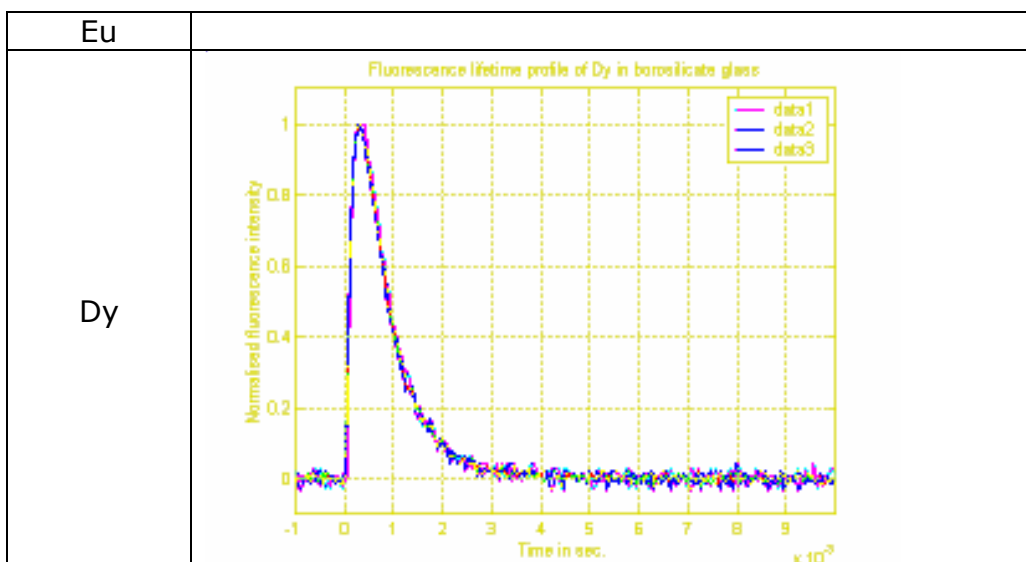


Figure 28 Eu, Dy and Tb fluorescent lifetimes in G2-03





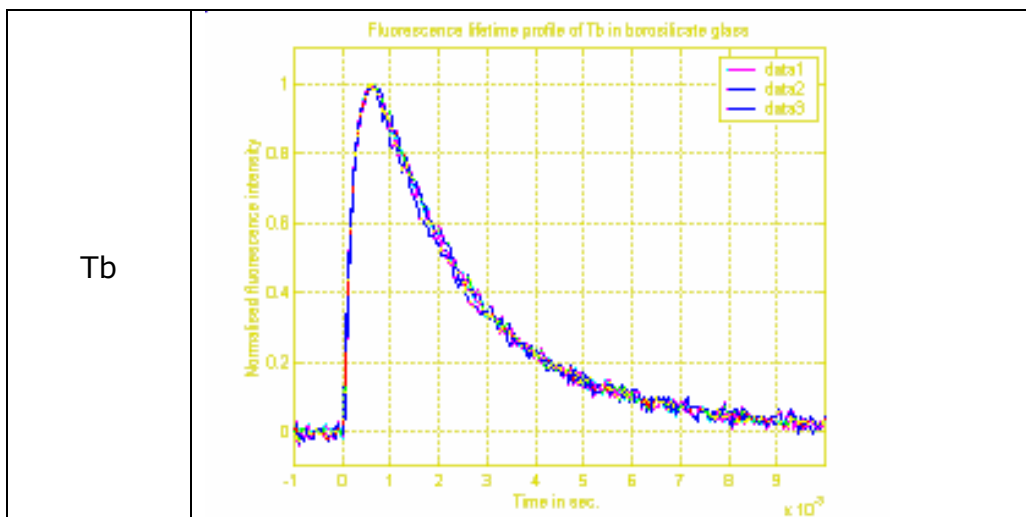


Figure 29 Eu, Dy and Tb fluorescent lifetimes in G2-04

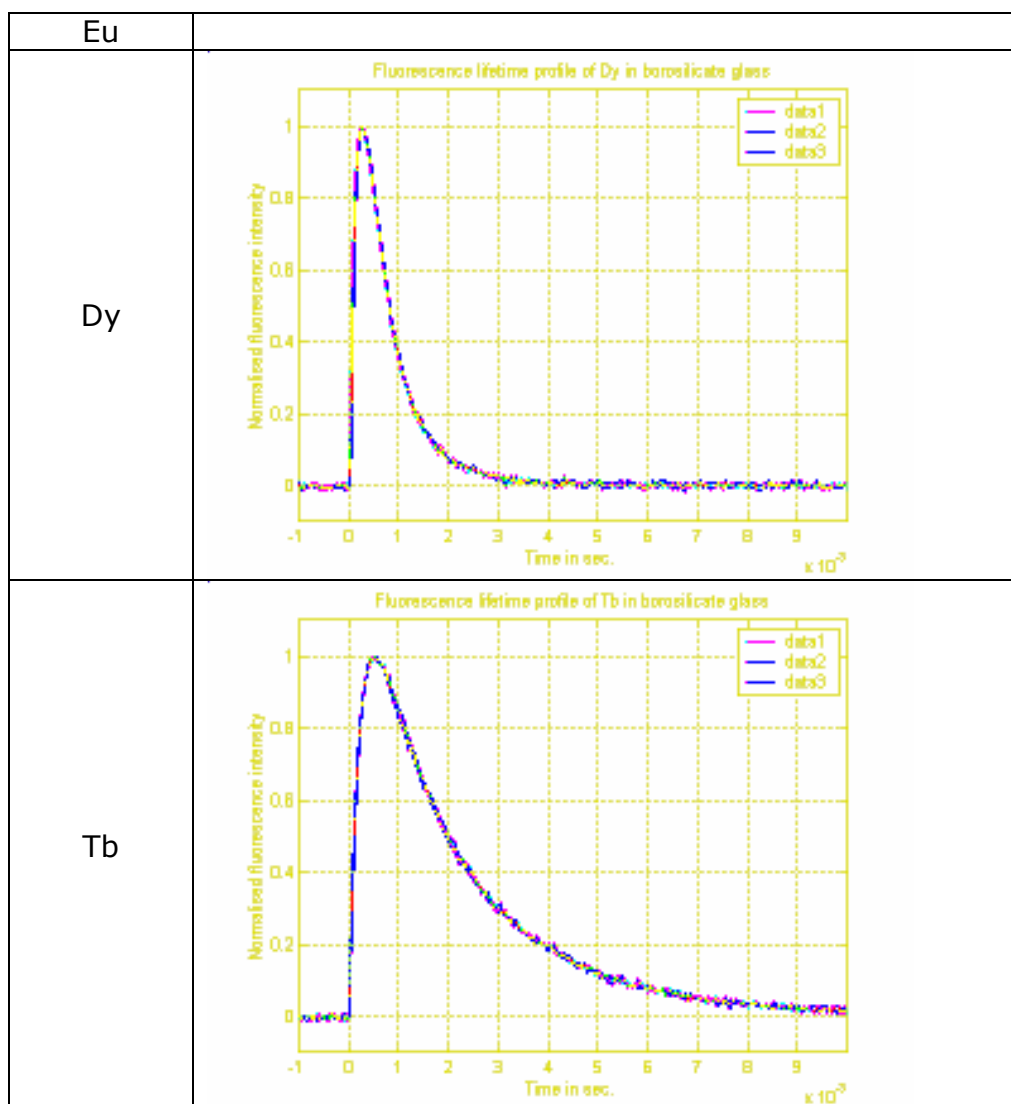


Figure 30 Eu, Dy and Tb fluorescent lifetimes in G2-05

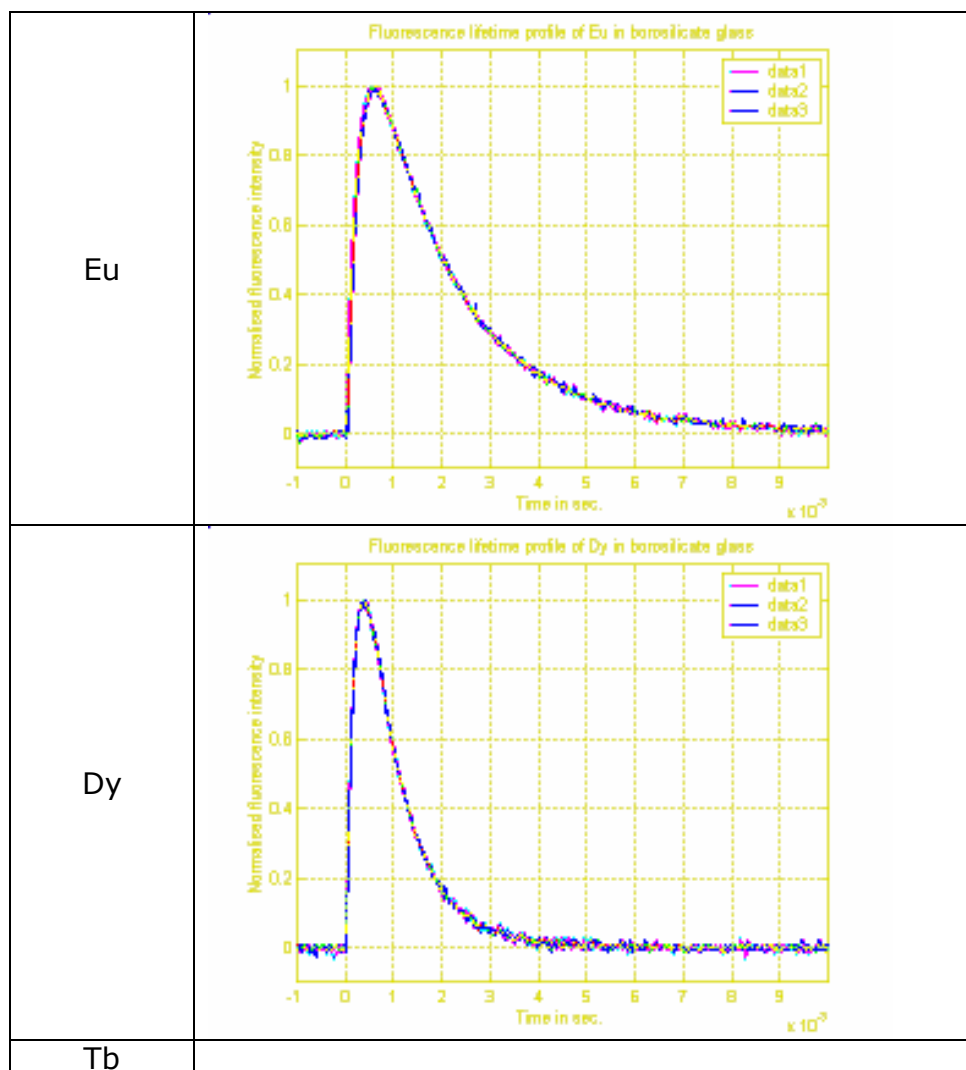


Figure 31 Eu, Dy and Tb fluorescent lifetimes in G2-06

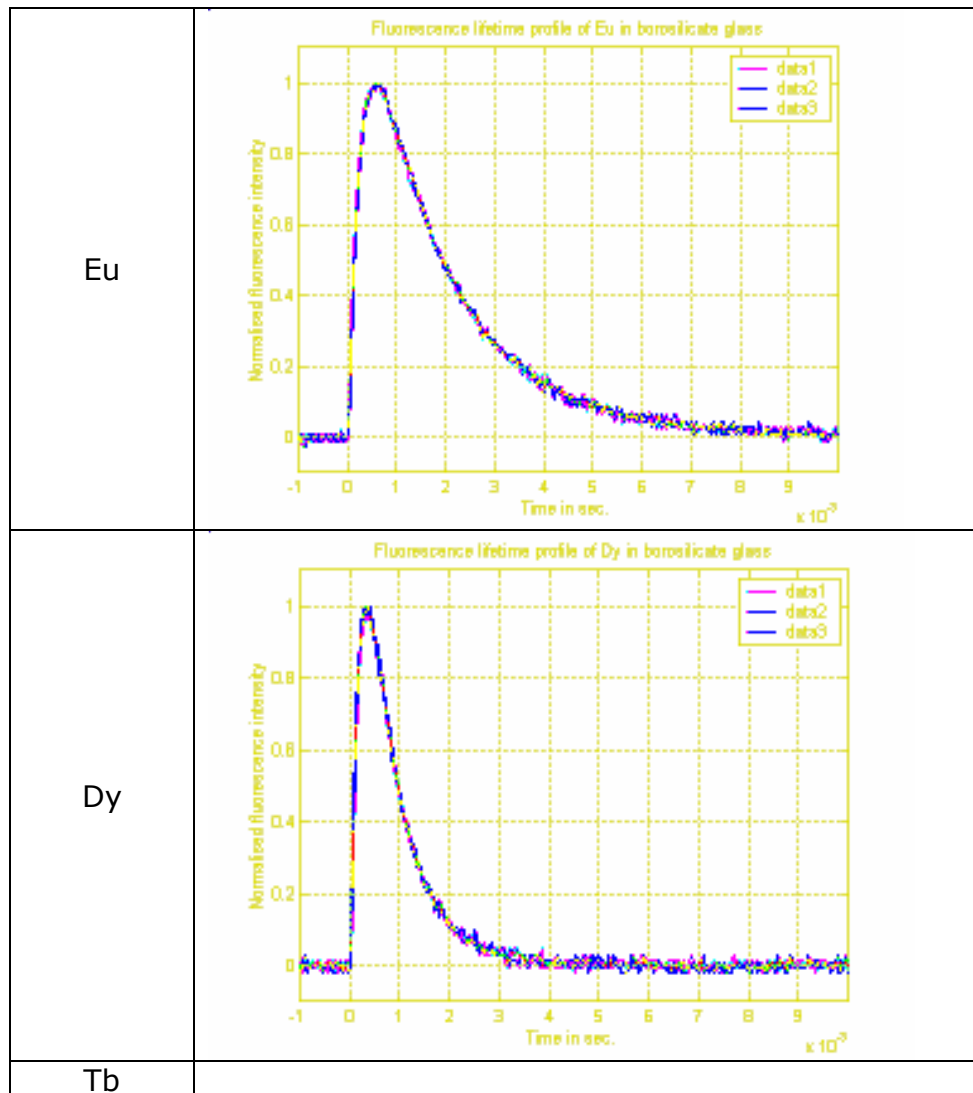


Figure 32 Eu, Dy and Tb fluorescent lifetimes in G2-07

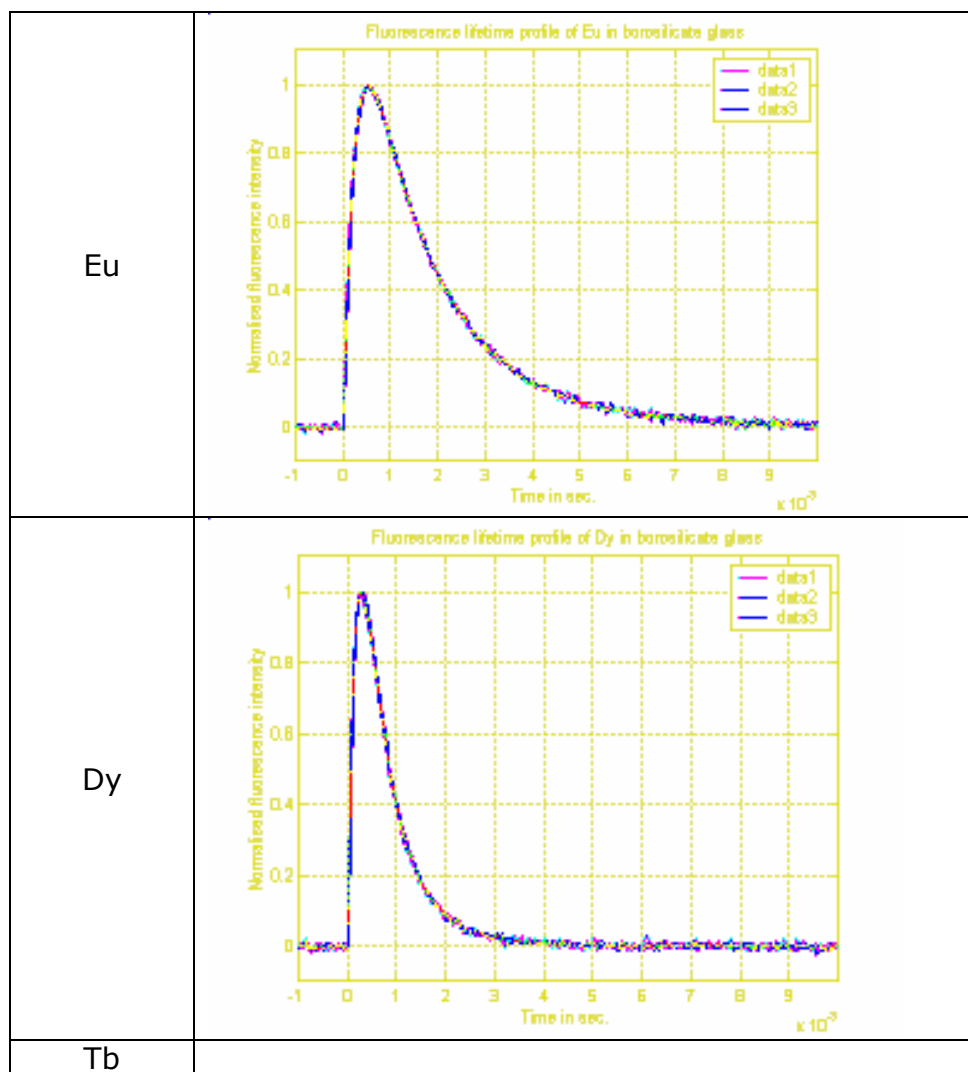


Figure 33 Eu, Dy and Tb fluorescent lifetimes in G2-08

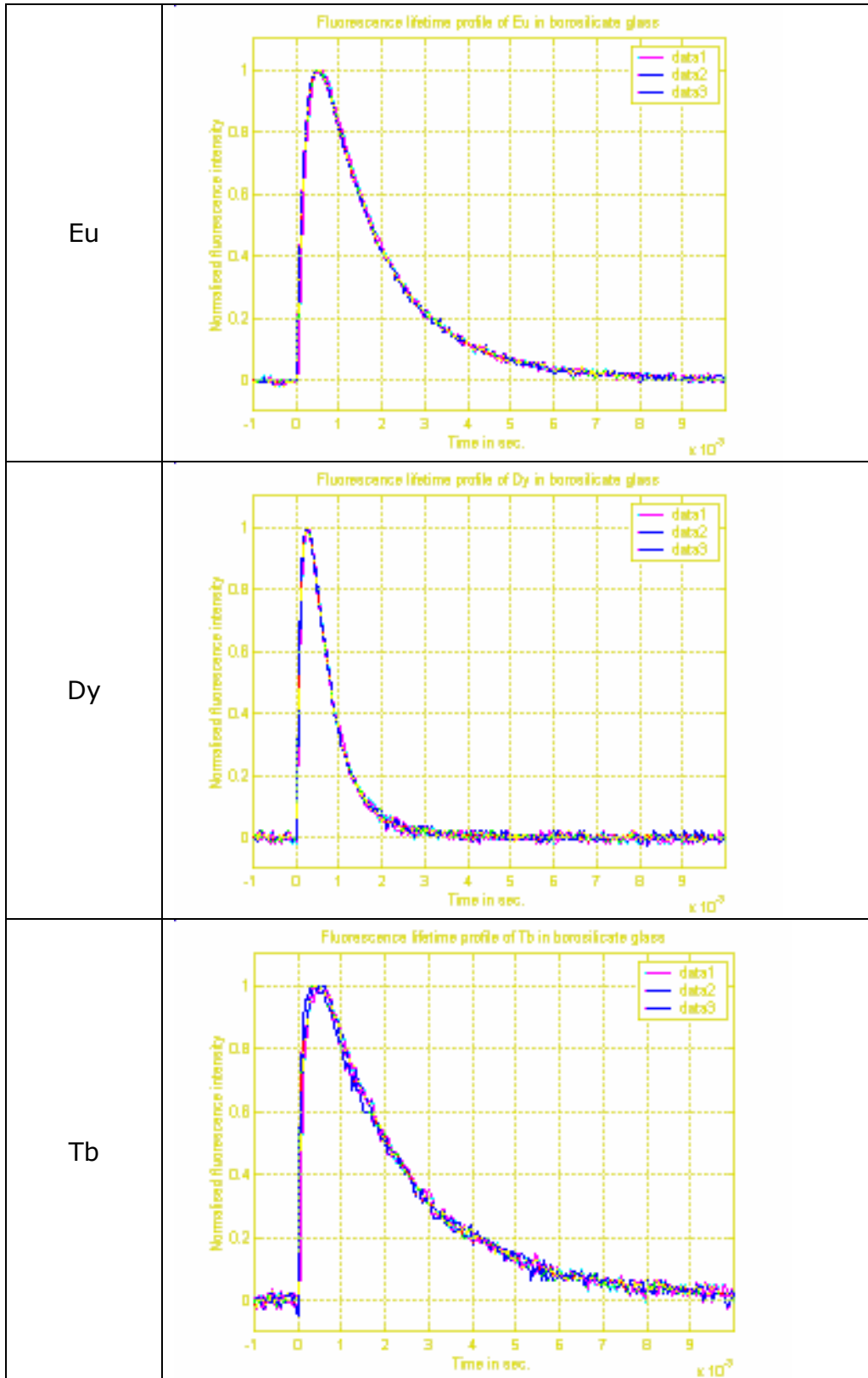


Figure 34 Eu, Dy and Tb fluorescent lifetimes in G2-09

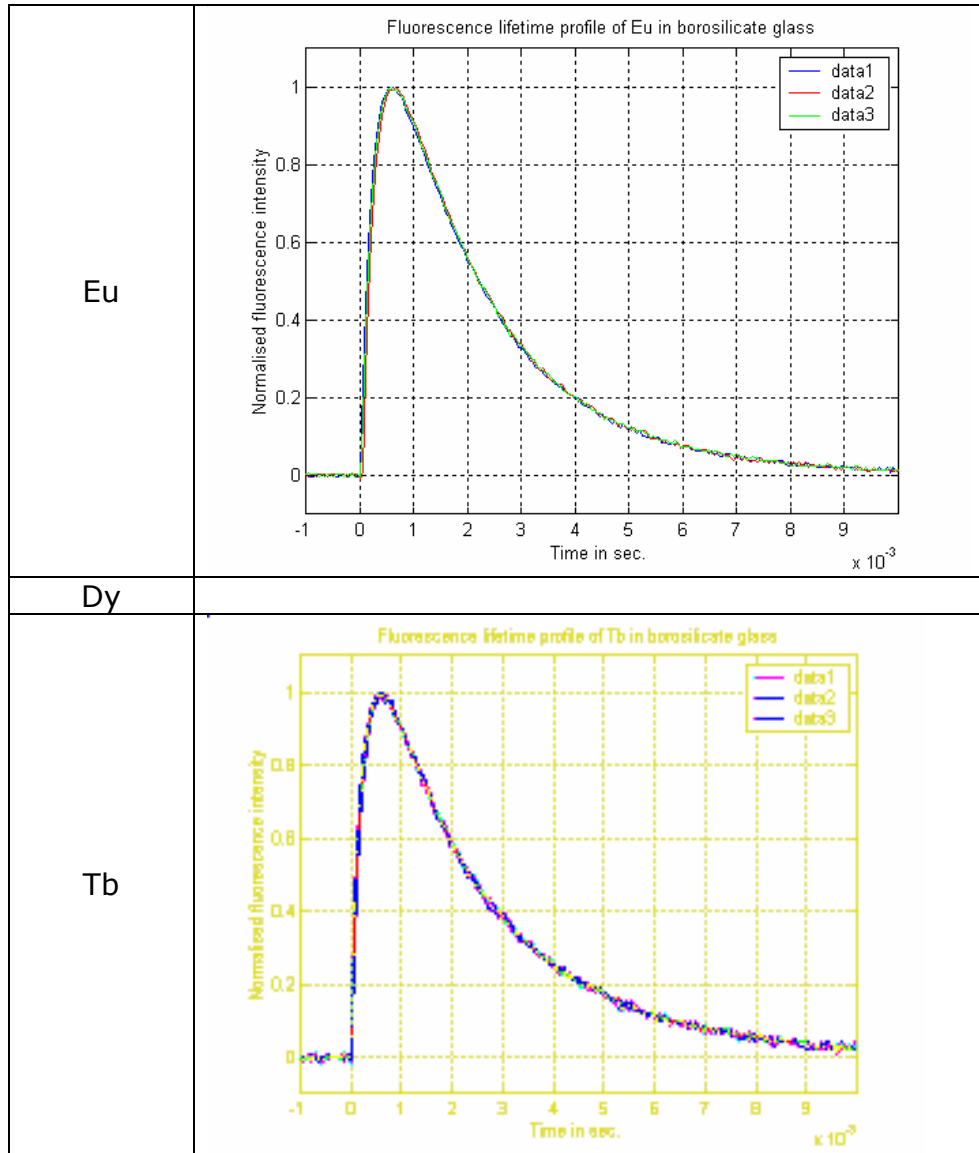


Figure 35 Eu, Dy and Tb fluorescent lifetimes in G2-10

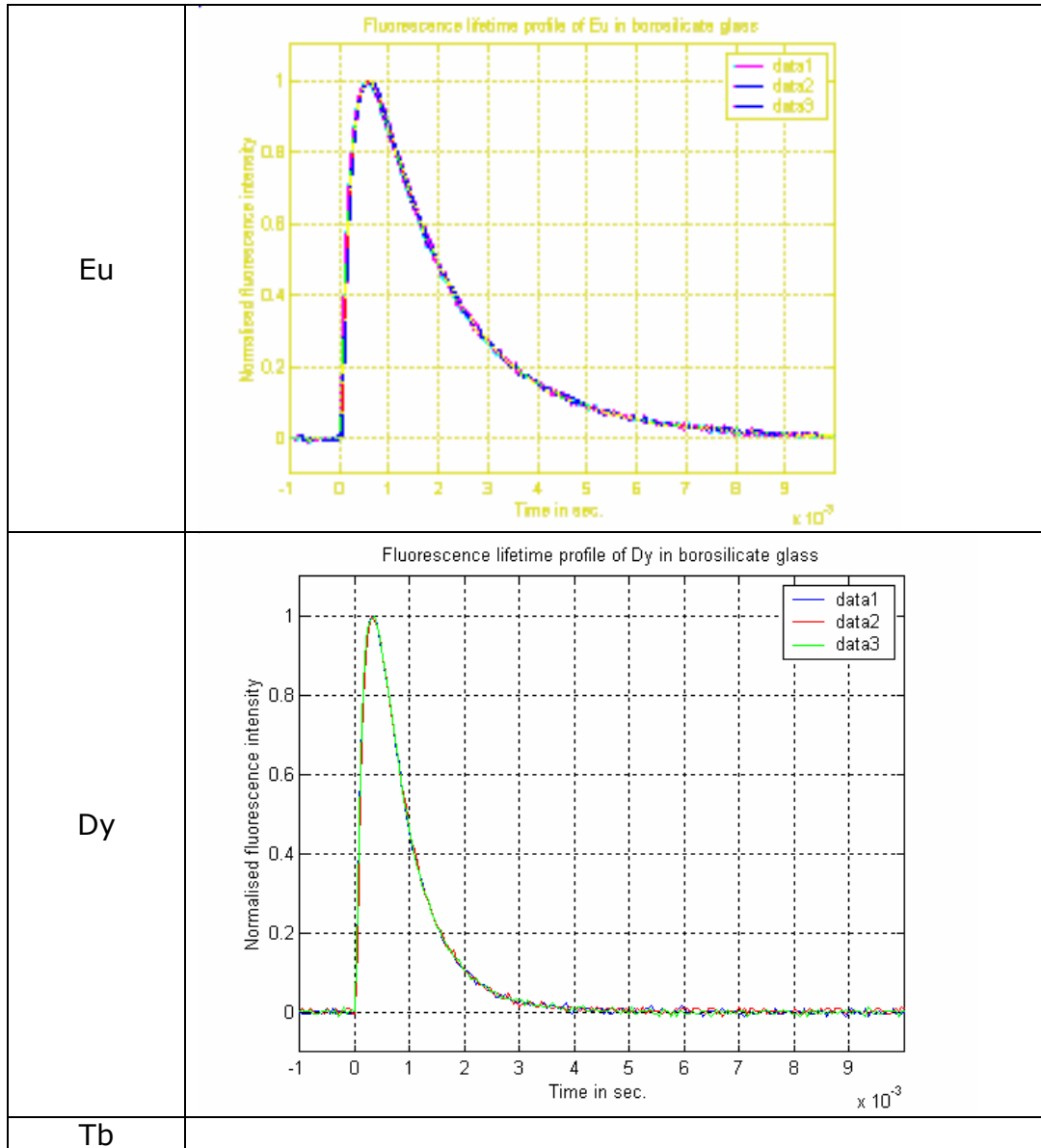


Figure 36 Eu, Dy and Tb fluorescent lifetimes in G2-11



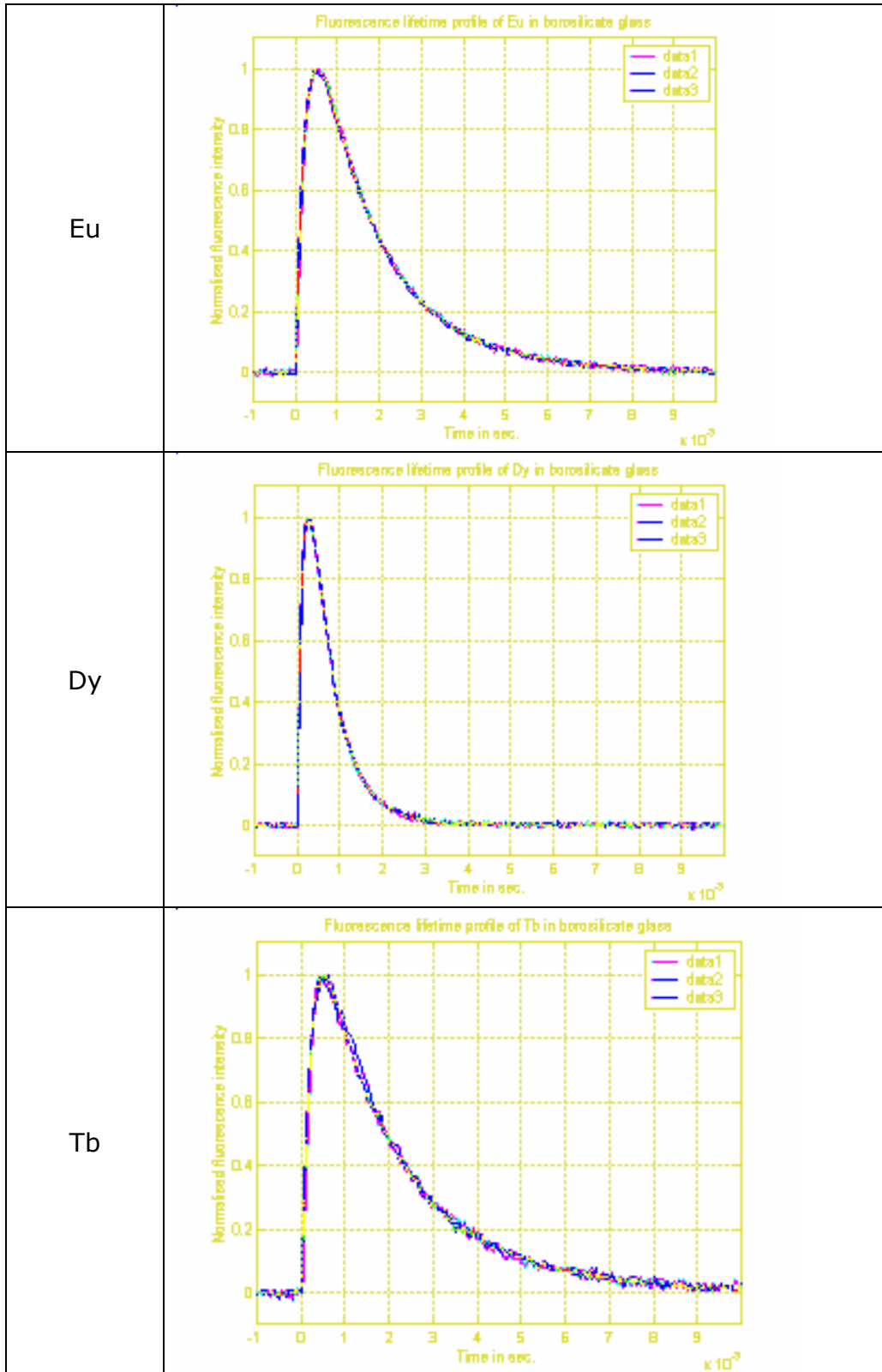


Figure 37 Eu, Dy and Tb fluorescent lifetimes in G2-12

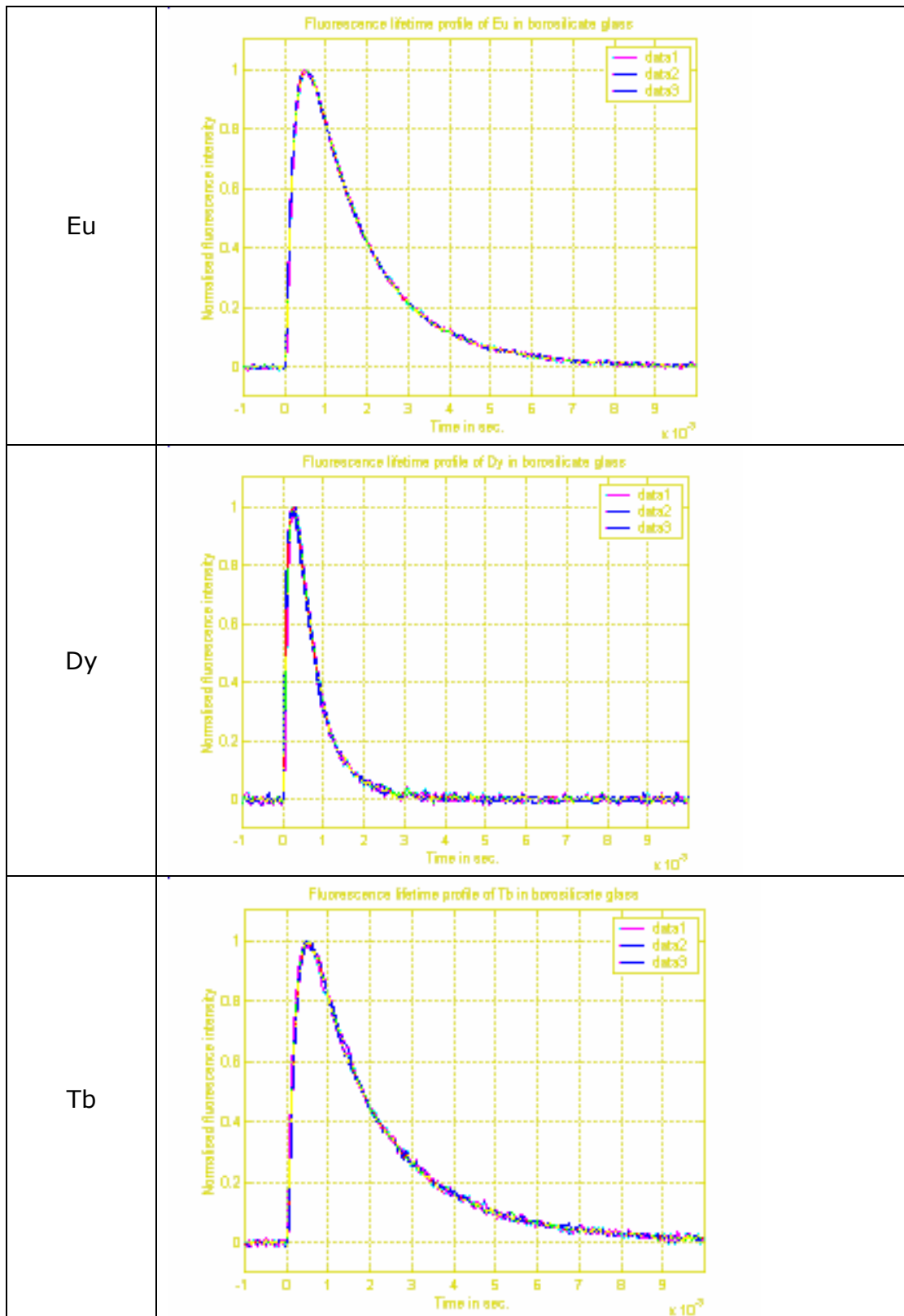


Figure 38 Eu, Dy and Tb fluorescent lifetimes in G2-13

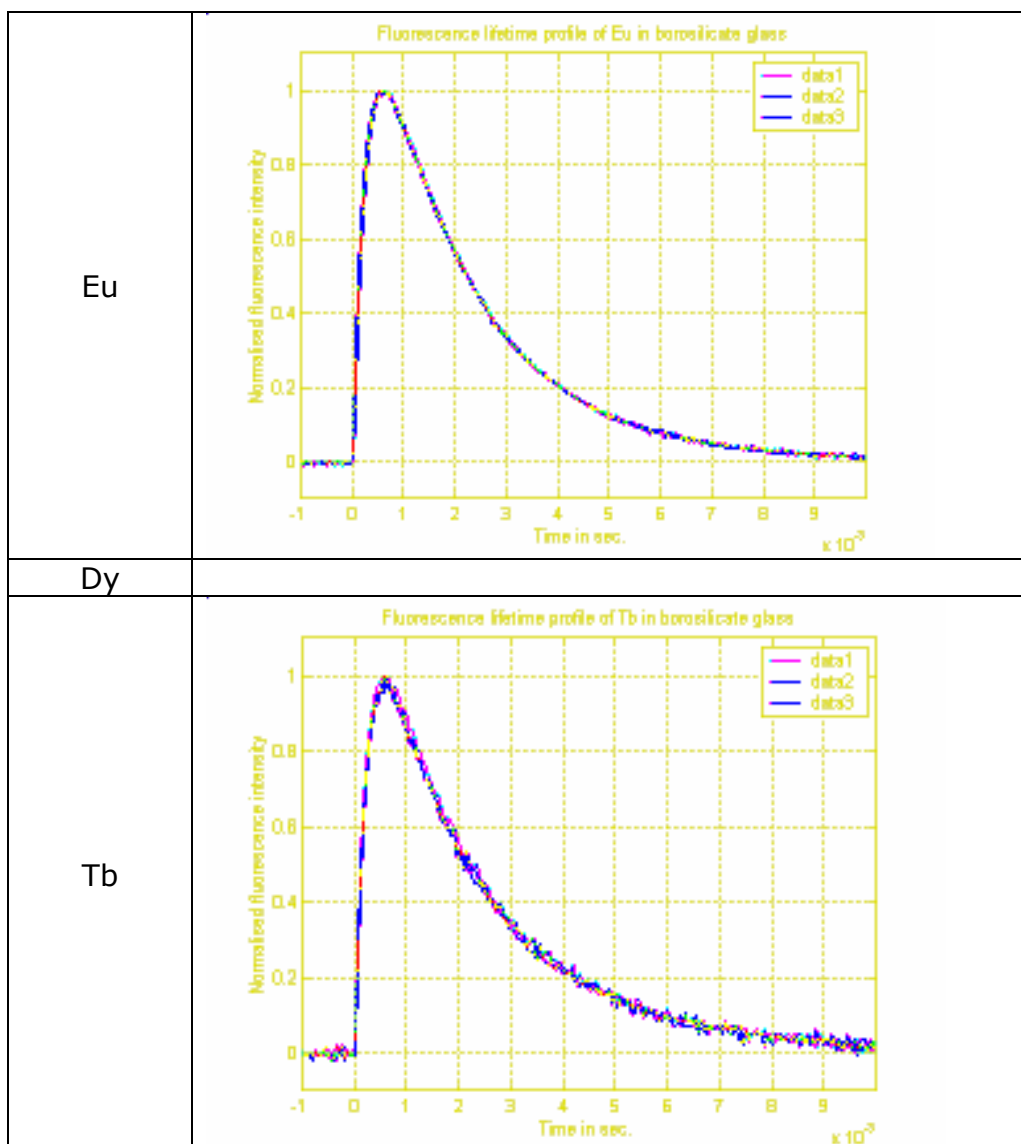


Figure 39 Eu, Dy and Tb fluorescent lifetimes in G2-14

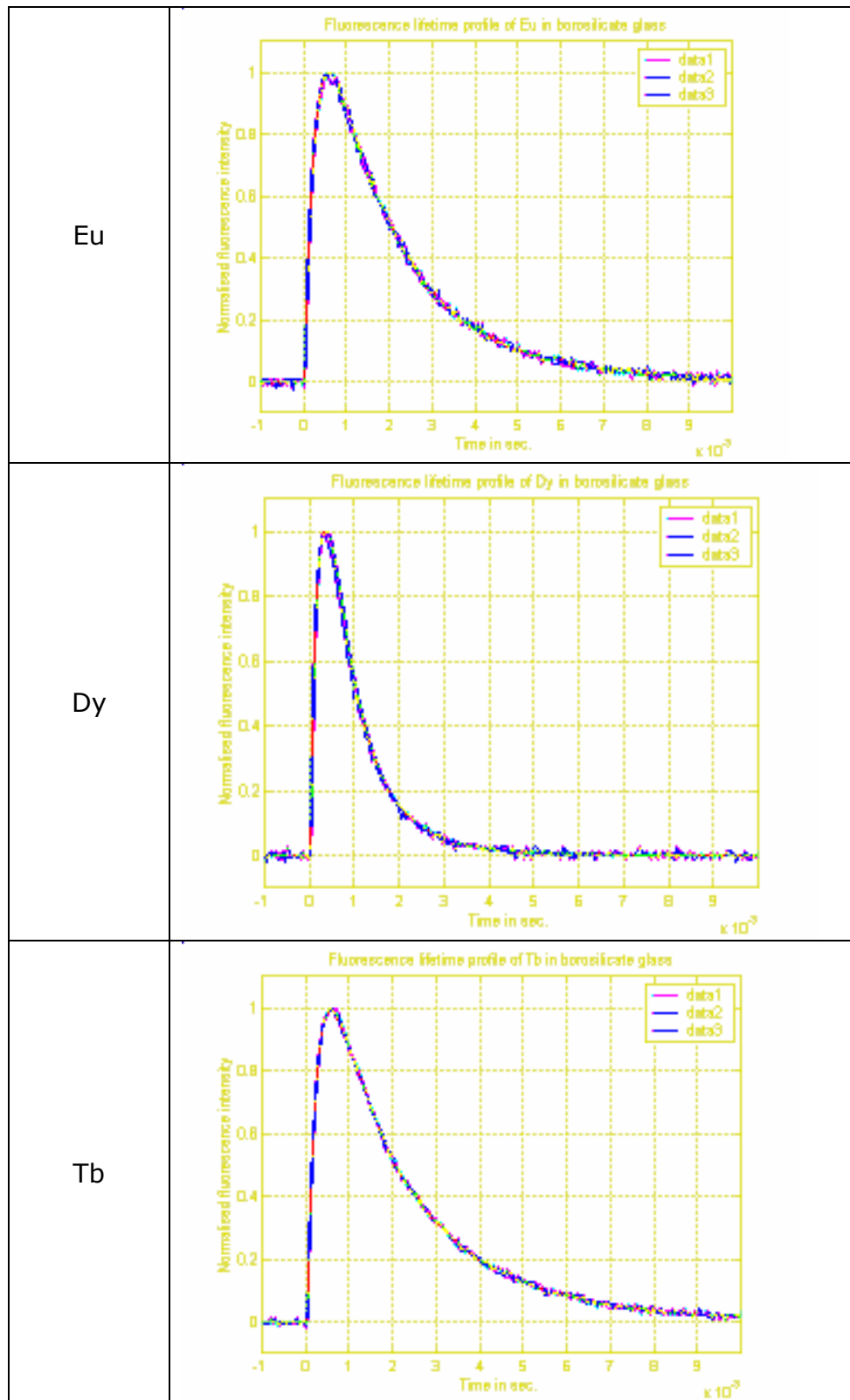


Figure 40 Eu, Dy and Tb fluorescent lifetimes in G2-15

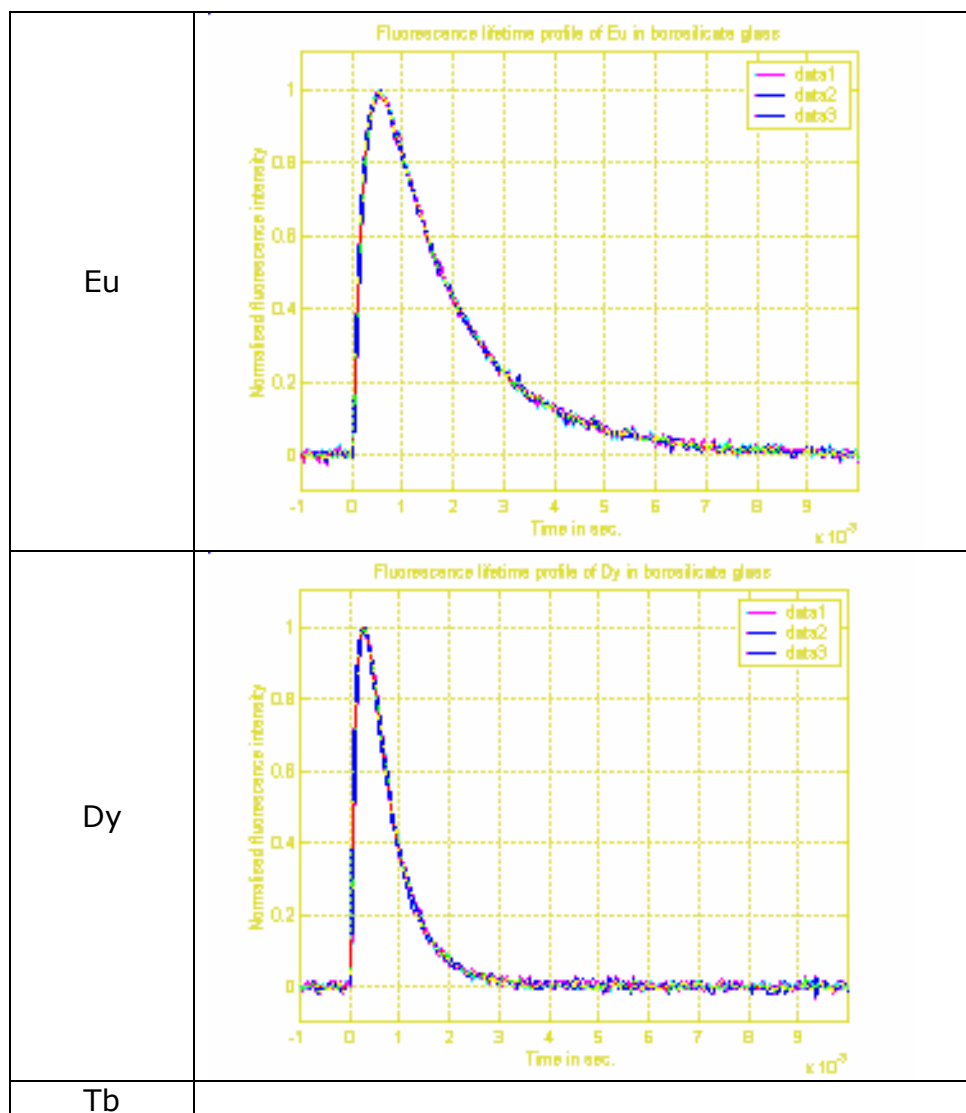


Figure 41 Eu, Dy and Tb fluorescent lifetimes in G2-16

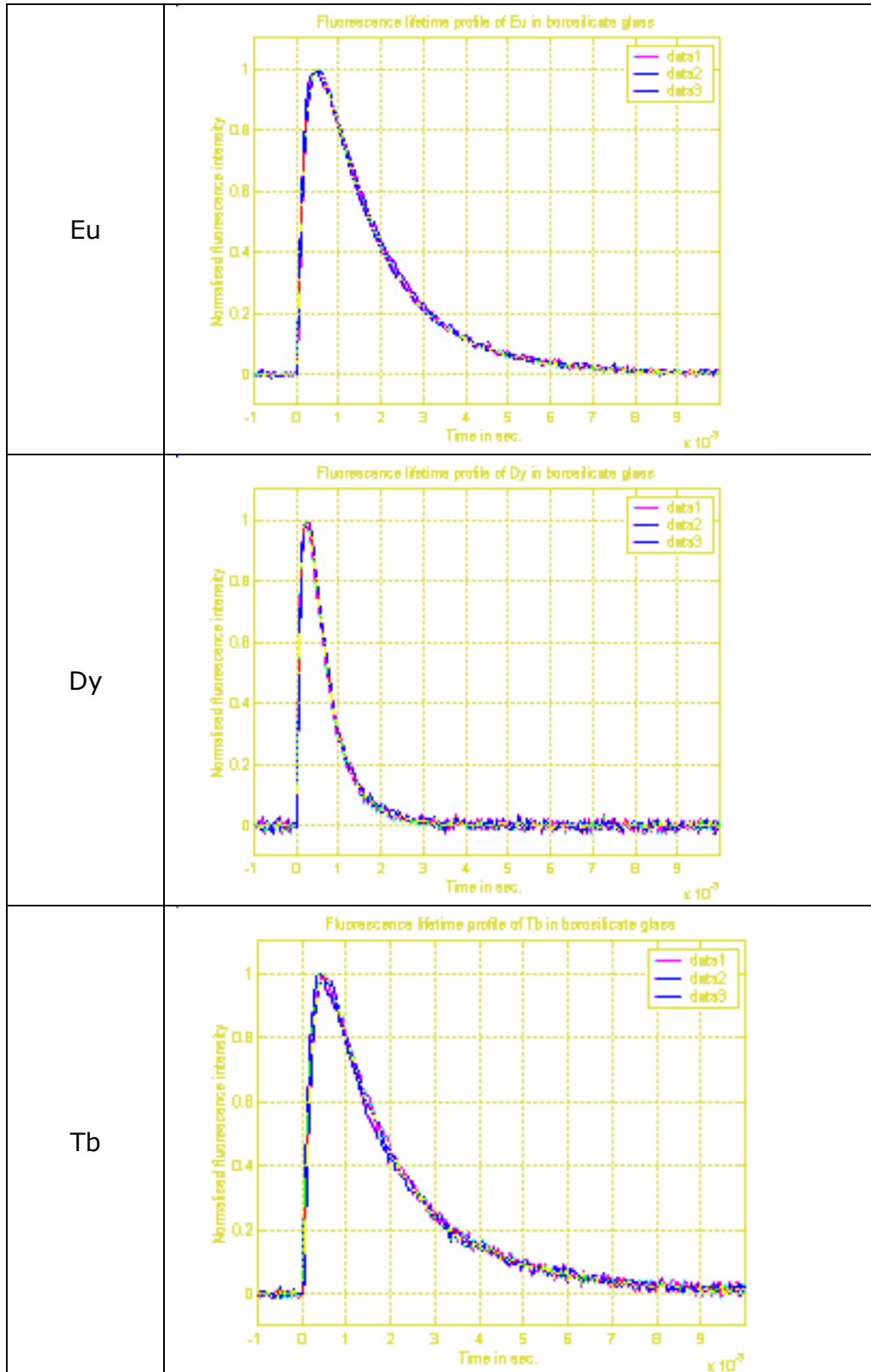


Figure 42 Eu, Dy and Tb fluorescent lifetimes in G2-17

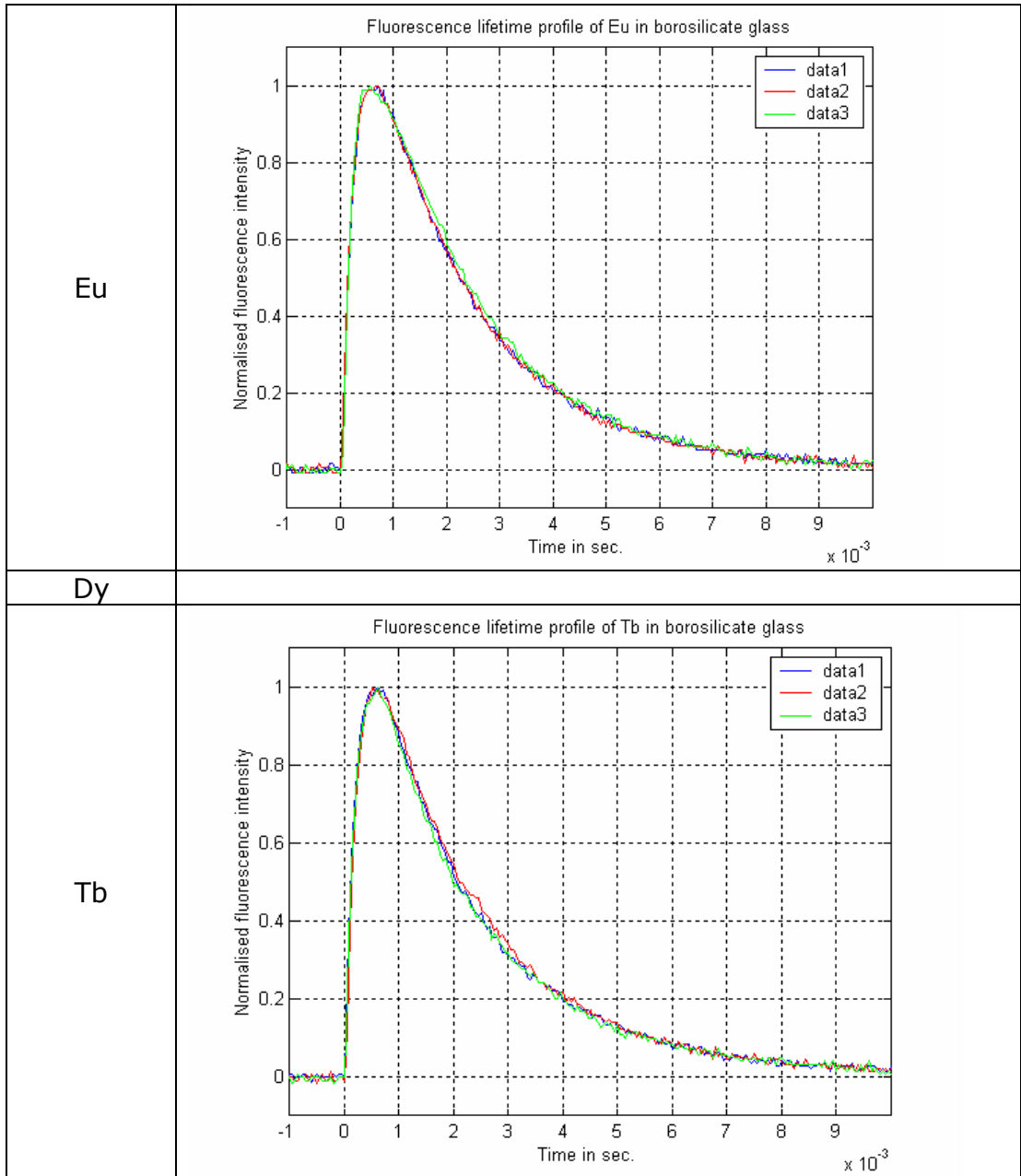


Figure 43 Eu, Dy and Tb fluorescent lifetimes in G2-18

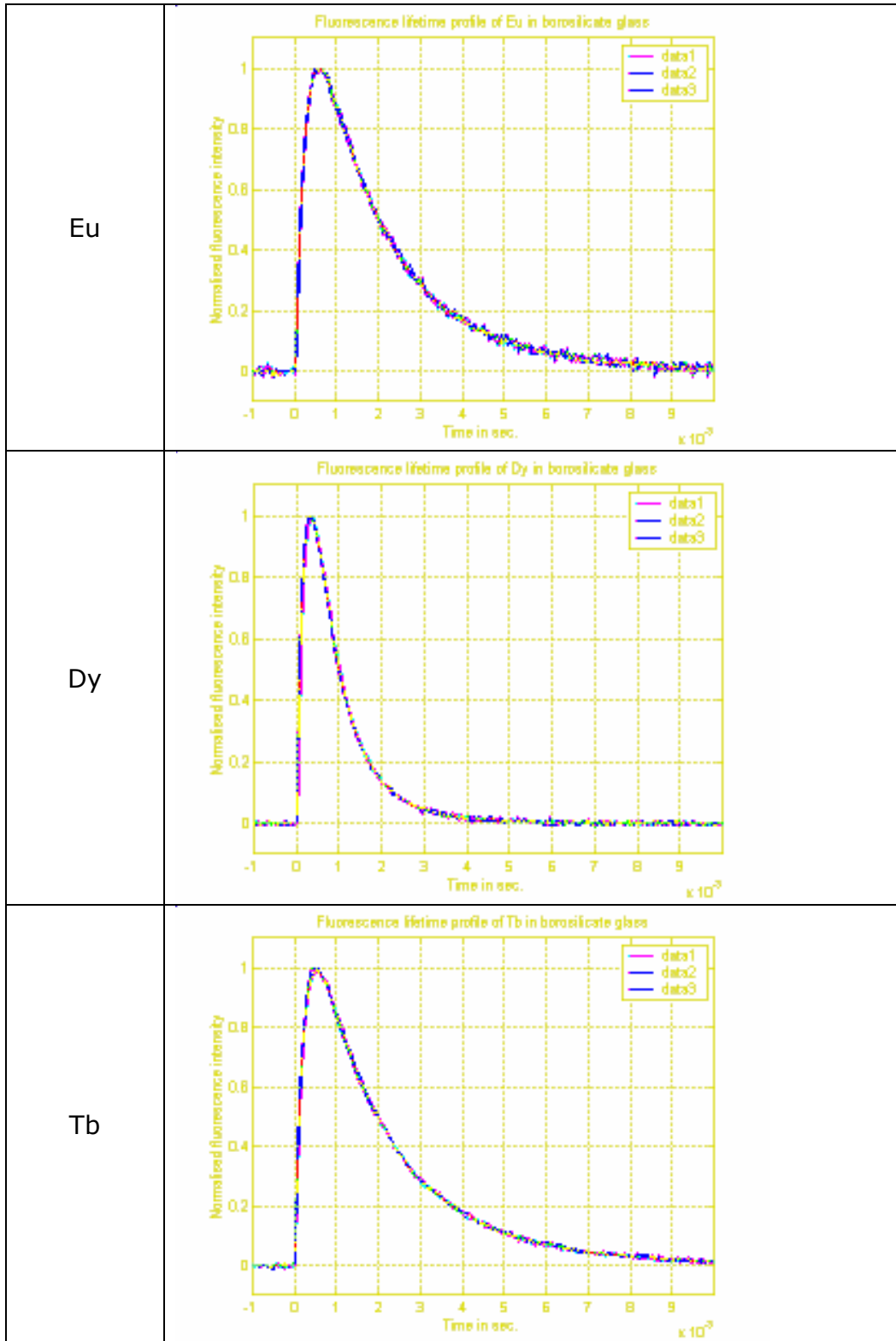


Figure 44 Eu, Dy and Tb fluorescent lifetimes in G2-19



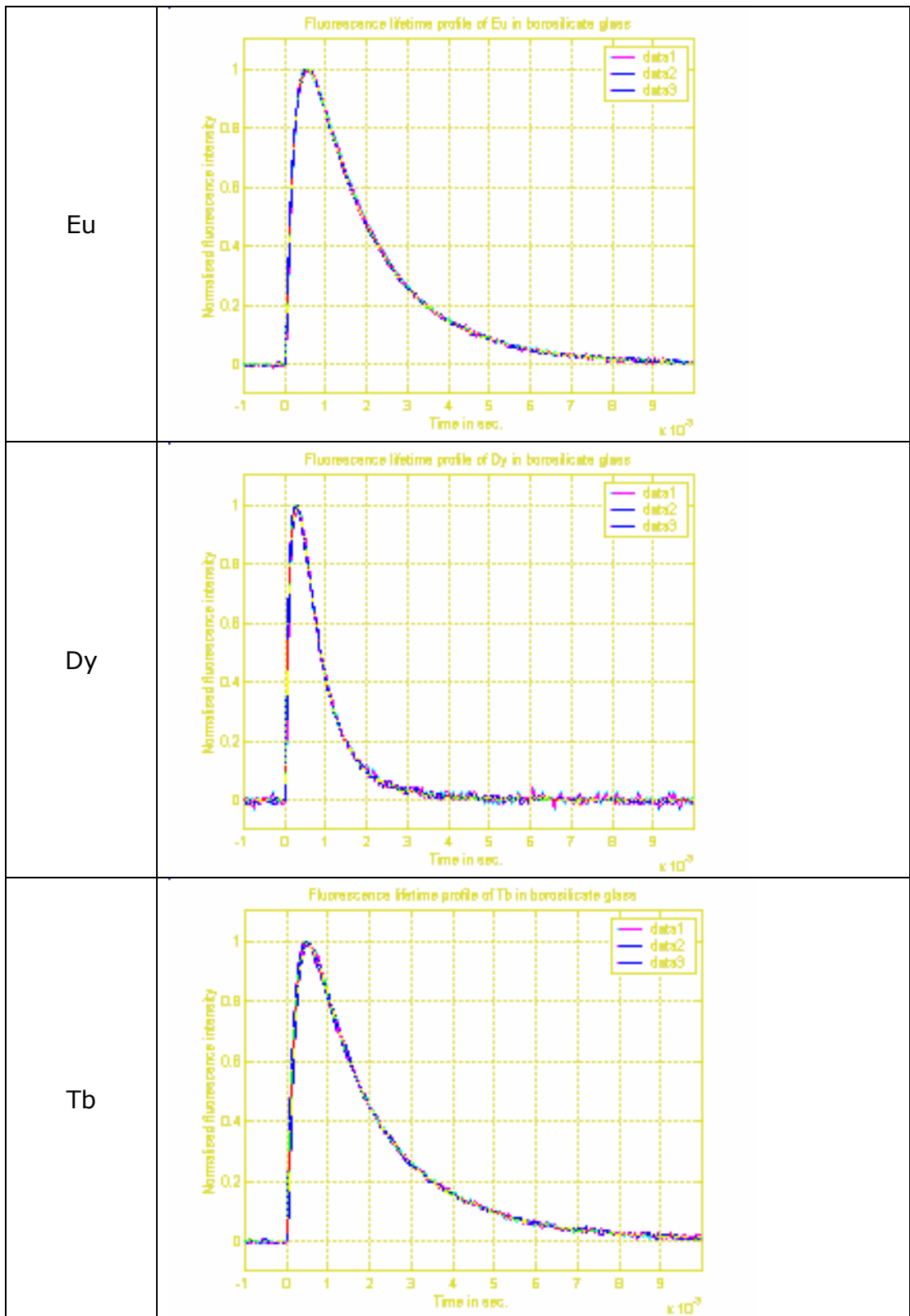


Figure 45 Eu, Dy and Tb fluorescent lifetimes in G2-20

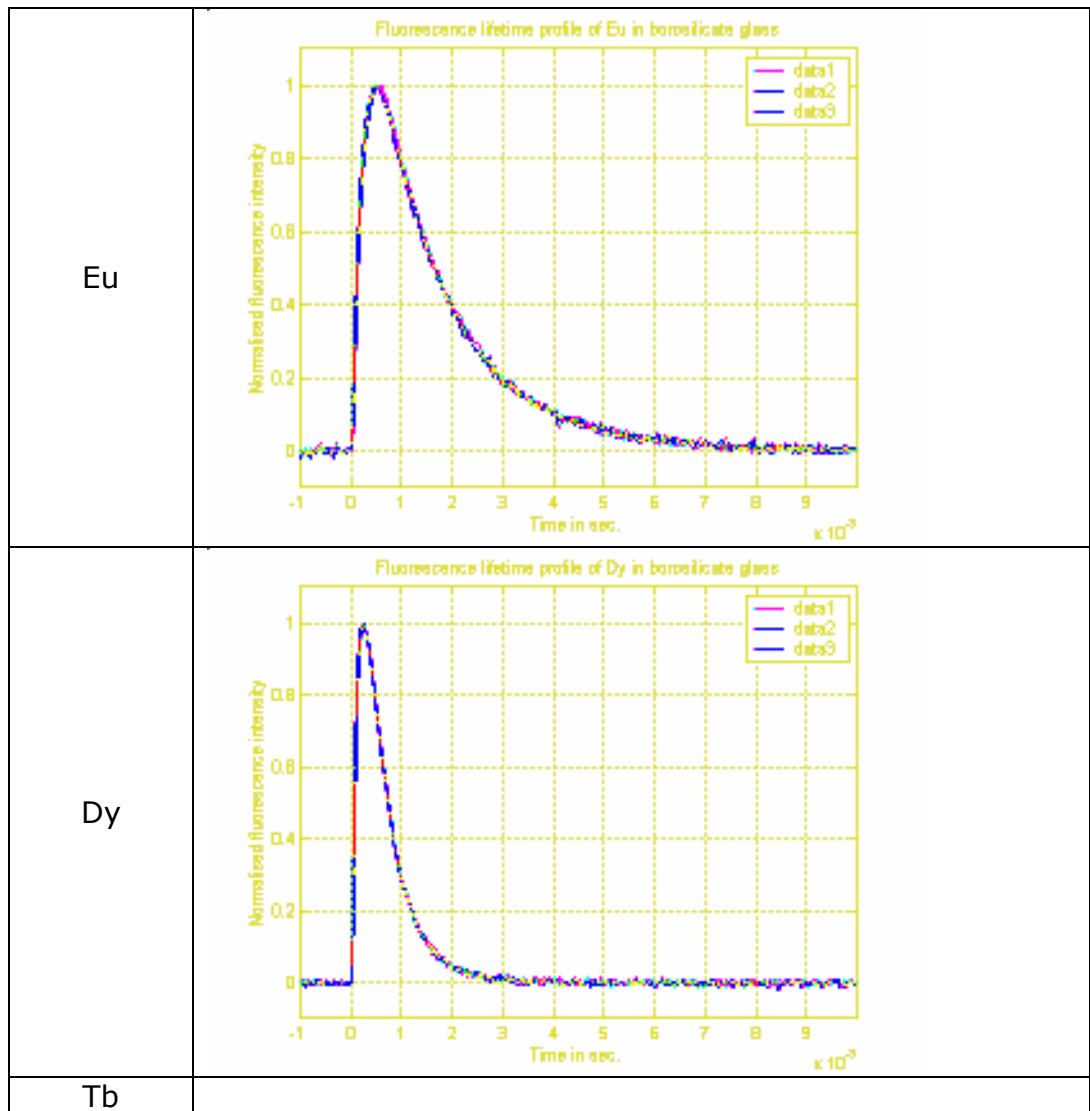


Figure 46 Eu, Dy and Tb fluorescent lifetimes in G2-21

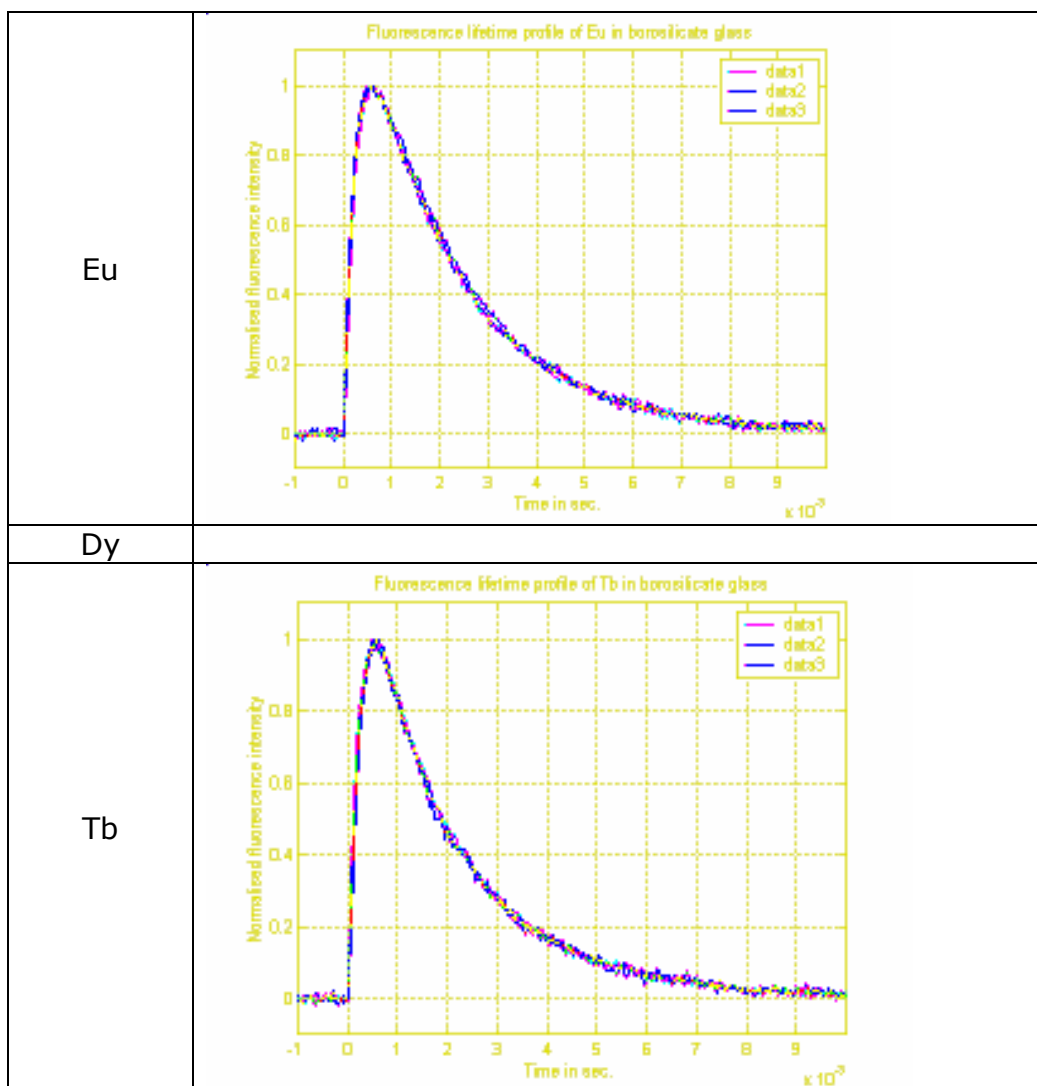


Figure 47 Eu, Dy and Tb fluorescent lifetimes in G2-22

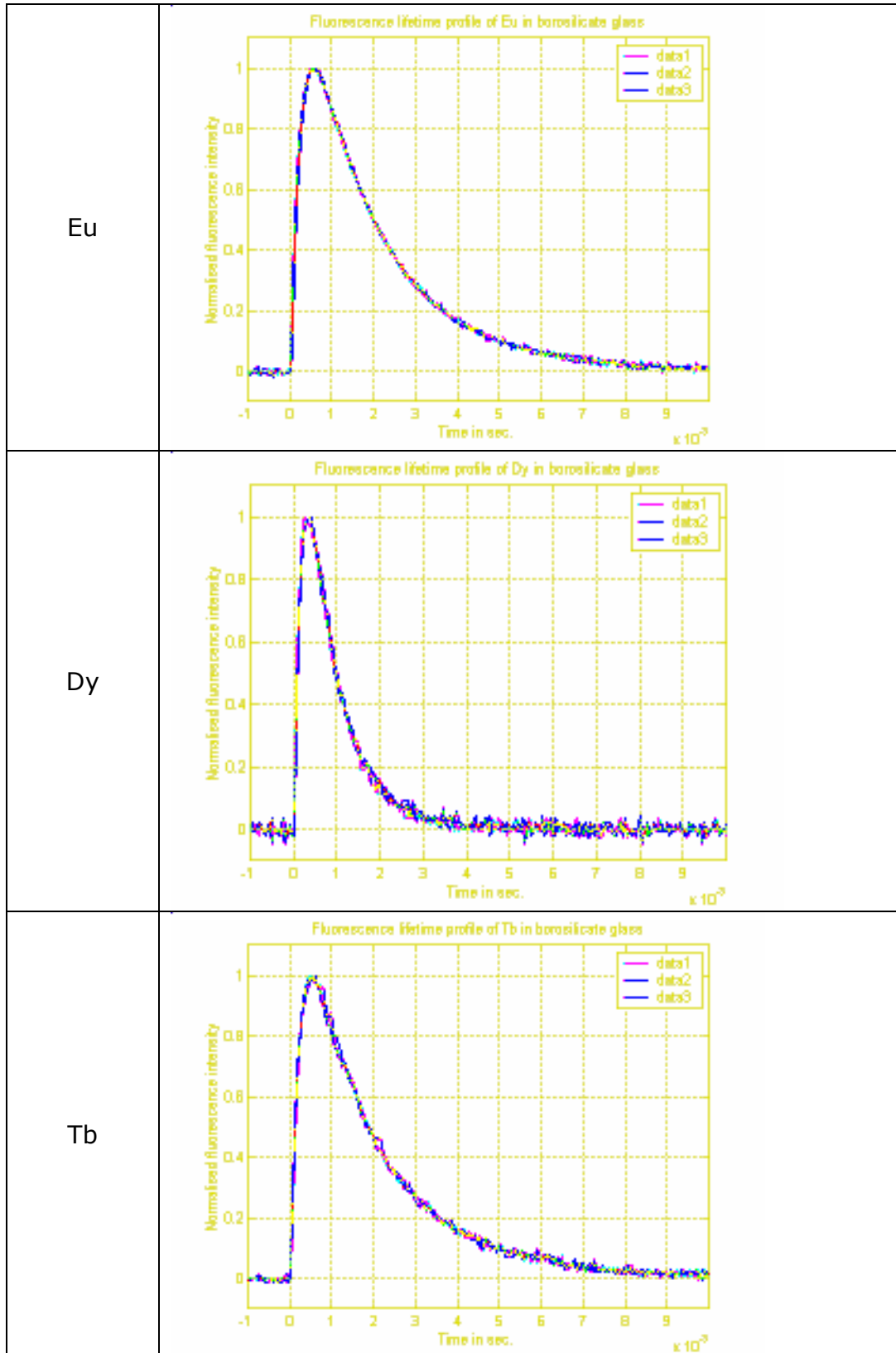


Figure 48 Eu, Dy and Tb fluorescent lifetimes in G2-23

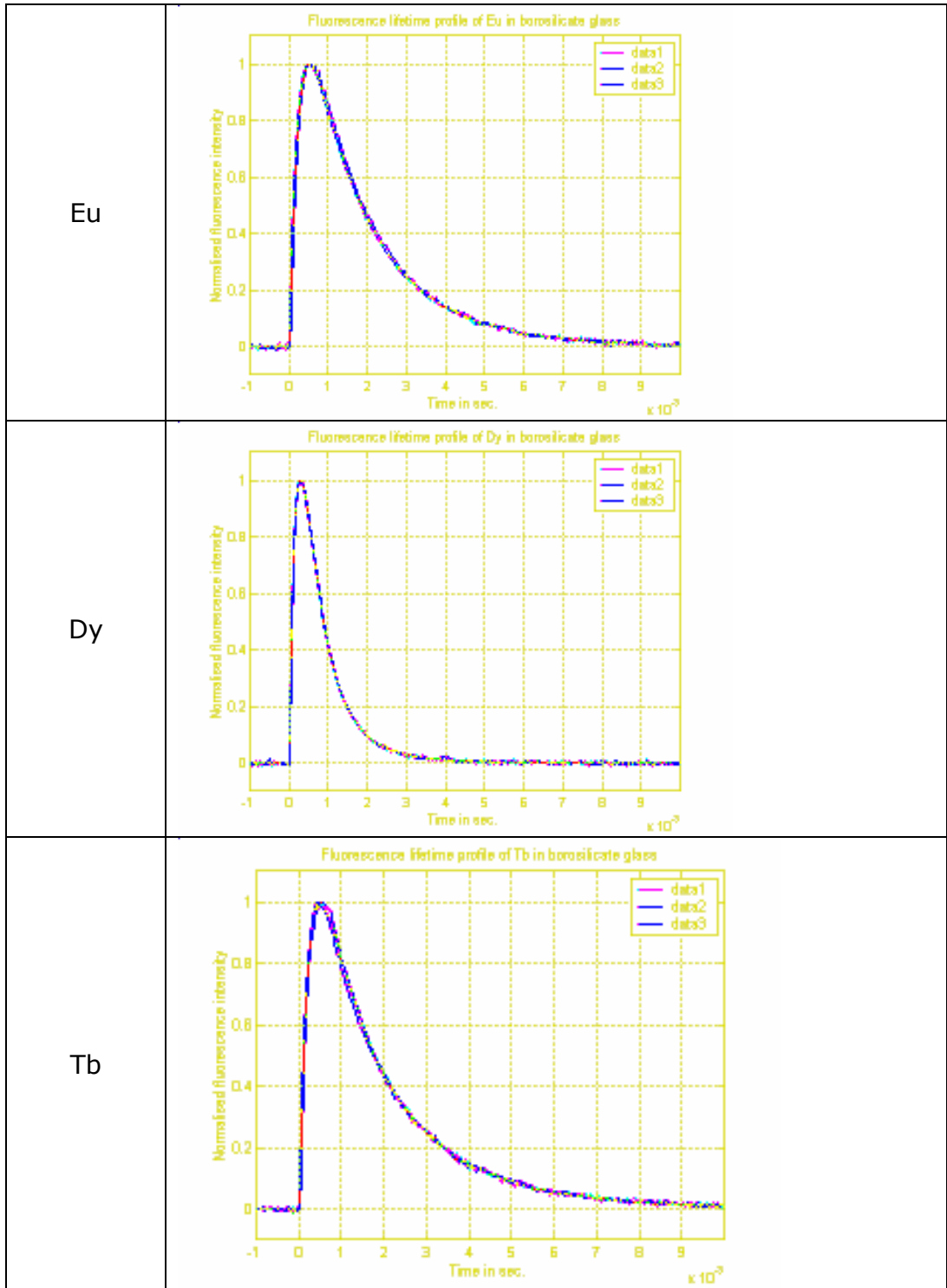


Figure 49 Eu, Dy and Tb fluorescent lifetimes in G2-24

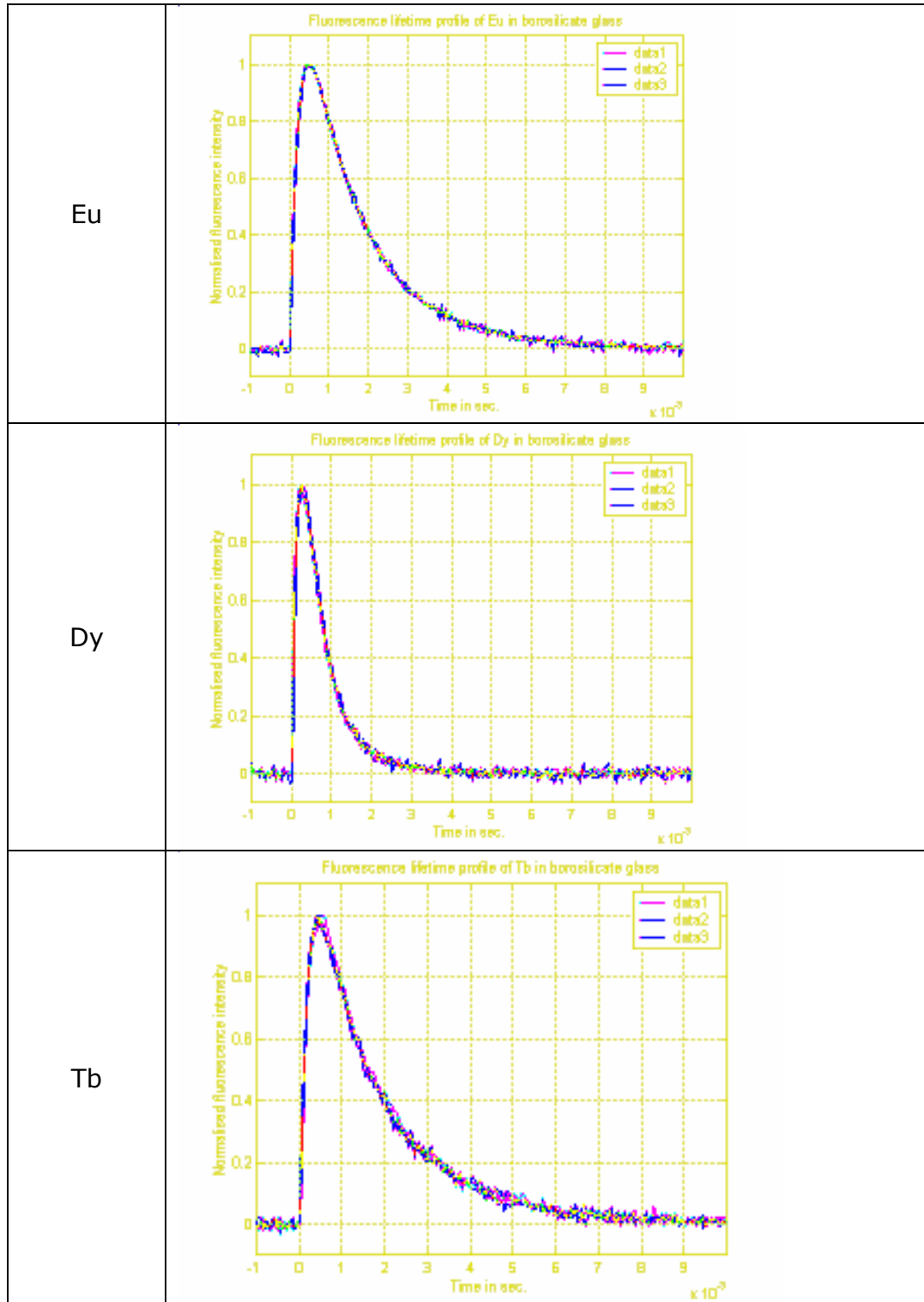


Figure 50 Eu, Dy and Tb fluorescent lifetimes in G2-25



**Appendix IV: Case Study GPS Data**



Development and Application of Novel Tracers for Environmental Applications  
 Appendix IV: Case Study GPS Data

---

<b>Point</b>	<b>Date and Time</b>	<b>GPS Position</b>
1	30/10/2008 09:18	N55 45.557 W6 19.398
2	30/10/2008 09:18	N55 45.546 W6 19.425
3	30/10/2008 09:19	N55 45.505 W6 19.544
4	30/10/2008 09:19	N55 45.461 W6 19.663
5	30/10/2008 09:19	N55 45.411 W6 19.793
6	30/10/2008 09:20	N55 45.362 W6 19.906
7	30/10/2008 09:20	N55 45.312 W6 20.016
8	30/10/2008 09:20	N55 45.263 W6 20.134
9	30/10/2008 09:21	N55 45.233 W6 20.253
10	30/10/2008 09:21	N55 45.210 W6 20.343
11	30/10/2008 09:21	N55 45.171 W6 20.413
12	30/10/2008 09:21	N55 45.101 W6 20.526
13	30/10/2008 09:22	N55 45.030 W6 20.625
14	30/10/2008 09:22	N55 44.973 W6 20.686
15	30/10/2008 09:22	N55 44.907 W6 20.763
16	30/10/2008 09:23	N55 44.837 W6 20.855
17	30/10/2008 09:23	N55 44.780 W6 20.931
18	30/10/2008 09:23	N55 44.741 W6 20.985
19	30/10/2008 09:24	N55 44.711 W6 21.050
20	30/10/2008 09:24	N55 44.683 W6 21.136
21	30/10/2008 09:24	N55 44.652 W6 21.219
22	30/10/2008 09:25	N55 44.618 W6 21.309
23	30/10/2008 09:25	N55 44.599 W6 21.405
24	30/10/2008 09:25	N55 44.594 W6 21.520
25	30/10/2008 09:25	N55 44.598 W6 21.660
26	30/10/2008 09:26	N55 44.607 W6 21.794
27	30/10/2008 09:26	N55 44.618 W6 21.914
28	30/10/2008 09:26	N55 44.624 W6 22.002
29	30/10/2008 09:27	N55 44.629 W6 22.045
30	30/10/2008 09:27	N55 44.636 W6 22.068
31	30/10/2008 09:27	N55 44.642 W6 22.080
32	30/10/2008 09:27	N55 44.641 W6 22.091
33	30/10/2008 09:28	N55 44.635 W6 22.100
34	30/10/2008 09:28	N55 44.629 W6 22.106
35	30/10/2008 09:28	N55 44.624 W6 22.110
36	30/10/2008 09:29	N55 44.618 W6 22.114
37	30/10/2008 09:29	N55 44.611 W6 22.119
38	30/10/2008 09:30	N55 44.603 W6 22.123
39	30/10/2008 09:30	N55 44.596 W6 22.126
40	30/10/2008 09:30	N55 44.587 W6 22.130
41	30/10/2008 09:31	N55 44.582 W6 22.133
42	30/10/2008 09:31	N55 44.576 W6 22.137
43	30/10/2008 09:31	N55 44.569 W6 22.140
44	30/10/2008 09:32	N55 44.562 W6 22.145
45	30/10/2008 09:32	N55 44.554 W6 22.150
46	30/10/2008 09:33	N55 44.547 W6 22.155
47	30/10/2008 09:33	N55 44.539 W6 22.159
48	30/10/2008 09:33	N55 44.533 W6 22.163
49	30/10/2008 09:34	N55 44.524 W6 22.168
50	30/10/2008 09:34	N55 44.517 W6 22.173
51	30/10/2008 09:34	N55 44.516 W6 22.183

Development and Application of Novel Tracers for Environmental Applications  
Appendix IV: Case Study GPS Data

---

52	30/10/2008 09:35	N55 44.516 W6 22.183
53	30/10/2008 09:35	N55 44.515 W6 22.178
54	30/10/2008 09:35	N55 44.510 W6 22.176
55	30/10/2008 09:35	N55 44.508 W6 22.176
56	30/10/2008 09:36	N55 44.505 W6 22.168
57	30/10/2008 09:36	N55 44.506 W6 22.176
58	30/10/2008 09:36	N55 44.506 W6 22.190
59	30/10/2008 09:37	N55 44.505 W6 22.201
60	30/10/2008 09:37	N55 44.500 W6 22.211
61	30/10/2008 09:38	N55 44.495 W6 22.222
62	30/10/2008 09:38	N55 44.499 W6 22.227
63	30/10/2008 09:38	N55 44.497 W6 22.223
64	30/10/2008 09:39	N55 44.490 W6 22.223
65	30/10/2008 09:39	N55 44.484 W6 22.225
66	30/10/2008 09:39	N55 44.477 W6 22.230
67	30/10/2008 09:40	N55 44.468 W6 22.236
68	30/10/2008 09:40	N55 44.462 W6 22.242
69	30/10/2008 09:40	N55 44.454 W6 22.248
70	30/10/2008 09:41	N55 44.446 W6 22.256
71	30/10/2008 09:41	N55 44.438 W6 22.263
72	30/10/2008 09:42	N55 44.431 W6 22.270
73	30/10/2008 09:42	N55 44.425 W6 22.278
74	30/10/2008 09:42	N55 44.420 W6 22.275
75	30/10/2008 09:42	N55 44.420 W6 22.273
76	30/10/2008 09:42	N55 44.424 W6 22.270
77	30/10/2008 09:43	N55 44.453 W6 22.255
78	30/10/2008 09:43	N55 44.507 W6 22.216
79	30/10/2008 09:44	N55 44.571 W6 22.169
80	30/10/2008 09:44	N55 44.623 W6 22.128
81	30/10/2008 09:45	N55 44.696 W6 22.074
82	30/10/2008 09:45	N55 44.761 W6 22.029
83	30/10/2008 09:45	N55 44.850 W6 21.974
84	30/10/2008 09:46	N55 44.917 W6 21.943
85	30/10/2008 09:46	N55 45.013 W6 21.914
86	30/10/2008 09:47	N55 45.131 W6 21.868
87	30/10/2008 09:47	N55 45.222 W6 21.827
88	30/10/2008 09:47	N55 45.250 W6 21.810
89	30/10/2008 09:48	N55 45.298 W6 21.816
90	30/10/2008 09:48	N55 45.322 W6 21.806
91	30/10/2008 09:48	N55 45.336 W6 21.796
92	30/10/2008 09:49	N55 45.337 W6 21.802
93	30/10/2008 09:49	N55 45.334 W6 21.813
94	30/10/2008 09:49	N55 45.330 W6 21.821
95	30/10/2008 09:50	N55 45.324 W6 21.829
96	30/10/2008 09:50	N55 45.317 W6 21.836
97	30/10/2008 09:51	N55 45.309 W6 21.843
98	30/10/2008 09:51	N55 45.302 W6 21.848
99	30/10/2008 09:51	N55 45.295 W6 21.854
100	30/10/2008 09:52	N55 45.286 W6 21.862
101	30/10/2008 09:52	N55 45.279 W6 21.868
102	30/10/2008 09:53	N55 45.272 W6 21.873
103	30/10/2008 09:53	N55 45.265 W6 21.878

Development and Application of Novel Tracers for Environmental Applications  
 Appendix IV: Case Study GPS Data

---

104	30/10/2008 09:54	N55 45.257 W6 21.884
105	30/10/2008 09:54	N55 45.251 W6 21.889
106	30/10/2008 09:54	N55 45.247 W6 21.892
107	30/10/2008 09:54	N55 45.254 W6 21.896
108	30/10/2008 09:55	N55 45.291 W6 21.848
109	30/10/2008 09:55	N55 45.337 W6 21.799
110	30/10/2008 09:56	N55 45.395 W6 21.736
111	30/10/2008 09:56	N55 45.466 W6 21.665
112	30/10/2008 09:57	N55 45.550 W6 21.562
113	30/10/2008 09:57	N55 45.616 W6 21.500
114	30/10/2008 09:58	N55 45.697 W6 21.441
115	30/10/2008 09:58	N55 45.770 W6 21.396
116	30/10/2008 09:58	N55 45.815 W6 21.366
117	30/10/2008 09:58	N55 45.816 W6 21.364
118	30/10/2008 09:59	N55 45.822 W6 21.353
119	30/10/2008 09:59	N55 45.820 W6 21.361
120	30/10/2008 10:00	N55 45.815 W6 21.371
121	30/10/2008 10:00	N55 45.810 W6 21.377
122	30/10/2008 10:01	N55 45.805 W6 21.382
123	30/10/2008 10:01	N55 45.798 W6 21.388
124	30/10/2008 10:02	N55 45.792 W6 21.392
125	30/10/2008 10:02	N55 45.787 W6 21.396
126	30/10/2008 10:02	N55 45.782 W6 21.400
127	30/10/2008 10:03	N55 45.774 W6 21.405
128	30/10/2008 10:03	N55 45.773 W6 21.415
129	30/10/2008 10:03	N55 45.777 W6 21.420
130	30/10/2008 10:03	N55 45.780 W6 21.417
131	30/10/2008 10:04	N55 45.800 W6 21.384
132	30/10/2008 10:04	N55 45.851 W6 21.313
133	30/10/2008 10:05	N55 45.901 W6 21.246
134	30/10/2008 10:05	N55 45.963 W6 21.175
135	30/10/2008 10:06	N55 46.024 W6 21.108
136	30/10/2008 10:06	N55 46.115 W6 21.027
137	30/10/2008 10:07	N55 46.199 W6 20.978
138	30/10/2008 10:07	N55 46.313 W6 20.925
139	30/10/2008 10:08	N55 46.392 W6 20.890
140	30/10/2008 10:08	N55 46.477 W6 20.843
141	30/10/2008 10:09	N55 46.520 W6 20.810
142	30/10/2008 10:09	N55 46.528 W6 20.797
143	30/10/2008 10:09	N55 46.532 W6 20.796
144	30/10/2008 10:10	N55 46.528 W6 20.808
145	30/10/2008 10:11	N55 46.523 W6 20.814
146	30/10/2008 10:11	N55 46.516 W6 20.816
147	30/10/2008 10:12	N55 46.508 W6 20.817
148	30/10/2008 10:13	N55 46.500 W6 20.819
149	30/10/2008 10:14	N55 46.491 W6 20.821
150	30/10/2008 10:14	N55 46.484 W6 20.825
151	30/10/2008 10:15	N55 46.477 W6 20.827
152	30/10/2008 10:15	N55 46.476 W6 20.828
153	30/10/2008 10:15	N55 46.483 W6 20.845
154	30/10/2008 10:15	N55 46.489 W6 20.835
155	30/10/2008 10:16	N55 46.511 W6 20.746

Development and Application of Novel Tracers for Environmental Applications  
 Appendix IV: Case Study GPS Data

---

156	30/10/2008 10:16	N55 46.535 W6 20.666
157	30/10/2008 10:17	N55 46.563 W6 20.579
158	30/10/2008 10:17	N55 46.569 W6 20.535
159	30/10/2008 10:17	N55 46.572 W6 20.493
160	30/10/2008 10:18	N55 46.573 W6 20.466
161	30/10/2008 10:18	N55 46.567 W6 20.456
162	30/10/2008 10:19	N55 46.560 W6 20.458
163	30/10/2008 10:19	N55 46.556 W6 20.450
164	30/10/2008 10:20	N55 46.560 W6 20.417
165	30/10/2008 10:20	N55 46.570 W6 20.391
166	30/10/2008 10:21	N55 46.577 W6 20.381
167	30/10/2008 10:21	N55 46.575 W6 20.390
168	30/10/2008 10:22	N55 46.569 W6 20.396
169	30/10/2008 10:22	N55 46.564 W6 20.400
170	30/10/2008 10:23	N55 46.559 W6 20.403
171	30/10/2008 10:23	N55 46.558 W6 20.411
172	30/10/2008 10:24	N55 46.573 W6 20.418
173	30/10/2008 10:24	N55 46.575 W6 20.393
174	30/10/2008 10:24	N55 46.565 W6 20.331
175	30/10/2008 10:25	N55 46.560 W6 20.282
176	30/10/2008 10:25	N55 46.564 W6 20.244
177	30/10/2008 10:26	N55 46.583 W6 20.218
178	30/10/2008 10:26	N55 46.614 W6 20.197
179	30/10/2008 10:27	N55 46.637 W6 20.164
180	30/10/2008 10:27	N55 46.659 W6 20.142
181	30/10/2008 10:28	N55 46.700 W6 20.118
182	30/10/2008 10:28	N55 46.724 W6 20.085
183	30/10/2008 10:29	N55 46.753 W6 20.047
184	30/10/2008 10:29	N55 46.767 W6 19.986
185	30/10/2008 10:29	N55 46.772 W6 19.848
186	30/10/2008 10:30	N55 46.776 W6 19.717
187	30/10/2008 10:30	N55 46.774 W6 19.581
188	30/10/2008 10:31	N55 46.778 W6 19.424
189	30/10/2008 10:31	N55 46.797 W6 19.225
190	30/10/2008 10:32	N55 46.813 W6 19.127
191	30/10/2008 10:32	N55 46.819 W6 19.092
192	30/10/2008 10:32	N55 46.817 W6 19.074
193	30/10/2008 10:33	N55 46.811 W6 19.066
194	30/10/2008 10:33	N55 46.806 W6 19.065
195	30/10/2008 10:34	N55 46.801 W6 19.067
196	30/10/2008 10:35	N55 46.794 W6 19.073
197	30/10/2008 10:35	N55 46.789 W6 19.080
198	30/10/2008 10:35	N55 46.786 W6 19.077
199	30/10/2008 10:35	N55 46.784 W6 19.070
200	30/10/2008 10:36	N55 46.780 W6 19.027
201	30/10/2008 10:36	N55 46.778 W6 18.912
202	30/10/2008 10:37	N55 46.769 W6 18.767
203	30/10/2008 10:37	N55 46.766 W6 18.627
204	30/10/2008 10:38	N55 46.759 W6 18.440
205	30/10/2008 10:39	N55 46.764 W6 18.279
206	30/10/2008 10:39	N55 46.775 W6 18.141
207	30/10/2008 10:39	N55 46.787 W6 18.044

Development and Application of Novel Tracers for Environmental Applications  
Appendix IV: Case Study GPS Data

---

208	30/10/2008 10:40	N55 46.787 W6 18.011
209	30/10/2008 10:40	N55 46.781 W6 17.995
210	30/10/2008 10:41	N55 46.775 W6 17.992
211	30/10/2008 10:41	N55 46.769 W6 17.994
212	30/10/2008 10:42	N55 46.764 W6 17.998
213	30/10/2008 10:43	N55 46.760 W6 18.004
214	30/10/2008 10:43	N55 46.754 W6 18.003
215	30/10/2008 10:43	N55 46.748 W6 17.961
216	30/10/2008 10:44	N55 46.745 W6 17.867
217	30/10/2008 10:45	N55 46.753 W6 17.768
218	30/10/2008 10:45	N55 46.756 W6 17.631
219	30/10/2008 10:46	N55 46.761 W6 17.500
220	30/10/2008 10:47	N55 46.752 W6 17.388
221	30/10/2008 10:47	N55 46.729 W6 17.280
222	30/10/2008 10:48	N55 46.706 W6 17.210
223	30/10/2008 10:48	N55 46.695 W6 17.182
224	30/10/2008 10:49	N55 46.685 W6 17.171
225	30/10/2008 10:49	N55 46.678 W6 17.171
226	30/10/2008 10:50	N55 46.670 W6 17.173
227	30/10/2008 10:51	N55 46.664 W6 17.181
228	30/10/2008 10:52	N55 46.657 W6 17.189
229	30/10/2008 10:53	N55 46.652 W6 17.197
230	30/10/2008 10:54	N55 46.647 W6 17.205
231	30/10/2008 10:55	N55 46.640 W6 17.212
232	30/10/2008 10:55	N55 46.634 W6 17.220
233	30/10/2008 10:56	N55 46.627 W6 17.231
234	30/10/2008 10:57	N55 46.617 W6 17.229
235	30/10/2008 10:58	N55 46.589 W6 17.183
236	30/10/2008 10:58	N55 46.548 W6 17.116
237	30/10/2008 10:59	N55 46.504 W6 17.035
238	30/10/2008 10:59	N55 46.428 W6 16.938
239	30/10/2008 11:00	N55 46.357 W6 16.878
240	30/10/2008 11:00	N55 46.277 W6 16.810
241	30/10/2008 11:01	N55 46.200 W6 16.748
242	30/10/2008 11:01	N55 46.146 W6 16.693
243	30/10/2008 11:02	N55 46.125 W6 16.662
244	30/10/2008 11:02	N55 46.114 W6 16.651
245	30/10/2008 11:02	N55 46.104 W6 16.647
246	30/10/2008 11:03	N55 46.098 W6 16.650
247	30/10/2008 11:04	N55 46.092 W6 16.655
248	30/10/2008 11:05	N55 46.086 W6 16.663
249	30/10/2008 11:05	N55 46.079 W6 16.670
250	30/10/2008 11:06	N55 46.053 W6 16.655
251	30/10/2008 11:06	N55 46.008 W6 16.643
252	30/10/2008 11:07	N55 45.961 W6 16.636
253	30/10/2008 11:08	N55 45.923 W6 16.642
254	30/10/2008 11:08	N55 45.882 W6 16.675
255	30/10/2008 11:09	N55 45.838 W6 16.708
256	30/10/2008 11:10	N55 45.812 W6 16.742
257	30/10/2008 11:10	N55 45.805 W6 16.767
258	30/10/2008 11:11	N55 45.798 W6 16.779
259	30/10/2008 11:11	N55 45.789 W6 16.785

Development and Application of Novel Tracers for Environmental Applications  
 Appendix IV: Case Study GPS Data

---

260	30/10/2008 11:12	N55 45.782 W6 16.791
261	30/10/2008 11:12	N55 45.775 W6 16.797
262	30/10/2008 11:13	N55 45.769 W6 16.807
263	30/10/2008 11:13	N55 45.759 W6 16.843
264	30/10/2008 11:14	N55 45.734 W6 16.894
265	30/10/2008 11:14	N55 45.704 W6 16.956
266	30/10/2008 11:15	N55 45.679 W6 17.011
267	30/10/2008 11:15	N55 45.656 W6 17.070
268	30/10/2008 11:16	N55 45.626 W6 17.138
269	30/10/2008 11:16	N55 45.593 W6 17.202
270	30/10/2008 11:17	N55 45.572 W6 17.245
271	30/10/2008 11:17	N55 45.573 W6 17.261
272	30/10/2008 11:17	N55 45.570 W6 17.264
273	30/10/2008 11:18	N55 45.570 W6 17.255
274	30/10/2008 11:18	N55 45.565 W6 17.261
275	30/10/2008 11:19	N55 45.563 W6 17.267
276	30/10/2008 11:19	N55 45.569 W6 17.277
277	30/10/2008 11:20	N55 45.563 W6 17.283
278	30/10/2008 11:20	N55 45.558 W6 17.290
279	30/10/2008 11:21	N55 45.560 W6 17.300
280	30/10/2008 11:21	N55 45.560 W6 17.305
281	30/10/2008 11:22	N55 45.551 W6 17.329
282	30/10/2008 11:22	N55 45.551 W6 17.334
283	30/10/2008 11:22	N55 45.549 W6 17.364
284	30/10/2008 11:22	N55 45.548 W6 17.372
285	30/10/2008 11:23	N55 45.550 W6 17.383
286	30/10/2008 11:23	N55 45.548 W6 17.385
287	30/10/2008 11:24	N55 45.545 W6 17.382
288	30/10/2008 11:24	N55 45.541 W6 17.389
289	30/10/2008 11:24	N55 45.537 W6 17.391
290	30/10/2008 11:24	N55 45.537 W6 17.389
291	30/10/2008 11:25	N55 45.541 W6 17.379
292	30/10/2008 11:25	N55 45.534 W6 17.376
293	30/10/2008 11:26	N55 45.532 W6 17.368
294	30/10/2008 11:26	N55 45.530 W6 17.360
295	30/10/2008 11:26	N55 45.534 W6 17.358
296	30/10/2008 11:27	N55 45.557 W6 17.357
297	30/10/2008 11:27	N55 45.584 W6 17.385
298	30/10/2008 11:28	N55 45.603 W6 17.414
299	30/10/2008 11:28	N55 45.610 W6 17.426
300	30/10/2008 11:28	N55 45.613 W6 17.421
301	30/10/2008 11:29	N55 45.623 W6 17.432
302	30/10/2008 11:29	N55 45.634 W6 17.439
303	30/10/2008 11:30	N55 45.655 W6 17.454
304	30/10/2008 11:30	N55 45.662 W6 17.498
305	30/10/2008 11:30	N55 45.642 W6 17.546
306	30/10/2008 11:30	N55 45.612 W6 17.585
307	30/10/2008 11:31	N55 45.575 W6 17.578
308	30/10/2008 11:31	N55 45.539 W6 17.548
309	30/10/2008 11:31	N55 45.513 W6 17.522
310	30/10/2008 11:32	N55 45.504 W6 17.521
311	30/10/2008 11:32	N55 45.493 W6 17.524

Development and Application of Novel Tracers for Environmental Applications  
Appendix IV: Case Study GPS Data

---

312	30/10/2008 11:33	N55 45.489 W6 17.530
313	30/10/2008 11:33	N55 45.487 W6 17.521
314	30/10/2008 11:33	N55 45.490 W6 17.522
315	30/10/2008 11:34	N55 45.511 W6 17.551
316	30/10/2008 11:34	N55 45.538 W6 17.603
317	30/10/2008 11:35	N55 45.566 W6 17.643
318	30/10/2008 11:35	N55 45.598 W6 17.678
319	30/10/2008 11:35	N55 45.603 W6 17.716
320	30/10/2008 11:36	N55 45.589 W6 17.778
321	30/10/2008 11:36	N55 45.564 W6 17.855
322	30/10/2008 11:37	N55 45.536 W6 17.934
323	30/10/2008 11:37	N55 45.503 W6 17.958
324	30/10/2008 11:37	N55 45.470 W6 17.957
325	30/10/2008 11:38	N55 45.421 W6 17.959
326	30/10/2008 11:38	N55 45.399 W6 17.968
327	30/10/2008 11:38	N55 45.375 W6 18.013
328	30/10/2008 11:39	N55 45.369 W6 18.033
329	30/10/2008 11:39	N55 45.367 W6 18.044
330	30/10/2008 11:40	N55 45.363 W6 18.050
331	30/10/2008 11:40	N55 45.357 W6 18.056
332	30/10/2008 11:41	N55 45.353 W6 18.062
333	30/10/2008 11:41	N55 45.347 W6 18.067
334	30/10/2008 11:41	N55 45.347 W6 18.070
335	30/10/2008 11:42	N55 45.352 W6 18.110
336	30/10/2008 11:42	N55 45.354 W6 18.154
337	30/10/2008 11:42	N55 45.359 W6 18.181
338	30/10/2008 11:42	N55 45.375 W6 18.177
339	30/10/2008 11:43	N55 45.426 W6 18.123
340	30/10/2008 11:43	N55 45.431 W6 18.120
341	30/10/2008 11:43	N55 45.449 W6 18.123
342	30/10/2008 11:43	N55 45.530 W6 18.212
343	30/10/2008 11:44	N55 45.603 W6 18.280
344	30/10/2008 11:44	N55 45.699 W6 18.361
345	30/10/2008 11:45	N55 45.766 W6 18.406
346	30/10/2008 11:45	N55 45.779 W6 18.408
347	30/10/2008 11:45	N55 45.784 W6 18.419
348	30/10/2008 11:46	N55 45.782 W6 18.427
349	30/10/2008 11:46	N55 45.780 W6 18.432
350	30/10/2008 11:46	N55 45.776 W6 18.437
351	30/10/2008 11:47	N55 45.771 W6 18.443
352	30/10/2008 11:47	N55 45.768 W6 18.447
353	30/10/2008 11:47	N55 45.764 W6 18.454
354	30/10/2008 11:48	N55 45.761 W6 18.460
355	30/10/2008 11:48	N55 45.757 W6 18.465
356	30/10/2008 11:49	N55 45.752 W6 18.471
357	30/10/2008 11:49	N55 45.749 W6 18.476
358	30/10/2008 11:49	N55 45.746 W6 18.482
359	30/10/2008 11:50	N55 45.743 W6 18.487
360	30/10/2008 11:50	N55 45.740 W6 18.492
361	30/10/2008 11:51	N55 45.738 W6 18.497
362	30/10/2008 11:51	N55 45.751 W6 18.499
363	30/10/2008 11:51	N55 45.752 W6 18.496

Development and Application of Novel Tracers for Environmental Applications  
 Appendix IV: Case Study GPS Data

---

364	30/10/2008 11:51	N55 45.777 W6 18.415
365	30/10/2008 11:52	N55 45.817 W6 18.282
366	30/10/2008 11:52	N55 45.857 W6 18.104
367	30/10/2008 11:53	N55 45.893 W6 17.940
368	30/10/2008 11:53	N55 45.926 W6 17.773
369	30/10/2008 11:53	N55 45.947 W6 17.683
370	30/10/2008 11:54	N55 45.952 W6 17.654
371	30/10/2008 11:54	N55 45.946 W6 17.639
372	30/10/2008 11:55	N55 45.940 W6 17.638
373	30/10/2008 11:55	N55 45.935 W6 17.643
374	30/10/2008 11:56	N55 45.930 W6 17.649
375	30/10/2008 11:56	N55 45.927 W6 17.654
376	30/10/2008 11:57	N55 45.923 W6 17.660
377	30/10/2008 11:57	N55 45.919 W6 17.667
378	30/10/2008 11:58	N55 45.914 W6 17.675
379	30/10/2008 11:58	N55 45.910 W6 17.682
380	30/10/2008 11:59	N55 45.906 W6 17.686
381	30/10/2008 11:59	N55 45.903 W6 17.684
382	30/10/2008 11:59	N55 45.879 W6 17.674
383	30/10/2008 11:59	N55 45.848 W6 17.708
384	30/10/2008 11:59	N55 45.794 W6 17.822
385	30/10/2008 12:00	N55 45.719 W6 17.980
386	30/10/2008 12:00	N55 45.668 W6 18.089
387	30/10/2008 12:01	N55 45.612 W6 18.179
388	30/10/2008 12:01	N55 45.537 W6 18.328
389	30/10/2008 12:02	N55 45.453 W6 18.502
390	30/10/2008 12:02	N55 45.395 W6 18.627
391	30/10/2008 12:02	N55 45.327 W6 18.754
392	30/10/2008 12:03	N55 45.252 W6 18.893
393	30/10/2008 12:03	N55 45.192 W6 19.030
394	30/10/2008 12:03	N55 45.176 W6 19.078
395	30/10/2008 12:04	N55 45.171 W6 19.094
396	30/10/2008 12:04	N55 45.167 W6 19.099
397	30/10/2008 12:04	N55 45.164 W6 19.102
398	30/10/2008 12:05	N55 45.160 W6 19.105
399	30/10/2008 12:05	N55 45.156 W6 19.110
400	30/10/2008 12:05	N55 45.153 W6 19.113
401	30/10/2008 12:06	N55 45.148 W6 19.116
402	30/10/2008 12:06	N55 45.144 W6 19.119
403	30/10/2008 12:07	N55 45.141 W6 19.123
404	30/10/2008 12:07	N55 45.137 W6 19.157
405	30/10/2008 12:07	N55 45.125 W6 19.216
406	30/10/2008 12:08	N55 45.105 W6 19.289
407	30/10/2008 12:08	N55 45.089 W6 19.378
408	30/10/2008 12:08	N55 45.075 W6 19.470
409	30/10/2008 12:08	N55 45.051 W6 19.576
410	30/10/2008 12:09	N55 45.011 W6 19.684
411	30/10/2008 12:09	N55 44.956 W6 19.810
412	30/10/2008 12:09	N55 44.936 W6 19.862
413	30/10/2008 12:10	N55 44.925 W6 19.887
414	30/10/2008 12:10	N55 44.919 W6 19.909
415	30/10/2008 12:10	N55 44.918 W6 19.919



Development and Application of Novel Tracers for Environmental Applications  
 Appendix IV: Case Study GPS Data

---

416	30/10/2008 12:11	N55 44.917 W6 19.923
417	30/10/2008 12:11	N55 44.914 W6 19.928
418	30/10/2008 12:12	N55 44.910 W6 19.930
419	30/10/2008 12:12	N55 44.905 W6 19.933
420	30/10/2008 12:12	N55 44.901 W6 19.935
421	30/10/2008 12:13	N55 44.896 W6 19.938
422	30/10/2008 12:13	N55 44.893 W6 19.940
423	30/10/2008 12:14	N55 44.888 W6 19.943
424	30/10/2008 12:14	N55 44.885 W6 19.946
425	30/10/2008 12:14	N55 44.885 W6 19.947
426	30/10/2008 12:14	N55 44.879 W6 19.981
427	30/10/2008 12:15	N55 44.848 W6 20.040
428	30/10/2008 12:15	N55 44.804 W6 20.107
429	30/10/2008 12:15	N55 44.755 W6 20.177
430	30/10/2008 12:15	N55 44.741 W6 20.218
431	30/10/2008 12:16	N55 44.706 W6 20.279
432	30/10/2008 12:16	N55 44.692 W6 20.305
433	30/10/2008 12:16	N55 44.689 W6 20.317
434	30/10/2008 12:17	N55 44.689 W6 20.324
435	30/10/2008 12:17	N55 44.687 W6 20.330
436	30/10/2008 12:17	N55 44.684 W6 20.333
437	30/10/2008 12:18	N55 44.681 W6 20.336
438	30/10/2008 12:18	N55 44.678 W6 20.340
439	30/10/2008 12:19	N55 44.674 W6 20.344
440	30/10/2008 12:19	N55 44.669 W6 20.350
441	30/10/2008 12:20	N55 44.666 W6 20.354
442	30/10/2008 12:20	N55 44.662 W6 20.358
443	30/10/2008 12:20	N55 44.659 W6 20.362
444	30/10/2008 12:21	N55 44.655 W6 20.366
445	30/10/2008 12:21	N55 44.653 W6 20.370
446	30/10/2008 12:21	N55 44.655 W6 20.415
447	30/10/2008 12:22	N55 44.647 W6 20.481
448	30/10/2008 12:22	N55 44.640 W6 20.585
449	30/10/2008 12:22	N55 44.634 W6 20.659
450	30/10/2008 12:22	N55 44.635 W6 20.770
451	30/10/2008 12:23	N55 44.635 W6 20.885
452	30/10/2008 12:23	N55 44.632 W6 20.994
453	30/10/2008 12:23	N55 44.631 W6 21.044
454	30/10/2008 12:23	N55 44.631 W6 21.078
455	30/10/2008 12:24	N55 44.631 W6 21.098
456	30/10/2008 12:24	N55 44.631 W6 21.106
457	30/10/2008 12:24	N55 44.630 W6 21.112
458	30/10/2008 12:25	N55 44.627 W6 21.118
459	30/10/2008 12:25	N55 44.624 W6 21.123
460	30/10/2008 12:25	N55 44.626 W6 21.127
461	30/10/2008 12:25	N55 44.628 W6 21.129
462	30/10/2008 12:25	N55 44.631 W6 21.119
463	30/10/2008 12:26	N55 44.628 W6 21.111
464	30/10/2008 12:26	N55 44.624 W6 21.110
465	30/10/2008 12:26	N55 44.624 W6 21.112
466	30/10/2008 12:27	N55 44.627 W6 21.120
467	30/10/2008 12:27	N55 44.624 W6 21.120

Development and Application of Novel Tracers for Environmental Applications  
 Appendix IV: Case Study GPS Data

---

468	30/10/2008 12:27	N55 44.627 W6 21.117
469	30/10/2008 12:27	N55 44.630 W6 21.127
470	30/10/2008 12:27	N55 44.636 W6 21.122
471	30/10/2008 12:28	N55 44.633 W6 21.113
472	30/10/2008 12:28	N55 44.631 W6 21.110
473	30/10/2008 12:28	N55 44.629 W6 21.106
474	30/10/2008 12:28	N55 44.633 W6 21.106
475	30/10/2008 12:29	N55 44.640 W6 21.118
476	30/10/2008 12:29	N55 44.646 W6 21.123
477	30/10/2008 12:29	N55 44.647 W6 21.115
478	30/10/2008 12:30	N55 44.647 W6 21.106
479	30/10/2008 12:30	N55 44.646 W6 21.112
480	30/10/2008 12:30	N55 44.647 W6 21.120
481	30/10/2008 12:31	N55 44.652 W6 21.115
482	30/10/2008 12:31	N55 44.646 W6 21.098
483	30/10/2008 12:31	N55 44.643 W6 21.094
484	30/10/2008 12:31	N55 44.641 W6 21.087
485	30/10/2008 12:32	N55 44.640 W6 21.078
486	30/10/2008 12:32	N55 44.647 W6 21.069
487	30/10/2008 12:32	N55 44.644 W6 21.068
488	30/10/2008 12:33	N55 44.642 W6 21.069
489	30/10/2008 12:33	N55 44.640 W6 21.074
490	30/10/2008 12:33	N55 44.637 W6 21.068
491	30/10/2008 12:33	N55 44.639 W6 21.060
492	30/10/2008 12:34	N55 44.642 W6 21.060
493	30/10/2008 12:34	N55 44.651 W6 21.058
494	30/10/2008 12:34	N55 44.661 W6 21.069
495	30/10/2008 12:34	N55 44.671 W6 21.081
496	30/10/2008 12:34	N55 44.671 W6 21.087
497	30/10/2008 12:35	N55 44.666 W6 21.106
498	30/10/2008 12:35	N55 44.658 W6 21.104
499	30/10/2008 12:35	N55 44.656 W6 21.093
500	30/10/2008 12:36	N55 44.661 W6 21.089
501	30/10/2008 12:36	N55 44.664 W6 21.086
502	30/10/2008 12:36	N55 44.664 W6 21.084
503	30/10/2008 12:36	N55 44.662 W6 21.072
504	30/10/2008 12:37	N55 44.660 W6 21.062
505	30/10/2008 12:37	N55 44.664 W6 21.059
506	30/10/2008 12:37	N55 44.672 W6 21.068
507	30/10/2008 12:38	N55 44.680 W6 21.069
508	30/10/2008 12:38	N55 44.680 W6 21.058
509	30/10/2008 12:38	N55 44.682 W6 21.051
510	30/10/2008 12:38	N55 44.697 W6 21.018
511	30/10/2008 12:39	N55 44.701 W6 21.010
512	30/10/2008 12:39	N55 44.703 W6 21.018
513	30/10/2008 12:39	N55 44.701 W6 21.021
514	30/10/2008 12:39	N55 44.686 W6 21.039
515	30/10/2008 12:40	N55 44.669 W6 21.053
516	30/10/2008 12:40	N55 44.662 W6 21.060
517	30/10/2008 12:40	N55 44.657 W6 21.086
518	30/10/2008 12:41	N55 44.652 W6 21.098
519	30/10/2008 12:41	N55 44.648 W6 21.103

Development and Application of Novel Tracers for Environmental Applications  
 Appendix IV: Case Study GPS Data

---

520	30/10/2008 12:41	N55 44.644 W6 21.104
521	30/10/2008 12:41	N55 44.640 W6 21.104
522	30/10/2008 12:42	N55 44.636 W6 21.099
523	30/10/2008 12:42	N55 44.633 W6 21.100
524	30/10/2008 12:42	N55 44.630 W6 21.092
525	30/10/2008 12:43	N55 44.630 W6 21.083
526	30/10/2008 12:43	N55 44.629 W6 21.074
527	30/10/2008 12:43	N55 44.635 W6 21.074
528	30/10/2008 12:44	N55 44.641 W6 21.080
529	30/10/2008 12:44	N55 44.645 W6 21.085
530	30/10/2008 12:44	N55 44.648 W6 21.084
531	30/10/2008 12:45	N55 44.656 W6 21.084
532	30/10/2008 12:45	N55 44.658 W6 21.089
533	30/10/2008 12:45	N55 44.657 W6 21.095
534	30/10/2008 12:45	N55 44.656 W6 21.100
535	30/10/2008 12:46	N55 44.654 W6 21.107
536	30/10/2008 12:46	N55 44.652 W6 21.112
537	30/10/2008 12:46	N55 44.653 W6 21.120
538	30/10/2008 12:46	N55 44.653 W6 21.123
539	30/10/2008 12:47	N55 44.661 W6 21.130
540	30/10/2008 12:47	N55 44.661 W6 21.125
541	30/10/2008 12:47	N55 44.658 W6 21.120
542	30/10/2008 12:48	N55 44.655 W6 21.121
543	30/10/2008 12:48	N55 44.652 W6 21.123
544	30/10/2008 12:48	N55 44.651 W6 21.125
545	30/10/2008 12:49	N55 44.648 W6 21.126
546	30/10/2008 12:49	N55 44.647 W6 21.120
547	30/10/2008 12:49	N55 44.653 W6 21.109
548	30/10/2008 12:49	N55 44.653 W6 21.104
549	30/10/2008 12:50	N55 44.652 W6 21.092
550	30/10/2008 12:50	N55 44.654 W6 21.080
551	30/10/2008 12:50	N55 44.660 W6 21.067
552	30/10/2008 12:50	N55 44.658 W6 21.060
553	30/10/2008 12:51	N55 44.655 W6 21.060
554	30/10/2008 12:51	N55 44.653 W6 21.056
555	30/10/2008 12:51	N55 44.655 W6 21.053
556	30/10/2008 12:51	N55 44.659 W6 21.058
557	30/10/2008 12:52	N55 44.660 W6 21.064
558	30/10/2008 12:52	N55 44.665 W6 21.072
559	30/10/2008 12:52	N55 44.669 W6 21.096
560	30/10/2008 12:52	N55 44.667 W6 21.111
561	30/10/2008 12:53	N55 44.666 W6 21.115
562	30/10/2008 12:53	N55 44.658 W6 21.117
563	30/10/2008 12:53	N55 44.657 W6 21.116
564	30/10/2008 12:53	N55 44.652 W6 21.110
565	30/10/2008 12:54	N55 44.649 W6 21.107
566	30/10/2008 12:54	N55 44.645 W6 21.097
567	30/10/2008 12:54	N55 44.644 W6 21.085
568	30/10/2008 12:55	N55 44.641 W6 21.082
569	30/10/2008 12:55	N55 44.638 W6 21.083
570	30/10/2008 12:55	N55 44.635 W6 21.086
571	30/10/2008 12:56	N55 44.632 W6 21.078

Development and Application of Novel Tracers for Environmental Applications  
 Appendix IV: Case Study GPS Data

---

572	30/10/2008 12:56	N55 44.628 W6 21.072
573	30/10/2008 12:56	N55 44.627 W6 21.063
574	30/10/2008 12:57	N55 44.633 W6 21.058
575	30/10/2008 12:57	N55 44.644 W6 21.059
576	30/10/2008 12:57	N55 44.645 W6 21.057
577	30/10/2008 12:57	N55 44.656 W6 21.051
578	30/10/2008 12:57	N55 44.657 W6 21.052
579	30/10/2008 12:58	N55 44.660 W6 21.074
580	30/10/2008 12:58	N55 44.661 W6 21.096
581	30/10/2008 12:58	N55 44.653 W6 21.108
582	30/10/2008 12:59	N55 44.644 W6 21.113
583	30/10/2008 12:59	N55 44.638 W6 21.113
584	30/10/2008 12:59	N55 44.636 W6 21.114
585	30/10/2008 13:00	N55 44.634 W6 21.117
586	30/10/2008 13:00	N55 44.629 W6 21.109
587	30/10/2008 13:00	N55 44.626 W6 21.103
588	30/10/2008 13:00	N55 44.622 W6 21.093
589	30/10/2008 13:01	N55 44.623 W6 21.083
590	30/10/2008 13:01	N55 44.625 W6 21.072
591	30/10/2008 13:01	N55 44.624 W6 21.063
592	30/10/2008 13:02	N55 44.629 W6 21.057
593	30/10/2008 13:02	N55 44.639 W6 21.054
594	30/10/2008 13:02	N55 44.644 W6 21.046
595	30/10/2008 13:02	N55 44.641 W6 21.034
596	30/10/2008 13:03	N55 44.645 W6 21.024
597	30/10/2008 13:03	N55 44.646 W6 21.023
598	30/10/2008 13:03	N55 44.658 W6 21.009
599	30/10/2008 13:04	N55 44.669 W6 21.015
600	30/10/2008 13:04	N55 44.684 W6 21.018
601	30/10/2008 13:04	N55 44.692 W6 21.023
602	30/10/2008 13:04	N55 44.695 W6 21.015
603	30/10/2008 13:05	N55 44.688 W6 20.992
604	30/10/2008 13:05	N55 44.679 W6 20.975
605	30/10/2008 13:05	N55 44.670 W6 20.964
606	30/10/2008 13:06	N55 44.658 W6 20.959
607	30/10/2008 13:06	N55 44.653 W6 20.962
608	30/10/2008 13:06	N55 44.650 W6 20.970
609	30/10/2008 13:07	N55 44.649 W6 20.975
610	30/10/2008 13:07	N55 44.648 W6 20.979
611	30/10/2008 13:07	N55 44.647 W6 20.982
612	30/10/2008 13:08	N55 44.645 W6 20.986
613	30/10/2008 13:08	N55 44.644 W6 20.990
614	30/10/2008 13:08	N55 44.649 W6 20.996
615	30/10/2008 13:08	N55 44.653 W6 21.025
616	30/10/2008 13:08	N55 44.655 W6 21.046
617	30/10/2008 13:09	N55 44.656 W6 21.060
618	30/10/2008 13:09	N55 44.656 W6 21.073
619	30/10/2008 13:09	N55 44.653 W6 21.091
620	30/10/2008 13:10	N55 44.648 W6 21.103
621	30/10/2008 13:10	N55 44.647 W6 21.107
622	30/10/2008 13:10	N55 44.645 W6 21.116
623	30/10/2008 13:11	N55 44.643 W6 21.121

Development and Application of Novel Tracers for Environmental Applications  
 Appendix IV: Case Study GPS Data

---

624	30/10/2008 13:11	N55 44.642 W6 21.125
625	30/10/2008 13:11	N55 44.641 W6 21.128
626	30/10/2008 13:12	N55 44.639 W6 21.132
627	30/10/2008 13:12	N55 44.638 W6 21.139
628	30/10/2008 13:12	N55 44.641 W6 21.149
629	30/10/2008 13:13	N55 44.641 W6 21.156
630	30/10/2008 13:13	N55 44.639 W6 21.160
631	30/10/2008 13:13	N55 44.637 W6 21.163
632	30/10/2008 13:14	N55 44.636 W6 21.177
633	30/10/2008 13:14	N55 44.631 W6 21.175
634	30/10/2008 13:14	N55 44.631 W6 21.173
635	30/10/2008 13:14	N55 44.626 W6 21.150
636	30/10/2008 13:15	N55 44.623 W6 21.139
637	30/10/2008 13:15	N55 44.621 W6 21.129
638	30/10/2008 13:15	N55 44.615 W6 21.117
639	30/10/2008 13:16	N55 44.612 W6 21.113
640	30/10/2008 13:16	N55 44.610 W6 21.115
641	30/10/2008 13:16	N55 44.608 W6 21.119
642	30/10/2008 13:16	N55 44.605 W6 21.119
643	30/10/2008 13:17	N55 44.598 W6 21.108
644	30/10/2008 13:17	N55 44.596 W6 21.098
645	30/10/2008 13:17	N55 44.603 W6 21.091
646	30/10/2008 13:17	N55 44.603 W6 21.090
647	30/10/2008 13:18	N55 44.612 W6 21.079
648	30/10/2008 13:18	N55 44.614 W6 21.078
649	30/10/2008 13:18	N55 44.626 W6 21.085
650	30/10/2008 13:19	N55 44.634 W6 21.092
651	30/10/2008 13:19	N55 44.644 W6 21.086
652	30/10/2008 13:19	N55 44.644 W6 21.084
653	30/10/2008 13:19	N55 44.648 W6 21.069
654	30/10/2008 13:19	N55 44.648 W6 21.064
655	30/10/2008 13:20	N55 44.651 W6 21.052
656	30/10/2008 13:20	N55 44.654 W6 21.052
657	30/10/2008 13:20	N55 44.666 W6 21.059
658	30/10/2008 13:20	N55 44.674 W6 21.066
659	30/10/2008 13:20	N55 44.679 W6 21.069
660	30/10/2008 13:21	N55 44.694 W6 21.062
661	30/10/2008 13:21	N55 44.703 W6 21.067
662	30/10/2008 13:21	N55 44.706 W6 21.066
663	30/10/2008 13:21	N55 44.716 W6 21.047
664	30/10/2008 13:22	N55 44.729 W6 21.035
665	30/10/2008 13:22	N55 44.747 W6 21.028
666	30/10/2008 13:22	N55 44.757 W6 21.008
667	30/10/2008 13:23	N55 44.769 W6 20.986
668	30/10/2008 13:23	N55 44.777 W6 21.002
669	30/10/2008 13:23	N55 44.772 W6 21.012
670	30/10/2008 13:23	N55 44.757 W6 21.007
671	30/10/2008 13:24	N55 44.750 W6 21.009
672	30/10/2008 13:24	N55 44.737 W6 21.013
673	30/10/2008 13:24	N55 44.724 W6 21.015
674	30/10/2008 13:25	N55 44.719 W6 21.022
675	30/10/2008 13:25	N55 44.718 W6 21.027

Development and Application of Novel Tracers for Environmental Applications  
 Appendix IV: Case Study GPS Data

---

676	30/10/2008 13:25	N55 44.710 W6 21.039
677	30/10/2008 13:25	N55 44.703 W6 21.046
678	30/10/2008 13:26	N55 44.689 W6 21.058
679	30/10/2008 13:26	N55 44.677 W6 21.068
680	30/10/2008 13:26	N55 44.667 W6 21.081
681	30/10/2008 13:27	N55 44.660 W6 21.094
682	30/10/2008 13:27	N55 44.654 W6 21.104
683	30/10/2008 13:27	N55 44.647 W6 21.112
684	30/10/2008 13:28	N55 44.642 W6 21.118
685	30/10/2008 13:28	N55 44.638 W6 21.125
686	30/10/2008 13:28	N55 44.635 W6 21.134
687	30/10/2008 13:29	N55 44.634 W6 21.139
688	30/10/2008 13:29	N55 44.632 W6 21.143
689	30/10/2008 13:29	N55 44.629 W6 21.145
690	30/10/2008 13:29	N55 44.628 W6 21.147
691	30/10/2008 13:30	N55 44.639 W6 21.154
692	30/10/2008 13:30	N55 44.639 W6 21.146
693	30/10/2008 13:30	N55 44.635 W6 21.129
694	30/10/2008 13:30	N55 44.632 W6 21.118
695	30/10/2008 13:31	N55 44.636 W6 21.104
696	30/10/2008 13:31	N55 44.640 W6 21.094
697	30/10/2008 13:31	N55 44.640 W6 21.089
698	30/10/2008 13:32	N55 44.641 W6 21.086
699	30/10/2008 13:32	N55 44.644 W6 21.100
700	30/10/2008 13:32	N55 44.645 W6 21.110
701	30/10/2008 13:33	N55 44.647 W6 21.120
702	30/10/2008 13:33	N55 44.647 W6 21.126
703	30/10/2008 13:33	N55 44.646 W6 21.131
704	30/10/2008 13:34	N55 44.644 W6 21.135
705	30/10/2008 13:34	N55 44.642 W6 21.139
706	30/10/2008 13:34	N55 44.641 W6 21.141
707	30/10/2008 13:34	N55 44.646 W6 21.148
708	30/10/2008 13:34	N55 44.671 W6 21.152
709	30/10/2008 13:35	N55 44.688 W6 21.159
710	30/10/2008 13:35	N55 44.699 W6 21.189
711	30/10/2008 13:35	N55 44.701 W6 21.247
712	30/10/2008 13:35	N55 44.690 W6 21.341
713	30/10/2008 13:35	N55 44.683 W6 21.470
714	30/10/2008 13:36	N55 44.676 W6 21.593
715	30/10/2008 13:36	N55 44.674 W6 21.697
716	30/10/2008 13:36	N55 44.662 W6 21.824
717	30/10/2008 13:36	N55 44.655 W6 21.941
718	30/10/2008 13:37	N55 44.652 W6 22.030
719	30/10/2008 13:37	N55 44.649 W6 22.069
720	30/10/2008 13:37	N55 44.649 W6 22.086
721	30/10/2008 13:37	N55 44.648 W6 22.094
722	30/10/2008 13:38	N55 44.645 W6 22.101
723	30/10/2008 13:38	N55 44.641 W6 22.107
724	30/10/2008 13:38	N55 44.638 W6 22.110
725	30/10/2008 13:39	N55 44.634 W6 22.114
726	30/10/2008 13:39	N55 44.630 W6 22.119
727	30/10/2008 13:39	N55 44.625 W6 22.124

Development and Application of Novel Tracers for Environmental Applications  
 Appendix IV: Case Study GPS Data

---

728	30/10/2008 13:40	N55 44.620 W6 22.129
729	30/10/2008 13:40	N55 44.615 W6 22.135
730	30/10/2008 13:40	N55 44.628 W6 22.133
731	30/10/2008 13:41	N55 44.645 W6 22.105
732	30/10/2008 13:41	N55 44.697 W6 22.052
733	30/10/2008 13:41	N55 44.757 W6 21.998
734	30/10/2008 13:42	N55 44.811 W6 21.942
735	30/10/2008 13:42	N55 44.864 W6 21.891
736	30/10/2008 13:42	N55 44.887 W6 21.875
737	30/10/2008 13:42	N55 44.932 W6 21.844
738	30/10/2008 13:43	N55 44.985 W6 21.792
739	30/10/2008 13:43	N55 45.051 W6 21.722
740	30/10/2008 13:43	N55 45.115 W6 21.655
741	30/10/2008 13:44	N55 45.189 W6 21.591
742	30/10/2008 13:44	N55 45.260 W6 21.527
743	30/10/2008 13:45	N55 45.327 W6 21.471
744	30/10/2008 13:45	N55 45.404 W6 21.394
745	30/10/2008 13:46	N55 45.470 W6 21.347
746	30/10/2008 13:46	N55 45.561 W6 21.289
747	30/10/2008 13:47	N55 45.649 W6 21.229
748	30/10/2008 13:47	N55 45.742 W6 21.173
749	30/10/2008 13:47	N55 45.821 W6 21.103
750	30/10/2008 13:48	N55 45.904 W6 21.037
751	30/10/2008 13:48	N55 46.004 W6 20.977
752	30/10/2008 13:49	N55 46.078 W6 20.927
753	30/10/2008 13:49	N55 46.147 W6 20.866
754	30/10/2008 13:49	N55 46.216 W6 20.782
755	30/10/2008 13:50	N55 46.287 W6 20.672
756	30/10/2008 13:50	N55 46.343 W6 20.548
757	30/10/2008 13:50	N55 46.401 W6 20.449
758	30/10/2008 13:51	N55 46.450 W6 20.358
759	30/10/2008 13:51	N55 46.496 W6 20.253
760	30/10/2008 13:51	N55 46.557 W6 20.173
761	30/10/2008 13:52	N55 46.629 W6 20.114
762	30/10/2008 13:52	N55 46.715 W6 20.084
763	30/10/2008 13:53	N55 46.746 W6 20.082
764	30/10/2008 13:53	N55 46.781 W6 20.090
765	30/10/2008 13:53	N55 46.796 W6 20.093
766	30/10/2008 13:54	N55 46.797 W6 20.108
767	30/10/2008 13:54	N55 46.792 W6 20.120
768	30/10/2008 13:55	N55 46.788 W6 20.127
769	30/10/2008 13:55	N55 46.784 W6 20.134
770	30/10/2008 13:55	N55 46.781 W6 20.141
771	30/10/2008 13:56	N55 46.781 W6 20.143
772	30/10/2008 13:56	N55 46.788 W6 20.140
773	30/10/2008 13:56	N55 46.788 W6 20.076
774	30/10/2008 13:56	N55 46.783 W6 19.949
775	30/10/2008 13:57	N55 46.773 W6 19.722
776	30/10/2008 13:57	N55 46.770 W6 19.533
777	30/10/2008 13:58	N55 46.771 W6 19.338
778	30/10/2008 13:58	N55 46.767 W6 19.142
779	30/10/2008 13:59	N55 46.764 W6 18.922

Development and Application of Novel Tracers for Environmental Applications  
 Appendix IV: Case Study GPS Data

---

780	30/10/2008 13:59	N55 46.760 W6 18.710
781	30/10/2008 14:00	N55 46.759 W6 18.505
782	30/10/2008 14:00	N55 46.765 W6 18.354
783	30/10/2008 14:00	N55 46.783 W6 18.108
784	30/10/2008 14:01	N55 46.795 W6 18.030
785	30/10/2008 14:01	N55 46.797 W6 17.994
786	30/10/2008 14:02	N55 46.792 W6 17.980
787	30/10/2008 14:02	N55 46.785 W6 17.977
788	30/10/2008 14:03	N55 46.778 W6 17.978
789	30/10/2008 14:03	N55 46.772 W6 17.979
790	30/10/2008 14:04	N55 46.770 W6 17.980
791	30/10/2008 14:04	N55 46.767 W6 17.982
792	30/10/2008 14:04	N55 46.761 W6 17.985
793	30/10/2008 14:05	N55 46.754 W6 17.990
794	30/10/2008 14:06	N55 46.750 W6 17.992
795	30/10/2008 14:06	N55 46.747 W6 17.994
796	30/10/2008 14:06	N55 46.742 W6 17.996
797	30/10/2008 14:07	N55 46.738 W6 17.998
798	30/10/2008 14:07	N55 46.733 W6 17.999
799	30/10/2008 14:08	N55 46.727 W6 18.000
800	30/10/2008 14:08	N55 46.720 W6 18.004
801	30/10/2008 14:09	N55 46.713 W6 18.007
802	30/10/2008 14:09	N55 46.709 W6 18.008
803	30/10/2008 14:10	N55 46.703 W6 18.010
804	30/10/2008 14:11	N55 46.695 W6 18.018
805	30/10/2008 14:11	N55 46.692 W6 18.023
806	30/10/2008 14:12	N55 46.685 W6 18.026
807	30/10/2008 14:12	N55 46.679 W6 18.030
808	30/10/2008 14:13	N55 46.676 W6 18.033
809	30/10/2008 14:13	N55 46.671 W6 18.036
810	30/10/2008 14:14	N55 46.666 W6 18.039
811	30/10/2008 14:14	N55 46.662 W6 18.043
812	30/10/2008 14:15	N55 46.656 W6 18.049
813	30/10/2008 14:15	N55 46.653 W6 18.054
814	30/10/2008 14:16	N55 46.648 W6 18.057
815	30/10/2008 14:16	N55 46.641 W6 18.063
816	30/10/2008 14:17	N55 46.638 W6 18.068
817	30/10/2008 14:17	N55 46.633 W6 18.072
818	30/10/2008 14:17	N55 46.630 W6 18.074
819	30/10/2008 14:18	N55 46.625 W6 18.076
820	30/10/2008 14:18	N55 46.621 W6 18.078
821	30/10/2008 14:18	N55 46.618 W6 18.050
822	30/10/2008 14:19	N55 46.609 W6 18.012
823	30/10/2008 14:19	N55 46.569 W6 17.951
824	30/10/2008 14:19	N55 46.501 W6 17.907
825	30/10/2008 14:19	N55 46.399 W6 17.871
826	30/10/2008 14:20	N55 46.290 W6 17.829
827	30/10/2008 14:20	N55 46.193 W6 17.765
828	30/10/2008 14:21	N55 46.109 W6 17.691
829	30/10/2008 14:21	N55 46.016 W6 17.610
830	30/10/2008 14:21	N55 45.909 W6 17.531
831	30/10/2008 14:22	N55 45.822 W6 17.467



Development and Application of Novel Tracers for Environmental Applications  
 Appendix IV: Case Study GPS Data

---

832	30/10/2008 14:22	N55 45.743 W6 17.415
833	30/10/2008 14:22	N55 45.654 W6 17.357
834	30/10/2008 14:23	N55 45.616 W6 17.314
835	30/10/2008 14:23	N55 45.591 W6 17.300
836	30/10/2008 14:23	N55 45.567 W6 17.306
837	30/10/2008 14:24	N55 45.563 W6 17.311
838	30/10/2008 14:24	N55 45.560 W6 17.312
839	30/10/2008 14:24	N55 45.559 W6 17.302
840	30/10/2008 14:24	N55 45.577 W6 17.275
841	30/10/2008 14:25	N55 45.581 W6 17.279
842	30/10/2008 14:25	N55 45.580 W6 17.289
843	30/10/2008 14:25	N55 45.588 W6 17.297
844	30/10/2008 14:26	N55 45.593 W6 17.263
845	30/10/2008 14:26	N55 45.594 W6 17.261
846	30/10/2008 14:26	N55 45.591 W6 17.249
847	30/10/2008 14:26	N55 45.586 W6 17.245
848	30/10/2008 14:27	N55 45.582 W6 17.244
849	30/10/2008 14:27	N55 45.580 W6 17.239
850	30/10/2008 14:27	N55 45.586 W6 17.234
851	30/10/2008 14:27	N55 45.600 W6 17.247
852	30/10/2008 14:28	N55 45.598 W6 17.258
853	30/10/2008 14:28	N55 45.594 W6 17.265
854	30/10/2008 14:29	N55 45.590 W6 17.269
855	30/10/2008 14:29	N55 45.586 W6 17.272
856	30/10/2008 14:29	N55 45.582 W6 17.277
857	30/10/2008 14:30	N55 45.579 W6 17.279
858	30/10/2008 14:30	N55 45.576 W6 17.283
859	30/10/2008 14:30	N55 45.573 W6 17.286
860	30/10/2008 14:31	N55 45.569 W6 17.289
861	30/10/2008 14:31	N55 45.565 W6 17.294
862	30/10/2008 14:31	N55 45.565 W6 17.299
863	30/10/2008 14:31	N55 45.554 W6 17.307
864	30/10/2008 14:32	N55 45.536 W6 17.310
865	30/10/2008 14:32	N55 45.534 W6 17.310
866	30/10/2008 14:32	N55 45.532 W6 17.301
867	30/10/2008 14:32	N55 45.534 W6 17.295
868	30/10/2008 14:32	N55 45.535 W6 17.295
869	30/10/2008 14:33	N55 45.534 W6 17.307
870	30/10/2008 14:33	N55 45.541 W6 17.307
871	30/10/2008 14:33	N55 45.541 W6 17.298
872	30/10/2008 14:34	N55 45.539 W6 17.296
873	30/10/2008 14:34	N55 45.537 W6 17.290
874	30/10/2008 14:34	N55 45.538 W6 17.291
875	30/10/2008 14:35	N55 45.542 W6 17.300
876	30/10/2008 14:35	N55 45.545 W6 17.306
877	30/10/2008 14:35	N55 45.546 W6 17.329
878	30/10/2008 14:35	N55 45.537 W6 17.332
879	30/10/2008 14:36	N55 45.532 W6 17.339
880	30/10/2008 14:36	N55 45.529 W6 17.331
881	30/10/2008 14:36	N55 45.532 W6 17.334
882	30/10/2008 14:37	N55 45.537 W6 17.344
883	30/10/2008 14:37	N55 45.540 W6 17.346

Development and Application of Novel Tracers for Environmental Applications  
 Appendix IV: Case Study GPS Data

---

884	30/10/2008 14:37	N55 45.540 W6 17.332
885	30/10/2008 14:38	N55 45.545 W6 17.316
886	30/10/2008 14:38	N55 45.543 W6 17.309
887	30/10/2008 14:39	N55 45.540 W6 17.305
888	30/10/2008 14:39	N55 45.544 W6 17.310
889	30/10/2008 14:39	N55 45.534 W6 17.349
890	30/10/2008 14:40	N55 45.532 W6 17.369
891	30/10/2008 14:40	N55 45.537 W6 17.382
892	30/10/2008 14:40	N55 45.544 W6 17.394
893	30/10/2008 14:41	N55 45.543 W6 17.384
894	30/10/2008 14:41	N55 45.540 W6 17.379
895	30/10/2008 14:41	N55 45.538 W6 17.348
896	30/10/2008 14:42	N55 45.541 W6 17.318
897	30/10/2008 14:42	N55 45.539 W6 17.307
898	30/10/2008 14:42	N55 45.540 W6 17.294
899	30/10/2008 14:43	N55 45.541 W6 17.283
900	30/10/2008 14:43	N55 45.540 W6 17.269
901	30/10/2008 14:43	N55 45.543 W6 17.266
902	30/10/2008 14:44	N55 45.546 W6 17.276
903	30/10/2008 14:44	N55 45.551 W6 17.288
904	30/10/2008 14:44	N55 45.554 W6 17.284
905	30/10/2008 14:44	N55 45.550 W6 17.277
906	30/10/2008 14:45	N55 45.543 W6 17.259
907	30/10/2008 14:45	N55 45.547 W6 17.262
908	30/10/2008 14:45	N55 45.551 W6 17.263
909	30/10/2008 14:46	N55 45.551 W6 17.254
910	30/10/2008 14:46	N55 45.550 W6 17.247
911	30/10/2008 14:46	N55 45.553 W6 17.249
912	30/10/2008 14:47	N55 45.555 W6 17.254
913	30/10/2008 14:47	N55 45.557 W6 17.262
914	30/10/2008 14:47	N55 45.554 W6 17.268
915	30/10/2008 14:48	N55 45.543 W6 17.278
916	30/10/2008 14:48	N55 45.540 W6 17.260
917	30/10/2008 14:48	N55 45.541 W6 17.251
918	30/10/2008 14:49	N55 45.547 W6 17.251
919	30/10/2008 14:49	N55 45.548 W6 17.252
920	30/10/2008 14:49	N55 45.554 W6 17.258
921	30/10/2008 14:49	N55 45.554 W6 17.284
922	30/10/2008 14:50	N55 45.551 W6 17.294
923	30/10/2008 14:50	N55 45.548 W6 17.297
924	30/10/2008 14:50	N55 45.544 W6 17.294
925	30/10/2008 14:51	N55 45.541 W6 17.294
926	30/10/2008 14:51	N55 45.540 W6 17.300
927	30/10/2008 14:51	N55 45.540 W6 17.314
928	30/10/2008 14:51	N55 45.536 W6 17.340
929	30/10/2008 14:52	N55 45.522 W6 17.368
930	30/10/2008 14:52	N55 45.517 W6 17.383
931	30/10/2008 14:52	N55 45.512 W6 17.396
932	30/10/2008 14:53	N55 45.507 W6 17.404
933	30/10/2008 14:53	N55 45.508 W6 17.410
934	30/10/2008 14:53	N55 45.515 W6 17.417
935	30/10/2008 14:53	N55 45.519 W6 17.411

Development and Application of Novel Tracers for Environmental Applications  
 Appendix IV: Case Study GPS Data

---

936	30/10/2008 14:54	N55 45.524 W6 17.405
937	30/10/2008 14:54	N55 45.529 W6 17.425
938	30/10/2008 14:54	N55 45.549 W6 17.447
939	30/10/2008 14:54	N55 45.557 W6 17.431
940	30/10/2008 14:55	N55 45.563 W6 17.390
941	30/10/2008 14:55	N55 45.560 W6 17.366
942	30/10/2008 14:55	N55 45.554 W6 17.339
943	30/10/2008 14:56	N55 45.552 W6 17.322
944	30/10/2008 14:56	N55 45.549 W6 17.315
945	30/10/2008 14:56	N55 45.546 W6 17.314
946	30/10/2008 14:57	N55 45.547 W6 17.307
947	30/10/2008 14:57	N55 45.550 W6 17.311
948	30/10/2008 14:57	N55 45.547 W6 17.354
949	30/10/2008 14:57	N55 45.535 W6 17.375
950	30/10/2008 14:57	N55 45.531 W6 17.361
951	30/10/2008 14:58	N55 45.533 W6 17.353
952	30/10/2008 14:58	N55 45.537 W6 17.346
953	30/10/2008 14:58	N55 45.534 W6 17.341
954	30/10/2008 14:59	N55 45.534 W6 17.335
955	30/10/2008 14:59	N55 45.537 W6 17.334
956	30/10/2008 14:59	N55 45.542 W6 17.333
957	30/10/2008 14:59	N55 45.548 W6 17.329
958	30/10/2008 15:00	N55 45.551 W6 17.333
959	30/10/2008 15:00	N55 45.549 W6 17.338
960	30/10/2008 15:00	N55 45.546 W6 17.343
961	30/10/2008 15:01	N55 45.543 W6 17.339
962	30/10/2008 15:01	N55 45.542 W6 17.336
963	30/10/2008 15:01	N55 45.542 W6 17.358
964	30/10/2008 15:01	N55 45.544 W6 17.402
965	30/10/2008 15:02	N55 45.535 W6 17.410
966	30/10/2008 15:02	N55 45.531 W6 17.405
967	30/10/2008 15:02	N55 45.531 W6 17.394
968	30/10/2008 15:03	N55 45.529 W6 17.387
969	30/10/2008 15:03	N55 45.527 W6 17.379
970	30/10/2008 15:03	N55 45.527 W6 17.368
971	30/10/2008 15:04	N55 45.528 W6 17.369
972	30/10/2008 15:04	N55 45.530 W6 17.401
973	30/10/2008 15:04	N55 45.530 W6 17.424
974	30/10/2008 15:05	N55 45.525 W6 17.437
975	30/10/2008 15:05	N55 45.524 W6 17.458
976	30/10/2008 15:05	N55 45.526 W6 17.476
977	30/10/2008 15:06	N55 45.526 W6 17.497
978	30/10/2008 15:06	N55 45.531 W6 17.500
979	30/10/2008 15:06	N55 45.531 W6 17.485
980	30/10/2008 15:07	N55 45.533 W6 17.469
981	30/10/2008 15:07	N55 45.536 W6 17.465
982	30/10/2008 15:07	N55 45.546 W6 17.451
983	30/10/2008 15:07	N55 45.559 W6 17.421
984	30/10/2008 15:08	N55 45.560 W6 17.407
985	30/10/2008 15:08	N55 45.561 W6 17.384
986	30/10/2008 15:08	N55 45.566 W6 17.363
987	30/10/2008 15:08	N55 45.568 W6 17.316

Development and Application of Novel Tracers for Environmental Applications  
Appendix IV: Case Study GPS Data

---

988	30/10/2008 15:09	N55 45.550 W6 17.302
989	30/10/2008 15:09	N55 45.524 W6 17.301
990	30/10/2008 15:09	N55 45.502 W6 17.302
991	30/10/2008 15:10	N55 45.498 W6 17.310
992	30/10/2008 15:10	N55 45.499 W6 17.320
993	30/10/2008 15:10	N55 45.497 W6 17.319
994	30/10/2008 15:10	N55 45.495 W6 17.318
995	30/10/2008 15:11	N55 45.495 W6 17.322
996	30/10/2008 15:11	N55 45.493 W6 17.325
997	30/10/2008 15:11	N55 45.492 W6 17.314
998	30/10/2008 15:11	N55 45.495 W6 17.322
999	30/10/2008 15:12	N55 45.500 W6 17.324
1000	30/10/2008 15:12	N55 45.499 W6 17.326
1001	30/10/2008 15:13	N55 45.498 W6 17.325
1002	30/10/2008 15:13	N55 45.499 W6 17.326
1003	30/10/2008 15:14	N55 45.497 W6 17.326
1004	30/10/2008 15:14	N55 45.496 W6 17.325
1005	30/10/2008 15:14	N55 45.495 W6 17.323
1006	30/10/2008 15:16	N55 45.496 W6 17.326
1007	30/10/2008 15:16	N55 45.497 W6 17.329
1008	30/10/2008 15:17	N55 45.497 W6 17.329
1009	30/10/2008 15:19	N55 45.498 W6 17.328

